REAL-TIME ESTIMATION OF DELAY AT SIGNALIZED INTERSECTIONS

By

JEFFREY W. BUCKHOLZ

A DISSERTATION PRESENTED TO THE GRADUATE SCHOOL
OF THE UNIVERSITY OF FLORIDA IN PARTIAL FULFILLMENT
OF THE REQUIREMENTS FOR THE DEGREE OF
DOCTOR OF PHILOSOPHY

UNIVERSITY OF FLORIDA

2007

To my dogs Zack and Sweet Pea,
who always provided me with free “fuzz therapy.”
I wish that service was still available.

ACKNOWLEDGMENTS

Special thanks go to Mr. Seokjoo Lee for his programming assistance and to Mr. Petra Vintu for checking the mathematical derivations

TABLE OF CONTENTS

page

ACKNOWLEDGMENTS 4

LIST OF TABLES 8

LIST OF FIGURES 10

ABSTRACT 14

CHAPTER

1 INTRODUCTION AND PROBLEM STATEMENT 16

Background Discussion 16
Problem Statement 19

2 OBJECTIVES AND RESEARCH APPROACH 22

3 CURRENT STATE OF THE ART 30

Real-Time Measurement of Intersection Delay 30
Vehicle Reidentification via Inductance Loops 36
Performance of Video Detection Systems 45
Signalized Intersection Queuing and Delay 52
Probe Monitoring 65
Extending the Body of Knowledge 67

4 ESTIMATING NON-VISIBLE DELAY 68

Data Analysis Programs 68
Prediction Algorithm for Non-Visible Delay 80
Non-Visible Queue Estimation Technique 80
Non-Visible Queue Adjustment Technique: 82
Non-Visible Queue Re-Adjustment Technique: 83
Examples 84
Queue Prediction 87
Stopped Delay Prediction 88
Control Delay Prediction 90
Variability Considerations 91
Limitations to the Delay Prediction Procedure 92

5 THEORETICAL BOUNDS FOR DELAY ESTIMATION 129

Derivation of the Bounds 131
Derivation of the Upper Bound 134
Derivation of the Lower Bound 138

Analysis of Bounds Summary 146
Derivation of Delay for Upper and Lower Bounds 148
Derivation of the Bounds with Visible Period 1 Queue 166
Derivation of Upper Bound with Visible Period 1 Queue 166
Derivation of Lower Bound with Visible Period 1 Queue 172
Analysis of Bounds Summary with Visible Period 1 Queue 173
Derivation of Delay with Visible Period 1 Queue 174
Derivation of the Bounds When Queue is Visible During Three Periods 176
Derivation of the Bounds When Analysis Time Frame is Greater Than One Hour 176
Derivation of the Five Period Upper Bound 177
Derivation of the Five Period Lower Bound 183
Five Period Analysis of Bounds Summary 197
Generalized Analysis of Bounds Summary 200
Historical Peak Hour Factors 203
Limitations to the Theoretical Bracketing Procedure 205

6 COMPARISONS WITH VEHICLE TRAJECTORY ANALYSIS 228

Trajectory Example 230
Cumulative Arrival/Departure Curve Example 232
Reconciling the Difference Between Cumulative Curves and Trajectories 233
Calculating Trajectory-Based Delay Components for the BuckQ Examples 236
Calculating Cumulative Curve Delay for the BuckQ Examples 237
Bracketing the Stopped Delay Prediction Results 240

7 PERIOD ISSUES DURING OVER-SATURATED FLOW 276

Simplified Example of Cycle-Period Issues in Calculating d_3 276
Residual Queue Discrepancy 281
Detailed Example of Cycle-Period Issues in Calculating d_3 283

8 CONCLUSIONS, APPLICATIONS, AND RECOMMENDATIONS 299

Research Findings 299
Application of the Research 301
Example 1: Signal System Retiming Evaluation 302
Example 2: Real-Time Traffic Signal Control 303
Example 3: Signalized Intersection Capacity Analysis 304
Potential Areas of Extended Research 304

APPENDIX

A DATA SETS FOR BUCKQ TESTING 308

B TYPICAL PEAK HOUR FACTORS 331

C GENERALIZED CYCLE-PERIOD DELAY EXAMPLE: 353

REFERENCES 376

BIOGRAPHICAL SKETCH 381

LIST OF TABLES

Table		page
4-1	Example summary - volume and capacity	122
4-2	Example summary - queue discharge, delay check and goodness-of-fit	123
4-3	Queue prediction	124
4-4	Stopped delay prediction	125
4-5	Control delay prediction	126
4-6	Comparison of variation in actual and predicted stopped delay	127
4-7	P-value determination for difference in median values	128
6-1	Calculation of cumulative curve delay conversion factors, volume pattern 625_700_650_350vph	249
6-2	Calculation of cumulative curve delay conversion factors, volume pattern 700_725_625_350vph	251
6-3	Calculation of cumulative curve delay conversion factors, volume pattern 700_700_700_350vph	253
6-4	Calculation of cumulative curve delay conversion factors, volume pattern 725_700_700_350vph	255
6-5	Cumulative curve delay for standard 4-period case	257
6-6	Cumulative curve delay with multiple visible periods	258
6-7	Stopped delay prediction results for 700_725_625_350vph volume pattern	259
6-8	Average stopped delay prediction results for 700_725_625_350vph volume pattern	262
6-9	Stopped delay prediction results for 700_700_700_350vph volume pattern	263
6-10	Average stopped delay prediction results for 700_700_700_350vph volume pattern	266
6-11	Stopped delay prediction results for 725_700_700_350vph volume pattern	267
6-12	Average stopped delay prediction results for 725_700_700_350vph volume pattern	270
6-13	Stopped delay prediction results for 625_700_650_350vph volume pattern	271
6-14	Average stopped delay prediction results for 625_700_650_350vph volume pattern	274

6-15 Prediction comparison 275

7-1 Generalized example of cycle-period delay discrepancies - data 292

7-2 Generalized example of cycle-period delay discrepancies – summary 293

7-3 Detailed example of cycle-period delay discrepancies, residual queue determination ...296

7-4 Detailed example of cycle-period delay discrepancies, delay comparison.....297

7-5 Detailed example of cycle-period delay discrepancies, delay comparison with modified d2 term.....297

7-6 Detailed example of cycle-period delay discrepancies, delay comparison with d_3 adjustment.....297

B1 US 1 machine counts (Southern St. Johns County) 334

B-2 US1 Machine counts (northern St. Johns County).....339

B-3 Atlantic Boulevard machine counts.....342

B-4 University Boulevard machine counts (Jacksonville).....345

B-5 SR A1A machine counts (Crescent Beach) 348

B-6 SR A1A machine counts (Ponte Vedra) PDF 17 KB 351

B-7 Appendix B data summary.....352

C-1 Generalized example of cycle-period delay discrepancies – data. 354

LIST OF FIGURES

Figure		page
4-1	Queue relationships	94
4-2	Signalized intersection delay components	95
4-3	Measured versus estimated delay	96
4-4	Visible and non-visible variables	97
4-5	Relationship between v/c ratio and ratio of control delay to stopped delay	98
4-6	Re-queuing that results in simultaneous queues	99
4-7	Re-queuing that does not result in simultaneous queues	100
4-8	Example of a blind period	101
4-9	Example of adjacent blind periods	102
4-10	Counters and queue status	103
4-11	Base case for P, C and X; stopped delay comparison	104
4-12	Effect of increasing the power constant on stopped delay comparison	105
4-13	Queue propagation example	106
4-14	Actual vehicle queues	107
4-15	Average queue length comparison	108
4-16	Maximum queue length comparison	109
4-17	98th percentile back of queue comparison	110
4-18	Vehicle re-queuing	111
4-19	Stopped delay comparison	112
4-20	Stopped delay prediction, 12 FOV	113
4-21	Comparison of actual and predicted stopped delay	114
4-22	Adjacent blind period counter v. stopped delay	115
4-23	Control delay comparison	116

4-24 Ratio of control delay to stopped delay 117
4-25 Graphical control delay comparison, ...118
4-26 Control delay estimates.....119
4-27 Control delay composition.....120
4-28 Ratio of control delay to stopped plus move-up delay 121
5-1 Cumulative arrival-departure curves and overflow delay.....207
5-2 Critical time and volume points for period 4.....208
5-3 Overflow delay in period 4 209
5-4 Maximum reasonable cumulative arrival curve.....210
5-5 Minimum reasonable cumulative arrival curve 211
5-6 Minimum overall reasonable cumulative arrival curve 212
5-7 Minimum reasonable cumulative arrival curve (minimum V_4 for minimum V_1 and V_2).....213
5-8 Minimum reasonable cumulative arrival curve (minimum V_4 for minimum V_1) 214
5-9 Period 1 delay for the upper bound.....215
5-10 Period 2 delay for the upper bound.....216
5-11 Period 3 and period 4 delay for the upper bound.....217
5-12 Reasonable overflow delay region for 600 vph capacity and 0.75 minimum PHF 218
5-13 Reasonable overflow delay region for 600 vph capacity and 0.80 minimum PHF 219
5-14 Reasonable overflow delay region for 600 vph capacity and 0.85 minimum PHF 220
5-15 Maximum delay estimation error for 0.75 minimum PHF 221
5-16 Maximum delay estimation error for 0.80 minimum PHF 222
5-17 Maximum delay estimation error for 0.85 minimum PHF 223
5-18 Maximum reasonable cumulative arrival curve with period 1 visible.....224
5-19 Minimum reasonable cumulative arrival curve with period 1 visible 225
5-20 Maximum reasonable cumulative arrival curve with 5 periods.....226

5-21 Minimum reasonable cumulative arrival curve with 5 periods 227

6-1 Trajectory example A) Complete chart B) Detailed view of circled area in upper right corner.....244

6-2 Cumulative arrival-departure curve example.....246

6-3 Trajectory conversion of cumulative curve example.....247

6-4 Delay and travel time components.....248

7-1 Cycle v. period initial queue delay analysis.....294

7-2 Cycle v. period "control delay" analysis.....295

7-3 Upward bias in HCM residual queue calculation 298

A-1 Queue discharge headway histogram.....309

A-2 Start-up lost time histogram.....310

A-3 Comparison of control delay and stopped delay by cycle length (g/C =0.30).....311

A-4 Comparison of control delay and stopped delay (g/C =0.30) 312

A-5 Comparison of control delay and stopped plus queue move-up delay by cycle length (g/C = 0.30).....313

A-6 Comparison of control delay and stopped delay plus queue move-up delay (g/C =0.30).....314

A-7 Relationship between v/c ratio and stopped delay.....315

A-8 Relationship between v/c ratio and stopped delay by cycle length 316

A-9 Relationship between v/c ratio and stopped plus queue move-up delay 317

A-10 Relationship between v/c ratio and stopped plus queue move-up delay by cycle length.....318

A-11 Relationship between v/c ratio and control delay.....319

A-12 Relationship between v/c ratio and control delay by cycle length.....320

A-13 Relationship between vehicle re-queues and control delay 321

A-14 Relationship between v/c ratio and vehicle re-queues.....322

A-15 Relationship between v/c ratio and vehicle re-queues by cycle length 323

A-16 Relationship between v/c ratio and cycles with phase failure 324
A-17 Relationship between v/c ratio and cycles with phase failure by cycle length 325
A-18 Percentage of cycles in 1 hour with phase failure by cycle length 326
A-19 Percentage of cycles in 1 hour with phase failure.....327
A-20 Linear relationship between ABPC and stopped delay.....328
A-21 Exponential relationship between ABPC and stopped delay.....329
A-22 Relationship between ABPC and control delay.....330
B-1 US 1 S. PM peak hour factor, southbound (outbound) flow 332
B-2 US 1 S. PM peak period factor, southbound (outbound) flow.....333
B-3 US 1 N. PM peak hour factor, northbound (outbound) flow 337
B-4 US 1 N. PM peak period factor, northbound (outbound) flow 338
B-5 Atlantic Boulevard PM peak hour factor, eastbound (outbound) flow.....340
B-6 Atlantic Boulevard PM peak period factor, eastbound (outbound) flow.....341
B-7 University Blvd. PM peak hour factor, northbound (outbound) flow 343
B-8 University Blvd. PM peak period factor, northbound (outbound) flow 344
B-9 SR A1A S. PM peak hour factor, southbound (outbound) flow.....346
B-10 SR A1A S. PM peak period factor, southbound (outbound) flow.....347
B-11 SR A1A N. PM peak hour factor, southbound (outbound) flow 349
B-12 SR A1A N. PM peak period factor, southbound (outbound) flow 350

Abstract of Dissertation Presented to the Graduate School
of the University of Florida in Partial Fulfillment of the
Requirements for the Degree of Doctor of Philosophy

REAL-TIME ESTIMATION OF DELAY AT SIGNALIZED INTERSECTIONS

By

Jeffrey W. Buckholz

December 2007

Chair: Ken Courage
Major: Civil and Coastal Engineering

To evaluate improvements at signalized intersections it is important to know the resulting change in vehicular delay. However, it is difficult to collect delay data during over-saturated conditions even though this is when knowledge of delay levels is critical. Extensive peak hour queuing thwarts our ability to collect key data, such as arrivals at the back of queue. This incomplete information makes it impossible to calculate the resulting delay.

The research presents a real-time procedure for estimating delay during over-saturated conditions with limited information. The procedure utilizes a series of adjustments to the measured arrival rate entering the field of view to estimate the true arrival rate at the back of the queue. An advantage of the procedure is that estimated queues and associated delay are calculated on a second-by-second basis in real time. A disadvantage is that no theoretical relationship exists between the measured arrival rate and the real arrival rate.

Fortunately, it is possible to calculate a set of theoretical upper and lower bounds on the solution space by using historical minimum peak hour factors. The theoretical bounds take the form of cumulative arrival curves. Delay is obtained through consideration of the area between these arrival curves and the associated departure curve. Trajectory analysis during over-

saturated conditions is used to reconcile the difference between stopped delay and the area between the curves.

This research also demonstrates that the Highway Capacity Manual (HCM) definition of an initial (residual) queue is incorrect. To identify the true residual queue, the situation must be evaluated at the end of the red interval and thruput during the subsequent green interval must be deducted. Failure to do so leads to overestimation of both the initial queue and the corresponding delay.

Another finding is that the random component of the HCM's incremental delay term incorrectly contributes to delay during over-saturated periods preceded by an initial queue. A remedial modification to the d_2 term is proposed.

Finally, it is demonstrated that the HCM's period-based queue accumulation procedure has drawbacks that can produce substantial errors in delay during over-saturated conditions. A remedial cycle-based counting technique is proposed.

CHAPTER 1
INTRODUCTION AND PROBLEM STATEMENT

Since the efficient operation of signalized intersections is a pertinent topic throughout the world, providing a real-time evaluation system that allows such intersections to be operated at maximum efficiency has the potential for tremendous benefit. Reductions in travel time would be the primary benefit, along with associated reductions in fuel usage and vehicle emissions. The benefits would accrue "24/7" in that signalized intersections function around the clock. In the United States alone there are approximately 265,000 signalized intersections and the delays at these signalized intersections contribute an estimated 25% to total highway system delay [1].

Background Discussion

To properly evaluate improvements made at a signalized intersection it is important to know the resulting change in various Measures of Effectiveness (MOEs), including what may be the most important MOE, vehicular delay. Delay is a particularly attractive measure of effectiveness because, as discussed by Hurdle [2], it can: "be measured; it has obvious economic worth; and it is easily understood by both technical and non-technical people." As recognized by Dowling [3], many MOEs (such as queue length, speed, stops, and density) are relatively invariant during highly over-saturated conditions where little vehicle movement occurs. Delay, on the other hand, continues to increase under such conditions, which is a highly desirable trait.

The benefit of corridor re-timing programs, signal phasing changes, and intersection geometric improvements can be properly evaluated only if a realistic assessment of the change in overall vehicular delay is determined. Collecting delay data by hand, as described in Chapter 16, Appendix A of the 2000 Highway Capacity Manual [4] is a labor-intensive task that must, by practical necessity, be limited to brief data collection periods. As Saito, et al. [5] put it:

> Manual field observations require large number of personnel and large amounts of other resources if delay estimates must be done frequently, such is the case if delay estimates are

> needed for Advanced Traffic Management Systems (ATMS's). The method is meant for occasional checks of delays at signalized intersections; it is not meant for continuous monitoring of the LOS (level of service) of signalized intersections. A more advantageous method would be to create automated methods of estimating delay from direct observation of queued vehicles. This significantly reduces the amount of data that needs to be collected and (eliminates) unnecessary assumptions. When such methods work, they allow traffic engineers to continuously monitor the LOS at intersections and estimate the arterial LOS …

In addition, it is particularly difficult to collect delay data during over-saturated conditions even though this is exactly when knowledge of delay levels is most critical. Consequently, under congested conditions, delay calculations that are based on manual information can be considered both piecemeal and of dubious accuracy. As Engelbrecht, et al. [6] explain

> From a practical point of view it is very difficult to accurately measure over-saturation delay in the field. Long queues and restricted sight distance may make the actual counting of queued vehicles impossible. Also, counting a large number of vehicles in a short 10-second interval may be very difficult. Furthermore, not all vehicles in the queue may be stationary at a single point in time, as internal shock waves due to the stopping and starting of traffic at the stop line may travel through the queue continuously. Because of the presence of non-stationary vehicles in the queue, transformation of the measured stopped delay into the overall delay predicted by most of the delay equations may be the most difficult task of all.

A properly automated method for collecting delay data, either on a cycle-by-cycle basis or on a periodic basis, could provide the needed evaluation data for all pertinent periods. Such a system would also provide reasonable estimations of delay, even during over-saturated conditions. Resulting delay data could then be used for project evaluation or for real-time modification of controller settings.

Using real-time delay obtained from intersection-based field measurements for project evaluation purposes (such as signal retiming evaluation) provides an important supplement to traditional before and after travel time runs, which completely ignore the delay experienced by side street motorists or main street left turn motorists. A rather large leap forward in project

evaluation could be taken if we are able to develop a widely applicable, robust procedure for calculating vehicular delay on the fly.

Video detection systems, vehicle re-identification systems using inductance loops, and probe monitoring all offer the potential of being able to calculate (or reasonably estimate) vehicular delay in real time.

Unfortunately, direct measurement of stopped delay via video detection or inductance loops falls prey to a number of practical limitations, ranging from detection inaccuracies to field of view limitations. The accuracy of any intersection-based delay measurement system is essentially limited by the detection technology available at the approaches under study. For example, if an intersection approach has video detection oriented to "see" from the stop bar to a point far upstream (the best case scenario) then the resulting estimation of delay can be expected to be relatively good whereas, if the approach only has a stop bar loop (other than no detection, the worst case scenario), then the delay estimation will be relatively poor.

In addition, the accurate estimation of approach delay is of most interest during peak periods when traffic demand is at its greatest. It is during these critical periods that extensive queues typically form; queues that can extend well beyond the field of view of any intersection-based detection system. Consequently, when we most need an accurate estimation of approach delay is exactly when we are least likely to obtain it from conventional detection systems.

Theoretical delay models for signalized intersection approaches, such as those described in the Highway Capacity Manual (HCM), offer another means of determining delay. One would expect that these models could be used in a real-time manner to obtain real-time delay results. However, to produce reasonable results the models must be based on reasonably accurate input data. If this needed data cannot be accurately obtained, then the models are of little value. This

brings us right back to the problems associated with obtaining accurate data under peak hour conditions. Extensive peak hour queuing essentially thwarts our ability to collect key approach data, such as the rate of vehicle arrivals at the back of the queue.

The use of probe vehicles provides a fresh alternative for collecting delay data. However, a host of challenging technical and privacy issues still need to be worked-out before probe vehicles can provide the needed detail to accurately estimate approach delay. On the technical side, a team of researchers in Florida recently discovered that cell phone technology, a promising probe alternative, is not accurate in congested traffic conditions and that the level of accuracy decreases rapidly as congestion increases.

Problem Statement

The latest edition of the Highway Capacity Manual provides a well-recognized analytical procedure for calculating control delay at signalized intersections, with control delay being defined as the sum of deceleration delay, stopped delay, queue move-up delay, and acceleration delay. This procedure has been automated in the form of the signalized intersection module of the HCS+ software suite. The HCS+ software offers a direct, user-friendly procedure for calculating lane group, approach, and intersection control delay and their associated levels of service. However, the HCM methodology assumes that, on a given approach, certain average conditions apply over the entire analysis period (saturation flow rate, start-up lost time, g/C ratio, arrival type) and that the vehicle arrival rate on the approach remains constant within each of the four 15-minute periods. In reality, conditions change on a cycle-by-cycle basis depending on random fluctuations in approach volumes and driver composition. For example, the considerable variation in cycle-by-cycle saturation flow rates at signalized intersections was documented in two recent papers, one citing data from the United States [7] and one citing data from Taiwan [8].

In addition to this cycle-by-cycle variation in conditions on a given approach, variations also occur between different approaches due to unique characteristics of the approach. For this reason, the HCM recommends collecting field data to establish such items as ideal saturation flow rate. The HCM recognizes that true site-specific delay can only be evaluated accurately by field measurement. Unfortunately, the field measurement of delay requires knowledge of the entire extent of the queue, and survey techniques required to capture the entire extent of the queue must utilize costly resources such as aerial surveillance or multiple coordinated ground observers. Less expensive observation techniques, such as a video camera located at a single point, can estimate delay only if the back of the queue is always in sight, which is typically not the case when peak hour congestion occurs.

Recognizing these limitations, a new procedure is needed that can reasonably estimate delay over a wide variety of conditions, including grossly over-saturated conditions. In order to properly measure delay during over-saturated conditions, multi-period analysis becomes a must in order to ensure that that no initial queues exist either at the start or at the end of the analysis. Keeping track of the various components of control delay (stopped delay, move-up delay, acceleration delay prior to the stop line, acceleration delay beyond the stop line, and deceleration delay) becomes more difficult as volume exceeds capacity for any significant length of time. Predicting control delay in real-time with limited information, and being able to do so even with over-saturated conditions, is the challenge addressed in the research at hand.

Key to this problem statement is the idea of limited information. Obviously, if we have perfect knowledge of each and every vehicle trajectory then we can rather easily compute a complete set of arrival rates, departure rates, queue lengths, and the resulting control delay. However, detailed vehicle trajectory information can be very difficult to obtain and trying to

secure it for more than a few locations quickly becomes cost-prohibitive given current technology. The crux of the problem is to find a method that uses more easily obtainable data to approximate the same delay information that a complete set of accurate vehicle trajectories would produce. The most easily obtainable data are usually data that occurs in proximity to the stop line. Current vehicle detection systems, including most video and inductance loop systems, are best suited to obtaining data at this location. The quest is to develop a practical, real-time delay estimation system that is supported by theoretical considerations and which also makes use of readily obtainable data.

CHAPTER 2
OBJECTIVES AND RESEARCH APPROACH

The following objectives were established for the research.

OBJECTIVE 1: Develop a methodology and associated real-time procedure that can reasonably estimate delay associated with vehicles that are beyond the reach of the detection system. The procedure should function during both under-saturated and over-saturated, obtaining reasonable estimates of vehicular delay even when queues are long and multiple phase failures occur.

OBJECTIVE 2: Identify variables to be used in the procedure that are important in the prediction of delay beyond the detection area (non-visible delay).

OBJECTIVE 3: Establish and clearly define any new terminology needed to document the methodology.

OBJECTIVE 4: If the proposed procedure is empirical in nature, develop theoretical limits on the solution space that can be established using readily available information.

OBJECTIVE 5: Ensure that all delay estimates are consistent with trajectory analysis and reflect the true nature of control delay.

OBJECTIVE 6: Ensure that all delay estimates are reconciled to the procedures contained in the 2000 Highway Capacity Manual and the current version of the HCS+ software. Document any needed modifications to the manual or the software based on the research.

OBJECTIVE 7: Provide examples of how the procedure could be used to address real-world traffic analysis or traffic control issues.

OBJECTIVE 8: Indicate areas of future research.

Objectives of the research would best be achieved using actual field data. However, detailed field data are not only expensive and time consuming to collect; one cannot safely or expeditiously manipulate field data in order to experiment at controlled volume levels or cycle lengths. Analyzing substantially over-saturated systems is also very difficult using actual field data as queue lengths can become quite extensive; spilling over into adjacent signalized intersections**.**

Therefore, theoretical research work was conducted in the laboratory using the CORSIM micro-simulation model. CORSIM allows us to quickly simulate a variety of real-world conditions in a relatively realistic manner and to accumulate important measures of

effectiveness, including delay. CORSIM was used because it is a well-accepted and well-understood model that has the capability to accommodate a wide range of input variables, including variable combinations that produce grossly over-saturated conditions with multiple phase failures. CORSIM also allows the user to vary the set of random number seeds to order to investigate changes in the results that occur due to random fluctuations. This ability is important since the stochastic nature of micro-simulation models can result in a level of variation that masks cause-and-effect relationships.

CORSIM was specifically used to examine how measured delay differs from actual delay when queues exceed the limits of the detection system. In order to investigate such differences, it was necessary to assume a certain "field of view" for the simulation runs. The field of view is defined as the number of vehicles on an intersection approach lane that can be accurately measured by the detection system when the vehicles are queued at the stop bar. A field of view of 12 vehicles was used in most of the examples associated with this theoretical work. This would be a reasonable field of view for a modern video detection system.

Using various fields of view and cycle lengths, a reasonably accurate method for estimating actual stopped delay was developed. For example, the back-of-queue on a single lane approach might extend to 20 vehicles whereas a video detection system may only be able to accurately "see" a queue extent of 12 vehicles. If this happens, the delay associated with the remaining 8 vehicles (the vehicles queued in the "blind" area) cannot be measured and must instead be estimated in some reasonably accurate manner. Knowing the time during which a queue existed in the "blind" area, which may extend over multiple cycles, and knowing the number of vehicles that "come into sight" after such a period of blind queuing, the procedures developed in this endeavor allow us to obtain a workable estimate of the "non-visible delay" that

occurred. The procedure developed is capable of handling both under-saturated conditions (having little or no “blindness”) and over-saturated conditions (with blind periods occurring over multiple cycles; referred to in this document as adjacent blind periods). The development of this procedure is one of the primary contributions to the literature dealing with signalized intersection delay.

A limited field of view produces a situation where arrivals at the back of the queue cannot be observed. This incomplete information makes it impossible to calculate the resulting delay. However, using the methodology contained in this dissertation, the delay can be reasonably estimated under a rather wide variety of conditions. The procedure that was developed in response to the challenge of estimating non-visible delay begins by calculating an "estimated arrival rate" (which is actually the departure rate). If the back end of the queue is not visible, the procedure modifies the estimated arrival rate upward using a power function in an attempt to predict the real arrival rate. This power function adjusts the rate in a manner that varies with the amount of time during which the back end of the queue is not visible. A major advantage of this approach is that the resulting estimated queues and associated delay are immediately calculated on a second-by-second basis, in real time. A major disadvantage of the approach is that there is no theoretical relationship between the departure rate and the real arrival rate. Hence, two different arrival patterns that result in the same number of vehicles crossing the stop line during the analysis period can produce similar delay results. This problem is most evident when the length of time that the end of the queue is not visible covers most of the analysis period.

Fortunately, it is possible to calculate a set of theoretical upper and lower bounds on the solution space by using information obtained at the end of the analysis period, when all queues are visible and the arrival rate equals the departure rate. In order to make any type of reasonable

delay estimation, all queues must dissipate prior to the end of the analysis period. Once queues become fully visible, an accurate calculation of the arrival rate can be made. Knowing this arrival/departure rate and knowing the total number of vehicles that have crossed the stop line during the entire hour we can, by assuming a reasonable minimum peak hour factor, work backwards through the period to identify minimum and maximum cumulative arrival curves. From these curves we can then calculate both lower and upper bounds on the overflow delay. These theoretical bounds can be used, in an ex post facto manner, to bracket the previously discussed real-time delay estimation procedure. They can also be used to identify an independent "most probable" arrival pattern by selecting an intermediate curve between the upper and lower bounds that minimizes the maximum percent error between the estimate and the actual delay**.** The development of these theoretical bounds is another important contribution to the literature dealing with signalized intersection delay.

The theoretical upper and lower bounds on the delay solution are calculated using cumulative arrival and departure curves. Vehicular delay is obtained through consideration of the area between these curves. Within this document it is demonstrated that, contrary to popular belief, the area between the arrival and departure curves is not the delay incurred by approaching vehicles. An evaluation of trajectory analysis during over-saturated conditions is used to reconcile the difference between the true delay and the area between the cumulative arrival and cumulative departure curves so that a consistent set of upper and lower bounds are provided. This reconciliation is another contribution to the literature dealing with signalized intersection delay.

The multi-period signalized intersection analysis procedure that is currently contained in the 2000 Highway Capacity Manual is codified as part of the HCS+ version 5.21 software suite.

The period-based procedure for queue accumulation that is described in this manual has certain drawbacks that can produce substantial errors when calculating control delay during over-saturated conditions. A description of these errors and the presentation of a cycle-based technique for eliminating them is yet another contribution to the literature dealing with signalized intersection delay.

The following detailed work tasks were developed in order to carry out this research approach:

TASK 1: Select a micro-simulation model for conducting the research and develop tools to extract needed information from the model.

TASK 2: Develop a comprehensive software tool that will facility the evaluation of real-time second-by-second delay estimation procedures for a one-hour analysis timeframe.

TASK 3: Develop data test sets for use in identifying the preferred delay estimation procedure. Various v/c ratios, cycle lengths, and fields of view should be reflected in this test set.

TASK 4: Using the test sets, identify the preferred delay estimation procedure.

TASK 5: Use the delay estimation procedure to analyze multiple replicates of four examples and document the results

TASK 6: Examine statistical variability issues by using a large number of replicates of a single example.

The first 6 tasks are documented in Chapter 4.

TASK 7: If the delay estimation procedure is empirical in nature, develop a theoretical technique for constraining the solution space.

Task 7 is documented in Chapter 5.

TASK 8: Develop a software tool for extracting trajectory information from the selected micro-simulation model.

TASK 9: Develop a software tool that will analyze all components of control delay associated with vehicle trajectories. The tool should summarize the resulting delay by 15-minute period for a one-hour analysis timeframe.

TASK 10: If necessary, modify the delay estimation procedure or the theoretical constraints to reflect true control delay concepts.

Tasks 8 through 10 are documented in Chapter 6.

TASK 11: Compare the results obtained with results produced by the 2000 Highway Capacity Manual and reconcile all differences.

Task 11 is documented in Chapter 7

TASK 12: Summarize the results and identify potential areas for further research.

Task 12 is documented in Chapter 8.

The end result of this research is the development of a theoretically constrained delay estimation procedure that is based on limited information. The delay estimation procedure makes use of available data to predict arrivals at the back of the non-visible queue as well as departures from the front of the non-visible queue at each point in time, information that would otherwise be unknown. Knowing the arrivals and departures we can predict the length of the non-visible queue at each point in time. This predicted non-visible queue length is then added to the measured visible queue length to obtain the total queue length with stopped delay being obtained directly from the queue length. Theoretical bounds based on historical minimum peak hour factors are then imposed on the delay estimate to ensure a reasonable result.

Use of the procedure to estimate control delay on an over-saturated intersection approach for a one-hour analysis time frame would proceed as follows:

1. Using the vehicle detection equipment for the approach of interest, real-time second-by-second data are collected on the number of vehicles crossing the stop bar, the number of vehicles entering the field of view, the length of the visible queue, and the presence or absence of a stationary vehicle in the last queue position of the field of view.

2. This data set is entered into the delay estimation software, which measures the length of the visible queue and estimates the length of the non-visible queue at every second of the one-hour analysis time frame. Second-by-second cumulative stopped delay is then calculated using this queue information.

3. The stopped delay prediction is converted to control delay using a series of conversion ratios that vary by cycle length and v/c ratio. The conversion ratio varies

between 1.2 and 1.4 with 1.3 being a typical value. The predicted control delay is considered the final control delay for use in real-time traffic control.

4. The time during the last 15-minute period at which the end of the queue becomes visible is recorded, as is the cumulative number of vehicles that have crossed the stop bar at that time. At the end of the one-hour analysis time frame, the cumulative number of vehicles that have crossed the stop bar is also recorded. This information is used to calculate the arrival rate during the last 15-minute period.

5. The minimum reasonable Peak Hour Factor (PHF) for the approach and time period in question is obtained from historical traffic counts. The analysis software constructs a theoretical set of minimum and maximum cumulative arrival curves using this minimum PHF and the calculated arrival rate during the last 15-minute period.

6. The analysis software then calculates the cumulative curve delay (overflow delay) associated with the minimum and maximum cumulative arrival curves.

7. The cumulative curve delay is then converted to stopped delay by the application of a correction factor (approximately 0.77) derived from trajectory analysis.

8. The corrected maximum theoretical stopped delay is used as an upper bound for the predicted stopped delay and the corrected minimum theoretical stopped delay is used as a lower bound. If the predicted stopped delay falls outside of the theoretical bounds during any of the four 15-minute periods, then the predicted delay is appropriately adjusted to remain within the bounds. The resulting "hybrid" stopped delay is considered the final stopped delay prediction. Note that the theoretical bracketing of the predicted stopped delay is carried-out in an ex post facto manner, after the analysis time frame has expired.

9. The hybrid stopped delay results are converted to control delay using a series of conversion ratios that vary by cycle length and v/c ratio. The conversion ratio varies between 1.2 and 1.4 with 1.3 being a typical value. The hybrid control delay is considered the final control delay prediction for project evaluation purposes.

By using the maximum amount of information available and by recognizing the true characteristics of overflow delay, this procedure produces, for over-saturated conditions, a delay estimate that is generally superior to that found in the Highway Capacity Manual – and does so in real time.. The proposed delay estimation technique should prove useful for both real-time traffic control and project evaluation. It is envisioned that the eventual end product of this theoretical research will be a self-contained delay estimation module that could be attached to

either a closed-loop or centralized signal control system, or could be inserted within the software of a local traffic signal controller.

CHAPTER 3
CURRENT STATE OF THE ART

A literature review was conducted to identify both past and ongoing research efforts affecting the area of interest. The studies obtained from this search can be segregated into the following general areas: Real Time Measurement of Intersection Delay, Vehicle Re-identification via Inductance Loops, Performance of Video Detection Systems, Signalized Intersection Queuing and Delay, and Probe Vehicle Monitoring. Quite a bit is known about intersection control delay, especially for under-saturated conditions - and for situations where all of the information needed to calculate delay is known. The current state of knowledge with respect to over-saturated conditions is more primitive and the results less tested.

Real-Time Measurement of Intersection Delay

In 1994, Maddula [9] studied signalized intersection delay using an AUTOSCOPE 2003 video detection system. This system is based on a tripwire approach and has count, presence and speed detectors. The system can provide interval data (from 10 seconds to 1 hour) and event data. The computational model developed makes use of a mandatory detection pattern that has 4 detectors in each lane. The first upstream detector (position 1) is located "as far upstream as possible such that section length includes all delay associated with the signal" and identifies the beginning of the **Approach Delay Section** (defined as the section where most, or all, of the approach delay is incurred) and reports arrival events. Position 2 is an additional upstream detector located between position 1 and the stop line. This detector accounts for vehicles changing lanes. It is used to estimate any missing data at other positions. Position 3 is at the stop line and defines the end of the approach delay section and reports departure events. Position 4 is beyond the stop bar and is used to determine the signal indication. Position 4 houses a directional detector.

The first step is the identification of each event in their chronological order. This step includes the removal of all events that lead to unrealistic headways (FILTER I).

The second step in the process is the use of the data from detector positions 3 and 4 to determine the signal status associated with every recorded event. The following user input is required to conduct the search: 1) beginning of red indication for first cycle, 2) limits of travel time between positions 3 and 4, and 3) limits of red indication for the phase. Each event is associated with a signal indication (red or green) and a cycle number. This step includes the removal of all events that lead to departures when there is no right-of-way (FILTER II).

The third and final step is the computation of the MOEs (throughput, stops, saturation headways, and saturation flow rate). Volume is computed from throughput and the estimated green time is treated as effective green time. Delay is then calculated using the 1985 HCM formula and LOS is identified via the HCM signalized intersection LOS table. The calculations are done using a computer program written in C called ADELAY. The inputs to ADELAY are an ASCII detection file from the video system with extension TXT (the events) and a text file with extension VXT (other required information) from the VIADET user interface program.

The report defines the **Approach Free Flow Time** as the time used by an unimpeded vehicle to traverse the approach delay section and defines the **Approach Time** as the time used by an impeded vehicle to traverse the approach delay section. **Approach Delay** (defined as the Approach Time minus the Approach Free Flow Time) is converted to **Stopped Delay** (defined as the time that the vehicle is stopped with stationary wheels) for comparison to field observations by dividing by a factor of 1.3 The raw data are converted to usable data using three filters:

- **FILTER I.** False detections (glare, reflections, turn signals) resulting in unrealistic headways (1 second is used as a minimum realistic headway)

- **FILTER II**. Detections at position 3 that lead to departures when there is no right of way (detections during red produced by pedestrians, crossing vehicles, etc.)
- **FILTER III.** Unrealistically high throughput (continuous detection due to shadows, turn signals) **Maximum Throughput** = Green Time / Minimum Headway

All vehicles that arrive on the approach delay section and depart before the end of the green of the current cycle are reported as throughput for the cycle. If a vehicle could not clear the intersection before the end of the green, it is reported as throughput for the next cycle. When the throughput reported at various positions in the lane is different (due to lane changing or detection errors), the maximum number of vehicles reported at any position is taken as the throughput for the cycle.

Every vehicle that arrives before the beginning of the green indication, minus the free flow travel time within a current cycle, is automatically treated as a stop. The free flow travel time for the vehicles that arrive after the stated time is calculated at 5 miles per hour (mph). If the travel time of the vehicle is more than this time, it is treated as a stop for that vehicle. (i.e. a vehicle is defined to have stopped if the actual travel time is more then the free flow travel time calculated at a speed of 5 mph.)

Reported departure times are used for determining saturation headways and calculating the saturation flow rate. Headways associated with the first 3 vehicles in the queue, and headways of more than 3 seconds, are not used. If the number of vehicles in the queue never exceeds three throughout the study, then default saturation flow rates are used that vary by lane type (1756 for a thru lane, 1946 for a single left turn lane, and 1651 for a dual left turn lane).

A preliminary study for a limited number of observations indicated that, for queues of passenger cars, average distance headway (front bumper to front bumper) is 25.1 feet and average spacing between cars is 9.0 feet. This yields an average car length of 16.1 feet.

The report defines the **Time-in-Queue Delay** (a.k.a. Time-in-Queue) as the time from the vehicle's first stop to the vehicle's exit across the stop line. The report also defines **Percentage of Vehicles Stopping** as the number of vehicles incurring Stopped Delay divided by the number of vehicles crossing the stop line.

Of the traffic parameters investigated, vehicle count, delay and level of service were obtained accurately from the data reported by VIDS (Video Image Detection System). However, throughput and stops were not. Minor changes in detector size, placement and orientation caused noticeable variation in the results. Data missing at a particular detector location was often available at another detector location, which argues for the use of multiple detection systems for evaluation.

The basic limitation of this work with respect to the research at hand is that it relied on a relatively optimum detection configuration and was not used for estimating delay during over-saturated conditions (a time when delay estimation is most critical).

In 1998, Lall, et al. [10], developed a speed-based procedure for calculating delay on a signalized intersection approach. For a 15 minute study period, traffic volumes and average speeds were recorded every 10 seconds using AUTOSCOPE at 5 distances from the stop bar (20 ft, 65 ft, 88 ft, 267 ft & 500 ft). Free-flow speeds (for vehicles not stopping) and "prevailing speeds" (for vehicles stopping) were calculated and associated travel times compared to estimate delay. The comparison checked well with "control delay" calculated for the approach using the HCM. If posted speed is used instead of prevailing speed the delay calculated is substantially higher and probably corresponds to "total delay", wherein total delay is defined as the difference

between the travel time actually experienced and the reference travel time that would result during ideal conditions. [1]

The authors noted that the longer the lens' focal length (view more zoomed in), the easier and more robust is vehicle tracking and detection. The shorter the focal length of the lens, the smaller the objects are on the image, but the larger the field of view. If the vehicle image is smaller than 5 pixels of the image that is analyzed by their video system, the tracking of vehicles becomes rather unreliable.

Two types of shadow problems were revealed. The first problem occurs when a tree, tall building or some other tall object is close to the section of roadway being monitored. On sunny days, the object's shadow will cover the monitored roadway at certain times of the day. If a vehicle enters the shadow, it may become barely visible, especially if the vehicle is dark. If a detection zone is located in the area covered by the shadow, the detection performance from this zone may be seriously impaired.

A second type of shadow problem occurs due to vehicle shadows. A shadow of a moving vehicle in one lane may sweep over the detection zone in another lane. This sweeping shadow may be taken for a vehicle. The authors "solved" the problem of thru lane vehicles activating left turn lane detection through the use of a 1.2 second detector delay setting (for a 6 foot detector length).

However, experience with this site indicates that the accuracy of video detection is adequate (the average maximum error is only about 5%). It is better than the accuracy of loop detectors at this location, which gave a maximum error rate of 10%.

[1] The important delay calculations contained in Tables 2 and 3 of this report cannot be followed given the information contained in the report and I contacted the primary author for clarification. Unfortunately, the author did not provide a response.

In 1999, Quiroga, et al. [11], developed a procedure based on linearly referenced GPS data that can be used to accurately measure both control delay and stopped delay. Algorithms were developed which accurately detect when a GPS-equipped probe vehicle either begins or ends acceleration or deceleration. More than 100 floating car travel time runs were made along two coordinated corridors having a background cycle length of 150 seconds. In addition to establishing the viability of this procedure for accurately determining stopped delay and control delay, the following was discovered:

1. A linear relationship exists between stopped delay and control delay. However, the line does not pass through the origin. It was found that control delay = (stopped delay + 19.3 seconds) x 1.04, which is quite different than the control delay = 1.3 x stopped delay formulation provided in the Highway Capacity Manual. The authors caution that other independent variables, such as length of the red interval, may be needed to properly generalize this equation.

2. An average end-acceleration distance of 427 feet downstream of the stop bar was established. An average begin-deceleration distance of 951 feet upstream of the stop bar was also established, but this distance obviously depends on the extent of queuing at the intersections.

3. Approximately 5% of the intersection control delay occurred after the vehicle crossed the stop bar.

In 2001, Saito, et al. [5], estimated stopped delay using simulated vehicle images generated by CORSIM and two image analysis methods: the gap method and the motion method. A simulation duration of 15 minutes was used. The simple algorithms that were developed produced promising results. The authors defined Percent Deviation using the following formula:

Percent Deviation = [Delay Estimated by Model – Delay Estimated by CORSIM]/(Delay Estimated by CORSIM) x 100

In 2004, Zheng, et al. [12], developed a methodology for using video image processing to accurately detect queue lengths and phase failures on a signalized intersection approach. A Trafcon video system was used to test the procedure on an actual intersection approach with a

field of view of about 18 vehicles. The camera was mounted 26 feet above the ground and was oriented at a 30-degree downward angle. The video algorithm extracts stopped vehicle information from the traffic stream, tracks the end of the queue, and identifies phase failures. Zheng concludes that:

> "The program based on this algorithm may provide reliable and accurate [phase] failure detections in real time for many traffic management and operation purposes if the camera that provides the video stream is correctly positioned to see the stop bar and a sufficient number of queued vehicles".

We can safely assume that, if the camera cannot see a sufficient number of queued vehicles (with a "sufficient number" obviously being to the end of the queue) then Zheng's technique will provide erroneous results; hence, the need for the extension provided in this research.

In 2004, Hoeschen, et al. [13], developed a procedure for using travel time between intersections (expressed as "segment delay") to approximate control delay. The approximation was found to be much better than using stopped delay to estimate control delay, especially for higher delay values. Control delay was approximated by subtracting mid-block delay from segment delay. The authors cautioned that queue spillback from a downstream intersection or non-recurring delay could negatively affect the results. The segment lengths for the research varied between ¼ mile and 1 mile in length. 300 feet was selected as the distance from the upstream intersection at which most vehicles had accelerated to running speed. 300 feet was also selected as the distance from the downstream intersection at which vehicles began decelerating.

Vehicle Reidentification via Inductance Loops

In 1999, Sun, et al. [14], examined the vehicle re-identification problem on freeways. A vehicle waveform pair can be formed by using one downstream waveform and one upstream waveform. The vehicle re-identification problem is to find the matching upstream vehicle from a set of upstream vehicle candidates given a downstream vehicle.

Inductive loop detector manufacturers are incorporating the ability to monitor and output vehicle inductance values (or waveforms). Detectors that output vehicle waveforms include detectors manufactured by: Peek/Sarasota, Intersection Development Corporation (IDC), and 3M.

The authors concluded that solution of the vehicle re-identification problem has the potential to yield reliable section measures such as travel times and densities. Implementation of their approach used conventional surveillance infrastructure; 6' by 6' freeway inductive loops spaced 1.2 miles apart on a 4 lane westbound stretch of freeway with no intervening ramps. Typical 6' x 6' loops produce a less distinctive waveform that is more difficult to re-identify compared with shorter (3.3') European loops. The 13 to 14 ms detector sampling period of most detectors is also problematic in that it misses sharp corners of the waveform.

Previous approaches that utilized sequences (Bohnke and Pfannersstill, 1986) are suitable for the case when sequences of vehicles are preserved from upstream to downstream. The preservation of sequences occurs when there is very little lane changing and the speeds across all traffic lanes are similar. The approach used in this study is suitable for cases where there is significant difference in lane speeds. This approach also has the potential to yield partial origin/destination demands and individual lane changing information.

This paper formulates and solves the vehicle re-identification problem as a lexicographic optimization problem using goal programming. Goal Programming is an optimization method wherein target values are set for each of the multiple objectives and then a single global objective, which is the sum of the deviations from the target values over all objectives, is optimized. Lexicographical Goal Programming is a goal programming procedure wherein the multiple objectives are introduced in a specified hierarchical order. The lexicographic method is

a sequential approach to solving the multi-objective optimization problem where each objective is ordered according to its importance. Multi-Objective Optimization is defined as the discovery of optimum points x* within a feasible set x that are as good as can be obtained when judged according to multiple criteria. A Pareto Set (a.k.a. an Efficient Frontier) is the optimum solution for multi-objective problems in that it contains all points (efficient points) for which there does not exist any other point that would be uniformly better on all objectives.

The results of the prior level of optimization constrain the feasible set for the current level of optimization. A lexicographic method has advantages over the traditional weighted average method in that the problem of specifying relevant weights when the multiple objectives are measured in different units is avoided and, by introducing the multiple objectives sequentially, the individual effect of each objective can be identified.

Five levels of optimization (multiple objectives) are used. The first three are implemented as goal programs. They are used to reduce the feasible set by eliminating unlikely waveform pairs.

- **Level 1:** travel time
- **Level 2:** vehicle inductance magnitude (the inductance magnitude is inversely proportional to the height of the vehicle)
- **Level 3:** vehicle electronic length (derived from occupancy time)

Maximum tolerances must be set for each level and a minimum tolerance must also be set for travel time. Level 4 uses a traditional weighted average utility function of the change in inductance magnitude, lane changes, and change in vehicle speed between the upstream and downstream detection points. Level 5 has a stochastic objective that is solved using Bayesian analysis. Calibration of the algorithms was performed with training data.

This research shows that the direct measurement of section measures of traffic system performance such as travel times and densities avoids the inaccuracies associated with estimating such values from "point" speeds and occupancies. This research also shows that values of "point" and section measures derived from freeway data differ significantly.

The authors also concluded that congestion causes more variability in the traffic stream which translates into more mismatches. The authors also cautioned that, when a higher percentage of trucks are matched (which often happens since they are longer and have more distinguishable features), speed results could be biased.

In a 2000 paper, Palen, et al. [15], discussed three phases of Caltrans detector research dealing with vehicle re-identification. Phase I initially used existing detectors with bivalent output only. **Bivalent Output** is defined as a detector output wherein just the presence or absence of a vehicle is reported. Vehicle lengths (calculated from loop-based time and distance data) and headway sequences were used to match platoons of vehicles. Vehicle lengths can only be calculated plus or minus 10% using conventional loop detection so additional sequence information based on headway distributions was needed to obtain useful results. Since model 170 traffic signal controllers lack the computational power needed to carry out the matching calculations for the sequence information, bivalent loop data was brought back to a web server via a wireless Internet Protocol (IP) modem. A stretch of I-80 near San Francisco currently uses this technique to obtain performance measures.

Phase II used commercially available scanning detector cards to obtain loop signatures. These signatures were used to match vehicles. This technique was applied to an intersection approach in Irvine, California having a 2070 controller. This process is more accurate than the Phase I process and loops can be spaced further apart.

Phase III examined new loop geometries.

In a 2001 study, Liu, et al. [16] used a vehicle re-identification algorithm developed at UC-Irvine to estimate the average and total delay by movement during each cycle at a signalized intersection, and these estimates were then fed to an on-line signal control algorithm to find the optimal green splits. Vehicle re-identification based on inductive loop signatures was used to estimate the delay. Knowing the prevailing free flow speed for the approaches, and the distance between detector stations, the minimum travel time for each movement can be derived. The delay of each vehicle was calculated by deducting this minimum travel time from the vehicle's actual travel time.

The analysis was conducted at the Alton/Irvine Center Drive intersection in Irvine, California with the microscopic simulation program Paramics used for online signal optimization as a complementary module to the existing signal controller. Paramics provides a framework that allows the user to customize many features of the underlying simulation model with access provided through an Application Programming Interface (API). Inductance loops were used for both vehicle detection and delay estimation in Paramics.

Thirty simulation runs were made for each scenario with each run comprising a 2-hour period. The use of multiple simulation runs permits statistical evaluation. Three measures of effectiveness were evaluated: total intersection delay, total throughput and average delay. The average delay-based on-line control algorithms performed better than the off-line case for both pre-timed and actuated signal control (as evidenced by a 10% reduction in delay).

In 2002 Sun, et al. [17], investigated the use of video cameras to improve the accuracy of vehicle re-identification using inductance loops. In this research, color information from video cameras was used to augment the inductive signature obtained from inductive loop detectors to

track individual vehicles. When inductive loop signatures alone are used, vehicles of the same model or even different models on the same body frame can be mismatched. On the other hand, the use of video alone can be sensitive to changes in illumination levels (night, dusk, dawn, rain, glare, etc.)

The test section was located in one direction of a 4-lane arterial. The two lanes of arterial traffic for the test section were treated separately; lane changing was ignored. Detector stations, each of which consisted of a speed trap (double inductance loops), were located 425 feet apart.

A traditional method of vehicle re-identification is license plate matching. Other potential methods of vehicle re-identification involve GPS, cellular, toll tags, or tracking beacons. Section measures can also be obtained via video using tripwire systems or through vehicle tracking. The advantages of using vehicle color are that it is not correlated with vehicle signatures (i.e. represents an independent identification measure), it can be extracted from imperfect video images, and it can be verified visually.

Linear feature fusion with six features was used in this study. The features used were: 1) vehicle signature, 2) vehicle velocity (distance between loops divided by turn-on time), 3) platoon traversal time (time between first and last vehicle in platoon crossing loop), 4) maximum inductive amplitude (inversely proportional to the cube of the distance from the ground to the vehicle undercarriage), 5) electronic length (length of metallic components only but includes the length of the magnetic field generated by the loop), 6) RGB triplet (color). The combined classifier score due to linear fusion is calculated using the following formula:

$$D_{linear} = E_{i=1,n}\, w_i\, d_i$$

Where i is an index from 1 to 6 for the six features and di are the feature values. The fusion weights (wi) are determined using an exhaustive search such that the re-identification accuracy is

maximized. The candidate upstream platoon that achieves the smallest D is matched to the downstream platoon. A time window constraint with upper and lower bounds is applied to identify candidate platoons.

The research concluded that the use of detector fusion provides system redundancy and yields better results than the use of either inductive signature information or vehicle color information alone. A re-identification rate of over 90% was obtained using multi-detector fusion whereas the rate was 87% for inductive signature information alone and only 75% for color alone.

The authors postulated that the results would be even better if the vehicle re-identification system could be tied into the arterial's signal control system since this would allow the direct estimation of lost time associated with starting and stopping. The tie-in would improve the accuracy and possibly yield real-time estimates of startup delays and saturation flow rates. The authors added that it is difficult to compute arterial travel times accurately using point measures (speed, occupancy, counts) since lost times associated with starting and stopping are not measured directly.

The authors provided the following definitions in the report:

- **Point Traffic Parameters** - traffic parameters that pertain to a particular point on the roadway (volume or flow, point speed, presence, occupancy)
- **Section Traffic Parameters** - traffic parameters that pertain to a section of roadway (link speed, travel time, origin/destination information)
- **Platoon Matching** - a method of vehicle re-identification that matches groups of vehicles rather than individual vehicles.

In 2002, Oh and Ritchie [18] used inductance loop signature data to track vehicles form upstream approach loops to receiving lane loops at a signalized intersection. Features used in the lexicographic optimization were maximum magnitude difference between front and back loops

(relates to vertical clearance), vehicle speed, and lane information. The matching rate was 32.5% for vehicles turning right, 51.7% for thru vehicles, and 62.5% for vehicles turning left, for an overall match rate of 46.7%. Left turns were eliminated from the analysis due to low absolute volume.

Cluster analysis was used to determine LOS categories based on reidentification delay (RD). Reidentification Delay is defined as the difference between the actual time required to traverse vehicle reidentification stations at a signalized intersection and a base travel time (such as that calculated from the speed limit). Two different aggregation methods were investigated, cycle-length based average (CBA) and fixed time average (FTA). A fixed interval of 60 seconds was used for FTA. K-means clustering, fuzzy clustering, and Self Organizing Map (2 layer neural network) methods were used in the clustering analysis. Wilk's lambda was used to compare the results:

Wilk's lambda = |W|/|B+W|

W = pooled within-group variance
B = between group variance

A lower Wilk's lambda value indicates better clustering. K-means clustering produced the best results, with the most appropriate number of clusters being 5. When compared to ground truth, reidentification delay errors were on the order of 26%

A rolling average RD based on 3 signal cycles was recommended to avoid signal control related stability problems associated with single cycle delay reporting. A recommended RD LOS classification system is presented with LOS I (excellent) through V (poor). The LOS table stratification values are similar to those contained in the HCM if LOS F is eliminated. Slightly different LOS stratification values are provided for right turn and thru movements.

Mean Absolute Percent Errors were calculated using the following formula:

$$MAPE = [E_{i=1,N}(ARD_i - AAD_i / AAD_i) \times 100] / N$$

MAPE = Mean Absolute Percent Error
ARD_i =Average Reidentification Delay at time step i
AAD_i =Average Actual Delay at time step i
N = total number of time steps

In a 2003 paper, Coifman and Ergueta [19] presented an improved algorithm for vehicle matching at a freeway inductive loop detector station having dual loops. This new algorithm, which includes four separate tests, performed significantly better than older algorithms developed in previous work by the authors. The algorithm should be applicable to any detector technology capable of extracting a reproducible vehicle signature. In this study, vehicles were matched based on length and lane changing was accounted for.

The algorithm matched between 35% and 65% of the vehicles, depending on lane. The authors noted that other researchers have estimated that matching 20% of the population is sufficient for travel time measurements. Matching percentage is improved as the speed decreases. The report defined a False Positive as a collection of incorrect matches and Effective Vehicle Length as Physical Vehicle Length plus Length of the Detection Zone. The algorithm is attractive in that it utilizes existing surveillance equipment and performs well under congested conditions.

In 2004, Coifman and Dhoorjaty [20] presented eight detector validation tests for freeway surveillance. Five of these tests can be applied to single-loop detectors while all of the tests can be applied to dual-loop detectors. The tests are used to compare the performance of different detector models and to identify permanent or transient hardware problems such as crosstalk between loops and shorts in the loop wire. Three of the tests could be applied to arterial loop detectors and these tests could be incorporated into the controller software for continuous

monitoring. The authors discovered that some detector units stay on a fraction of a second after the vehicle passes and some are prone to flicker (turning on and off multiple times as a vehicle passes). A large variability in detector operation was noticed from one model to the next and, in the case of one of the detectors, from one software revision to the next within the same model.

In a 2007 paper, Jeng, et al. [21] described an inductance loop based vehicle re-identification algorithm (RTREID-2) that produced excellent results when compared to GPS information from control vehicles.

Performance of Video Detection Systems

In 1999, Washburn and Nihan [22] evaluated the Mobilizer, a video image detection system based on vehicle tracking developed by Condition Monitoring Systems. Preliminary results indicated that the Mobilizer is capable of matching vehicles in successive fields-of-view with a reasonable degree of accuracy and that the travel time estimates provided by the system are statistically valid. Two sites were evaluated, one on an arterial and one on a freeway. For both of these sites, a departing FOV (Field of View) was used. The arterial had 76% correct matches while 78% of the freeway matches were correct. The system can be instructed to not consider matches that fall outside of dynamic travel time ranges, ranges that are adjusted in real-time by the system, however, the system does not currently utilize color information and the system does not consider matches of vehicles that change lanes. The system was only evaluated under free flow conditions.

In 2001, Grenard, et al. [23], evaluated various video detection systems (Autoscope, VideoTrak and Odetics) for signalized intersections. They discovered that:

- The effective length of the detection zone increased from an average of 23.7 feet during the day to an average of 67.7 feet at night, which could cause the signal to operate less efficiently. The percentage increase in effective detection length at night due to headlight glare ranged between 50% and 500%; this adds 2 seconds of detection time.

- False video detections became slightly larger at night with rain due to headlight glare.

- Video detection frequently only detects the headlights at night so the call is lost if the video detection zone ends just a few feet in front of the stop bar. Extending the video detection zone somewhat past the stop bar would help to remedy this situation, but at the expense of detecting additional pedestrians or crossing/left turning traffic. This produces both safety (due to missed calls) and efficiency problems. Illuminating the intersection eliminates this problem.

- The video detection systems tested sometimes "stuck on" for substantial periods of time.

- During dawn and dusk, sunlight causes so much glare that the camera is often unable to distinguish between the absence and presence of vehicles.

- Wet pavement does not significantly impact the likelihood of a T0L1 error (loop on when no vehicle is present) but traffic volume does (probably due to spillover). Neither wet pavement nor traffic volume significantly impact the likelihood of a T1L0 error (loop off when vehicle is present).

- Under base (optimal) conditions, the video detection system has a false detection rate of 2% to 6% and a missed vehicle presence of between 7% and 8%

- The authors distinguished between **Error**, defined as video results compared to actual or ground truth and **Discrepancy**, defined as video results compared to another type of detection system (such as loops). **Discrepant calls** include false calls and missed calls (discrepancies of less than 3/10 of a second were not recorded). **Discrepant Call Frequency** is defined as the number of discrepant calls per cycle. **Error Rate** is defined as the ratio of discrepant calls to true calls and **Relative Error Rate** is defined as the ratio of the error rate to the average error rate.

- Under worst-case conditions (rain, night, wet pavement, average count, heavy camera motion) video detection misses between 16% and 20% of vehicle presence time and indicates false detection during about 40% of the vehicle absence time.

- The authors defined **Activation Distance** as the distance a vehicle is from the stop bar when it is detected by the video detection system, and **Blanking Band** as a process used to remove all discrepancies smaller than a user-defined value.

- Due to the imprecision of night detection, the authors recommended that video detection not be used to provide dilemma zone protection.

- The authors cited past work in this area: MacCarley's 1992 evaluation of video detection found that several conditions caused significant degradation in video detection performance: non-optimum camera placement, day-to-night transition, headlight reflections on wet pavement, shadows, fog, heavy rain with error rates of 20% to 40% for most tests performed. MacCarley's 1998 evaluation of video detection found that several additional conditions caused significant degradation in video detection performance: transverse lighting, low

lighting and vehicles that have a low contrast to the pavement. 65% of all vehicles were detected correctly with an 8.3% false detection rate. 64.9% of all red-green transitions would have been actuated correctly if video were used instead of properly functioning loops. Middleton's 1999 evaluation of video detection found that video detection: 1.) consistently over-counted by as much as 40% to 50% at night, 2.) at dawn and dusk sun angles produced glare that caused undercount rates of 10% to 40%, 3.) undercounted by 6% to 8% during heavy rain. The most consistent period of error was between midnight and 5:00 am. Middleton and Parker's 2000 evaluation of video detection found that video detection: 1.) over-counted both day and night during wet pavement conditions because of headlight reflections, 2.) had reduced accuracy at night and when long shadows occurred.

The authors provided the following formulas for calculating detection errors:

Missed Detection Rate (MDR) = Number of Actual Detection Events Missed By Loop/Total Number of Actual Vehicle Arrivals (discrete definition)

$P(L=0|_{T=1})$ = D(L=0 & T=1)/D(T=1) where D=Duration, T=Ground Truth, L=Loop, 1=On, 0=Off (continuous definition)

False Detection Rate (FDR) - Number of False Detection Events Reported By Loop/Total Number of Inductive Loop Events (discrete definition)

$P(L=1|_{T=0})$ = D(L=1 & T=0)/D(L=1) where D=Duration, T=Ground Truth, L=Loop, 1=On, 0=Off (continuous definition)

$P(L=1|_{T=0})$ = D(L=1 & T=0)/D(T=0) where D=Duration, T=Ground Truth, L=Loop, 1=On, 0=Off (revised continuous definition)

For the likelihood (probability) of a detection discrepancy the following formulas apply:

The probability of video detection being off when loop detection is on = $P(V=0|_{L=1})$ = D(V=0 & L=1)/D(L=1) where D=Duration, V=Video, L=Loop, 1=On, 0=Off

The probability of video detection being on when loop detection is off = $P(V=1|_{L=0})$ = D(V=1 & L=0)/D(L=0) where D=Duration, V=Video, L=Loop, 1=On, 0=Off

For the likelihood (probability) of a detection error the following formulas apply:

The probability of video detection being off when a vehicle is present = $P(V=0|_{T=1})$ = $P(L=1|_{T=1})$ x $P(V=0|_{L=1})$ + $P(L=0|_{T=1})$ x [1-$P(V=1|_{L=0})$]

The probability of video detection being on when a vehicle is not present = $P(V=1|_{T=0})$ = $P(L=1|_{T=0})$ x [1-$P(V=0|_{L=1})$] + $P(L=0|_{T=0})$ x $P(V=1|_{L=0})$

In 2002, Bonneson and Abbas [24] investigated the operation of Video Imaging Vehicle Detection Systems (VIVDS) in Texas. It was estimated that about 10% of the intersections in

Texas were using VIVDS and that Texas DOT was installing VIVDS at about ½ of all newly constructed intersections. They identified the following VIVDS manufacturers: Image Sensing Systems (Autoscope system used by Econolite), Iteris (Vantage system used by Naztec and Eagle), Peek Traffic Systems (VideoTrak system), Traficon, Nestor Traffic Systems and Transformation Systems. A review of VIVDS product manuals revealed that these manuals do not describe techniques for the effective use of delay, extend, or passage time settings in conjunction with a VIVDS installation.

Their report made the following points:

- Detection zones can be linked via Boolean logic functions (AND, OR, NOT, etc.)
- VIVDS can provide reliable presence detection when the detection zone is relatively long (say, 40 ft or more). However, its limited ability to measure gaps between vehicles compromises the usefulness of several controller features that rely on such information (such as volume-density control).
- A VIVDS system is sometimes used to provide advance detection on high-speed intersection approaches. However, some engineers are cautious about this use because of difficulties associated with the accurate detection of vehicles that are distant from the camera. Of those agencies that use a VIVDS for advance detection, the most conservative position is that it should not be used to monitor vehicle presence at distances more than 300 feet from the stop line.
- The minimum camera height (in feet) for advanced detection is calculated using the formula:

$$H_a = (x_l + x_c)/R$$

Where x_1 is the distance in feet between the stop line and the upstream edge of the detection, calculated as: $x_l = 1.47 t_{bz} V_{95}$, and:

x_c = distance in feet between camera and stop line
R = distance-to-height ratio (17 in Texas)
T_{bz} = travel time from the start of the dilemma zone to the stop line (5 seconds)
V_{95} = 95th percentile speed in mph (= 1.07 x V_{85})

Table 4-2 in the report provides the resulting minimum required camera heights for advanced detection. The required height varies between 24 feet and 36 feet.

- A camera's field of view is impacted by the following factors: camera height (distance from ground to camera), camera offset (lateral distance from camera to the lane or lanes being monitored), distance (longitudinal distance from the detection zone to the camera), pitch angle (angle of downward "tilt" of the camera relative to the ground), and focal length (which determines the relative size of objects in the camera's field of view). **Detection Design** is defined as the selection of camera location and the calibration of its field of view whereas **Detection Layout** involves locating detection zones, determining the number of detection zones, and identifying the settings or detection features used with each zone.

- The "10 ft to 1 ft" rule states that, if camera set up is optimal, one should be able to extend out 10 feet for every 1 feet of camera elevation to a maximum distance of around 300 feet. However, Texas DOT staff indicated acceptable operations using 17 feet instead of 10 feet.

- Detection accuracy will improve as camera height increases within the range of 20 to 40 feet. Increased height improves the camera's field of view of each approach traffic lane by minimizing the adverse effects of occlusion. Three types of occlusion are present with most camera locations: adjacent-lane, same-lane and cross-lane. Increasing camera height tends to decrease call error, provided there is no increase in camera motion. Cameras mounted above 34 feet may experience unacceptable camera motion unless located on a stable pole. **Adjacent-Lane Occlusion** (Horizontal Occlusion) occurs when the blocked and blocking vehicles are in adjacent lanes, which can result in false detections in adjacent lanes. Table 4-1 of the paper provides minimum required camera heights to reduce adjacent-lane occlusion. The required height depends on the lateral offset, whether the offset is to the left or to the right, and the lane configuration, and varies between 20 feet and 63 feet. The minimum required height is lowest for a camera mounted in the center of the approach, 20 feet. **Same-Lane Occlusion** (Vertical Occlusion) occurs when the blocked and blocking vehicles are in the same lane, which can result in a low vehicle count. The extent of this problem increases as the distance from the stop line increases. Same lane occlusion is associated with an increase in the effective length of a vehicle. Consequently, passage settings must be reduced to yield operation equivalent to that obtained with an inductance loop. **Cross-Lane Occlusion** occurs when a vehicle crosses between the camera and the intersection approach being monitored, which can result in false detections.

- The optimal field of view for a camera is one that has the stop line parallel to the bottom edge of the view and in the bottom one-half of this view. The optimal field of view also includes all approach traffic lanes. The focal length should be adjusted such that the approach width, measured at the stop line, represents 90% to 100% of the horizontal width of the view. The view must exclude the horizon.

- Detection accuracy is significantly degraded by glare from the sun and, sometimes, from strong reflections from smooth surfaces. Sun glare typically causes problems for the eastbound and westbound approaches. A larger pitch angle can reduce the impact of sun glare and a camera equipped with an automatic iris (or electronic shutter) will minimize

the adverse effects of reflection. An infrared filter can also reduce the adverse effects of glare. VIVDS processors have the ability to detect excessive glare or reflection and automatically invoke maximum recall for the troubled approach. **Detection Accuracy** is defined as the number of times that VIVDS reports detection when a vehicle is in the detection zone, or reports no detection when a vehicle is not in the detection zone.

- Most VIVDS have separate image-processing algorithms for daytime and nighttime conditions. The daytime algorithm searches for vehicle edges and shadows. During nighttime hours, the VIVDS searches for the vehicle headlights and the associated light reflected from the pavement. Research has found that the nighttime algorithm is less accurate than the daytime algorithm and also has a tendency to place calls before the vehicle actually reaches the detection zone. Intersection lighting can minimize the extent of this problem.

- The detection design should avoid having pavement markings cross the boundaries of a detection zone since camera movement combined with high-contrast images may confuse the image processor and trigger false calls.

- The following equations are provided for determining the required length of a stop line detection zone:

$$l_{sl} = v_q\,(MAH\text{-}PT) - l_v$$

$$l_v^* = (l_v - l_{ro}) + x_c(h_v/h_c)$$

l_{sl} = length of stop line detection zone in feet
v_q = maximum queue discharge speed at the stop line (use 40 ft/sec)
MAH = Maximum Allowable Headway (use 3 seconds)
PT = controller Passage Time in seconds
l_v^* = effective length of vehicle in feet
l_v = length of design vehicle (use 16.7 feet)
l_{ro} = distance from back axle to back bumper of design vehicle (use 4.3 feet)
x_c = distance between the camera and the stop line in feet
h_v = height of design vehicle (use 4.5 feet)
h_c = height of camera in feet

- The detection zone length should be approximately equal to the length of a passenger car in order to maximize sensitivity. Stop line detection typically consists of multiple detection zones. For reliable queue service, detection zones should extend at least 40 feet from the stop line**.** **Zone Location** is defined as the distance between the upstream edge of the detection zone and the stop line.

- The camera field of view should be established to avoid inclusion of objects that are brightly lit in the evening hours, especially those that flash or vary in intensity. If these sources are located near a detection zone, they can trigger false calls. The light from

these sources can also cause the cameras to reduce its sensitivity by closing its iris, which results in reduced detection accuracy.

- Each VIVDS detection zone has a directional mode that allows it to recognize calls only for traffic moving in a specified direction. However, this mode appears to reduce the sensitivity of the detection zone.

- During daytime hours, swaying power lines, support cables or signal heads can trigger false calls as they move into and out of the detection zone.

- The performance of VIVDS is adversely affected by environmental conditions such as fog, precipitation, and wind. Condensation and dirt buildup on the camera lens can further degrade VIVDS operation.

- Shadows can extend into a detection zone and trigger false calls or compromise the VIVDS ability to detect vehicles.

- Delay settings are sometimes used to reduce the frequency of false calls. For example, a few seconds of delay is often set for stop line detection zones on the minor street approach. The delay eliminates false calls at night caused by right-turning vehicles from the major road whose headlights sweep across the detection zone. It also eliminates false calls due to cross-lane occlusion caused by tall vehicles on the major road.

- A lens adjustment module is an essential VIVDS-related installation device. It connects to the back of the camera and is used during camera installation to adjust the camera's zoom and focus settings. Having this device facilitates camera replacements or adjustments. Enough room is needed in the controller cabinet to house the needed VIVDS equipment. Standard RG-59 coaxial cable is good for up to a distance of about 500 feet for connecting the camera to the hardware in the controller cabinet.

- Satisfactory operation of a VIVDS requires verification of the initial layout and periodic on-site performance checks (at least every 6 months is recommended).

- A review of some existing VIVDS installations in Texas indicated that there was more than one discrepant call each cycle with about 1.8 discrepant calls per true call. About 80% of the discrepant calls averaged less than 2 seconds per call and were typically associated with the VIVDS registering a call slightly before or after its true arrival or departure time. Wholly missed or false calls were less frequent and often had a duration in excess of 2 seconds. During approximately 20% of the signal cycles, a phase experienced about 4 missed calls with the total duration of these missed calls being about 25 seconds per cycle.

In 2003, Oh and Leonard [25] obtained validation results for the PEEK VideoTrak 900 image processing system. The test site was on I-75 in Atlanta. The test results showed huge

volume errors in some case, especially at night. The system also provided lower speeds than true speeds at night. The farther the lane was from the camera, the more inaccurate was the count.

Signalized Intersection Queuing and Delay

In 1977, Riley and Gardner [26] investigated various techniques for measuring delay at signalized intersections. Four possible techniques were listed:

- **Point Sample**
  1st Advantage: self-correcting, each sample is independent of the previous one
  2nd Advantage: not dependent upon signal indications
  Disadvantage: accuracy reduced when counts become high (an upward bias exists such that an adjustment factor of 0.92 is recommended)

- **Input-Output** (a.k.a. Interval Sample)
  Disadvantage: field data must be corrected for vehicles that enter or leave the study area between the input and output points (at driveways or cross streets)

- **Path Trace**
  Disadvantage: a very large sample of vehicles is needed to provide an estimate of delay having reasonable confidence

- **Modeling**

As part of their work, the authors concluded that; "Once the recommended field data corrections have been made, stopped delay per vehicle multiplied by 1.3 will yield a good estimate of approach delay per vehicle."

In 1984, Hurdle [2] proposed the use of delay models that take more account of variations in travel demand over time. Hurdle noted that: "… any steady-state model that does not assume completely uniform arrivals will predict that the queue length, and therefore the delay, approach infinity as the v/c ratio approaches unity. This is, of course, the reason that systems with a high v/c ratio take a long time to settle into a steady state; it simply takes a long time for such long queues to form, particularly since vehicles keep leaking through the signal. As a result, one seldom sees real delays as large as those predicted for high v/c ratios. This discrepancy is not a

result of faulty mathematics but of the unrealistic assumption that the system is in a steady state. If vehicles continued to arrive at a rate v nearly equal to the capacity c, the giant queues really would form, but in reality the peak period ends and v decreases long before a steady state is reached. As a result, steady-state models are useful for predicting delays only at lightly loaded intersections." Hurdle added: "…there is one group of models, the steady-state queuing models, that work well when v/c is considerably less than one and another type, the deterministic queuing models, that work well when v/c is considerably more than one. In between, there are problems." He also stated: "What modeling approaches make very clear is that the development of the queue is very dependent on the details of the arrival pattern … more information about arrival patterns must be provided than is now customary."

In 1992, Bonneson [27] developed a discharge headway model for signalized intersections that was based on non-constant acceleration behavior. Bonneson mentions that, in 1977, Messer & Fambro found that, except for the first position, driver response by queue position was fairly constant at 1.0 second. The first driver experienced an additional delay of 2 seconds. Messer & Fambro also found that the average length of roadway occupied by each queue position is about 25 feet. Bonneson found this distance to be 25.9 feet.

Bonneson used regression analysis to obtain an approximate equation for the Standard Deviation (SD) of delay: $SD = 0.42 \times (\text{mean delay})^{0.7}$. The Maximum Error (ME) in the calculated delay at the 95% confidence interval is then: $ME = 1.96 \times SD = 0.82 \times (\text{mean delay})^{0.7}$.

Bonneson concluded that the minimum discharge headway of a traffic movement is a complex process that is dependent on driver response time, desired speed, and traffic pressure. The discharge headway model developed in his research indicates that the minimum discharge

headway of a traffic movement is not reached until the eighth or higher queue position. Bonneson also concluded that:

- A rather strong inverse linear relationship exists between vehicle acceleration and stop line speed.
- For the driver acceleration model developed, the maximum acceleration ranges between 6 and 8 ft/sec/sec with an average of 6.63 (this is similar to a value of 6.0 found by Evans and Rothery).
- For the stop line speed model developed, stop line speed increases with queue position in an exponential manner to a maximum value between 46.7 and 51.0 ft/sec with a median value of about 49 ft/sec (33 mph).
- Traffic pressure (vehicles per lane per cycle) is a significant factor (p=0.001) in reducing discharge headways.
- Based on the calibrated model, the start-up lost time for a typical through movement with a common desired speed of 49 fps and a maximum acceleration of 6.63 ft/sec/sec is 3.67 seconds
- Based on the calibrated model, the minimum discharge headway for a typical through movement of an at-grade intersection with a common desired speed of 49 fps and a nominal traffic pressure of 5 veh/ln/cycle is 1.81 seconds

The following formulas are provided in the report:

Briggs Models Based on Constant Acceleration

Calibrated Discharge Headway Model:

Headway of nth vehicle = $h_n = T + [2dn/A]^{1/2} – [2d(n-1)/A]^{1/2}$
(if $nd < d_{max} = V_q^2/ 2A$)

Headway of nth vehicle = $h_n = T + d/V_q$
(if $nd >= d_{max}$)

V_q = desired speed of queued traffic (29.4 ft/sec)
d = distance between vehicles in a stopped queue (19.65 feet)
T = driver starting response time (1.22 seconds)
A = constant acceleration of queued vehicles (3.67 ft/sec/sec)
d_{max} = distance traveled to reach speed V_q
n = queue position

Bonneson Models Based on Non-Constant Acceleration

Calibrated Stop Line Speed Model:

Stop Line Speed for vehicle n = $V_{sl(n)} = V_{max} (1 – e^{-nk})$

$k = -0.290 + 24.0/V_{max}$

Calibrated Discharge Headway Model:

Headway of nth vehicle = $h_n = (tau)N_1 + T(d/V_{max})$
$+ 0.357[(V_{sl(n)} - V_{sl(n-1)}/A_{max}] – 0.0086v – 0.23AGI$

Calibrated Minimum Discharge Headway Model:

Minimum Headway = $H = T + d/V_{max} – 0.0086v – 0.23AGI$

Calibrated Start-Up Lost Time Model:

Start-Up Lost Time = $K_s = 1.03 + 0.357V_{max}/A_{max}$

n = queue position
tau = additional response time for first queued driver (1.03 sec)
d = distance between vehicles in a stopped queue (25.25 feet)
T = driver starting response time (1.57 sec)
v = **traffic pressure** in vehicles per cycle per lane
V_{max} = common desired speed of queued traffic in feet per second
A_{max} = maximum acceleration in feet per second per second
N_1 = 1 for first queued vehicle, 0 otherwise
AGI = 1 for at-grade intersection, 0 for single point urban interchange

In 1997, Fambro & Rouphail [28] proposed a new set of delay equations that were, for the most part, incorporated into the 2000 Highway Capacity Manual. The only difference is that the formulas recommended for the d3 term were replaced by different formulas included in Appendix F of Chapter 16 of the 2000 HCM.

Simulation (TRAF-SIM) data were used to validate the over-saturation and variable demand component of the generalized delay model because of the difficulty in measuring over-saturation delay in the field

The following parameters are defined in this study:

- **I** = parameter for variance-to-mean ratio of arrivals from upstream signal. Isolated signals have the highest I value (I=1.0 → Variance=Mean →Poisson Distribution). The I value varies between 0.09 and 1.0 at coordinated intersections.

- The **k** value produces less delay for actuated signals with snappy extension intervals (down to 2 seconds). The amount of the delay decrease depends on the degree of saturation, with greater decreases experienced when the degree of saturation is low (toward 0.5) and no decreases experienced when the degree of saturation is high (at 1.0)

- Including a **T** parameter in the generalized delay model to account for the duration of the analysis period improves delay estimates under oversaturated conditions. Longer periods of oversaturation and higher degrees of oversaturation result in longer delays. It is important to note that part of the estimated delay during oversaturated conditions occurs after the analysis period.

The following definitions are given in the report:

- **Stopped Delay** = the time an individual vehicle spends stopped in a queue while waiting to enter an intersection.

- **Average Stopped Delay** = the total Stopped Delay experienced by all vehicles arriving during a designated period divided by the total volume of all vehicles arriving during the same period (used to determine LOS in 1985 and 1994 HCM).

- **Signal Delay (a.k.a. Control Delay)** = deceleration delay + queue move-up delay + Stopped Delay + acceleration delay

  The following formulas are provided in the report:

- **Control Delay (delay per vehicle for each lane group)** = d1 (Uniform Delay) + d2 (Incremental Delay due to Random and Overflow Queues) + d3 (Incremental Delay due to Oversaturation Queues at the start of the analysis period)

  $d_1 = PF[0.5C\{1-(g/C)\}^2]/[1-(g/C)\min(X,1.0)]$

  PF = $(1-P)f_{PA}/[1-g/C]$ (from 2000 HCM)
  X = v/c for lane group (aka degree of saturation)
  C = average cycle length (seconds)
  G = average effective green time (seconds)

  $d_2 = 900T[(X-1) + \{(X-1)^2+8kIX/Tc\}^{1/2}]$

  I = upstream filtering/metering factor obtained from Exhibit 15-7 of 2000 HCM
  k = incremental delay factor obtained from Exhibit 16-13 of 2000 HCM
  c = capacity of lane group (vph)
  T = duration of analysis period (hours)

d_3 = (See Appendix F of 2000 HCM)

In 1997, Engelbrecht, Fambro, et al. [6] proposed a generalized delay model that handles over-saturated conditions at signalized intersections. The delay equations calculate delays consistent with the more accurate path-trace method of delay measurement rather than the less accurate (but easier to carry-out) queue-sampling method. Delays estimated by the proposed generalized model were in close agreement with those simulated by TRAF-NETSIM.

The path-trace method measures individual vehicle delays from arrival to departure, even if the departure occurs after the end of the analysis period. Delay measurement using this technique is typically complicated. However, advances in intelligent transportation system technology may reduce the difficulty associated with this technique.

The queue-sampling method records the number of stopped vehicles at periodic intervals (such as every 10 seconds), multiplies this by the length of the sampling period, and then divides by the number of vehicles arriving during the analysis period.

For the path-trace method and queue count methods to be compatible, two conditions must hold: 1.) There must not be a residual queue at the start of the analysis period, and 2.) Queue counts must continue until all vehicles that arrived during the analysis period have cleared the intersection. All vehicles joining the back of the queue after the end of the analysis period should be excluded from this count.

TRAF-NETSIM calculates delay by subtracting the free-flow travel time from the actual travel time to yield overall delay. However, the actual travel time includes not only intersection, or control delay, but also some delay as a result of interactions between vehicles on the link itself, or traffic delay. In the analysis, the authors decided to ignore this discrepancy, as it is very

difficult to separate control and traffic delay, and the error is assumed to be small, especially under over-saturated conditions.

The following TRAF-NETSIM input values (representative of over-saturated conditions) were analyzed:

Analysis Period (T) = 15 & 30 minutes
Cycle Length (C) = 60, 90, 120 seconds
Saturation flow (s) = 1800 & 3600 vphg
G/C ratio = 0.3, 0.5 & 0.7
Degree of Saturation (X) = 1.0, 1.1, 1.2, 1.3 & 1.4 (0.9 was also included)

The authors point out that equilibrium (in TRAF-NETSIM) can never be reached for over-saturated conditions, as capacity is less than demand and outflow will always be less than inflow. The initialization will terminate before equilibrium can be reached, leaving an initial queue of unknown size. This queue will delay vehicles when it clears, increasing the delay experienced by vehicles that arrive during the analysis period. Therefore, the authors decided to use 3 periods in the analysis: an initial 60-second period with very low flow; the actual analysis period of duration T; and a final period of duration T, again with very low flow (TRAF-NETSIM can not handle zero flow). The first period is needed to initialize the network without transferring a queue to the second period, the second period is the actual analysis period, and the third period dissipates the over-saturation queue that built up over the second period.

Not all of the input scenarios yielded usable results. In some scenarios, the simulated delays were incorrect because of queue spillback

In 2000, Tarko and Tracz [29] investigated uncertainty in saturation flow predictions and concluded that standard errors reached 8 to 10%. They identified three primary sources of error: temporal variance, omission of one or more capacity factors in the predictive model, and inadequate functional relationships between model variables and saturation flow rates. The data

were collected on Polish highways but the authors conclude that the results should be transferable to other countries.

Using data from over 1100 signal cycles, Tarko and Tracz discovered that the saturation flow rate increases rapidly during the first 6 seconds of the green indication to a value of about 1400 pcphg (headway of 2.6 sec/veh), then slowly increases to a value of about 1600 pcphg (headway of 2.2 sec/veh) after another 20 seconds. Past this 25 second mark the rate stabilizes. This type of behavior occurred in all of the lanes investigated although the length of the periods varied somewhat. Consequently, the length of the counting period has an effect on the saturation flow rate that is obtained.

Tarko and Tracz also found that the percent of heavy vehicles in the traffic stream has an effect on the headway of passenger cars, with the headway varying between 2.2 sec/veh when no heavy vehicles are present to 2.6 sec/veh when the traffic stream is composed of 30% heavy vehicles. Heavy vehicles also have longer headways than passenger cars, which is another factor that reduces the saturation flow rate. Tarko and Tracz recommend the use of a Passenger Car Equivalence (PCE) factor of 2.4, which is substantially higher than the value of 2.0 used in the 2000 Highway Capacity Manual or the 1.2 default factor used by CORSIM.

Tarko and Tracz proposed various predictive models for saturation flow that included the following statistically significant independent variables: ratio of heavy vehicles, lane width, turning radius (infinite for straight lanes), and lane location (near curb or middle). The authors conclude by stating that: “Where possible, the saturation flow rates should be determined through direct field measurement”. This provides more support for the research at hand.

In 2002, Li and Prevedouros [30] studied three methods for describing the discharge process of a standing queue at an approach of a signalized intersection. Method 1 (M1) entails

measurements of headways based on the first 12 vehicles in a standing queue. Method 2 (M2 or HCM Method) entails measurements of headways based on all vehicles in a standing queue. Method 3 (M3) is the same as M2 except that arrivals which join the standing queue are included.

According to the HCM, the saturation headway is estimated by averaging the headways from the 5th vehicle to the last vehicle in a standing queue. The 2000 HCM suggests a base saturation flow rate of 1900 pc/h/ln for thru lanes, which corresponds to a saturation headway of 1.895 seconds (3600/1900) and 1800 pc/h/ln (a 2 second saturation headway) for protected left turn lanes. Start–Up Lost Time (SULT) is derived from the first four vehicles in a standing queue. The 2000 HCM mentions typical observed values of between 1 and 2 seconds for thru lanes.

Li and Prevedouros collected data on two lanes of a five-lane approach (3 thru lanes and a dual left turn lane) of a signalized intersection in Honolulu, Hawaii. The outside thru lane and the inside left turn lane were measured. These lanes were considered to be of 'ideal" design and no queues with heavy vehicles were used in the analysis. A vehicle was considered to be discharged when its rear axle passed the stop line. Observations containing fewer than four vehicles at the end of a queue were not included.

Start-Up Response Time (SRT) was defined by the author's as the time from the beginning of green to when the first vehicle's rear axle passes the stop line. The following relationship between SRT and SULT was provided:

Start-Up Lost Time = SULT = SRT + 4*(H_4-h)
Saturation Headway = h = (T_N-T_4)/(N-4)
Average Headway = H_i = (T_i – T_{i-4})/4
Where:
T_i = time when rear axle of vehicle i passes the stop line (T_0 = SRT)

N = last vehicle in the queue

The saturation headways (h) derived by the three methods (M1, M2 and M3) are statistically different.

For thru movements:

h = 1.90 sec (s = 1895 pc/h/ln) for M1, std dev = 0.21
h = 1.92 sec (s = 1875 pc/h/ln) for M2, std dev = 0.20
h = 1.98 sec (s = 1818 pc/h/ln) for M2, std dev = 0.22

The minimum headway was not reach until the 9th to 12th vehicle instead of the 5th vehicle as implied by the HCM. If queue arrivals are included (M3), both the mean and standard deviations of the headways increase after the 12th vehicle.

For protected left turn movements:

h = 2.04 sec (s = 1765 pc/h/ln) for M1 (1765/1895 = 0.931 LT factor), std dev = 0.23
h = 2.01 sec (s = 1791 pc/h/ln) for M2 (1791/1875 = 0.955 LT factor), std dev = 0.23

Headways decrease as queue position increases (motorists may be aware of the limited green time and tailgate so as to not experience a phase failure). After the first 12 vehicles the saturation flow rate remained well above 1800 pc/h/ln. Queues of medium length discharge more efficiently than do short queues. After the 16th vehicle in the queue the saturation flow rates of the left turn movement were larger than for the thru movement. The Start-Up Response Time (SRT) for left turn movements (1.42 seconds) is less than for thru movements (1.76 seconds), indicating a heightened awareness of left turning drivers to the display of the green.

There was a high standard deviation of SRT for both movement types (0.61 for thru's and 0.74 for LT's), indicating a big variation amongst drivers. However, SRT was not sensitive to queue length. The calculated SULT was well above the 1 to 2 seconds of the HCM (2.89 for thru's and 2.38 for LT's under peak period conditions and 3.03 for thru's and 2.53 for LT's

under off-peak conditions.) As with the SRT's, the SULT's also have high standard deviations (1.36 for peak thru's and 1.32 for peak LT's; 1.5 for off-peak thru's and 1.3 for off-peak LT's).

Linear regression models (one for thru movements and one for LT movements) were developed that indicate a negative correlation between SULT and queue length (i.e. long queues produced shorter start-up loss times).

Distribution tests showed that thru movement headways were lognormally distributed without a shift and that LT headways were lognormally distributed with a shift of 1 second. SRT was normally distributed for both movements.

In 2002, Cohen [31] used the Pitt car-following system to examine the effects of lane changing and a heterogeneous vehicle mix on queue discharge headways.

In the Pitt car-following model, the first vehicle in the queue begins to move across the stop line after the lost time (start-up delay) has expired. The second vehicle in the queue then responds to the motion of the leader through the car-following system with no additional explicit lost time added. The effect of lost time on subsequent vehicles is modeled through the sluggishness of the car-following system.

Based on the results of the study, it can be concluded that trucks not only have longer headways than cars, but they also increase the headways of the vehicles behind them. The closer to the front of the queue that the truck is located, the greater the overall negative effect on queue discharge. In addition, for trucks further back in the queue the major item affecting its equivalency factor is its greater length whereas, for trucks near the head of the queue, the major item is vehicle performance limitations. Queue Discharge Headway is defined as the difference in stop line crossing times between each vehicle pair.

Lane changing also has a substantial effect on discharge headways, particularly if the lane change takes place close to the stop line. For thru lanes with short adjacent turn lanes (where lane changing is apt to take place) the saturation flow rate will be lowered on the basis of the percentage of turns.

The results of the study also suggest that the start-up wave in a discharging queue will slow down as it progresses upstream. Acceleration rates decrease as one progresses upstream in the queue (each vehicle accelerates more slowly than its leader). Consequently, it takes longer for gaps to open between pairs of vehicles in the queue and the presence of these gaps is the necessary requirement for the follower to begin to move. Start-Up Wave (a.k.a. Green Wave, Expansion Wave) is defined as the rate at which vehicles in the queue begin to move. (With movement defined as the time at which a speed of 1 ft/sec is achieved.)

In addition, the study results indicate that the discharge headway distribution is almost flat beyond the fifth vehicle in the queue, which is consistent with the HCM.

The author notes that the best approach for calibration of the Pitt car-following model is to measure in the field the crossing times of both the front and rear of each vehicle in the queue as it discharges across the stop line. These measurements allow the plotting of two curves, the front-to-front time headway curve and the rear-to-front time spacing curve. Unfortunately, this type of detailed data set is usually not collect in queue discharge studies.

The author explains that the NETSIM queue discharge mechanism is limited in that it is based on the assumption that vehicles in a queue discharge from the intersection at equal time headways (other than stochastic variations) subject to start-up delays applied to the first 3 vehicles in the queue. The effect of lane changing is ignored completely and the effect of commercial vehicles is treated heuristically using vehicle equivalency factors.

In 2003, Mousa [32] presented a microscopic stochastic simulation model developed to emulate the traffic movement at signalized intersections and estimate vehicular delays, including acceleration and deceleration delay. By analyzing 48 cases with a fixed g/C ratio of 0.475, it was found that the ratio of total delay to stopped delay is directly proportional to both the degree of saturation and the approach speed, and inversely proportional to the cycle length. The effect is greatest for degree of saturation and cycle length and least for approach speed. For the 48 simulated cases, the saturation flow obtained from simulation ranged from 1692 vph to 1807 vph, with an average value of 1770 vph and a standard deviation of 28 vph.

Approach speeds ranging from 30 to 50 mph and cycle lengths varying between 60 and 150 seconds were considered and tested in this study. Different levels of degree of saturation, ranging between 0.5 and 0.9, are also considered. The ratio of total delay to stopped delay was found to be between 1.5 and 3.0 with the minimum ratio resulting from the longest cycle length (150 seconds) and the lowest degree of saturation (0.5) and the maximum ratio resulting from the shortest cycle length (60 seconds) and the highest degree of saturation (0.9).

A sufficient length of approach was considered in the analysis to ensure that all acceleration/deceleration delays incurred by individual vehicles were executed within the simulated length.

In 2004, Rakha and Zhang [33] authored a paper that demonstrated the consistency that exists between queuing theory and shock-wave analysis and that highlighted the common errors that are made with regard to delay estimation using shock-wave analysis. The authors point out that the main difference between shock-wave analysis and queuing models is the way vehicles are assumed to queue upstream of the bottleneck. Queuing analysis assumes “vertical stacking” of the queue whereas shock-wave analysis considers the horizontal extent of the queue.

Maximum queue reach (a.k.a. back of queue) can only be identified using shock-wave analysis. The authors show that the size of the queue obtained from shock-wave analysis is the same as the size of the queue obtained from deterministic queuing theory if the queuing theory value is adjusted by a factored equal to total travel time divided by total delay.

In 2004, Perez-Cartagena and Tarko [34] demonstrated that, based on studies conducted in Indiana, town size and lateral lane location (right-most lane or not) are important variables in identifying the base saturation flow rate for a signalized intersection. Saturation flow rates were estimated using the Headway Method and weighted regression analysis. The authors also discovered that small communities tend to have considerably lower values of saturation flow than large communities, indicating that drivers in large communities are more aggressive than drivers in small communities. The reduction in saturation flow rate was about 8% for medium size towns and 21% for small towns (as compared to large towns).

Kebab, et al. [35] developed an efficient field procedure for measuring approach delay at a signalized intersection that segregated the delay by movement. The procedure produced good results in comparison to ground truth obtained from video.

One section of a 2006 paper by Brilon, et al. [36] discussed variation in capacity that occurs at signalized intersections due to "the randomness of driver behavior and interaction between vehicles". The authors concluded that their stochastic concept of capacity "provides better plausibility than the assumption of constant-value capacities" and that "the implications of random capacities on delay distributions should be investigated by further research".

Probe Monitoring

The most promising alternative method for obtaining the type of globally applicable delay estimates (estimates applicable to over-saturated as well as under-saturated conditions) addressed in this paper is the use of probe vehicles. A considerable body of work is being conducted in this

area, including the potential use of cell phone data to track individual vehicles and the results of the work are starting to show up in the literature.

A 2005 article by Jiang, et al. [37] examined the collection of signalized intersection delay data using vehicles outfitted with global positioning system (GPS) technology. It was determined that, compared to manually measured delays, the GPS approach provided the same accuracy with considerably lower labor requirements.

A 2007 paper by Ko, et al. [38] also examined the collection of signalized intersection delay data using vehicles outfitted with global positioning system (GPS) technology. Their technique included algorithms for analyzing speed profiles and acceleration profiles in order to automatically identify critical control delay points, such as deceleration onset points and accelerating ending points. This automated process permits the analysis of large data sets and provides consistent results. However, the approach experienced some difficulty in handling over-capacity conditions and closely spaced intersections.

A 2007 paper by Comert and Certin [39] used probe vehicles to estimated queue lengths on a signalized intersection approach. The best estimate of queue length was provided for high volume, but under-saturated, conditions. The results are subject to sampling errors (a common characteristic of probe use) and the procedure was not tested under congested conditions.

A 2007 Florida Department of Transportation report authored by Wunnava, et al. [40] of Florida Atlantic University investigated cell phone tracking. The authors concluded that a host of both technical and privacy issues need to be worked-out before probe vehicles can provide the needed detail to accurately estimate approach delay:

> … the team also found that the cell phone technology is not accurate in congested traffic conditions, where the data is more important than in the free-flow traffic conditions, and the accuracy decreases rapidly as the congestion increases… Additional issues remain such as: (1) privacy of the cell phone users whose phone transmissions are being probed by the

cell companies for location data, (2) irregular and transient cell data for travel time and speed computations, especially during congested traffic and severe weather conditions, (3) limited capabilities of the travel time providers to follow changes by the cell companies in their data formats and structures, and (4) incompatibility of data when switching from one travel time provider to another.

If these issues, some of which are political in nature, cannot be addressed satisfactorily then obtaining widespread delay information from probes may never occur.

Extending the Body of Knowledge

Although a number of researchers have investigated sampling techniques designed to improve the estimation of travel time and delay along the through lanes of an arterial corridor (such as through vehicle re-identification or the use of instrumented probes), the research effort described herein is unique in that it attempts to estimate delay in a manner that is directly applicable to the minor movements of the intersection as well as the major thru movements, and it utilizes information from all approaching vehicles, not a restricted sample. In addition, none of the previous research has dealt with the real-world problem of queues that extend beyond the detection system for some period of time; either short-lived queues that occur during under-saturated conditions because of spurts in activity or longer-lived, recurring queues that occur during over-saturated conditions. This appears to be the only research that is attempting to intelligently "estimate that which cannot be easily measured" with respect to intersection delay.

The basic problem that is being addressed is the need to establish a methodology that can intelligently estimate delay associated with vehicles that are beyond the reach of the detection system. This means obtaining reasonable estimates of vehicular delay even when queues are long and multiple phase failures occur. The use of incomplete information, combined with a concentration on over-saturated conditions, represent a deviation from the research conducted to date.

CHAPTER 4
ESTIMATING NON-VISIBLE DELAY

This chapter describes the methodology that was established to predict non-visible delay under conditions of limited information and the associated analysis procedure that was developed. Variables important to the procedure are discussed and a series of new technical terms relevant to the procedure are introduced (Objectives 1, 2 and 3).

Research activities were conducted using CORSIM (CORridor SIMulation) microscopic traffic simulation software and TRAFVU (TRAFfic Visualization Utility) software that are contained within the TSIS (Traffic Software Integrated Systems) software package. The CORSIM software, which was developed by the Federal Highway Administration (FHWA), consists of the FRESIM (FREeway SIMulation) component and the NETSIM (NETwork SIMulation) component. TRAFVU is an object-oriented, graphics postprocessor for CORSIM that displays traffic networks, animates simulated traffic and traffic controls, and reports measures of effectiveness for the network under study.

The CORSIM runs made use of a very simple case, the intersection of 2 one-way streets, each having a single approach lane. No trucks were placed into the traffic stream and no turns were allowed. A random (Poisson) arrival pattern was set with arrival rates varying each 15-minutes during a one-hour analysis time frame. The intersection was controlled by a 2-phase semi-actuated traffic signal and delay data were collected and analyzed only for the actuated side street approach. Goodness-of-fit testing using the chi-square technique was used to ensure that a random (Poisson) arrival distribution was actually produced by CORSIM.

Data Analysis Programs

In order to obtain the data needed for analysis, a visual basic program called TSDViewer [41] was developed which reads the output file of CORSIM and produces, on a second-by-

second basis, a variety of information pertaining to the number of vehicles crossing various checkpoints and arriving and departing queues. TSDViewer automates the data collection process from the CORSIM runs by reading CORSIM's output file (the .tsd file for CORSIM 5.1 and the .ts0 for CORSIM 6.0) and producing an Excel worksheet containing the following information:

- The time at which each vehicle enters the approach link,
- The time at which each vehicle enters the delay zone,
- The speed of each vehicle when it enters the delay zone,
- The time at which each vehicle enters the Field of View (FOV),
- The time at which each vehicle arrives at the Back of Queue (BOQ),
- The time at which each vehicle departs the queue,
- The time at which each vehicle crosses the stop bar (leaves the link),
- The time at which each vehicle leaves the delay zone,
- The signal indication (red, yellow, or green) at each time point,
- If two queues exist simultaneously, the time at which vehicles arrive at the back of queue 2,
- If two queues exist simultaneously, the time at which vehicles depart queue 2,
- The number of vehicles experiencing 1 phase failure,
- The number of vehicles experiencing 2 phase failures,
- The number of vehicles experiencing 3 phase failures, and so on up to a maximum of 15

This information can be used to calculate, on a second-by-second basis, both queue length and back of queue position. Stopped delay is then calculated using the queue length. An example that shows the relationship between queue length and back of queue position is provided in Figure 4-1. It is important to recognize that the back of queue is not itself a length, but rather a position. As is shown in Figure 4-1, the value for the back of queue position can be quite large even if the corresponding queue length is small.

A visual basic program named DTDiagram [42] was also developed as part of this research. This program reads the CORSIM output file and produces trajectory information (a series of time-distance points) for each vehicle. The data produced by DTDiagram is read by BuckTRAJ [43], another visual basic program that was developed as part of this research to calculate, for each vehicle, all of the components of control delay.

The programs developed allow the researcher to quickly simulate a variety of real-world conditions in a relatively realistic manner and to accumulate the associated MOEs, such as delay. The researcher can then compare "actual delay" obtained from CORSIM against the "predicted delay" obtained from the techniques developed in this research. The use of simulation allowed many different scenarios to be run in order to compare actual versus predicted delay, allowing us to see how well our proposed delay estimation methodology performed. Essentially, micro-simulation provided a source of verification against which our delay prediction methodology could be developed and refined.

The pivotal task of the research was the creation of an automated analysis procedure that can use the outputs of TSDViewer to produce queue and delay information that is required for proper evaluation of candidate delay estimation procedures. The analysis procedure must be able to, on a second-by-second basis, estimate the non-visible queue, add this queue to the visible queue, calculate the associated stopped delay, and then compare the result to the "true" control delay as calculated by CORSIM.

For the purposes of this study, **stopped delay** is defined as the delay experienced by vehicles when they are at a complete stop (zero acceleration and zero velocity). Also for the purposes of this study, a vehicle is considered queued when it comes to a complete stop (zero acceleration and zero velocity). These are slightly more conservative definitions than those used by CORSIM. CORSIM considers a vehicle to be stopped when its speed is less than 3 feet/second and considers a vehicle to be queued when its speed is less than 9 feet/second and its acceleration is less than 2 feet/second/second. The zero-velocity-zero-acceleration complete stop definition was chosen since it is easier to correlate with both video images of vehicle queues and

queues observed in the field. Much less discretion is needed to determine when a car stops than when its acceleration and speed simultaneously fall below a certain set of values.

Control delay (D_C) is defined, both by CORSIM and in general, as the sum of initial deceleration delay (D_D), stopped delay (D_S), queue move-up delay (D_{MU}), and final acceleration delay (D_A). Acceleration delay can be further subdivided into acceleration delay that occurs prior to the stop bar (D_{A1}) and acceleration delay that occurs after the stop bar (D_{A2}). Figure 4-2 depicts the delay elements.

Total delay is defined as the sum of control delay, which is caused by the presence of the traffic signal, and the delay associated with vehicular interactions that occur on the link (called "interaction delay" in this study). Others have called this "cruise delay" or "traffic delay" instead of interaction delay since it is the delay resulting from cruise speeds that are lower than the free flow speed due to the presence of other traffic.

Ideally, we would like to have a tool that provides "accurate real-time measurement of control delay". However, given the limitations of almost all detection systems, the best we can hope for, and what has been developed in this research, is a procedure that provides a "reasonably accurate real-time estimate of stopped delay". By applying an appropriate factor (such as the commonly-used 1.3 value) or range of factors, we then scale-up the stopped delay estimate to obtain a "reasonably accurate real-time estimate of control delay". Absent the instrumentation of every vehicle, control delay cannot be accurately measured using current vehicle detection systems for the following reasons:

1. Since vehicle detection systems are primarily used to allocate green time at a signal, there is usually no detection in the departure lanes. Consequently, final acceleration delay cannot be measured.

2. Queue lengths often extend beyond the limits of the detection system, especially during peak hours. When this happens, we can only measure the stopped delay and

queue move-up time that occurs within the limits (or **field of view**) of the detection system. Any stopped delay or queue move-up time that occurs outside the field of view cannot be measured.

3. Motorists usually begin their initial deceleration far in advance of any signalized intersection queue, often well beyond the field of view of the detection system. So, most of the time, initial deceleration delay cannot be measured either.

In order to make use of existing detection systems it becomes necessary to measure that portion of the delay that can be observed and then intelligently estimate what cannot be observed (see Figure 4-3). The result is the methodology produced by this research, a methodology that measures visible stopped delay; stopped delay that occurs within the Field of View (FOV) of the detection system and then uses various analytical techniques to predict non-visible stopped delay; stopped delay that occurs outside the FOV. The portion of the queue that is outside the FOV is referred to in this research as the non-visible queue (see Figure 4-4) and the period of time during which non-visible queues are present is referred to as the blind period.

During this research, a set of factors were identified that can be used to convert predicted stopped delay to predicted control delay. Previous research by Mousa [32] suggests that the use of a single 1.3 value is too simplistic. His simulation work suggests that the ratio of total delay to stopped delay varies from a value of 1.5 to 3 depending mainly on cycle length and degree of saturation. Figure 4-5 summarizes the relationship between this ratio and both the v/c ratio and cycle length for over-saturated conditions.

For each CORSIM run, a certain Field of View (FOV) was assumed. Measured visible locked-wheel stopped delay (delay occurring within this FOV) was added to the predicted non-visible stopped delay to produce a total value for predicted stopped delay. This predicted value was then compared to the actual value of locked-wheel stopped delay assuming an infinite FOV. Finally, the predicted stopped delay was factored-up to obtain a predicted value for control delay.

This predicted control delay was then compared to the actual value of control delay, again assuming an infinite FOV. As might be expected, these comparisons are more favorable when traffic volumes are lower, or when the FOV is larger. In this case, queue lengths seldom go beyond the FOV and most of the delay can be directly measured. Conversely, when traffic volumes are higher, or the FOV is relatively short, the delay comparisons are less favorable since, under these conditions, the queue frequently extends beyond the FOV requiring most of the delay to be estimated.

CORSIM accumulates control delay on a link basis and, by necessity, the link numbering changes at signalized intersections. The unfortunate result is that CORSIM's estimate of control delay does not include any final acceleration delay that occurs past the stop bar. This forces the development of an alternate measure of "control delay" to use as the CORSIM reference value. This was accomplished by setting up a delay zone that begins well in advance of the intersection and ends a few hundred feet downstream of the intersection. The location of the start and end points for this delay zone were chosen carefully. The start point was set far enough in advance of the intersection (upstream) so that all initial deceleration delay is accounted for, but not so far in advance that a significant amount of pre-signal interaction delay occurs. Likewise, the end point was set far enough past the intersection (downstream) so that all final acceleration delay is accounted for but not so far past that a significant amount of post-signal interaction delay occurs.

The best location for the start point depends on the physical extent of the queuing that is expected and was set in an iterative fashion. Given a fixed g/C ratio, the physical extent of the queuing depends on both arrival volume and cycle length. For the range of variables considered in this study, the location of the delay zone start point was located either 1600, 2600 or 3600 feet

in advance of the stop bar with corresponding CORSIM upstream link lengths of 2000, 3000, or 4000 feet used.

The best location for the end point was determined using the acceleration charts contained in AASHTO's Geometric Design of Highways and Streets [44]. For example, using Exhibit 2-24 in this AASHTO manual we see that, on level terrain, approximately 300 feet is required for passenger cars to accelerate from a stop to 34 mph. Consequently, a delay zone that ends 300 feet past the stop bar is a reasonable configuration for a road with a posted speed limit of 35 mph. Since the link speeds used in our study were kept constant at 30 mph, 300 feet was chosen as a reasonable downstream distance from the stop bar with a corresponding CORSIM downstream link length of 1000 feet. The resulting delay zone length was either 1900 feet, 2900 feet, or 3900 feet.

If the start of the delay zone is positioned far enough upstream then all vehicles should enter the delay zone at their free-flow speed (with free-flow speed being defined as the speed at which the vehicle would travel had the signal not existed). The time it takes for a vehicle to cover the length of the delay zone at its free-flow speed is defined as its free travel time. With the delay zone boundaries properly established, the control delay is simply the difference between the actual time it takes a given vehicle to traverse the delay zone and the vehicle's free travel time. Although some interaction delay may occur near the start point and the end point of the delay zone, it should be relatively minor in nature and should not significantly affect the results.

For all CORSIM runs over-capacity conditions existed for at least a portion of the one-hour analysis time frame, resulting in substantial levels of queuing. Such queues behave in a manner consistent with shock-wave theory and when traffic volumes become very high in

relation to the capacity of the approach in question, vehicle re-queuing causes the formation of one queue at the stop bar and another queue further upstream. The resulting simultaneous queues are separated by vehicles moving between them, as is demonstrated in Figure 4-6. When this occurs, it is often the case that vehicles arrive and depart both queues at the same time. The analysis programs track both queues in order to provide accurate queuing information. In this research, whenever there are two simultaneous queues, the queue closest to the stop bar is referred to as queue 2 and the one furthest from the stop bar as queue 1. When either of the two queues dissipates, the remaining queue is referred to as queue 1. The analysis programs were designed to handle a maximum of two simultaneous queues since three simultaneous queues are only present under extremely congested conditions, conditions for which almost any prediction methodology would be grossly inaccurate.

Re-queuing events are associated with phase failures, which occur when a vehicle joins the back of a queue and the next green interval is of insufficient duration to allow the vehicle to pass through the intersection. Phase failures tend to occur under congested conditions, but can also occur during uncongested conditions because of poor signal timings. Poor signal timings might include insufficient maximum intervals, extension intervals that are too short for the detection system, or even insufficient minimum intervals if the approach utilizes an upstream detection system. Re-queuing is a necessary condition for the formation of simultaneous queues; however, it is not a sufficient one. As shown in Figure 4-7, re-queuing may not result in the formation of simultaneous queues.

Unusual or atypical events can also result in phase failures and associated re-queuing. For example, a vehicle that does not respond in a reasonable time to the green indication (because it is temporarily stalled, the driver is not paying attention, etc.) may cause an actuated approach to

gap-out prematurely, forcing this vehicle and all vehicles behind it to re-queue. CORSIM does not model such atypical events, but they do occur periodically in the real world. As Courage & Fambro [45] put it; “Simulation models introduce a stochastic element into the departure headways based on a theoretical distribution. They are therefore able to invoke premature phase terminations to some extent, but they do not deal with anomalous driver behavior”.

A phase failure may be either “liberal” or “strict”. A strict phase failure occurs when a vehicle that was queued when the signal turned green is forced to re-queue when the signal turns yellow then red. A liberal phase failure occurs when a vehicle joins the back of the queue during the green indication but is forced to re-queue when the signal turns yellow then red. It should be noted that the analysis process developed for this research recognizes both types of phase failures, whereas CORSIM only reports strict phase failures.

It is worth noting that the number of vehicle re-queues is equal to the number of vehicle stops if the first stop is ignored.

When the side street approach under investigation receives the red indication, vehicles begin to queue at the stop bar. The time during which the entire queue is within the FOV and can be “seen” by the detection system is referred to as the visible period.

Eventually, the queue fills-up the FOV and the detection system can no longer measure the exact queue length. When this occurs, the system transitions from a visible period into a blind period and the prediction process must begin for the non-visible queue. Figure 4-8 provides an example of a blind period. During this blind period, vehicles attach themselves to the end of the non-visible queue at some unknown rate, referred to as the actual arrival rate. The portion of the blind period during which vehicles can attach themselves to the back of the non-visible queue, but cannot leave the front of the non-visible queue since the signal has not yet turned green and

there are vehicles queued ahead of them, is referred to as the rising queue blind period (which occurs from time T-7 to time T-34 in Figure 4-8).

Eventually the side street approach receives the green indication and vehicles on that approach begin to cross the stop bar. The visible queue shrinks from the front until the last vehicle in the FOV begins to move and the visible queue becomes zero. At this point, vehicles can begin to depart the non-visible queue from the front while they continue to attach to the back of the non-visible queue at the unknown rate. We refer to this portion of the blind period where vehicles can both attach themselves to the back of the non-visible queue and leave the front of the non-visible queue, as the falling queue blind period (which occurs from time T-34 to time T-72 in Figure 4-8). The length of the non-visible queue is typically falling during this period since vehicles almost always depart the front of the queue at a much faster rate than they arrive at the back of the queue.

For example, assume a field of view (FOV) of 12 vehicles. When the visible queue extends to a point where the 12th position is filled by a queued vehicle, the rising queue portion of the blind period begins. After some period of time the signal turns green and, eventually, the vehicle in position 12 moves forward. When this vehicle moves forward the rising queue portion of the blind period ends and the falling queue portion of the blind period begins. After some additional period of time, a gap of sufficient duration (such as 5 seconds) is encountered between successive vehicles entering the FOV, signaling that the end of the queue has come into view. When this happens, the blind period has ended (which occurs at time T-72 in Figure 4-8).

A review of the Figure 4-8 example reveals that the non-visible queue actually shrinks to zero well before the end of the falling queue portion of the blind period (somewhere abound time

T-50). However, because of the limited FOV, we cannot be certain that the non-visible queue has dissipated until time T-72.

Many blind periods may exist over a given analysis time frame, with the number of blind periods depending on the number of times that the end of the actual queue goes out of, and then comes back into, the field of view.

If a vehicle does not enter the queue FOV for some sufficiently long period of time (for our Figure 4-8 example, 5 seconds), and if another queue does not fill the FOV prior to this 5-second period, then the blind period is considered to have ended and the system returns to a visible state where the actual queue length is known. When this occurs it is assumed that there no longer exists a non-visible queue (i.e., the non-visible queue has been "flushed out"). However, if this 5-second headway does not occur before the FOV is once again filled with queued vehicles, then the system transitions from one blind period into another with no intervening period of visibility. When this happens, adjacent blind periods occur (see Figure 4-9). As one might expect, the problem of estimating the length of non-visible queues and their associated delay becomes more difficult (and, hence, more approximate) as the frequency of adjacent blind periods increases.

As we shall soon discover, the number of adjacent blind periods is an important variable when attempting to predict the length of the non-visible queue and its associated stopped delay. The non-visible delay estimation algorithm contained within our analysis software makes use of two counters (labeled A and D for Ascending and Descending) that are tied to the rising queue/falling queue status as shown in Figure 4-10.

One important variable in the queue formation/dissipation process is the average time it takes a vehicle to depart the queue once the vehicle ahead of it has begun to move. This time, referred to by Long [46] as the queue startup lag time (or by others, and in this research, as the

queue departure time), is 1 second in CORSIM. However, field studies by Long at 4 sites in Florida involving 140 queues of at least 16 vehicles in length (for a total sample of 1893) resulted in a slightly longer average startup lag time of 1.15 seconds with a standard deviation of 0.52 seconds. Long also references work by Herman, et al., in 1971 that indicated an average startup lag time of 1.0 sec and work by Messer and Fambro in 1977 that produced an average startup lag time of 1.1 sec. One must use the 1 second startup lag time when trying to replicate CORSIM behavior, however, the 1.15 second value measured by Long would be applicable when analyzing actual field data.

The necessary computations for carrying-out the delay estimation procedure were incorporated into a software tool called "BuckQ". BuckQ is a visual basic application program for Excel which reads the data provided by TSDViewer and produces a variety of useful information based on this data. BuckQ provides, for a one-hour analysis time frame having four 15-minute periods, a second-by-second tabulation of items such as queue length, back of queue position, stopped delay, move-up delay and control delay. It also provides a host of ancillary capabilities, including automated calculation of: start-up-lost-time, saturation flow, and capacity by cycle; HCM queuing and delay information by 15-minute period; and arrival type by 15-minute period. In addition, BuckQ allows evaluation of arrival patterns using a chi-squared goodness-of-fit test and provides extensive graphing capabilities. However, the most important feature of BuckQ is its ability to accommodate second-by-second queue and delay prediction procedures and its ability to compare the results of these procedures to CORSIM results. Using BuckQ, delay prediction algorithms can be tested to see how well they perform and the results presented in a graphical format.

The following information is compiled by BuckQ on a second-by-second basis for the entire 3600-second (60-minute) analysis period:

- Length of queue 1
- Length of queue 2
- Actual stopped delay
- Back of Queue position for queue 1
- Back of Queue position for queue 2
- Length of visible queue 1 (constrained by FOV)
- Length of visible queue 2 (constrained by FOV)
- Visible stopped delay
- Visibility status
  = 1 when there is a "rising queue blind period"
  = -1 when there is a "falling queue" blind period"
  = 0 when there is no blind period

Development, testing and refinement of the various software programs was carried out using a large number of data sets covering a wide range of near-saturated and over-saturated arrival patterns and three cycle lengths (80, 120 and 160 seconds). The extensive testing was necessary to ensure that both programs functioned properly over a wide variety of conditions, including grossly over-saturated conditions.

Prediction Algorithm for Non-Visible Delay

One of the central elements of this research is the development of a predictive algorithm that determines a reasonable value for the delay associated with the non-visible portion of the queue. The first component of the algorithm is an estimation technique that uses the rate of arrivals into the FOV to estimate the arrival rate at the back of the non-visible queue.

Non-Visible Queue Estimation Technique

Estimated NVQ Length = f(vehicles entering FOV during blind period, length of the blind period, departure rate)

This technique assumes that vehicles arrive at the back of the queue at a uniform rate during the full extent of the blind period. The arrival rate is calculated using the number of

vehicles that enter the FOV during the blind period. For example, if the blind period last for 32 seconds and 8 vehicles enter the FOV, then the estimated arrival rate is 8 vehicles/32 seconds or 0.25 vehicles/second. All of these vehicles enter the FOV during the falling queue portion of the blind period, a time when traffic is freely flowing thru the FOV.

Vehicles are also assumed to depart the non-visible queue at a constant rate of 1 vehicle per second during the Falling Queue Blind Period. Since the departure rate is almost always greater than the arrival rate, the non-visible queue shrinks in size and, if sufficient green time is provided, eventually disappears during this period.

As discussed previously, the blind period ends when a 5 second (or greater) gap occurs between vehicles entering the FOV since a gap of this size suggests that we have come to the end of the non-visible queue of vehicles. The blind period thus gives way to a period of visibility during which we know for sure what the true queue length is because we can observe it.

In reality, it may or may not be true that a 5 second headway signals the end of the blind period. It may be that the last vehicle in the non-visible queue passed some time ago or, conversely, it may be that there are more vehicles in the non-visible queue but that some "sleeper" (a slow truck, someone fiddling with their radio, etc.) has allowed a large gap to form in front of him or her. The use of a five-second headway is a reasonable compromise between these two situations, at least when we are dealing with a stream of traffic composed solely of passenger cars. In any event, given a limited field of view, selection of some reasonably prudent headway value that is neither too long nor too short under most circumstances is the best that can be done.

Initial experiments have verified that this particular technique does a good job of estimating non-visible queues and delays when a period of visibility follows the blind period.

However, when traffic volumes intensify, it is often the case that the FOV fills with queued vehicles without a 5-second headway being observed. In this case, "adjacent blind periods" occur. The problem with adjacent blind periods is twofold: 1) The true number of vehicles that arrived during the blind period is unknown because the FOV fills-up and all of the arrivals do not come into the FOV, and 2) One never really knows where the true end of the queue is, forcing non-visible queue length estimations to be made that depend on previous non-visible queue length estimations. Additional adjustments are needed to handle adjacent blind periods.

When adjacent blind periods occur, the number of vehicles entering the FOV during the blind period may substantially underestimate the number of vehicles that arrived at the back of the non-visible queue during the blind period. A second "adjustment technique" is needed to augment the initial "estimation technique" when this occurs.

Non-Visible Queue Adjustment Technique:

Adjusted NVQ Length = f(vehicles entering FOV during blind period, length of the blind period, departure rate, adjacent blind period counter) = f(estimated arrival rate, departure rate, adjacent blind period counter)

The adjacent blind period counter increments by a value of 1 whenever a blind period is followed by another blind period, and resets to zero when a period of visibility occurs. The estimated arrival rate is increased using an additive power function of the following form:

$$AR_{adj} = AR_{est} + [(ABPC + C)^{P}]/X$$

Where: AR_{adj} = Adjusted Arrival Rate
AR_{est} = Estimated Arrival Rate
ABPC = Adjacent Blind Period Counter
C, P, X = Constants

The longer the end of the queue stays "out of view", the higher the ABPC becomes and the more the adjusted arrival rate is increased in comparison to the estimated arrival rate. Extensive

testing suggests that the following constants provide good predictive abilities, even during highly over-saturated conditions where some vehicles experience as many as six phase failures:

P = 0.4
C = 66
X = 30

These constants can be varied to change the shape of the predicted cumulative delay curve. Figure 4-11 is the base condition where P, C and X equal the values just listed. If P, the power constant, is increased from 0.40 to 0.41 while holding C and X constant, the entire curve shifts upward as shown in Figure 4-12. If C, the additive constant, is increased while keeping P and X at their original values, then the curve both increases and flattens out. If X, the division constant, is decreased while keeping P and C at their original values, then the tail end of the curve shifts upward. The optimum combination of P, C and X that results in a predicted cumulative stopped delay curve that most closely follows the actual cumulative stopped delay curve is obtained through trial and error.

Non-Visible Queue Re-Adjustment Technique:

Re-Adjusted NVQ Length = f(vehicles entering FOV during blind period, length of the blind period, departure rate, adjacent blind period counter, average headway, average free flow speed, average vehicle length) = f(adjusted arrival rate, average headway, average free flow speed, average vehicle length)

As a queue becomes longer the back of the queue propagates closer to its source of arrivals. This tends to increase the effective arrival rate of vehicles at the end of the queue. Hurdle [2] recognized this fact in his investigation of intersection delay:

> "Another way of thinking about the model is to say that, in the model, vehicles do not line up along the street but form a vertical stack at the stop line. The real queue is always somewhat longer than the model predicts because the queue engulfs some vehicles that the model assumes are still driving to the vertical stack at the stop line".

Figure 4-13 provides an example. In this example, an additional arrival effectively occurs once every 60 seconds due to queue propagation. This adjustment becomes significant as volume exceeds capacity and queues become extensive.

Examples

To demonstrate the analysis procedure, four examples based on a 120 second cycle length were developed. Each example uses a different set of arrival rates that result in over-capacity conditions at some point during the one-hour analysis time frame. Three runs (replications) were made for each example with a different random number set used for each of the three replications: See Table B-29.

Tables 4-1 and 4-2 summarize the characteristics of these examples while Tables 4-3 through 4-5 summarize the predictive results.

The first column of each table lists the Random Number (RN) set that was used and the second column provides an abbreviation of the file name that includes the 15-minute volumes that were input into CORSIM. Considering the first row, random number set 1 was used and the 15-minute input volumes were 625 vph, 700 vph, 650 vph and 350 vph. The input volume for the last 15-minute period was always set at a relatively low value so that all residual queues would clear by the end of the one-hour analysis time frame. This ensured that all delay was accounted for.

Because of the random fluctuation in arrivals, the arrival flow rates input into CORSIM are, in almost every case, not the same as the arrival flow rates that actually enter the link. For example, the 625, 700, 650, 350 vph input flow rates associated with random number set 1 (the row 1 values) produce link entry flow rates of 640, 692, 628 and 364 vph. By the time these entering vehicle reach the back of the queue, the arrival flow rates have changed once again to the 676, 688, 652, 360 vph values shown in Table 4-1. It is these arrival at BOQ (Back of

Queue) volumes that are of interest because it is these volumes that contribute directly to the formation of queues and the associated stopped delay. Arrival at BOQ volumes are also provided for the hour as a whole and for the first 45 minutes of the hour (the portion of the hour during which near or over capacity conditions exist).

Also provided in Table 4-1 are the approach capacity values for each 15-minute period; along with the capacity value for the first 45 minutes of the hour. BuckQ automatically calculates the capacity values by applying the methodology described in Chapter 16, Appendix H of the Highway Capacity Manual [4] to traffic stream information obtained from CORSIM. In order to calculate the capacity our analysis procedure determines, for each 15-minute period, the needed intermediate variables such as queue discharge Headway (H), Start-Up Lost Time (SULT), and effective green time (g). The Extension of Effective Green (EEG) is determined for the first 45-minutes of the hour by minimizing the sum of the squared deviations between the cycle-by-cycle capacity values calculated using the Highway Capacity Manual procedure and actual cycle-by-cycle thruput. A review of Table 4-1 indicates that the calculated capacity values show considerable variation. This is not surprising when one considers the substantial degree of variation in driver behavior that has been incorporated into CORSIM, including variations in driver aggressiveness associated with departing the queue (which affects both SULT and H) and in making use of the yellow and all red change interval time (which affects the EEG). All drivers do not behave the same and CORSIM correctly recognizes this.

Volume-to-capacity ratios are calculated for each 15-minute period and for the first 45 minutes of the hour. These values are also provided in Table 4-1. For individual 15-minute periods, the v/c ratio varies from a low of 0.92 (RN set 2 for file 625_700_650_350) to a high of 1.24 (RN set 1 for file 725_700_700_350). For the first 45 minutes of the hour, the v/c ratio

varies from a low of 1.02 (RN set 2 for file 625_700_650_350) to a high of 1.12 (RN set 1, 2 or 3 for file 725_700_700_350).

A review of the average values shows that, for the first 45-minutes, both volume and v/c ratio steadily increase as one moves down the table, while capacity remains constant at 644 vph. The average volume increases from a low of 664 vph to a high of 722 vph while the average v/c ratio increases from 1.03 to 1.12

The first section of Table 4-2 summarizes various values used for capacity analysis, including cycle length, green time, queue discharge headway, saturation flow rate, and start-up lost time. Our analysis procedure calculates these values on both a cycle-by-cycle basis and a 15-minute period basis - as well as for the entire hour, but only the hourly values are presented here. As the v/c ratio increases, the amount of green time (G) increases to its maximum setting of 38 seconds, and the cycle length (C) increases to its maximum value of 120 seconds. This makes sense for an actuated approach. The extension of effective green, start-up lost time, queue discharge headway, and saturation flow rate all remain about the same as the v/c ratio increases, which also seems reasonable. The overall average queue discharge headway of 1.81 seconds is very close to the 1.80 CORSIM input value. However, the overall average start-up lost time value of 2.7 seconds is significantly greater than the 2.0 second mean start-up delay input into CORSIM. The difference is due to a definition inconsistency. CORSIM only applies the mean start-up delay to the first vehicle, adding additional delay (of about 0.7 seconds) to subsequent vehicles. In other words, CORSIM's mean start-up delay is not the same as start-up lost time.

The next section of Table 4-2 provides a quality control check on the results for actual stopped delay and control delay during the one hour analysis time frame. This check is made by comparing the values obtained from our analysis procedure to similar values found in the

CORSIM output report. Considering the delay definitions used in CORSIM, we would expect CORSIM Stop Time to approximately equal the actual stopped delay obtained from our procedure, and we would expect CORSIM Queue Delay to be slightly greater than the actual stopped delay. This is true in every case. We would also expect CORSIM Delay Time to approximately equal the actual control delay obtained from our procedure, and we would expect CORSIM control delay to be slightly less than the actual control delay. Once again, this is true in every case. As we might expect, the amount of both stopped delay and control delay increases as the v/c ratio increases.

The final section of Table 4-2 summarizes, for the Poisson distribution, the chi-square goodness-of-fit test results based on 20-second arrival intervals. During only one of the forty-eight 15-minute periods examined (2% of the time) did the test statistic exceed the 95th percentile reference statistic. CORSIM 6.0 appears to be generating truly random arrivals. It is important to use 20-second arrival intervals when conducting this test since the use of longer intervals reduces the number of available data points while the use of shorter intervals can give rise to truncation effects that distort the results. The truncation effects arise because unsafe headways of less than 1.5 seconds are rarely encountered within the CORSIM traffic stream.

Queue Prediction

Table 4-3 summarizes the queue prediction results for our analysis procedure as compared to actual queues. Comparisons are made of average queue length, maximum queue length, maximum back of queue position, and 98th percentile back of queue position. Figure 4-14 depicts actual queue length as a function of v/c ratio while Figures 4-15 through 4-17 compare actual and predicted queue results for the average queue length, the maximum queue length, and the 98th percentile back of queue, respectively. Figures 4-14 through 4-17 all demonstrate that, as might be expected, queue length tends to increase linearly as a function of the v/c ratio. A

review of Figures 4-15 through 4-17 also indicates that our procedure is fairly good at predicting all of these queues, with the amount of error increasing somewhat as the v/c ratio increases. The procedures contained in the Highway Capacity Manual, provide information on the 98th percentile back of queue. A review of Figure 4-17 indicates that the HCM procedures grossly overestimate the 98th percentile back of queue.

Also provided in Table 4-3 is information on the number of (liberal) phase failures, the percentage of cycles experiencing a phase failure, and the number of vehicle re-queues. Phase failures are defined in relation to the cycle and, as such, are insensitive to the number of vehicles involved. For example, a phase failure occurs for a given cycle if only one vehicle is forced to re-queue, or if 100 vehicles are forced to re-queue. For this reason, the number of vehicle re-queues is a much better indicator of the extent of congestion than the number of phase failures. Figure 4-18 demonstrates that the number of vehicle re-queues tends to increase linearly as a function of v/c ratio.

Stopped Delay Prediction

Table 4-4 summarizes the stopped delay prediction results for our analysis procedure as compared to actual stopped delay. Figure 4-19 indicates that the procedure does a pretty good job of predicting stopped delay over all v/c ratios.

Figure 4-20 shows the relative contribution of each segment of the prediction methodology. For the examples under consideration, visible delay makes-up about 60% of total stopped delay when the v/c ratio is near 1.02 but only 20% of total stopped delay when the v/c ratio climbs to 1.12 This clearly demonstrates the need for this predictive procedure, at least for the rather typical case where the cycle length is 120 seconds and the field of view is limited to 12 vehicles. The first step in the predictive process uses an estimated arrival rate based on vehicles entering the field of view to predict the non-visible queue. This alteration increases the

percentage of captured stopped delay to about 80% when the v/c is near 1.02 and to about 30% when the v/c is near 1.12. The results become reasonable for relatively low over-saturated v/c ratios but not for the higher ratios. The second step in the predictive process uses an adjusted arrival rate obtained from a power function adjustment that increases the estimated arrival rate based on the number of adjacent blind periods. This alteration increases the percentage of captured stopped delay to about 115% when the v/c is near 1.02 and to about 65% when the v/c is near 1.12. The results are still reasonable for relatively low over-saturated v/c ratios, and are greatly improved for the higher ratios, but the error for the higher ratios is still quite significant. The third step in the predictive process adjusts the non-visible queue length and associated delay due to queue propagation. This alteration has little or no affect on the percentage of captured stopped delay when the v/c is close to one but increases the percentage of captured stop delay to about 90% when the v/c is high. The results are now reasonable over all v/c ratios although a slight upward bias of about 15% exists near the lower oversaturated v/c ratios and a slight downward bias of about 10% exists near the higher v/c ratios. A tremendous improvement in stopped delay estimation is clearly provided by our procedure. Figure 4-21 provides another way of visualizing the final predictive results.

The maximum individual over-estimation of delay is 27% and the maximum individual under-estimation is 17.5%. If the results are averaged over the three random number replicates, as is documented at the bottom of 4-4, the maximum over-estimation is 13% and the maximum under-estimation is 11%.

If we graph the sum of the Adjacent Blind Period Counter (ABPC) against stopped delay (either actual or predicted) as shown in Figure 4-22, a strong linear relationship exists. This

provides rather strong support for our use of the ABPC as the explanatory variable in our arrival rate adjustment process.

Control Delay Prediction

Table 4-5 summarizes the control delay prediction results as compared to actual control delay. Figure 4-23 indicates that the analysis procedure also does a reasonably good job of predicting control delay over all v/c ratios, even if we use a constant ratio of 1.3 to convert our predicted stopped delay into predicted control delay. This conversion factor actually varies somewhat by v/c ratio as shown in Figure 4-24. (Previous work has demonstrated that this factor also varies by cycle length; but that is not of concern here since we have restricted our analysis to a single cycle length.) Also included in Figure 4-23 is control delay as predicted by HCM procedures. The HCM procedures tend to over-predict control delay for the lower over-saturated v/c ratios.

Figures 4-25 and 4-26 provide two other ways of visualizing these comparisons between actual control delay, predicted control delay, and HCM calculated control delay.

Control delay is composed of stopped delay, acceleration/deceleration delay, and queue move-up delay. As shown in Figure 4-27, the percentage of stopped delay for our example remains relatively constant at about 80% of the control delay. This is consistent with the fact that the control delay/stopped delay ratio does not change much as the v/c ratio increases. However, the percentage of queue move-up delay increases dramatically (more than doubles) as the v/c ratio increases and the percentage of acceleration/deceleration delay falls correspondingly. Recurrent cycle failures and extensive re-queuing associated with high v/c ratios produces this steady and dramatic increase in queue move-up delay. Figure 4-28 provides factors that convert “stopped delay plus queue move-up delay” to control delay. A review of this

figure reveals that there is much more variation in this new ratio than with a ratio based only on stopped delay.

Variability Considerations

To investigate the degree of variability associated with the actual cumulative stopped delay, and with the predicted stopped delay, ten replicate runs were made for the 700_725_625_350 volume pattern using the sets of random number seeds found in Table B-30.

The last number in the set produces vehicle behavior variation associated with various driver aggressiveness characteristics, including driver response to the amber interval, the amount of start-up lost time experienced by the first vehicle in the queue, the discharge headway of the vehicle, and the free flow speed of the vehicle.

Table 4-6 provides a comparison between the actual 1-hour cumulative stopped delay and the predicted stopped delay. A review of the embedded graph in this table shows that the variation in the predicted stopped delay is very similar to the variation in the actual stopped delay, with only of the 10 data points (the one associated with random number set 8) exhibiting a somewhat unfavorable comparison. This similarity in variation provides some reassurance that the prediction procedure is behaving appropriately. It is also encouraging to discover that, as is shown in Table 4-6, the 95% confidence interval for the mean actual stopped delay includes the mean predicted stopped delay.

Formal statistical testing was conducted to determine whether a significant difference exists between the actual and predicted median stopped delay. The non-parametric Fisher Sign Test, which does not require a symmetrical distribution, was used to test the null hypothesis that the mean of the differences between the actual and predicted median delay is zero. Table 4-7 contains the test, which produces a p-value of about 0.11 The p-value is not significant so we cannot reject the null hypothesis that the mean of the differences is indeed zero, which reinforces

the idea that the prediction procedure does a relatively good job of estimating the total cumulative stopped delay.

Limitations to the Delay Prediction Procedure

Our analysis procedure includes a new technique for predicting delay on a signalized intersection approach under conditions of limited information. Although the usefulness of the technique is evident, limitations on the use of the technique should be understood. These limitations include the following:

1. As the size of the field of view decreases, the accuracy of the technique also decreases. Testing to date has concentrated on a field of view of 12 vehicles with additional runs made at a field of view of 8 vehicles. Reasonable results are obtained with these fields of view up to a v/c ratio of about 1.12 for the over-saturated periods. More testing is needed to determine the maximum v/c ratio that can be accommodated with smaller fields of view.

2. The current delay prediction technique can produce rather inaccurate delay forecasts if "sleepers" are present at critical points in the non-visible queue. A "sleeper" is defined as a motorist that does not exhibit normal car-following behavior within the queue; leaving a large gap between his or her vehicle and the preceding vehicle in the queue. This type of lethargic driver behavior can be caused by in-vehicle distractions or by simple daydreaming. Under the current analysis methodology, the abnormally large gap between vehicles caused by sleepers can result in a false conclusion that the end of the queue has been reached. This causes the adjacent blind period counter to be lower than desired which results in a correspondingly low adjusted arrival rate. The end result is an underestimation of delay.

3. Our analysis procedure is essentially a queue prediction technique that uses predicted queue length to calculate expected stopped delay. Consequently, by its very nature, the procedure is relegated to directly predicting stopped delay, not control delay. The emphasis on stopped delay makes sense when one considers the limited information made available to the program. The program assumes no knowledge of various items important in the direct calculation of control delay; including vehicle free flow speeds and delay associated with both deceleration and acceleration - most of which occurs outside the field of view. Changing stopped delay to control delay requires the application of a delay ratio. Typical delay ratios (such as the commonly used 1.30 value) will need to be applied and there will be some inherent error in this factoring process.

4. If a motorist joins the queue and experiences delay but then, prior to entering the field of view, becomes impatient and leaves the queue (known in the queuing literature as "reneging"), the delay experienced by this motorist will not be accounted for. Any

"delay" associated with motorists that decided not to join the queue due to its excessive length (known in the literature as "balking") would also not be accounted for.

5. The research to date has concentrated on random arrivals at an isolated intersection. Some initial experimentation was conducted with platooned arrivals and, based on that work, it is clear that the delay situation can change quite a bit depending on the relative offsets of the upstream intersection and the intersection under study. This platoon progression effect is well documented in the literature. Consequently, the analysis procedure is less suitable for use on coordinated approaches, especially during under-saturated or near-saturated conditions. For over-saturated conditions, platoon progression effects on coordinated approaches tend to be minimized since all approaching vehicle are forced to join the queue. The analysis procedure should perform well under these conditions.

6. Work completed to date is based on a single micro-simulation tool and is subject to all limitations and characteristics of the CORSIM software.

A final drawback is that the analysis procedure is still in the form of a research tool that is oriented towards evaluating simulation runs. Converting the procedure to a practical engineering tool that can be field implemented at a real intersection is an important extension that will require additional effort.

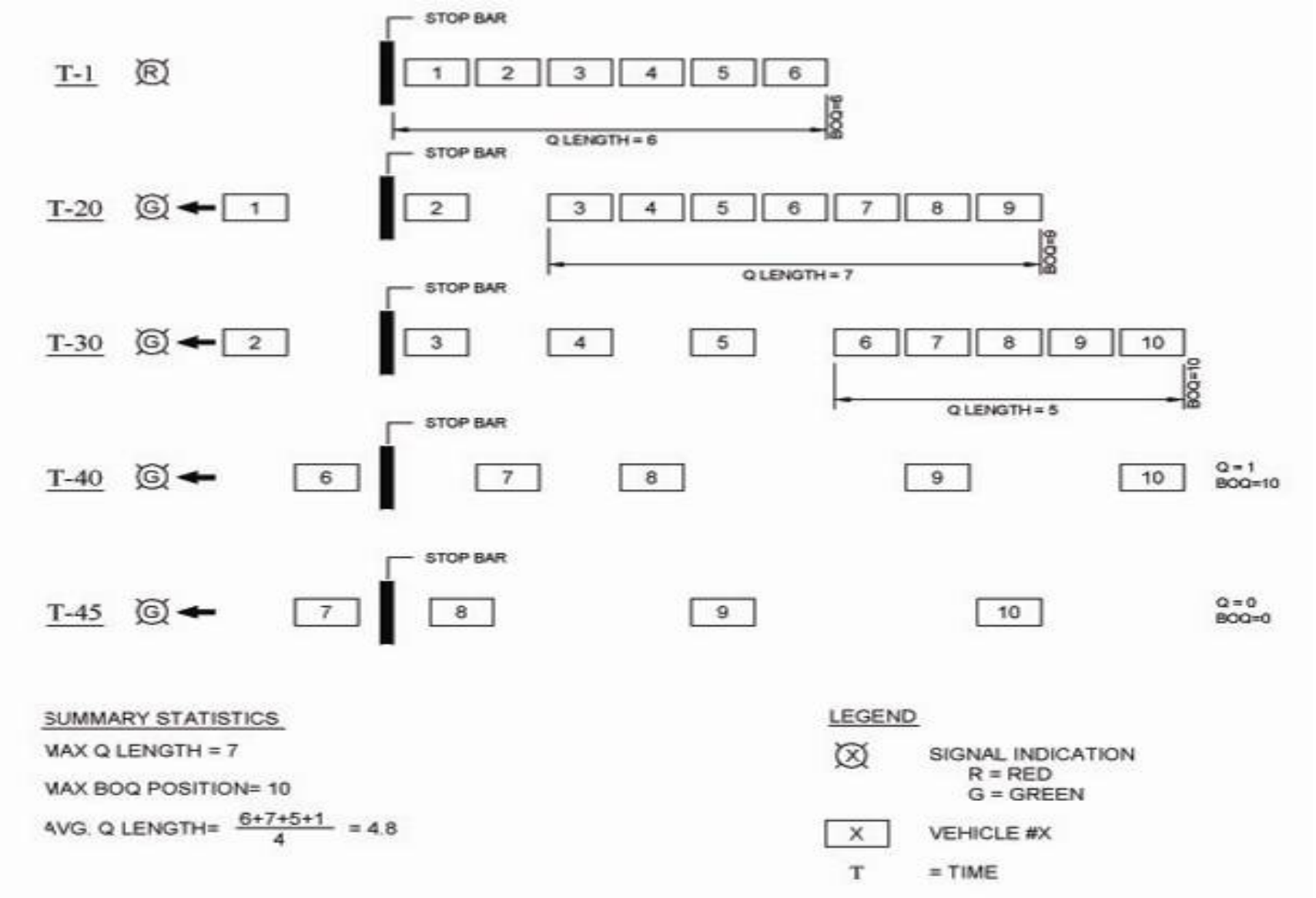

Figure 4-1. Queue relationships

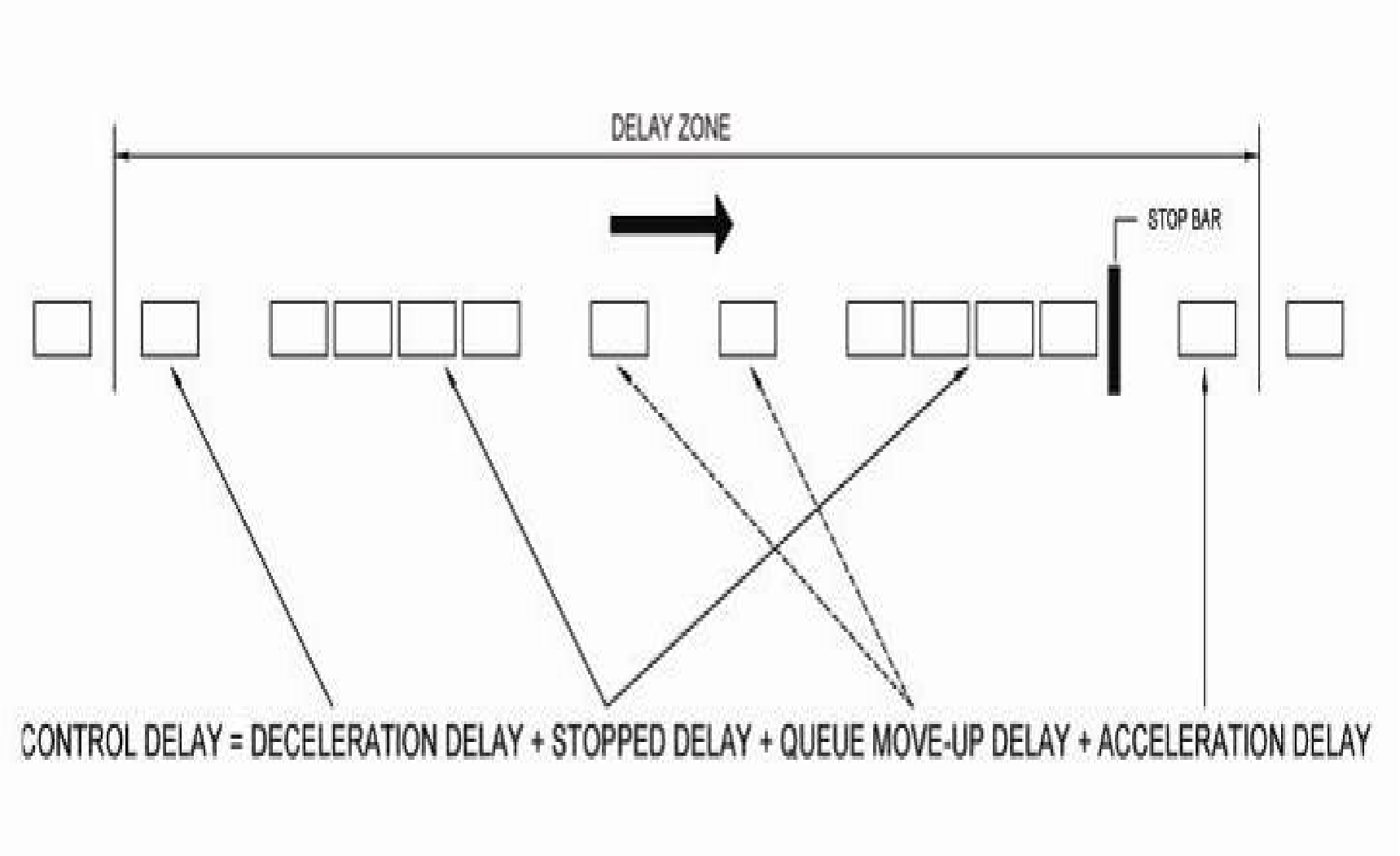

Figure 4-2. Signalized intersection delay components

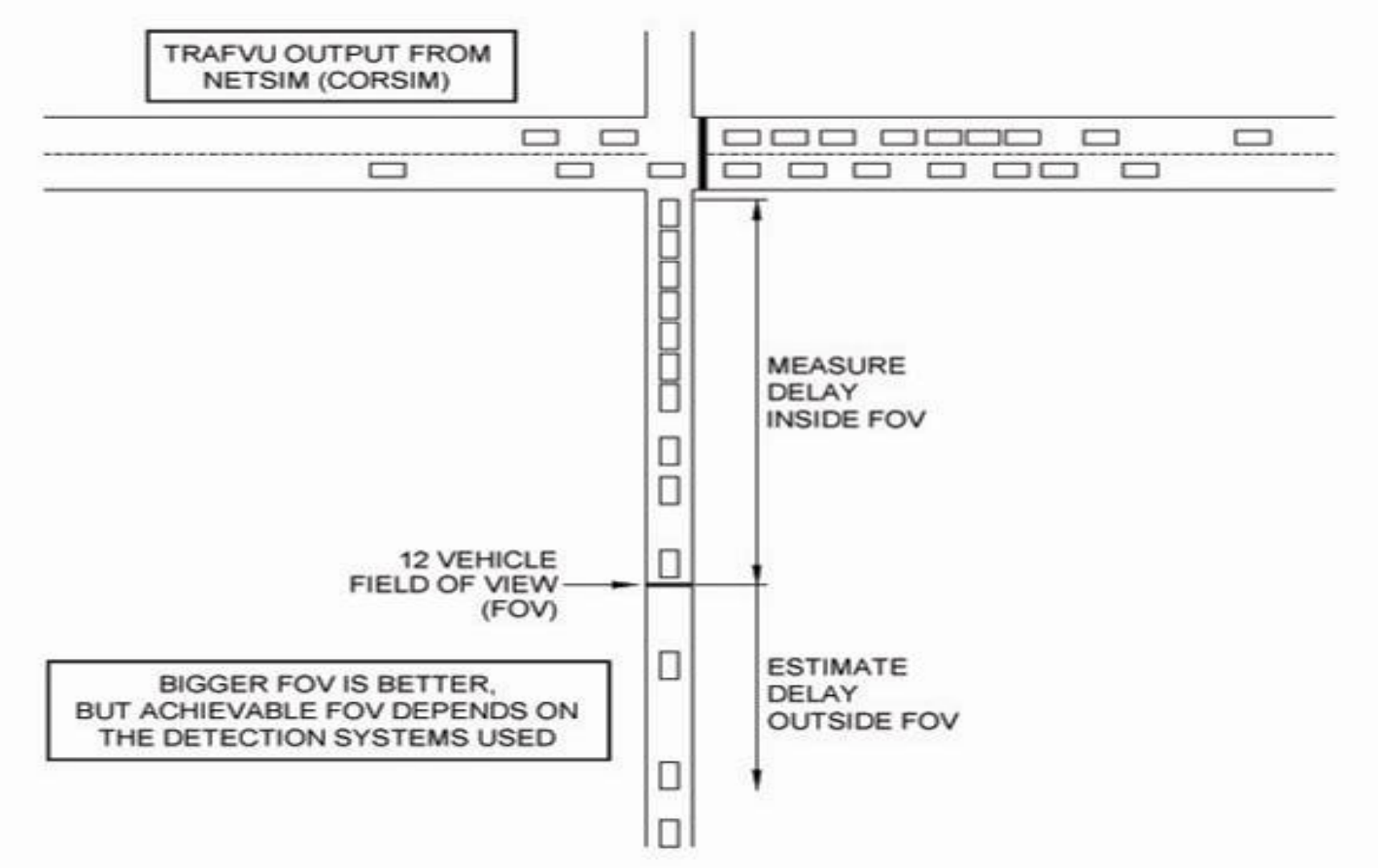

Figure 4-3. Measured versus estimated delay

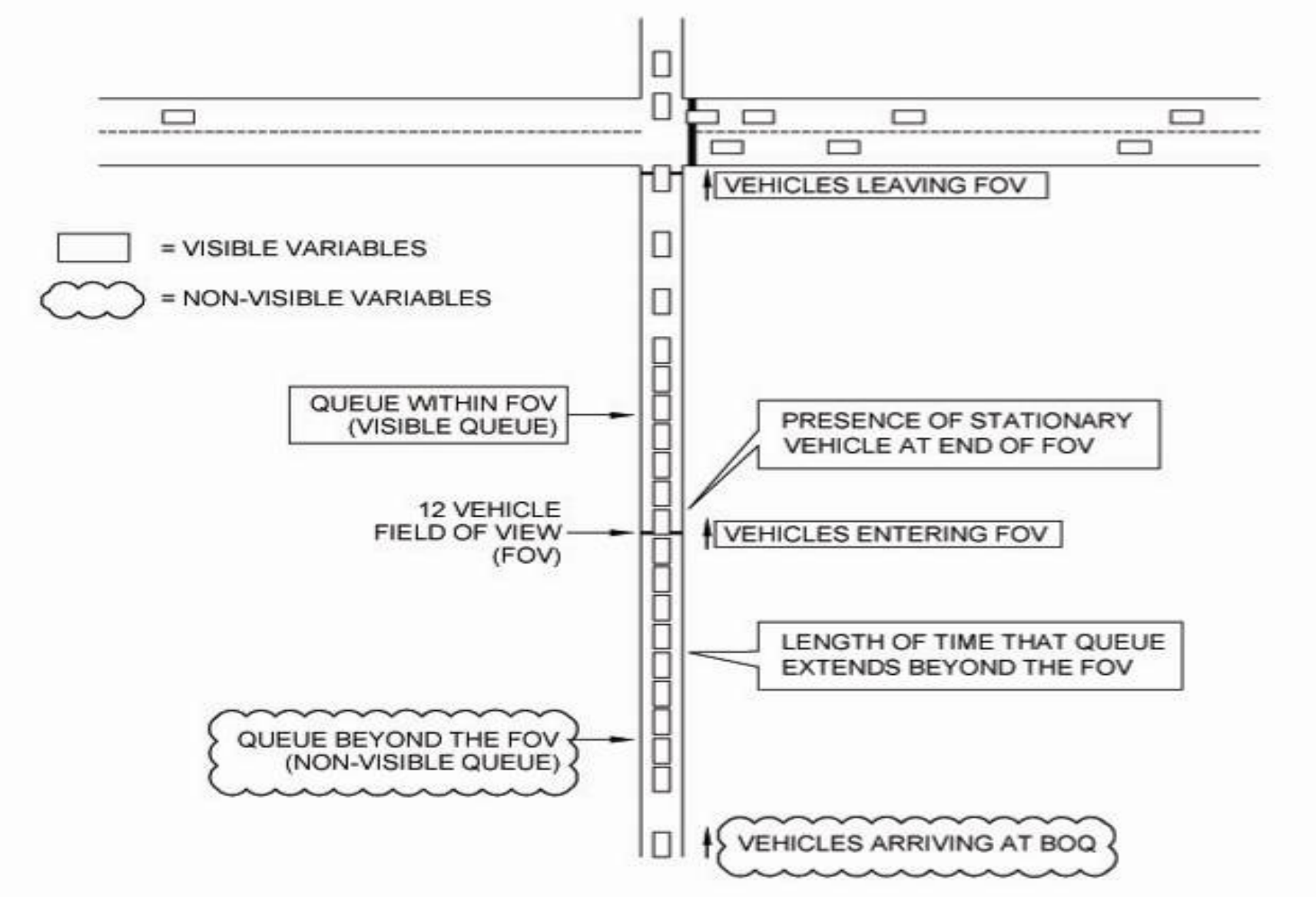

Figure 4-4. Visible and non-visible variables

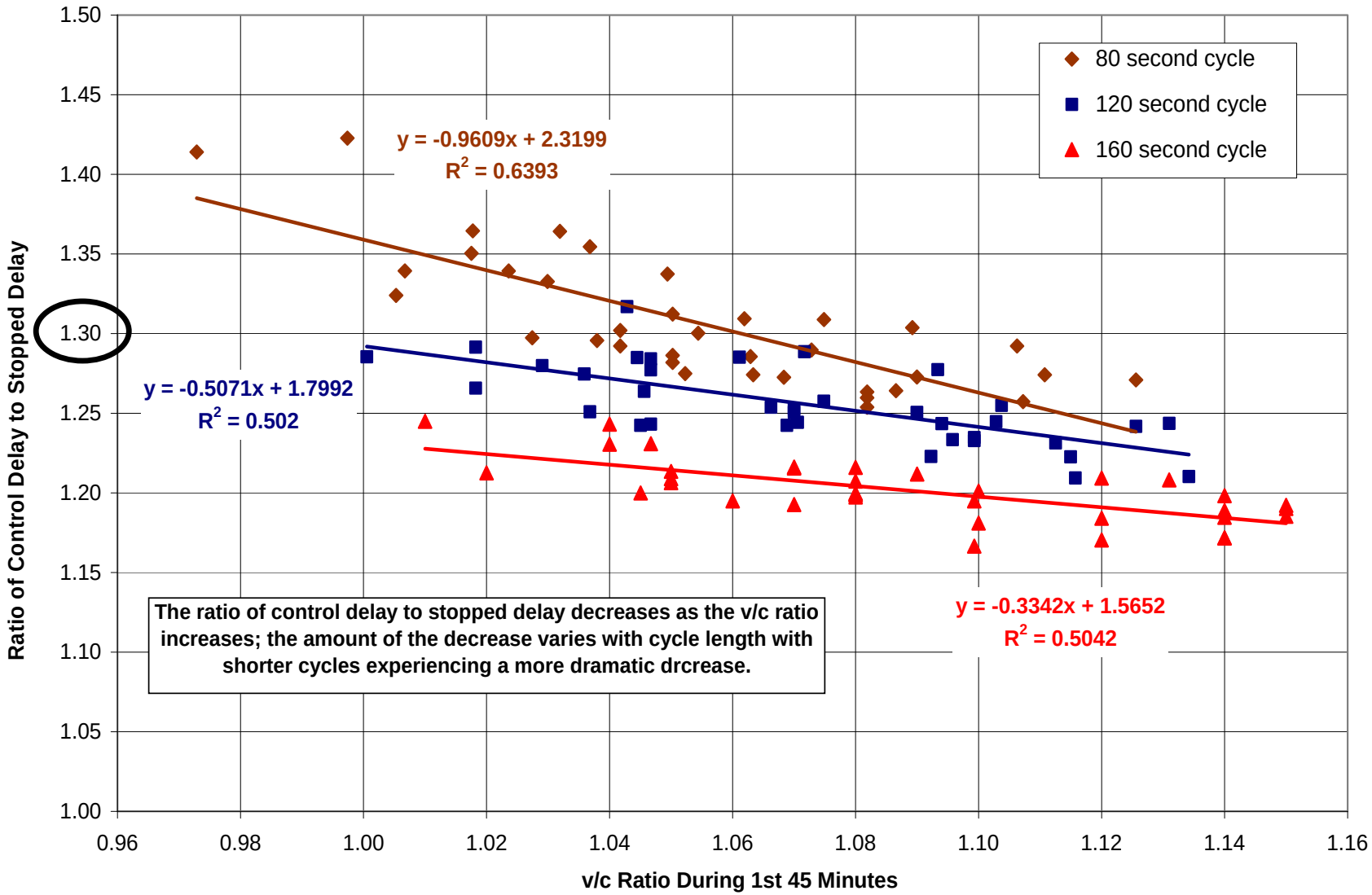

Figure 4-5. Relationship between v/c ratio and ratio of control delay to stopped delay

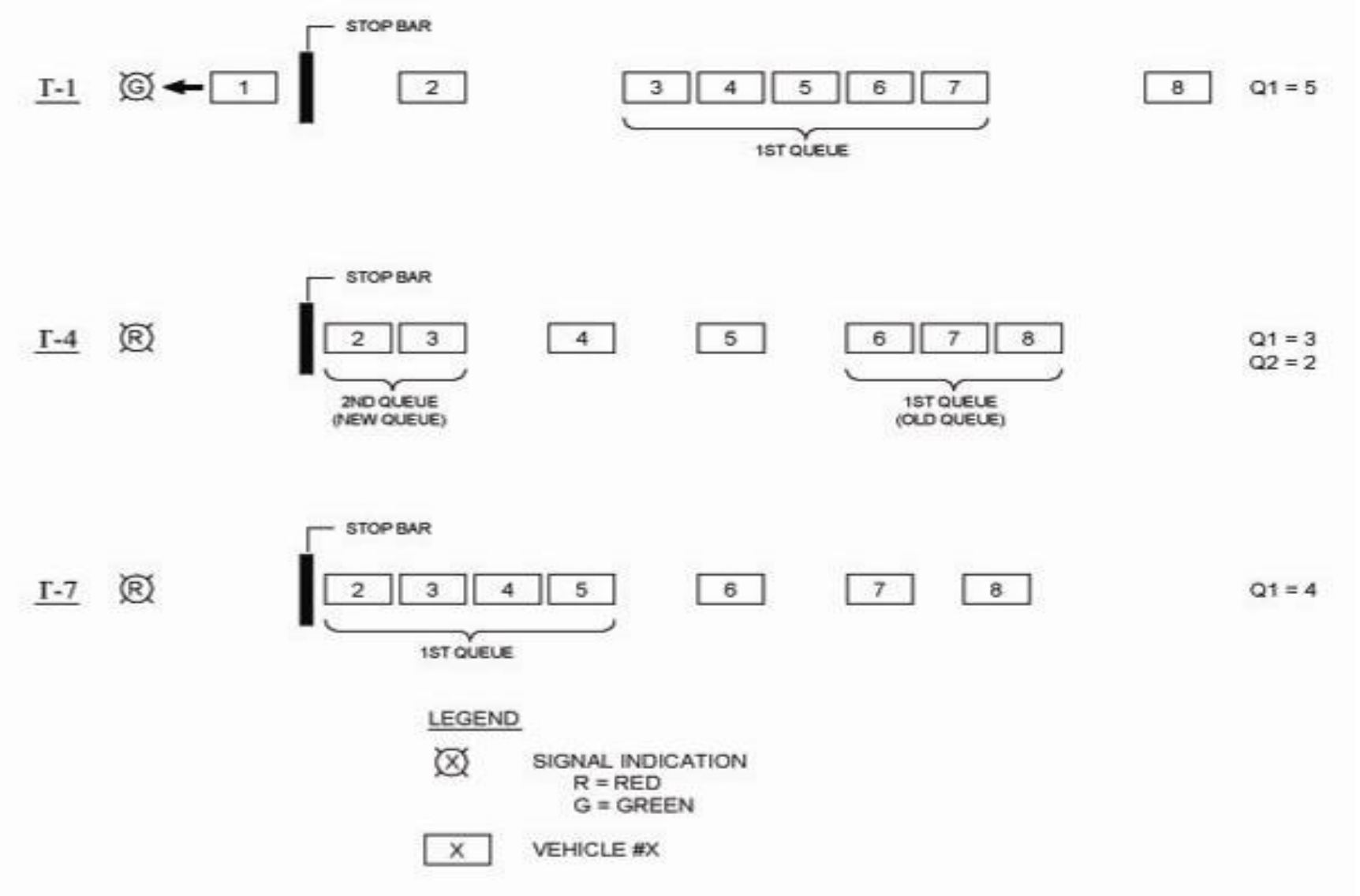

Figure 4-6. Re-queuing that results in simultaneous queues

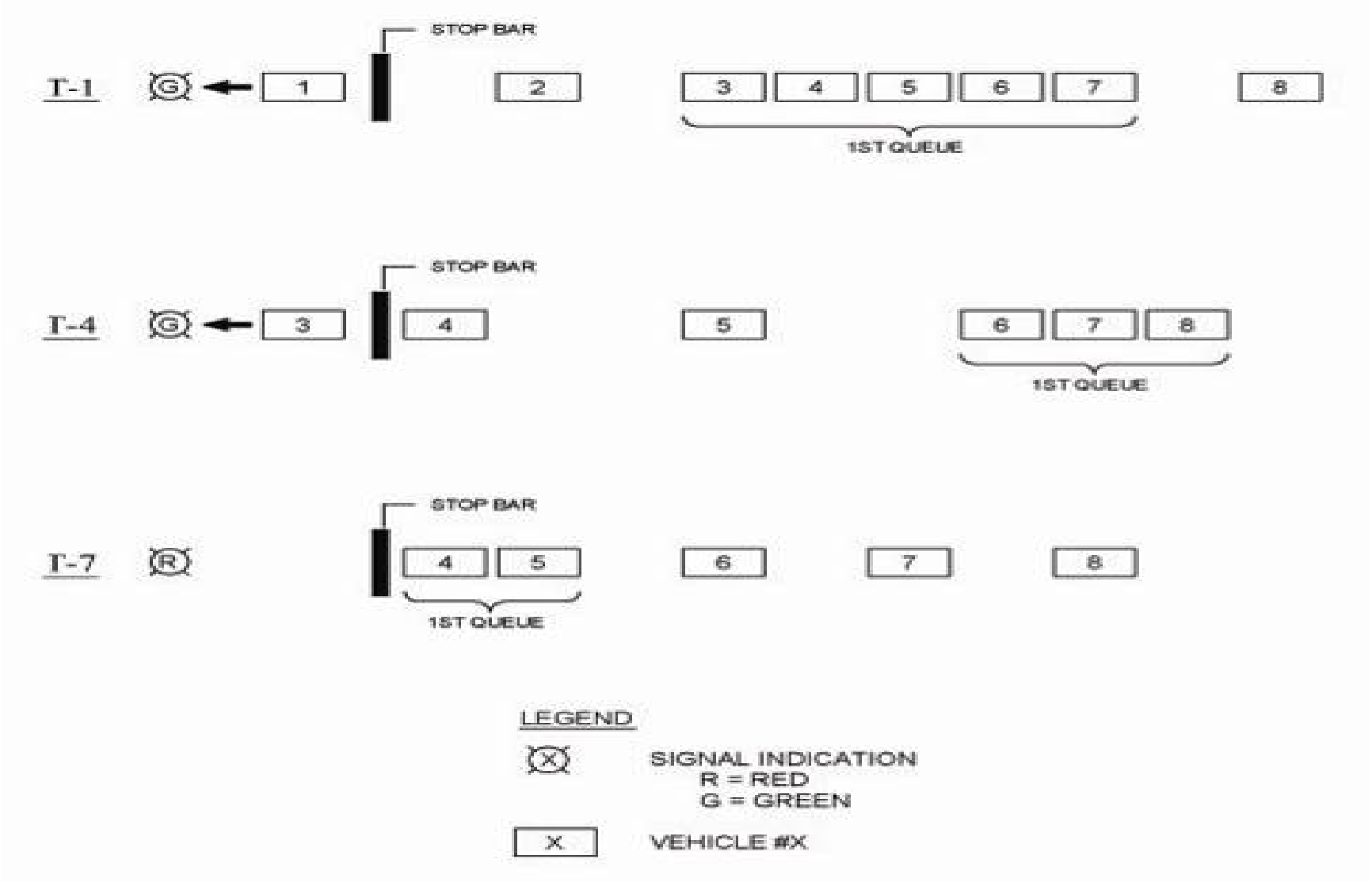

Figure 4-7. Re-queuing that does not result in simultaneous queues

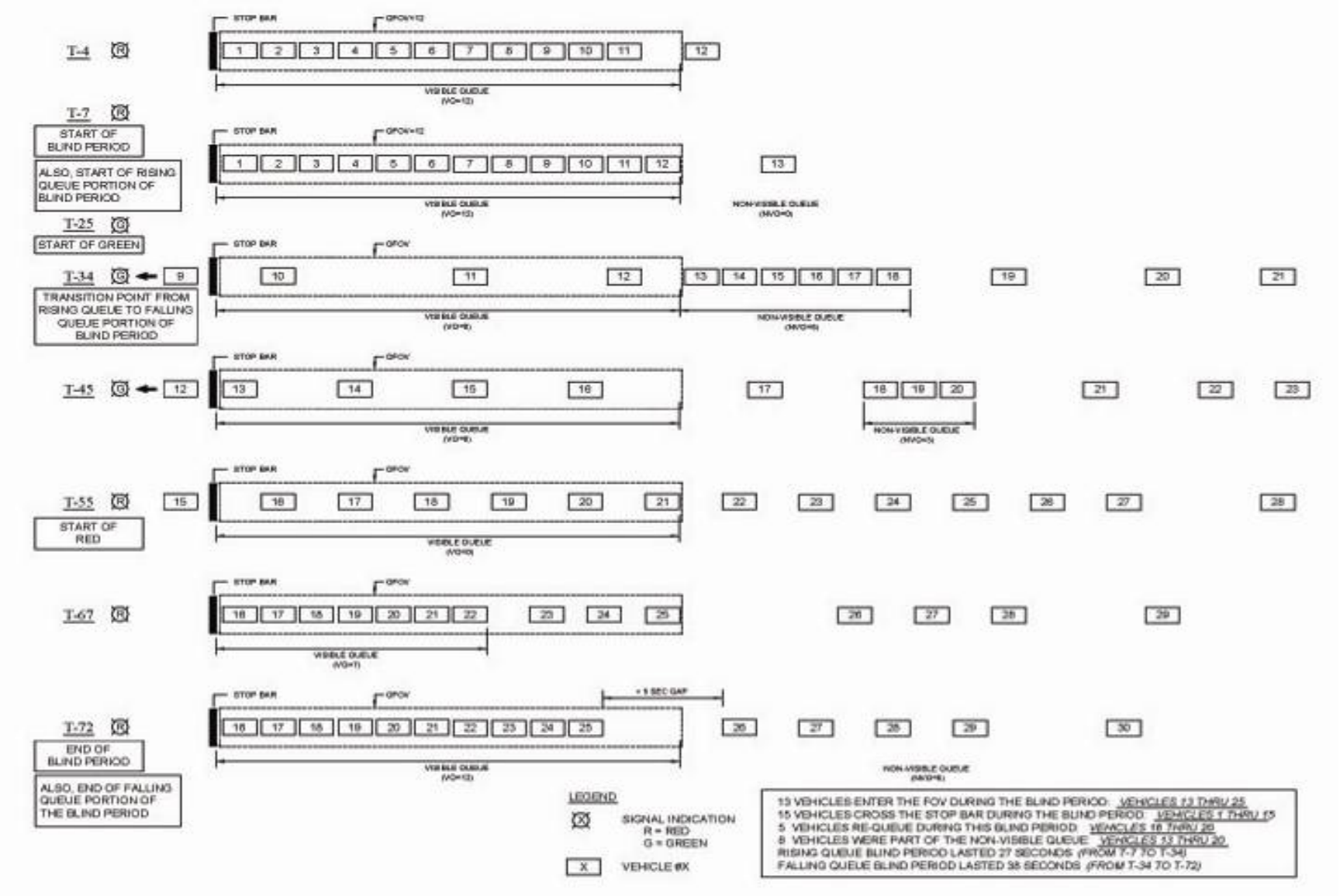

Figure 4-8. Example of a blind period

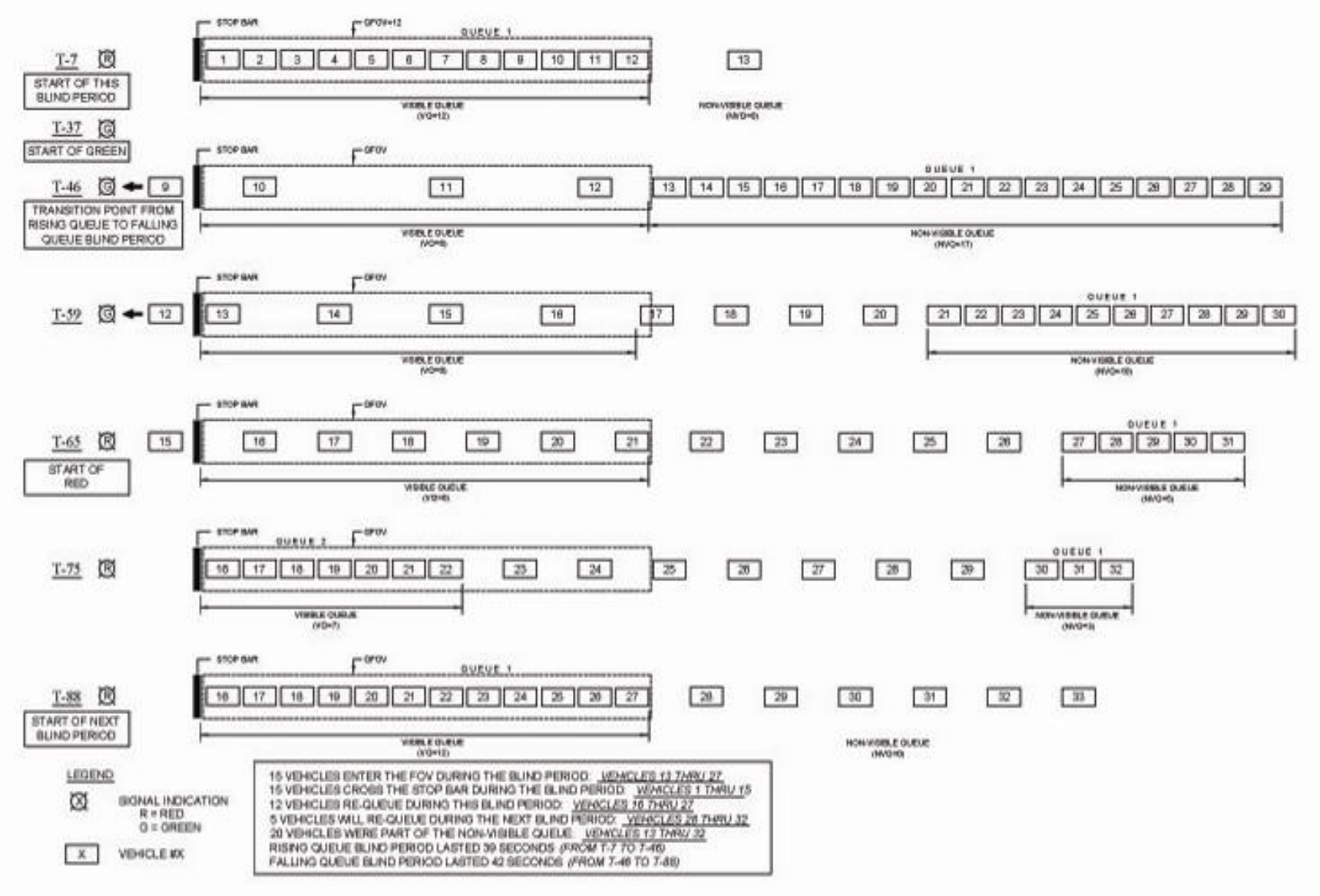

Figure 4-9. Example of adjacent blind periods

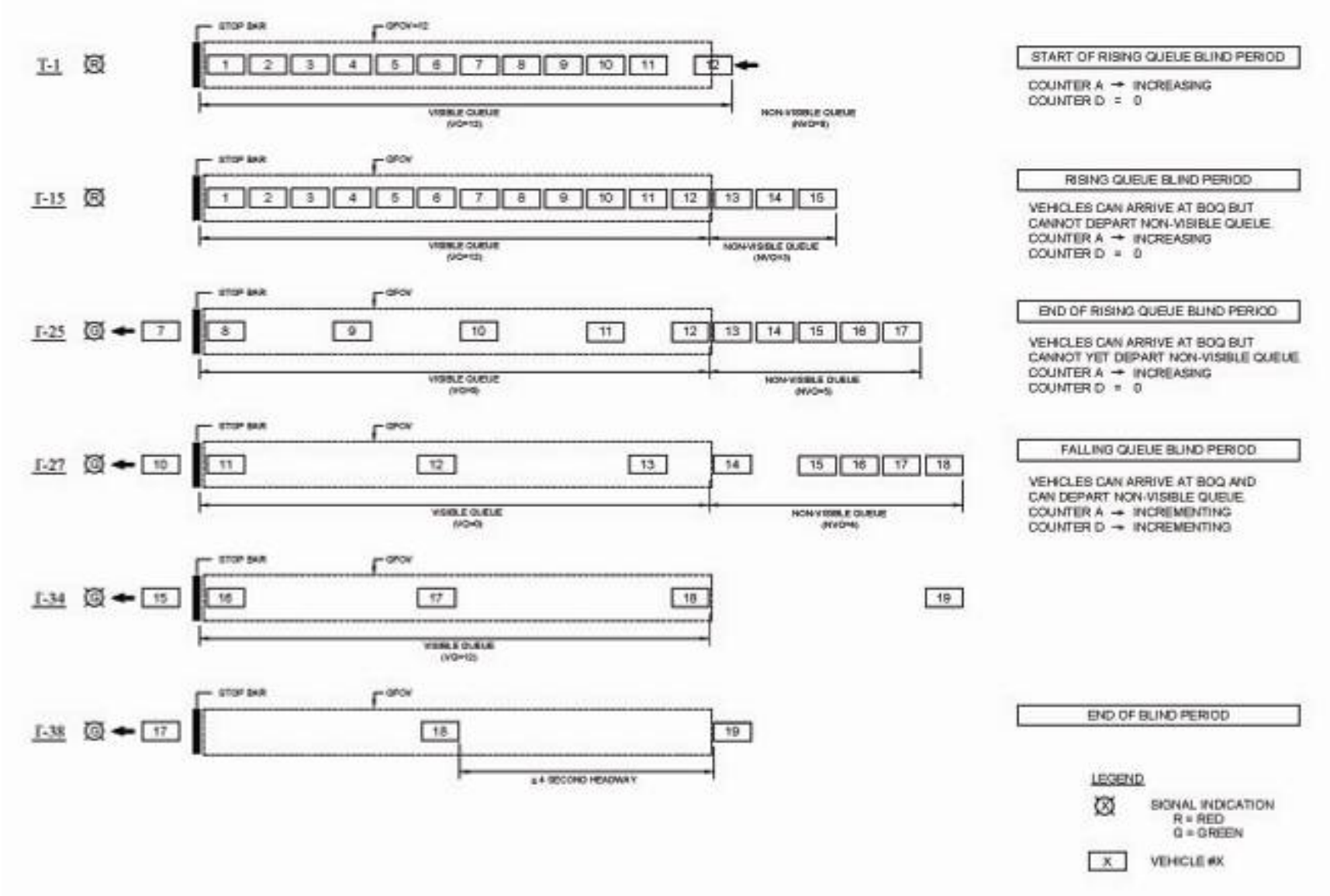

Figure 4-10. Counters and queue status

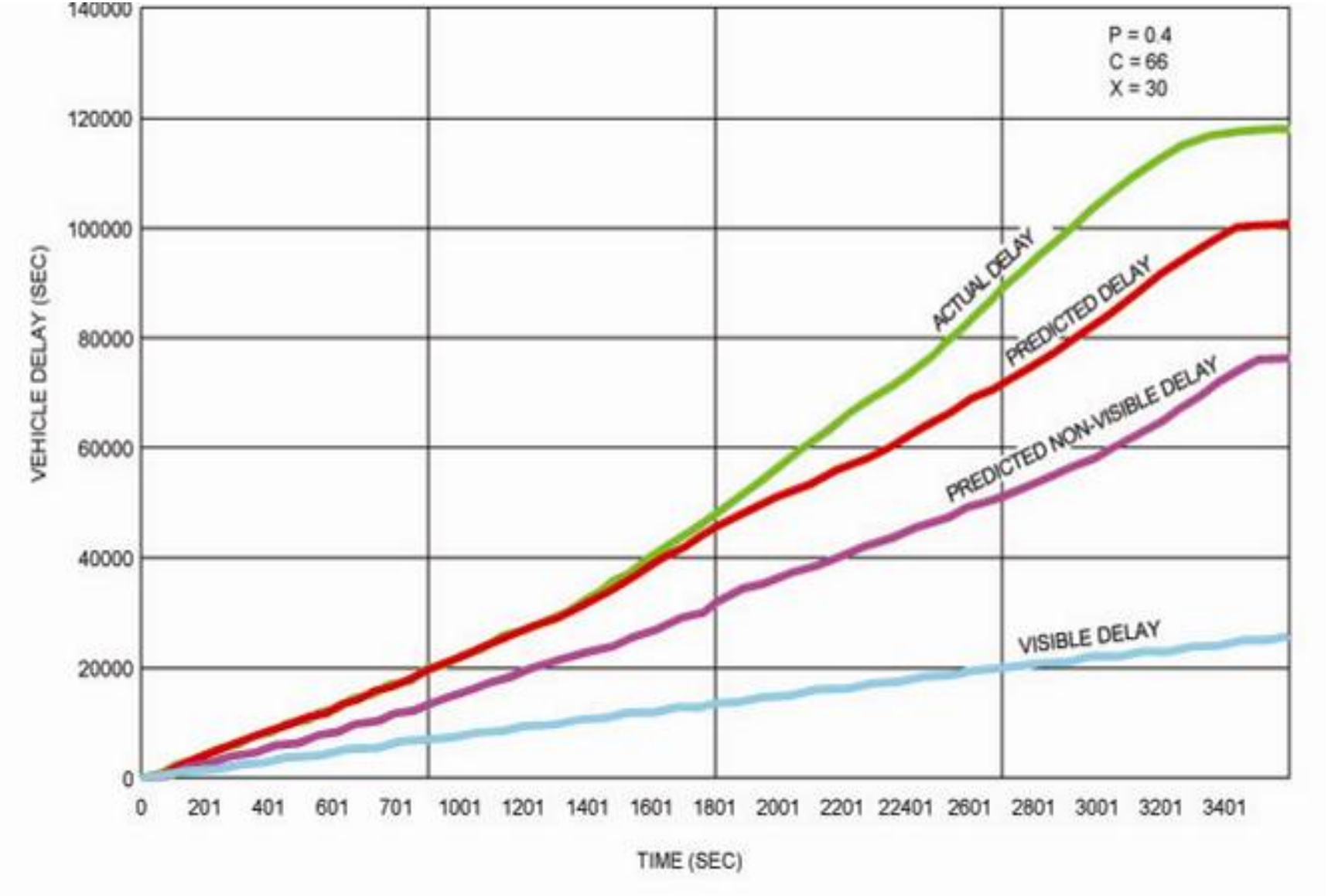

Figure 4-11. Base case for P, C and X; stopped delay comparison

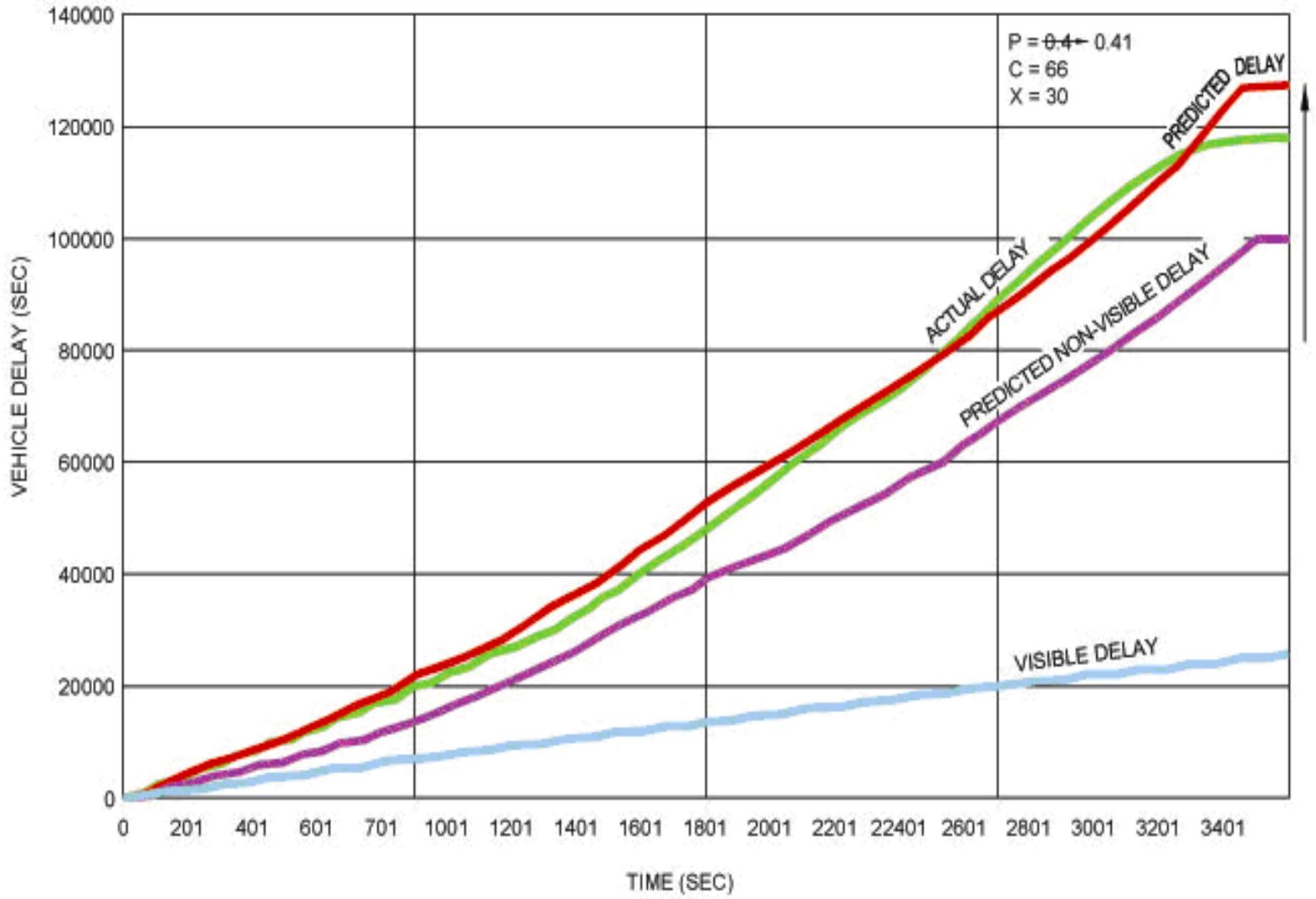

Figure 4-12. Effect of increasing the power constant on stopped delay comparison

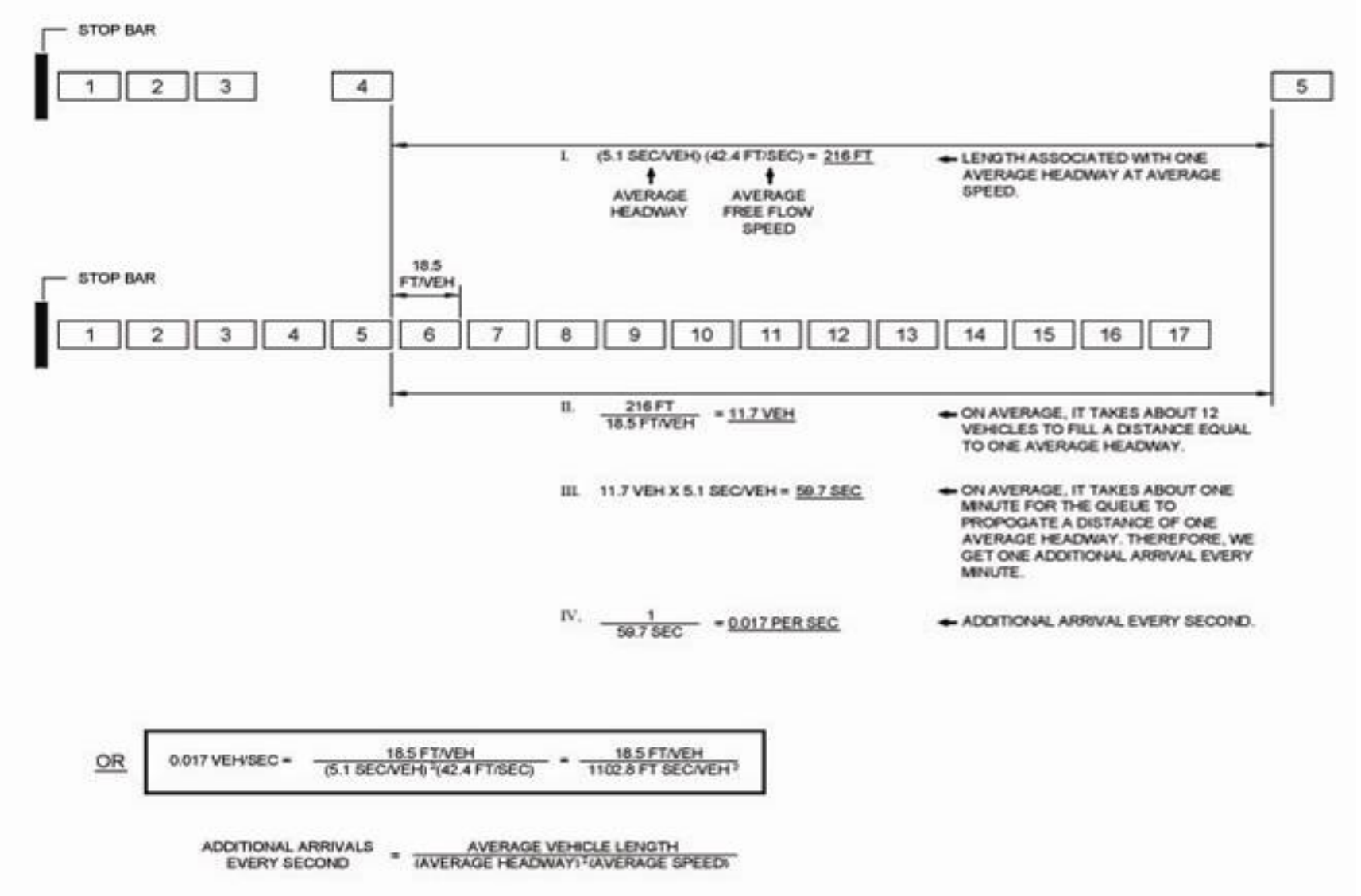

Figure 4-13. Queue propagation example

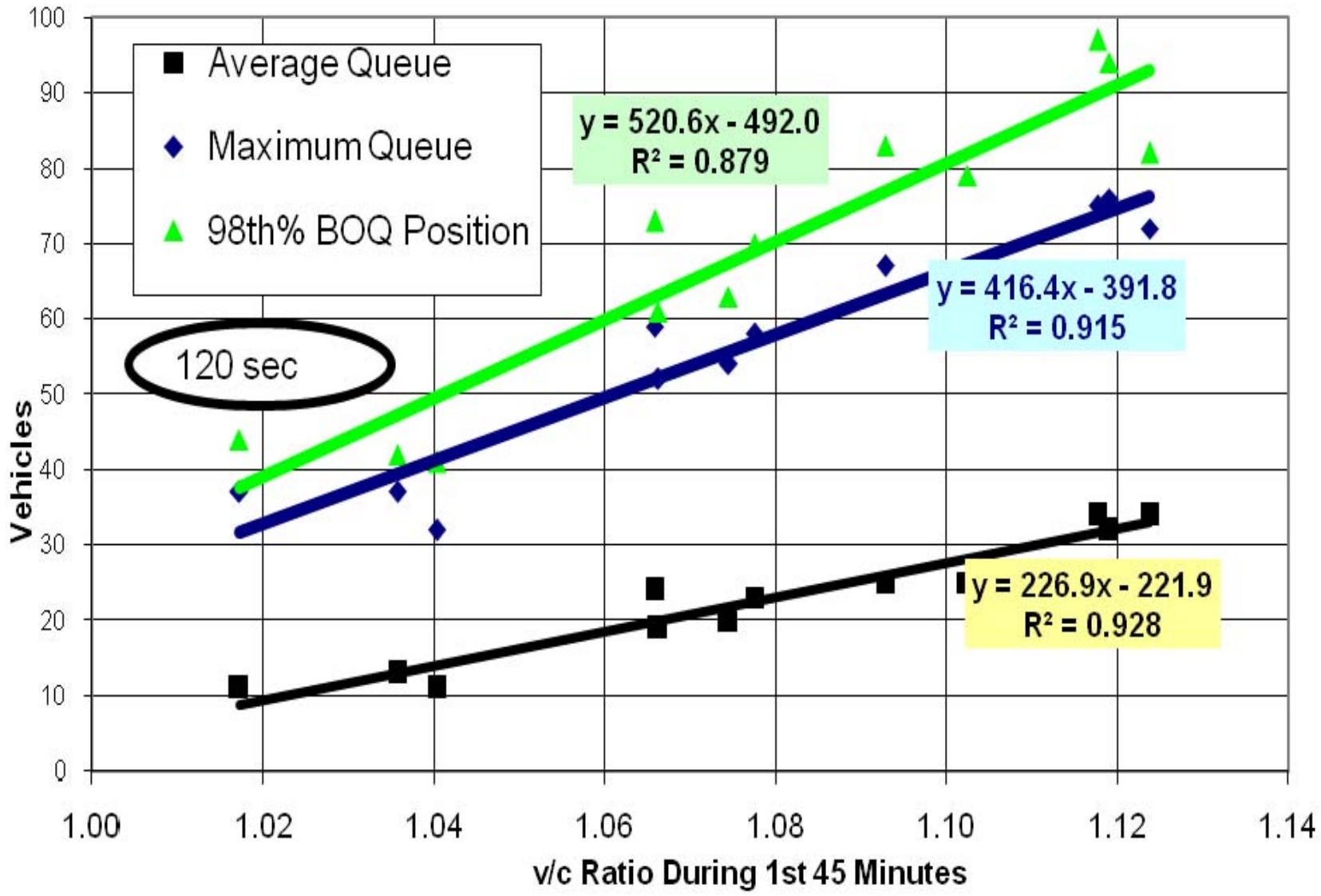

Figure 4-14. Actual vehicle queues

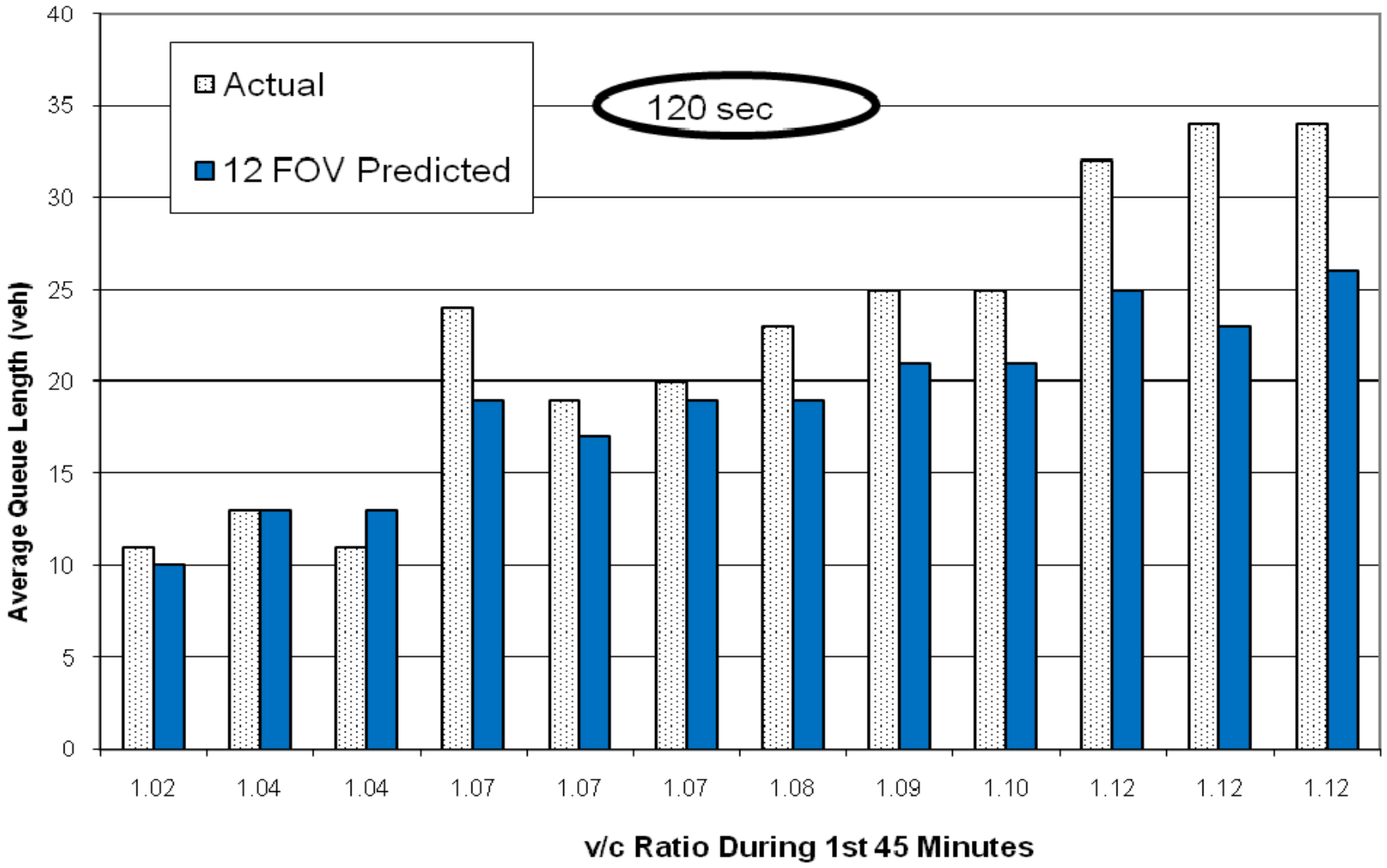

Figure 4-15. Average queue length comparison

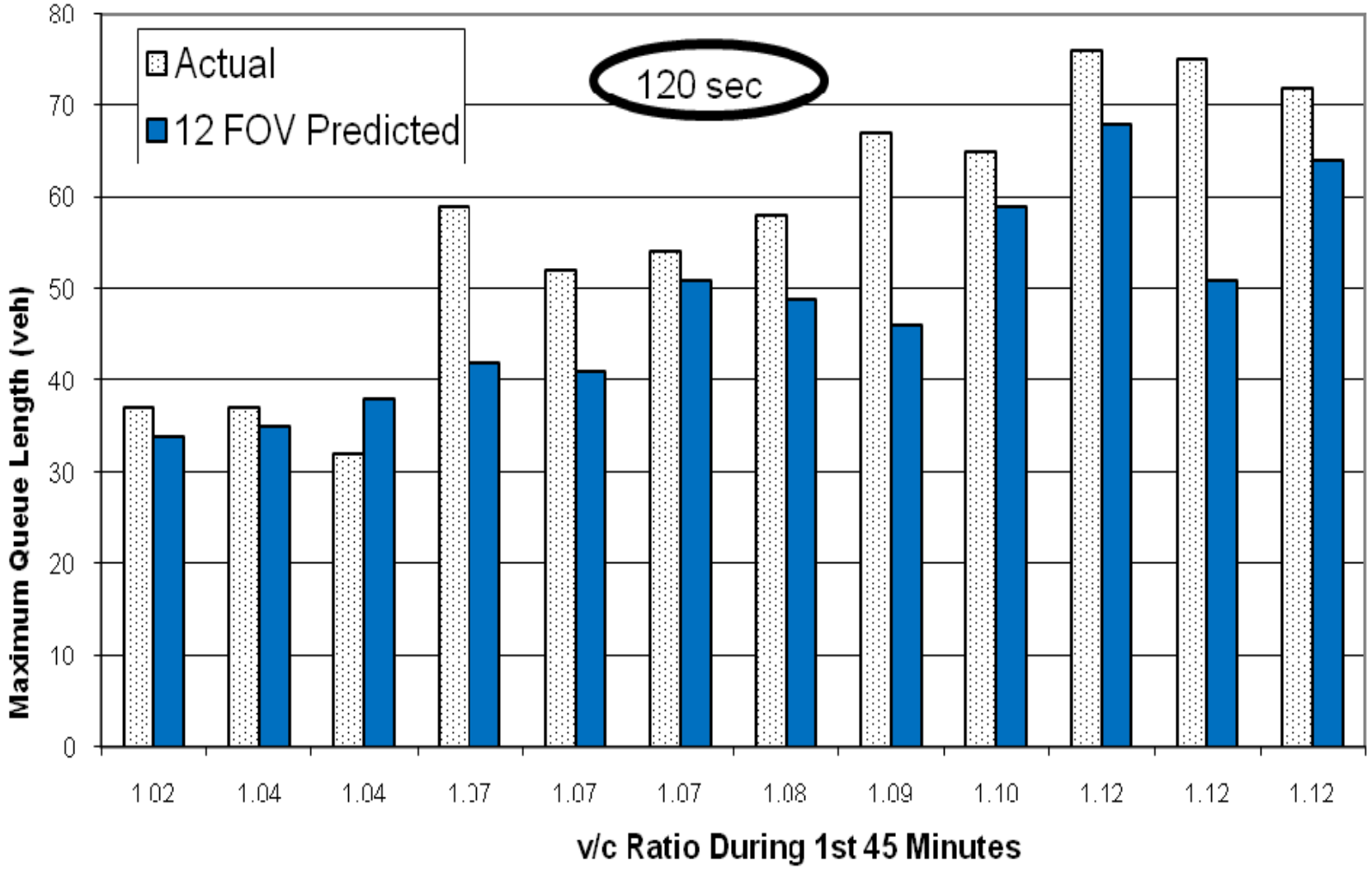

Figure 4-16. Maximum queue length comparison

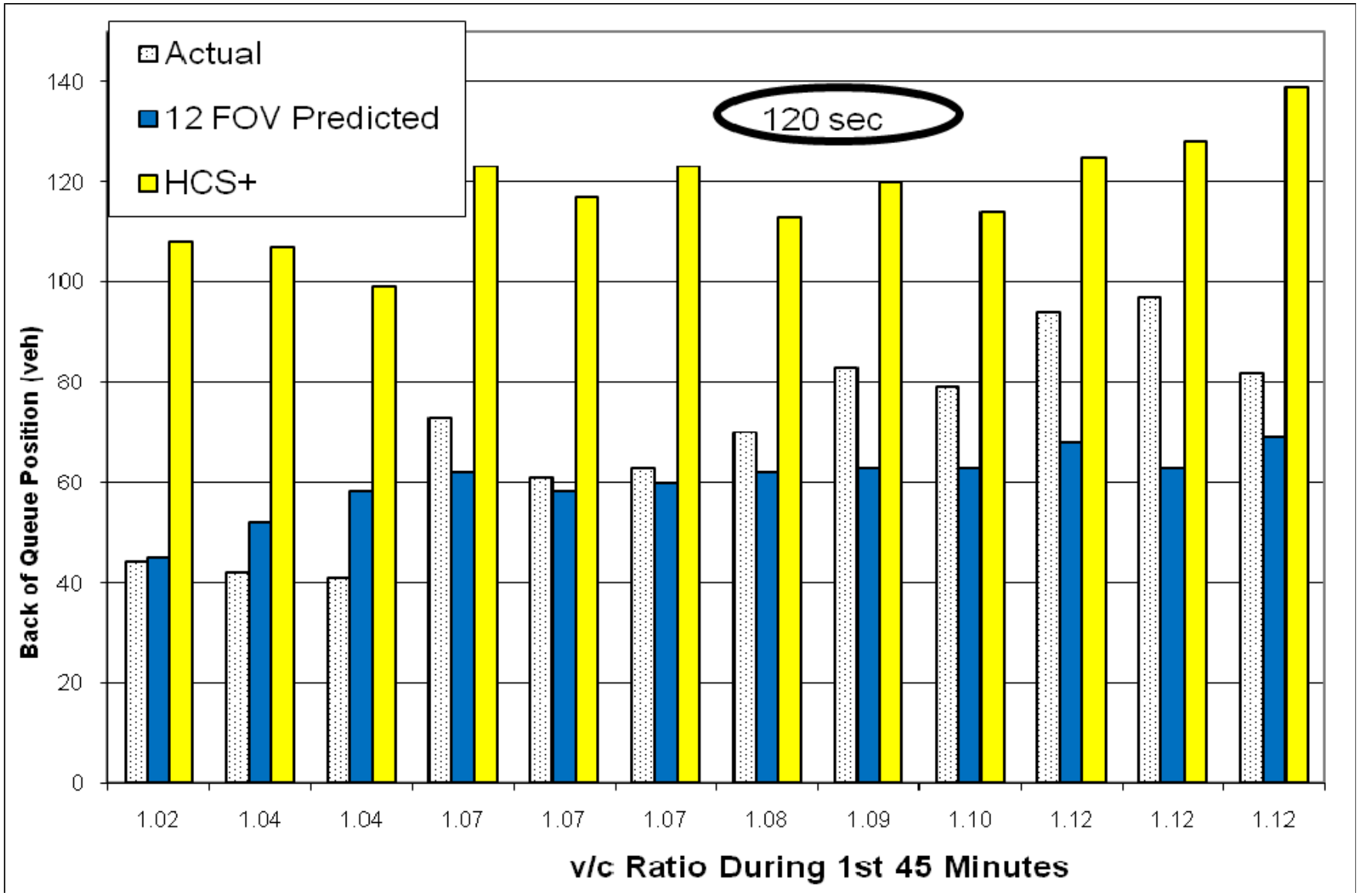

Figure 4-17. 98th percentile back of queue comparison

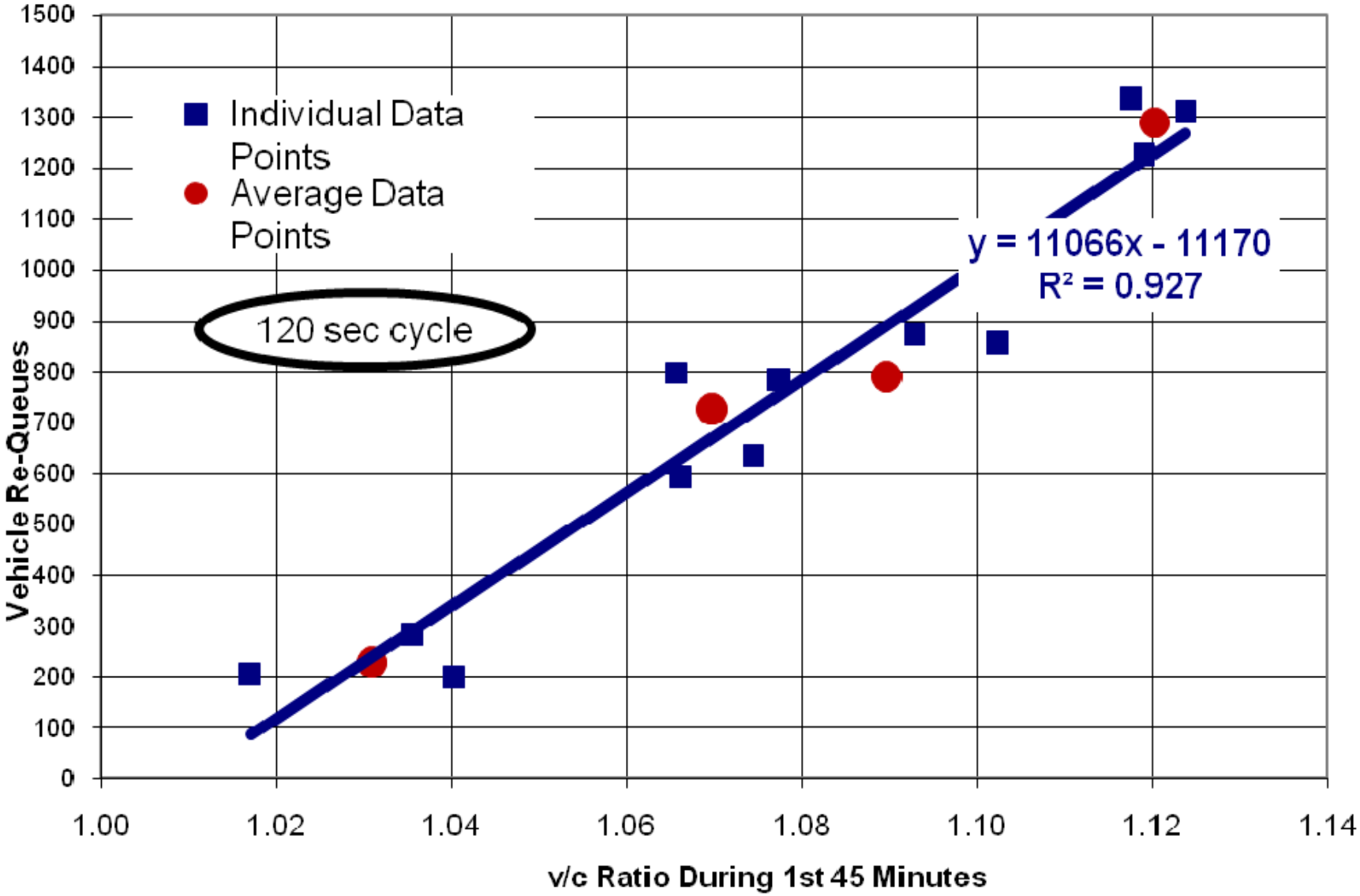

Figure 4-18. Vehicle re-queuing

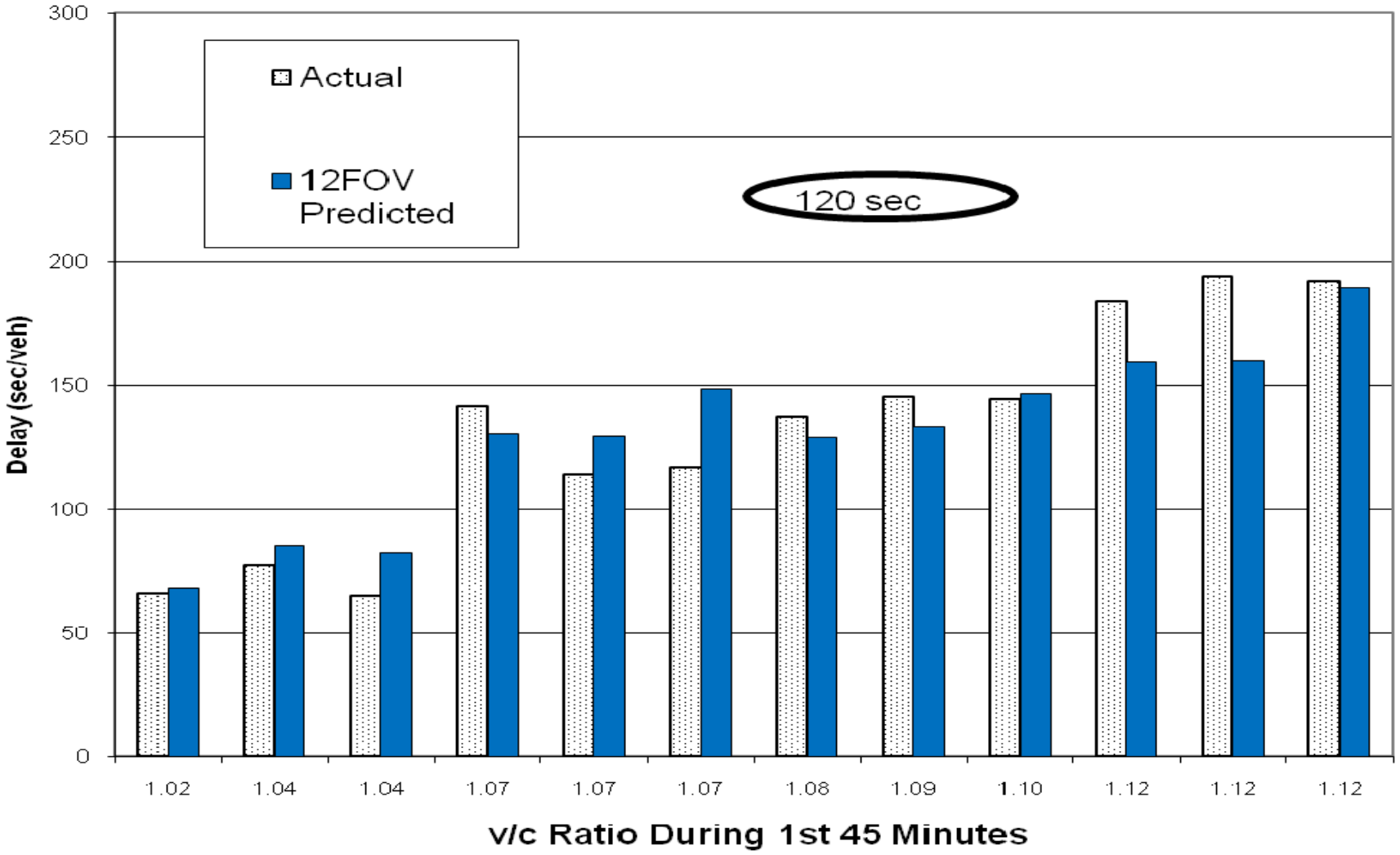

Figure 4-19. Stopped delay comparison

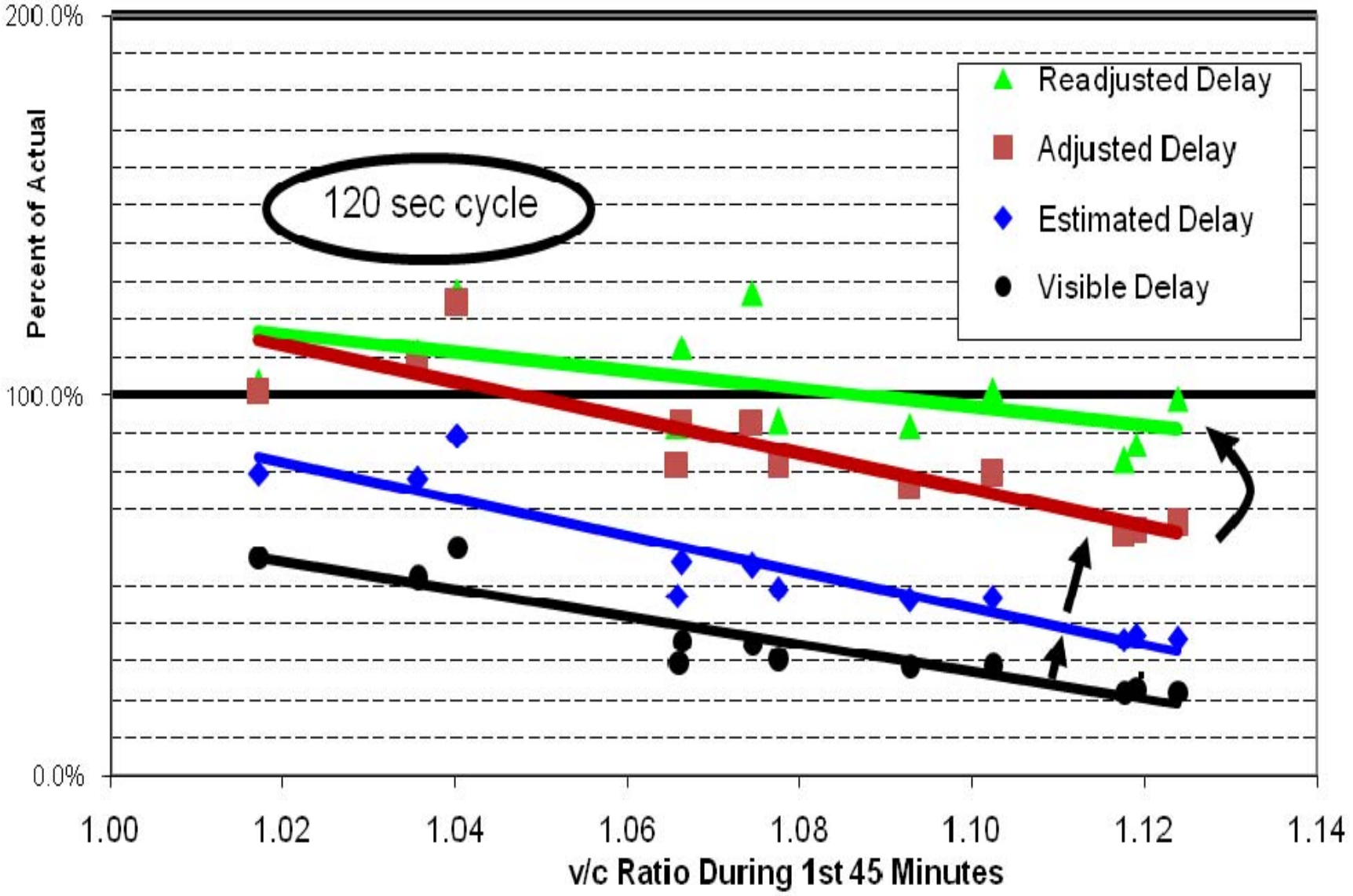

Figure 4-20. Stopped delay prediction, 12 FOV

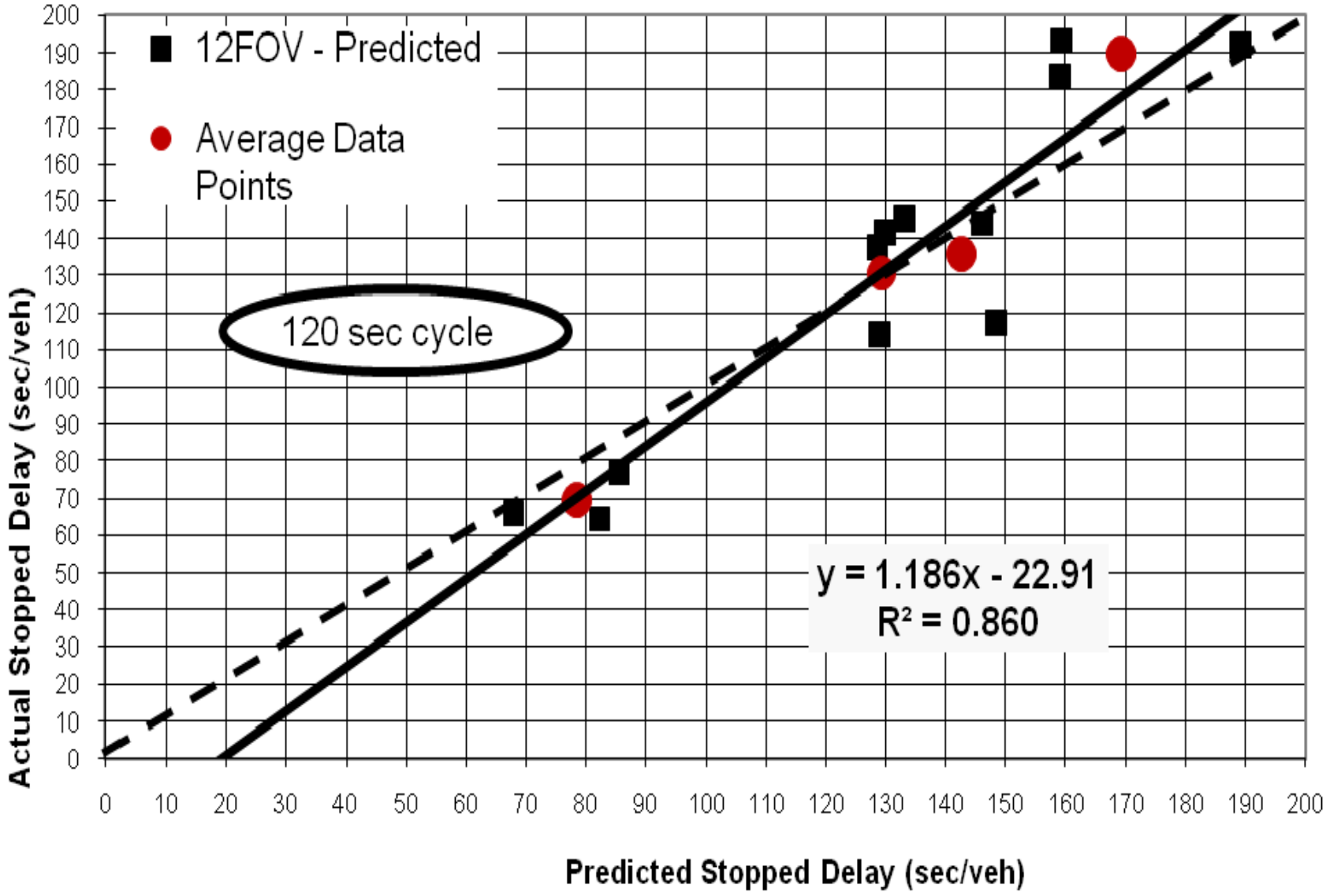

Figure 4-21. Comparison of actual and predicted stopped delay

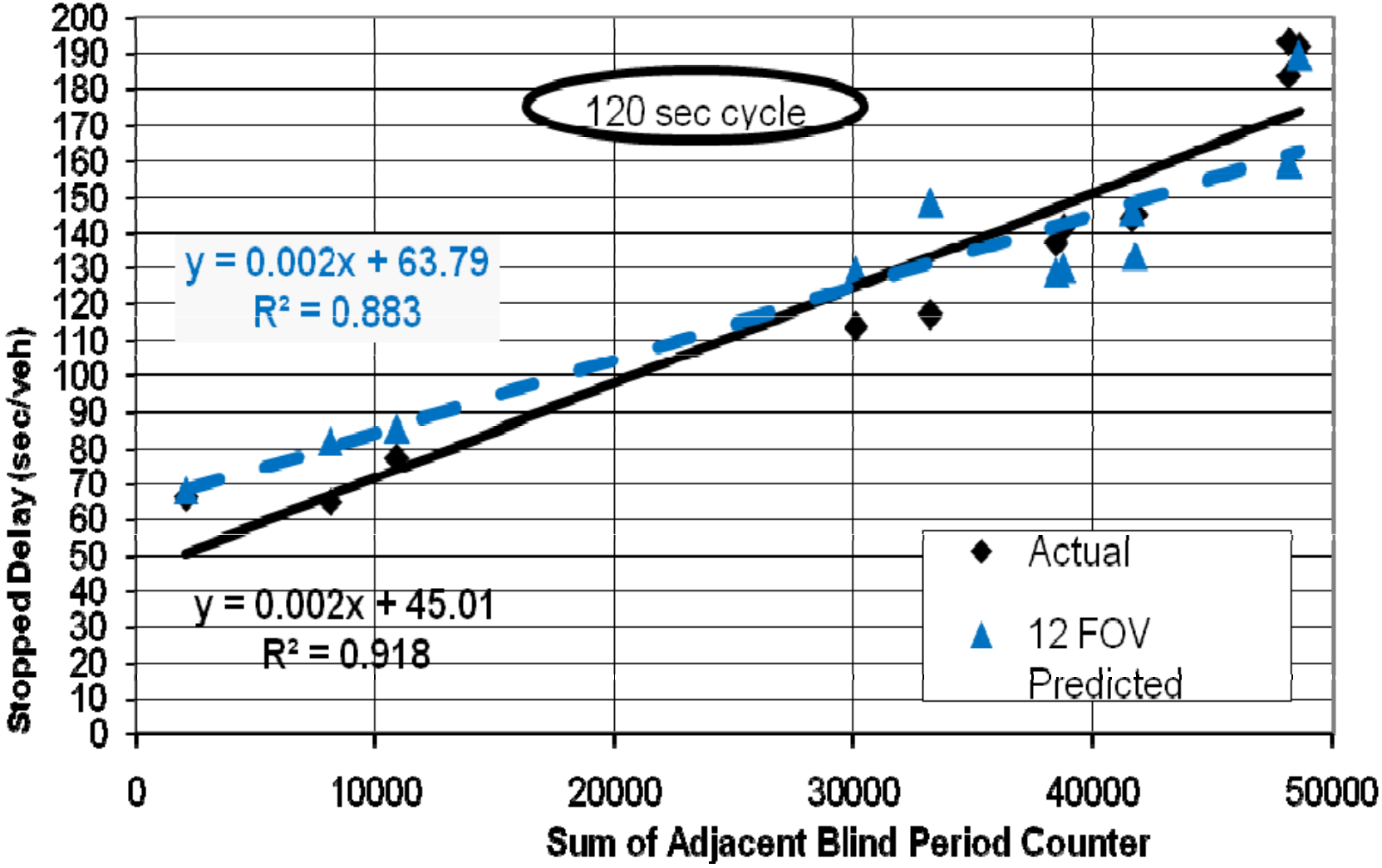

Figure 4-22. Adjacent blind period counter v. stopped delay

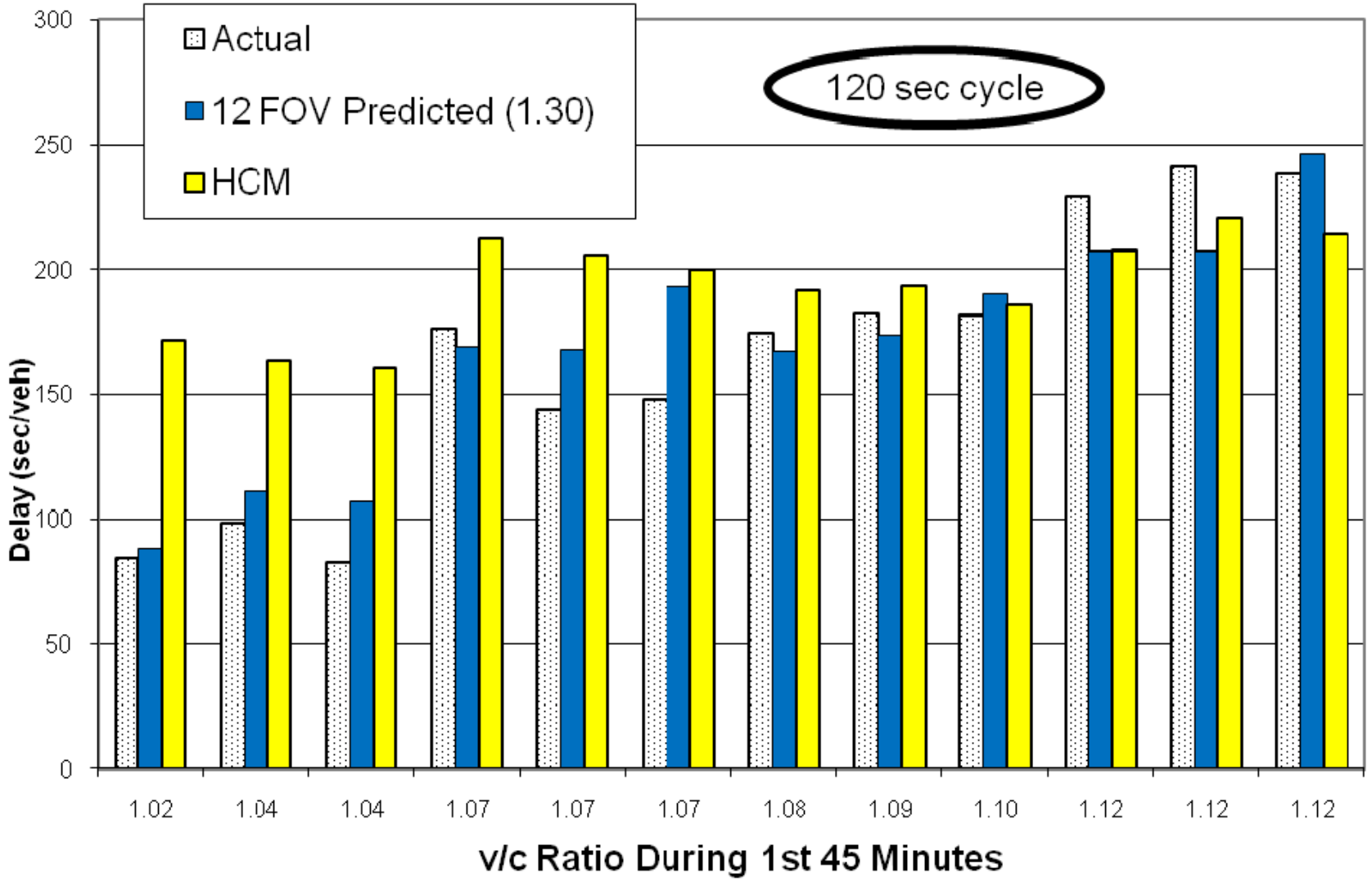

Figure 4-23. Control delay comparison

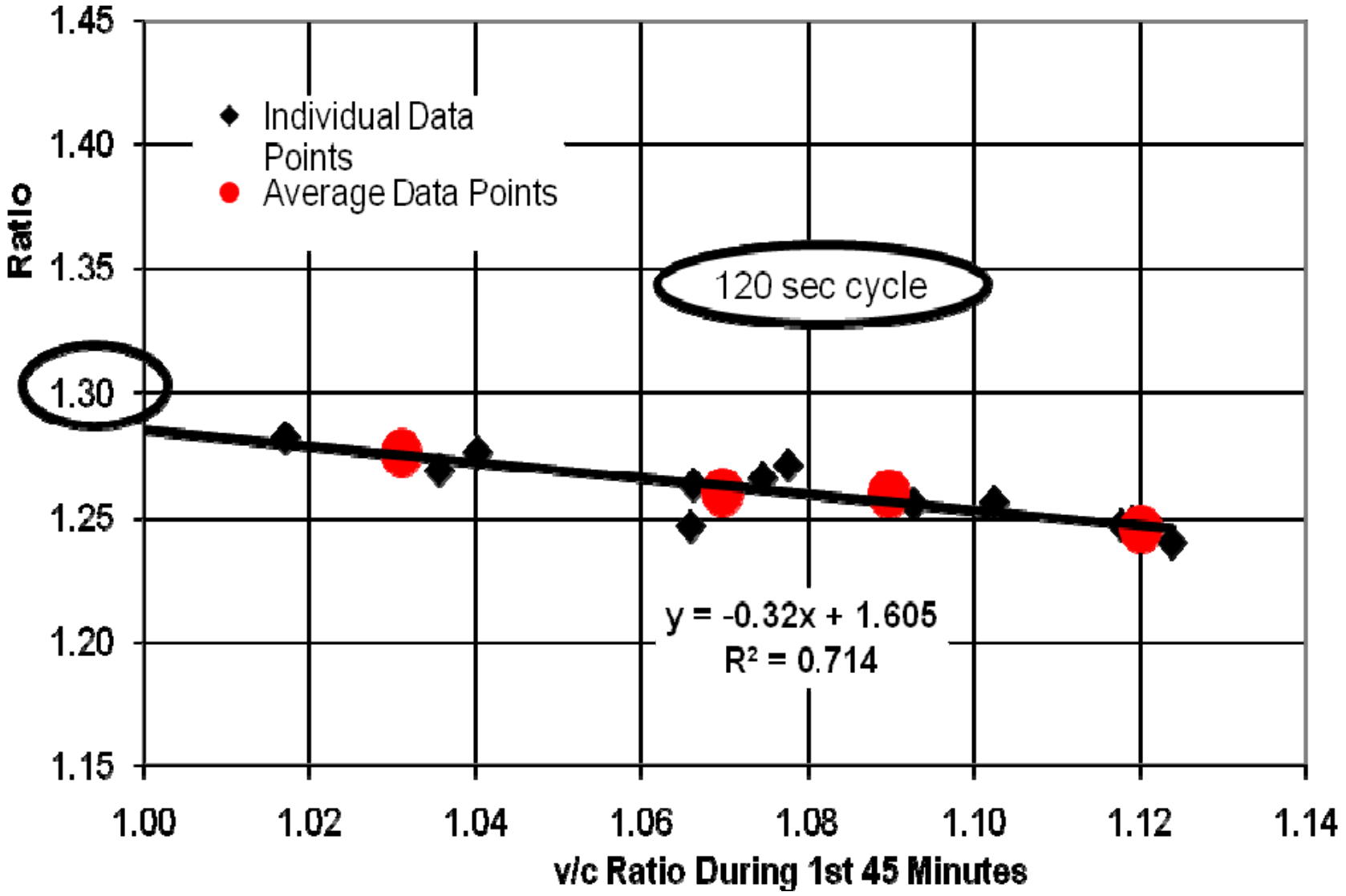

Figure 4-24. Ratio of control delay to stopped delay

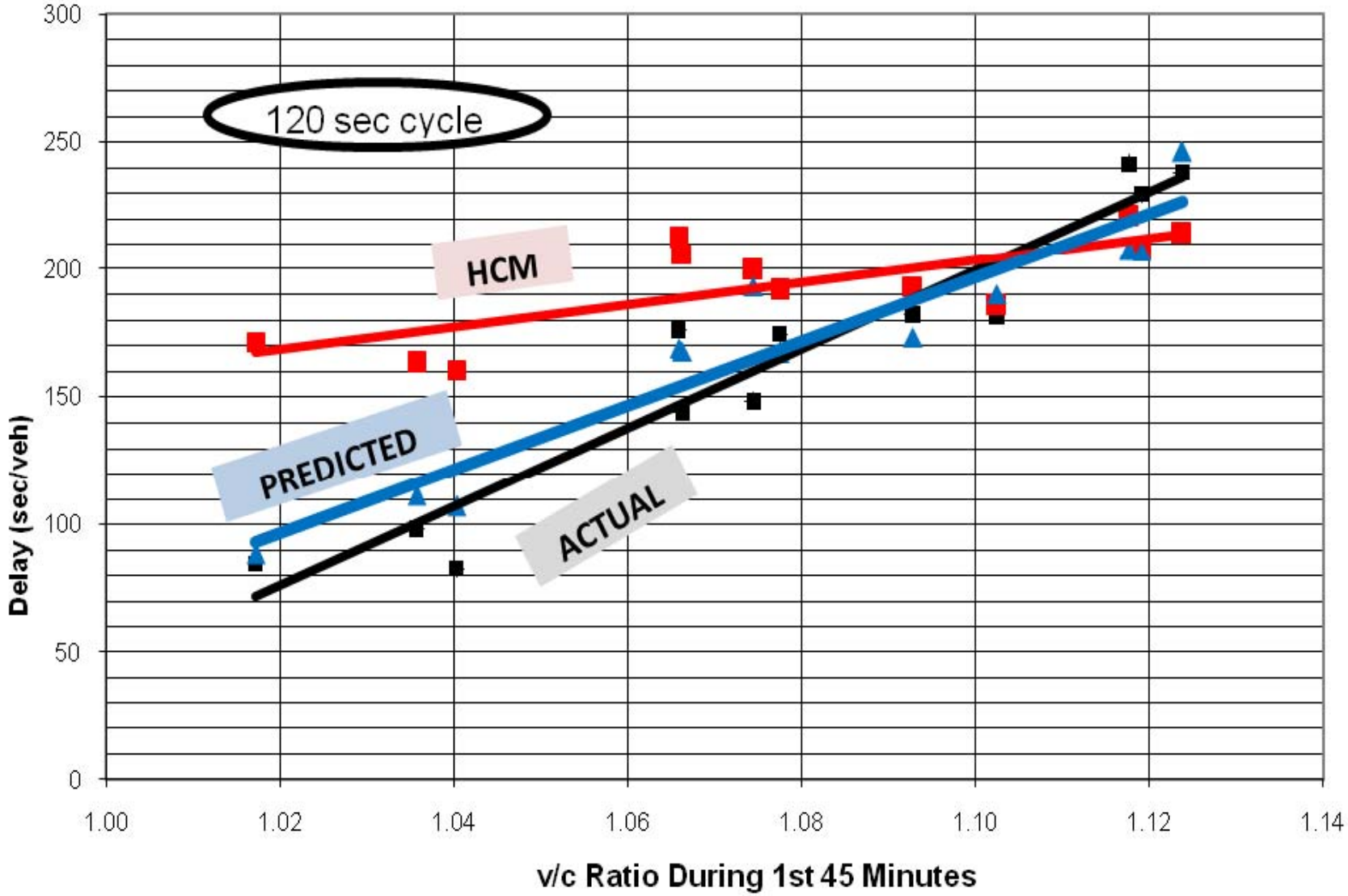

Figure 4-25. Graphical control delay comparison,

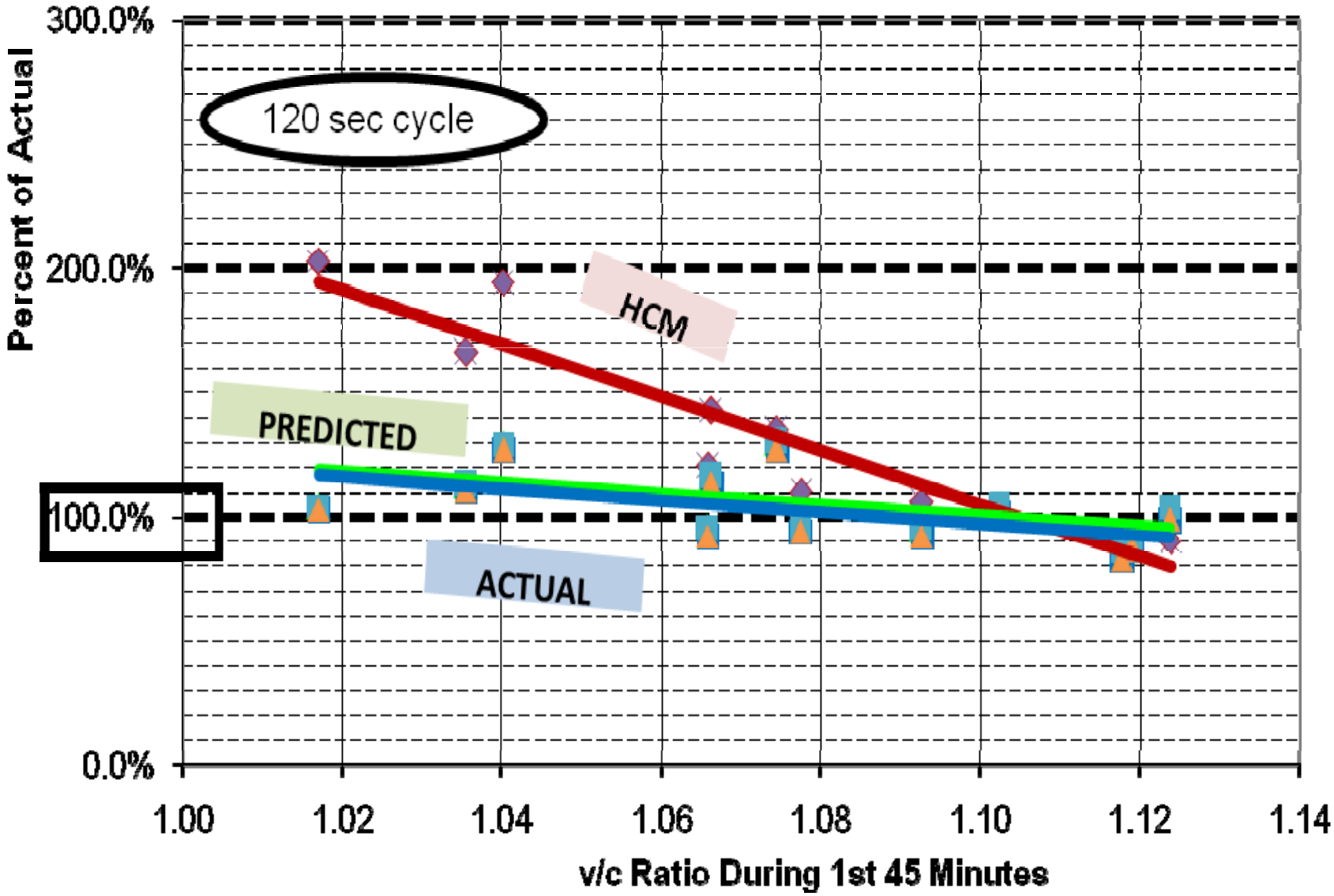

Figure 4-26. Control delay estimates

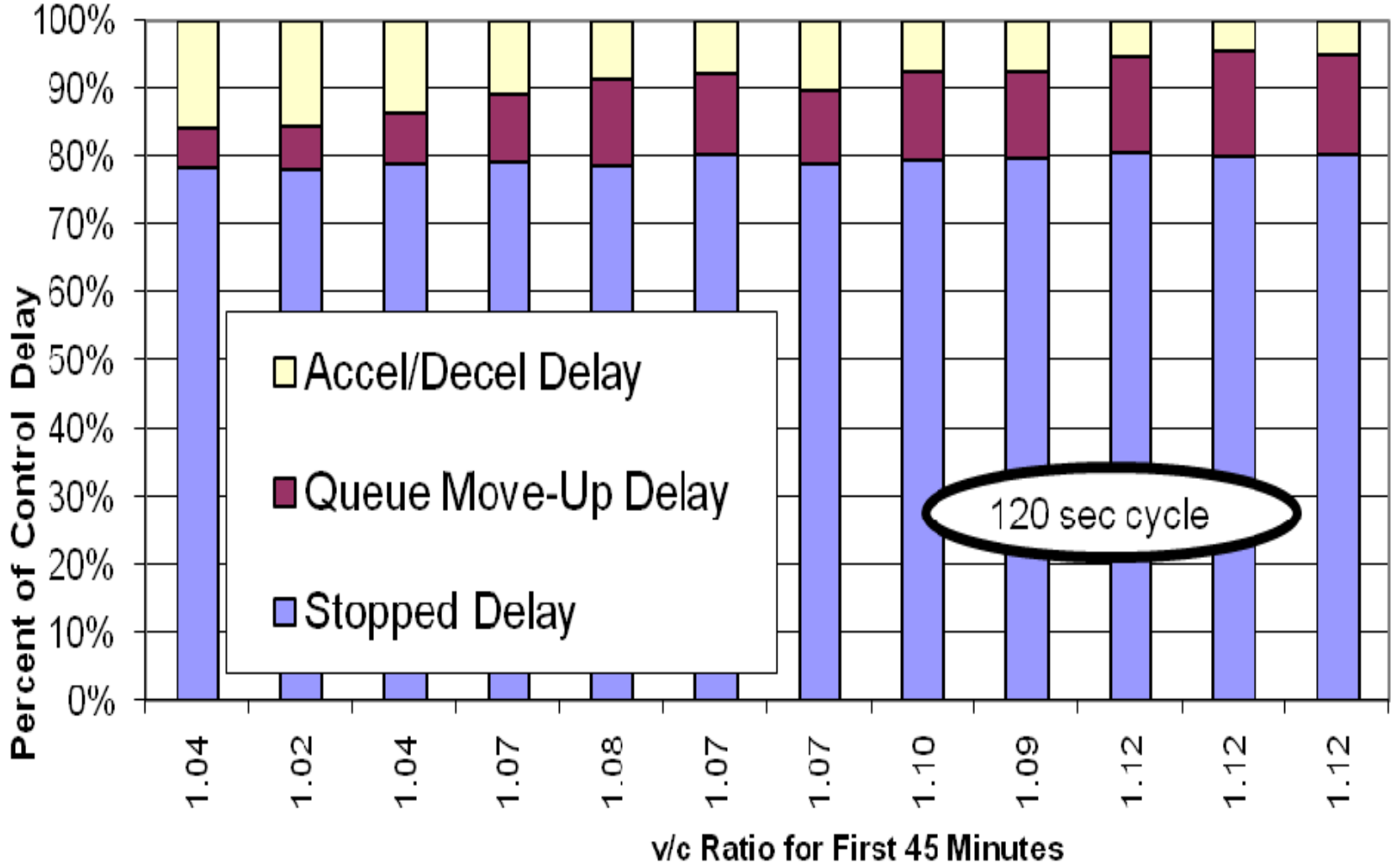

Figure 4-27. Control delay composition

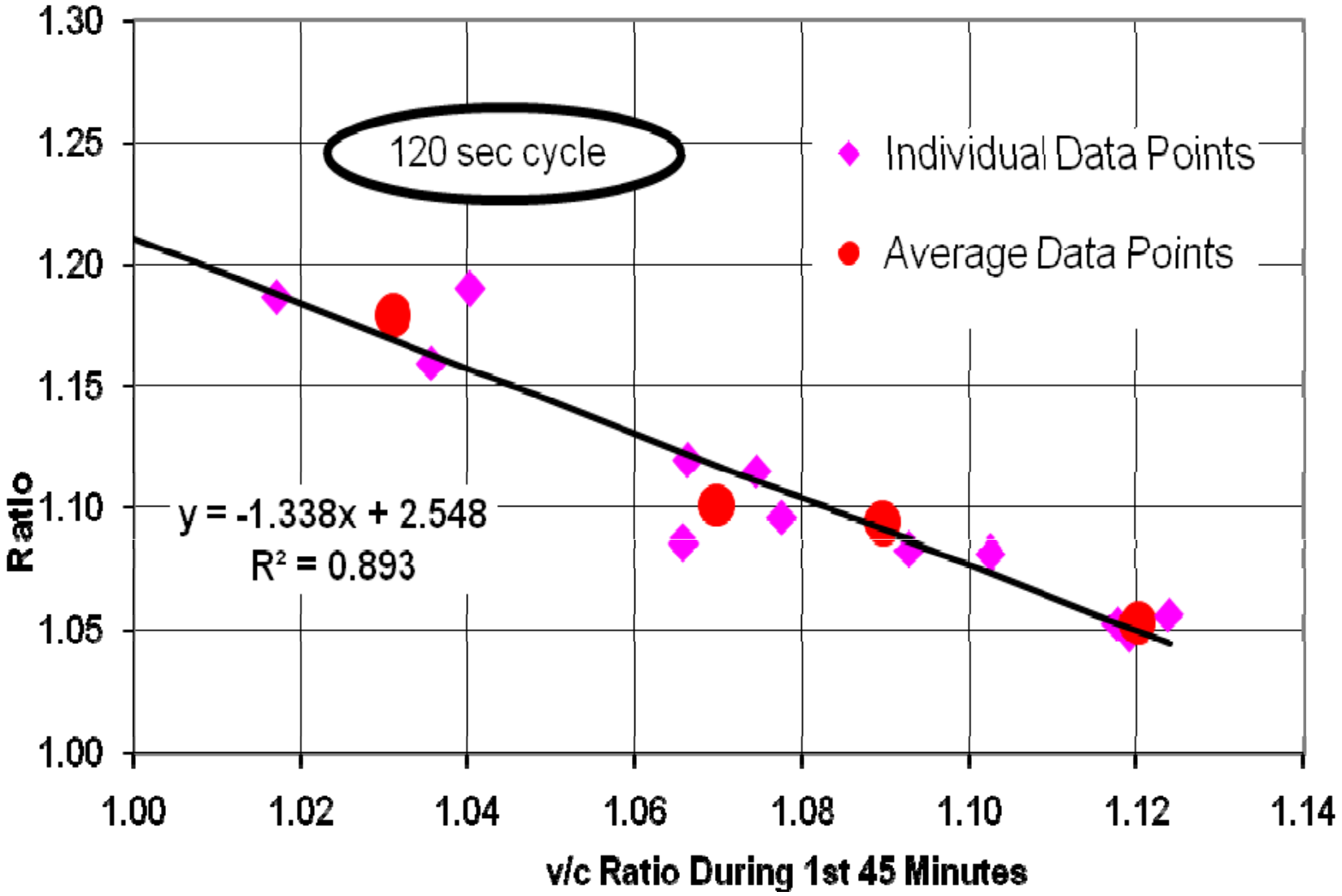

Figure 4-28. Ratio of control delay to stopped plus move-up delay

Table 4-1. Example summary - volume and capacity

File Name	Random	Arrival at Back of Queue Volumes			Calculated Capacity and Volume-to-Capacity Ratio									
15 min input volumes	Number Set	15 min volumes	1st 45 minutes	1 hour	1st 15 minutes		2nd 15 minutes		3rd 15 minutes		4th 15 minutes		1st 45 minutes	
			v										c	v/c
625_700_650_350vph	1	676 688 652 360	672	594	616	1.10	668	1.03	656	0.99	511	0.70	646	**1.04**
625_700_650_350vph	2	608 676 672 364	652	580	663	0.92	642	1.05	623	1.08	492	0.74	641	**1.02**
625_700_650_350vph	3	648 668 688 344	668	587	643	1.01	649	1.03	642	1.07	499	0.69	645	**1.04**
700_725_625_350vph	1	708 740 628 348	692	606	631	1.12	659	1.12	656	0.96	547	0.64	649	**1.07**
700_725_625_350vph	2	720 728 624 368	691	610	648	1.11	661	1.10	610	1.02	604	0.61	641	**1.08**
700_725_625_350vph	3	692 732 632 364	685	605	648	1.07	635	1.15	646	0.98	556	0.65	643	**1.07**
700_700_700_350vph	1	708 704 680 380	697	618	631	1.12	659	1.07	656	1.04	602	0.63	649	**1.07**
700_700_700_350vph	2	720 688 712 344	707	616	648	1.11	661	1.04	610	1.17	625	0.55	641	**1.10**
700_700_700_350vph	3	692 712 704 360	703	617	648	1.07	635	1.12	646	1.09	614	0.59	643	**1.09**
725_700_700_350vph	1	788 692 708 340	729	632	637	1.24	648	1.07	661	1.07	618	0.55	649	**1.12**
725_700_700_350vph	2	728 724 700 356	717	627	663	1.10	639	1.13	623	1.12	645	0.55	641	**1.12**
725_700_700_350vph	3	752 704 700 364	719	630	648	1.16	635	1.11	646	1.08	610	0.60	643	**1.12**
		vph			vph		vph		vph		vph		vph	
Averages														
625_700_650_350vph		644 677 671 356	664	587	641	1.01	653	1.04	640	1.05	501	0.71	644	**1.03**
700_725_625_350vph		707 733 628 360	689	607	642	1.10	652	1.13	637	0.99	569	0.63	644	**1.07**
700_700_700_350vph		707 701 699 361	702	617	642	1.10	652	1.08	637	1.10	614	0.59	644	**1.09**
725_700_700_350vph		756 707 703 353	722	630	649	1.16	641	1.10	643	1.09	624	0.57	644	**1.12**

Table 4-2. Example summary - queue discharge, delay check and goodness-of-fit

		Queue Discharge Data, Average Over All Cycles							BuckQ Delay Check						Goodness-of-Fit Test			
File Name 15 min input volumes	Random Number Set	Cycle Length	Green Time	g/C ratio	Discharge Headway	Sat Flow Rate	Lost Time	Ext. of Green	Actual Stopped Delay	CORSIM Stop Time	CORSIM Queue Delay	CORSIM Control Delay	Actual Control Delay	CORSIM Delay Time	(20-sec arrival intervals) 95% Ref. Statistic = 9.49			
		C	G	g=G+EEG-SULT	H	S	SULT	EEG	d_S	=	<	<		=	Chi-Square Test Statistic			
625_700_650_350vph	1	118.5	35.7	0.31	1.80	2004	2.74	3.4	64.7	65.0	66.7	76.6	82.6	81.9	3.4	**16.9**	6.4	2.2
625_700_650_350vph	2	116.7	34.7	0.30	1.79	2009	2.73	3.4	65.9	66.8	68.7	78.9	84.5	83.5	6.9	2.6	5.6	2.2
625_700_650_350vph	3	117.6	35.6	0.31	1.81	1994	2.95	3.3	77.3	77.8	79.9	91.9	98.1	97.1	2.5	7.5	4.3	2.5
700_725_625_350vph	1	118.8	36.6	0.32	1.80	1999	2.56	3.4	113.9	113.4	116.7	133.4	143.9	141.9	5.2	4.4	5.4	0.9
700_725_625_350vph	2	119.1	37.1	0.31	1.79	2007	2.92	3.3	137.2	136.9	141.4	163.6	174.4	172.4	3.7	4.0	1.4	8.3
700_725_625_350vph	3	118.9	36.9	0.32	1.82	1980	2.60	3.3	141.3	139.8	143.8	165.4	176.1	175.4	5.4	5.4	2.1	3.9
700_700_700_350vph	1	119.8	37.6	0.32	1.81	1991	2.49	3.4	117.0	117.4	120.9	138.6	148.1	147.3	5.2	7.9	4.6	3.8
700_700_700_350vph	2	119.5	37.5	0.32	1.80	1998	2.71	3.3	144.3	142.4	147.1	169.8	181.3	178.8	3.7	2.9	3.1	2.6
700_700_700_350vph	3	120.0	38.0	0.32	1.82	1974	2.53	3.3	145.0	143.9	148.2	171.1	182.1	181.3	5.4	2.4	3.7	1.1
725_700_700_350vph	1	120.0	38.0	0.32	1.81	1985	2.65	3.4	191.8	190.8	197.0	225.8	237.9	236.5	3.3	2.6	7.8	0.7
725_700_700_350vph	2	120.0	38.0	0.32	1.79	2007	2.75	3.3	183.8	183.4	189.5	218.6	229.5	229.1	6.9	3.1	1.0	4.6
725_700_700_350vph	3	120.0	38.0	0.32	1.83	1971	2.52	3.3	193.3	192.3	198.5	229.4	241.1	240.6	1.0	3.0	6.5	6.6
		sec	sec		sec/veh	vphg	sec	sec	sec/veh									
Averages																		
625_700_650_350vph		117.6	35.3	0.30	1.80	2002	2.8	3.4	69.3	69.9	71.8	82.5	88.4	87.5				
700_725_625_350vph		118.9	36.9	0.31	1.80	1995	2.7	3.3	130.8	130.0	134.0	154.1	164.8	163.2				
700_700_700_350vph		119.8	37.7	0.31	1.81	1988	2.6	3.3	135.4	134.6	138.7	159.8	170.5	169.1				
725_700_700_350vph		120.0	38.0	0.32	1.81	1988	2.6	3.3	189.6	188.8	195.0	224.6	236.2	235.4				
ALL		**119.1**	**37.0**	**0.32**	**1.81**	**1993**	**2.7**	**3.3**										

Table 4-3. Queue prediction

File Name	RN	Vol		QUEUING														PHASE FAILURES		
				Average Queue Length			Maximum Queue Length			Maximum Back of Queue Position			98th Percentile Back of Queue Position					Actual Phase	% of Cycles	Actual Vehicle
15 min input vol	Set	45min	v/c	A	P	%Err	A	P	%Err	A	P	%Err	A	P	%Err	HCM	%Err	Fail	w/ PF	Re-Q's
12FOV		**v**	**v/c**																	
625_700_650_350	1	**672**	**1.04**	11	13	**18%**	32	38	**19%**	45	58	**29%**	41	58	**41%**	99	**141%**	21	**70%**	197
625_700_650_350	2	**652**	**1.02**	11	10	**-9%**	37	34	**-8%**	45	47	**4%**	44	45	**2%**	108	**145%**	19	**63%**	204
625_700_650_350	3	**668**	**1.04**	13	13	**0%**	37	35	**-5%**	45	53	**18%**	42	52	**24%**	107	**155%**	24	**80%**	281
700_725_625_350	1	**692**	**1.07**	19	17	**-11%**	52	41	**-21%**	62	58	**-6%**	61	58	**-5%**	117	**92%**	24	**80%**	591
700_725_625_350	2	**691**	**1.08**	23	19	**-17%**	58	49	**-16%**	74	63	**-15%**	70	62	**-11%**	113	**61%**	27	**90%**	782
700_725_625_350	3	**685**	**1.07**	24	19	**-21%**	59	42	**-29%**	75	63	**-16%**	73	62	**-15%**	123	**68%**	27	**90%**	797
700_700_700_350	1	**697**	**1.07**	20	19	**-5%**	54	51	**-6%**	72	65	**-10%**	63	60	**-5%**	123	**95%**	25	**83%**	635
700_700_700_350	2	**707**	**1.10**	25	21	**-16%**	65	59	**-9%**	81	65	**-20%**	79	63	**-20%**	114	**44%**	28	**93%**	854
700_700_700_350	3	**703**	**1.09**	25	21	**-16%**	67	46	**-31%**	85	64	**-25%**	83	63	**-24%**	120	**45%**	28	**93%**	872
725_700_700_350	1	**729**	**1.12**	34	26	**-24%**	72	64	**-11%**	97	68	**-30%**	82	69	**-16%**	139	**70%**	29	**97%**	1308
725_700_700_350	2	**717**	**1.12**	32	25	**-22%**	76	68	**-11%**	99	68	**-31%**	94	68	**-28%**	125	**33%**	29	**97%**	1224
725_700_700_350	3	**719**	**1.12**	34	23	**68%**	75	51	**-32%**	103	63	**-39%**	97	63	**-35%**	128	**32%**	29	**97%**	1334
		vph		veh	veh		veh	veh		veh	veh		veh	veh						

Cycles per Hour: 30.0

Averages

625_700_650_350		**664**	**1.03**	12	12	**3%**	35	36	**1%**	45	53	**17%**	42	52	**22%**	105	**147%**	21	**71%**	227
700_725_625_350		**689**	**1.07**	22	18	**-17%**	56	44	**-22%**	70	61	**-13%**	68	61	**-11%**	118	**73%**	26	**87%**	723
700_700_700_350		**702**	**1.09**	23	20	**-13%**	62	52	**-16%**	79	65	**-18%**	75	62	**-17%**	119	**59%**	27	**90%**	787
725_700_700_350		**722**	**1.12**	33	25	**-26%**	74	61	**-18%**	100	66	**-33%**	91	67	**-27%**	131	**44%**	29	**97%**	1289

A = Actual
P = Predicted

Table 4-4. Stopped delay prediction

File Name 15 min input volumes	Random Number Set	Volume 1st 45 min	v/c Ratio	Stopped Delay Actual	Stopped Delay BuckQ Predicted		% of Time Queue Not Visible	Stopped Delay Prediction Steps Visible	BuckQ Estimated	BuckQ Adjusted	BuckQ Readjusted	Sum of Adjacent Blind Period Counter
12FOV		**v**	**v/c**	d_S	d_{SP}							ABPC
625_700_650_350vph	1	**672**	**1.04**	64.7	82.2	127.0%	70%	60%	89%	124%	128%	8131
625_700_650_350vph	2	**652**	**1.02**	65.9	67.9	103.0%	63%	57%	80%	101%	104%	2118
625_700_650_350vph	3	**668**	**1.04**	77.3	85.5	110.6%	77%	52%	78%	108%	111%	10921
700_725_625_350vph	1	**692**	**1.07**	113.9	129.1	113.3%	83%	36%	56%	93%	113%	30098
700_725_625_350vph	2	**691**	**1.08**	137.2	128.5	93.7%	88%	31%	49%	82%	93%	38508
700_725_625_350vph	3	**685**	**1.07**	141.3	130.0	92.0%	88%	30%	47%	82%	92%	38761
700_700_700_350vph	1	**697**	**1.07**	117.0	148.6	127.0%	86%	35%	55%	93%	127%	33220
700_700_700_350vph	2	**707**	**1.10**	144.3	146.2	101.3%	92%	29%	47%	79%	101%	41636
700_700_700_350vph	3	**703**	**1.09**	145.0	133.3	91.9%	92%	29%	46%	76%	92%	41762
725_700_700_350vph	1	**729**	**1.12**	191.8	189.3	98.7%	98%	22%	36%	66%	99%	48604
725_700_700_350vph	2	**717**	**1.12**	183.8	159.2	86.6%	96%	23%	37%	65%	87%	48170
725_700_700_350vph	3	**719**	**1.12**	193.3	159.5	82.5%	99%	22%	36%	63%	83%	48199
		vph		secs/veh								
Averages												
625_700_650_350vph		**664**	**1.03**	69	79	113%	70%	57%	82%	111%	114%	7057
700_725_625_350vph		**689**	**1.07**	131	129	99%	86%	32%	51%	86%	99%	35789
700_700_700_350vph		**702**	**1.09**	135	143	105%	90%	31%	49%	83%	107%	38873
725_700_700_350vph		**722**	**1.12**	190	169	89%	98%	22%	36%	65%	90%	48324
ALL						**107%**	**82%**	**40%**	**61%**	**93%**	**107%**	

Table 4-5. Control delay prediction

File Name 15 min input volumes	Random Number Set	Volume 1st 45 min	v/c Ratio	1.XX Control Delay/ Stopped Delay	1.XX Control Delay/ Stop+QMU Delay	Actual Stopped Plus Queue Move-Up Delay	Control Delay: Actual	Control Delay: HCM		Control Delay: 1.XX BuckQ Pred		Control Delay: 1.30 BuckQ Pred		Percentage of Control Delay: Stopped Delay	Stop & Q Move-Up	Queue Move-Up	Accel./ Decel.
12FOV		v	v/c			$d_S + d_{MU}$	d_C	d_{CH+}		d_{CPX}		d_{CP3}					
625_700_650_350vph	1	672	1.04	1.28	1.19	69.4	82.6	160.5	194%	104.9	127%	106.9	129%	78%	84%	6%	16%
625_700_650_350vph	2	652	1.02	1.28	1.19	71.2	84.5	171.3	203%	87.1	103%	88.3	104%	78%	84%	6%	16%
625_700_650_350vph	3	668	1.04	1.27	1.16	84.6	98.1	163.2	166%	108.5	111%	111.2	113%	79%	86%	7%	14%
700_725_625_350vph	1	692	1.07	1.26	1.12	128.5	143.9	205.8	143%	163.1	113%	167.8	117%	79%	89%	10%	11%
700_725_625_350vph	2	691	1.08	1.27	1.10	159.2	174.4	191.7	110%	163.3	94%	167.1	96%	79%	91%	13%	9%
700_725_625_350vph	3	685	1.07	1.25	1.09	162.2	176.1	212.3	121%	162.0	92%	169.0	96%	80%	92%	12%	8%
700_700_700_350vph	1	697	1.07	1.27	1.12	132.8	148.1	199.6	135%	188.1	127%	193.2	130%	79%	90%	11%	10%
700_700_700_350vph	2	707	1.10	1.26	1.08	167.6	181.3	185.5	102%	183.7	101%	190.1	105%	80%	92%	13%	8%
700_700_700_350vph	3	703	1.09	1.26	1.08	168.1	182.1	193.0	106%	167.4	92%	173.3	95%	80%	92%	13%	8%
725_700_700_350vph	1	729	1.12	1.24	1.06	225.1	237.9	214.0	90%	234.8	99%	246.1	103%	81%	95%	14%	5%
725_700_700_350vph	2	717	1.12	1.25	1.05	218.8	229.5	207.4	90%	198.8	87%	207.0	90%	80%	95%	15%	5%
725_700_700_350vph	3	719	1.12	1.25	1.05	228.9	241.1	220.6	91%	198.9	83%	207.4	86%	80%	95%	15%	5%
		vph				secs/veh	secs/veh	secs/veh		secs/veh		secs/veh					
Averages																	
625_700_650_350vph		664	1.03	1.28	1.18	75.1	88.4	165.0	187%	100.2	113%	102.1	115%	78%	85%	7%	15%
700_725_625_350vph		689	1.07	1.26	1.10	150.0	164.8	203.3	123%	162.8	99%	168.0	102%	79%	91%	12%	9%
700_700_700_350vph		702	1.09	1.26	1.09	156.2	170.5	192.7	113%	179.7	105%	185.5	109%	79%	92%	12%	8%
725_700_700_350vph		722	1.12	1.25	1.05	224.3	236.2	214.0	91%	210.9	89%	220.1	93%	80%	95%	15%	5%
ALL				1.26	1.11				142%		107%		110%	79%	89%	10%	11%

Table 4-6. Comparison of variation in actual and predicted stopped delay

Random Number Set	Cumulative 1-Hour Stopped Delay (sec) Actual	Predicted
1	68622	77325
2	83364	77713
3	85601	78925
4	80081	69056
5	59339	57874
6	95345	91536
7	94206	78308
8	111432	73012
9	66737	67418
10	78859	75952
Mean	**82359**	**74712**
Std Deviation	15441	8836
CV	0.19	0.12
Std. Error	**4883**	**2794**
95% C.I.	9571	5477
Lower	72788	69235
Upper	91929	80189

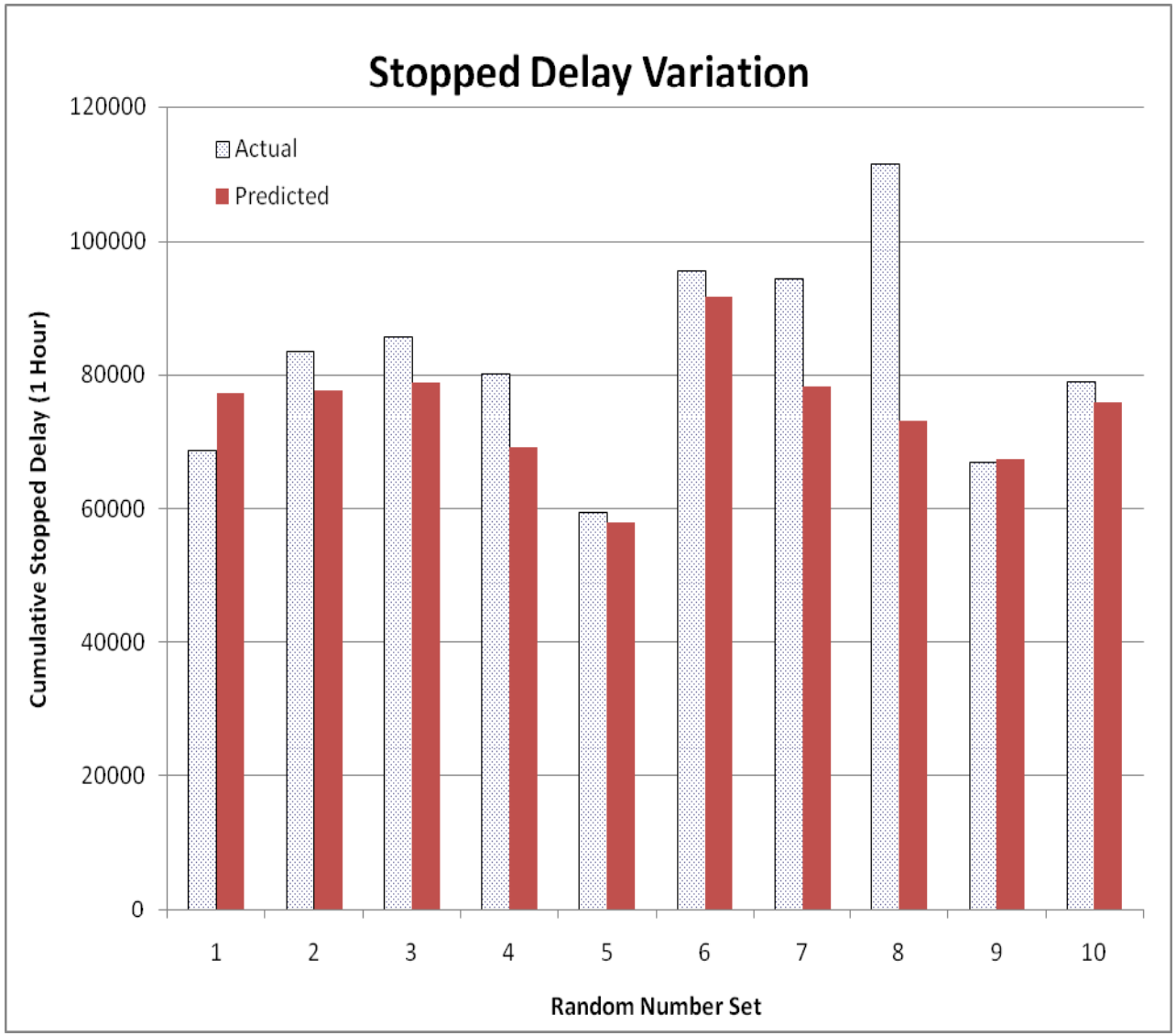

Table 4-7. P-value determination for difference in median values

Fisher SignTest
For paired replicates

Null hypothesis: Differences between actual and predicted median delay is zero

Random Number Set	**Cumulative 1-Hour Stopped Delay (sec)** Actual	Predicted	Difference	Mu
RN	X	Y	Z = Y - X	u
1	68622	77325	8703	1
2	83364	77713	-5651	0
3	85601	78925	-6676	0
4	80081	69056	-11025	0
5	59339	57874	-1465	0
6	95345	91536	-3809	0
7	94206	78308	-15898	0
8	111432	73012	-38420	0
9	66737	67418	681	1
10	78859	75952	-2907	0
			B =	**2**

From Reference Table with n = 10 and b = B = 2: p/2 = 0.0547, **p = 0.1094**

CHAPTER 5
THEORETICAL BOUNDS FOR DELAY ESTIMATION

This chapter describes the development of theoretical limits on the solution space for the empirical delay prediction procedure (Objective 4).

The delay estimation procedure presented in the previous chapter begins by calculating an "estimated arrival rate", which is actually the departure rate. Then, if the back end of the queue is not visible, the procedure modifies the estimated arrival rate upward using a power function to predict the real arrival rate. This power function adjusts the rate in a manner that, in essence, varies with the amount of time during which the back end of the queue is not visible. A major advantage of this approach is that the resulting estimated queues and associated delay can be immediately calculated on a second-by-second basis, in real time. A major disadvantage of the approach is that there is no relationship between the departure rate and the real arrival rate. Under the right circumstances, errors can accumulate to the point that the delay estimation is no longer reasonable. The potential for this is highest when the length of time that the end of the queue is not visible covers most of the analysis time frame.

However, it is possible to calculate a set of theoretical upper and lower bounds on the solution space by using information obtained at the end of the analysis period when the arrival rate does equal the departure rate. In order to make any type of reasonable delay estimation, all queues must dissipate prior to the end of the analysis time frame. Once this occurs, a calculation of the arrival rate (which is equal to the departure rate) during the final portion of the analysis time frame, the last 15 minutes of the hour, can be made. Knowing this final arrival/departure rate and knowing the total number of vehicles that have crossed the stop bar during the entire hour we can, by assuming a reasonable minimum peak hour factor, work backwards through the period to identify arrival curves that serve as both lower and upper bounds. These theoretical

results can be used, in an ex post facto manner, to "bracket" the real-time delay estimation procedure presented in the previous chapter. These bounds can also be used to identify an independent "most probable" delay pattern by selecting an intermediate curve between the upper and lower bounds that minimizes the maximum percent error between the estimate and the actual delay.

Chapter 16 of the 2000 Highway Capacity Manual [4] contains a widely recognized and well-accepted procedure for calculating per-vehicle control delay at signalized intersections. In the 2000 HCM, this control delay has three components: d1 (uniform delay), d2 (incremental delay) and d3 (initial queue delay). Component d2 can be further subdivided into an over-saturation element and a random delay element. The random delay element is based on a coordinate transformation technique originally proposed by Whiting and refined for signalized delay applications by Akcelik [47]. In 2007, Courage [48] demonstrated the relationships between overflow delay, deterministic queue delay, incremental delay and initial queue delay. Courage showed that overflow delay and deterministic queue delay (both of which can be calculated using the area between the cumulative arrival curve and the uniform cumulative departure curve) were each composed of initial queue delay and the over-saturation portion of the incremental delay. The random portion of the control delay is not reflected in the cumulative arrival and departure curves, nor is the portion of the control delay associated with acceleration or deceleration. In addition, queue move-up delay is not explicitly depicted in the cumulative arrival and cumulative departure curves although its effect is somewhat implied within the general treatment of delay as the area between the curves. Appendix F of the 2000 HCM discusses the relationship between the initial queue delay and deterministic queue delay. Five

specific arrival “cases” are discussed and the proper way to account for initial queue delay and deterministic delay for each case is explained.

The theoretical delay literature is extended in this chapter through the development of a theoretical framework for establishing the upper and lower bounds of the overflow delay given a terminal arrival rate and a minimum Peak Hour Factor (PHF). The mathematical bracketing of overflow delay using this type of information represents a new aspect of delay estimation.

Derivation of the Bounds

During a period of over-saturated flow on a signalized intersection approach, the cumulative number of arrivals at the back of the queue exceeds the cumulative number of departures from the stop bar, with resulting queue formation. Let us assume that over-saturated flow begins immediately at the start of a one-hour observation period and that, at some point near the end of the hour, it is replaced by a period of under-saturated flow that causes the queue to dissipate before the hour expires. Let us also assume that the component 15-minute flow rates follow a reasonable pattern that result in some minimum Peak Hour Factor (PHF). Figure 5-1 graphically depicts the analysis setting.

Both the cumulative arrival curve and the cumulative departure curve are monotonically increasing functions. If we have enough information to construct both of these curves, then the “delay” during the period can be found by simply calculating the area between the curves. However, if we are dependent upon detection devices located at the intersection then, during periods of over-saturated flow, we will only be able to measure the attributes of the departure curve, not the arrival curve, since the end of the queue will be beyond our Field of View (FOV).

Under these circumstances we can still obtain, after the one-hour analysis period ends, a reasonable estimation of the delay that occurred during the period. We cannot know with certainty the delay that occurred because we have no direct knowledge of the shape of the arrival

curve. However, we can obtain an estimate of the most-likely amount of delay and can put limits on the expected error associated with that estimate.

The delay estimation begins by measuring the following values: 1.) the total number of vehicles that arrived during the analysis period; which also equals the number of vehicles that departed during the analysis period since it is assumed that the overflow queue fully dissipates, 2.) the overflow queue clearance time, or the time point at which the cumulative arrival curve and the cumulative departure curves intersect; which is also the time at which the overflow queue is reduced to zero, and 3.) the total number of vehicles that have arrived when the overflow queue clearance time was reached.

Using this information, the arrival rate during the last 15-minute period (period 4) of the hour can be calculated:

$$AR_4 = (CA_{60}-CA_C)/(T_{60}-T_C) \quad (1)$$

Where: AR_4 = Arrival Rate during period 4 (veh/sec)
CA_{60} = Cumulative Arrivals at time point 60 (end of the hour)
CA_C = Cumulative Arrivals at overflow queue Clearance time point
T_{60} = Time point 60 (3600 seconds)
T_C = Time point when overflow queue Clears

In the example shown in Figure 5-2, the arrival rate is calculated to be:

$$AR_4 = (575 \text{ veh} – 540 \text{ veh})/(3600 \text{ sec} – 3240 \text{ sec}) = 0.0972 \text{ veh/sec}$$

This can be converted to an hourly flow rate by multiplying by 3600 sec/hour:

$$V_4 = (0.0972 \text{ veh/sec})(3600 \text{ sec/hour}) = 350 \text{ veh/hr}$$

The cumulative number of arriving vehicles at the beginning of the last 15-minute period is calculated by multiplying this terminal hourly flow rate by the duration of the period and then subtracting the resulting value from the cumulative number of arriving vehicles at time point 60:

$$CA_{45} = CA_{60} – (AR_4)(t_4) \text{ , or}$$
$$CA_{45} = CA_{60} – V_4 \quad (2)$$

Where: AR_4 = Arrival Rate during period 4 (veh/sec)
V_4 = Arrival Flow Rate during period 4 (veh/hr)
CA_{60} = Cumulative Vehicles at time point 60 (end of the hour)
CA_{45} = Cumulative Vehicles at time point 45
t_4 = Duration of the 4^{th} 15-minute time period (sec)

Continuing the Figure 5-2 example, the cumulative number of arrivals at the beginning of the last 15-minute time period is calculated as:

CA_{45} = 575 veh – (0.0972 veh/sec)(900 sec) = 487.5 veh

Given this value, we can now calculate the amount of overflow delay that occurs during the last 15-minute period (see Figure 5-3):

OD_4 = Area between Cumulative Arrival Curve and Uniform Departure Curve

$$OD_4 = 0.5\,(t_{4S})^2(UDR_4 - AR_4) = 0.5(T_c - T_{45})^2(UDR_4 - AR_4) \quad (3)$$

Where: OD_4 = Overflow Delay during period 4 (veh-sec)
UDR_4 = Uniform Departure Rate during period 4 (veh/sec)
AR_4 = Arrival Rate during period 4 (veh/sec)
t_{4S} = Duration of over-saturated flow during 4^{th} 15-min time period (sec)

For our example, the overflow delay during period 4 is calculated to be:

OD_4 = 0.5 (3240 sec – 2700 sec)^2(0.1667 veh/sec – 0.0972 veh/sec) = 10,133 veh-sec

And the arrival rate in vehicles per hour during period 4 (V_4) is calculated as:

V_4 = (575 veh – 487.5 veh)(4/hr) = 350 veh/hr

Calculating the overflow delay for the other three periods is not as straightforward. The arrival rate during each period cannot be definitively established since one can only measure the departure rate, not the true arrival rate, and since the extent of the queue is only visible to the end of the Field of View. However, even with this limited information, one can still develop a “best estimate” of the overflow delay. This is done by identifying both a “maximum reasonable delay” arrival curve and a “minimum reasonable delay” arrival curve. Maximum and minimum delay

curves are then calculated which correspond to each of these arrival curves and a check conducted to ensure that the delay estimated by the BuckQ analysis procedure falls within these bounds. We can also use the theoretical bounds to establish an independent "best" estimate of the overflow delay by construction an intermediate delay curve that minimizes the "maximum percent error" in delay at each time point.

Two reasonable assumptions are required in order to bracket the estimated overflow delay on both the low and high side. The first assumption is that the arrival rate observed during the final 15-minute period is the lowest rate experienced during the hour. The second assumption is that the PHF (Peak Hour Factor) is greater than or equal to some reasonable minimum value (such as 0.75) that is specified in advance. The minimum PHF value can be easily obtained through an examination of historical traffic counts for the approach under study.

A third assumption is also inherent in the proposed methodology; the assumption that the arrival rate is constant over each 15 minute period. If the rival rate varies during a given 15-minute period then the cumulative arrival curve will appear curvilinear in nature. This can be problematic when dealing with the lower bound.

Derivation of the Upper Bound

Conservation of flow principals dictate that the average of the arrival flow rates during each of the four 15-minute periods must equal the arrival rate over the entire 1-hour period:

$$(V_1 + V_2 + V_3 + V_4)/4 = CA_{60} \quad (4)$$

Where: V_i = Arrival Flow Rate during period i (veh/hr)
CA_{60} = Cumulative Arrivals at time point 60 (veh)

Equation (4) constitutes the first constraint on the solution space for both the minimum and maximum reasonable delay curves. Continuing our example, equation (4) becomes:

$$(V_1 + V_2 + V_3 + 350 \text{ veh/hr})/4 = 575 \text{ veh/hr}$$

$V_1 + V_2 + V_3 = 1950$ veh/hr

Maximum overall delay is obtained when the highest 15-minute flow rates occur at the start of the hour. Consequently, when identifying the maximum reasonable delay curve, the PHF is defined as follows:

$PHF = (V_1+V_2+V_3+V_4)/[(4)Max(V_1,V_2,V_3,V_4)]$

$PHF = (V_1+V_2+V_3+V_4)/4V_1$ (5)

Equation (5) constitutes the second constraint on the solution space for the maximum reasonable delay curve. Assuming a minimum PHF of 0.75 and continuing our example, equation (5) becomes:

$0.75 = (V_1+V_2+V_3+350 \text{ veh/hr})/4V_1$

$3V_1 = (V_1+V_2+V_3+350 \text{ veh/hr})$

$2V_1 – V_2 – V_3 = 350$ veh/hr

Equations (4) and (5) cannot be uniquely solved since we have only 2 equations to solve for 3 unknown variables (V_1, V_2 and V_3). However, an examination of the solution space for this problem indicates that we can obtain an additional equation by attempting to set V_2 as high as possible (in a continued attempt to maximize delay). In this case, the upper limit for V_2 is V_1. V_2 cannot be greater than V_1 or delay would not be maximized.

With V_1 forming the upper limit for V_2 we have the additional equation:

$V_1 = V_2$ (6)

We can now solve for all of the Vi's. Substituting equation (6) into equation (4) produces:

$V_1 + V_1 + V_3 + V_4 = 4CA_{60}$

$2V_1 + V_3 + V_4 = 4CA_{60}$

$V_3 = 4CA_{60} – V_4 – 2V_1$ (7)

And substituting equations (6) and (7) into equation (5) produces:

$$PHF = (V_1 + V_1 + (4CA_{60} - V_4 - 2V_1) + V_4)/(4V_1)$$

$$PHF = (V_1 + V_1 + 4CA_{60} - V_4 - 2V_1 + V_4)/(4V_1)$$

$$PHF = (4CA_{60})/(4V_1)$$

$$4V_1PHF = 4CA_{60}$$

$$V_1 = CA_{60}/PHF \quad (8)$$

Substituting equation (8) into equation (6) produces:

$$V_2 = CA_{60}/PHF \quad (9)$$

And substituting equations (8) and (9) into equation (4) yields:

$$CA_{60}/PHF + CA_{60}/PHF + V_3 + V_4 = 4CA_{60}$$

$$V_3 = 4CA_{60} - 2CA_{60}/PHF - V_4$$

$$V_3 = 2CA_{60}(2 - 1/PHF) - V_4 \quad (10)$$

Continuing our example and utilizing equations (8), (9), and (10):

$$V_1 = 575/0.75 = 766.7 \text{ veh/hr}$$

$$V_2 = 575/0.75 = 766.7 \text{ veh/hr}$$

$$V_3 = 2(575 \text{ veh/hr})(2 - 1/(0.75)) - 350 \text{ veh/hr} = 416.7 \text{ veh/hr}$$

So, for our example, the cumulative arrival curve that produces the maximum reasonable delay has quartile hourly flow rates of: **766.7 vph, 766.7 vph, 416.7 vph, and 350.0 vph.** This upper bound curve is depicted in Figure 5-4.

In this example, V_1 was a feasible upper limit for V_2, which results in maximum delay. However, it is possible that V_1 may not be a feasible upper limit for V_2. This occurs when the value of V_4 is too high to allow V_1 to equal V_2 without violating the minimum PHF requirement.

To account for this possibility, equation (10) must be restricted so that V_3 is greater than or equal to V_4. And since maximum delay occurs when V_3 is minimized (which, in turn, maximizes V_2 subject to the PHF constraint), V_3 must equal V_4. In other words, If V_1 does not form the upper limit for V_2 then maximum delay will be obtained when $V_3 = V_4$, which is the minimum V_3 given our initial assumption that V_3 must be greater than V_4. The value of V_4 at which this restriction occurs can be found by setting V_3 equal to V_4 in equation (10):

$$V_3 = 2CA_{60}(2 - 1/PHF) - V_3$$

$$2V_3 = 2CA_{60}(2 - 1/PHF)$$

$$V_3 = CA_{60}(2 - 1/PHF) = V_4 \quad (11)$$

For our example:

$$V_3 = 575(2 - 1/0.75) = 383.3 \text{ veh/hr}$$

$$V_4 = V_3 = 383.3 \text{ veh/hr}$$

Consequently, in our example, if V_4 is less than 383.3 then $V_1 = V_2$ and equation (10) can be used to calculate V_3. Otherwise, V_3 must be set equal to V_4 and the remaining equations solved accordingly. In general, V_3 must be set equal to V_4 if $V_4 > CA_{60}(2 - 1/PHF)$. If V_1 does not form the upper limit for V_2 then we have the additional equation:

$$V_3 = V_4 \quad (12)$$

We can once again solve for all of the Vi's. Substituting equation (12) into equation (4) produces:

$$V_1 + V_2 + V_4 + V_4 = 4CA_{60}$$

$$V_1 + V_2 + 2V_4 = 4CA_{60}$$

$$V_2 = 4CA_{60} - V_1 - 2V_4 \quad (13)$$

And substituting equations (12) and (13) into equation (5) produces:

$$PHF = (V_1 + (4CA_{60} - V_1 - 2V_4) + V_4 + V_4)/(4V_1)$$

$$PHF = (V_1 + 4CA_{60} - V_1 - 2V_4 + 2V_4)/(4V_1)$$

$$PHF = (4CA_{60})/(4V_1)$$

$$4V_1PHF = 4CA_{60}$$

$$V_1 = CA_{60}/PHF \quad (8)$$

This is the same result as before for V_1. Substituting equation (8) into equation (13) produces:

$$V_2 = 4CA_{60} - CA_{60}/PHF - 2V_4$$

$$V_2 = (4 - 1/PHF)CA_{60} - 2V_4 \quad (14)$$

If, in our example, V_4 was actually 385 instead of 350, then setting $V_1 = V_2$ and using equation (10) would result in a value for V_3 of:

$$V_3 = 2(575 \text{ vph})(2 - 1/0.75) - 385 \text{ vph} = 381.6 \text{ vph}$$

But this is not acceptable, since $V_3 = 381.6$ would be less than $V_4 = 385$, which violates our original assumption that the last period must be the period with the lowest flow rate. Rather, if $V_4 = 385$ vph, then V_3 must be set equal to V_4 and equation (13) used to solve for V_2 (The value of V_1 does not change):

$$V_2 = (4 - 1/0.75)(575 \text{ vph}) - 2(385 \text{ vph}) = 763.3$$

So, for this modified example, the cumulative arrival curve that produces the maximum reasonable delay has quartile hourly flow rates of: 766.7 vph, 763.3 vph, 385.0 vph, and 385.0 vph.

Derivation of the Lower Bound

We previously discussed how conservation of flow principals dictate that the average of the arrival rates during each of the four 15-minute periods must equal the arrival rate over the entire 1 hour period:

$$(V_1 + V_2 + V_3 + V_4)/4 = CA_{60} \quad (4)$$

Where:

V_i = Arrival Rate during period i (veh/hr)
CA_{60} = Cumulative Arrivals at time point 60 (veh)

For our example, equation (4) became:

$$(V_1 + V_2 + V_3 + 350 \text{ veh/hr})/4 = 575 \text{ veh/hr}$$

$$V_1 + V_2 + V_3 = 1950 \text{ veh/hr}$$

Minimum delay occurs when the vertical distance between the arrival curve and the departure curve (the nominal queue length) is continually minimized, without the end of the queue becoming visible. This happens when the nominal queue length equals the Field of View (FOV). Under these conditions, the minimum value for V_1 is:

$$V_1 = [(UDR_1)(t_1) + FOV] \text{ x 4 periods/hr, or}$$

$$V_1 = C_1 + 4FOV \quad (15)$$

Where: V_1 = Arrival Rate during period 1 (veh/hr)
UDR_1 = Uniform Departure Rate during period 1 (veh/sec)
FOV = Field of View (veh)
t_1 = Duration of 1st 15-min time period (sec/period) = 900 sec/period
C_1 = Capacity during period 1 (veh/hr)

V_1 cannot be any lower than this value or the end of the queue would be visible at the end of period 1 and no estimation of the delay associated with the overflow queue would be required. If V_1 equals this absolute lower bound, then we can continue to minimize delay by having V_2 equal the following:

$$V_2 = [(UDR_2)(t_2)] \text{ x 4 periods/hr, or}$$

$$V_2 = C_2 \quad (16)$$

This produces a cumulative arrival curve for period 2 that parallels the uniform departure curve for period 2. Assuming a FOV of 12, we continue our example as follows:

V_1 = [(0.1667 veh/sec)(900 sec/period) + 12 veh] x 4 periods/hr = 600 + 48 = 648 veh/hr

V_2 = [(0.1667 veh/sec)(900 sec/period)] x 4 periods/hr = 600 veh/hr

We can now solve for all of the Vi's. Substituting equations (15) and (16) into equation (4) produces:

$$C_1 + 4FOV + C_2 + V_3 + V_4 = 4CA_{60}$$

$$V_3 = 4CA_{60} - C_1 - C_2 - 4FOV - V_4 \quad (17)$$

For our example:

V_3 = 4/hr (575 veh) – (600 veh/hr) – (600 veh/hr) – 4/hr (12 veh) – 350 veh/hr = 702 veh/hr

So, for our example, the cumulative arrival curve that produces the minimum reasonable delay has quartile hourly flow rates of: **648.0 vph, 600.0 vph, 702.0 vph, and 350.0 vph.** This lower bound curve is depicted in Figure 5-5.

When calculating the upper bound arrival curves, the minimum PHF is always maintained; it represents a constraint on the solution space that is always in effect. However, this is not so with the lower bound. Under lower bound conditions the PHF may or may not pose a constraint. Substituting equations (15) and (16) into equation (5), and recognizing that V_3 is the highest 15-minute volume in this situation, the following is produced:

$$PHF = (V_1+V_2+V_3+V_4)/[(4)Max(V_1,V_2,V_3,V_4)] \quad (5)$$

$$PHF = (V_1+V_2+V_3+V_4)/4V_3$$

$$PHF = (C_1 + 4FOV + C_2 + V_3 + V_4) / 4V_3$$

$$PHF = (C_1 + C_2 + 4FOV + V_3 + V_4) / 4V_3 \quad (5B)$$

Substituting equation (17) into equation (5B) produces:

$$PHF = (C_1 + C_2 + 4FOV + 4CA_{60} - C_1 - C_2 - 4FOV - V_4 + V_4) / 4 (4CA_{60} - C_1 - C_2 - 4FOV - V_4)$$

$$PHF = 4CA_{60} / 4(4CA_{60} - C_1 - C_2 - 4FOV - V_4)$$

$$PHF = CA_{60} / (4CA_{60} - C_1 - C_2 - 4FOV - V_4) \quad (18)$$

Continuing our example:

PHF = (575 veh/hr)/[(4(575 veh/hr) – (600 veh/hr) – (600 veh/hr) – 4/hr(12 veh) – 350 veh/hr]

PHF = 575 veh/hr / 702 veh/hr = 0.819

The actual peak hour factor is considerably larger than the minimum required value of 0.75. In this example, it was feasible for both V_1 and V_2 to meet their absolute minimum lower bounds. However, it is possible that V_1 may be able to meet its absolute minimum lower bound while V_2 cannot, or even that both V_1 and V_2 cannot meet their absolute minimum lower bounds. This restriction occurs when the value of V_4 is too low to allow V_1 and/or V_2 to meet their absolute minimum lower bounds without either violating the minimum PHF requirement, the conservation of flow equation, or causing the nominal queue length to shrink to a value that is less than the FOV (thus eliminating the need for delay estimation).

If V_1 and V_2 are at their absolute minimum lower bound, then the maximum value for V_4 can be calculated by setting V_3 equal to its lowest possible bound which, as with V_2, is parallel to the cumulative departure curve:

$$V_3 = C_3 \tag{19}$$

Substituting equation (19) into equation (17) yields:

$$C_3 = 4CA_{60} - C_1 - C_2 - 4FOV - V_4$$

$$V_4 = 4CA_{60} - C_1 - C_2 - C_3 - 4FOV \tag{20}$$

Or, for our example:

V_4 = 4/hr (575 veh) – (600 veh/hr) – (600 veh/hr) – (600 veh/hr) – 4/hr (12 veh)

V_4 = 2300 veh/hr – 1800 veh/hr – 48 veh/hr

V_4 = 452 veh/hr

The result is graphically depicted in Figure 5-6. This arrival curve produces the overall minimum delay and has quartile hourly flow rates of: **648.0 vph, 600.0 vph, 600.0 vph, and 452.0 vph.**

Once again, the PHF does not impose a constraint in this situation. Under conditions of overall minimum delay, V_1 is always the highest 15-minute volume, therefore:

$$PHF = (V_1+V_2+V_3+V_4)/[(4)Max(V_1,V_2,V_3,V_4)] = (V_1+V_2+V_3+V_4)/4V_1 \quad (5)$$

$$PHF = (C_1 + 4FOV + C_2 + C_3 + V_4) / 4(C_1 + 4FOV)$$

$$PHF = (C_1 + C_2 + C_3 + 4FOV + V_4) / 4(C_1 + 4FOV) \quad (21)$$

Continuing our example:

PHF=[600veh/hr+600veh/hr+600veh/hr+4/hr(12 veh)+452veh/hr]/4(600 veh/hr+4/hr(12 veh))

PHF = 2300 veh/hr / 2592 veh/hr = 0.887

The actual peak hour factor is once again considerably larger than the minimum required value of 0.75 If V_1 and V_2 are at their absolute minimum lower bound, then the minimum value for V_4 can be calculated by setting V_3 equal to its highest possible value while maintaining the minimum required peak hour factor and preserving conservation of flow. Substituting equations (15) and (16) into equation (4):

$$(C_1 + 4FOV + C_2 + V_3 + V_4)/4 = CA_{60}$$

$$C_1 + C_2 + 4FOV + V_3 + V_4 = 4CA_{60}$$

$$V_4 = 4(CA_{60} - FOV) - C_1 - C_2 - V_3 \quad (22)$$

Equation (22) is merely a rearrangement of equation (17). Substituting equations (15) and (16) into equation (5) and recognizing that V_3 has the highest arrival volume for this situation:

$$PHF = (C_1 + 4FOV + C_2 + V_3 + V_4) / 4V_3$$

$$4PHFV_3 = C_1 + C_2 + 4FOV + V_3 + V_4$$

$$4PHFV_3 - V_3 = C_1 + C_2 + 4FOV + V_4 \quad (23)$$

Substituting equation (22) into equation (23) yields:

$$4PHFV_3 - V_3 = C_1 + C_2 + 4FOV + 4CA_{60} - C_1 - C_2 - 4FOV - V_3$$

$$4PHFV_3 = 4CA_{60}$$

$$V_3 = CA_{60} / PHF \quad (24)$$

Now substituting equation (24) back into equation (22) gives:

$$V_4 = 4CA_{60} - C_1 - C_2 - 4FOV - CA_{60} / PHF$$

$$V_4 = (4 - 1/PHF)CA_{60} - C_1 - C_2 - 4FOV \quad (25)$$

Using the example values we obtain:

$$V_3 = 575/0.75 = 766.7 \text{ veh/hr}$$

and $V_4 = (4\text{-}1/0.75)(575) - 600 - 600 - 4(12) = 1533.3 - 1200 - 48$

$$V_4 = 285.3 \text{ veh/hr}$$

So, V_4=285.3 vph is the lowest possible V_4 value that will allow both V_1 and V_2 to meet their absolute minimum lower bounds (see Figure 5-7).

We have now examined the case where V_1, V_2 and V_3 are all at their minimum values, and we have examined the case where V_1 and V_2 are at their minimum values but V_3 is not. The next arrangement of interest is when only V_1 is at its minimum value. Substituting equation (15) into equation (4) yields:

$$(C_1 + 4FOV + V_2 + V_3 + V_4)/4 = CA_{60}$$

Solving for V_2:

$$V_2 = 4CA_{60} - C_1 - 4FOV - V_4 - V_3 \quad (26)$$

For this situation, minimum delay is obtained when V_3 is maximized, subject to the peak hour constraint. Therefore:

$$PHF = (V_1+V_2+V_3+V_4) / [4Max(V_1,V_2,V_3,V_4)] = (V_1+V_2+V_3+V_4)/4V_3 \quad (5)$$

Substituting equations (15) and (26) into equation (5) yields:

$$PHF = (C_1 + 4FOV + 4CA_{60} - C_1 - 4FOV - V_4 - V_3 + V_3 + V_4)/4V_3$$

$$PHF = (4CA_{60})/4V_3$$

Solving for V_3:

$$V_3 = (CA_{60})/PHF \quad (27)$$

Now substituting equation (27) back into equation (26) gives:

$$V_2 = 4CA_{60} - C_1 - 4FOV - V_4 - (CA_{60})/PHF$$

$$V_2 = (4 - 1/PHF)CA_{60} - C_1 - 4FOV - V_4 \quad (28)$$

We recognize that the highest possible value for V_4 will occur when V_2 is as low as possible, which occurs when:

$$V_2 = C_2 \quad (16)$$

Substituting equation (16) into equation (28) produces:

$$C_2 = (4 - 1/PHF)CA_{60} - C_1 - 4FOV - V_4$$

Solving for V_4:

$$V_4 = (4 - 1/PHF)CA_{60} - C_1 - C_2 - 4FOV \quad (25)$$

This formula is consistent with the results obtained previously. We also recognize that the lowest possible V_4 will occur when V_2 is as high as possible, which is when $V_2 = V_3$:

$$V_2 = V_3 \quad (29)$$

Substituting equations (27) and (29) into equation (28) produces:

$$(CA_{60})/PHF = (4 - 1/PHF)CA_{60} - C_1 - 4FOV - V_4$$

Solving for V_4:

$$V_4 = (4 - 1/PHF)CA_{60} - C_1 - 4FOV - (CA_{60})/PHF$$

$$V_4 = 4CA_{60}/hr - (CA_{60})/PHF - C_1 - 4FOV - (CA_{60})/PHF$$

$$V_4 = 4CA_{60}/hr - 2(CA_{60})/PHF - C_1 - 4FOV$$

$$V_4 = 2CA_{60}(2 - 1/PHF) - C_1 - 4FOV \quad (30)$$

Using our example values we obtain:

$$V_4 = 2(575 \text{ veh/hr})(2\text{-}1/0.75) - 600 \text{ veh/hr} - 4/hr(12 \text{ veh}) = 118.7 \text{ veh/hr}$$

So, $V_4 = 118.7$ vph is the lowest possible V_4 value that will allow V_1 to meet its absolute minimum lower bound (see Figure 5-8). If V_4 falls below the value given in equation (30) then V_1 (along with V_2 and V_3) will no longer be at its minimum value. For this situation, minimum delay is obtained when V_3 is maximized, subject to the peak hour constraint, and when $V_2 = V_3$. Therefore:

$$PHF = (V_1+V_2+V_3+V_4)/[(4)Max(V_1,V_2,V_3,V_4)] = (V_1+V_2+V_3+V_4)/4V_3 \quad (5)$$

Substituting equation (29) into equation (5) yields:

$$PHF = (V_1 + V_3 + V_3 + V_4)/4V_3$$

$$PHF = (V_1 + 2V_3 + V_4)/4V_3$$

$$4V_3PHF = V_1 + 2V_3 + V_4$$

$$4V_3PHF - 2V_3 = V_1 + V_4$$

$$V_1 = 4V_3PHF - 2V_3 - V_4 \quad (31)$$

Substituting equations (29) and (31) into equation (4) produces:

$$(4V_3PHF - 2V_3 - V_4 + V_3 + V_3 + V_4)/4 = CA_{60}$$

$$4V_3PHF/4 = CA_{60}$$

$$V_3 = CA_{60}/PHF \quad (27)$$

Substituting equation (27) into equation (29) yields:

$$V_2 = CA_{60}/PHF \quad (32)$$

The value for V_1 can be determined by substituting equations (27) and (32) into equation (4), which produces:

$$(V_1 + CA_{60}/PHF + CA_{60}/PHF + V_4)/4 = CA_{60}$$

$$V_1 + 2CA_{60}/PHF + V_4 = 4CA_{60}$$

$$V_1 = 4CA_{60} - 2CA_{60}/PHF - V_4$$

$$V_1 = 2CA_{60}(2 - 1/PHF) - V_4 \quad (33)$$

Analysis of Bounds Summary

The results of the analysis of the bounds can be summarized as follows:

UPPER BOUND

$V_1 = CA_{60}/PHF$ (8)

If $V_4 < CA_{60}(2 - 1/PHF)$ (11)

Then: $V_2 = CA_{60}/PHF$ (9)
$V_3 = 2CA_{60}(2 - 1/PHF) - V_4$ (10)

If $V_4 > CA_{60}(2 - 1/PHF)$ (11)

Then: $V_2 = CA_{60}(4 - 1/PHF) - 2V_4$ (14)
$V_3 = V_4$ (12)

LOWER BOUND

If $V_4 = 4CA_{60} - C_1 - C_2 - C_3 - 4FOV$ (20)

Then: $V_1 = C_1 + 4FOV$ (15)
$V_2 = C_2$ (16)
$V_3 = C_3$ (19)
$PHF = CA_{60} / (4CA_{60} - C_1 - C_2 - 4FOV - V_4)$ (18)

If $V_4 < 4CA_{60} - C_1 - C_2 - C_3 - 4FOV$ (20)
And $V_4 >= (4 - 1/PHF)CA_{60} - C_1 - C_2 - 4FOV$ (25)

Then: $V_1 = C_1 + 4FOV$ (15)
$V_2 = C_2$ (16)
$V_3 = 4CA_{60} - C_1 - C_2 - 4FOV - V_4$ (17)
$PHF = (C_1 + C_2 + C_3 + 4FOV + V_4) / 4(C_1 + 4FOV)$ (21)

If $V_4 < (4 - 1/PHF)CA_{60} – C_1 – C_2 – 4FOV$ (25)
And $V_4 >= 2CA_{60}(2- 1/PHF) – C_1 – 4FOV$ (30)

Then: $V_1 = C_1 + 4FOV$ (15)
$V_2 = (4 – 1/PHF)CA_{60} – C_1 – 4FOV – V_4$ (28)
$V_3 = CA_{60}/PHF$ (27)

If $V_4 < 2CA_{60}(2- 1/PHF) – C_1 – 4FOV$ (30)

Then: $V_1 = 2CA_{60}(2 – 1/PHF) - V_4$ (33)
$V_2 = CA_{60}/PHF$ (32)
$V_3 = CA_{60}/PHF$ (27)

For our example, the values are:

UPPER BOUND

V_1 = 575 vph/0.75 = **766.7 vph**

Is **V_4 = 350 vph** < 575 vph (2 – 1/0.75) = 383.3 vph ?
YES

Then:
V_2 = 575 vph/0.75 = **766.7 vph**
V_3 = 2(575 vph)(2 – 1/0.75) – 350 vph = **416.7 vph**

LOWER BOUND

Is **V_4 = 350 vph** > $4CA_{60} – C_1 – C_2 – C_3 – 4FOV$?
Is V_4 = 350 vph > 4(575 vph) – 3(600 vph) – 4/hr (12 veh) = 2300 – 1800 – 48 = 452?
NO

Is V_4 = 350 vph > $(4 - 1/PHF)CA_{60} – C_1 – C_2- 4FOV$?
Is V_4 = 350 vph > (4 - 1/0.75)575 vph – 2(600 vph) – 4/hr(12 veh)?
Is V_4 = 350 vph > 1533.3 vph – 1200 vph – 48 vph = 285.3 vph?
YES

Then: **V_1** = C_1 + 4FOV = 600 vph + 4/hr(12 veh) = 600 vph + 48 vph = **648 vph**
V_2 = C_2 = **600 vph**
$V_3 = 4CA_{60} – C_1 – C_2– 4FOV – V_4$
V_3 = 4(575 vph) – 2(600 vph) – 4/hr(12 veh) – 350 vph
V_3 = 2300 vph – 1200 vph – 48 vph – 350 vph = **702 vph**

Is V_4 = 350 vph < $2CA_{60}(2- 1/PHF) – C_1 – 4FOV$?
Is V_4 = 350 vph < 2(575 vph)(2- 1/0.75) – 600 vph – 4/hr(12 veh)?

Is $V_4 = 350$ vph < 766.67 vph $- 600$ vph $- 48$ vph $= 118.7$ vph?

NO

Derivation of Delay for Upper and Lower Bounds

Figure 5-9 shows the first two periods of the upper bound curve for our example. The Overflow Delay for period 1 (OD_1) is simply the area between the arrival and departure curves within period 1. On the other hand, the Deterministic Queue Delay for period 1 (DQD_1) is composed of two elements: the in-period delay for period 1 (Dp_1) and the out-of-period delay for period 1 (Dc_1). Both of these elements of the period 1 Deterministic Queue Delay are associated with vehicles that arrive at the back of the queue during period 1, however, only the in-period delay actually occurs during period 2.

For period 1, the in-period DQD equals the Overflow Delay, and can be calculated using the following formulas:

$$CA_{15} = (V_1/3600 \text{ sec/hr})(T_{15} - T_0) \quad (34)$$

$$UCD_{15} = (C_1/3600 \text{ sec/hr})(T_{15} - T_0) \quad (35)$$

$$OD_1 = Dp_1 = 0.5(T_{15} - T_0)(CA_{15} - UCD_{15}) \quad (36)$$

Substituting equations (34) and (35) into equation (36) yields:

$$OD_1 = Dp_1 = 0.5(T_{15} - T_0)[(V_1/3600 \text{ sec/hr})(T_{15} - T_0) - (C_1/3600 \text{ sec/hr})(T_{15} - T_0)]$$

$$OD_1 = 0.5(T_{15} - T_0)(T_{15} - T_0)(V_1 - C_1)/3600 \text{ sec/hr}$$

$$OD_1 = Dp_1 = (T_{15} - T_0)^2(V_1 - C_1)/7200 \text{ sec/hr} \quad (37)$$

Where:
- CA_{15} = Cumulative Arrivals at time point 15 (veh)
- UCD_{15} = Uniform Cumulative Departures at time point 15 (veh)
- OD_1 = Overflow Delay during period 1 (sec)
- C_1 = Capacity during period 1 (veh/sec)
- V_1 = Arrival Rate during period 1 (veh/hr)
- T_0 = Time Point at Beginning of 15 minutes (sec) = 0 sec
- T_{15} = Time Point at End of First 15 minutes (sec) = 900 sec

For our example:

CA_{15} = (766.7 veh/hr/3600 sec/hr)(900 sec) = **191.7 veh**

C_1 = 600.0 veh

$OD_1 = Dp_1 = (900 \text{ sec})^2(766.7 \text{ veh/hr} - 600 \text{ veh/hr})/7200 \text{ sec/hr}$

$OD_1 = Dp_1$ = 18,750 veh-sec

The out-of-period portion of the DQD for period 1, which actually occurs in period 2, is calculated using the following formulas. Accumulating departures:

$$UCD_{C1} = UCD_{15} + (C_2/3600 \text{ sec/hr})(T_{C1} - T_{15}) \quad (38)$$

A critical time point occurs when the last arriving vehicle during period 1 departs. This occurs when:

$$UCD_{C1} = CA_{15} \quad (39)$$

Where:

UCD_{Ci} = Uniform Cumulative Departures at time point Ci (veh)
C_i = Capacity during period i (veh/sec)
T_{Ci} = Critical Time Point (T_{C1} is the critical time point at which the number of Uniform Cumulative Departures = CA_{15})
CD_{Ci} = Cumulative Departures at Critical Time Point T_{Ci} (sec)

Substituting equation (39) into equation (38) and solving for T_{C1} yields:

$$CA_{15} = UCD_{15} + (C_2/3600 \text{ sec/hr})(T_{C1}) - (C_2/3600 \text{ sec/hr})(T_{15})$$

$$(CA_{15} - UCD_{15}) + (C_2/3600 \text{ sec/hr})(T_{15}) = (C_2/3600 \text{ sec/hr})(T_{C1})$$

$$T_{C1} = 3600 \text{ sec/hr } (CA_{15} - UCD_{15})/C_2 + T_{15} \quad (40)$$

For period 1, the out-of-period DQD can be calculated using the following formula:

$$Dc_1 = 0.5(T_{C1} - T_{15})(CA_{15} - UCD_{15}) \quad (41)$$

For our example:

T_{C1} = 3600 sec/hr (191.7 veh – 150.0 veh)/600 veh/hr + 900 sec = **1150 sec**

And:

$Dc_1 = 0.5(1150 \text{ sec} – 900 \text{ sec})(191.7 \text{ veh} – 150 \text{ veh}) =$

$Dc_1 = 5208$ veh-sec

Figure 5-10 shows the second and third periods of the upper bound curve for our example. The Overflow Delay for period 2 (OD_2) is still simply the area between the arrival and departure curves within period 2. On the other hand, the Deterministic Queue Delay for period 2 (DQD_2) is now composed of four elements: the in-period over-saturation delay for period 2 (Dp_2), the out-of-period over-saturation delay for period 2 (Dc_2), the in-period initial queue delay for period 2 (D_{IQA2}) and the out-of-period initial queue delay for period 2 (D_{IQB2}). All four components of the period 2 Deterministic Queue Delay are associated with vehicles that arrive at the back of the queue during period 2, however, only the in-period delay and in-period initial queue delay actually occur during period 2, the out-of-period delay and out-of-period initial queue delay occur during period 3. The in-period DQD for Period 2 can be calculated using the following formulas:

Accumulating arrivals:

$$CA_{30} = (V_2/3600 \text{ sec/hr})(T_{30} – T_{15}) + CA_{15} \quad (42)$$

Accumulating departures:

$$UCD_{30} = (C_2/3600 \text{ sec/hr})(T_{30} – T_{15}) + UCD_{15} \quad (43)$$

By inspection we see that the bottom boundary of the area for Dp_2 begins at point C_{15} and is parallel to the departure curve. Defining UCD_{30A} as the cumulative number of vehicles obtained when this parallel boundary line reaches T_{30} (1800 sec), we have:

$$UCD_{30A} = (C_2/3600 \text{ sec/hr})(T_{30} – T_{15}) + CA_{15} \quad (44)$$

The in-period over-saturation delay is then calculated as:

$$Dp_2 = 0.5(T_{30} - T_{15})(CA_{30} - UCD_{30A}) \quad (45)$$

For our example:

CA_{30} = (766.7 veh/hr/3600 sec/hr)(1800 sec - 900 sec) + 191.7 veh = **383.3 veh**

UCD_{30} = (600 veh/hr/3600 sec/hr)(1800 sec - 900 sec) + 150 veh = **300.0 veh**

UCD_{30A} = (600 veh/hr/3600 sec/hr)(1800 sec - 900 sec) + 191.7 veh = **341.7 veh**

$Dp_2 = 0.5(1800 \text{ sec} - 900 \text{ sec})(383.3 \text{ veh} - 341.7 \text{ veh})$

$Dp_2 = (450 \text{ sec})(41.6 \text{ veh})$

Dp_2 = 18,750 veh-sec

The out-of-period over-saturation delay for period 2, which actually occurs in period 3, is calculated using the following formulas. Accumulating departures:

$$UCD_{C2A} = UCD_{30A} + (C_3/3600 \text{ sec/hr})(T_{C2A} - T_{30}) \quad (46)$$

A critical time point occurs when the last arriving vehicle during period 2 would have departed had there not been an initial queue at the beginning of time period 2:

$$UCD_{C2A} = CA_{30} \quad (47)$$

Substituting equation (47) into equation (46) and solving for T_{C2A} yields:

$CA_{30} = UCD_{30A} + (C_3/3600 \text{ sec/hr})(T_{C2A}) - (C_3/3600 \text{ sec/hr})(T_{30})$

$(CA_{30} - UCD_{30A}) + (C_3/3600 \text{ sec/hr})(T_{30}) = (C_3/3600 \text{ sec/hr})(T_{C2A})$

$$T_{C2A} = (3600 \text{ sec/hr})(CA_{30} - UCD_{30A})/C_3 + T_{30} \quad (48)$$

For period 2, the out-of-period over-saturation delay can be calculated using the following formula:

$$Dc_2 = 0.5(T_{C2A} - T_{30})(CA_{30} - UCD_{30A}) \quad (49)$$

For Figure 5-10 to be an accurate representation of the delay situation, the nominal queue length at T_{30} must be greater than the nominal queue length at T_{15}. If it is less, then both D_{P2} and D_{C2} are equal to zero. The nominal queue length at T_{30} is calculated as:

$$Q_{30} = CA_{30} - UCD_{30} \quad (50)$$

And the nominal queue length at T_{15} is:

$$Q_{15} = CA_{15} - UCD_{15} \quad (51)$$

Consequently:

If $Q_{30} > Q_{15}$ then equations (45) and (49) hold, otherwise $Dp_2 = Dc_2 = 0$

For our example:

$\mathbf{Q_{30}} = CA_{30} - UCD_{30} = 383.3$ veh – 300 veh **= 83.3 veh**

which is greater than:

$\mathbf{Q_{15}} = CA_{15} - UCD_{15} = 191.7$ veh – 150 veh = **41.7 veh**

Therefore, equations (45) and (49) hold:

$Dp_2 = 0.5(T_{30} - T_{15})(CA_{30} - UCD_{30A}) = 0.5(1800 \text{ sec} - 900 \text{ sec})(383.3 \text{ veh} - 341.7 \text{ veh})$

Dp_2 = 18,750 veh-sec

$T_{C2A} = (3600 \text{ sec/hr})(CA_{30} - UCD_{30A})/C_3 + T_{30}$

$T_{C2A} = (3600 \text{ sec/hr.})(383.3 \text{ veh} - 341.7 \text{ veh})/600 \text{ veh/hr} + 1800 \text{ sec}$

$T_{C2A} = 2050$ sec

$Dc_2 = 0.5(T_{C2A} - T_{30})(CA_{30} - UCD_{30A}) = 0.5(2050 \text{ sec} - 1800 \text{ sec})(383.3 \text{ veh} - 341.7 \text{ veh})$

Dc_2 = 5208 veh-sec

An inspection of Figure 5-10 reveals that the in-period initial queue delay for period 2 is represented by a trapezoid and a triangle. The trapezoid has a base of $T_{C1} - T_{15}$ and a height of $UCD_{30} - CA_{15}$. The triangle also has a base of $T_{C1} - T_{15}$ but its height is UCD_{30A}-UCD_{30}. Consequently:

$$D_{IQA2} = (T_{C1} - T_{15})(UCD_{30} - CA_{15}) + 0.5(T_{C1} - T_{15})(UCD_{30A} - UCD_{30})$$

$$D_{IQA2} = (T_{C1} - T_{15})[(UCD_{30} - CA_{15}) + 0.5(UCD_{30A} - UCD_{30})] \quad (52)$$

The total out-of-period delay for period 2, which actually occurs in period 3, is calculated using the following formulas. Accumulating departures:

$$UCD_{C2} = UCD_{30} + (C_3/3600 \text{ sec/hr})(T_{C2} - T_{30}) \quad (53)$$

Another critical time point occurs when the last vehicle arriving during period 2 departs:

$$UCD_{C2} = CA_{30} \quad (54)$$

Substituting equation (54) into equation (53) and solving for T_{C2} yields:

$$CA_{30} = UCD_{30} + (C_3/3600 \text{ sec/hr})(T_{C2}) - (C_3/3600 \text{ sec/hr})(T_{30})$$

$$(CA_{30} - UCD_{30}) + (C_3/3600 \text{ sec/hr})(T_{30}) = (C_3/3600 \text{ sec/hr})(T_{C2})$$

$$T_{C2} = (3600 \text{ sec/hr})(CA_{30} - UCD_{30})/C_3 + T_{30} \quad (55)$$

For period 2, the total out-of-period delay can be calculated using the following formula:

$$D_{T2} = 0.5(T_{C2} - T_{30})(CA_{30} - UCD_{30}) \quad (56)$$

The out-of-period initial queue delay for period 2 is then calculated by simply subtracting the out-of-period over-saturation delay from the total out-of-period delay:

$$D_{IQB2} = D_{T2} - D_{C2}$$

$$D_{IQB2} = 0.5(T_{C2} - T_{30})(CA_{30} - UCD_{30}) - D_{C2} \quad (57)$$

For Figure 5-10 to be an accurate representation of the delay situation such that equations (52) and (57) apply, the nominal queue length at T_{30} must be greater than the nominal queue length at T_{15}. If it is less, then both D_{IQA2} and D_{IQB2} are calculated using different equations, as we shall soon see for period 3. For our example the nominal queue length at T_{30} was previously shown to be greater than the nominal queue length at T_{15}. Therefore:

$$D_{IQA2} = (T_{C1} - T_{15})[(UCD_{30} - CA_{15}) + 0.5(UCD_{30A} - UCD_{30})]$$

D_{IQA2} = (1150 sec – 900 sec)[(300 veh – 191.7 veh) + 0.5(341.7 veh – 300 veh)]

D_{IQA2} = (1150 sec – 900 sec)[(300 veh – 191.7 veh) + 0.5(341.7 veh – 300 veh)]

D_{IQA2} = 32,292 veh–sec

T_{C2} = (3600 sec/hr)(CA_{30} – UCD_{30})/C_3 + T_{30}

T_{C2} = (3600 sec/hr)(383.3 veh – 300 veh)/600 veh/hr + 1800 sec

T_{C2} = 2300 sec

D_{IQB2} = 0.5(T_{C2} – T_{30})(CA_{30} – UCD_{30}) – D_{C2}

D_{IQB2} = 0.5(2300 sec – 1800 sec)(383.3 veh – 300 veh) – 5208 veh-sec

D_{IQB2} = 15,625 veh–sec

Figure 5-11 shows the third and fourth periods of the upper bound curve for our example. The Overflow Delay for period 3 (OD_2) is still simply the area between the arrival and departure curves within period 3. On the other hand, since the queue at the end of the period is smaller than the queue at the beginning of the period, the Deterministic Queue Delay for period 3 (DQD_3) is now composed of the following two elements: the in-period initial queue delay for period 3 (D_{IQA3}) and the out-of-period initial queue delay for period 3 (D_{IQB3}). Both components of the period 3 Deterministic Queue Delay are associated with vehicles that arrive at the back of the queue during period 3, however, only the in-period initial queue delay actually occurs during period 3, the out-of-period initial queue delay occurs during period 4. The in-period DQD for Period 3 can be calculated using the following formulas:

Accumulating arrivals:

$$CA_{45} = (V_3/3600 \text{ sec/hr})(T_{45} - T_{30}) + CA_{30} \quad (58)$$

Accumulating departures:

$$UCD_{45} = (C_3/3600 \text{ sec/hr})(T_{45} - T_{30}) + UCD_{30} \quad (59)$$

For our example:

$\mathbf{CA_{45}}$ = (416.7 veh/hr/3600 sec/hr)(2700 sec – 1800 sec) + 383.3 veh = **487.5 veh**

$\mathbf{UCD_{45}}$ = (600 veh/hr/3600 sec/hr)(2700 sec – 1800 sec) + 300 veh = **450.0 veh**

An inspection of Figure 5-11 reveals that the in-period initial queue delay for period 3 can be calculated by taking the difference of two triangles. The larger triangle has a base of $T_{45} - T_{30}$ and a height of $CA_{45} - CA_{30}$. The smaller triangle has a base of $T_{45} - T_{C2}$ and a height of $UCD_{45} - CA_{30}$. Consequently:

$$D_{IQA3} = 0.5(T_{45} - T_{30})(CA_{45} - CA_{30}) - 0.5(T_{45} - T_{C2})(UCD_{45} - CA_{30})$$

$$D_{IQA3} = 0.5[(T_{45} - T_{30})(CA_{45} - CA_{30}) - (T_{45} - T_{C2})(UCD_{45} - CA_{30})] \quad (60)$$

The out-of-period initial queue delay for period 3, which actually occurs in period 4, is calculated using the following formulas. Accumulating departures:

$$UCD_{C3} = UCD_{45} + (C_4/3600 \text{ sec/hr})(T_{C3} - T_{45}) \quad (61)$$

A critical time point occurs when the last vehicle arriving during period 3 departs:

$$UCD_{C3} = CA_{45} \quad (62)$$

Substituting equation (62) into equation (61) and solving for T_{C3} yields:

$$CA_{45} = UCD_{45} + (C_4/3600 \text{ sec/hr})(T_{C3}) - (C_4/3600 \text{ sec/hr})(T_{45})$$

$$(CA_{45} - UCD_{45}) + (C_4/3600 \text{ sec/hr})(T_{45}) = (C_4/3600 \text{ sec/hr})(T_{C3})$$

$$T_{C3} = (3600 \text{ sec/hr})(CA_{45} - UCD_{45})/C_4 + T_{45} \quad (63)$$

For period 3, the out-of-period initial queue delay can be calculated using the following formula:

$$D_{IQB3} = 0.5(T_{C3} - T_{45})(CA_{45} - UCD_{45}) \quad (64)$$

For our example:

$$D_{IQA3} = 0.5[(T_{45} - T_{30})(CA_{45} - CA_{30}) - (T_{45} - T_{C2})(UCD_{45} - CA_{30})]$$

$$D_{IQA3}=0.5[(2700\text{sec}-1800\text{sec})(487.5\text{veh}-383.3\text{veh})-(2700 \text{ sec}-1800 \text{ sec})(450 \text{ veh}-383.3 \text{ veh})]$$

$$D_{IQA3}=0.5[(2700\text{sec}-1800\text{sec})(487.5\text{veh}-383.3\text{veh})-(2700 \text{ sec}-2300 \text{ sec})(450 \text{ veh}-383.3 \text{ veh})]$$

D_{IQA3} = 33,542 veh-sec

$T_{C3} = (3600 \text{ sec/hr})(CA_{45} - UCD_{45})/C_4 + T_{45}$

$T_{C3} = (3600 \text{ sec/hr})(487.5 \text{ veh} - 450 \text{ veh})/600 \text{ veh/hr.} + 2700 \text{ sec}$

$T_{C3} = 2923 \text{ sec}$

$D_{IQB3} = 0.5(T_{C3} - T_{45})(CA_{45} - UCD_{45})$

$D_{IQB3} = 0.5(2925 \text{ sec} - 2700 \text{ sec})(487.5 \text{ veh} - 450 \text{ veh})$

D_{IQB3} = 4219 sec

For Figure 5-11 to be an accurate representation of the delay situation, the nominal queue length at T_{45} must be less than the nominal queue length at T_{30}. If it is greater, then both D_{IQA3} and D_{IQB3} are calculated as shown previously for period 2:

$$D_{IQA3} = (T_{C2} - T_{30})[(UCD_{45} - CA_{30}) + 0.5(UCD_{45A} - UCD_{45})] \quad (52B)$$

$$D_{IQB3} = 0.5(T_{C3} - T_{45})(CA_{45} - UCD_{45}) - D_{C3} \quad (57B)$$

The nominal queue length at T_{45} is calculated as:

$$Q_{45} = CA_{45} - UCD_{45} \quad (65)$$

For our example:

Q_{45} = $CA_{45} - UCD_{45}$ = 487.5 veh – 450 veh **= 37.5 veh**

Which is less than the previously calculated value for Q_{30} of 83.3 vehicles, therefore our calculations are correct. In general:

If $Q_{i+1} > Q_i$ then equations (52) and (57) hold, otherwise equations (60) and (64) hold

Figure 5-11 shows that the Deterministic Queue Delay for period 4 (DQD_4) is composed of just one element, the initial queue delay (D_{IQ4}). An inspection of Figure 5-11 reveals that this delay can be calculated by taking the difference of two triangles. The larger triangle has a base

of $T_{C4} - T_{45}$ and a height of $CA_{C4} - CA_{45}$. The smaller triangle has a base of $T_{C4} - T_{C3}$ and a height of $CA_{C4} - CA_{45}$. Consequently:

$$D_{IQ4} = 0.5(T_{C4} - T_{45})(CA_{C4} - CA_{45}) - 0.5(T_{C4} - T_{C3})(CA_{C4} - CA_{45})$$

$$D_{IQ4} = 0.5(CA_{C4} - CA_{45})(T_{C4} - T_{45} - T_{C4} + T_{C3})$$

$$D_{IQ4} = 0.5(CA_{C4} - CA_{45})(T_{C3} - T_{45}) \quad (66)$$

For our example:

$$D_{IQ4} = 0.5(CA_{C4} - CA_{45})(T_{C3} - T_{45}) = 0.5(540 \text{ veh} - 487.5 \text{ veh})(2925 \text{ sec} - 2700 \text{ sec})$$

D_{IQ4} = 5906 veh-sec

It should be pointed out that the period 4 delay situation that is represented in Figure 5-11 corresponds to the Case III situation described in Appendix F of the 2000 Highway Capacity Manual [4] whereas the period 3 situation represented in Figure 5-11 corresponds to CASE IV. In addition, the period 2 situation represented in Figure 5-10 corresponds to Case V and the period 1 situation represented in Figure 5-9 corresponds to Case II of Appendix F.

The total overflow delay for the one-hour analysis period is obtained by simply summing the individual 15-minute period overflow delays. Inspection of Figures 5-9 through 5-11 indicates that

$$OD_1 = D_{P1} \quad (67)$$

$$OD_2 = D_{C1} + D_{P2} + D_{IQA2} \quad (68)$$

$$OD_3 = D_{C2} + D_{IQB2} + D_{P3} + D_{IQA3} \quad (69)$$

$$OD_4 = D_{C3} + D_{IQB3} + D_{IQ4} \quad (70)$$

Therefore:

$$OD_T = OD_1 + OD_2 + OD_3 + OD_4 \quad (71)$$

$$OD_T = D_{P1} + D_{C1} + D_{P2} + D_{C2} + D_{IQA2} + D_{IQB2} + D_{P3} + D_{C3} + D_{IQA3} + D_{IQB3} + D_{IQ4} \quad (72)$$

For our example:

$\mathbf{OD_1 = D_{P1} = 18{,}750\ veh\text{-}sec}$

$OD_2 = D_{C1} + D_{P2} + D_{IQA2} = 5208\ veh\text{-}sec + 18{,}750\ veh\text{-}sec + 32{,}292\ veh\text{-}sec$

$\mathbf{OD_2 = 56{,}250\ veh\text{-}sec}$

$OD_3 = D_{C2} + D_{IQB2} + D_{P3} + D_{IQA3} = 5208\ veh\text{-}sec + 15{,}625\ veh\text{-}sec + 0\ veh\text{-}sec + 33{,}542\ veh\text{-}sec$

$\mathbf{OD_3 = 54{,}375\ veh\text{-}sec}$

$OD_4 = D_{C3} + D_{IQB3} + D_{IQ4} = 0\ veh\text{-}sec + 4219\ veh\text{-}sec + 5906\ veh\text{-}sec$

$\mathbf{OD_4 = 10{,}125\ veh\text{-}sec}$

$OD_T = OD_1 + OD_2 + OD_3 + OD_4$

$OD_T = 18{,}750\ veh\text{-}sec + 56{,}250\ veh\text{-}sec + 54{,}375\ veh\text{-}sec + 10{,}125\ veh\text{-}sec$

$\mathbf{OD_T = 139{,}500\ veh\text{-}sec}$

The total overflow delay for the hour can also be obtained by summing all of the deterministic queue delays.

$$DQD_1 = D_{P1} + D_{C1} \quad (73)$$

$$DQD_2 = D_{P2} + D_{C2} + D_{IQA2} + D_{IQB2} \quad (74)$$

$$DQD_3 = D_{P3} + D_{C3} + D_{IQA3} + D_{IQB3} \quad (75)$$

$$DQD_4 = D_{IQ4} \quad (76)$$

Therefore:

$$DQD_T = DQD_1 + DQD_2 + DQD_3 + DQD_4 \quad (77)$$

$$DQD_T = D_{P1}+D_{C1}+D_{P2}+D_{C2}+D_{IQA2}+D_{IQB2}+D_P+D_{C3}+D_{IQA3}+D_{IQB3}+D_{IQ4} \quad (78)$$

For our example:

$DQD_1 = D_{P1} + D_{C1} = 18{,}750\ veh\text{-}sec + 5208\ veh\text{-}sec$

$\mathbf{DQD_1 = 23{,}958\ veh\text{-}sec}$

$DQD_2 = D_{P2} + D_{C2} + D_{IQA2} + D_{IQB2}$

$DQD_2 = 18{,}750$ veh-sec + 5208 veh-sec + 32,292 veh-sec + 15,625 veh-sec

$DQD_2 = 71{,}875$ veh-sec

$DQD_3 = D_{P3} + D_{C3} + D_{IQA3} + D_{IQB3}$

$DQD_3 = 0$ veh-sec + 0 veh-sec + 33,542 veh-sec + 4219 veh-sec

$DQD_3 = 37{,}760$ veh-sec

$DQD_4 =$ $D_{IQ4} =$ **5906 veh-sec**

$DQD_T = DQD_1 + DQD_2 + DQD_3 + DQD_4$

$DQD_T = 23{,}958$ veh-sec + 71,875 veh-sec + 37,760 veh-sec + 5906 veh-sec

$DQD_T = 139{,}500$ veh-sec

The deterministic delay values can be changed to a "per-vehicle" basis by dividing the deterministic queue delay for each period by the vehicles **arriving** during that period.

$$dqd_1 = DQD_1/CA_{15} \quad (79)$$

$$dqd_2 = DQD_2/(CA_{30} - CA_{15}) \quad (80)$$

$$dqd_3 = DQD_3/(CA_{45} - CA_{30}) \quad (81)$$

$$dqd_4 = DQD_4/(CA_{60} - CA_{45}) \quad (82)$$

$$dqd_T = DQD_T/CA_{60} \quad (83)$$

where: dqd_i = Per Vehicle Deterministic Queue Delay for Period i (T = Total)

For our example:

$dqd_1 = DQD_1/CA_{15} =$ 23,958 sec/191.7 veh

$dqd_1 = 125.0$ sec/veh

$dqd_2 = DQD_2/(CA_{30} - CA_{15}) = 71{,}875$ sec/(383.3 veh – 191.7 veh)

$dqd_2 = 375.0$ sec/veh

$dqd_3 = DQD_3/(CA_{45} - CA_{30}) =$ 37,760 sec/(487.5 veh – 383.3 veh)

dqd_3 = 362.5 sec/veh

$dqd_4 = DQD_4/(CA_{60} - CA_{45})$ = 5906 sec/(575 veh – 487.5 veh)

dqd_4 = 67.5 sec/veh

$dqd_T = DQD_T/CA_{60}$= 139,500 sec/575 veh

dqd_T = 242.6 sec/veh

The overflow delay for each period can be changed to a "per-vehicle" basis by dividing the overflow delay for each period by the **average of the vehicles arriving and departing** during that period.

$$od_1 = OD_1/[(CA_{15} + UCD_{15})/2] \quad (84)$$

$$od_2 = OD_2/[(CA_{30} + UCD_{30})/2 - (CA_{15} + UCD_{15})/2] \quad (85)$$

$$od_3 = OD_3/[(CA_{45} + UCD_{45})/2 - (CA_{30} + UCD_{30})/2] \quad (86)$$

$$od_4 = OD_4/[CA_{60} - (CA_{45} + UCD_{45})/2] \quad (87)$$

$$od_T = OD_T/CA_{60} \quad (88)$$

where: od_i = Per Vehicle Overflow Delay for Period i (T = Total)

For our example:

$od_1 = OD_1/[(CA_{15}+UCD_{15})/2]$=18,750 sec/[191.7 veh + 150 veh)/2]=18,750veh-sec/170.9 veh

od_1 = 109.8 sec/veh

$od_2 = OD_2/[(CA_{30} + UCD_{30})/2 - (CA_{15} + UCD_{15})/2]$

od_2 = 56,250 sec/[(383.3 veh + 300 veh)/2 – (191.7 veh + 150 veh)/2]

od_2 = 56,250 sec/(341.7 veh – 170.9 veh)

od_2 = 329.3 sec/veh

$od_3 = OD_3/[(CA_{45} + UCD_{45})/2 - (CA_{30} + UCD_{30})/2]$

od_3 = 54,375 sec/[(487.5 veh + 450 veh)/2 – (383.3 veh + 300)/2]

od_3 = 54,375 sec/(468.8 veh – 341.7 veh)

od_3 = 427.9 sec/veh

$od_4 = OD_4/[CA_{60} – (CA_{45} + UCD_{45})/2]$

od_4 = 10,125 sec/[575 veh – (487.5 veh + 450 veh)/2] = 10,125 veh-sec/(575 veh – 468.8 veh)

od_4 = 95.3 sec/veh

$od_T = OD_T/CA_{60}$ = 139,500 sec /575 veh

od_T = 242.6 sec/veh

i. Delay Summary

The results of the overflow delay derivation can be summarized as follows:

PERIOD 1

$DQD_1 = D_{P1} + D_{C1}$ (73)

$OD_1 = D_{P1}$ (67)

Where: $Dp_1 = (T_{15} – T_0)^2(V_1 – C_1)/7200$ sec/hr (37)

$Dc_1 = 0.5(T_{C1} – T_{15})(CA_{15} – UCD_{15})$ (41)

PERIOD 2

$DQD_2 = D_{P2} + D_{C2} + D_{IQA2} + D_{IQB2}$ (74)

$OD_2 = D_{C1} + D_{P2} + D_{IQA2}$ (68)

Where, <u>if $Q_{30} > Q_{15}$</u>:

$Dp_2 = 0.5(T_{30} – T_{15})(CA_{30} – UCD_{30A})$ (45)

$Dc_2 = 0.5(T_{C2A} – T_{30})(CA_{30} – UCD_{30A})$ (49)

$D_{IQA2} = (T_{C1} – T_{15})[(UCD_{30}\text{-}CA_{15}) + 0.5(UCD_{30A} – UCD_{30})]$ (52)

$D_{IQB2} = 0.5(T_{C2} – T_{30})(CA_{30} – UCD_{30}) – D_{C2}$ (57)

$Dc_1 = 0.5(T_{C1} – T_{15})(CA_{15} – UCD_{15})$ (41)

Or, if $Q_{30} < Q_{15}$:

$D_{P2} = 0$

$D_{C2} = 0$

$D_{IQA2} = 0.5[(T_{30} - T_{15})(CA_{30} - CA_{15}) - (T_{30} - T_{C1})(UCD_{30} - CA_{15})]$ (60A)

$D_{IQB2} = 0.5(T_{C2} - T_{30})(CA_{30} - UCD_{30})$ (64A)

$Dc_1 = 0.5(T_{C1} - T_{15})(CA_{15} - UCD_{15})$ (49)

PERIOD 3

$DQD_3 = D_{P3} + D_{C3} + D_{IQA3} + D_{IQB3}$ (75)

$OD_3 = D_{C2} + D_{IQB2} + D_{P3} + D_{IQA3}$ (69)

Where, if $Q_{45} < Q_{30}$:

$D_{P3} = 0$

$D_{C3} = 0$

$D_{IQA3} = 0.5[(T_{45} - T_{30})(CA_{45} - CA_{30}) - (T_{45} - T_{C2})(UCD_{45} - CA_{30})]$ (60)

$D_{IQB3} = 0.5(T_{C3} - T_{45})(CA_{45} - UCD_{45})$ (64)

$Dc_2 = 0.5(T_{C2A} - T_{30})(CA_{30} - UCD_{30A})$ (49)

$D_{IQB2} = 0.5(T_{C2} - T_{30})(CA_{30} - UCD_{30}) - D_{C2}$ (57)

Or, if $Q_{45} > Q_{30}$:

$D_{P3} = 0.5(T_{45} - T_{30})(CA_{45} - UCD_{45A})$ (45)

$D_{C3} = 0.5(T_{C3A} - T_{45})(CA_{45} - UCD_{45A})$ (49)

$D_{IQA3} = (T_{C2} - T_{30})[(UCD_{45} - CA_{30}) + 0.5(UCD_{45A} - UCD_{45})]$ (52B)

$D_{IQB3} = 0.5(T_{C3} - T_{45})(CA_{45} - UCD_{45}) - D_{C3}$ (57B)

$Dc_2 = 0.5(T_{C2} - T_{30})(CA_{30} - UCD_{30})$ (41)

$D_{IQB2} = 0.5(T_{C2} - T_{30})(CA_{30} - UCD_{30}) - D_{C2}$ (57)

PERIOD 4

$DQD_4 = D_{IQ4}$ (76)

$OD_4 = D_{C3} + D_{IQB3} + D_{IQ4}$ (70)

Where: $D_{IQ4} = 0.5(CA_{C4} - CA_{45})(T_{C3} - T_{45})$ (66)

$D_{C3} = 0$

$D_{IQB3} = 0.5(T_{C3} - T_{45})(CA_{45} - UCD_{45})$ (64)

ALL PERIODS

$DQD_T = DQD_1 + DQD_2 + DQD_3 + DQD_4$ (77)

$OD_T = OD_1 + OD_2 + OD_3 + OD_4$ (71)

$DQD_T = OD_T = D_{P1} + D_{C1} + D_{P2} + D_{C2} + D_{IQA2} + D_{IQB2} + D_{P3} + D_{C3} + D_{IQA3} + D_{IQB3} + D_{IQ4}$ (72)

Using the above formulas we can, for a given capacity, construct a series of feasible delay regions for each minimum Peak Hour Factor (PHF). Figure 5-12 shows an example set of feasible delay regions for a minimum PHF of 0.75, while Figures 5-13 and 5-14 show similar examples for minimum PHF's of 0.80 and 0.85, respectively. We can fit a series of quadratic curves to the data with a rather high degree of correlation as is shown in the three figures. An inspection of these figures provides some interesting information:

- As we would expect, the amount of delay increases as the observed hourly arrival volume (CA_{60}) increases
- As the observed hourly arrival volume (CA_{60}) approaches capacity, the shape of the feasible region morphs from triangular to bullet-shaped and the area between the minimum delay curve and the maximum delay curve increases.
- As the minimum PHF increases, the area between the minimum delay curve and the maximum delay curve decreases. This makes sense since a higher peak hour factor indicates lower variability in the 15-minute flow rates and thus lower variability in the associated delay. We can provide tighter bounds on our solution space for delay when we have higher minimum peak hour factors.

- As the minimum PHF increases, the minimum observable arrival flow rate for period 4 (V_4) increases. For example, when the PHF = 0.75 the minimum observable arrival flow rate is theoretically zero whereas, when the PHF = 0.85, the minimum observable arrival flow is approximately 275 vph.

The value of V_4 at which the difference between the maximum delay curve and the minimum delay curve is the greatest can be determined by setting equal to zero the first derivative of the difference between the two curve formulas and solving for X (where $X = V_4$). For example, given a PHF of 0.75 and 585 for the value of CA_{60}, the value of X_{MAX} is calculated as follows:

Delay Difference = $(400.03-0.1727X-0.0007X^2) – (404.05-1.2365X+0.00106X^2)$

Delay Difference = $- 4.02 + 1.0638X - 0.00176X^2$

d(Delay Difference)/dX = 0 at X_{MAX}: $1.0638 – 2(0.00176)X_{MAX} = 0$

$1.0638 = 0.00352\ X_{MAX}$

$X_{MAX} = 302$ veh/hr

So the maximum difference in delay occurs at a value of V_4 = 302 vph. The associated maximum delay difference is therefore:

Maximum Delay Difference = $- 4.02 + 1.0638X_{MAX} - 0.00176X^2_{MAX}$

Maximum Delay Difference = $- 4.02 + 1.0638(302) - 0.00176(302)^2$

Maximum Delay Difference = 156.7 sec/veh

We can also calculate the delay value associated with the maximum delay curve and the delay value associated with the minimum delay curve at this point:

Maximum Delay = $400.03 – 0.1727X – 0.0007X^2$

Maximum Delay = $400.03 – 0.1727(302) – 0.0007(302)^2$

Maximum Delay = 284.0 sec/veh

Minimum Delay = $404.05 – 1.2365X + 0.00106X^2$

Minimum Delay = $404.05 – 1.2365(302) + 0.00106(302)^2$

Minimum Delay = 127.3 sec/veh

It can be shown that the following equation holds when we desire to have an intermediate estimate that yields equivalent percentage errors when compared against both minimum and maximum possible values:

$$Y = 2UL/(U+L) \quad (89)$$

Where: Y = Estimate that yields equivalent percentage errors
U = Upper Value (in this case the Maximum Delay)
L = Lower Value (in this case the Minimum Delay)

Therefore, our delay estimate for the example would be:

$Y = 2(284.0)(127.3)/(284.0 + 127.3) = 175.8$ sec/veh

With a maximum potential percentage error of: $(175.8 – 127.3)/127.3 = (284.0 – 175.8)/284.0 = 38.1\%$ Although the maximum delay difference occurs towards the center of the region, the highest percentage error occurs near the far right end of the region where the average delay is least and the ratio of the delay difference to the average delay is greatest. Continuing our PHF = 0.75 and CA_{60} = 585 example, at X = 492 the delay difference is:

Delay Difference = $– 4.02 + 1.0638X – 0.00176X^2$

Delay Difference = $– 4.02 + 1.0638(492) – 0.00176(492)^2$

Delay Difference = 93.3 sec/veh

While the minimum and maximum delay are:

Maximum Delay = $400.03 – 0.1727X – 0.0007X^2$

Maximum Delay = $400.03 – 0.1727(492) – 0.0007(492)^2$

Maximum Delay = 145.6 sec/veh

Minimum Delay = $404.05 – 1.2365X + 0.00106X^2$

Minimum Delay = $404.05 – 1.2365(492) + 0.00106(492)^2$

Minimum Delay = 52.7 sec/veh

Our delay estimate for this case would then be:

Y = 2(145.6)(52.7)/(145.6 + 52.7) = 77.4 sec/veh

And our maximum potential percentage error would be (77.4 – 52.7)/52.7 = (145.6 – 77.4)/145.6 = 46.9%.

Continuing these types of calculations, we can plot the maximum percentage error as a function of the observed flow rate. For a minimum PHF of 0.75, this yields the set of curves shown in Figure 5-15. Figures 5-16 and 5-17 provide a similar set of curves for a minimum PHF of 0.80 and 0.85, respectively. These curves clearly show that the maximum percentage error of the estimate increases as the observed flow rate increases. Looking at the PHF=0.75 graph, the percentage error is only 20% at an observed terminal flow rate of 150 vph, whereas the percentage error is close to 50% when the terminal flow rate rises to 350 vph. The curves also show that the overall worst percentage error decreases as the PHF increases, from about 55% for a PHF of 0.75 to approximately 35% for a PHF of 0.85.

Derivation of the Bounds with Visible Period 1 Queue

If the end of the queue remains visible during a long enough portion of period 1 such that an arrival rate can be determined for the first 15 minutes of the hour, then the bound equations can be simplified as follows.

Derivation of Upper Bound with Visible Period 1 Queue

Conservation of flow principals still dictate that the average of the arrival flow rates during each of the four 15-minute periods must equal the arrival rate over the entire 1 hour period:

$$(V_1 + V_2 + V_3 + V_4)/4 = CA_{60} \quad (4)$$

Where: V_i = Arrival Flow Rate during period i (veh/hr)

CA_{60} = Cumulative Arrivals at time point 60 (veh)

Equation (4) continues to constitute the first constraint on the solution space for both the minimum and maximum reasonable delay curves. Using the previous example, equation (4) becomes:

$(V_1 + V_2 + V_3 + 350 \text{ veh/hr})/4 = 575 \text{ veh/hr}$

$V_1 + V_2 + V_3 = 1950 \text{ veh/hr}$

With period 1 visible, the arrival rate for period 1 can be set equal to the capacity of period 1 for the purposes of overflow delay calculation. The overflow delay during period 1 equals zero and there is no residual queue at the start of period 2. Maximum overall delay is obtained when the highest 15-minute flow rate occurs during period 2. Consequently, when identifying the maximum reasonable delay curve, the PHF is defined as follows:

$PHF = (V_1 + V_2 + V_3 + V_4)/[(4)\text{Max}(V_1,V_2,V_3,V_4)]$

$PHF = (V_1 + V_2 + V_3 + V_4)/4V_2$ (5C)

Equation (5B) constitutes the second constraint on the solution space for the maximum reasonable delay curve. Given a minimum PHF of 0.75, equation (5B) becomes:

$0.75 = (V_1 + V_2 + V_3 + 350 \text{ veh/hr})/4V_2$

$3V_2 = (V_1 + V_2 + V_3 + 350 \text{ veh/hr})$

$2V_2 - V_1 - V_3 = 350 \text{ veh/hr}$

With a visible period 1 we know that:

$V_1 = C_1$ (6B)

Consequently, equations (4) and (5B) can be uniquely solved since we have 2 equations to solve for 2 unknown variables (V_2 and V_3). Substituting equation (6B) into equation (4) produces:

$C_1 + V_2 + V_3 + V_4 = 4CA_{60}$

$$2V_1 + V_3 + V_4 = 4CA_{60}$$

$$V_3 = 4CA_{60} - V_4 - V_2 - C_1 \quad (7B)$$

And substituting equations (6B) and (7B) into equation (5B) produces:

$$PHF = (C_1 + V_2 + (4CA_{60} - V_4 - V_2 - C_1) + V_4)/(4V_2)$$

$$PHF = (C_1 + V_2 + 4CA_{60} - V_4 - V_2 - C_1 + V_4)/(4V_2)$$

$$PHF = (4CA_{60})/(4V_2)$$

$$4V_2PHF = 4CA_{60}$$

$$V_2 = CA_{60}/PHF \quad (8B)$$

Substituting equation (8B) into equation (7B) yields:

$$V_3 = 4CA_{60} - V_4 - CA_{60}/PHF - C_1$$

$$V_3 = CA_{60}(4\text{-}1/PHF) - V_4 - C_1 \quad (10B)$$

Continuing our example and utilizing equations (6B), (8B), and (10B):

$V_1 = 600$ veh/hr

$V_2 = 575/0.75 = 766.7$ veh/hr

$V_3 = (575 \text{ veh/hr})\,(4 - 1/(0.75)) - 350 \text{ veh/hr} - 600 \text{ veh/hr} = 583.3 \text{ veh/hr}$

So, for our example, the cumulative arrival curve that produces the maximum reasonable delay when visibility exists through period 1 has quartile hourly flow rates of: **600.0 vph, 766.7 vph, 583.3 vph, and 350.0 vph.** This upper bound curve is depicted in Figure 5-18.

A minimum value exists for V_4 if the minimum PHF is to be maintained. The minimum V_4 value is obtained when V_3 is maximized. Since V_3 cannot exceed V_2, this occurs when:

$$V_2 = V_3 \quad (29)$$

Substituting equations (6B) and (29B) into equation (5B) and solving for V_2 produces:

$$PHF = (V_1 + V_2 + V_3 + V_4)/4V_2$$

$$PHF = (C_1 + V_2 + V_2 + V_4)/4V_2$$

$$4V_2PHF = C_1 + 2V_2 + V_4$$

$$4V_2PHF - 2V_2 = C_1 + V_4$$

$$2V_2(2PHF - 1) = C_1 + V_4$$

$$V_2 = (C_1 + V_4) / 2(2PHF - 1) \quad (90)$$

Substituting equations (6B) and (29B) into equation (4) yields:

$$(V_1 + V_2 + V_3 + V_4)/4 = CA_{60}$$

$$V_1 + V_2 + V_3 + V_4 = 4CA_{60}$$

$$C_1 + V_2 + V_2 + V_4 = 4CA_{60}$$

$$C_1 + 2V_2 + V_4 = 4CA_{60}$$

And then substituting in equation (90) and solving for V_4 yields:

$$C_1 + 2(C_1 + V_4) / 2(2PHF - 1) + V_4 = 4CA_{60}$$

$$(C_1 + V_4) / (2PHF - 1) + V_4 = 4CA_{60} - C_1$$

$$(C_1 + V_4) + (2PHF - 1)V_4 = (4CA_{60} - C_1)(2PHF - 1)$$

$$C_1 + V_4 (1+ (2PHF - 1)) = (4CA_{60} - C_1)(2PHF- 1)$$

$$C_1 + 2PHFV_4 = (4CA_{60} - C_1)(2PHF- 1)$$

$$2PHFV_4 = (4CA_{60} - C_1)(2PHF - 1) - C_1$$

$$V_4 = [(4CA_{60} - C_1)(2PHF -1) - C_1] / 2PHF \quad (91)$$

Continuing our example:

$$V_4 = [(4(575 \text{ vph}) - 600 \text{ vph})(2(0.75) - 1) - 600 \text{ vph}] / 2(0.75)$$

$$V_4 = [(1700 \text{ vph})(0.5) - 600 \text{ vph}] / 1.5 = (850 \text{ vph} - 600 \text{ vph}) / 1.5$$

$V_4 = 166.7$ vph

The value of V_4 can be no lower than this if the minimum PHF is to be maintained.

A maximum value also exists for V_4 if the minimum PHF is to be maintained. The maximum V_4 value is obtained when V_3 is minimized. Since V_3 cannot be less than V_4, this occurs when:

$$V_3 = V_4 \quad (12)$$

Substituting equations (6B) and (12) into equation (5C) and solving for V_2 produces:

$$PHF = (V_1 + V_2 + V_3 + V_4)/4V_2$$

$$PHF = (C_1 + V_2 + V_4 + V_4)/4V_2$$

$$4V_2PHF = C_1 + V_2 + 2\ V_4$$

$$4V_2PHF - V_2 = C_1 + 2V_4$$

$$V_2(4PHF - 1) = C_1 + 2V_4$$

$$V_2 = (C_1 + 2V_4) / (4PHF - 1) \quad (92)$$

Substituting equations (6B) and (12) into equation (4) yields:

$$(V_1 + V_2 + V_3 + V_4)/4 = CA_{60}$$

$$V_1 + V_2 + V_3 + V_4 = 4CA_{60}$$

$$C_1 + V_2 + V_4 + V_4 = 4CA_{60}$$

$$C_1 + V_2 + 2V_4 = 4CA_{60}$$

And then substituting in equation (92) and solving for V_4 yields:

$$C_1 + (C_1 + 2V_4) / (4PHF - 1) + 2V_4 = 4CA_{60}$$

$$(C_1 + 2V_4) / (4PHF - 1) + 2V_4 = 4CA_{60} - C_1$$

$$(C_1 + 2V_4) + 2(4PHF - 1)V_4 = (4CA_{60} - C_1)(4PHF - 1)$$

$$C_1 + 2V_4\ (1 + (4PHF - 1)) = (4CA_{60} - C_1)(4PHF - 1)$$

$$C_1 + 8PHFV_4 = (4CA_{60} - C_1)(4PHF - 1)$$

$$8PHFV_4 = (4CA_{60} - C_1)(4PHF - 1) - C_1$$

$$V_4 = [(4CA_{60} - C_1)(4PHF - 1) - C_1] / 8PHF \quad (93)$$

Continuing our example:

$V_4 = [(4(575 \text{ vph}) - 600 \text{ vph})(4(0.75) - 1) - 600 \text{ vph}] / 8(0.75)$

$V_4 = [(1700 \text{ vph})(2) - 600 \text{ vph}] / 6 = (3400 \text{ vph} - 600 \text{ vph}) / 6$

$V_4 = 466.7$ vph $= V_3$

The value of V_4 can be no higher than this if the minimum PHF is to be maintained. The corresponding value for V_2 can be obtained using equation (92):

$V_2 = (600 \text{ vph} + 2(466.7 \text{ vph})) / (4(0.75) - 1)$

$V_2 = 1533.4 \text{ vph} / 2$

$V_2 = 766.7$ vph

However, an additional constraint applies in that the value for V_3 must be high enough so that the end of the queue does not come within view by the end of the third period. In other words:

$$V_1 + V_2 + V_3 > C_1 + C_2 + C_3 + 4FOV \quad (94)$$

The minimum acceptable value of V_3 is obtained when the equality holds for this equation:

$600 \text{ vph} + 766.7 \text{ vph} + V_3 = 600 \text{ vph} + 600 \text{ vph} + 600 \text{ vph} + 4/\text{hr}(12 \text{ veh})$

$1366.7 \text{ vph} + V_3 = 1848 \text{ vph}$

$V_3 = 481.3$ vph

And the corresponding value for V_4 is obtained via conservation of flow:

$(600 \text{ vph} + 766.7 \text{ vph} + 481.3 \text{ vph} + V_4)/4 = 575 \text{ veh}$

$(600 \text{ vph} + 766.7 \text{ vph} + 481.3 \text{ vph} + V_4)/4 = 575 \text{ veh}$

$1848 \text{ vph} + V_4 = (575 \text{ veh})(4/\text{hr})$

$V_4 = 452$ vph

This is less than the previously calculated value of 466.7 vph and is therefore the true minimum value of V_4.

Derivation of Lower Bound with Visible Period 1 Queue

Conservation of flow principals continue to dictate that the average of the arrival rates during each of the four 15-minute periods must equal the arrival rate over the entire 1-hour period:

$$(V_1 + V_2 + V_3 + V_4)/4 = CA_{60} \quad (4)$$

Where:

V_i = Arrival Rate during period i (veh/hr)
CA_{60} = Cumulative Arrivals at time point 60 (veh)

For our example, equation (4) became:

$(V_1 + V_2 + V_3 + 350$ veh/hr$)/4 = 575$ veh/hr

$V_1 + V_2 + V_3 = 1950$ veh/hr

Minimum delay occurs when the vertical distance between the arrival curve and the departure curve (the nominal queue length) is continually minimized, without the end of the queue becoming visible. This happens when the nominal queue length equals the Field of View (FOV). Under these conditions, the minimum value for V_2 is:

$V_2 = [(UDR_2)(t_2) + FOV]$ x 4 periods/hr, or

$$V_2 = C_2 + 4FOV \quad (15B)$$

Where:

V_2 = Arrival Rate during period 2 (veh/hr)
UDR_2 = Uniform Departure Rate during period 2 (veh/sec)
FOV = Field of View (veh)
t_2 = Duration of 2nd 15-min time period (sec/period) = 900 sec/period
C_2 = Capacity during period 2 (veh/hr)

V_2 cannot be any lower than this value or the end of the queue would be visible at the end of period 2 and no estimation of the delay associated with the overflow queue would be required.

Assuming a FOV of 12, we continue our example as follows:

$V_1 = C_1 = 600$ veh/hr

$V_2 = [(0.1667 \text{ veh/sec})(900 \text{ sec/period}) + 12 \text{ veh}] \times 4 \text{ periods/hr} = 600 + 48 = 648$ veh/hr

We can now solve for V_3. Substituting equation (15B) into equation (4) produces:

$$C_1 + C_2 + 4FOV + V_3 + V_4 = 4CA_{60}$$

$$V_3 = 4CA_{60} - 4FOV - C_1 - C_2 - V_4$$

$$V_3 = 4(CA_{60} - FOV) - C_1 - C_2 - V_4 \quad (17B)$$

For our example:

$V_3 = 4/\text{hr}\ (575 \text{ veh} - 12 \text{ veh}) - (600 \text{ veh/hr}) - (600 \text{ veh/hr}) - 350 \text{ veh/hr} = 702$ veh/hr

So, for our example, when the first period is visible the cumulative arrival curve that produces the minimum reasonable delay has quartile hourly flow rates of: **600.0 vph, 648.0 vph, 702.0 vph, and 350.0 vph.** This lower bound curve is depicted in Figure 5-19.

Analysis of Bounds Summary with Visible Period 1 Queue

The results of the analysis of the bounds can be summarized as follows when the first period is a visible period:

UPPER BOUND

$V_1 = C_1$

$V_2 = CA_{60}/PHF \quad (8B)$

$V_3 = CA_{60}(4 - 1/PHF) - V_4 - C_1 \quad (10B)$

LOWER BOUND

$V_1 = C_1$

$V_2 = C_2 + 4FOV \quad (15B)$

$V_3 = 4(CA_{60} - FOV) - C_1 - C_2 - V_4$ (18B)

For our example, the values are:

UPPER BOUND

V_1 = 600 vph

V_2 = 575 vph/0.75 = **766.7 vph**

V_3 = 575 vph (4 - 1/0.75) – 350 vph – 600 vph = **583.3 vph**

V_4 = 350 vph

LOWER BOUND

V_1 = 600 vph

V_2 = 600 vph + 4/hr(12veh) = **648 vph**

V_3 = 4/hr(575 veh – 12 veh) – 600 vph – 600 vph – 350 vph = **702 vph**

V_4 = 350 vph

Derivation of Delay with Visible Period 1 Queue

The calculation of Overflow Delay and Deterministic Queue Delay proceeds as before, with the exception that there is no Overflow Delay or Deterministic Queue Delay during period 1 ($DO_1 = DQD_1 = 0$). The results are summarized as follows:

PERIOD 1

$DQD_1 = OD_1 = 0$

PERIOD 2

$DQD_2 = D_{P2} + D_{C2}$ (73B)

$OD_2 = D_{P2}$ (67B)

Where: $Dp_2 = (T_{30} - T_{15})^2(V_2 - C_2)/7200$ sec/hr (37B)

$Dc_2 = 0.5(T_{C2} - T_{30})(CA_{30} - UCD_{30})$ (41B)

PERIOD 3

$DQD_3 = D_{P3} + D_{C3} + D_{IQA3} + D_{IQB3}$ (75)

$OD_3 = D_{C2} + D_{P3} + D_{IQA3}$ (95)

Where, <u>if $Q_{45} < Q_{30}$</u>:

$D_{P3} = 0$

$D_{C3} = 0$

$D_{IQA3} = 0.5[(T_{45} - T_{30})(CA_{45} - CA_{30}) - (T_{45} - T_{C2})(UCD_{45} - CA_{30})]$ (60)

$D_{IQB3} = 0.5(T_{C3} - T_{45})(CA_{45} - UCD_{45})$ (64)

$Dc_2 = 0.5(T_{C2} - T_{30})(CA_{30} - UCD_{30})$ (49)

Or, <u>if $Q_{45} > Q_{30}$</u>:

$D_{P3} = 0.5(T_{45} - T_{30})(CA_{45} - UCD_{45A})$ (45)

$D_{C3} = 0.5(T_{C3A} - T_{45})(CA_{45} - UCD_{45A})$ (49B)

$D_{IQA3} = (T_{C2} - T_{30})[(UCD_{45} - CA_{30}) + 0.5(UCD_{45A} - UCD_{45})]$ (52)

$D_{IQB3} = 0.5(T_{C3} - T_{45})(CA_{45} - UCD_{45}) - D_{C3}$ (57B)

$Dc_2 = 0.5(T_{C2} - T_{30})(CA_{30} - UCD_{30})$ (41)

PERIOD 4

$DQD_4 = D_{IQ4}$ (76)

$OD_4 = D_{C3} + D_{IQB3} + D_{IQ4}$ (70)

Where: $D_{IQ4} = 0.5(CA_{C4} - CA_{45})(T_{C3} - T_{45})$ (66)

$D_{C3} = 0$

$D_{IQB3} = 0.5(T_{C3} - T_{45})(CA_{45} - UCD_{45})$ (64)

ALL PERIODS

$DQD_T = DQD_1 + DQD_2 + DQD_3 + DQD_4$ (77)

$$OD_T = OD_1 + OD_2 + OD_3 + OD_4 \quad (71)$$

$$DQD_T = OD_T = D_{P2} + D_{C2} + D_{P3} + D_{C3} + D_{IQA3} + D_{IQB3} + D_{IQ4} \quad (72B)$$

Derivation of the Bounds When Queue is Visible During Three Periods

If the end of the queue remains visible during three of the four 15-minute analysis periods such that an arrival rate at the back of the queue can be determined for three of the four periods, then the bounds converge to a single unique solution. Conservation of flow principals still dictate that the average of the arrival flow rates during each of the four 15-minute periods must equal the arrival rate over the entire 1 hour period:

$$(V_1 + V_2 + V_3 + V_4)/4 = CA_{60} \quad (4)$$

Where:

V_i = Arrival Flow Rate during period i (veh/hr)
CA_{60} = Cumulative Arrivals at time point 60 (veh)

Consequently:
$V_1 = 4CA_{60} - V_2 - V_3 - V_4$, or
$V_2 = 4CA_{60} - V_1 - V_3 - V_4$, or
$V_3 = 4CA_{60} - V_1 - V_2 - V_4$, or
$V_4 = 4CA_{60} - V_1 - V_2 - V_3$

In general: $V_i = 4CA_{60} - E_j V_{j<>i}$

The calculation of Overflow Delay and Deterministic Queue Delay proceeds as before.

Derivation of the Bounds When Analysis Time Frame is Greater Than One Hour

The analysis procedure can be expanded to a time frame greater than one hour. However, to do so we must replace the Peak Hour Factor, which is based on four 15-minute periods, with a newly defined **"Peak Period Factor"** that is consistent with the actual number of 15-minute periods under consideration. For example, the Peak Period Factor for a 5-period analysis time frame (P5F) would be calculated as follows:

$$P5F = (V_1 + V_2 + V_3 + V_4 + V_5) / [(5)Max(V_1,V_2,V_3,V_4,V_5)] \quad (96)$$

In general: $PNF = (E^N V_i) / (N)Max(V_i)$

The conservation of flow equation would continue to apply for the expanded number of periods. For 5 periods it would be:

$$(V_1 + V_2 + V_3 + V_4 + V_5) / 5 = CA_5 \quad (97)$$

Where:

V_i = Arrival Rate during period i (veh/analyis timeframe)
CA_5 = Cumulative Arrivals at the end of the last (5^{th}) period (veh/analysis timeframe)

In general: $(E^N V_i) / N = CA_N$

Equation (97), the conservation of flow equation, constitutes the first constraint on the solution space for both the minimum and maximum reasonable delay curves.

Note that both V_i and CA are expressed in terms of vehicles per analysis time frame. When the analysis time frame is not exactly one hour, as is the case here, V_i must be divided by the analysis time frame (atf) to obtain the period flow rate in vehicles per hour. If V_1 = 766.7 vehicles/analysis time frame then the equivalent hourly flow rate would be 766.7 vehicles per analysis time frame / 1.25 hours per analysis time frame = 766.7 veh/atf / 1.25 hr/atf = 613.3 vehicles/hour.

Derivation of the Five Period Upper Bound

Maximum overall delay is obtained when the highest 15-minute volume occurs at the start of the analysis time frame. Consequently, when identifying the maximum reasonable delay curve, P5F is defined as follows:

$$P5F = (V_1 + V_2 + V_3 + V_4 + V_5)/[(5)\text{Max}(V_1,V_2,V_3,V_4,V_5)]$$

$$PHF = (V_1 + V_2 + V_3 + V_4 + V_5)/5V_1 \quad (96B)$$

Equation (96B) constitutes the second constraint on the solution space for the maximum reasonable delay curve.

Equations (96B) and (97) cannot be uniquely solved since we have only 2 equations to solve for 4 unknown variables (V_1, V_2, V_3 and V_4). However, an examination of the solution space for this problem indicates that we can obtain additional equations by attempting to set V_2 and V_3 as high as possible (in a continued attempt to maximize delay). In this case, the upper limit for V_2 and V_3 is V_1. V_2 and V_3 cannot be greater than V_1 or delay would not be maximized. With V_1 forming the upper limit for V_2 and V_3 we have the additional equations:

$$V_1 = V_2 \quad (98)$$

$$V_1 = V_3 \quad (99)$$

We now have 4 equations and 4 unknowns and we can solve for all of the Vi's. Substituting equations (98) and (99) into conservation of flow equation (97) produces:

$$V_1 + V_1 + V_1 + V_4 + V_5 = 5CA_5$$

$$3V_1 + V_4 + V_5 = 5CA_5$$

$$V_4 = 5CA_5 - V_5 - 3V_1 \quad (100)$$

Substituting equations (98), (99) and (100) into peak period factor equation (96) and recognizing that V_1 will have the largest value when delay is maximized:

$$P5F = (V_1 + V_1 + V_1 + (5CA_5 - V_5 - 3V_1) + V_5)/(5V_1)$$

$$P5F = (3V_1 + 5CA_5 - V_5 - 3V_1 + V_5)/(5V_1)$$

$$P5F = (5CA_5)/(5V_1)$$

$$5V_1P5F = 4CA_5$$

$$V_1 = CA_5/P5F \quad (101)$$

Substituting equation (101) into equations (98) and (99) produces:

$$V_2 = CA_5/P5F \quad (102)$$

$$V_3 = CA_5/P5F \quad (103)$$

And substituting equations (101), (102) and (103) into conservation of flow equation (97) yields:

$$CA_5/P5F + CA_5/P5F + CA_5/P5F + V_4 + V_5 = 5CA_5$$

$$V_4 = 5CA_5 - 3CA_5/P5F - V_5$$

$$V_4 = CA_5\,(5 - 3/P5F) - V_5 \qquad (104)$$

Continuing our example and utilizing equations (101), (102), (103) and (104):

$$V_1 = 575/0.75 = 766.7 \text{ veh/atf}$$

$$V_2 = 575/0.75 = 766.7 \text{ veh/atf}$$

$$V_3 = 575/0.75 = 766.7 \text{ veh/atf}$$

$$V_4 = (575 \text{ veh/atf})\,(5 - 3/(0.75)) - 350 \text{ veh/atf} = 225.0 \text{ veh/atf}$$

However, this solution violates our initial requirement that V_4 (225 vpatf) be greater than or equal to V_5 (350 vpatf). Consequently, in this case, we must re-work our solution with equation (99) eliminated, replaced with:

$$V_4 = V_5 \qquad (105)$$

Substituting equations (98) and (105) into conservation of flow equation (97) produces:

$$V_1 + V_1 + V_3 + V_5 + V_5 = 5CA_5$$

$$2V_1 + V_3 + 2V_5 = 5CA_5$$

$$V_3 = 5CA_5 - 2V_5 - 2V_1 \qquad (106)$$

And substituting equations (98), (105) and (106) into peak period factor equation (96) produces:

$$P5F = (V_1 + V_1 + (5CA_5 - 2V_5 - 2V_1) + V_5 + V_5)/(5V_1)$$

$$P5F = (2V_1 + 5CA_5 - 2V_5 - 2V_1 + 2V_5)/(5V_1)$$

$$P5F = (5CA_5)/(5V_1)$$

$$5V_1P5F = 5CA_5$$

$$V_1 = CA_5/P5F \qquad (101)$$

Substituting equation (101) into equations (98) produces:

$$V_2 = CA_5/P5F \quad (102)$$

These are the same equations for V_1 and V_2 that were previously obtained. However, substituting equations (101), (102) and (105) into equation (97) now yields:

$$CA_5/P5F + CA_5/P5F + V_3 + V_5 + V_5 = 5CA_5$$

$$V_3 = 5CA_5 - 2CA_5/P5F - 2V_5$$

$$V_3 = CA_5\,(5 - 2/P5F) - 2V_5 \quad (107)$$

Continuing our example and utilizing equations (101), (102), (104) and (107):

$V_1 = 575/0.75 = 766.7$ veh/atf

$V_2 = 575/0.75 = 766.7$ veh/atf

$V_3 = (575$ veh/atf$)\,(5 - 2/(0.75)) - 2(350$ veh/atf$) = 641.7$ veh/atf

$V_4 = 350$ veh/atf

This is an acceptable solution. So, for our example, the cumulative arrival curve that produces the maximum reasonable delay has period flow rates of: **766.7 vpatf, 766.7 vpatf, 641.7 vpatf, 350 vpatf and 350 vpatf.** This upper bound curve is depicted in Figure 5-20. Dividing by 1.25, the length of the analysis time frame in hours, converts these values into hourly flow rates: **613.3 vph, 613.3 vph, 513.3 vph, 280 vph and 280 vph**

In this example, V_1 was a feasible upper limit for V_2 but was not a feasible upper limit for V_3. However, it is possible that V_1 may be a feasible upper limit for both V_2 and V_3. This occurs when the value of V_5 is low enough to allow V_3 to equal V_1 without forcing V_4 to be lower than V_5. The value of V_5 at which this restriction occurs can be found by setting V_4 equal to V_5 in equation (104):

$$V_4 = CA_5\,(5 - 3/P5F) - V_4$$

$$2V_4 = CA_5\,(5 - 3/P5F)$$

$$V_4 = CA_5\,/2(5 - 3/P5F) = V_5 \qquad (108)$$

For our example:

$$V_4 = 575\,/2(5 - 3/0.75)$$

$$V_4 = V_5 = 287.5 \text{ veh/atf}$$

Therefore, in our example, if V_5 is less than 287.5 then $V_1 = V_3$ and equation (104) can be used to calculate V_4. In general, equation (104) can be used to calculate V_4 if $V_5 < (CA_5\,/2)(5 - 3/P5F)$. If $V_5 > CA_5\,/2(5 - 3/P5F)$ then V_4 must be set equal to V_5 and the remaining equations solved accordingly. This will yield an acceptable answer as long as V_1 can serve as an upper limit for V_2, which occurs if V_5 is not too high. If V_1 does not form the upper limit for V_2 then we have the additional equation:

$$V_3 = V_5 \qquad (109)$$

And we must re-work our solution with equations (98) and (99) eliminated. Substituting equations (105) and (109) into equation (97) produces:

$$V_1 + V_2 + V_5 + V_5 + V_5 = 5CA_5$$

$$V_1 + V_2 + 3V_5 = 5CA_5$$

$$V_2 = 5CA_5 - 3V_5 - V_1 \qquad (110)$$

And substituting equations (105), (109) and (110) into conservation of flow equation (97) produces:

$$P5F = (V_1 + (5CA_5 - 3V_5 - V_1) + V_5 + V_5 + V_5)/(5V_1)$$

$$P5F = (V_1 + 5CA_5 - 3V_5 - V_1 + 3V_5)/(5V_1)$$

$$P5F = (5CA_5)/(5V_1)$$

$$5V_1P5F = 5CA_5$$

$$V_1 = CA_5/P5F \quad (101)$$

This is the same equation for V_1 that was previously obtained. However, substituting equations (101), (105) and (109) into equation (97) now yields:

$$CA_5/P5F + V_2 + V_5 + V_5 + V_5 = 5CA_5$$

$$V_2 = 5CA_5 - CA_5/P5F - 3V_5$$

$$V_2 = CA_5\,(5 - 1/P5F) - 3V_5 \quad (111)$$

If we modify our example such that V_5 is actually 450 instead of 350, then setting $V_1 = V_2$ and using equation (107) would result in a value for V_3 of:

$$V_3 = 575 \text{ vpatf}\,(5 - 2/0.75) - 2(450 \text{ vpatf}) = 441.7\text{vpatf}$$

But this is not acceptable, since $V_3 = 441.7$ would be less than $V_4 = V_5 = 450$, which violates our original assumption that the last period must be the period with the lowest flow rate. Rather, if $V_5 = 450$, then V_3 must be set equal to V_5 and equation (111) used to solve for V_2 (The value of V_1 does not change):

$$V_2 = 575 \text{ vpatf}\,(5 - 1/0.75) - 3(450 \text{ vpatf}) = 763.3 \text{ vpatf}$$

So, for this modified example, the cumulative arrival curve that produces the maximum reasonable delay has period flow rates of: 766.7 vpatf, 763.3 vpatf, 450.0 vpatf, 450.0 vpatf and 450.0 vpatf. Or, expressed as hourly flow rates: 613.3 vph, 613.3 vph, 360.0 vph, 360.0 vph and 360.0 vph.

In the original example, V_1 is a feasible upper limit for V_2 but in the modified example it is not. The value of V_5 is too high in the modified example to allow V_2 to equal V_1 without forcing V_3 to be lower than V_5. The value of V_5 at which this restriction occurs can be found by setting V_3 equal to V_5 in equation (105):

$$V_3 = CA_5\,(5 - 2/P5F) - 2V_3$$

$$3V_3 = CA_5\,(5 - 2/P5F)$$

$$V_3 = CA_5\,/3(5 - 2/P5F) = V_5 \quad (112)$$

For our original example:

$$V_3 = 575\,/3(5 - 2/0.75)$$

$$V_3 = V_5 = 447.2 \text{ vpatf}$$

Consequently, if V_5 is less than 447.2 then $V_1 = V_2$ and equation (105) can be used to calculate V_3. In general, equation (105) can be used to calculate V_3 if $V_5 > CA_5\,/2(5 - 3/P5F)$ and $V_5 < CA_5\,/2(5 - 3/P5F)$. If $V_5 > CA_5\,/3(5 - 2/P5F)$ then V_3 must be set equal to V_5 and the remaining equations solved accordingly. Equation (109) must be used to solve for V_2 when this occurs since V_2 no longer equals V_1.

Derivation of the Five Period Lower Bound

Minimum delay occurs when the vertical distance between the arrival curve and the departure curve (the nominal queue length) is continually minimized, without the end of the queue becoming visible. This happens when the nominal queue length equals the Field of View (FOV). Under these conditions, the minimum value for V_1 is:

$$V_1 = [(UDR_1)(t_1) + FOV] \text{ x 5 periods/atf, or}$$

$$V_1 = C_1 + 5FOV \quad (113)$$

V_1 cannot be any lower than this value or the end of the queue would be visible at the end of period 1 and no estimation of the delay associated with the overflow queue would be required. If V_1 equals this absolute lower bound, then we can continue to minimize delay by having V_2 and V_3 equal their respective capacities:

$$V_2 = C_2 \quad (114)$$

$$V_3 = C_3 \quad (115)$$

This produces a cumulative arrival curve for periods 2 and 3 that parallels the uniform departure curve for these periods. We continue our ongoing example as follows:

V_1 = [(0.1667 veh/sec)(900 sec/period) + 12 veh] x 5 periods/atf = 600 + 60 = 660 veh/atf

V_2 = [(0.1667 veh/sec)(900 sec/period)] x 5 periods/hr = 600 veh/atf

V_3 = [(0.1667 veh/sec)(900 sec/period)] x 5 periods/hr = 600 veh/atf

We can now solve for V_4. Substituting equations (113), (114) and (115) into conservation of flow equation (97) produces:

$$C_1 + 5FOV + C_2 + C_3 + V_4 + V_5 = 5CA_5$$

$$V_4 = 5CA_5 - C_1 - C_2 - C_3 - 5FOV - V_5 \quad (116)$$

For our example:

V_4=5/atf (575 veh)–(600 veh/atf)–(600 veh/atf)–(600 veh/atf)–5/hr (12 veh)–350 veh/atf=665 veh/atf

The resulting P5F is found by substituting equations (113), (114) and (115) into equation (96):

$$P5F = (C_1 + 5FOV + C_2 + C_3 + V_4 + V_5) / (5V_4)$$

And then substituting in equation (114) for V_4:

$$P5F = (C_1 + 5FOV + C_2 + C_3 + 5CA_5 - C_1 - C_2 - C_3 - 5FOV - V_5 + V_5) / (5V_4)$$

$$P5F = (5CA_5) / (5V_4)$$

$$P5F = CA_5 / V_4 \quad (117)$$

$$P5F = 575 \text{ vpatf} / 665 \text{ vpatf} = 0.865$$

Which is greater then the minimum required value of 0.75

So, for our example, the cumulative arrival curve that produces the minimum reasonable delay has period flow rates of: **660 vpatf, 600 vpatf, 600 vpatf, 665 vpatf, and 350 vpatf.** This lower bound curve is depicted in Figure 5-21. Dividing by 1.25, the length of the analysis time

frame in hours, converts these values into hourly flow rates: **528 vph, 480 vph, 480 vph, 532 vph and 280 vph**

If V_1, V_2 and V_3 are all at their lower limit, then the **maximum** value for V_5 can be calculated by setting V_4 equal to its **lowest** possible value. As with V_2 and V_3, V_4's lowest possible value occurs when it parallels its cumulative departure curve:

$$V_4 = C_4 \tag{118}$$

We can now solve for he maximum value of V_5. Substituting equation (118) into equation (116) produces:

$$C_4 = 5CA_5 - C_1 - C_2 - C_3 - 5FOV - V_5$$

$$V_5 = 5CA_5 - C_1 - C_2 - C_3 - 5FOV - C_4$$

For our example:

V_5 = 5/atf (575 veh)–(600 veh/atf) – (600 veh/atf) – (600 veh/atf) – 5/hr (12 veh) – 600 veh/atf

V_5 = 415 veh/atf

If V_1, V_2 and V_3 are all at their lower limit, then the **minimum** value for V_5 can be calculated by setting V_4 equal to its **highest** possible value while maintaining the minimum required PHF and preserving conservation of flow. Recognizing that V_4 will have the highest flow rate for this situation:

$$P5F = (V_1 + V_2 + V_3 + V_4 + V_5)/(5V_4) \tag{119}$$

Substituting equations (113), (114) and (116) into the peak period equation (119) yields:

$$P5F = (C_1 + 5FOV + C_2 + C_3 + V_4 + V_5)/(5V_4)$$

$$5P5F\ V_4 = C_1 + 5FOV + C_2 + C_3 + V_4 + V_5$$

$$5P5F\ V_4 - V_4 = C_1 + 5FOV + C_2 + C_3 + V_5$$

$$V_4 = (C_1 + 5FOV + C_2 + C_3 + V_5) / (5P5F - 1) \tag{120}$$

Substituting equation (120) into equation (116) produces:

$$(C_1 + 5FOV + C_2 + C_3 + V_5) / (5P5F - 1) = 5CA_5 - C_1 - C_2 - C_3 - 5FOV - V_5$$

$$V_5 = 5CA_5 - C_1 - C_2 - C_3 - 5FOV - (C_1 + 5FOV + C_2 + C_3 + V_5) / (5P5F - 1)$$

$$V_5 (5P5F - 1) = (5P5F - 1) (5CA_5 - C_1 - C_2 - C_3 - 5FOV) - C_1 - 5FOV - C_2 - C_3 - V_5$$

$$5P5F\ V_5 - V_5 = (5P5F - 1) (5CA_5 - C_1 - C_2 - C_3 - 5FOV) - C_1 - 5FOV - C_2 - C_3 - V_5$$

$$5P5F\ V_5 = (5P5F - 1)(5CA_5 - C_1 - C_2 - C_3 - 5FOV) + (5CA_5 - C_1 - 5FOV - C_2 - C_3) - 5CA_5$$

$$5P5F\ V_5 = (5P5F - 1 + 1) (5CA_5 - C_1 - C_2 - C_3 - 5FOV) - 5CA_5$$

$$V_5 = [(5P5F) (5CA_5 - C_1 - C_2 - C_3 - 5FOV) - 5CA_5] / 5P5F$$

$$V_5 = (5CA_5 - C_1 - C_2 - C_3 - 5FOV) - CA_5 / P5F$$

$$V_5 = 5CA_5 - C_1 - C_2 - C_3 - 5FOV) - CA_5 / P5F$$

$$V_5 = CA_5 (5\text{-}1/P5F) - C_1 - C_2 - C_3 - 5FOV \qquad (121)$$

For our example:

$$V_5 = 5/atf\ (575\ veh) - (600\ veh/atf) - (600\ veh/atf) - (600\ veh/atf) - 5/hr\ (12\ veh) - [575\ veh / 0.75]$$

$$V_5 = 1015\ veh/atf - 766.7\ veh/atf$$

$$\mathbf{V_5 = 248.3\ veh/atf}$$

The corresponding value of V_4 is found by inserting this value for V_5 into formula (120):

$$V_4 = (600\ vpatf + 5\ (12) + 600\ vpatf + 600\ vpatf + 248.3\ vpatf) / (5(0.75) - 1)$$

$$V_4 = (2108.3\ vpatf) / 2.75$$

$$\mathbf{V_4 = 766.67\ vpatf}$$

If V_1, V_2, V_3 and V_4 are all at their lower limits then the value of V_5 is fixed due to conservation of flow. Substituting equations (113), (114), (115) and (118) into equation (96) yields:

$$(C_1 + 5FOV + C_2 + C_3 + C_4 + V_5) / 5 = CA_5$$

$$V_5 = 5CA_5 - 5FOV - C_1 - C_2 - C_3 - C_4 \qquad (122)$$

For our example:

$V_5 = 5/atf(575\ veh) - 600\ vpatf - 600\ vpatf - 600\ vpatf - 600\ vpatf$

$V_5 = 475\ vpatf$

The corresponding P5F value is obtained by substituting equations (113), (114) and (115) into equation (96B):

$$P5F = (V_1 + V_2 + V_3 + V_4 + V_5)/5V_1 \quad (96B)$$

$$P5F = (C_1 + 5FOV + C_2 + C_3 + C_4 + V_5)/5(C_1 + 5FOV)$$

And then substituting in equation (122):

$$P5F = (C_1 + 5FOV + C_2 + C_3 + C_4 + 5CA_5 - 5FOV - C_1 - C_2 - C_3 - C_4)/5(C_1 + 5FOV)$$

$$P5F = (5CA_5)/5(C_1 + 5FOV)$$

$$P5F = CA_5/(C_1 + 5FOV) \quad (123)$$

For our example:

$P5F = 575\ vpatf\ /660\ vpatf$

$P5F = 0.871$

If V_1 and V_2 are at their lower limit, then the **minimum** value for V_5 can be calculated by setting V_3 and V_4 equal to their **highest** possible values while maintaining the minimum required PHF and preserving conservation of flow. Recognizing that V_4 will need to have the higher flow rate to minimize delay:

$$P5F = (V_1 + V_2 + V_3 + V_4 + V_5)/(5V_4) \quad (124)$$

Substituting equations (113) and (114) into equation (124) yields:

$$P5F = (C_1 + 5FOV + C_2 + V_3 + V_4 + V_5)/(5V_4)$$

$$5P5F\ V_4 = C_1 + 5FOV + C_2 + V_3 + V_4 + V_5$$

$$5P5F\ V_4 - V_4 = C_1 + 5FOV + C_2 + V_3 + V_5$$

$$V_4 = (C_1 + 5FOV + C_2 + V_3 + V_5) / (5P5F - 1) \quad (125)$$

Substituting equations (113) and (114) into equation (97) yields:

$$(C_1 + 5FOV + C_2 + V_3 + V_4 + V_5) / 5 = CA_5$$

$$C_1 + 5FOV + C_2 + V_3 + V_4 + V_5 = 5CA_5$$

$$V_3 = 5CA_5 - C_1 - C_2 - 5FOV - V_5 - V_4$$

Substituting in equation (125) produces:

$$V_3 = 5CA_5 - C_1 - C_2 - 5FOV - V_5 - [(C_1 + 5FOV + C_2 + V_3 + V_5) / (5P5F - 1)]$$

$$(5P5F - 1)V_3 = (5P5F - 1)5CA_5 - (5P5F - 1)C_1 - (5P5F - 1)C_2 - (5P5F - 1)5FOV - (5P5F - 1)V_5 - C_1 - 5FOV - C_2 - V_3 - V_5$$

$$(5P5F - 1)V_3 = 25P5F\ CA_5 - 5CA_5 - 5P5F\ C_1 + C_1 - 5P5F\ C_2 + C_2 - 25P5FFOV + 5FOV - 5P5F\ V_5 + V_5 - C_1 - 5FOV - C_2 - V_3 - V_5$$

$$(5P5F - 1)V_3 = 25P5F\ CA_5 - 5CA_5 - 5P5F\ C_1 - 5P5F\ C_2 - 25P5FFOV - 5P5F\ V_5 - V_3$$

$$(5P5F - 1)V_3 + V_3 = 25P5F\ CA_5 - 5CA_5 - 5P5F\ C_1 - 5P5F\ C_2 - 25P5FFOV - 5P5F\ V_5$$

$$5P5F\ V_3 - V_3 + V_3 = 25P5F\ CA_5 - 5CA_5 - 5P5F\ C_1 - 5P5F\ C_2 - 25P5FFOV - 5P5F\ V_5$$

$$5P5F\ V_3 = 25P5F\ CA_5 - 5CA_5 - 5P5F\ C_1 - 5P5F\ C_2 - 25P5FFOV - 5P5F\ V_5$$

$$V_3 = (25P5F\ CA_5 - 5CA_5 - 5P5F\ C_1 - 5P5F\ C_2 - 25P5FFOV - 5P5F\ V_5) / 5P5F$$

$$V_3 = 5CA_5 - CA_5 / P5F - C_1 - C_2 - 5FOV - V_5$$

$$V_3 = CA_5\ (5 - 1/ P5F) - C_1 - C_2 - 5FOV - V_5 \quad (126)$$

Substituting equation (126) into equation (125) produces:

$$V_4 = (C_1 + 5FOV + C_2 + CA_5\ (5 - 1/ P5F) - C_1 - C_2 - 5FOV - V_5 + V_5) / (5P5F - 1)$$

$$V_4 = CA_5\ (5 - 1/ P5F) / (5P5F - 1)$$

$$V_4 = CA_5\ (5 - 1/ P5F) / (5P5F - 1)$$

This can be simplified by showing that $(5 - 1/ P5F) / (5P5F - 1) = 1/P5F$:

$$(5 - 1/ P5F) / (5P5F - 1) = 5 /(5P5F - 1) - 1/ P5F/(5P5F - 1)$$

$$(5 - 1/ P5F) / (5P5F - 1) = 5 /(5P5F - 1) - 1/ [P5F(5P5F - 1)]$$

$$(5 - 1/ P5F) / (5P5F - 1) = 5\ P5F / [P5F\ (5P5F - 1)] - 1/ [P5F(5P5F - 1)]$$

$$(5 - 1/ P5F) / (5P5F - 1) = (5\ P5F - 1) / [P5F\ (5P5F - 1)]$$

$$(5 - 1/ P5F) / (5P5F - 1) = 1 / P5F$$

Therefore:

$$V_4 = CA_5 / P5F \qquad (127)$$

Continuing our example:

$$V_4 = 575 / 0.75$$

$$\mathbf{V_4 = 766.7\ vpatf}$$

And using equation (126):

$$V_3 = 575\ (5 - 1/0.75) - 600 - 600 - 5(12veh) - V_5$$

$$V_3 = 2108.3\ vpatf - 1260\ vpatf - V_5$$

$$V_3 = 848.3\ vpatf - V_5$$

The value of V_5 is minimized when V_3 is maximized. The maximum value of V_3 is constrained by the PHF equation:

$$P5F = (V_1 + V_2 + V_3 + V_4 + V_5)/(5V_3)$$

$$P5F = (C_1 + 5FOV + C_2 + V_3 + V_4 + V_5)/(5V_3)$$

$$5P5F\ V_3 = C_1 + 5FOV + C_2 + V_3 + V_4 + V_5$$

$$5P5F\ V_3 - V_3 = C_1 + 5FOV + C_2 + V_4 + V_5$$

$$V_3 = (C_1 + 5FOV + C_2 + V_4 + V_5) / (5P5F - 1)$$

Substituting in equation (127) we obtain:

$$V_3 = (C_1 + 5FOV + C_2 + CA_5 /5P5F + V_5) / (5P5F - 1)$$

And substituting in conservation of flow equation (126) produces:

$$CA_5\ (5 - 1/ P5F) - C_1 - C_2 - 5FOV - V_5 = (C_1 + 5FOV + C_2 + CA_5 / P5F + V_5) / (5P5F - 1)$$

$$CA_5\,(5 - 1/\,P5F) - C_1 - C_2 - 5FOV = (C_1 + 5FOV + C_2 + CA_5\,/\,P5F + V_5)\,/\,(5P5F - 1) + V_5$$

$$(5P5F-1)[CA_5(5 -1/\,P5F)-C_1- C_2- 5FOV] = C_1 + 5FOV + C_2 + CA_5\,/P5F + V_5 + V_5\,(5P5F - 1)$$

$$V_5\,(1+5P5F-1) = (5P5F - 1)[CA_5(5 - 1/\,P5F) - C_1 - C_2 - 5FOV] - C_1 - 5FOV - C_2 - CA_5\,/\,P5F$$

$$5P5F\;V_5 = (5P5F - 1)[CA_5(5 - 1/\,P5F) - C_1 - C_2 - 5FOV] - C_1 - 5FOV - C_2 - CA_5\,/\,P5F$$

$$V_5 = \{[CA_5(5 - 1/\,P5F) - C_1 - C_2 - 5FOV]\,(5P5F - 1) - C_1 - 5FOV - C_2 - CA_5\,/\,P5F\}/\,5P5F$$

$$V_5 = \{[5CA_5 - CA_5/\,P5F - C_1 - C_2 - 5FOV]\,(5P5F - 1) - C_1 - 5FOV - C_2 - CA_5\;P5F\}/\,5P5F$$

$$V_5 = (25P5FCA_5 - 5CA_5 - 5P5FC_1 - 5P5FC_2 - 25P5FFOV - 5CA_5 + CA_5/P5F + C_1 + C_2 + 5FOV - C_1 - 5FOV - C_2 - CA_5/P5F)/5P5F$$

$$V_5 = (25P5FCA_5 - 5CA_5 - 5P5FC_1 - 5P5F\;C_2 - 25P5F\;FOV - 5CA_5)/\,5P5F$$

$$V_5 = 5CA_5 - CA_5/5P5F - C_1 - C_2 - 5\;FOV - CA_5/5P5F$$

$$V_5 = 5CA_5 - 2CA_5/5P5F - C_1 - C_2 - 5\;FOV$$

$$V_5 = CA_5(5 - 2/P5F) - C_1 - C_2 - 5FOV \qquad (128)$$

Substituting this equation into equation (126) produces the formula for V_3:

$$V_3 = CA_5\,(5 - 1/\,P5F) - C_1 - C_2 - 5FOV - CA_5(5 - 2/P5F) + C_1 + C_2 + 5FOV$$

$$V_3 = CA_5\,(5 - 1/\,P5F) - CA_5(5 - 2/P5F)$$

$$V_3 = CA_5\,[(5 - 1/\,P5F) - (5 - 2/P5F)]$$

$$V_3 = CA_5\,(5 - 1/\,P5F - 5 + 2P5F)$$

$$V_3 = CA_5\,(-\,1/\,P5F + 2/P5F)$$

$$V_3 = CA_5\,(1/\,P5F)$$

$$V_3 = CA_5\,/\,P5F \qquad (129)$$

For our example V_3 and V_5 are calculated as follows:

$$V_3 = 575\,/\,0.75$$

V_3 = 766.7 vpatf

$$V_5 = (575)(5 - 2/0.75) - 600 - 600 - 5(12)$$

$V_5 = (575)(2.33) - 1260$

V_5 = 81.7 vpatf

So we see that, if V_1 and V_2 are at their lower limit, then the minimum possible value for V_5 is 81.7 vpatf.

If V_1 is held to its lower limit, then the **minimum** value for V_5 can be calculated by setting V_2, V_3 and V_4 equal to their **highest** possible values while maintaining the minimum required PHF and preserving conservation of flow. Recognizing that V_4 will still have the highest flow rate for this situation:

$$P5F = (V_1 + V_2 + V_3 + V_4 + V_5)/(5V_4) \quad (124)$$

Substituting equation (113) into peak period factor equation (124) yields:

$$P5F = (V_1 + V_2 + V_3 + V_4 + V_5)/(5V_4)$$

$$5P5F\ V_4 = V_1 + V_2 + V_3 + V_4 + V_5$$

$$5P5F\ V_4 - V_4 = V_1 + V_2 + V_3 + V_5$$

$$V_4 = (V_1 + V_2 + V_3 + V_5) / (5P5F - 1) \quad (130)$$

Substituting equation (113) into conservation of flow equation (97) yields:

$$(C_1 + 5FOV + V_2 + V_3 + V_4 + V_5) / 5 = CA_5$$

$$C_1 + 5FOV + V_2 + V_3 + V_4 + V_5 = 5CA_5$$

$$V_3 = 5CA_5 - C_1 - 5FOV - V_2 - V_5 - V_4 \quad (131)$$

The value of V_5 is minimized when V_3 is maximized. The maximum value of V_3 is constrained by the PHF equation:

$$P5F = (V_1 + V_2 + V_3 + V_4 + V_5)/(5V_3)$$

$$P5F = (C_1 + 5FOV + C_2 + V_3 + V_4 + V_5)/(5V_3)$$

$$5P5F\ V_3 = C_1 + 5FOV + C_2 + V_3 + V_4 + V_5$$

$$5P5F\ V_3 - V_3 = C_1 + 5FOV + C_2 + V_4 + V_5$$

$$V_3 = (C_1 + 5FOV + C_2 + V_4 + V_5) / (5P5F - 1)$$

Substituting in equation (127) we obtain:

$$V_3 = (C_1 + 5FOV + C_2 + CA_5\ (5 - 1/\ P5F)/(5P5F - 1) + V_5) / (5P5F - 1)$$

$$V_3 = (C_1 + 5FOV + C_2 + CA_5 / P5F + V_5) / (5P5F - 1)$$

And substituting in conservation of flow equation (126) produces:

$$CA_5\ (5 - 1/\ P5F) - C_1 - C_2 - 5FOV - V_5 = (C_1 + 5FOV + C_2 + CA_5 / P5F + V_5) / (5P5F - 1)$$

$$CA_5\ (5 - 1/\ P5F) - C_1 - C_2 - 5FOV = (C_1 + 5FOV + C_2 + CA_5 / P5F + V_5) / (5P5F - 1) + V_5$$

The value of V_5 is minimized when V_3 and V_4 are maximized. The maximum value of V_4 was provided previously as equation (127):

$$V_4 = CA_5 / P5F$$

For V_3 to be maximized it must also share this P5F-constrained value:

$$V_3 = CA_5 / P5F \qquad (132)$$

Substituting equation (113), (127) and (132) into conservation of flow equation (97) and solving for V_2 we obtain:

$$(V_1 + V_2 + V_3 + V_4 + V_5) / 5 = CA_5$$

$$(C_1 + 5FOV + V_2 + 2CA_5/\ P5F + V_5) / 5 = CA_5$$

$$C_1 + 5FOV + V_2 + 2CA_5/\ P5F + V_5 = 5CA_5$$

$$V_2 = 5CA_5 - C_1 - 5FOV - 2CA_5 / P5F - V_5$$

$$V_2 = CA_5(5 - 2/P5F) - C_1 - 5FOV - V_5 \qquad (133)$$

The value of V_5 is minimized when V_2 is maximized. The maximum value of V_2 is constrained by the PHF equation:

$$P5F = (V_1 + V_2 + V_3 + V_4 + V_5)/(5V_2)$$

$$P5F = (C_1 + 5FOV + V_2 + V_3 + V_4 + V_5)/(5V_2)$$

$$5P5F\ V_2 = C_1 + 5FOV + V_2 + V_3 + V_4 + V_5$$

$$5P5F\ V_2 - V_2 = C_1 + 5FOV + V_3 + V_4 + V_5$$

$$V_2 = (C_1 + 5FOV + V_3 + V_4 + V_5) / (5P5F - 1)$$

Substituting in equations (127) and (130) we obtain:

$$V_2 = (C_1 + 5FOV + CA_5/ P5F + CA_5/ P5F + V_5) / (5P5F - 1)$$

$$V_2 = (C_1 + 5FOV + 2CA_5 / P5F + V_5) / (5P5F - 1) \qquad (134)$$

And substituting in conservation of flow equation (133) produces:

$$CA_5(5 - 2/P5F) - C_1 - 5FOV - V_5 = (C_1 + 5FOV + 2CA_5 / P5F + V_5) / (5P5F - 1)$$

$$CA_5(5 - 2/P5F) - C_1 - 5FOV = (C_1 + 5FOV + 2CA_5 / P5F + V_5) / (5P5F - 1) + V_5$$

$$(5P5F - 1)\ [CA_5(5 - 2/P5F) - C_1 - 5FOV] = C_1 + 5FOV + 2CA_5 / P5F + V_5 + V_5\ (5P5F - 1)$$

$$V_5 + V_5\ (5P5F - 1) = (5P5F - 1)\ [CA_5(5 - 2/P5F) - C_1 - 5FOV] - C_1 - 5FOV - 2CA_5 / P5F$$

$$V_5 + 5P5F\ V_5 - V_5 = (5P5F - 1)\ [5CA_5 - 2\ CA_5/P5F - C_1 - 5FOV] - C_1 - 5FOV - 2CA_5 / P5F$$

$$5P5FV_5 = 25\ P5F\ CA_5 - 10CA_5 - 5P5F\ C_1 - 25\ P5F\ FOV$$
$$- 5CA_5 + 2CA_5/P5F + C_1 + 5FOV - C_1 - 5\ FOV\ 2CA_5/P5F$$

$$5P5F\ V_5 = 25\ P5F\ CA_5 - 15CA_5 - 5P5F\ C_1 - 25\ P5F\ FOV$$

$$V_5 = 5CA_5 - 3CA_5 /P5F - C_1 - 5FOV$$

$$V_5 = CA_5(5-3 /P5F) - C_1 - 5FOV \qquad (135)$$

Continuing our example:

$$V_5 = 575(5 - 3 /0.75) - 600 - 5(12)$$

$$V_5 = 575(1) - 600 - 60$$

$$V_5 = -\ 85\ vpatf$$

And using equation (132):

$$V_2 = (600 + 5(12) + 2(575) / 0.75 - 85) / (5(0.75) - 1)$$

$$V_2 = (600 + 60 + 1533.3 - 85) / 2.75$$

$V_2 = 2108.3 / 2.75$

$V_2 = 766.7$ vpatf

This is obviously not a feasible solution since V_5 is negative. In this particular case, the value for V_2 cannot be maximized with respect to its peak period factor. Once again, using equation (134):

$V_2 = 575\ (5 - 2/0.75) - 600 - 5(12) - V_5$

$V_2 = 575\ (2.33) - 660 - V_5$

$V_2 = 1341.7 - 660 - V_5$

$V_2 = 681.7 - V_5$

And since V_5 is minimized when V_2 is maximized:

V_2 = 681.7 vpatf

V_5 = 0 vpatf

So we see that if V_1 is at its lower limit, then the minimum possible value for V_5 is 0, which occurs when V_2 = 681.7 vpatf. If V_1 is **not** held to its lower limit, then the **minimum** value for V_5 can be calculated by setting V_1, V_2, V_3 and V_4 equal to their **highest** possible values while maintaining the minimum required PHF and preserving conservation of flow. Recognizing that V_4 will continue to have the highest flow rate for this situation:

$P5F = (V_1 + V_2 + V_3 + V_4 + V_5)/(5V_4)$ (124)

$P5F = (V_1 + V_2 + V_3 + V_4 + V_5)/(5V_4)$

$5P5F\ V_4 = V_1 + V_2 + V_3 + V_4 + V_5$

$5P5F\ V_4 - V_4 = V_1 + V_2 + V_3 + V_5$

$V_4 = (V_1 + V_2 + V_3 + V_5) / (5P5F - 1)$ (136)

Rearranging conservation of flow equation (97) yields:

$$(V_1 + V_2 + V_3 + V_4 + V_5) / 5 = CA_5$$

$$V_1 + V_2 + V_3 + V_4 + V_5 = 5CA_5$$

$$V_2 = 5CA_5 - V_1 - V_3 - V_5 - V_4 \quad (137)$$

The value of V_5 is minimized when V_3 and V_4 are maximized. The maximum values of V_3 and V_4 were provided previously as equations (127) and (132):

$$V_4 = CA_5 / P5F$$

$$V_3 = CA_5 / P5F$$

For V_2 to be maximized it must also share this P5F-constrained value:

$$V_2 = CA_5 / P5F \quad (138)$$

Substituting equation (127), (132) and (138) into conservation of flow equation (97) and solving for V_1 we obtain:

$$(V_1 + V_2 + V_3 + V_4 + V_5) / 5 = CA_5$$

$$(V_1 + 3CA_5/P5F + V_5) / 5 = CA_5$$

$$V_1 + 3CA_5/ P5F + V_5 = 5CA_5$$

$$V_1 = 5CA_5 - 3CA_5 / P5F - V_5$$

$$V_1 = CA_5(5 - 3/P5F) - V_5 \quad (139)$$

For our example V_1 equals:

$$V_1 = 575\ (5 - 3/0.75) - V_5$$

$$V_1 = 575\ (1.00) - V_5$$

$$V_1 = 575 - V_5$$

And since V_5 is minimized when V_1 is maximized:

V_1 = 575 vpatf

However, this is not a feasible solution for this example since V_1 must be greater than C_1 + 5FOV (which is 600 + (5)12 = 660 vpatf) or the end of the queue will be visible during the first period. As we discovered previously, V_2 cannot reach its maximum peak period factor value of CA_5 / P5F for this example without causing V_1 to drop to a value that is too low.

In general, for V_2 to reach its maximum peak period factor constrained value while maintaining a minimum non-negative value for V_5 (i.e. zero), the value of V_1 must satisfy equation (139) and conservation of flow must be maintained. Since V_1 must continue to equal C_1+ 5FOV for the queue to remain non-visible, this places a maximum value on C_1 of:

$$C_1 + 5FOV = CA_5(5 - 3/P5F) - V_5$$

$$C_1 <= CA_5(5 - 3/P5F) - 0 - 5FOV$$

$$C_1 <= CA_5(5 - 3/P5F) - 5FOV \quad (140)$$

For our example, the maximum value that C_1 can be if V_2 is to be maximized is:

$$C_1 = 575(5 - 3/0.75) - 5(12)$$

$$C_1 = 515$$

And since conversation of flow must be maintained:

$$(V_1 + V_2 + V_3 + V_4 + V_5) / 5 = CA_5$$

$$V_1 + CA_5 / P5F + CA_5 / P5F + CA_5 / P5F + V_5 = 5CA_5$$

$$V_1 + 3CA_5 / P5F + V_5 = 5CA_5$$

$$C_1 + 5FOV + 3CA_5 / P5F + V_5 = 5CA_5$$

$$C_1 = 5CA_5 - 3CA_5 / P5F - 5FOV - V_5$$

$$C_1 = CA_5(5 - 3/ P5F) - 5FOV - V_5$$

For our example:

$$515 = (575)(5 - 3/0.75) - 5(12) - V_5$$

$V_5 = (575)(1) – 60 - 515$

$V_5 = 0$

Which checks.

Five Period Analysis of Bounds Summary

For the 5 period case the results of the analysis of the bounds can be summarized as follows where the V_i's are expressed in terms of vehicles per analysis time frame:

UPPER BOUND

$V_1 = CA_5/P5F$ (101)

If $V_5 < (CA_5/2)(5 – 3/P5F)$ (108)

Then: $V_2 = CA_5/P5F$ (102)
$V_3 = CA_5/P5F$ (103)
$V_4 = CA_5(5 – 3/P5F) – V_5$ (104)

If $V_5 > (CA_5/2)(5 – 3/P5F)$ (108)
And $V_5 < (CA_5/3)(5 – 2/P5F)$ (112)

Then: $V_2 = CA_5/P5F$ (102)
$V_3 = CA_5 (5 – 2/P5F) – 2V_5$ (107)
$V_4 = V_5$ (105)

If $V_5 > (CA_5/3)(5 – 2/P5F)$ (112)

Then: $V_2 = CA_5 (5 – 1/P5F) – 3V_5$ (111)
$V_3 = V_5$ (109)
$V_4 = V_5$ (105)

LOWER BOUND

If $V_5 = 5CA_5 – C_1 – C_2 – C_3 – C_4 – 5FOV$ (122)

Then: $V_1 = C_1 + 5FOV$ (113)
$V_2 = C_2$ (114)
$V_3 = C_3$ (115)
$V_4 = C_4$ (118)
$P5F = CA_5 / (C_1 + 5FOV)$ (123)

If $V_5 < 5CA_5 – C_1 – C_2 – C_3 – C_4 – 5FOV$ (122)
And $V_5 >= CA_5 (5\text{-}1/P5F) – C_1 – C_2 – C_3 – 5FOV$ (121)

Then: $V_1 = C_1 + 5FOV$ (113)
$V_2 = C_2$ (114)

$V_3 = C_3$ (115)
$V_4 = 5CA_5 – C_1 – C_2 – C_3 – 5FOV – V_5$ (116)
$P5F = CA_5 / V_4$ (117)

If $V_5 < CA_5 (5 – 1/P5F) – C_1 – C_2 – C_3 – 5FOV$ (121)
And $V_5 >= CA_5(5 – 2/P5F) – C_1 – C_2 – 5FOV$ (128)

Then: $V_1 = C_1 + 5FOV$ (113)
$V_2 = C_2$ (114)
$V_3 = CA_5(5–1/P5F) – C_1 – C_2 – 5FOV – V_5$ (126)
$V_4 = CA_5 /P5F$ (127)
$P5F = CA_5 / V_4$ (117)

If $V_5 < CA_5(5 – 2/P5F) – C_1 – C_2 – 5FOV$ (128)
And $V_5 >= CA_5(5 – 3/PHF) – C_1 – 5FOV$ (137)

Then: $V_1 = C_1 + 5FOV$ (113)
$V_2 = CA_5 (5 – 2/P5F) – C_1 – 5FOV – V_5$ (133)
$V_3 = CA_5/ P5F$ (132)
$V_4 = CA_5 / P5F$ (127)
$P5F = CA_5 / V_4$ (117)

If $V_5 < CA_5(5 – 3/PHF) – C_1 – 5FOV$ (137)

Then: $V_1 = CA_5 (5 – 3/P5F) - V_5$ (139)
$V_2 = CA_5 / P5F$ (138)
$V_3 = CA_5 / P5F$ (129)
$V_4 = CA_5 / P5F$ (127)
$P5F = CA_5 / V_4$ (117)
$C_1 <= CA_5(5 – 3/P5F) – 5FOV$ (138)

For our example, the values are:

UPPER BOUND

$V_1 = 575/0.75$
$V_1 = 766.7$ vpatf
(V_1 = 766.7/1.25 = **613.3 vph)**

Is $V_5 = 350 < (575 /2)(5 – 3/0.75)$?
Is $V_5 = 350 < (575 /2)(1)$?
Is $V_5 = 350 < \underline{287.5}$? NO

Is $V_5 = 350 < (575 /3)(5 – 2/0.75)$?
Is $V_5 = 350 < (191.7)(2.33)$?
Is $V_5 = 350 < \underline{447.2}$? **YES**

(V_5 = 350/1.25 = **280 vph)**

$V_2 = CA_5/P5F = 575/0.75$
$V_2 = 766.7$ vpatf
(V_2 = 766.7/1.25 = **613.3 vph)**
$V_3 = 575(5 – 2/0.75) – 2(350) = 575(2.33) – 2(350)$
$V_3 = 641.7$ vpatf
(V_3 = 641.7/1.25 = **513.3 vph)**
$V_4 = 350$ vpatf
(V_4 = 350/1.25 = **280 vph)**

Is $V_5 > (575/3)(5 – 2/0.75)$?
Is $V_5 > (191.7)(2.33)$?
Is $V_5 > 447.2$? NO

LOWER BOUND

Is $V_5 = 350 = 5(575) – 600 – 600 – 600 – 600 – 5(12)$?
Is $V_5 = 350 = 2875 – 2400 – 60$?
Is $V_5 = 350 = 415$? NO

Is $V_5 = 350 < 5(575) – 600 – 600 – 600 – 600 – 5(12)$?
Is $V_5 = 350 < \underline{415}$? **YES**

AND

Is $V_5 = 350 > 575\ (5 – 1/0.75) – 600 – 600 – 600 – 5(12)$?
Is $V_5 = 350 > 2108.3 – 1800 – 60$?
Is $V_5 = 350 > \underline{248.3}$? **YES**

(V_5 = 350/1.25 = **280 vph)**

$V_1 = 600 + 5(12)$
$V_1 = 660$ vpatf
(V_1 = 660/1.25 = **528 vph)**
$V_2 = C_2$
$V_2 = 600$ vpatf
(V_2 = 600/1.25 = **480 vph)**
$V_3 = C_3$
$V_3 = 600$ vpatf
(V_3 = 600/1.25 = **480 vph)**
$V_4 = 5(575) – 600 – 600 – 600 – 5(12) – 350$
$V_4 = 2875 – 1800 – 60 – 350$
$V_4 = 665$ vpatf
(V_4 = 665/1.25 = **532 vph)**
P5F = 575 / 665
P5F = 0.865

Is $V_5 = 350 < 575\ (5 – 1/0.75) – 600 – 600 – 600 – 5(12)$?
Is $V_5 = 350 < 2108.3 – 1800 – 60$?

Is $V_5 = 350 <$ 248.3? NO

Is $V_5 = 350 < 575(5 – 2/0.75) – 600 – 600 – 5(12)$?
Is $V_5 = 350 < 1341.7 – 1200 – 60$?
Is $V_5 = 350 <$ 81.7? NO

Is $V_5 = 350 < 575(5 – 3/0.75) – 600 – 5(12)$?
Is $V_5 = 350 < 575 – 600 – 60$?
Is $V_5 = 350 <$ – 85? NO (Not Feasible)

Only Feasible If:
$C_1 <= 575(5 – 3/0.75) – 5(12)$
$C_1 <= 575 – 60$
$C_1 <=$ 515 (but $C_1 = 600$)

Generalized Analysis of Bounds Summary

The conservation of flow equation and the peak period factor equation can be generalized to any number of periods as follows:

$$(E^N V_i) / N = CA_N$$

$$(E^N V_i) / [N \, Max(V_i)] = PNF$$

where N is the number of periods in the analysis time frame and the V_i's are expressed in terms of vehicles per analysis time frame. The corresponding analysis of bounds results can be generalized as well:

UPPER BOUND

$V_1 = CA_N/PNF$

If $V_N < (CA_N/(N–3))(N – (N–2)/PNF)$

Then: $V_{N-3} = CA_N/PNF$
$V_{N-2} = CA_N/PNF$
$V_{N-1} = CA_N(N – (N–2)/PNF) – (N–4)V_N$

If $V_N > (CA_N/(N–3))(N – (N–2)/PNF)$
And $V_N < (CA_N/(N–2))(N – (N–3)/PNF)$

Then: $V_{N-3} = CA_N/PNF$

$V_{N-2} = CA_N(N - (N-3)/PNF) - (N-3)V_N$
$V_{N-1} = V_N$

If $V_N > (CA_N/(N-2))(N - (N-3)/PNF)$

Then: $V_{N-3} = CA_N(N - (N-4)/PNF) - (N-2)V_N$
$V_{N-2} = V_N$
$V_{N-1} = V_N$

LOWER BOUND

If $V_N = NCA_N - (E^{N-1}C_i) - NFOV$

Then: $V_{N-4} = C_{N4} + NFOV$
$V_{N-3} = C_{N-3}$
$V_{N-2} = C_{N-2}$
$V_{N-1} = C_{N-1}$
$PNF = CA_N / (C_{N-4} + NFOV)$

If $V_N < CA_N(N-(N-5)/PNF) - (E^{N-1}C_i) - NFOV$
And $V_N >= CA_N(N - (N-4)/PNF) - (E^{N-2}C_i) - NFOV$

Then: $V_{N-4} = C_{N-4} + NFOV$
$V_{N-3} = C_{N-3}$
$V_{N-2} = C_{N-2}$
$V_{N-1} = CA_N(N - (N-5)/P5F) - (E^{N-2}C_i) - NFOV - V_N$
$PNF = CA_N / V_{N-1}$

If $V_N < CA_N(N - (N-4)/PNF) - (E^{N-2}C_i) - NFOV$
And $V_N >= CA_N(N - (N-3)/PNF) - (E^{N-3}C_i) - NFOV$

Then: $V_{N-4} = C_{N-4} + NFOV$
$V_{N-3} = C_{N-3}$
$V_{N-2} = CA_N(N - (N-4)/P5F) - (E^{N-3}C_i) - NFOV - V_N$
$V_{N-1} = CA_N /PNF$
$PNF = CA_N / V_{N-1}$

If $V_N < CA_N(N - (N-3)/PNF) - (E^{N-3}C_i) - NFOV$
And $V_N >= CA_N(N - (N-2)/PHF) - (E^{N-4}C_i) - NFOV$

Then: $V_{N-4} = C_{N-4} + NFOV$
$V_{N-3} = CA_N(N - (N-3)/PNF) - (E^{N-4}C_i) - NFOV - V_N$
$V_{N-2} = CA_N / PNF$
$V_{N-1} = CA_N / PNF$
$PNF = CA_N / V_{N-1}$

If $V_N < CA_N(N - (N-2)/PHF) - (E^{N-4}C_i) - NFOV$

Then: $V_{N-4} = CA_N(N - (N-2)/PNF) - (E^{N-5}C_i) - V_N$

$$V_{N-3} = CA_N / PNF$$
$$V_{N-2} = CA_N / PNF$$
$$V_{N-1} = CA_N / PNF$$
$$PNF = CA_N / V_{N-1}$$

$$C_1 <= CA_N(N - (N–2)/P5F) - NFOV$$

And these equations can be further generalized to the following:

UPPER BOUND

$V_1 = CA_N/PNF$ (141)

For j = 1:
When $V_N > V_{NLL} = (CA_N/2)[N - (N–2)/PNF]$ (142)

Then:

For $1 < k < N–1$: $V_k = CA_N/PNF$ (143)

For k = N–1: $V_k = 2V_{NUL} – V_N$ (144)

For k = N: $V_k = V_N$ (145)

For j = 2 to N–3:
When $V_N > V_{NLL} = (CA_N/j)(N - (N–j)/PNF)$ (146)
And $V_N < V_{NUL} = (CA_N/(j +1))[N - (N–j–1)/PNF]$ (147)

Then:

For $1 < k < N–j$: $V_k = CA_N/PNF$ (143)

For k = N–j: $V_k = V_{NUL}(j +1) - jV_N$ (148)

For $N >= k > N–j$: $V_k = V_N$ (145)

For j = N–2:
When $V_N > V_{NLL} = (CA_N/(N–2))(N - 2/PNF)$ (149)

Then:

For k = 1: $V_k = CA_N/PNF$ (143)

For k = 2: $V_k = (N–1)V_{NUL} – (N–2)V_N$ (150)

For $N >= k > 2$: $V_k = V_N$ (145)

LOWER BOUND

For j = 1 to N–2:

If j = 1

And $V_N = V_{NUL} = NCA_N – (E^{N-1} C_i) – NFOV$ (151)

Then: $PNF = CA_N / (C_1 + NFOV)$ (152)

For k = 1: $V_k = C_k + NFOV$ (153)

For N–1 > k > 1: $V_k = C_k$ (154)

Otherwise:

When $V_N < V_{NUL} = CA_N (N – (j–1)/PNF) – (E^{N-j} C_i) – NFOV$ (155)

And $V_N > V_{NLL} = CA_N (N – (j)/PNF) – (E^{N-j-1} C_i) – NFOV$ (156)

Then: $PNF = CA_N / V_{N-1}$ (157)

For k = 1: $V_k = C_k + NFOV$ (153)

For 1 < k < N–j: $V_k = C_k$ (154)

For k = N–j: $V_k = V_{NUL} + C_k – V_N$ (158)

For N–1 > k > N–j: $V_k = CA_N /PNF$ (159)

For j = N–1:

If $V_N < V_{NUL} = CA_N (2/PNF) – C_1 – NFOV$ (160)

And $C_1 <= CA_N(N – (N–2)/P5F) – NFOV$ (161)

Then: $PNF = CA_N / V_{N-1}$ (152)

For k = 1: $V_k = V_{NUL} + C_k – V_N$ (153)

For N–1 > k > 1: $V_k = CA_N /PNF$ (159)

Historical Peak Hour Factors

This theoretical bracketing procedure for estimated delay is dependent upon the ability to identify a minimum peak hour factor for each approach under consideration. Fortunately,

information on peak hour factors is routinely collected as part of the data collection effort for most intersection evaluations. Consequently, historical peak hour factors are rather easy to identify, at least for intersections that are not over-saturated. Appendix B contains a sample of historical PHF information for various locations in Jacksonville, Florida.

Tarko and Perez-Cartagena [49] proposed the following prediction model for the Peak Hour Factor (PHF) based on time of day, population, and peak hour volume:

$$PHF = 1 - \exp(-2.23 + 0.435\,AM + 0.209\,POP - 0.258\,VOL)$$

Where: AM = 1 if AM, 0 Otherwise
VOL= Peak Hour Volume (1000's/hour)
POP = Population (1,000,000's)

Applying this equation to our four examples and assuming that we are dealing with the weekday PM peak hour at an intersection that is situated in a city of 1,000,000 people yields the following results:

625_700_650_350vph: PHF = 1 – exp (-2.23 + 0 + 0.209(1.0) – 0.258 (581.25/1000)) = **0.89**

700_725_625_350vph: PHF = 1 – exp (-2.23 + 0 + 0.209(1.0) – 0.258 (600/1000)) = **0.89**

700_700_700_350vph: PHF = 1 – exp (-2.23 + 0 + 0.209(1.0) – 0.258 (612.5/1000)) = **0.89**

725_700_700_350vph: PHF = 1 – exp (-2.23 + 0 + 0.209(1.0) – 0.258 (618.75/1000)) = **0.89**

These expected peak hour factors are well above the 0.80 minimum PHF assumed in our analysis. If the AM peak hour were under consideration, the PHF would fall to a value of 0.82, which is still above the minimum assumed value.

Hellinga and Abdy [50] investigated the variability of peak hour traffic volumes and the Peak Hour Factor (PHF) at 10 urban locations in Waterloo and Kitchener, Ontario, Canada. The average PHF for their 10-location urban data set varied between 0.88 and 0.94 with an overall

average PHF of 0.92. Their minimum PHF varied between 0.47 and 0.87 with an average minimum PHF of 0.78

One fortunate aspect of the use of peak hour factors is that low peak hour factors (factors below a value of about 0.80) are typically encountered only on low volume approaches where queues tend to remain small and delay can be directly measured. As volumes rise on an intersection approach, the associated peak hour factor tends to rise as well.

Through the use of minimum historical peak hour factors we can develop a reasonable set of lower and upper bounds for the overflow delay. After making the necessary modifications discussed in the next chapter, these bounds can be used to bracket the results of our delay prediction procedure. The required historical peak hours are readily available or can be easily derived from archived traffic count information.

Limitations to the Theoretical Bracketing Procedure

The peak hour factor based technique for theoretically bracketing delay represents a novel approach for keeping delay estimates within reasonable limits. Although the usefulness of the technique is evident, limitations on the use of the technique should be understood. These limitations include the following:

1. The technique assumes that the flow rate remains constant within each 15-minute period, which results in a piecewise linear cumulative arrival curve. This constant arrival rate assumption is made by many analysis procedures, including those contained within the Highway Capacity Manual. If the cumulative arrival curve is actually curvilinear then the bounds, especially the lower bound, may be incorrect.

2. The technique also assumes that the arrival rate observed during the final 15-minute period is the lowest rate experienced during the analysis time frame. One could conceive of circumstances where this would not be the case, especially for a long analysis time frame of greater than an hour.

3. If the end of the queue remains beyond the field of view for more than four 15-minute periods then a peak period factor will need to be used to establish the upper and lower bounds instead of the peak hour factor. Historical peak hour factors are readily available and, as was previously discussed, there even exists an equation to predict the

peak hour factor given volume, population and time-of-day information. However, since the concept of a peak period factor is introduced in this research, no information on peak period factors is directly available. Fortunately, historical peak period factors can be easily derived from archived traffic count information.

4. If, for some reason, an unusual level of peak period flow occurs such that the minimum peak period factor is violated, then the upper bound will be incorrect. Extreme peak period flows could be due to some unusual event, such as a serious accident, a special activity in the area or a weather-related incident.

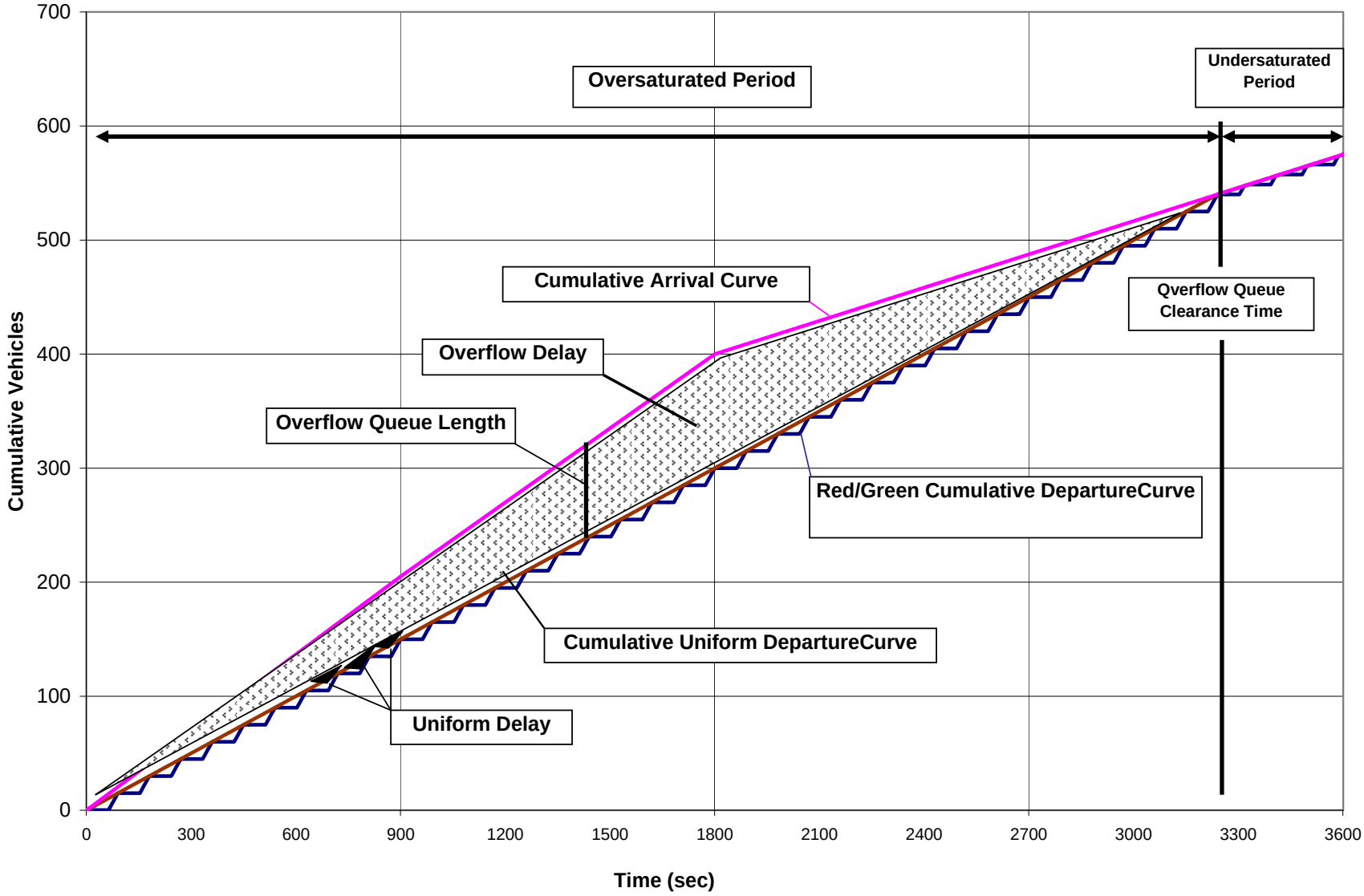

Figure 5-1. Cumulative arrival-departure curves and overflow delay

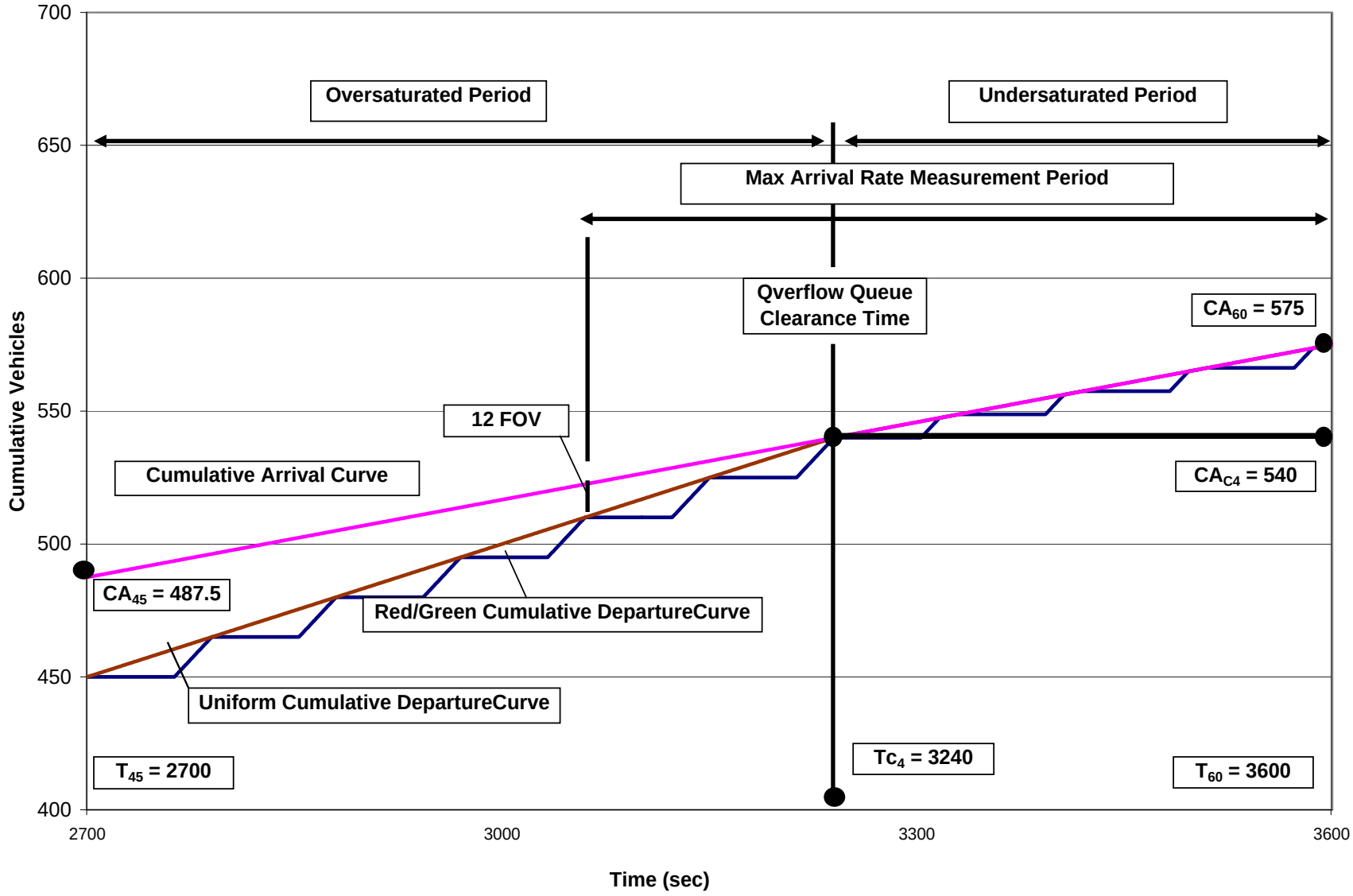

Figure 5-2. Critical time and volume points for period 4

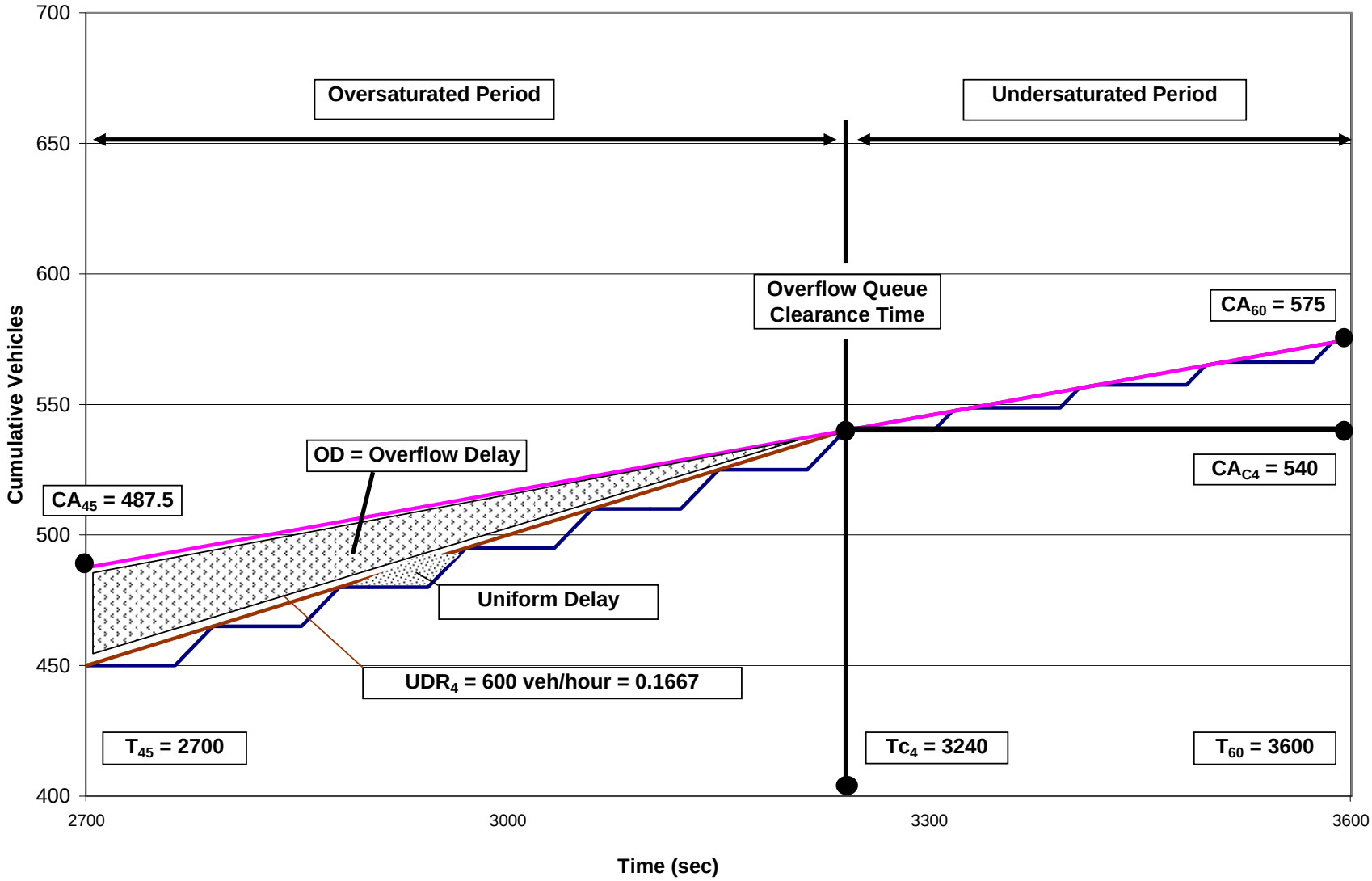

Figure 5-3. Overflow delay in period 4

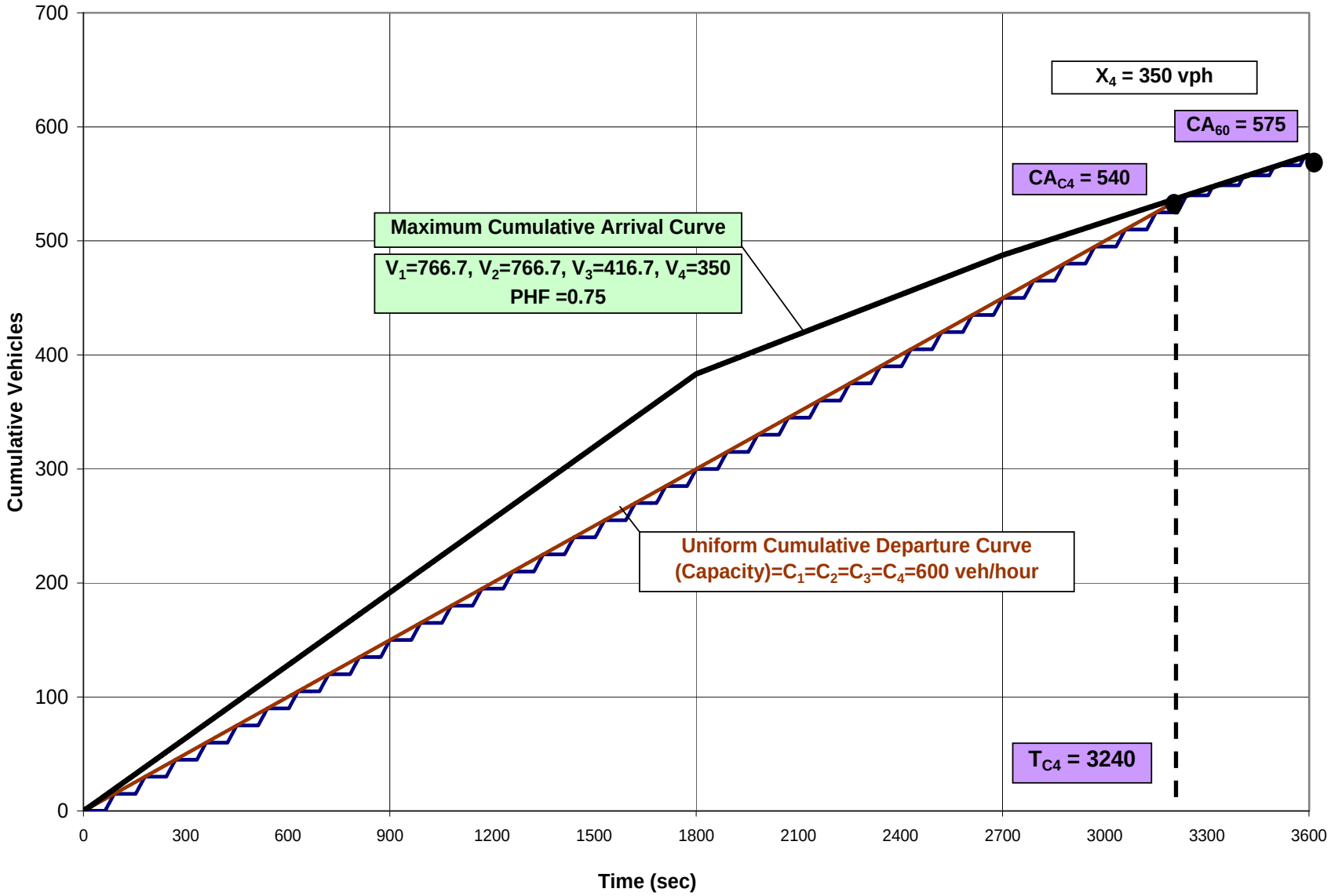

Figure 5-4. Maximum reasonable cumulative arrival curve

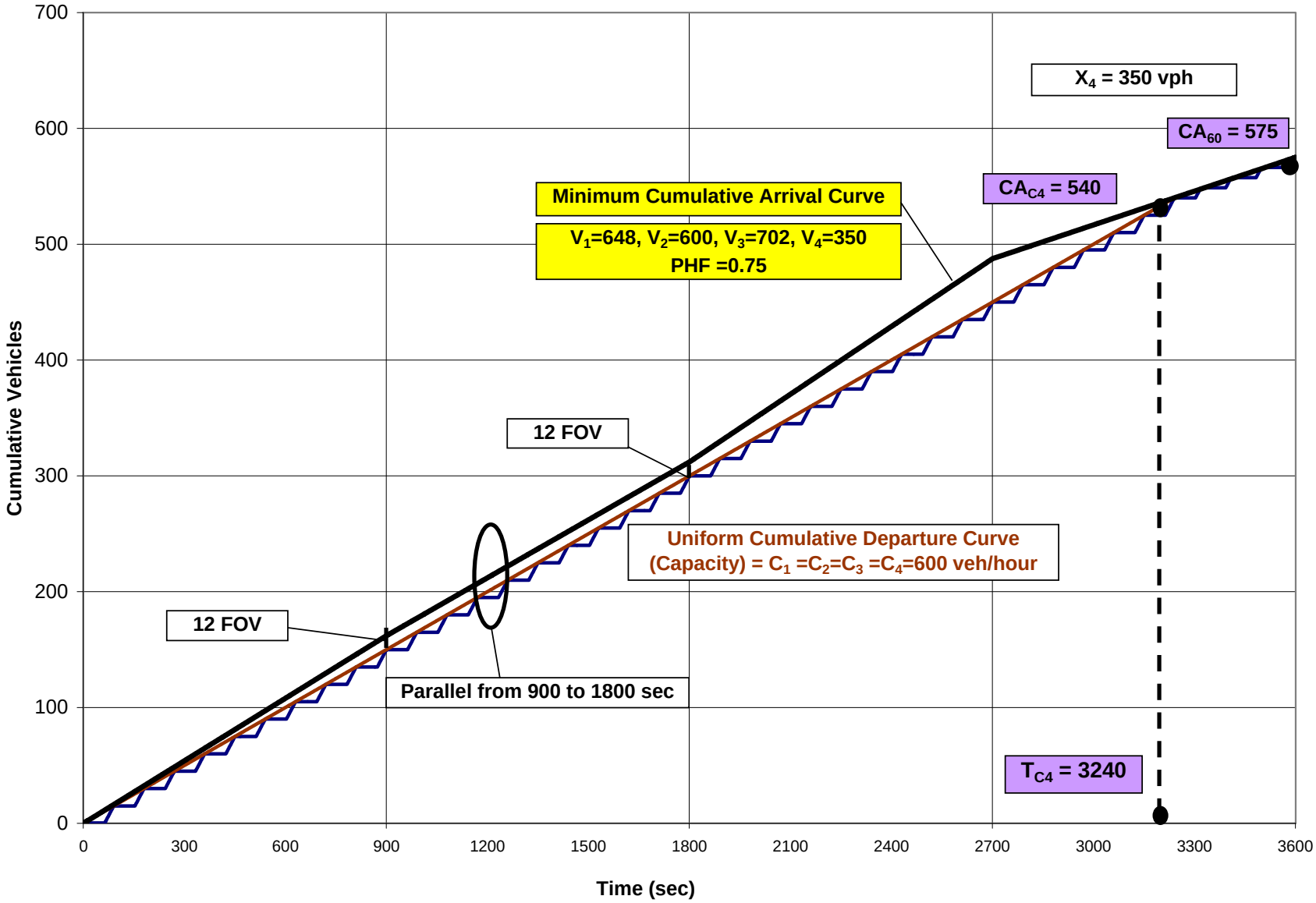

Figure 5-5. Minimum reasonable cumulative arrival curve

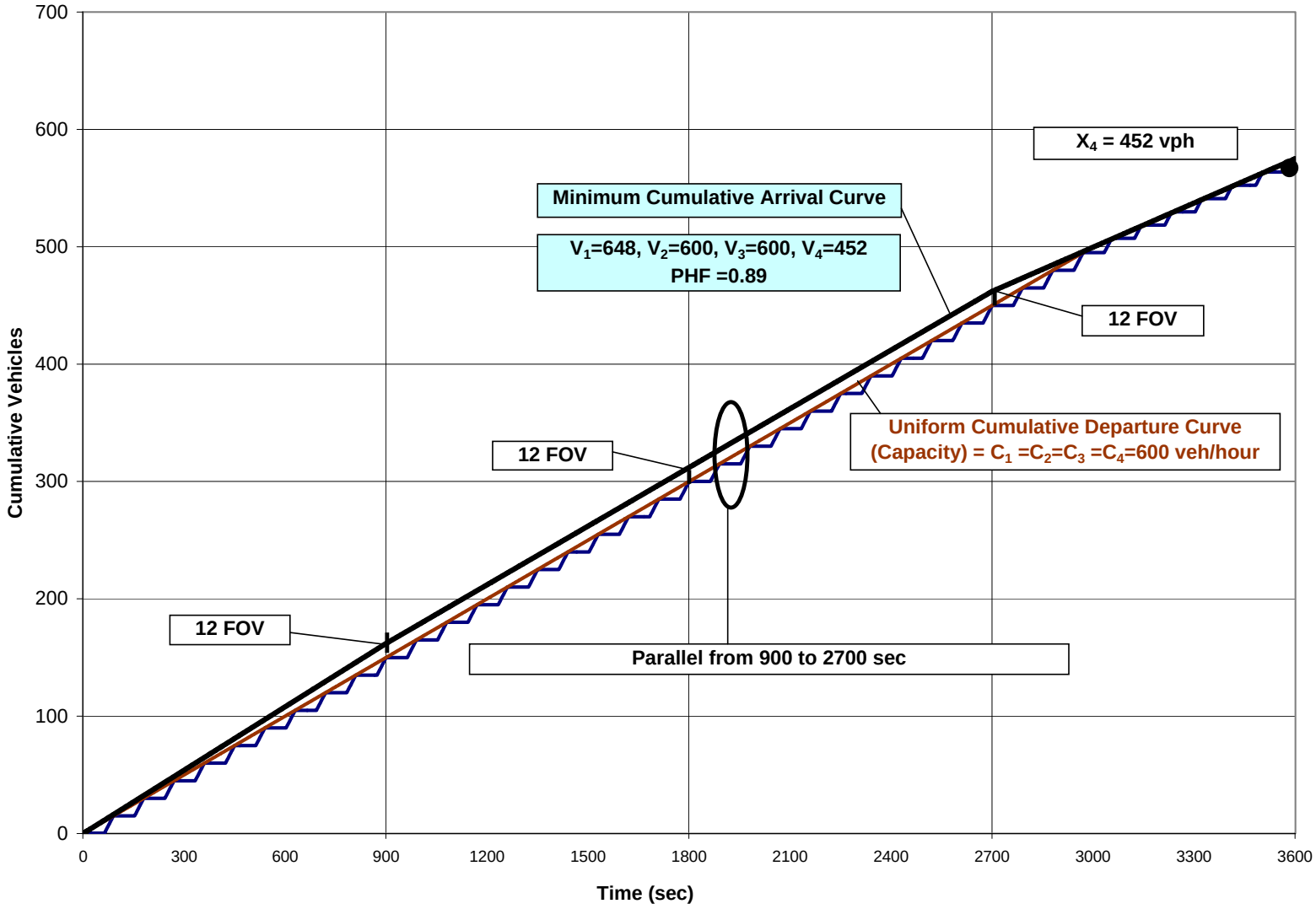

Figure 5-6. Minimum overall reasonable cumulative arrival curve

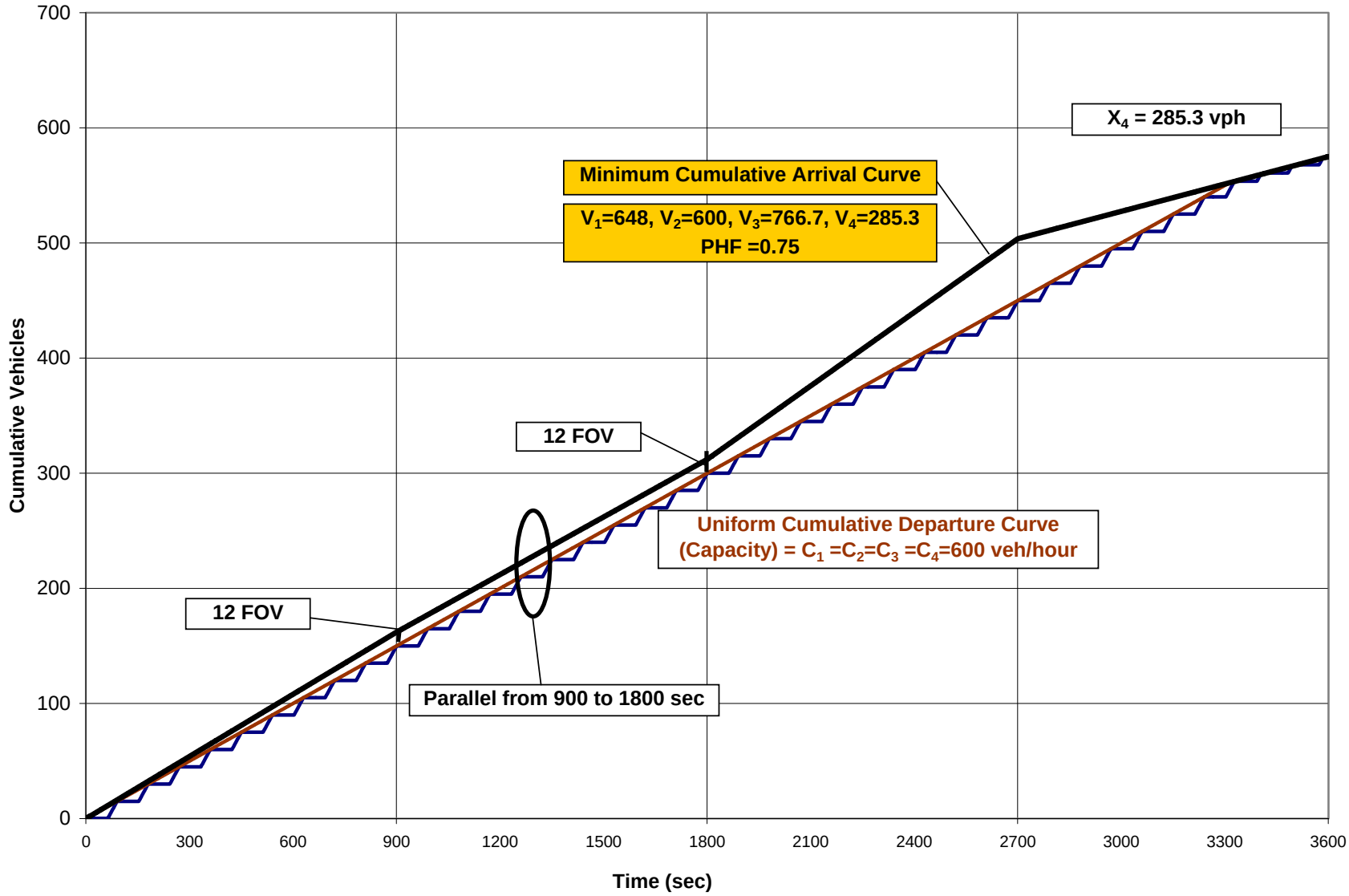

Figure 5-7. Minimum reasonable cumulative arrival curve (minimum V_4 for minimum V_1 and V_2)

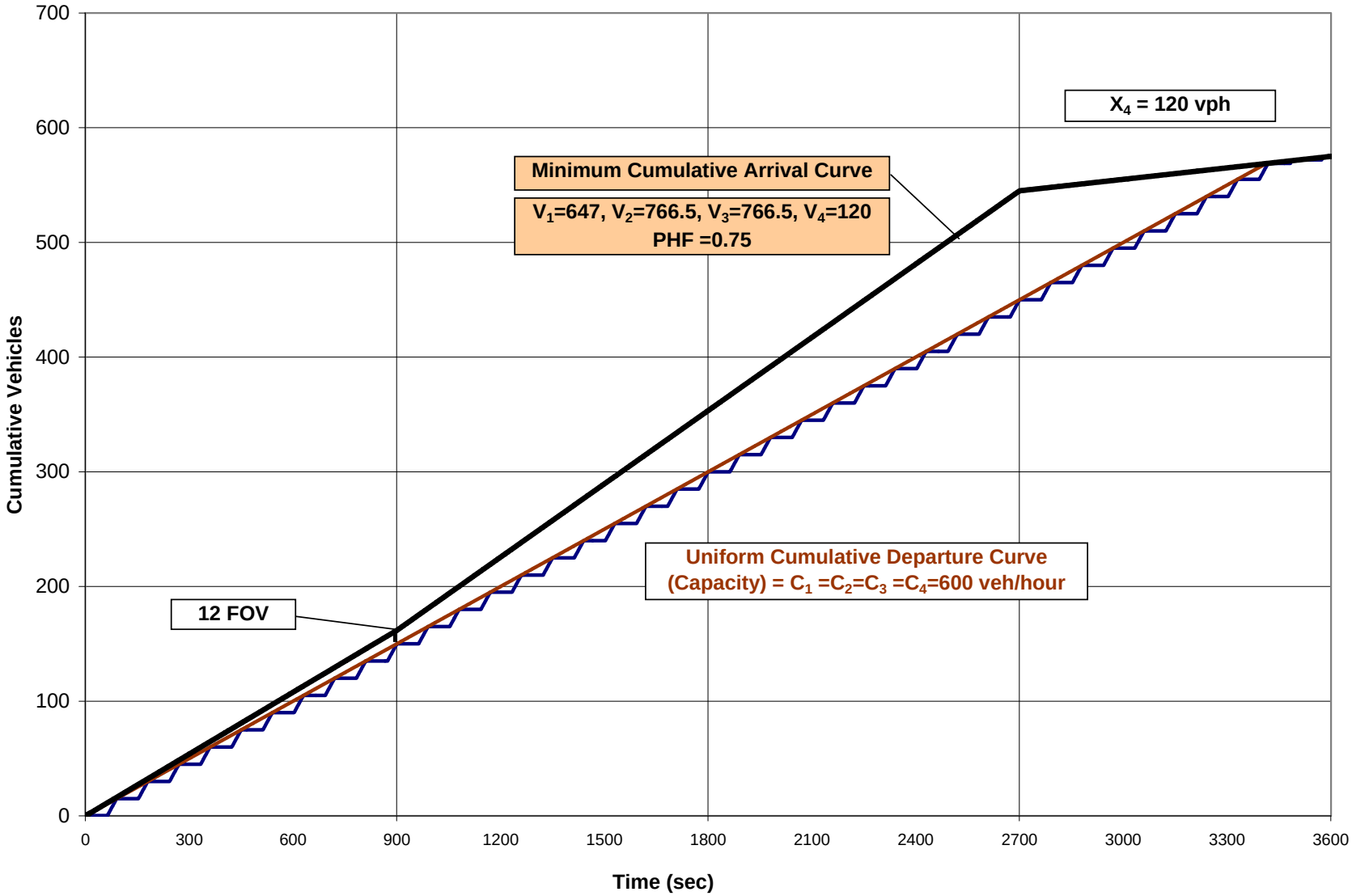

Figure 5-8. Minimum reasonable cumulative arrival curve (minimum V_4 for minimum V_1)

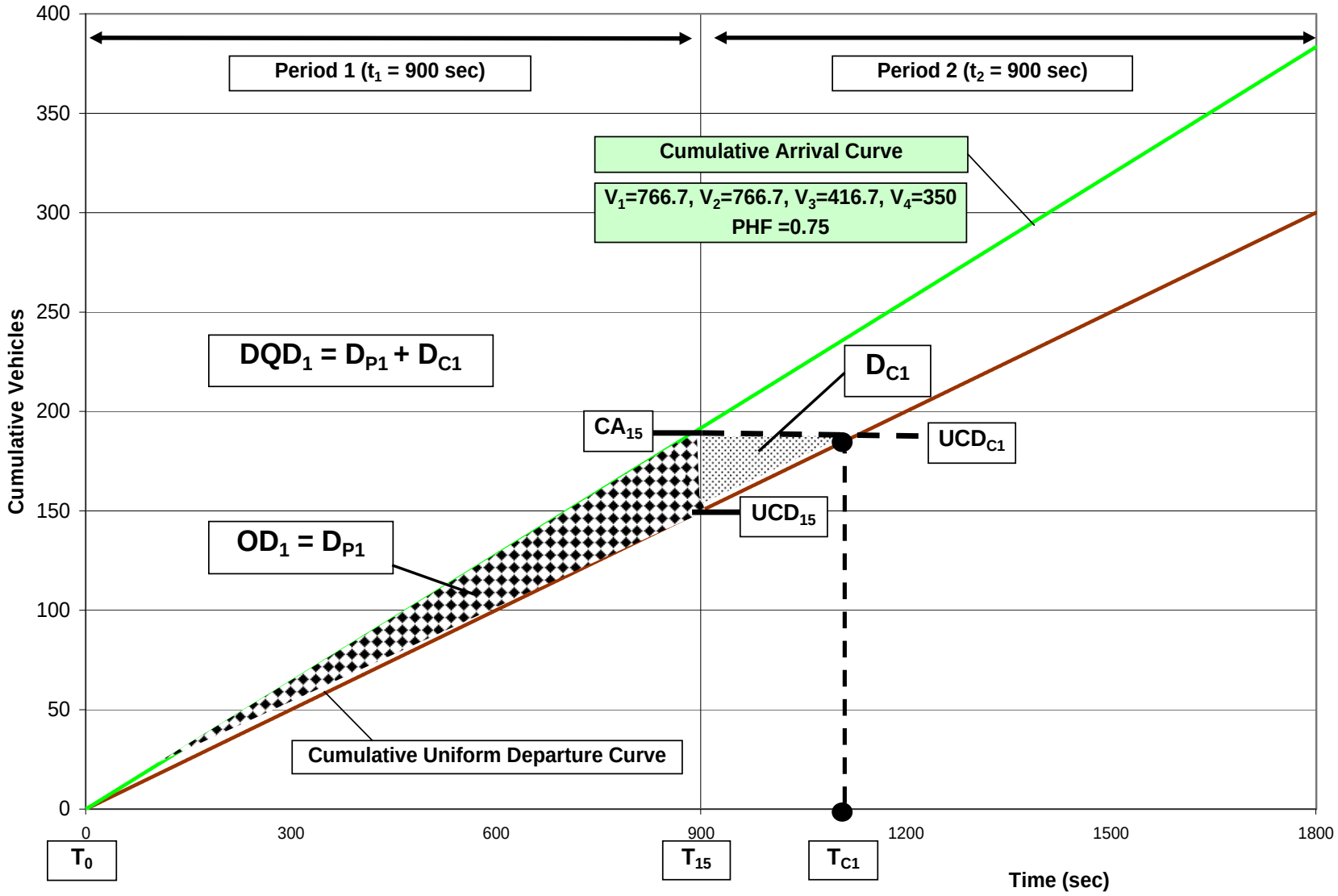

Figure 5-9. Period 1 delay for the upper bound

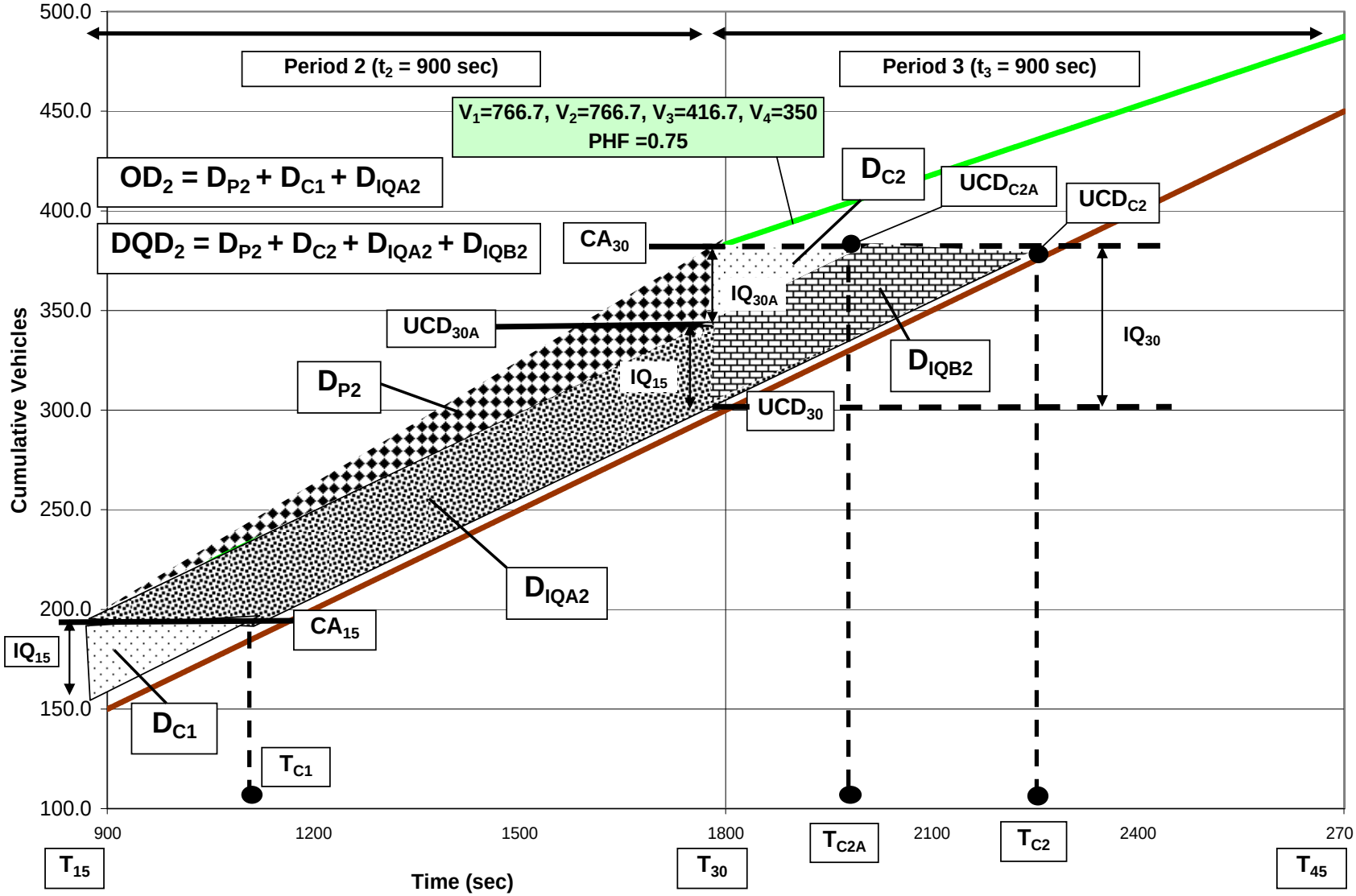

Figure 5-10. Period 2 delay for the upper bound

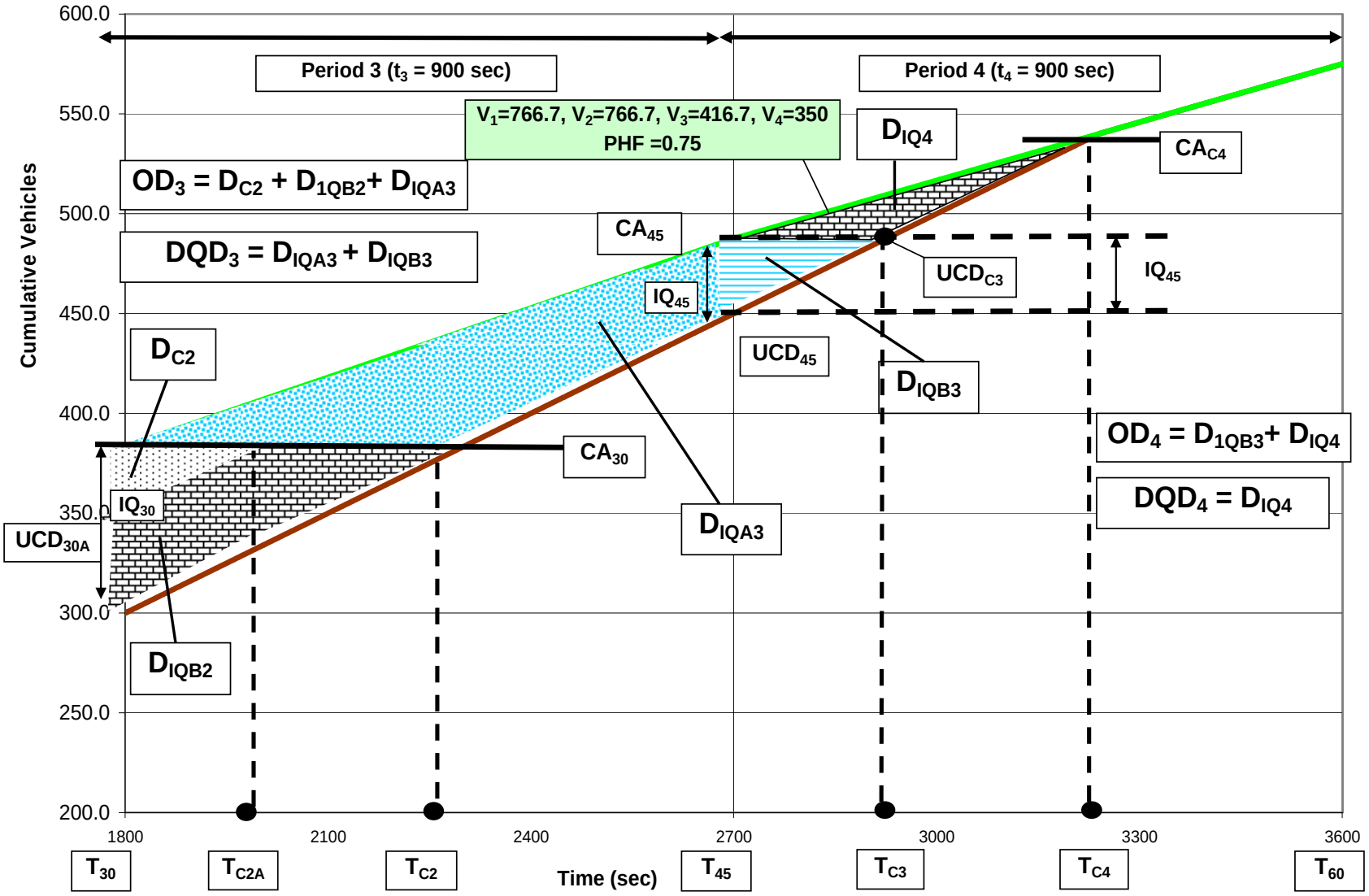

Figure 5-11. Period 3 and period 4 delay for the upper bound

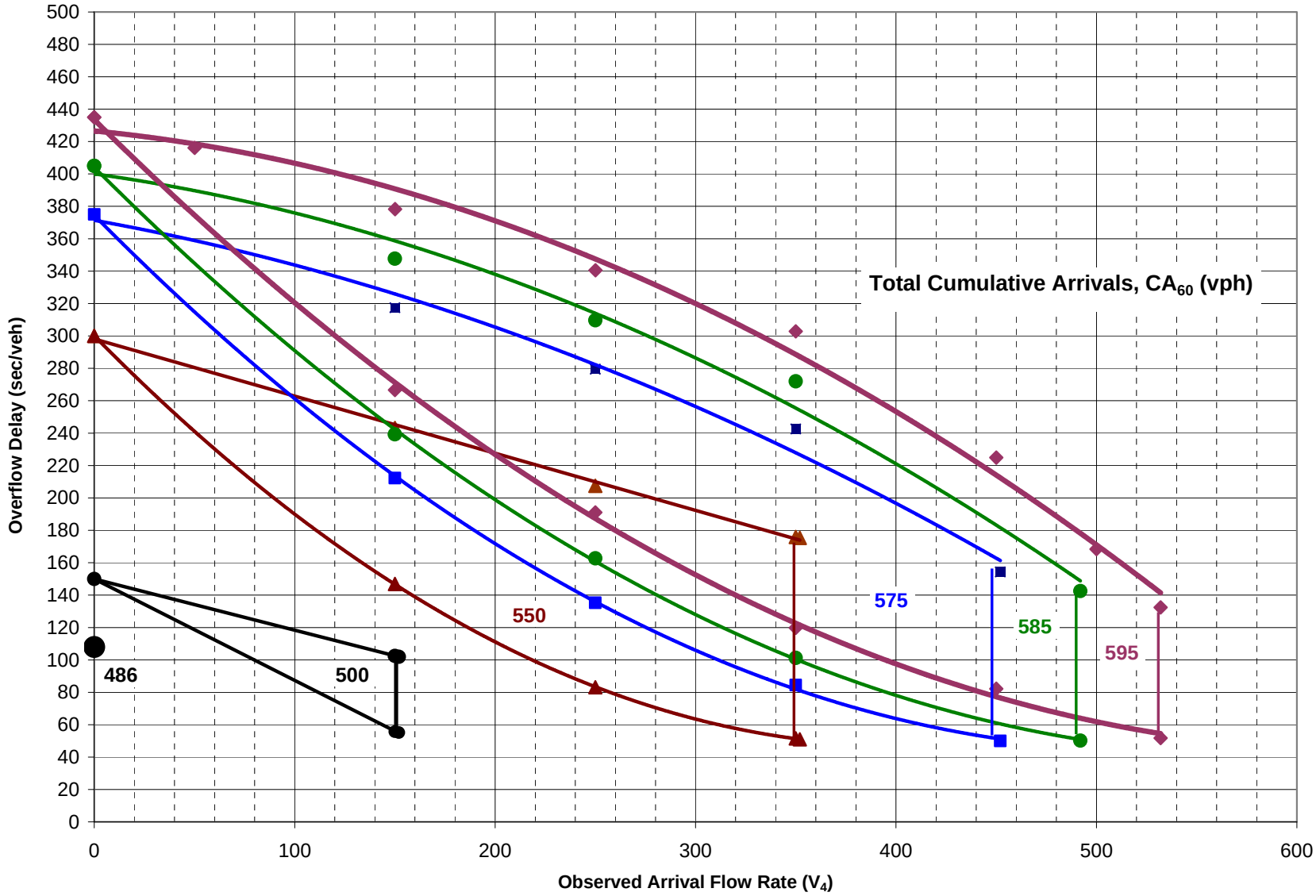

Figure 5-12. Reasonable overflow delay region for 600 vph capacity and 0.75 minimum PHF

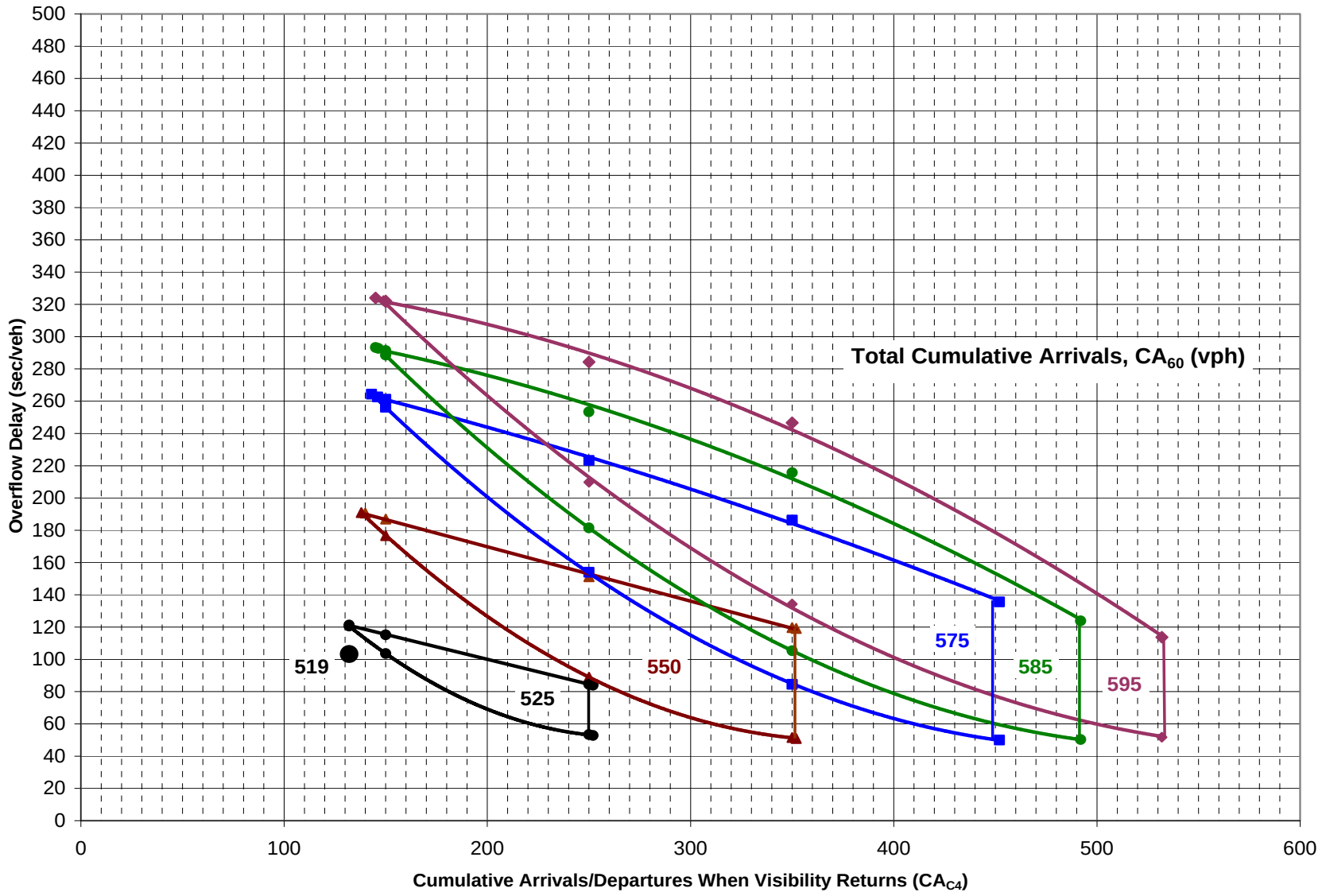

Figure 5-13. Reasonable overflow delay region for 600 vph capacity and 0.80 minimum PHF

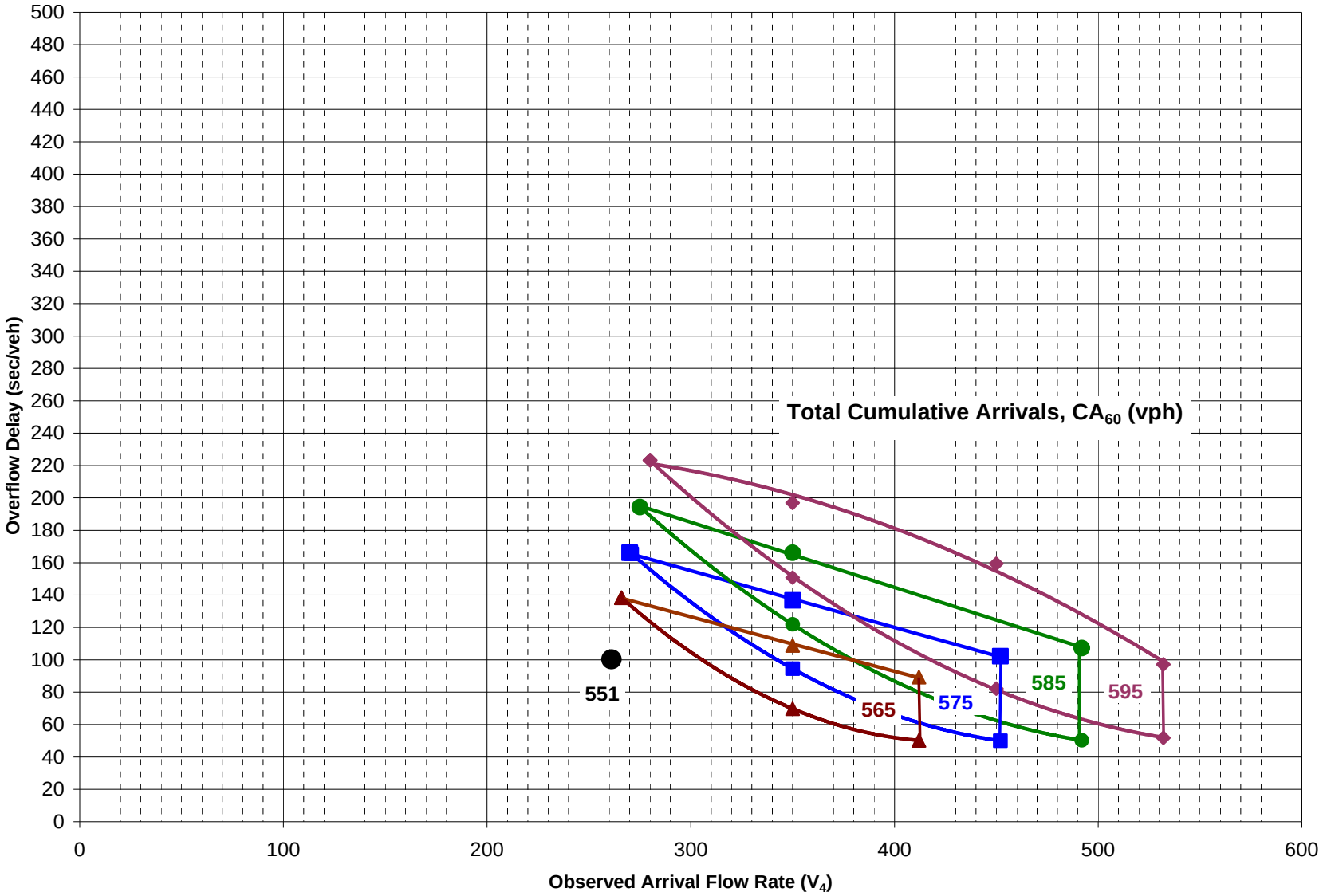

Figure 5-14. Reasonable overflow delay region for 600 vph capacity and 0.85 minimum PHF

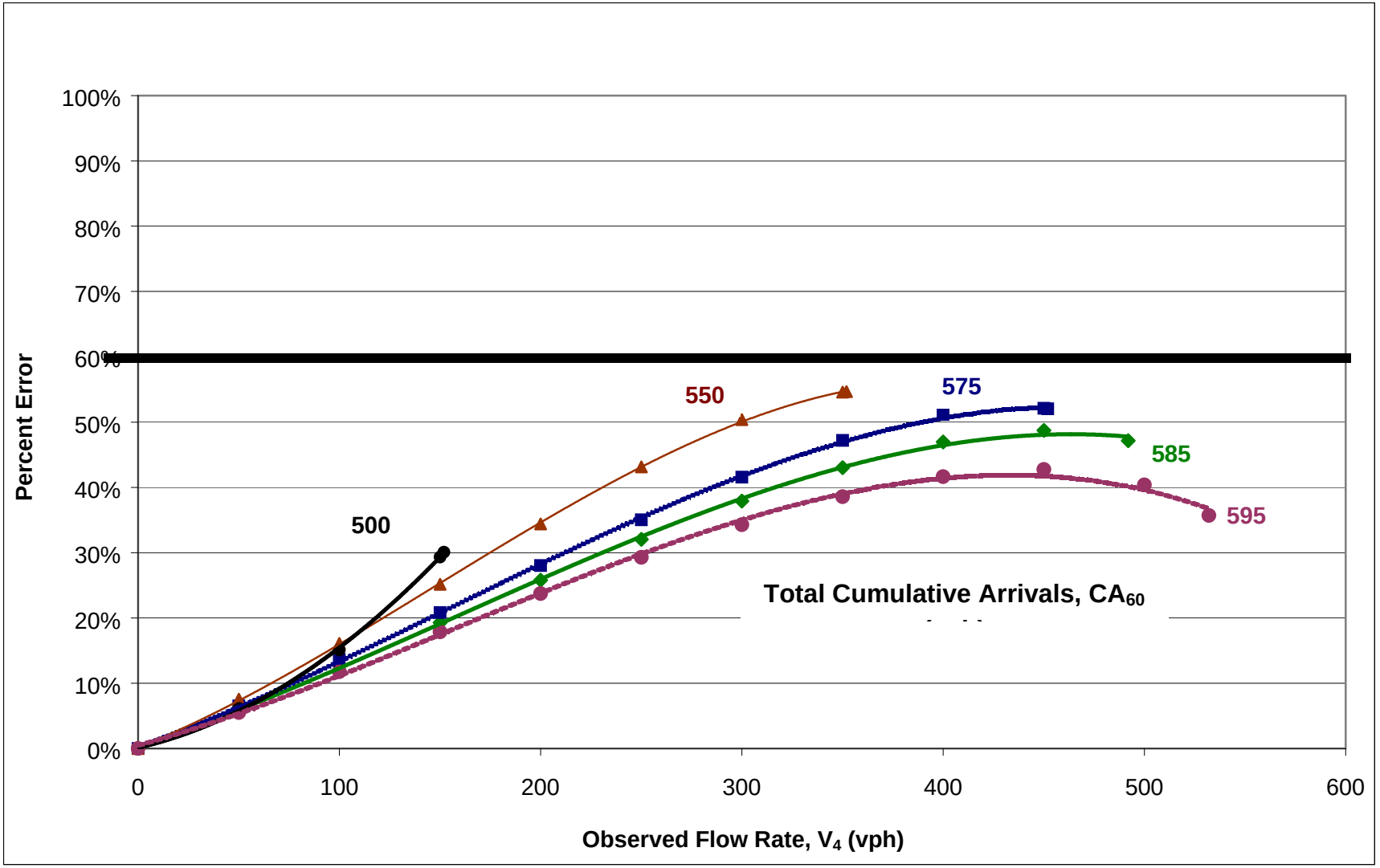

Figure 5-15. Maximum delay estimation error for 0.75 minimum PHF

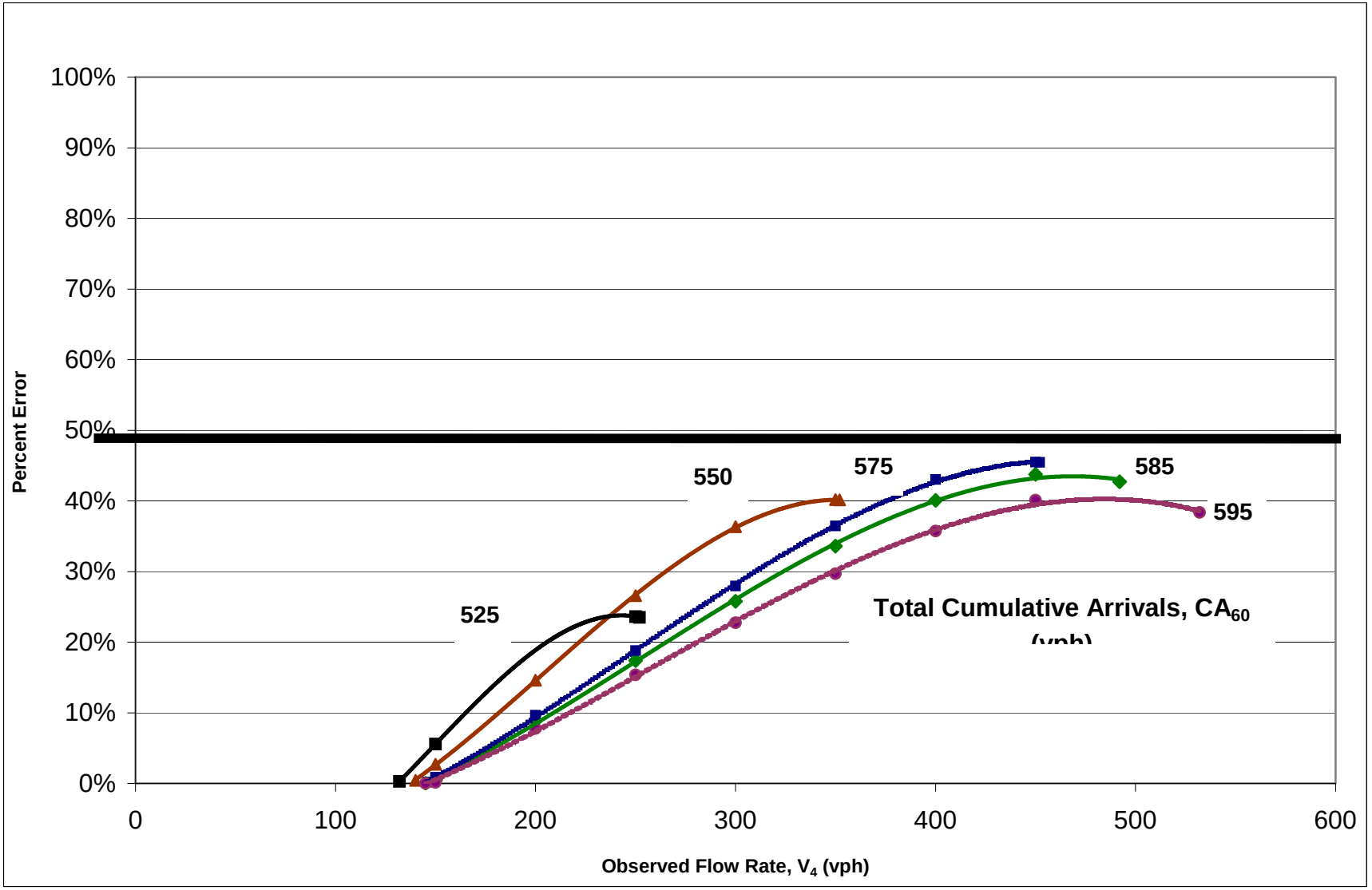

Figure 5-16. Maximum delay estimation error for 0.80 minimum PHF

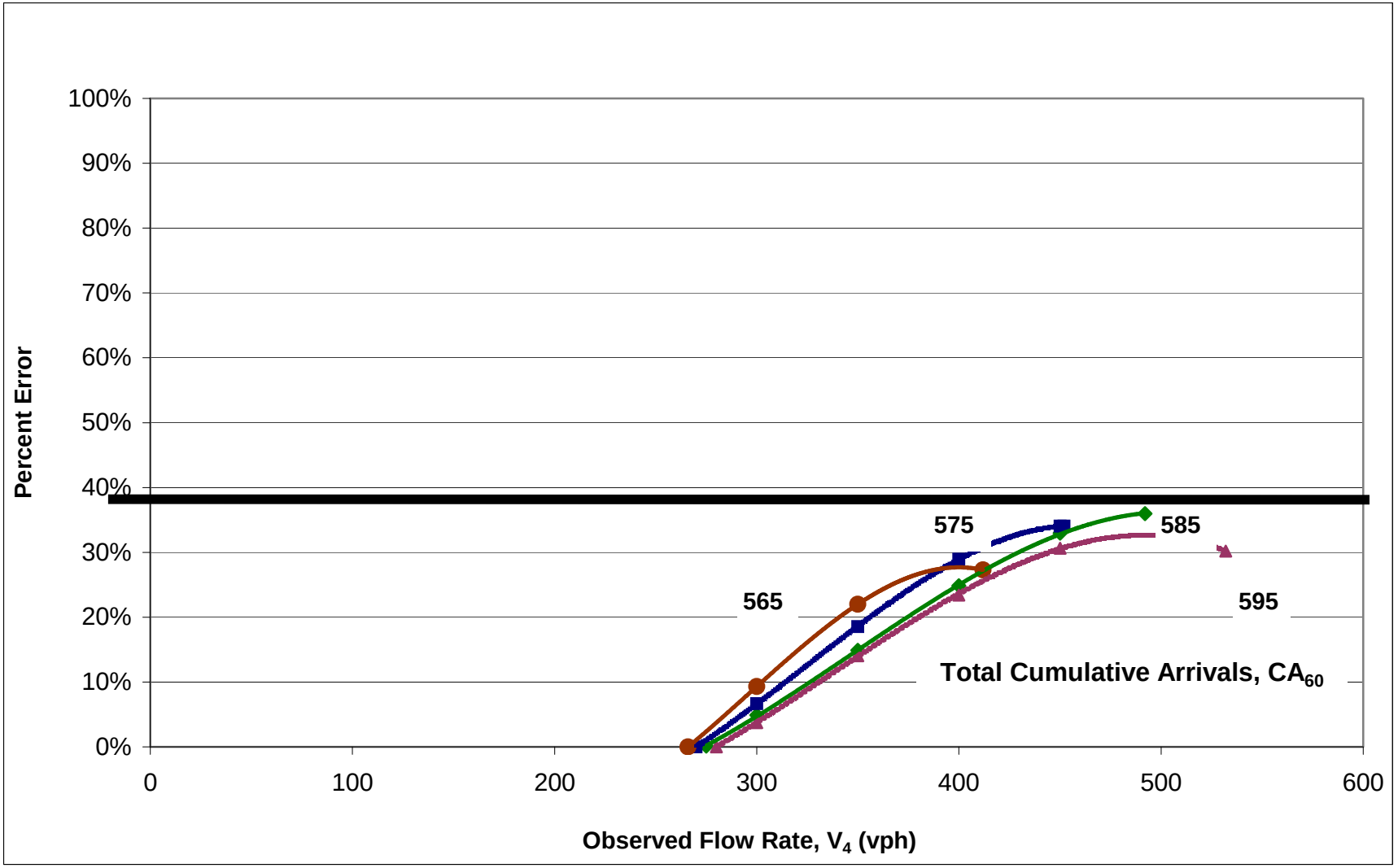

Figure 5-17. Maximum delay estimation error for 0.85 minimum PHF

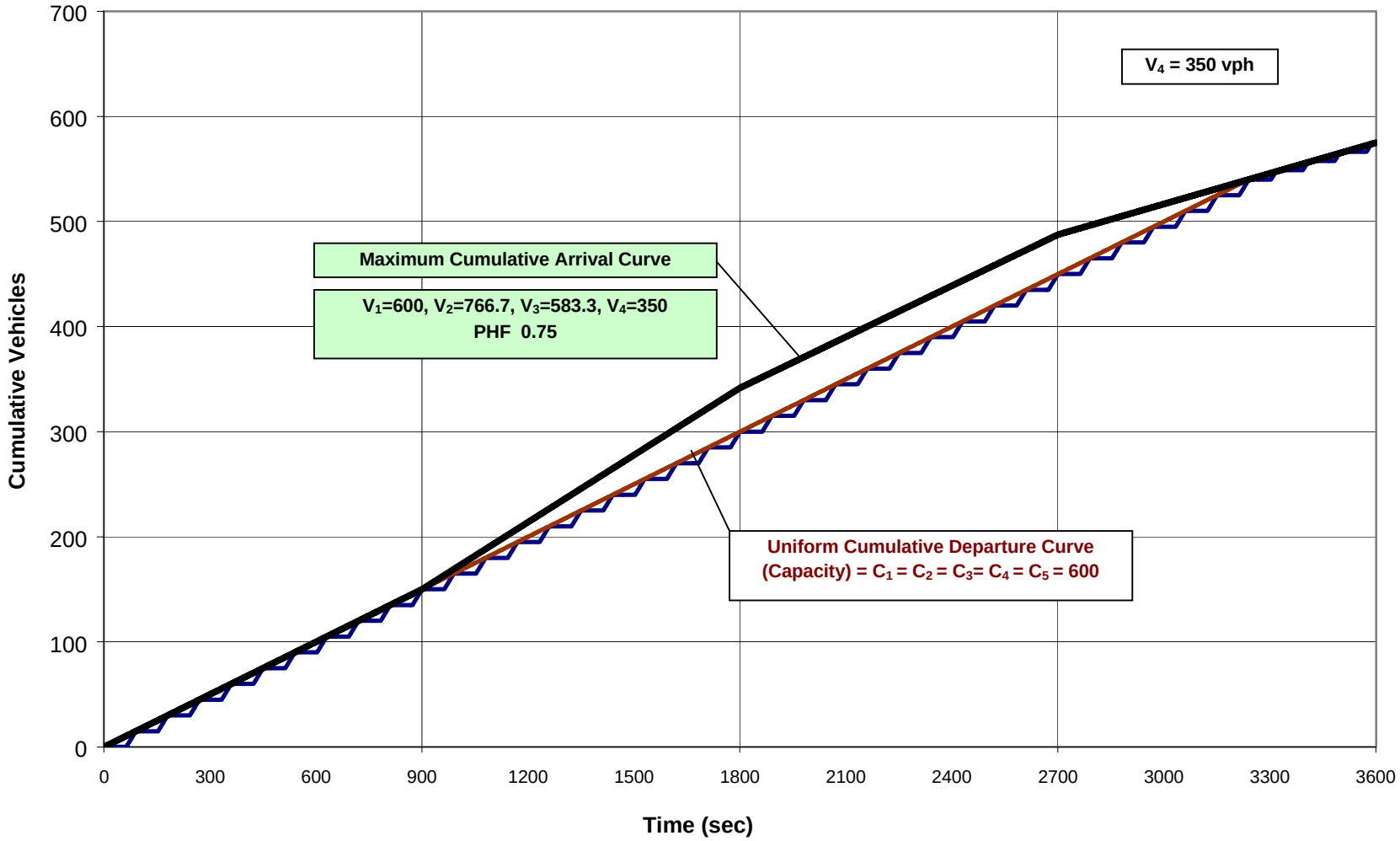

Figure 5-18. Maximum reasonable cumulative arrival curve with period 1 visible

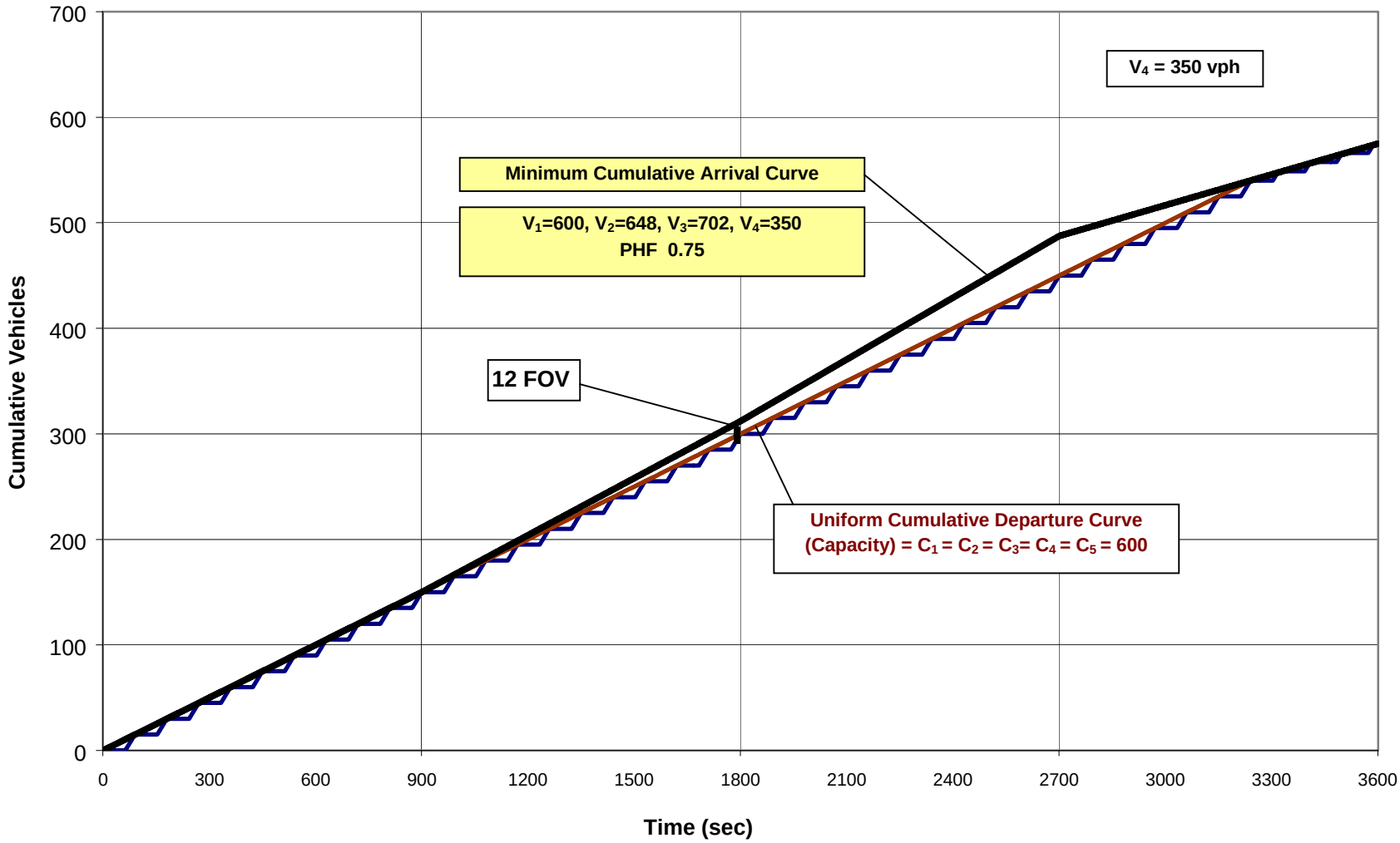

Figure 5-19. Minimum reasonable cumulative arrival curve with period 1 visible

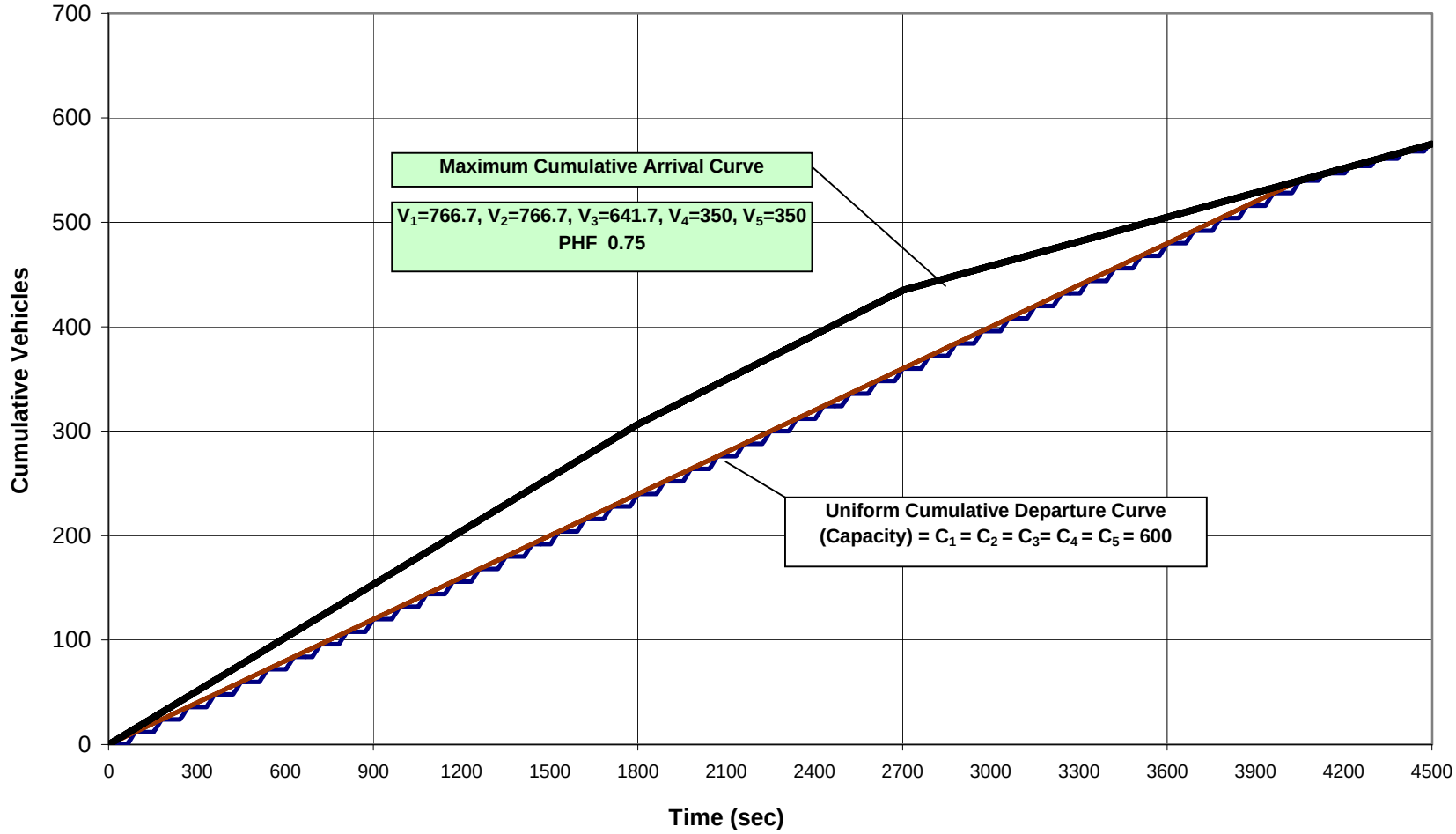

A

Figure 5-20. Maximum reasonable cumulative arrival curve with 5 periods

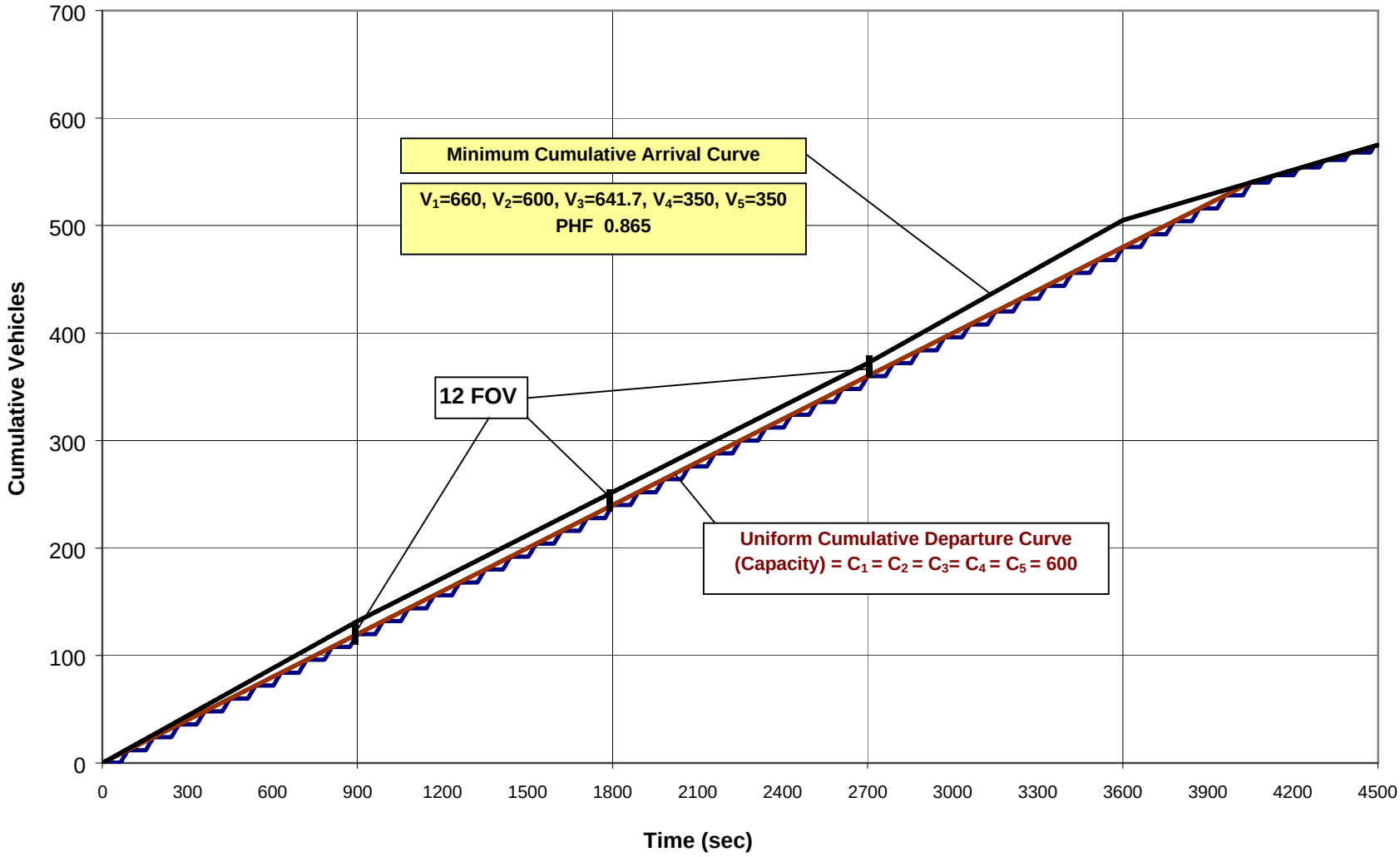

Figure 5-21. Minimum reasonable cumulative arrival curve with 5 periods

CHAPTER 6
COMPARISONS WITH VEHICLE TRAJECTORY ANALYSIS

This chapter describes a process for reconciling cumulative curve delay and control delay obtained from trajectory analysis. This reconciliation ensures that the delay limits associated with the theoretical bounds properly represent delay and are consistent with trajectory analysis (Objective 5).

The area between the cumulative arrival curve and the cumulative departure curve does not represent either stopped delay or control delay, but rather a mixture of various delay and travel time components. Trajectory analysis is used to demonstrate this fact and to establish the true relationship between overflow delay and both stopped delay and control delay.

Appendix F of Chapter 16 of the 2000 HCM discusses the relationship between the initial queue delay and deterministic queue delay using cumulative arrival curves. Five specific arrival "cases" are discussed and the proper way to account for initial queue delay and deterministic delay for each case is explained.

Unfortunately, the random portion of the control delay is not reflected in the cumulative arrival and departure curves, nor is the portion of the control delay associated with deceleration or post-stop bar acceleration. In addition, queue move-up delay and pre-stop bar acceleration delay are over-represented when using a cumulative arrival/cumulative departure approach. To prove these statements, an example has been prepared. The following technical terms are referred to in the presentation of this example:

Delay Zone = Segment length over which control delay is measured. It includes a portion of the approach link at the intersection and a portion of the departure link. For our examples, the delay zone is 3900 feet long with 3600 feet on the approach link and 300 feet on the departure link.

Stopped Delay = Time that the vehicle is stopped in a queue (stationary wheels)

Acceleration Distance = Distance that the vehicle covers while accelerating from a complete stop to its desired free flow speed

Pre-Stop Bar Free Speed Acceleration Time = Time that the vehicle would have taken to travel from the front of the queue to the stop bar had it been able to move at its desired free flow speed

Acceleration Delay = Time that the vehicle takes to accelerate form a complete stop to its desired free flow speed minus the time that the vehicle would have taken to traverse the acceleration distance had it been able to travel consistently at its desired free flow speed

Pre-Stop Bar Acceleration Delay = Time that the vehicle takes to travel from the front of the queue to the stop bar minus the time that the vehicle would have taken to traverse this distance had it been able to travel consistently at its desired free flow speed

Deceleration Distance = Distance that the vehicle covers while decelerating from its free flow speed to a complete stop

Deceleration Delay = Time that the vehicle takes to decelerate form a its free flow speed to a complete stop minus the time that the vehicle would have taken to traverse the deceleration distance had it been able to travel consistently at its desired free flow speed

Move-Up Time = Time that it takes the vehicle to travel between queues

Free Speed Move-Up Time = Time that the vehicle would have taken to travel between queues if it had been able to move at its desired free flow speed

Move-Up Delay = Time that the vehicle is delayed while traveling between queues = Move-Up Time – Free Speed Move-Up Time

Control Delay = Time that the vehicle is delayed due to intersection control = Time that the vehicle takes to traverse the delay zone minus the time that the vehicle would have taken to traverse the delay zone had it been able to travel consistently at its desired free flow speed = Deceleration Delay + Stopped Delay + Move-Up Delay + Acceleration Delay

Interaction Delay = Delay resulting from travel speeds that are lower than the desired free flow speed due to restrictions caused by other vehicles. It is not part of control delay.

Figures 50 through 53 document the differences between delay as represented by cumulative arrival curves and true control delay as given by an analysis of vehicle trajectories. As Dowling [3] has correctly noted:

> Comparison of results between tools and methods is possible only if the analyst looks at the lowest common denominator shared by all field data collection and analytical tools: **vehicle trajectories**. At this microscopic level, the analyst can compare field data to analysis tool outputs, whether the tool is microscopic or macroscopic. By computing

macroscopic MOEs from the vehicle trajectory data the analyst can compare the results of macroscopic and microscopic tools to field data **and to each other** in a consistent manner. This is the only appropriate method for comparing results between tools, validating the model results against field data, or using the outputs of other tools to compute level of service as defined by the Highway Capacity Manual.

Trajectory Example

Figure 6-1 provides an instructive example of how control delay accumulates for a single vehicle traversing a signalized intersection using the true method for analyzing delay, trajectory analysis. In this example, the vehicle initially travels at a free flow speed of 40 feet per second. It enters the delay zone at distance 0 and travels at the free flow speed for 60 seconds until it reaches a distance of 2400 feet. The vehicle then decelerates to a stop over a distance of 1000 feet, taking another 60 seconds to cover this distance. The 60 seconds of deceleration time can be decomposed into 35 seconds of deceleration delay and 25 seconds of time traveling at the free flow speed. The average speed during deceleration is 16.7 fps (1000 feet/60 seconds).

The vehicle then stops for 80 seconds, all of which is delay time. No progress forward is made. The speed is zero during this period. The vehicle takes 50 seconds to move up from its first stop to a second stop. The 50 seconds of move-up time can be decomposed in 40 seconds of move-up delay and 10 seconds of time traveling at the free flow speed. The average speed during move-up is 8 fps (400 feet/50 seconds). The vehicle then stops for another 90 seconds, all of which is delay time. No progress forward is made and the speed is zero during this period.

The vehicle then accelerates back to the free flow speed. A portion of this acceleration occurs prior to the stop bar. The vehicle travels 200 feet in 20 seconds to reach the stop bar. This 20 seconds of pre-stop bar acceleration time can be decomposed into 15 seconds of acceleration delay and 5 seconds of time traveling at the free flow speed. The remainder of the acceleration occurs after the stop bar. The vehicle travels 300 feet in 10 seconds to reach the end of the delay measurement zone. This 10 seconds of post-stop bar acceleration time can be

decomposed into 2.5 seconds of acceleration delay and 7.5 seconds of time traveling at the free flow speed. The average speed during acceleration is 16.7 fps: (200 feet + 300 feet)/(20 seconds+10 seconds).

Summarizing, the vehicle experience 262.5 seconds of delay which is composed of 35 seconds of deceleration delay, 170 seconds of stop delay, 40 seconds of move-up delay, and 17.5 seconds of acceleration delay. The vehicle spends an additional 107.5 seconds of time traveling at the free flow speed: 25 seconds of which occurs during the deceleration period, 10 seconds of which occurs during move up, and 12.5 seconds of which occurs during acceleration (the remaining 60 seconds occurs at the start of the period under free-flow conditions).

Trajectory analysis gives a true picture of vehicular delay. The only component of delay that is not represented by this single-vehicle diagram is interaction delay, which is not a part of control delay.

In setting up our trajectory analysis, we would like to minimize the amount of interaction delay that is captured by making the delay zone as short as possible. The longer we make the delay zone, the more unwanted interaction delay between vehicles will occur. However, attempts to reduce interaction action delay by reducing the length of the delay zone can lead to a situation where significant amounts of deceleration or acceleration delay go unmeasured because they occur outside the delay zone. Free flow speeds may not be accurately obtained as well if the delay zone is too short. Consequently, a certain unknown amount of interaction delay will almost always be included in our control delay measurement. Fortunately, under most conditions of interest, interaction delay is relatively small in comparison to control delay and can be ignored.

Cumulative Arrival/Departure Curve Example

Figure 6-2 tracks the vehicle previously shown in Figure 6-1, but this time using a typical set of cumulative arrival and cumulative departure curves. As in Figure 6-1, Vehicle X stops at the back of the queue (thus "arriving") at time point 120 and vehicle X eventually crosses the stop bar (thus "departing") at time point 360. In a traditional cumulative arrival/cumulative departure analysis, the type of analysis discussed in Appendix F of Chapter 16 of the Highway Capacity Manual, control delay is equated to the area between the two curves.

There are three principal problems with this approach**.** The first and most obvious is that **none of the deceleration delay is accounted for in the area between the curves** since, by definition, all of the deceleration delay occurs before the vehicle arrives at the back of the queue.

Analyzing the movement of vehicles between the two cumulative curves, we can see the second problem with this view of delay; **it includes two time components that are not delay at all**: Free Speed Move-Up Time and Free Speed Acceleration Time Prior to the Stop Bar. Upon arriving at time point 120 there are 24 other vehicles situated between the stop bar and Vehicle X. Contrary to popular belief, the vertical distance of 24 vehicles is not necessarily the length of the queue at time 120 because some of the vehicles may be in motion, either moving-up between queues or accelerating towards the stop bar just prior to departure. This is an important distinction because, as we observed during the trajectory analysis, the time spent by vehicles in motion can only partially be construed as delay time. This leads us to conclude that the horizontal distance covered by vehicle X is not the delay experienced by Vehicle X since it includes the free flow speed portion of the move-up time as well as the free flow speed portion of the pre-stop bar acceleration delay.

This means that, once more contrary to popular belief, the time spent by Vehicle X between the cumulative arrival and cumulative departure curves is not its control delay, or even its stopped delay, but is rather made-up of the following 5 components:

1.) Stopped delay
2.) Move-up delay
3.) Free Speed Move-Up Time
4.) Pre-Stop Bar Acceleration Delay
5.) Pre-Stop Free Speed Acceleration Time

To convert this time to pure delay, we must subtract out the two free flow speed time components.

The third problem is that **none of the post-stop bar acceleration delay is accounted for** in the area between the curves.

Reconciling the Difference Between Cumulative Curves and Trajectories

Continuing our example, Figure 6-3 shows the simplified cumulative arrival/cumulative departure curve view of the world converted into a trajectory analysis. This view ignores deceleration delay, as well as the portion of acceleration delay that occurs downstream of the stop bar. This can be represented graphically by having vehicles approach the queue at free-flow speed (Line A on the figure) and depart the stop line at free flow speed (Line B in the figure). In the naïve world of cumulative arrival and departure curves, the vehicle is added to the cumulative arrival curve, and delay time begins, when the vehicle arrives at the back of the first queue. The vehicle is then added to the cumulative departure curve, and delay time ends, when the vehicle departs the stop bar. In this example, delay time begins at T = 120 seconds and ends at T = 360 seconds, for a total delay value of 240 seconds, 22.5 seconds less than the 262.5 seconds of delay obtained through proper trajectory analysis.

It is possible to reconcile the 262.5 seconds of delay produced through proper trajectory analysis and the 240 seconds of delay given by the cumulative curves. First, the deceleration

delay (35 seconds) is added to the cumulative curve delay (240 seconds) to obtain an adjusted delay of 275 seconds. The portion of the acceleration delay that occurs downstream from the stop bar (2.5 seconds) is also added in to obtain a new adjusted delay of 277.5 seconds. Finally, as previously discussed, it is necessary to subtract out the free flow speed portion of the move-up time (10 seconds) and the free flow speed portion of the pre-stop bar acceleration time (5 seconds) to obtain a final adjusted delay of 262.5 seconds, which now matches the delay from the trajectory analysis. This last adjustment is required because the cumulative procedure fails to account for the fact that not all of the time spent between arrival at the back of the queue and departure from the stop bar is delay time, some of the time is being productively used to cover the distance (600 feet in this case) between the back of the queue and the stop bar (600 feet/40 fps = 15 seconds).

The Highway Capacity Manual delay formula also contains a random element of delay that is not directly reflected in the cumulative arrival and departure curves. Consequently, the delay calculated via these formulas would be somewhat higher than 240 seconds. Unfortunately, this delay element is added in a macroscopic fashion, which makes it impossible to translate into the microscopic situation shown here.

Since some of the errors in the cumulative arrival/cumulative departure procedure result in the control delay being underestimated (failure to include deceleration delay or acceleration delay past the stop bar) while others result in the delay being overestimated (inclusion of free flow speed move-up time and free flow speed pre-stop bar acceleration time), the errors may, to a large degree, cancel each other out. For example, initial simulation testing has shown that, under a rather wide range of over-saturated conditions, the free flow speed move-up time and free flow speed pre-stop bar acceleration time make up about 10% of the control delay.

Coincidentally, the acceleration delay and post-stop bar deceleration delay also sum to about this 10% value, producing overall delay results that look fairly good. However, it should be recognized that this counter-balancing effect is not guaranteed, and conditions can arise wherein the errors become significant.

Summarizing, a comparison of the control delay obtained from trajectory analysis and that obtained from cumulative arrival/departure curves shows that the cumulative curves omit certain valid portions of the control delay, while including other portions of time that are not delay at all. To guarantee a true measure of control delay, the delay values obtained from these curves must be adjusted by adding in the deceleration delay and the post-stop bar acceleration delay, and by subtracting out the free flow speed portion of both the move-up time and the pre-stop bar acceleration time.

Figure 6-4 illustrates the various delay-related travel time components in relation to a set of cumulative arrival and departure curves. In Chapter 5 it was shown how a reasonable set of cumulative arrival and cumulative delay curves associated with minimum and maximum delay could be constructed using minimum peak hour factors. Recognizing the relationships depicted in Figure 6-4, stopped delay (D_S) can be obtained from these cumulative curves by converting the area between the curves ($A_{CC} = D_{CC} + T_{CC}$) as follows:

$$A_{CC} = D_{CC} + T_{CC} = D_S + D_{MU} + D_{A1} + T_{MU} + T_{A1} \quad (162)$$

Let E_{CC}=Non-Stopped Delay Portion of Cumulative Curve Area=$D_{MU} + D_{A1} + T_{MU} + T_{A1}$

Therefore: $A_{CC} = D_S + E_{CC}$

$$A_{CC} = D_S + D_S (E_{CC} / D_S)$$

$$A_{CC} = D_S (1 + E_{CC} / D_S)$$

$$D_S = A_{CC} [1/(1 + E_{CC} / D_S)] \quad (163)$$

So, if the non-stopped delay elements associated with the area between the cumulative curves equals 35% of the stopped delay (E_{CC} / D_S = 0.35), then 74% of the area between the cumulative curves is associated with stopped delay: $D_S = A_{CC} [1/(1 + 0.35)] = 0.74 A_{CC}$

Calculating Trajectory-Based Delay Components for the BuckQ Examples

Trajectory-based delay was calculated for the twelve BuckQ data sets (four examples, each with three random number seeds) using the BuckTRAJ program. The results of the trajectory analysis can be used to identify the non-stopped delay portion of the cumulative arrival area based on equations 162 and 163. Tables 6-1 through 6-4 summarize the resulting percentages that are used to convert the overflow delay, as reflected in the area between the cumulative curves, into stopped delay. The conversion percentages are fairly stable regardless of the volume levels or period, ranging from 74% to 79% and averaging about 77%. It is quite interesting to note that using the area between the cumulative arrival curves as a measure of stopped delay can be expected to produce results that are more than 20% too high. The results of our BuckTRAJ runs were also used to investigate the relationship between the area between the cumulative arrival curves and control delay. As a review of Tables 6-1 through 6-4 indicates, the conversion percentages are also relatively stable for this case, ranging from 93% to 103% and averaging about 98%. Given these results, it appears that using the area between the cumulative curves to approximate control delay is not unreasonable since the various delay errors inherent in using the cumulative curves almost exactly compensate for one another.

Changing cumulative curve delay to stopped delay requires the application of these delay conversion factors. To obtain the true factors for the situation at hand, a complete trajectory analysis is required. However, if we have enough information to conduct a complete trajectory analysis then we can determine the control delay directly and our entire delay estimation procedure is not needed. Since we don't have this information, typical conversion factors (such

as the 77% factor evident from our four examples) will need to be applied to the upper and lower delay bounds and there will be some inherent error in this conversion process.

Calculating Cumulative Curve Delay for the BuckQ Examples

The formulas contained in sections B, D and E of Chapter 5 were applied to our four BuckQ examples in order to calculate the area between the cumulative arrival curve and the cumulative departure curve (which equals the overflow delay plus the uniform delay). Each random number replicate for the four examples was examined separately, resulting in twelve sets of delay calculations. The random number results were not aggregated since it is the explicit intent of our delay estimation procedure to detect variations in delay due to these random variations. Nine of the twelve data sets are representative of a "standard" analysis situation wherein the true arrival rate can only be determined for period 4. The formulas contained in Section B of Chapter 5 pertain in this case. However, two of the three data sets associated with the lowest volume arrival pattern (625_700_650_350vph) have visible queues during period 1, allowing an arrival rate to be calculated for this period as well. The formulas contained in Section D of Chapter 5 pertain to this case. The remaining 625_700_650_350vph data set has visible queues during all but one period and the formulas contained in Section E of Chapter 5 pertain to this case.

The cumulative curve delay for the 4-period Upper Bound assuming a minimum PHF of 0.80 was calculated and the resulting maximum cumulative overflow delay values for each 15-minute period are provided on the right side of Table 6-5. The cumulative curve delay for the 4-period Lower Bound was also calculated and the resulting minimum cumulative overflow delay values for each 15-minute period are provided on the left side of Table 6-5. The middle of Table 6-5 provides similar values for the "estimated actual" delay. This is the delay obtained from the cumulative curve formulas when the actual arrival rates are used.

The cumulative curve delay was calculated for the Upper Bound when queues are visible throughout period 1. The resulting maximum cumulative overflow delay values for each 15-minute period are provided on the right side of Table 6-6. Cumulative curve delay was also calculated for the cumulative Lower Bound curve for the case where period 1 queues are visible. The resulting minimum cumulative overflow delay values for each 15-minute period are provided on the left side of Table 6-6. The middle of Table 6-6 provides similar values for the estimated actual delay.

Also included in Table 6-6 are the delay results for the case when all but one period is visible. In this case, it is not necessary to establish upper and lower bounds since there is a single, known delay solution

The cumulative curves do not address random delay. Random delay is an additional source of delay that stems from headway variations in the arriving traffic stream. When volume on an intersection approach exceeds the capacity of the approach then residual queues form and the effect of random arrivals on delay is minimal. In effect, the residual queues "absorb" the randomness. However, when no residual queues exist, then this variation in vehicle arrivals leads to the under-utilization of some cycles, as the green time is "starved" due to episodes of infrequent arrivals, and to the over-utilization of other cycles as the green time is "swamped" by closely spaced arrivals. This random component of delay is recognized by the Highway Capacity Manual [4] and is included as an element in the HCM's d_2 term.

To account for the effect of random delay, the random component of the HCM's d_2 term is included as part of the cumulative curve delay for a given 15-minute period whenever a residual queue does not exist at the beginning of that 15-minute period. The presence of a residual queue is determined by comparing the cumulative number of arrivals at the beginning of the period to

the cumulative number of departures at the beginning of the period. If this value is greater than the overall thruput for the approach, then a residual queue exists and the random delay component is calculated and added to the other components of the cumulative curve delay (overflow delay and uniform delay). Otherwise the random delay is given a value of zero.

Thruput is calculated for each 15-minute period by dividing the number of signals cycles that occur during the period into the 15-minute capacity of that period. For example, if the hourly capacity for the first 15-minute period is 600 vph and the average cycle length is 120 seconds, then the average thruput for the first 15-minute period is: (600/4)/(3600/120) = 150 / 7.5 = 20 vehicles. The maximum of the four period thruputs is used as the overall thruput.

This random delay adjustment is not applied to the lower bound since the lower bound represents a minimum condition and a lack of variation in the traffic stream can lead to situations where the random delay component is very close to zero even though no residual queue exists.

In general:

$$\text{Cumulative Curve Delay } (A_{CC}) = \text{Overflow Delay (OD)} + \text{Uniform Delay } (D_U) + \text{Random Delay } (D_R) * I \quad (164)$$

Where I = 0 if a residual queue exists at the start of the period, and 1 otherwise

This can be reflected in the d_2 term of the Highway Capacity Manual control delay equation by modifying the 8kIX component to be 8kIX(T-min(t,T))/T. The modified d_2 term thus becomes:

$$d_2 = 900T[(X-1)+\text{sqrt}[(X-1)^2 + 8kIX(T-\min(t,T)/cT^2] \quad (165)$$

It is interesting to note that, during over-saturated conditions, variations in cycle-to-cycle vehicle arrival patterns have much less of an effect on delay than variations in cycle-to-cycle capacity stemming from relative driver aggressiveness. The amount of start-up lost time experienced during a given cycle and the degree to which motorists utilize the yellow and all red

change intervals as green time are the important random variables when over-saturated conditions exist.

Bracketing the Stopped Delay Prediction Results

As discussed in section D of this chapter, the cumulative curve delay must be multiplied by the conversion factors provided in Tables 6-1 through 6-4 to obtain stopped delay. Once this is done, the minimum and maximum reasonable delay curves (the curves associated with the minimum PHF lower and upper bounds) can be used to bracket our prediction results and create an envelope of reasonable delay. If the prediction results fall outside this envelope then abandoning the prediction process would be a reasonable course of action. When this occurs, the prediction results can either be replaced by the "minimum percent error" estimate obtained from the minimum and maximum delay curves as was described in Chapter 5 (see equation. 89), or a "hybrid" prediction curve can be constructed that makes uses of the theoretical boundary whenever the prediction curve lies outside of it.

To illustrate how this theoretical bracketing is used, a series of tables with embedded cumulative delay figures have been developed based on our four examples. Table 6-7 addresses volume pattern 700_725_625_350vph with a separate analysis provided for each of the three random number sets. The "corrected" delay values provided in this table are cumulative curve values that have been multiplied by the required conversion factor. The reference value against which all delay results are evaluated is actual stopped delay as identified through simulation. Also provided in the table is the BuckQ prediction as well as the "minimum percent error" estimate. A review of the embedded figures shows that predicted delay (delay estimated by our limited-information second-by-second procedure based on a power function) falls well within the theoretical envelope for all three runs. The heavy dashed lines delineate the theoretical constraint on the solution space using a minimum PHF of 0.80 while the dotted PHF Min %

Error line is the theoretical "best estimate". Table 6-8 provides a comparison of the average results for the three runs. The prediction continues to fall well within the theoretical envelope and underestimates the final cumulative stopped delay by only 2% whereas the "minimum percent error" estimate obtained from the theoretical curves underestimates delay by 10%. The "estimated actual" delay obtained from using the true arrival rates to construct the cumulative curves deviates from simulation by 13%.

Tables 6-9 and 6-10 address volume pattern 700_700_700_350vph. A review of the embedded figures in Table 6-9 shows that the prediction falls just outside the theoretical envelope for two of the three runs. (A review of the cumulative arrival and departure curves for these two cases reveals that the cumulative arrival curve is curvilinear between the end of period 3 and the start of period 4, violating the linear assumption. It is this violation that causes the resulting delay to be slightly less than the minimum.) Table 6-10 provides a comparison of the average results for the three runs. The prediction falls well within the theoretical envelope for the average, overestimating the final cumulative stopped delay by just 5 percent. The "minimum percent error" estimate obtained from the theoretical curves overestimates the delay by 13%. The "estimated actual" delay obtained from using the true arrival rates to construct the cumulative curves deviates from the simulation by 9%.

Tables 6-11 and 6-12 address the highest volume pattern: 725_700_700_350vph. A review of the embedded figures in Table 6-11 shows that the prediction continues to falls within the theoretical envelope for all three runs. Table 6-12 provides a comparison of the average results for the three runs. Once again, the prediction falls well within the theoretical envelope, this time underestimating the final cumulative stopped delay by 10 percent. The "minimum percent error" estimate obtained from the theoretical curves underestimates the delay by 14%.

The “estimated actual” delay obtained from using the true arrival rates to construct the cumulative curves deviates from the simulation by 5%.

Tables 6-13 and 6-14 deal with the lowest volume pattern: 625_700_650_350vph. As discussed previously, the theoretical delay envelope is not pertinent when the arrival rate can be determined for three of the four periods, which happens with the second run. For this run, the theoretical curves are omitted. A review of the remaining two embedded figures in Table 6-13 shows that the prediction falls outside the theoretical envelope for one of the two runs. When this occurs, the theoretical upper bound overrides our predicted values, producing a hybrid solution that is much more accurate. Table 6-14 provides a comparison of the average results for the three runs. The prediction falls inside the theoretical envelope when the results are averaged and the resulting delay overestimation is only 14%. The “minimum percent error” estimate obtained from the theoretical curves overestimates the delay by 2% while the “estimated actual” delay obtained from using the true arrival rates to construct the cumulative curves deviates from the simulation by less than ¼ of a percent.

Table 6-15 summarizes the delay prediction results for all four volume pattern examples presented in the dissertation. A review of this table indicates that the hybrid procedure does the best job of estimating actual stopped delay with the average percent error being only 11% after the fourth period. Even the intermediate periods are predicted with reasonable accuracy, having an average percent error of 14% or less. If averages are considered instead of individual runs, the average percent error falls to 8% for the fourth period with a percent error of 12% or less for any period. These values compare very favorably to the 65% error that would occur if our prediction procedure was not used and only visual delay were taken into account.

The final results are relatively satisfying. Using limited information, our analysis procedure does a reasonable job of predicting stopped delay under a variety of over-saturated volume patterns and the improvement over directly measurable delay is dramatic. In addition, the predictions tend to fall within theoretically justifiable limits.

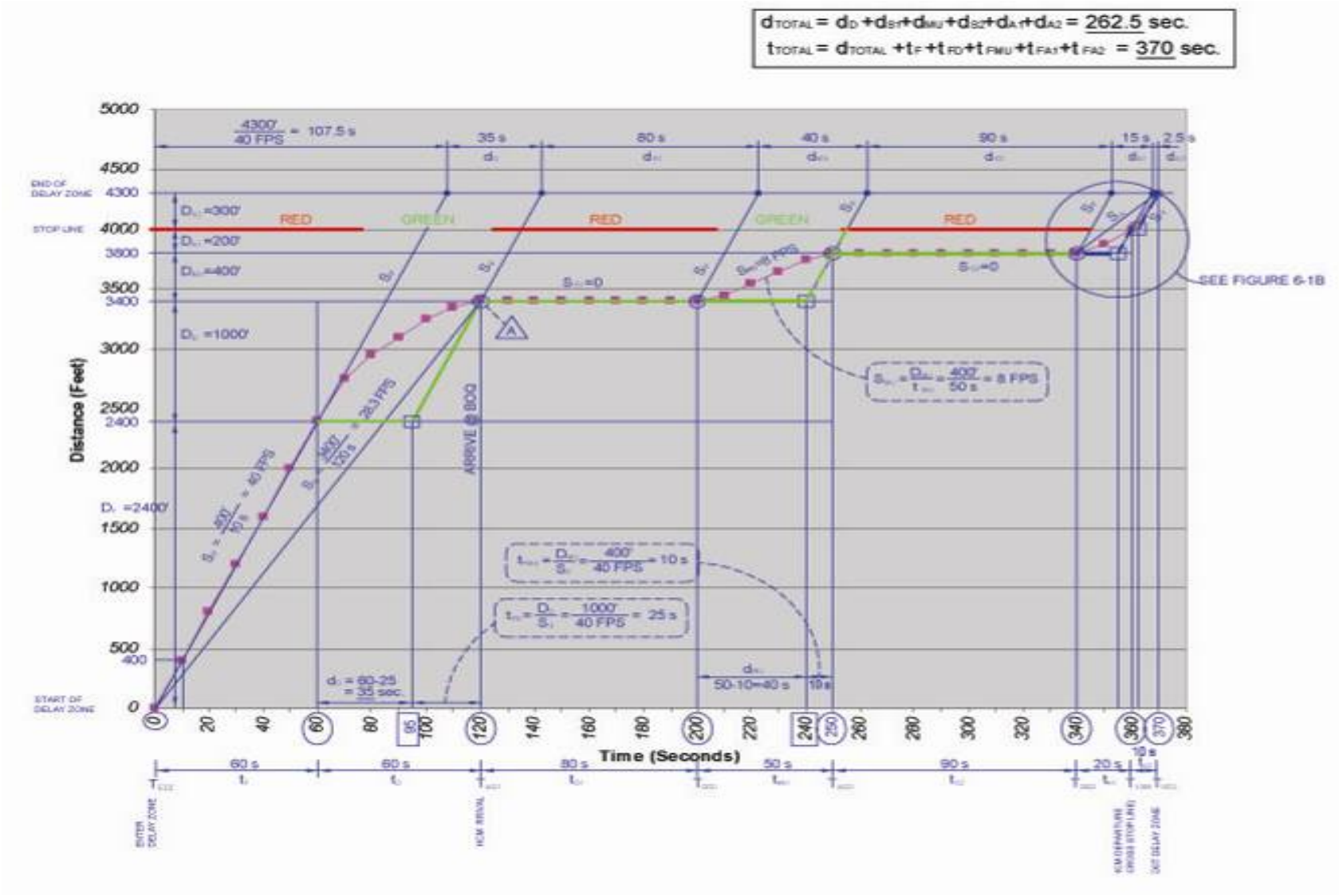

Figure 6-1. Trajectory example A) Complete chart B) Detailed view of circled area in upper right corner.

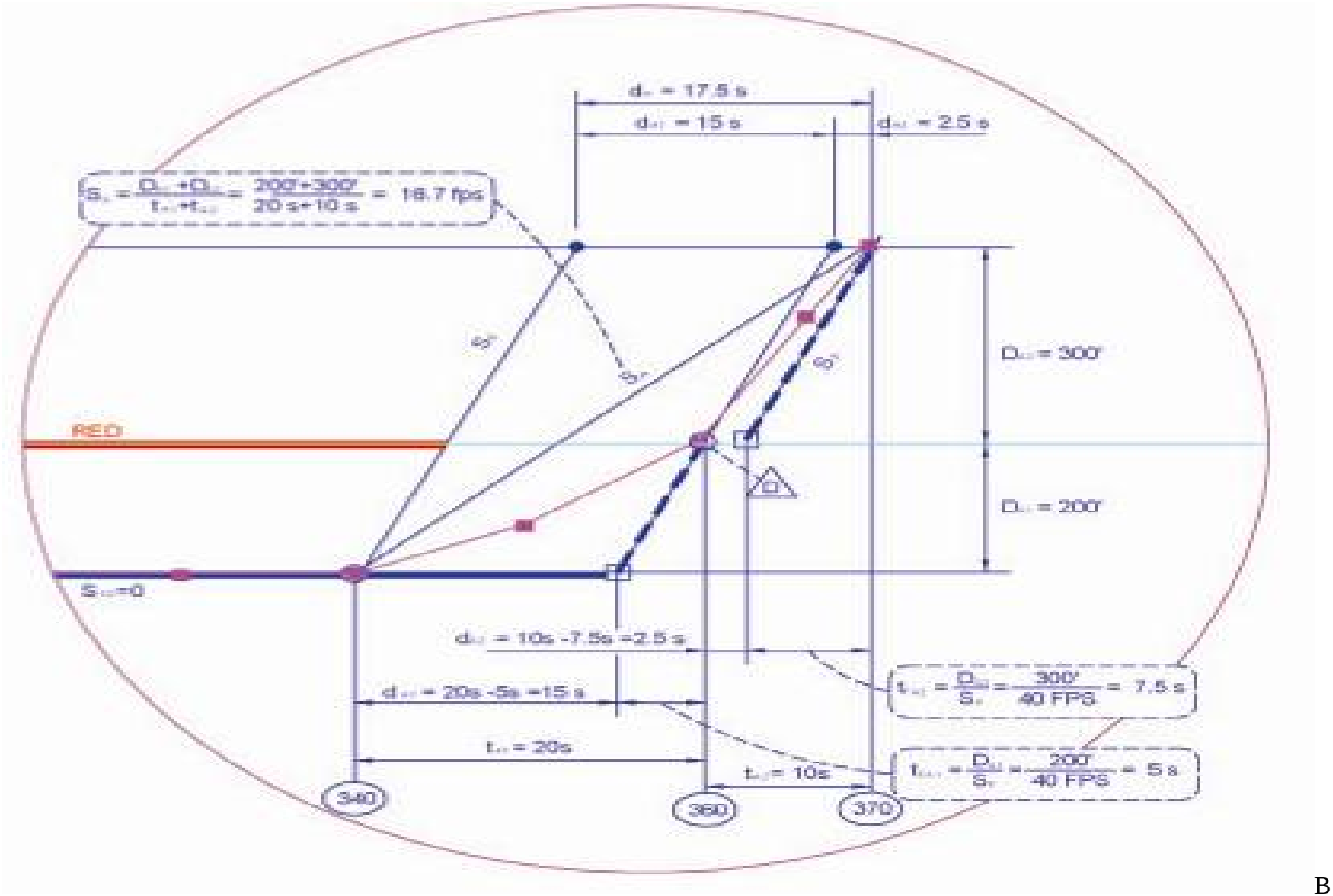
RED
45°
45°
60°
D = 300'
D = 200'
S = 0
d = 17.5 s
d = 15 s
d = 2.5 s
d = 10s -7.5s =2.5 s
d = 20s -5s =15 s
t = 20s
t = 10s
340
360
370
40 FPS
40 FPS

B

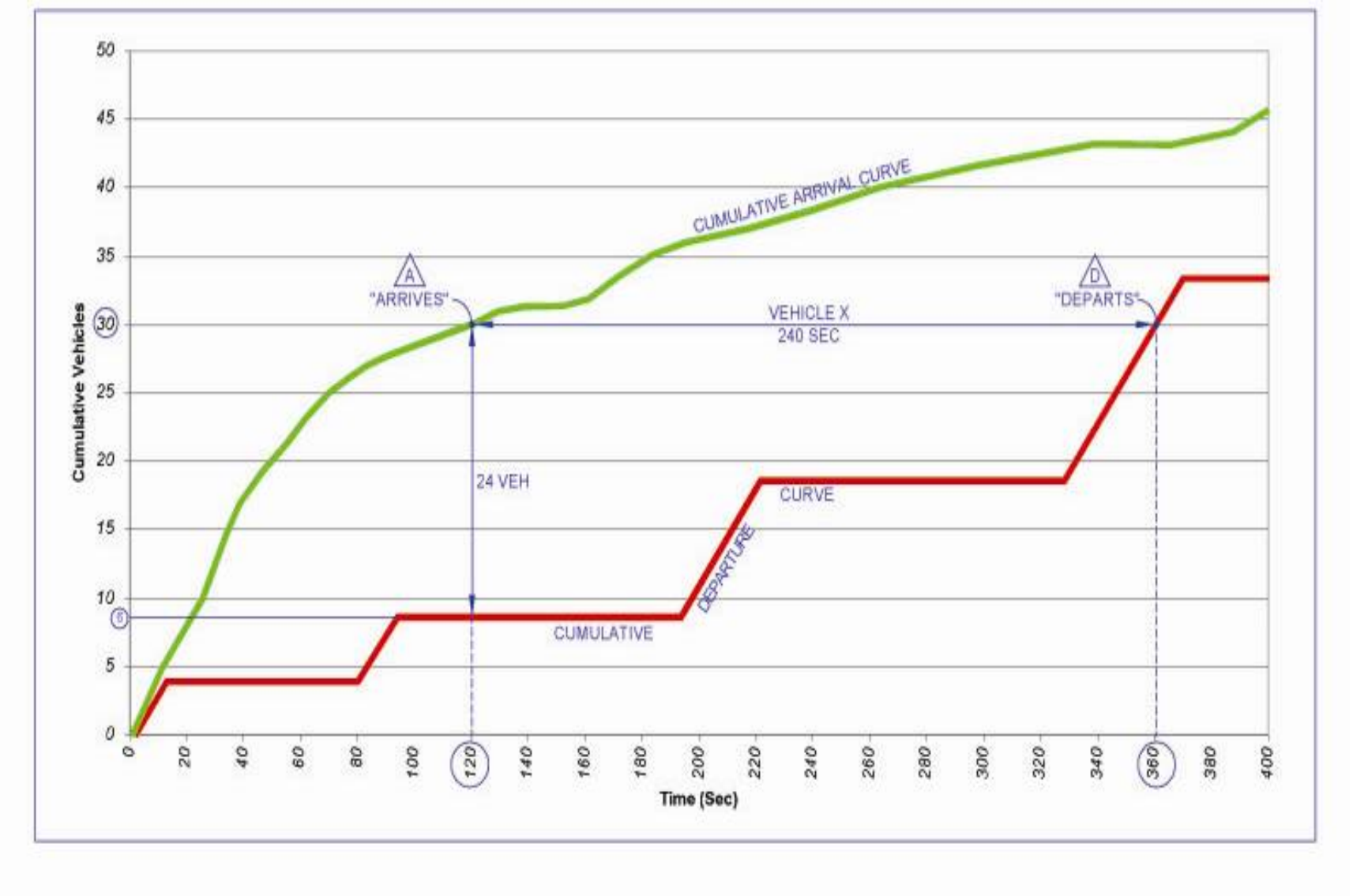

Figure 6-2. Cumulative arrival-departure curve example

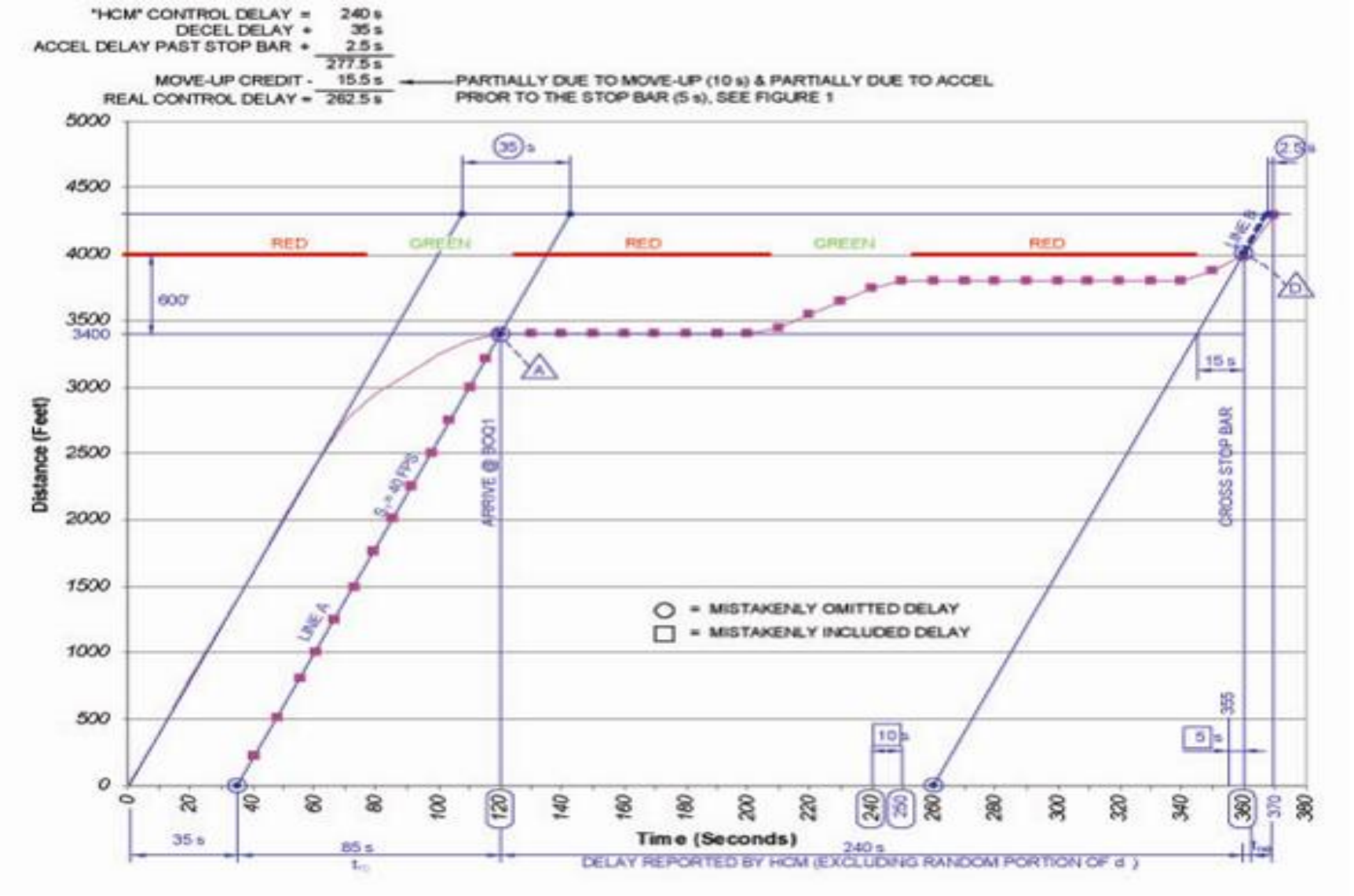

Figure 6-3. Trajectory conversion of cumulative curve example

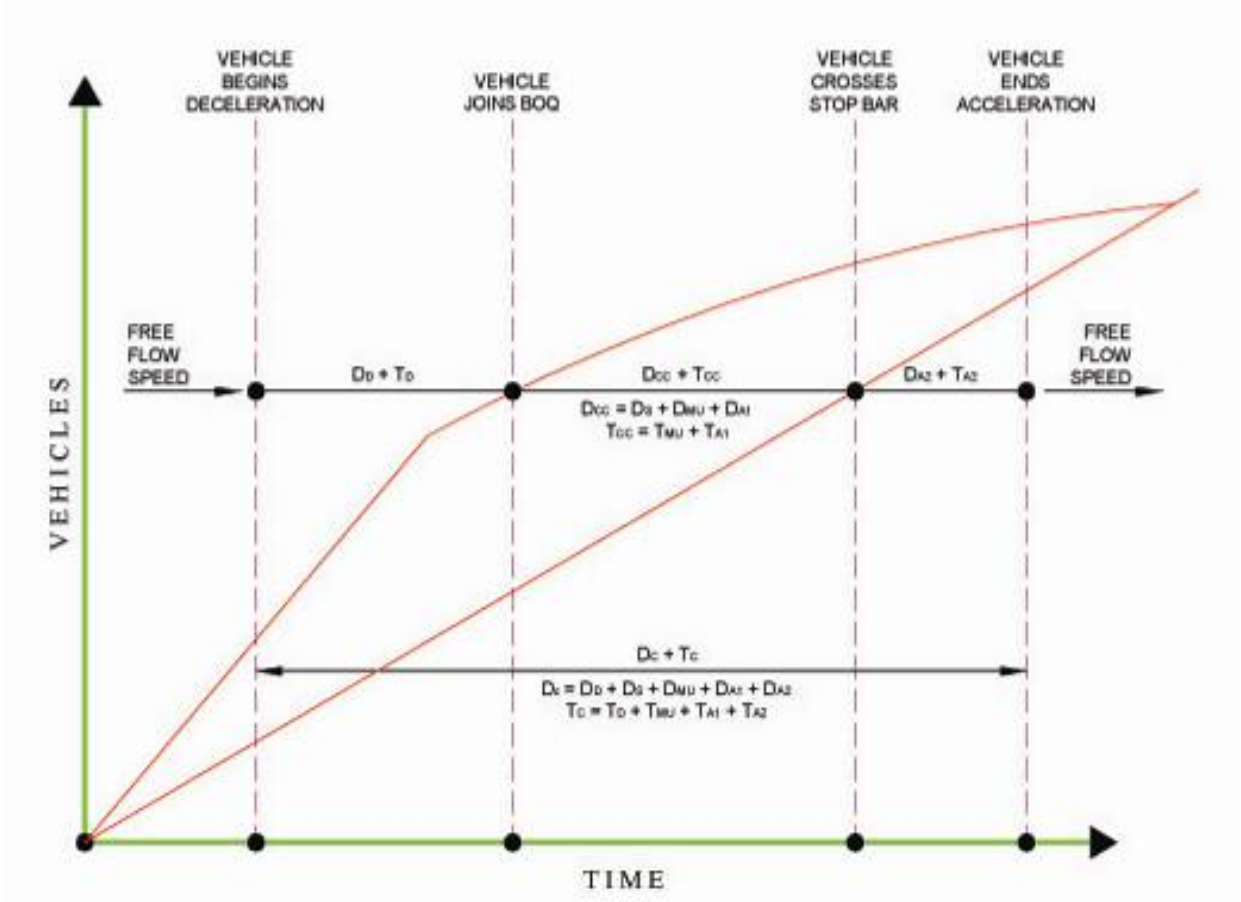

WHERE:

D_C	=	CONTROL DELAY
T_C	=	FREE SPEED TIME
D_D	=	DECELERATION DELAY
T_D	=	FREE SPEED DECELERATION TIME
D_{CC}	=	CUMULATIVE CURVE DELAY
T_{CC}	=	CUMULATIVE CURVE FREE SPEED TIME
D_S	=	STOPPED DELAY
D_{MU}	=	MOVE-UP DELAY
D_{A1}	=	PRE-STOP BAR ACCELERATION DELAY
D_{A2}	=	POST-STOP BAR ACCELERATION DELAY
T_{MU}	=	FREE SPEED MOVE-UP TIME
T_{A1}	=	PRE-STOP BAR FREE SPEED SPEED ACCELERATION TIME
T_{A2}	=	POST-STOP BAR FREE SPEED ACCELERATION TIME

Figure 6-4. Delay and travel time components.

Table 6-1. Calculation of cumulative curve delay conversion factors, volume pattern 625_700_650_350vph

Random Number Set 1	Variable	Source	Period 1	2	3	4
Stopped Delay	D_S	BuckQ	8223	19035	33144	38126
Queue Move-Up Delay	D_{MU}	BuckQ	399	932	2538	2725
Free Speed Queue Move-Up Time	T_{MU}	BuckQ	268	669	1732	1842
Accel/Decel Delay		BuckQ	2461	4824	7268	8285
Pre-Stop Bar Accel Delay as % of Accel/Decel Delay		BuckTRAJ	45%	40%	42%	43%
Pre-Stop Bar Acceleration (A1) Delay	D_{A1}	Calculated	1107	1930	3053	3563
Free Speed Pre-Stop Bar Accel Time as % of A1Delay		BuckTRAJ	72%	88%	86%	82%
Free Speed Pre-Stop Bar Acceleration Time	T_{A1}	Calculated	797	1698	2625	2921
Non-Stopped Delay Portion of Cumulative Curve Area	E_{CC}	Calculated	2572	5229	9948	11051
Non-Stopped Delay Portion as % of Stopped Delay	E_{CC}/D_S	Calculated	31%	27%	30%	29%
Factor That Converts Overflow Delay to Stopped Delay	F_S	Calculated	**76%**	**78%**	**77%**	**78%**

Random Number Set 2	Variable	Source	Period 1	2	3	4
Stopped Delay	D_S	BuckQ	6424	15372	32476	38385
Queue Move-Up Delay	D_{MU}	BuckQ	35	533	2731	3105
Free Speed Queue Move-Up Time	T_{MU}	BuckQ	28	398	1591	1870
Accel/Decel Delay		BuckQ	1821	4479	6973	7924
Pre-Stop Bar Accel Delay as % of Accel/Decel Delay		BuckTRAJ	46%	46%	46%	47%
Pre-Stop Bar Acceleration (A1) Delay	D_{A1}	Calculated	838	2060	3208	3724
Free Speed Pre-Stop Bar Accel Time as % of A1Delay		BuckTRAJ	70%	73%	73%	72%
Free Speed Pre-Stop Bar Acceleration Time	T_{A1}	Calculated	586	1504	2342	2681
Non-Stopped Delay Portion of Cumulative Curve Area	E_{CC}	Calculated	1487	4495	9871	11381
Non-Stopped Delay Portion as % of Stopped Delay	E_{CC}/D_S	Calculated	23%	29%	30%	30%
Factor That Converts Overflow Delay to Stopped Delay	F_S	Calculated	**81%**	**77%**	**77%**	**77%**

Table 6-1. Continued

Random Number Set 3	Variable	Source	Period 1	2	3	4
Stopped Delay	D_S	BuckQ	9858	22344	39242	45610
Queue Move-Up Delay	D_{MU}	BuckQ	435	1560	3691	4327
Free Speed Queue Move-Up Time	T_{MU}	BuckQ	331	1076	2300	2617
Accel/Decel Delay		BuckQ	2513	4767	7222	8326
Pre-Stop Bar Accel Delay as % of Accel/Decel Delay		BuckTRAJ	39%	43%	45%	46%
Pre-Stop Bar Acceleration (A1) Delay	D_{A1}	Calculated	980	2050	3250	3830
Free Speed Pre-Stop Bar Accel Time as % of A1Delay		BuckTRAJ	84%	84%	79%	77%
Free Speed Pre-Stop Bar Acceleration Time	T_{A1}	Calculated	823	1722	2567	2949
Non-Stopped Delay Portion of Cumulative Curve Area	E_{CC}	Calculated	2569	6408	11808	13723
Non-Stopped Delay Portion as % of Stopped Delay	E_{CC}/D_S	Calculated	26%	29%	30%	30%
Factor That Converts Overflow Delay to Stopped Delay	F_S	Calculated	**79%**	**78%**	**77%**	**77%**

All Values are Cumulative

Table 6-2. Calculation of cumulative curve delay conversion factors, volume pattern 700_725_625_350vph

Random Number Set 1	Variable	Source	Period 1	2	3	4
Stopped Delay	D_S	BuckQ	12465	32341	59334	68622
Queue Move-Up Delay	D_{MU}	BuckQ	926	3472	7433	8807
Free Speed Queue Move-Up Time	T_{MU}	BuckQ	644	2405	4888	5544
Accel/Decel Delay		BuckQ	3394	6910	9114	9934
Pre-Stop Bar Accel Delay as % of Accel/Decel Delay		BuckTRAJ	38%	35%	38%	39%
Pre-Stop Bar Acceleration (A1) Delay	D_{A1}	Calculated	1290	2419	3463	3874
Free Speed Pre-Stop Bar Accel Time as % of A1Delay		BuckTRAJ	71%	89%	86%	84%
Free Speed Pre-Stop Bar Acceleration Time	T_{A1}	Calculated	916	2152	2978	3254
Non-Stopped Delay Portion of Cumulative Curve Area	E_{CC}	Calculated	3775	10448	18763	21480
Non-Stopped Delay Portion as % of Stopped Delay	E_{CC}/D_S	Calculated	30%	32%	32%	31%
Factor That Converts Overflow Delay to Stopped Delay	F_S	Calculated	**77%**	**76%**	**76%**	**76%**

Random Number Set 2	Variable	Source	Period 1	2	3	4
Stopped Delay	D_S	BuckQ	15661	38310	69620	83364
Queue Move-Up Delay	D_{MU}	BuckQ	1187	4184	11605	13341
Free Speed Queue Move-Up Time	T_{MU}	BuckQ	900	2837	6156	7260
Accel/Decel Delay		BuckQ	3119	6490	9438	10307
Pre-Stop Bar Accel Delay as % of Accel/Decel Delay		BuckTRAJ	37%	37%	38%	40%
Pre-Stop Bar Acceleration (A1) Delay	D_{A1}	Calculated	1154	2401	3586	4123
Free Speed Pre-Stop Bar Accel Time as % of A1Delay		BuckTRAJ	78%	80%	75%	75%
Free Speed Pre-Stop Bar Acceleration Time	T_{A1}	Calculated	900	1921	2690	3092
Non-Stopped Delay Portion of Cumulative Curve Area	E_{CC}	Calculated	4141	11343	24037	27816
Non-Stopped Delay Portion as % of Stopped Delay	E_{CC}/D_S	Calculated	26%	30%	35%	33%
Factor That Converts Overflow Delay to Stopped Delay	F_S	Calculated	**79%**	**77%**	**74%**	**75%**

Table 6-2. Continued

Random Number Set 3	Variable	Source	Period 1	2	3	4
Stopped Delay	D_S	BuckQ	13743	38723	73079	85601
Queue Move-Up Delay	D_{MU}	BuckQ	1089	4886	10666	12720
Free Speed Queue Move-Up Time	T_{MU}	BuckQ	775	2997	6415	7458
Accel/Decel Delay		BuckQ	3145	6416	8969	10050
Pre-Stop Bar Accel Delay as % of Accel/Decel Delay		BuckTRAJ	33%	36%	37%	40%
Pre-Stop Bar Acceleration (A1) Delay	D_{A1}	Calculated	1038	2310	3319	4020
Free Speed Pre-Stop Bar Accel Time as % of A1Delay		BuckTRAJ	88%	82%	83%	79%
Free Speed Pre-Stop Bar Acceleration Time	T_{A1}	Calculated	913	1894	2754	3176
Non-Stopped Delay Portion of Cumulative Curve Area	E_{CC}	Calculated	3815	12087	23154	27374
Non-Stopped Delay Portion as % of Stopped Delay	E_{CC}/D_S	Calculated	28%	31%	32%	32%
Factor That Converts Overflow Delay to Stopped Delay	F_S	Calculated	**78%**	**76%**	**76%**	**76%**

All Values are Cumulative

Table 6-3. Calculation of cumulative curve delay conversion factors, volume pattern 700_700_700_350vph

Random Number Set 1	Variable	Source	Period 1	2	3	4
Stopped Delay	D_S	BuckQ	12465	29923	57995	72168
Queue Move-Up Delay	D_{MU}	BuckQ	928	3042	7153	9787
Free Speed Queue Move-Up Time	T_{MU}	BuckQ	642	2132	4699	5925
Accel/Decel Delay		BuckQ	3420	6568	9013	10084
Pre-Stop Bar Accel Delay as % of Accel/Decel Delay		BuckTRAJ	38%	37%	38%	40%
Pre-Stop Bar Acceleration (A1) Delay	D_{A1}	Calculated	1300	2430	3425	4034
Free Speed Pre-Stop Bar Accel Time as % of A1Delay		BuckTRAJ	71%	86%	85%	81%
Free Speed Pre-Stop Bar Acceleration Time	T_{A1}	Calculated	923	2090	2911	3267
Non-Stopped Delay Portion of Cumulative Curve Area	E_{CC}	Calculated	3792	9694	18188	23013
Non-Stopped Delay Portion as % of Stopped Delay	E_{CC}/D_S	Calculated	30%	32%	31%	32%
Factor That Converts Overflow Delay to Stopped Delay	F_S	Calculated	**77%**	**76%**	**76%**	**76%**

Random Number Set 2	Variable	Source	Period 1	2	3	4
Stopped Delay	D_S	BuckQ	15661	36773	69423	88873
Queue Move-Up Delay	D_{MU}	BuckQ	1185	4090	11561	14343
Free Speed Queue Move-Up Time	T_{MU}	BuckQ	902	2781	6196	7938
Accel/Decel Delay		BuckQ	3092	6138	9307	10171
Pre-Stop Bar Accel Delay as % of Accel/Decel Delay		BuckTRAJ	37%	39%	39%	41%
Pre-Stop Bar Acceleration (A1) Delay	D_{A1}	Calculated	1144	2394	3630	4170
Free Speed Pre-Stop Bar Accel Time as % of A1Delay		BuckTRAJ	78%	80%	76%	76%
Free Speed Pre-Stop Bar Acceleration Time	T_{A1}	Calculated	892	1915	2759	3169
Non-Stopped Delay Portion of Cumulative Curve Area	E_{CC}	Calculated	4123	11180	24145	29620
Non-Stopped Delay Portion as % of Stopped Delay	E_{CC}/D_S	Calculated	26%	30%	35%	33%
Factor That Converts Overflow Delay to Stopped Delay	F_S	Calculated	**79%**	**77%**	**74%**	**75%**

Table 6-3. Continued

Random Number Set 3	Variable	Source	Period 1	2	3	4
Stopped Delay	D_S	BuckQ	13743	36400	71981	89605
Queue Move-Up Delay	D_{MU}	BuckQ	1085	4644	10854	14263
Free Speed Queue Move-Up Time	T_{MU}	BuckQ	779	2889	6545	8195
Accel/Decel Delay		BuckQ	3103	5920	8611	10066
Pre-Stop Bar Accel Delay as % of Accel/Decel Delay		BuckTRAJ	33%	37%	38%	42%
Pre-Stop Bar Acceleration (A1) Delay	D_{A1}	Calculated	1024	2190	3272	4228
Free Speed Pre-Stop Bar Accel Time as % of A1Delay		BuckTRAJ	88%	81%	82%	78%
Free Speed Pre-Stop Bar Acceleration Time	T_{A1}	Calculated	901	1774	2683	3298
Non-Stopped Delay Portion of Cumulative Curve Area	E_{CC}	Calculated	3789	11498	23354	29983
Non-Stopped Delay Portion as % of Stopped Delay	E_{CC}/D_S	Calculated	28%	32%	32%	33%
Factor That Converts Overflow Delay to Stopped Delay	F_S	Calculated	**78%**	**76%**	**76%**	**75%**

All Values are Cumulative

Table 6-4. Calculation of cumulative curve delay conversion factors, volume pattern 725_700_700_350vph

Random Number Set 1	Variable	Source	Period 1	2	3	4
Stopped Delay	D_S	BuckQ	23943	55507	96463	121786
Queue Move-Up Delay	D_{MU}	BuckQ	3060	8310	16446	21141
Free Speed Queue Move-Up Time	T_{MU}	BuckQ	2083	5259	9856	12256
Accel/Decel Delay		BuckQ	3623	6277	8591	10068
Pre-Stop Bar Accel Delay as % of Accel/Decel Delay		BuckTRAJ	32%	35%	37%	41%
Pre-Stop Bar Acceleration (A1) Delay	D_{A1}	Calculated	1159	2197	3179	4128
Free Speed Pre-Stop Bar Accel Time as % of A1Delay		BuckTRAJ	86%	92%	88%	83%
Free Speed Pre-Stop Bar Acceleration Time	T_{A1}	Calculated	997	2021	2797	3426
Non-Stopped Delay Portion of Cumulative Curve Area	E_{CC}	Calculated	7299	17787	32278	40951
Non-Stopped Delay Portion as % of Stopped Delay	E_{CC}/D_S	Calculated	30%	32%	33%	34%
Factor That Converts Overflow Delay to Stopped Delay	F_S	Calculated	**77%**	**76%**	**75%**	**75%**

Random Number Set 2	Variable	Source	Period 1	2	3	4
Stopped Delay	D_S	BuckQ	19909	48528	89649	116151
Queue Move-Up Delay	D_{MU}	BuckQ	2117	7524	17590	22139
Free Speed Queue Move-Up Time	T_{MU}	BuckQ	1515	4341	8819	11428
Accel/Decel Delay		BuckQ	2837	5827	8079	8568
Pre-Stop Bar Accel Delay as % of Accel/Decel Delay		BuckTRAJ	38%	39%	40%	44%
Pre-Stop Bar Acceleration (A1) Delay	D_{A1}	Calculated	1078	2273	3232	3770
Free Speed Pre-Stop Bar Accel Time as % of A1Delay		BuckTRAJ	88%	80%	77%	77%
Free Speed Pre-Stop Bar Acceleration Time	T_{A1}	Calculated	949	1818	2488	2903
Non-Stopped Delay Portion of Cumulative Curve Area	E_{CC}	Calculated	5659	15956	32129	40240
Non-Stopped Delay Portion as % of Stopped Delay	E_{CC}/D_S	Calculated	28%	33%	36%	35%
Factor That Converts Overflow Delay to Stopped Delay	F_S	Calculated	**78%**	**75%**	**74%**	**74%**

Table 6-4. Continued

Random Number Set 3	Variable	Source	Period 1	2	3	4
Stopped Delay	D_S	BuckQ	20321	52124	96875	122534
Queue Move-Up Delay	D_{MU}	BuckQ	2470	8095	16789	22567
Free Speed Queue Move-Up Time	T_{MU}	BuckQ	1663	4923	9891	12556
Accel/Decel Delay		BuckQ	3272	6005	8309	9584
Pre-Stop Bar Accel Delay as % of Accel/Decel Delay		BuckTRAJ	36%	39%	41%	44%
Pre-Stop Bar Acceleration (A1) Delay	D_{A1}	Calculated	1178	2342	3407	4217
Free Speed Pre-Stop Bar Accel Time as % of A1Delay		BuckTRAJ	92%	84%	83%	79%
Free Speed Pre-Stop Bar Acceleration Time	T_{A1}	Calculated	1084	1967	2828	3331
Non-Stopped Delay Portion of Cumulative Curve Area	E_{CC}	Calculated	6395	17327	32914	42671
Non-Stopped Delay Portion as % of Stopped Delay	E_{CC}/D_S	Calculated	31%	33%	34%	35%
Factor That Converts Overflow Delay to Stopped Delay	F_S	Calculated	**76%**	**75%**	**75%**	**74%**

All Values are Cumulative

Table 6-5. Cumulative curve delay for standard 4-period case

Volume Pattern	Random Number Set	0.80 PHF LOWER BOUND Period 1	2	3	4	ESTIMATED ACTUAL Period 1	2	3	4	0.80 PHF UPPER BOUND Period 1	2	3	4
700_725_625_350vph	1	11753	29234	56730	68776	19463	58276	99671	112335	23701	70376	118010	130107
	2	12034	29541	61707	81296	19862	54020	96973	116386	22508	66509	117687	137276
	3	11935	29204	56654	70758	19807	57213	104156	124531	21796	66487	114469	128573
700_700_700_350vph	1	11753	37021	83274	107397	19463	55002	94147	111382	25291	77028	138979	163129
	2	12034	38978	92930	125614	19862	49520	93373	119362	23276	69808	135023	167708
	3	11935	29204	60601	79204	19807	54963	105506	132882	23306	73060	128363	146966
725_700_700_350vph	1	11829	39043	90783	121695	29297	81598	144363	178994	26505	83981	153946	184858
	2	12169	36563	86182	118668	21714	61722	120097	156275	23279	73553	140755	173241
	3	11935	32588	72744	100593	25848	73605	135397	171951	24969	80207	144540	172389

Table 6-6. Cumulative curve delay with multiple visible periods

Volume Pattern	Random Number Set	0.80 PHF LOWER BOUND Period 1	2	3	4	ESTIMATED ACTUAL Period 1	2	3	4	0.80 PHF UPPER BOUND Period 1	2	3	4
625_700_650_350vph	1	6227	18342	37939	44698	10649	24184	47491	53956	11793	28562	49797	55113
	2					9718	24633	39689	49616				
	3	6583	18588	40481	48428	12078	25698	46675	54024	12288	31676	63073	71020

Table 6-7. Stopped delay prediction results for 700_725_625_350vph volume pattern

120 second cycle

Min PHF = 0.80

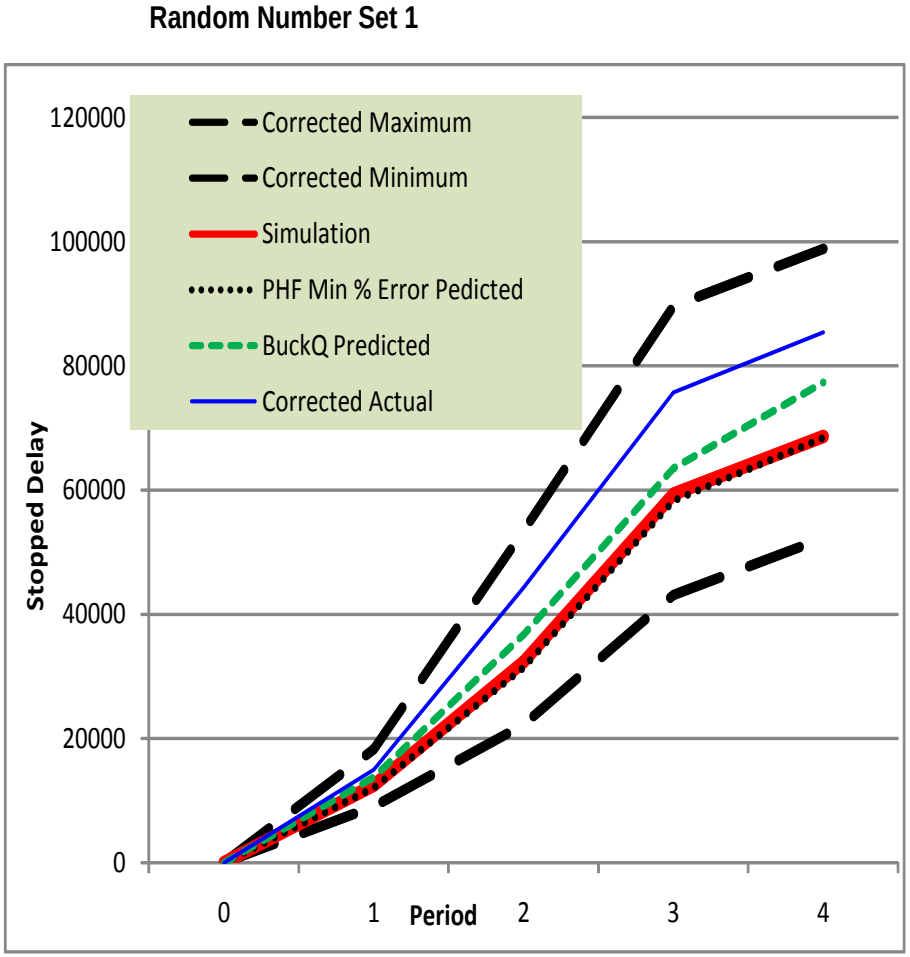

	Cumulative Stopped Delay				
Period:	0	1	2	3	4
S*g/L Capacity:		629	659	655	639
Arrivals at BOQ:		716	740	628	348
Actual PHF:		0.82			
Simulation	**0**	**12465**	**32341**	**59334**	**68622**
OD tp D_S Conversion %		77%	76%	76%	76%
Actual		19463	58276	99671	112335
Corrected Actual	0	14987	44290	75750	85374
% Error		20.2%	36.9%	27.7%	**24%**
Maximum	0	23701	70376	118010	130107
Corrected Maximum	0	18250	53486	89687	98882
Minimum	0	11753	29234	56730	68776
Corrected Minimum	0	9050	22218	43115	52270
PHF Min % Error Pedicted	0	12100	31394	58235	68389
% Error		-3%	-3%	-2%	**0%**
BuckQ Predicted	0	13796	36748	63544	77325
% Error		11%	14%	7%	**13%**

Table 6-7. Continued

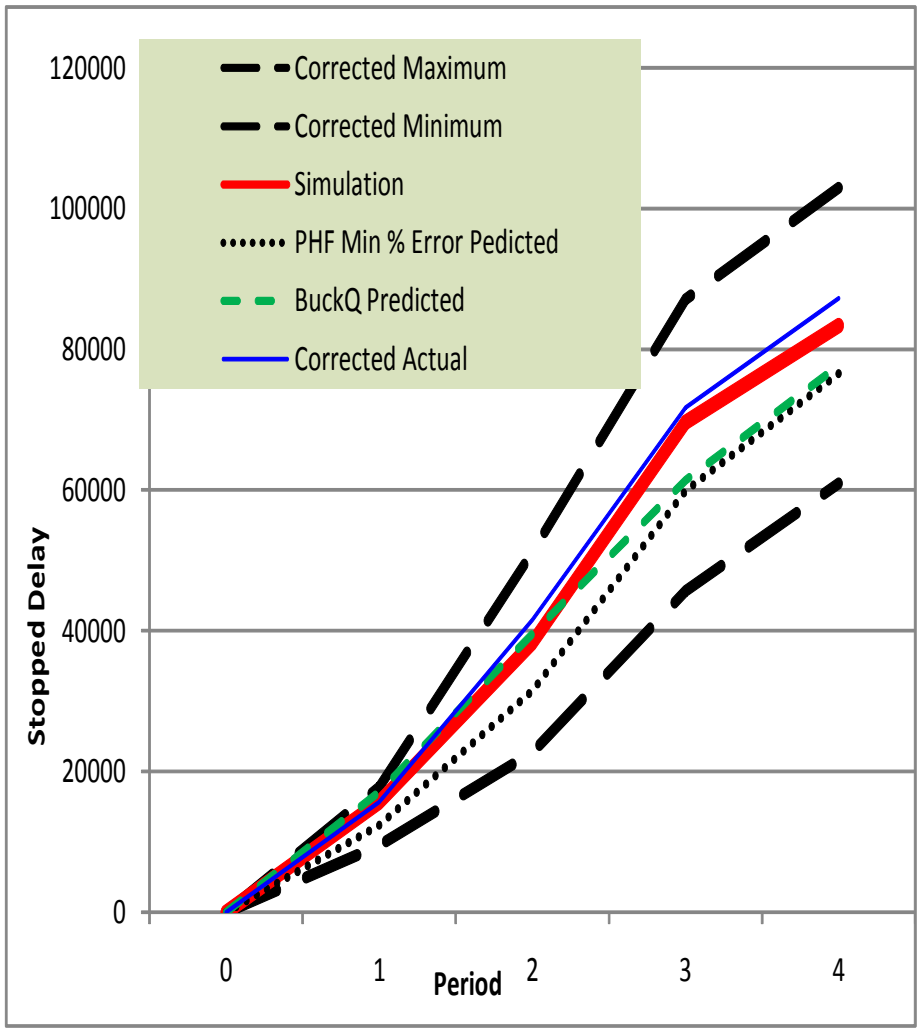

S*g/L Capacity:		648	660	609	604
Arrivals at BOQ:		720	728	624	368
Actual PHF:		0.84			
Simulation	**0**	**15661**	**38310**	**69620**	**83364**
OD tp D_S Conversion %		79%	77%	74%	75%
Actual		19862	54020	96973	116386
Corrected Actual	0	15691	41595	71760	87290
% Error		0.2%	8.6%	3.1%	**5%**
Maximum	0	22508	66509	117687	137276
Corrected Maximum	0	17781	51212	87088	102957
Minimum	0	12034	29541	61707	81296
Corrected Minimum	0	9507	22747	45663	60972
PHF Min % Error Pedicted	0	12390	31501	59912	76588
% Error		-21%	-18%	-14%	**-8%**
BuckQ Predicted	0	17080	39625	61400	77713
% Error		9%	3%	-12%	**-7%**

Table 6-7. Continued

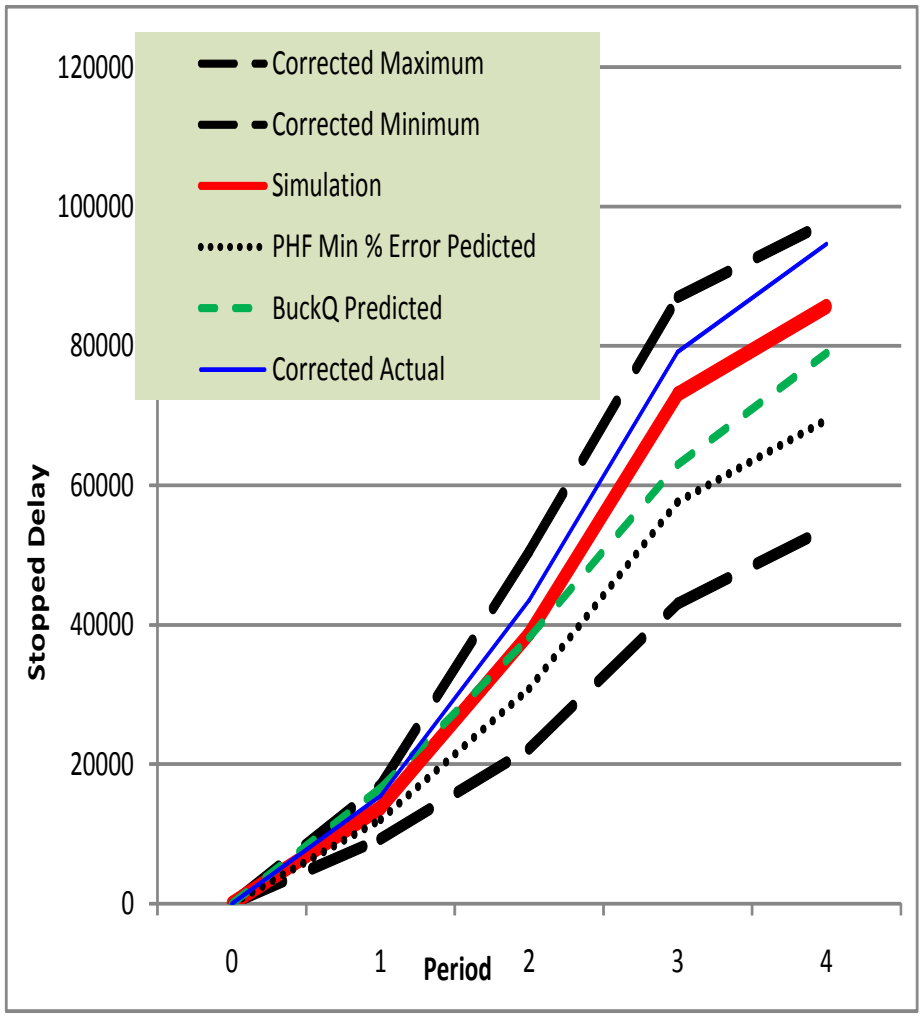

S*g/L Capacity:		647	635	645	561
Arrivals at BOQ:		736	732	632	364
Actual PHF:		0.84			
Simulation	**0**	**13743**	**38723**	**73079**	**85601**
OD tp D_S Conversion %		78%	76%	76%	76%
Actual		19807	57213	104156	124531
Corrected Actual	0	15449	43482	79158	94644
% Error		12.4%	12.3%	8.3%	**11%**
Maximum	0	21796	66487	114469	128573
Corrected Maximum	0	17001	50530	86996	97715
Minimum	0	11935	29204	56654	70758
Corrected Minimum	0	9309	22195	43057	53776
PHF Min % Error Pedicted	0	12031	30843	57604	69374
% Error		-12%	-20%	-21%	**-19%**
BuckQ Predicted	0	16567	38141	62987	78925
% Error		21%	-2%	-14%	**-8%**

Table 6-8. Average stopped delay prediction results for 700_725_625_350vph volume pattern

120 second cycle

Min PHF = 0.80

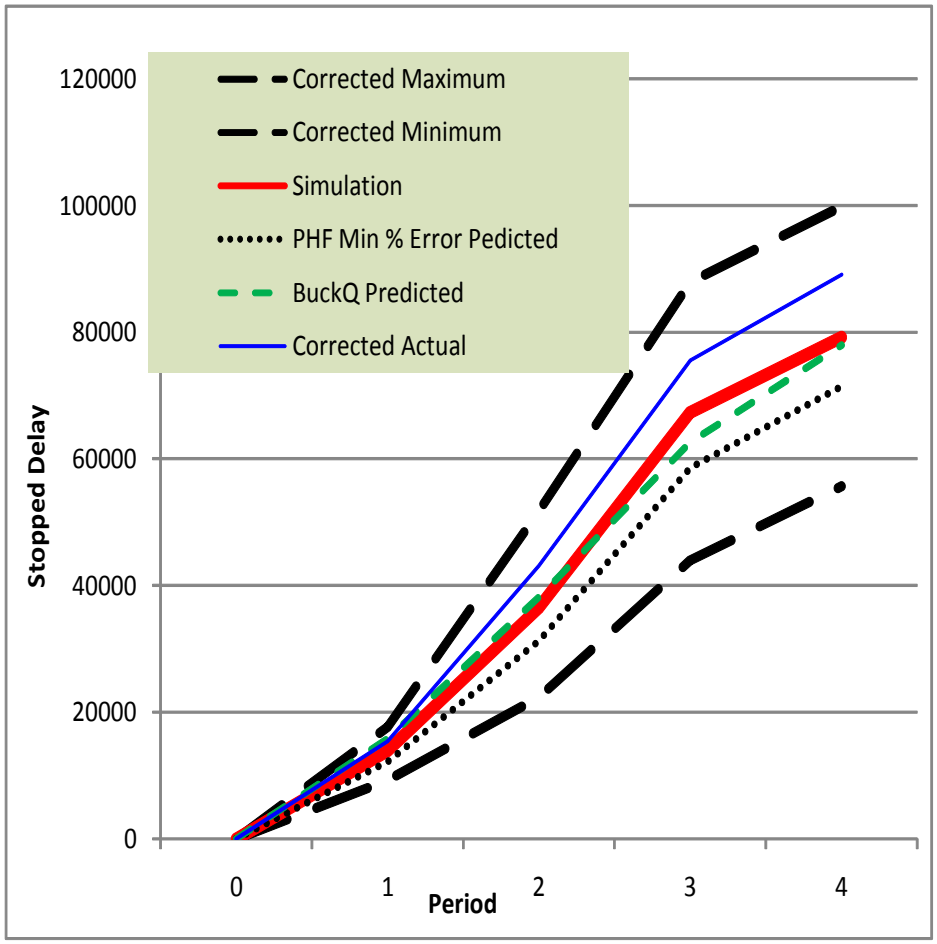

		Cumulative Stopped Delay			
Period:	0	1	2	3	4
S*g/L Capacity:		641	651	636	601
Arrivals at BOQ:		724	733	628	360
Actual PHF:		0.83			
Simulation	**0**	**13956**	**36458**	**67344**	**79196**
OD tp D_S Conversion %		78%	76%	75%	76%
Actual		19711	56503	100266	117751
Corrected Actual	0	15374	43131	75534	89098
% Error		10.2%	18.3%	12.2%	**13%**
Maximum	0	22669	67791	116722	131985
Corrected Maximum	0	17681	51747	87930	99869
Minimum	0	11907	29326	58364	73610
Corrected Minimum	0	9288	22386	43967	55698
PHF Min % Error Pedicted	0	12173	31246	58584	71450
% Error		-13%	-14%	-13%	**-10%**
BuckQ Predicted	0	15814	38171	62644	77988
% Error		13%	5%	-7%	**-2%**

Table 6-9. Stopped delay prediction results for 700_700_700_350vph volume pattern

120 second cycle

Min PHF = 0.80

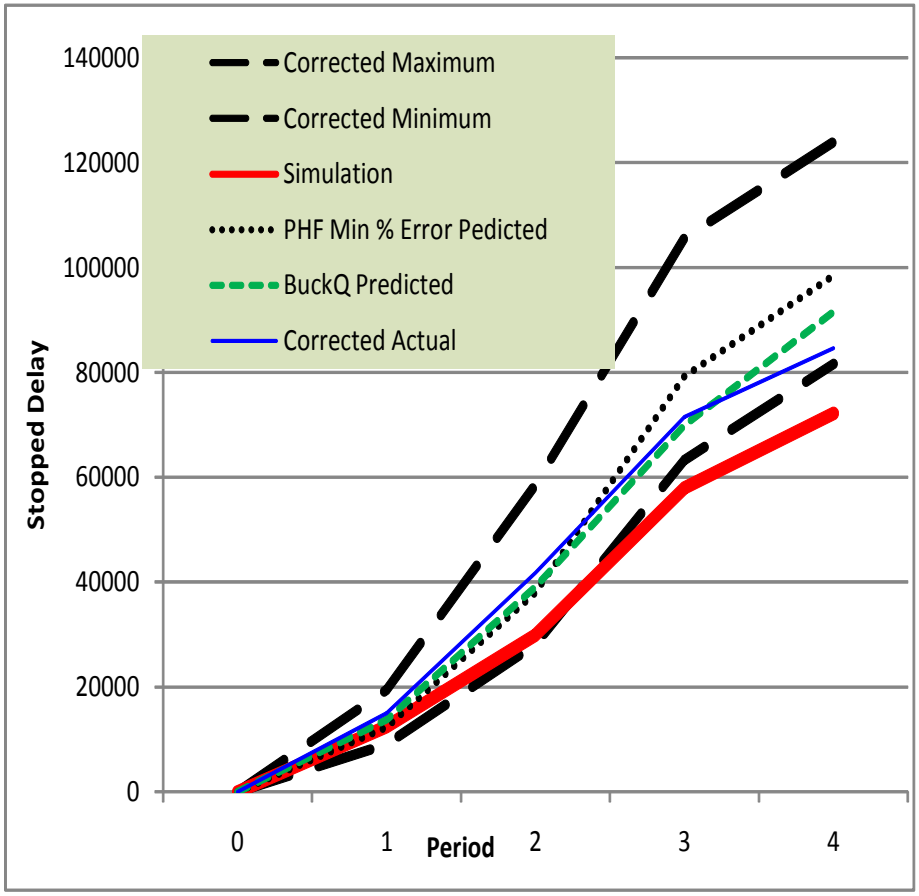

		Cumulative Stopped Delay			
Period:	0	1	2	3	4
S*g/L Capacity:		629	659	655	596
Arrivals at BOQ:		716	704	680	380
Actual PHF:		0.87			
Simulation	**0**	**12465**	**29923**	**57995**	**72168**
OD tp D_S Conversion %		77%	76%	76%	76%
Actual		19463	55002	94147	111382
Corrected Actual	0	14987	41802	71551	84651
% Error		20.2%	39.7%	23.4%	**17%**
Maximum	0	25291	77028	138979	163129
Corrected Maximum	0	19474	58541	105624	123978
Minimum	0	11753	37021	83274	107397
Corrected Minimum	0	9050	28136	63288	81622
PHF Min % Error Pedicted	0	12357	38006	79151	98437
% Error		-1%	27%	36%	**36%**
BuckQ Predicted	0	13813	39068	69887	91541
% Error		11%	31%	21%	**27%**

Table 6-9. Continued

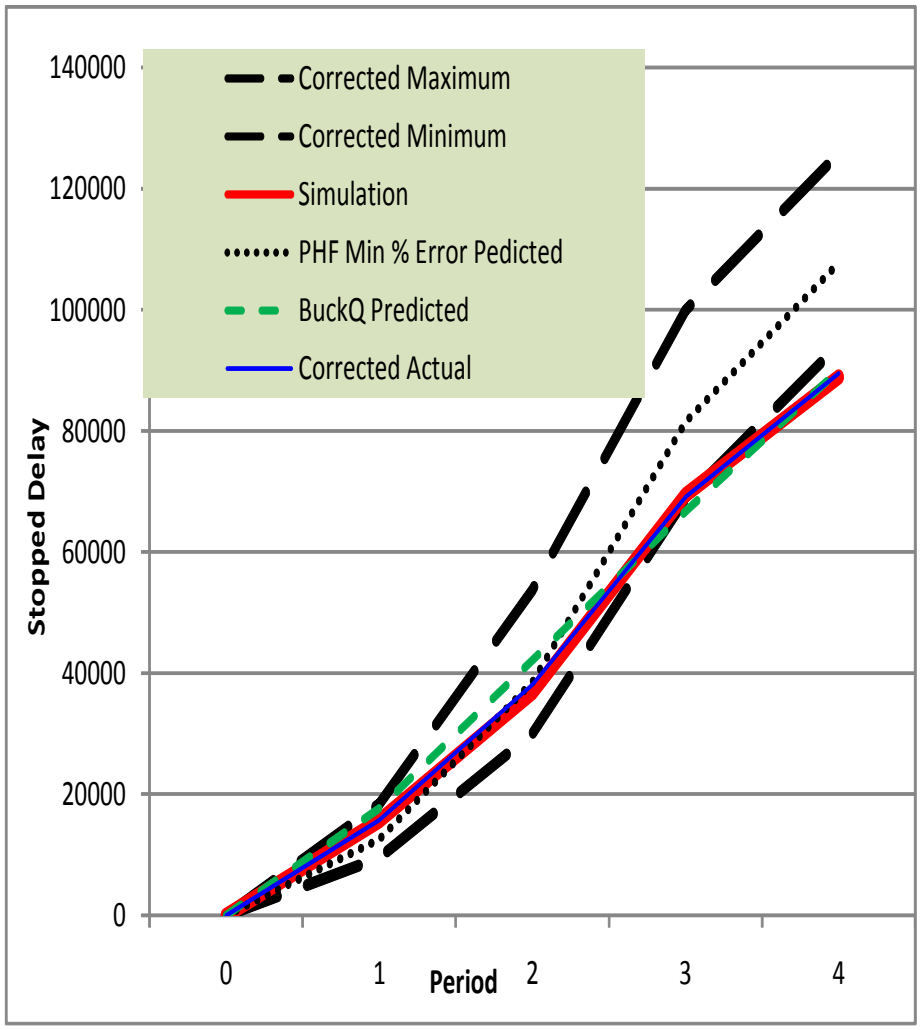

S*g/L Capacity:		648	660	609	612
Arrivals at BOQ:		736	688	712	344
Actual PHF:		0.84			
Simulation	**0**	**15661**	**36773**	**69423**	**88873**
OD tp D_S Conversion %		79%	77%	74%	75%
Actual		19862	49520	93373	119362
Corrected Actual	0	15691	38130	69096	89522
% Error		0.2%	3.7%	-0.5%	**1%**
Maximum	0	23276	69808	135023	167708
Corrected Maximum	0	18388	53752	99917	125781
Minimum	0	12034	38978	92930	125614
Corrected Minimum	0	9507	30013	68768	94211
PHF Min % Error Pedicted	0	12534	38519	81467	107730
% Error		-20%	5%	17%	**21%**
BuckQ Predicted	0	17698	42183	66738	90042
% Error		13%	15%	-4%	**1%**

Table 6-9. Continued

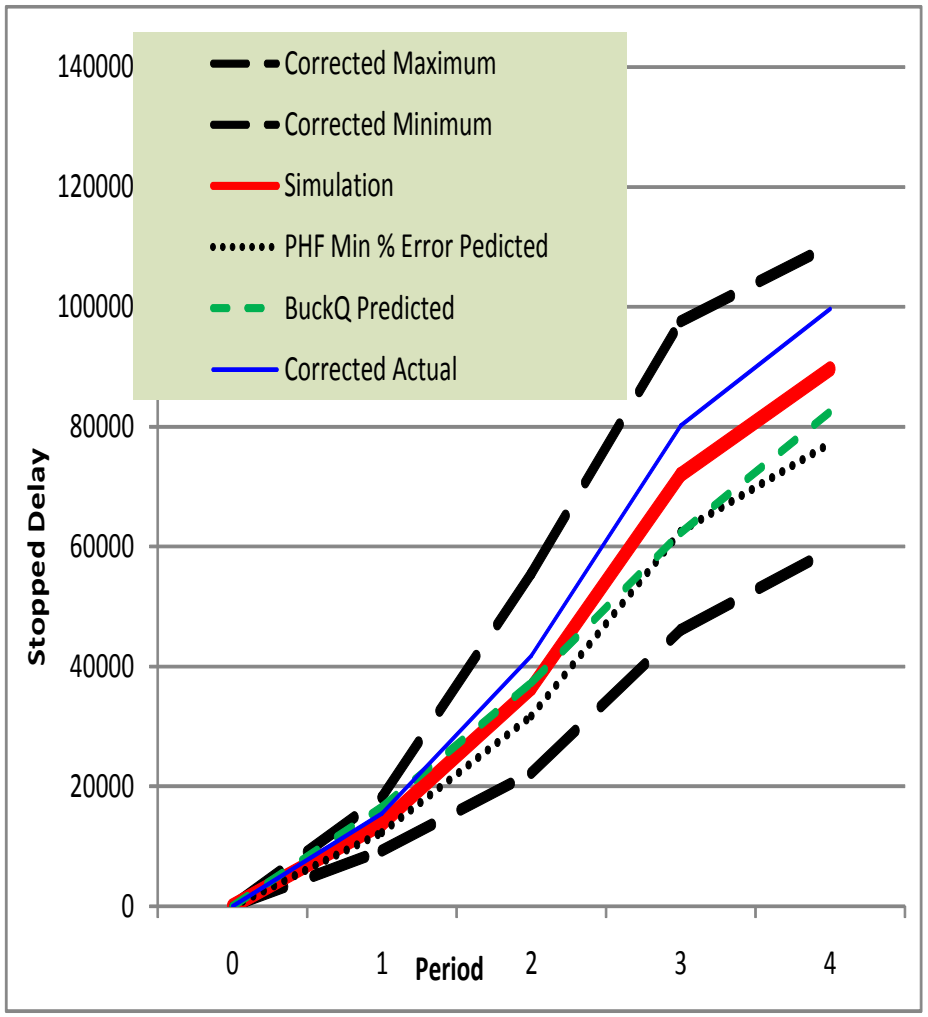

S*g/L Capacity:		642	635	645	613
Arrivals at BOQ:		736	712	704	360
Actual PHF:		0.85			
Simulation	**0**	**13743**	**36400**	**71981**	**89605**
OD tp D_S Conversion %		78%	76%	76%	75%
Actual		19807	54963	105506	132882
Corrected Actual	0	15449	41772	80184	99662
% Error		12.4%	14.8%	11.4%	**11%**
Maximum	0	23306	73060	128363	146966
Corrected Maximum	0	18179	55525	97556	110224
Minimum	0	11935	29204	60601	79204
Corrected Minimum	0	9309	22195	46057	59403
PHF Min % Error Pedicted	0	12313	31713	62573	77201
% Error		-10%	-13%	-13%	**-14%**
BuckQ Predicted	0	16586	37329	62358	82487
% Error		21%	3%	-13%	**-8%**

Table 6-10. Average stopped delay prediction results for 700_700_700_350vph volume pattern

120 second cycle

Min PHF = 0.80

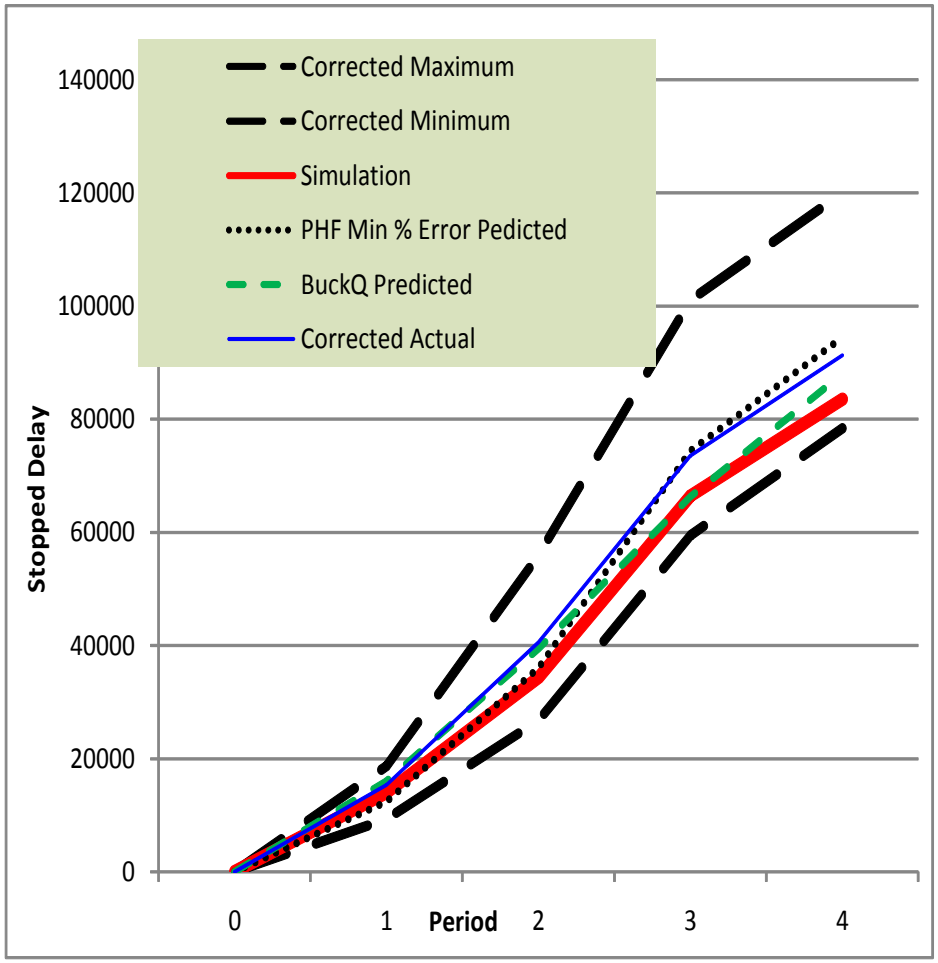

		Cumulative Stopped Delay			
Period:	0	1	2	3	4
S*g/L Capacity:		640	651	636	607
Arrivals at BOQ:		729	701	699	361
Actual PHF:		0.85			
Simulation	**0**	**13956**	**34365**	**66466**	**83549**
OD tp D_S Conversion %		78%	76%	75%	75%
Actual		19711	53162	97675	121209
Corrected Actual	0	15374	40580	73582	91311
% Error		10.2%	18.1%	10.7%	**9%**
Maximum	0	23958	73299	134122	159267
Corrected Maximum	0	18687	55951	101038	119982
Minimum	0	11907	35068	78935	104072
Corrected Minimum	0	9288	26768	59464	78401
PHF Min % Error Pedicted	0	12401	36079	74397	94456
% Error		-11%	5%	12%	**13%**
BuckQ Predicted	0	16032	39527	66328	88023
% Error		15%	15%	0%	**5%**

Table 6-11 - Stopped delay prediction results for 725_700_700_350vph volume pattern

120 second cycle
Min PHF = 0.80

Random Number Set 1

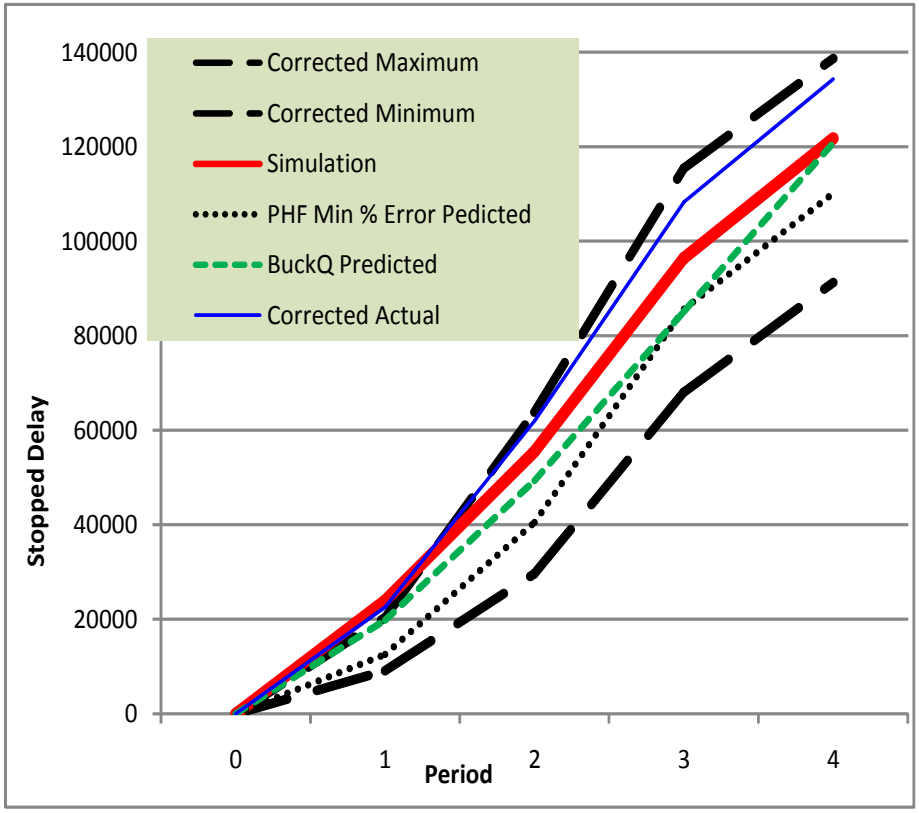

		Cumulative Stopped Delay			
Period:	0	1	2	3	4
S*g/L Capacity:		635	648	660	616
Arrivals at BOQ:		788	692	708	340
Actual PHF:		0.80			
Simulation	**0**	**23943**	**55507**	**96463**	**121786**
OD tp D_S Conversion %		77%	76%	75%	75%
Actual		29297	81598	144363	178994
Corrected Actual	0	22559	62014	108272	134245
% Error		-5.8%	11.7%	12.2%	**10%**
Maximum	0	26505	83981	153946	184858
Corrected Maximum	0	20409	63826	115460	138644
Minimum	0	11829	39043	90783	121695
Corrected Minimum	0	9108	29673	68087	91271
PHF Min % Error Pedicted	0	12595	40511	85660	110077
% Error		-47%	-27%	-11%	**-10%**
BuckQ Predicted	0	19817	49338	85163	120764
% Error		-17%	-11%	-12%	**-1%**

Table 6-11. Continued

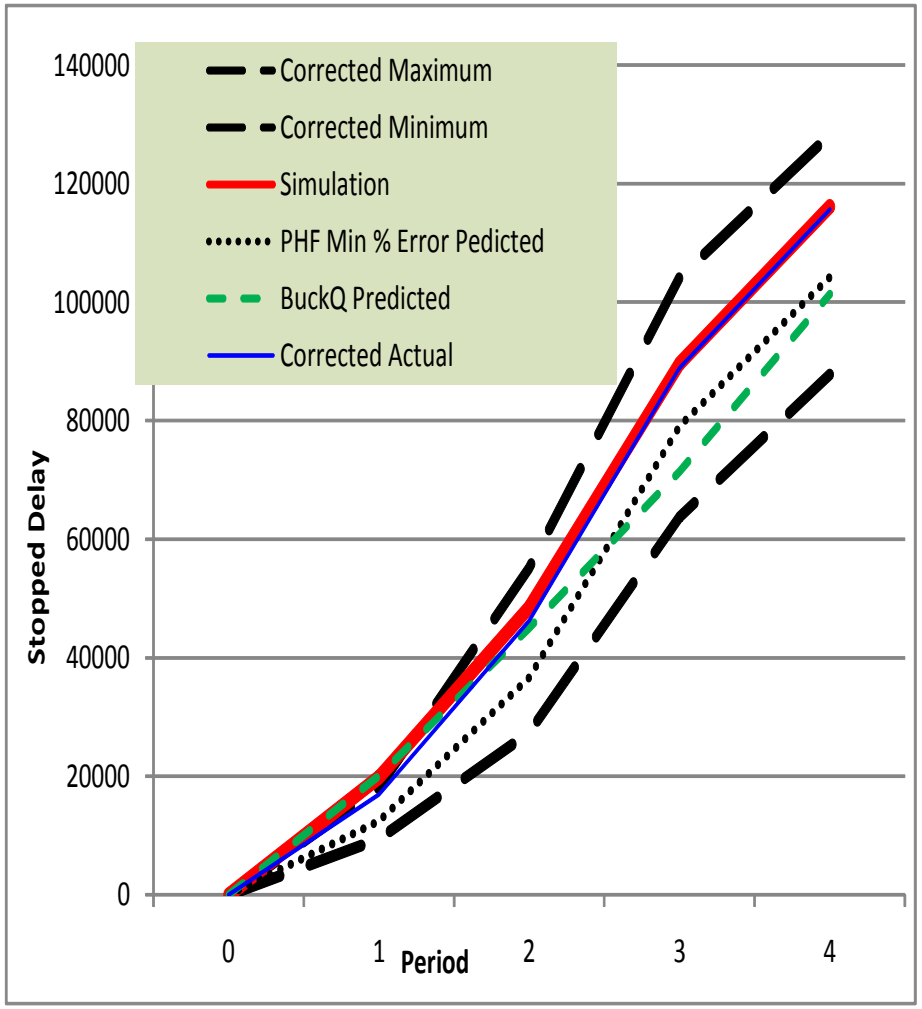

S*g/L Capacity:		662	638	621	644
Arrivals at BOQ:		768	724	700	356
Actual PHF:		0.83			
Simulation	**0**	**19909**	**48528**	**89649**	**116151**
OD tp D_S Conversion %		78%	75%	74%	74%
Actual		21714	61722	120097	156275
Corrected Actual	0	16937	46292	88872	115643
% Error		-14.9%	-4.6%	-0.9%	**0%**
Maximum	0	23279	73553	140755	173241
Corrected Maximum	0	18158	55165	104159	128198
Minimum	0	12169	36563	86182	118668
Corrected Minimum	0	9492	27422	63775	87814
PHF Min % Error Pedicted	0	12467	36634	79111	104231
% Error		-37%	-25%	-12%	**-10%**
BuckQ Predicted	0	20074	45086	71435	101389
% Error		1%	-7%	-20%	**-13%**

Table 6-11. Continued

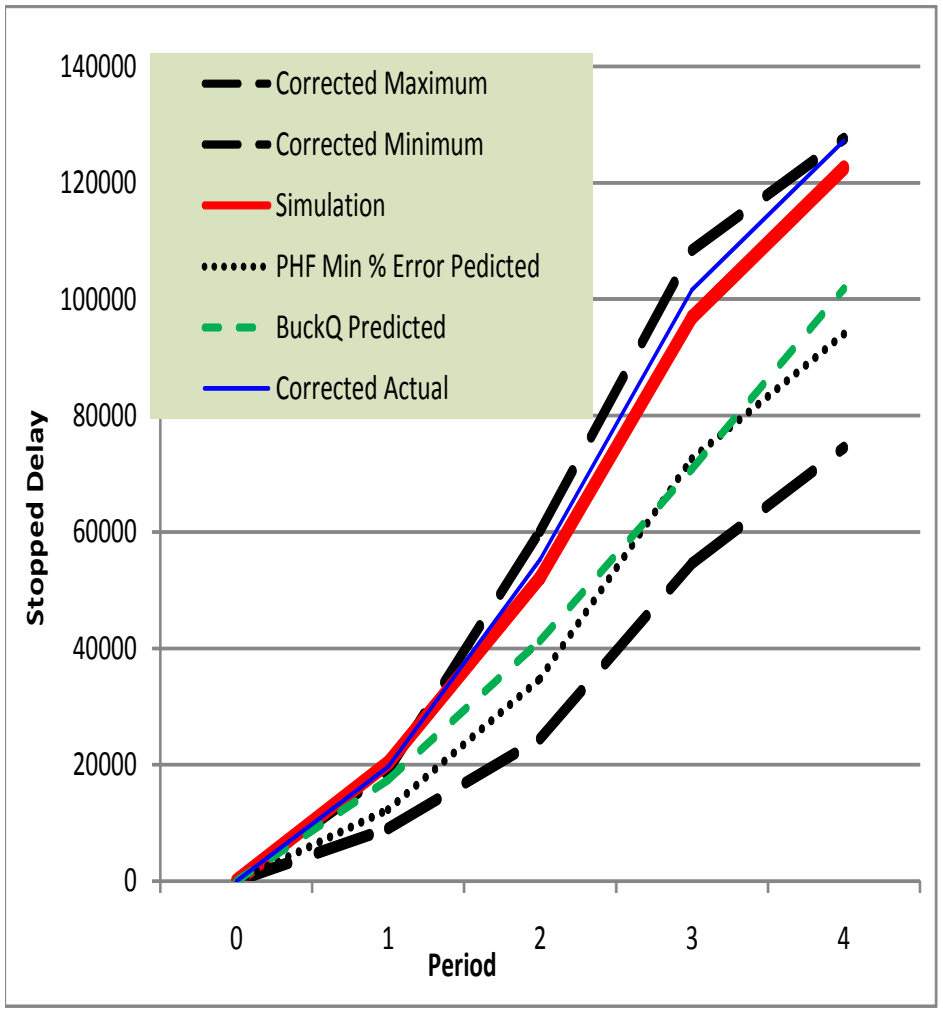

S*g/L Capacity:		647	635	645	610
Arrivals at BOQ:		796	704	700	364
Actual PHF:		0.81			
Simulation	**0**	**20321**	**52124**	**96875**	**122534**
OD tp D_S Conversion %		76%	75%	75%	74%
Actual		25848	73605	135397	171951
Corrected Actual	0	19645	55203	101548	127243
% Error		-3.3%	5.9%	4.8%	**4%**
Maximum	0	24969	80207	144540	172389
Corrected Maximum	0	18977	60155	108405	127568
Minimum	0	11935	32588	72744	100593
Corrected Minimum	0	9071	24441	54558	74439
PHF Min % Error Pedicted	0	12274	34759	72585	94017
% Error		-40%	-33%	-25%	**-23%**
BuckQ Predicted	0	17366	41246	70799	101785
% Error		-15%	-21%	-27%	**-17%**

Table 6-12. Average stopped delay prediction results for 725_700_700_350vph volume pattern

120 second cycle

Min PHF = 0.80

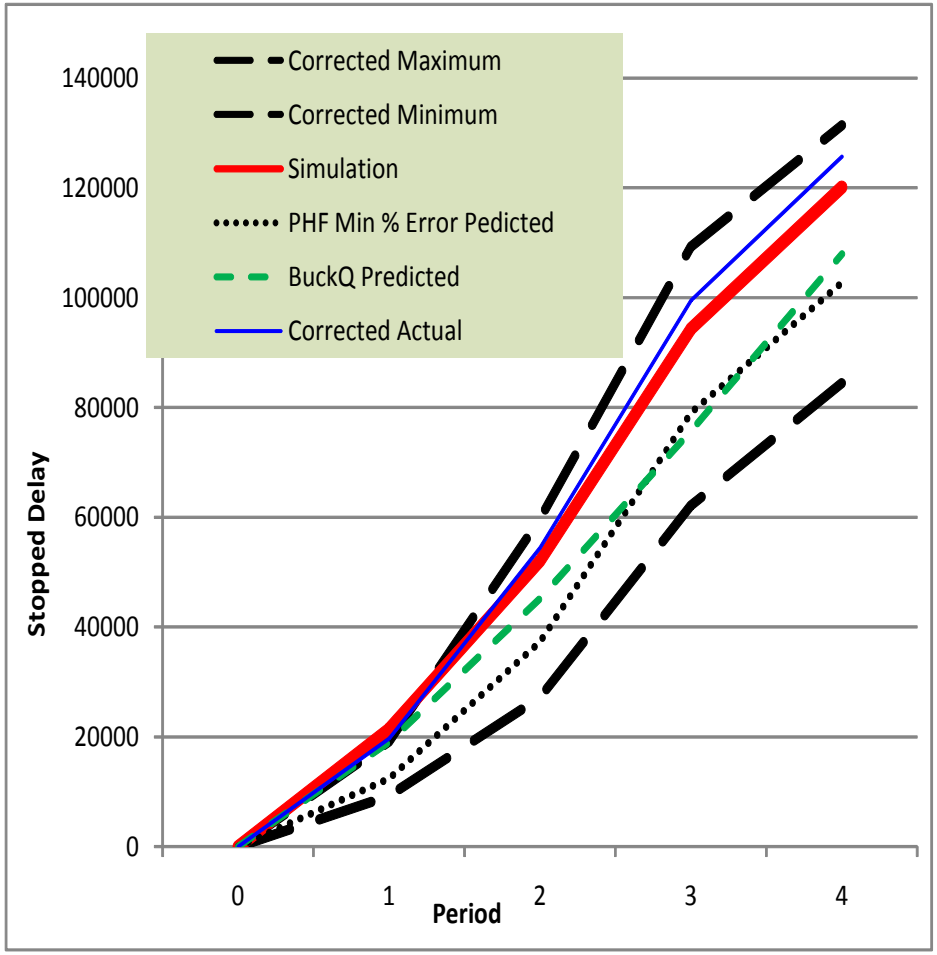

	Cumulative Stopped Delay				
Period:	0	1	2	3	4
S*g/L Capacity:		648	640	642	623
Arrivals at BOQ:		784	707	703	353
Actual PHF:		0.81			
Simulation	**0**	**21391**	**52053**	**94329**	**120157**
OD tp D_S Conversion %		77%	75%	75%	74%
Actual		25620	72308	133286	169073
Corrected Actual	0	19727	54472	99520	125678
% Error		-7.8%	4.6%	5.5%	**5%**
Maximum	0	24918	79247	146414	176829
Corrected Maximum	0	19187	59699	109322	131443
Minimum	0	11978	36065	83236	113652
Corrected Minimum	0	9223	27169	62150	84481
PHF Min % Error Pedicted	0	12445	37302	79119	102775
% Error		-42%	-28%	-16%	**-14%**
BuckQ Predicted	0	19086	45223	75799	107979
% Error		-11%	-13%	-20%	**-10%**

Table 6-13 - Stopped delay prediction results for 625_700_650_350vph volume pattern

120 second cycle

Min PHF = 0.80

Random Number Set 1

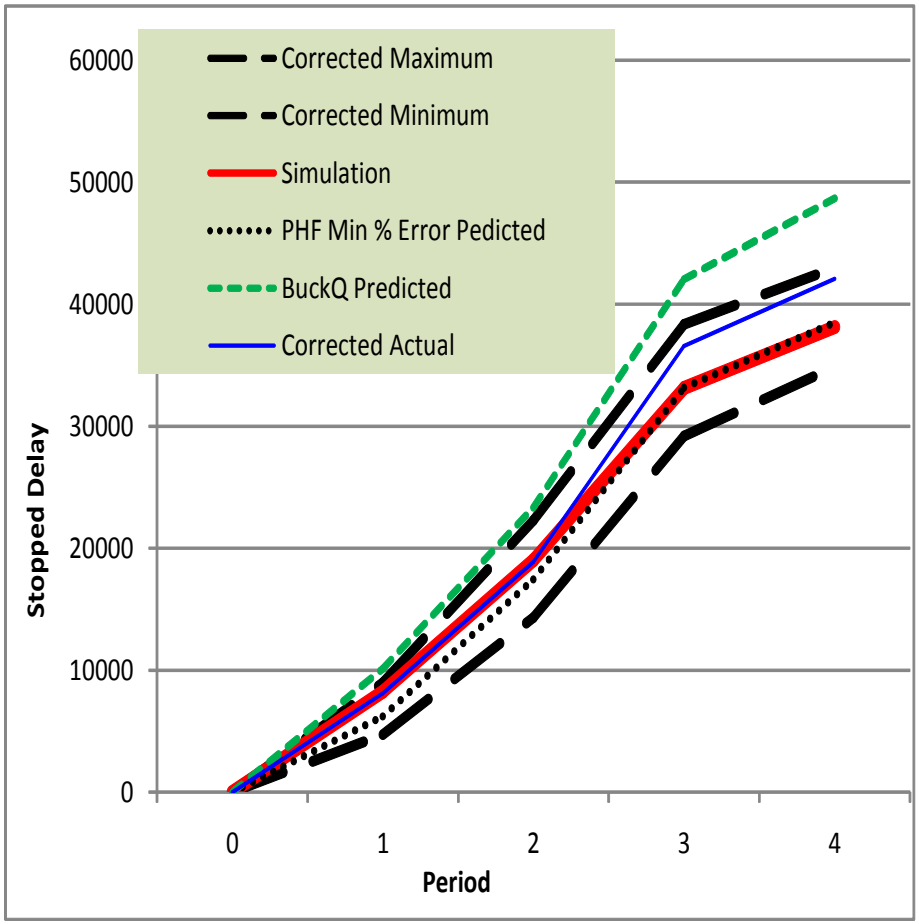

		Cumulative Stopped Delay			
Period:	0	1	2	3	4
S*g/L Capacity:		612	669	655	516
Arrivals at BOQ:		676	688	652	360
Actual PHF:		0.86			
Simulation	**0**	**8223**	**19035**	**33144**	**38126**
OD tp D_S Conversion %		76%	78%	77%	78%
Actual		10649	24184	47491	53956
Corrected Actual	0	8093	18864	36568	42086
% Error		-1.6%	-0.9%	10.3%	**10%**
Maximum	0	11793	28562	49797	55113
Corrected Maximum	0	8963	22279	38343	42988
Minimum	0	6227	18342	37939	44698
Corrected Minimum	0	4733	14307	29213	34865
PHF Min % Error Pedicted	0	6194	17424	33161	38503
% Error		-25%	-8%	0%	**1%**
BuckQ Predicted	0	10115	23332	42062	48662
% Error		23%	23%	27%	**28%**

Table 6-13. Continued

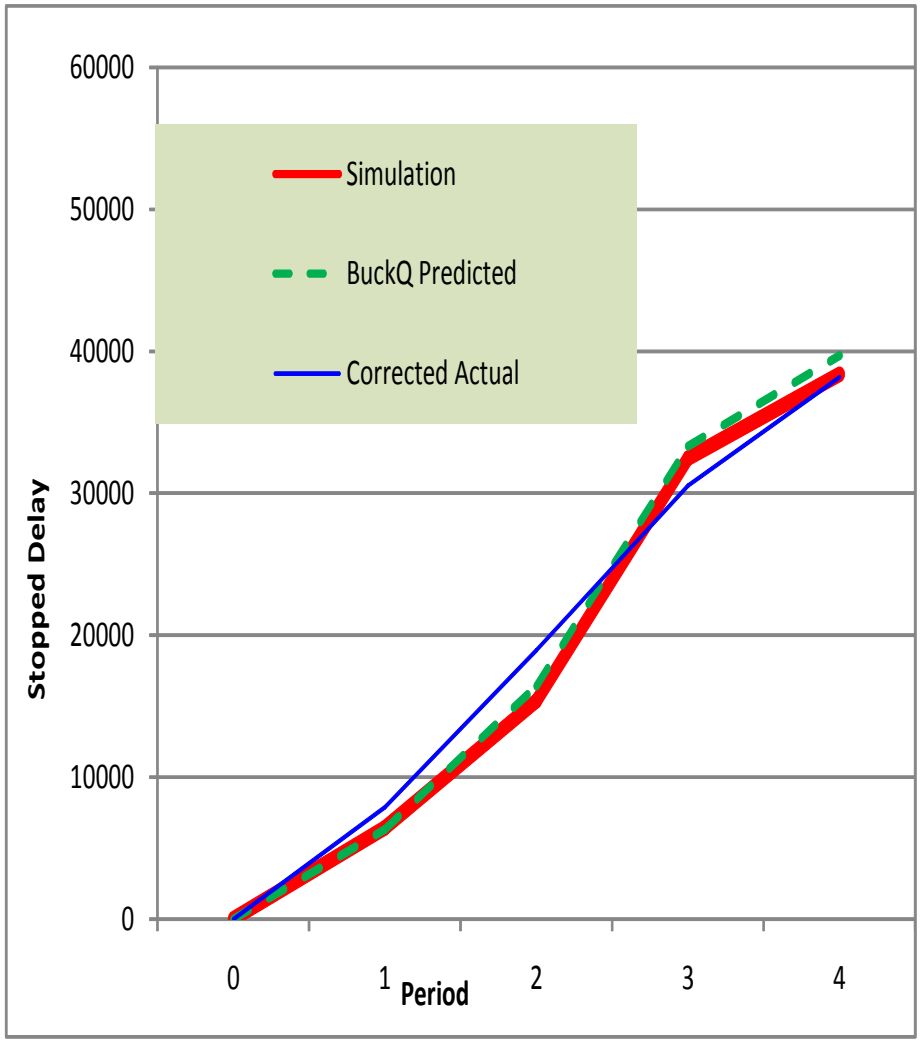

S*g/L Capacity:		665	643	623	497
Arrivals at BOQ:		628	676	672	364
Actual PHF:		0.87			
Simulation	**0**	**6424**	**15372**	**32476**	**38385**
OD tp D_S Conversion %		81%	77%	77%	77%
Actual		9718	24633	39689	49616
Corrected Actual	0	7872	18967	30561	38204
% Error		22.5%	23.4%	-5.9%	**0%**
BuckQ Predicted	0	6342	16427	33318	39729
% Error		-1%	7%	3%	**4%**

Table 6-13. Continued

Random Number Set 3

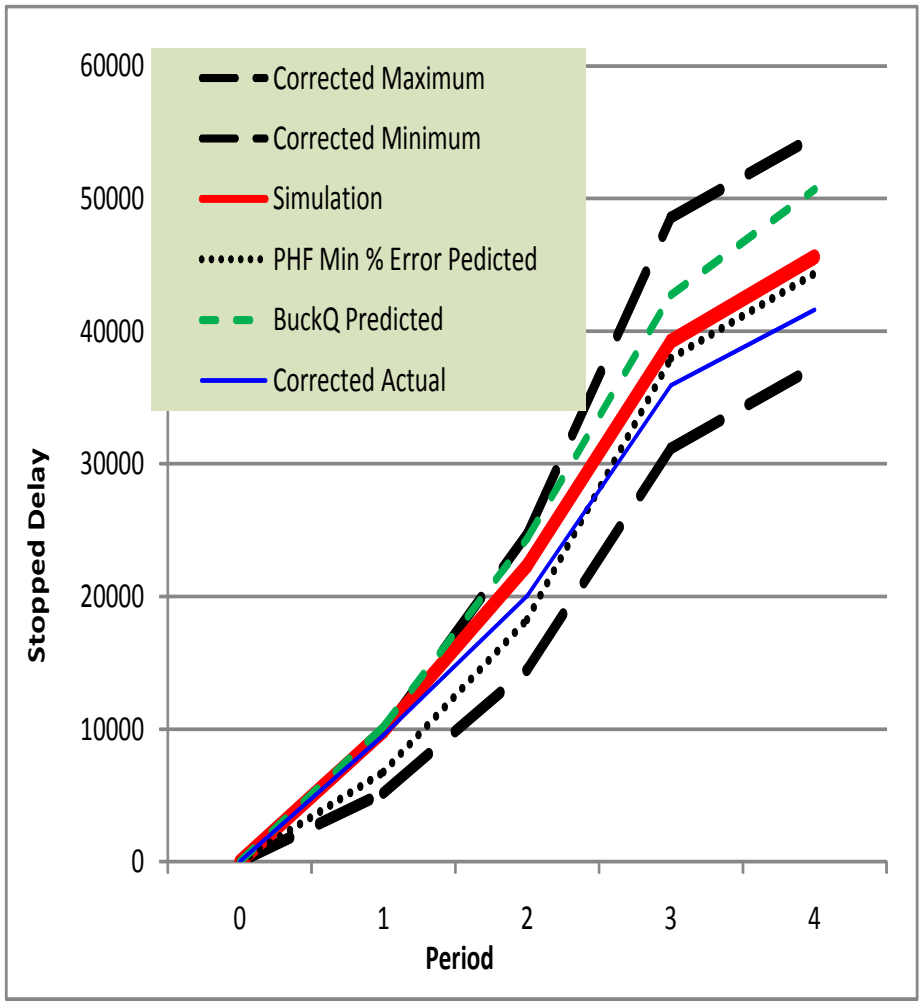

S*g/L Capacity:		643	650	641	524
Arrivals at BOQ:		672	668	688	344
Actual PHF:		0.86			
Simulation	**0**	**9858**	**22344**	**39242**	**45610**
OD tp D_S Conversion %		79%	78%	77%	77%
Actual		12078	25698	46675	54024
Corrected Actual	0	9542	20044	35940	41598
% Error		-3.2%	-10.3%	-8.4%	**-9%**
Maximum	0	12288	31676	63073	71020
Corrected Maximum	0	9708	24708	48566	54685
Minimum	0	6583	18588	40481	48428
Corrected Minimum	0	5200	14499	31170	37289
PHF Min % Error Pedicted	0	6773	18274	37971	44342
% Error		-31%	-18%	-3%	**-3%**
BuckQ Predicted	0	10197	24353	42741	50672
% Error		3%	9%	9%	**11%**

Table 6-14. Average stopped delay prediction results for 625_700_650_350vph volume pattern

120 second cycle

Min PHF = 0.80

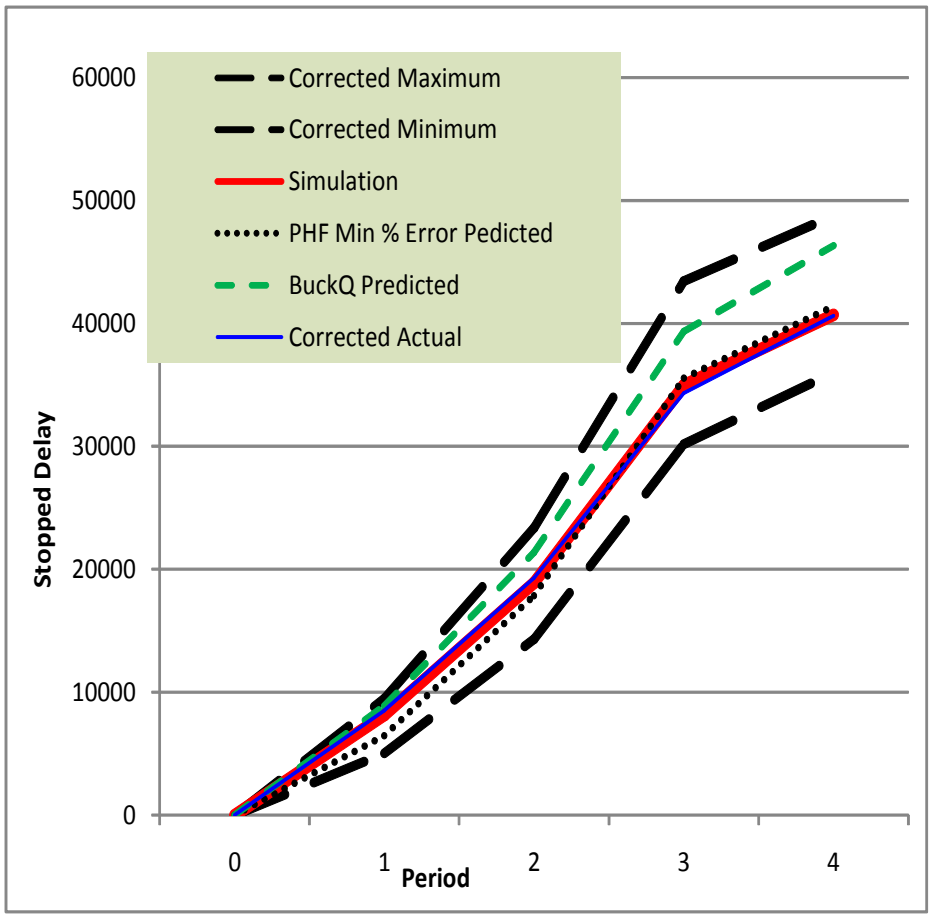

	Cumulative Stopped Delay				
Period:	0	1	2	3	4
S*g/L Capacity:		640	654	640	512
Arrivals at BOQ:		659	677	671	356
Actual PHF:		0.87			
Simulation	**0**	**8168**	**18917**	**34954**	**40707**
OD tp D_S Conversion %		79%	78%	77%	77%
Actual		10815	24838	44618	52532
Corrected Actual	0	8508	19291	34356	40625
% Error		4.2%	2.0%	-1.7%	**0%**
Maximum	0	12041	30119	56435	63066
Corrected Maximum	0	9472	23393	43455	48771
Minimum	0	6405	18465	39210	46563
Corrected Minimum	0	5039	14341	30192	36009
PHF Min % Error Pedicted	0	6484	17849	35566	41422
% Error		-21%	-6%	2%	**2%**
BuckQ Predicted	0	8885	21371	39374	46354
% Error		9%	13%	13%	**14%**

Table 6-15. Prediction comparison

Volume Pattern	Random Number Set		Percent Difference From Ground Truth, Period 1	Period 2	Period 3	Period 4	Visual	Average % Difference From Ground Truth, Period 1	Period 2	Period 3	Period 4	Visual
625_700_650_350vph	1	PHF Min % Error	-25%	-8%	0%	1%	-40%					
		Predicted	23%	23%	27%	28%						
		Hybrid	9%	17%	16%	13%						
	2	PHF Min % Error					-43%	-21%	-6%	2%	2%	-44%
		Predicted	-1%	7%	3%	4%		9%	13%	13%	14%	
		Hybrid						9%	13%	13%	14%	
	3	PHF Min % Error	-31%	-18%	-3%	-3%	-48%					
		Predicted	3%	9%	9%	11%						
		Hybrid	-2%	9%	9%	11%						
700_725_625_350vph	1	PHF Min % Error	-3%	-3%	-2%	0%	-64%					
		Predicted	11%	14%	7%	13%						
		Hybrid	11%	14%	7%	13%						
	2	PHF Min % Error	-21%	-18%	-14%	-8%	-69%	-13%	-14%	-13%	-10%	-68%
		Predicted	9%	3%	-12%	-7%		13%	5%	-7%	-2%	
		Hybrid	9%	3%	-12%	-7%		13%	5%	-7%	-2%	
	3	PHF Min % Error	-12%	-20%	-21%	-19%	-70%					
		Predicted	21%	-2%	-14%	-8%						
		Hybrid	21%	-2%	-14%	-8%						
700_700_700_350vph	1	PHF Min % Error	-1%	27%	36%	36%	-65%					
		Predicted	11%	31%	21%	27%						
		Hybrid	11%	31%	21%	27%						
	2	PHF Min % Error	-20%	5%	17%	21%	-71%	-11%	5%	12%	13%	-69%
		Predicted	13%	15%	-4%	-1%		15%	15%	0%	5%	
		Hybrid	13%	15%	-1%	6%		15%	15%	0%	5%	
	3	PHF Min % Error	-10%	-13%	-13%	-14%	-71%					
		Predicted	21%	3%	-13%	-8%						
		Hybrid	21%	3%	-13%	-8%						
725_700_700_350vph	1	PHF Min % Error	-47%	-27%	-11%	-10%	-78%					
		Predicted	-17%	-11%	-12%	-1%						
		Hybrid	-17%	-11%	-12%	-1%						
	2	PHF Min % Error	-37%	-25%	-12%	-10%	-77%	-42%	-28%	-16%	-14%	-78%
		Predicted	1%	-7%	-20%	-13%		-11%	-13%	-20%	-10%	
		Hybrid	-9%	-7%	-20%	-13%		-11%	-13%	-20%	-10%	
	3	PHF Min % Error	-40%	-33%	-25%	-23%	-78%					
		Predicted	-15%	-21%	-27%	-17%						
		Hybrid	-15%	-21%	-27%	-17%						
Average of Absolute Percent Difference		PHF Min % Error	22%	18%	**14%**	13%	65%	22%	13%	11%	10%	65%
		Predicted	**12%**	**12%**	**14%**	12%		**12%**	**12%**	**10%**	**8%**	
		Hybrid	13%	**12%**	**14%**	**11%**		**12%**	**12%**	**10%**	**8%**	
							Total					Total
Frequency of Best Prediction		PHF Min % Error	4	4	**6**	4	18	2	**2**	**2**	1	7
		Predicted	5	**7**	5	**6**	23	**3**	**2**	**2**	**3**	**10**
		Hybrid	**6**	**7**	**6**	**6**	**25**	**3**	**2**	**2**	**3**	**10**

CHAPTER 7
PERIOD ISSUES DURING OVER-SATURATED FLOW

This chapter describes deficiencies in the Highway Capacity Manual that can lead to incorrect delay values during over-saturated conditions. These deficiencies must be corrected before meaningful comparisons can be made to the predicted delay from our analysis procedure. Methods for correcting these deficiencies are presented (Objective 6).

Correctly identifying the size of the residual queue is very important for accurately calculating delay during over-saturated conditions. If the size of the residual queue is not correctly identified at the start of each 15-minute period then the resulting delay calculations for that period can be off by a substantial amount. The value of the d_3 delay term is directly tied to the length of the residual queue while the correct application of the random portion of the d_2 delay term depends on whether or not a residual queue is present. As the following discussion demonstrates, a cycle-by-cycle approach is required to accurately identify the residual queue, and use of the period approach contained in the Highway Capacity Manual [4] would not provide the desired result.

Simplified Example of Cycle-Period Issues in Calculating d_3

Formula F16-6 in the Highway Capacity Manual is touted as yielding the residual queue. The formula is:

$$Q_{b,i+1}=\max[0,Q_{b,i}+c_iT(X_i-1)]$$

Assuming that, at the start of the hour, there is no residual queue ($Q_{b,i} = 0$) then, if the volume is greater than the capacity for the first 15 minutes, this equation becomes:

$$Q_{b2} = cT(X-1)$$

Recognizing that $X = v/c$, we can further simplify this equation to:

$$Q_{b2}=cT(v/c-1)$$

$$Q_{b2} = Tv - cT$$

Where v = volume in vph and c = capacity in vph. If we call V the volume for the first 15-minute period then V = Tv (or v = V/T) and if we call C the capacity for the first 15-minute period, then C = Tc (or c = C/T). The equation then simply reduces to:

$$Q_{b2} = T(V/T) - (C/T)T$$

$$Q_{b2} = V - C \qquad (166)$$

So, the residual queue for the start of period 2 equals the difference between the arriving vehicles (15-minute volume) and the departing vehicles (15-minute capacity) for period 1.

However, this is not the correct procedure for determining the residual queue and Tables 7-1 and 7-2 show why. The simple example illustrated in these tables has just two 15-minute periods. The first period starts with no residual queue and the last period ends with little or no residual queue. However, a sizeable residual queue does exist at the end of the first 15-minute period and a value for d_3 is calculated for the second 15-minute period based on this value. Uniform arrivals are used to keep the example simple (and to avoid having to deal with the d_2 term) but the results can be generalized to any arrival situation. Table 7-1 provides the second-by-second cumulative arrival, cumulative departure and queue length information while the resulting residual queue, thruput, and associated d_3 values are provided in Table 7-2. (The full data set associated with Table 7-1 is provided in Appendix C.)

This example will demonstrate that the HCM formula consistently over-predicts the length of the residual queue and the associated value for d_3. In other words, there is an upward bias in the HCM formula and this bias can be substantial.

The uniform arrival rate for the first 15-minute period is V=180 vehicles (or v=720 vph) and the uniform arrival rate for the second 15-minute period is V=130 vehicles (or v=520 vph).

Again, to keep the example simple, vehicles are assumed to depart at constant 2-second headways whenever the indication is green and the effective green time is assumed to equal the actual green time. Obviously, no departures occur when the signal is red.

Columns B through F of Table 7-1 pertain to a 60 second cycle length with 20 seconds of green time and 40 seconds of red time. The start of the red for this cycle occurs at the start of the first period, which results in the green time ending at the end of the first period. In other words, the cycle is in complete synch with the period demarcation points. This is the best case situation and, even in this case, the residual queue at the end of the first period is over-predicted by 4 vehicles and the resulting d_3 is too high by about 15%.

There are 15 cycles during each 15-minute period (900/60 = 15) and 150 vehicles (C = 10 x 15 =150) will pass the stop bar during each 15-minute period for a capacity of c = 600 vph. 180/15 = 12 vehicles will arrive each cycle, with 4 arriving on the green and 8 arriving on the red. A traffic technician counting from time 0 to time 900 seconds would count 180 arriving vehicles (at either the stop bar or back of queue) and would count 150 vehicles departing. A queue of 30 vehicles is present at time 900 and the approach is just beginning to receive the green indication at this time. The modified HCM formula (166) would produce a residual queue at the end of period 1 of 180 – 150 = 30 vehicles and a corresponding value for d_3 in period 2 of 180.0 sec/veh. **However, 4 of these 30 vehicles arrived during the previous green period and are not part of the residual queue.** The true residual queue is 26 and the correct value for d_3 is 156.0 sec/vehicle.

The best way to obtain the residual queue is to look at the last end-of-red (start-of-green) time point within period 1 which, for this example, is time point 880. At this time there are 176 cumulative arrivals and 140 cumulative departures, which result in 36 “queued” vehicles. (These

vehicles may not actually be stationary; they are simply vehicles situated between the back of queue and the stop bar, whether moving or stationary.) However, this 36-vehicle "queue" at the end of red is not the residual queue either. We must subtract out vehicles that will clear the stop bar on the next green (the thruput), which for this example is 10. 36 – 10 = 26 is the true residual queue, which matches our previous result.

Another source of error occurs if the start-of-red does not match up with the period demarcation point and the period thruput is used, instead of the period capacity, to calculate the HCM residual queue and associated d_3. An example is provided in columns G through K. The counted thruput for period 1 is only 144 vehicles (576 vph), considerably less than the 600 vph capacity, which produces an (incorrect) residual queue of 36 vehicles and an associated d_3 value of 216.0 veh/sec. This type of error also occurs if the cycle length does not divide evenly into 900 seconds. If one is bent on using the erroneous HCM period-based approach, then one can at least avoid this type of error by always using the calculated capacity, not the thruput. This is one instance in queue accumulation and dissipation where the theoretical capacity is preferable to the thruput.

The largest delay discrepancy is found with the 162-second cycle example analyzed in columns AF through AJ. At time 900 there are 180 cumulative arrivals and 135 cumulative departures, for an HCM residual queue of 45 vehicles. Consequently, the associated value for d_3 is a whopping 250.0 sec/veh if one uses thruput instead of capacity. Using capacity continues to produce a value of 30 for the residual queue and a corresponding value of 180.0 sec/veh for d_3. This is much closer to the truth but both values are still much too high.

The last end-of-red in period 1 occurs at time 756. There are 151 cumulative arrivals and 108 cumulative departures at this time, which produce 43 "queued" vehicles. Since we have 54

seconds of green time, the thruput is 27 vehicles (1 vehicle every 2 seconds), so the residual queue is 43 - 27 = 16 and the associated value for d_3 is only 97.2 seconds/vehicle, a hugh difference of almost 100%.

Even for the best possible case, a cycle in synch with the period demarcation points, there is an upward bias in both the residual queue and d_3. The upward bias get worse if we have a cycle length that does not divide evenly into 900 seconds, as shown in columns Q through AE. And the bias gets even worse if the cycle length is a large one, as is shown in columns AF through AT. The substantial difference in d_3 that occurs between a cycle-based approach and a period-based approach can be readily seen in Figure 7-1. The true cycle-based delay is always less than the period-based delay.

A further demonstration of the loss of accuracy associated with period-based analysis can be made by comparing the "actual control delay" (as obtained by summing up the actual queue lengths on a second-by-second basis) with the control delay obtained by adding the d_1 term to the previously calculated d_3 term. The results are presented in Figure 7-2. The cycle-based analysis is much closer to the actual delay than the period-based analysis in every case. Also shown in Figure 7-2 is the control delay value provided by CORSIM. As with the actual control delay, the CORSIM delay results are much closer to the cycle-based results than the period-based results. It should be noted that, because of CORSIM initialization issues and because this spreadsheet example uses vertical queuing while CORSIM uses true horizontal queuing, an exact comparison between the spreadsheet results and CORSIM cannot be made. However, in this particular case, the differences caused by these items appear to be minor.

The solution to the period-cycle problem is to always start and stop the counts at the end-of-red (start-of-green), and to keep track of how much time transpires for each count "period".

For the 162-second example just discussed, the traffic technician would, for the first period, start counting at end-of-red time 108 and stop counting at end-of-red time 756. This makes period 1 of length 648 seconds (756-108). The cumulative arrivals during that period would be 130 and the cumulative departures would be 108 (the two 108's are just a coincidence). The calculated arrival rate would be 130 x 900/648 = 180 (or 720 vph) and the calculated departure rate (capacity) would be 108 x 900/648 = 150 (or 600 vph). Both of these values check as the stipulated arrival rate and capacity. The residual queue and associated d_3 value would be calculated as discussed in the previous paragraph. For period 2, we would start counting at time 756 and the process would be repeated. **This type of counting discipline is needed to obtain correct delay values when over-saturated conditions are present.**

Residual Queue Discrepancy

It is very important to understand what is meant by the term "initial queue". It can be argued that the term "residual queue" is preferable since it better represents the item of interest**. The residual queue for a particular lane is the number of "queued" vehicles that exist at the start-of-green for that lane, minus the thruput of the lane**. The thruput of the lane is the number of vehicles that depart the stop bar during the subsequent green interval. To find the residual queue at the end of each 15-minute period, one would evaluate the cycle that falls closest to this time point.

The term "queue" is used loosely here to represent the number of vehicles situated between the stop line and the back of queue. Under congestion, some of these vehicles may be moving while some may be stopped, so there is no guarantee that they are all queued. The term "caged" vehicles is coined in this research to describe these vehicles. (The word "trapped" was considered for use, but this word has numerous other potential meanings in traffic engineering whereas "caged" does not.)

It should be pointed out that the residual queue is not the number of vehicles between the stop bar and the back of queue when the signal turns red (end-of-green) since these "caged" vehicles include vehicles that arrived during the green interval. Only the portion of the caged vehicles that arrived during the red interval represent the residual queue. In other words, only those vehicles that experience a strict phase failure contribute to the residual queue; vehicles experiencing a liberal phase failure do not.

Figure 7-3 uses another simple example to illustrate the difference between the true residual queue and the residual queue calculated using the HCM approach. The HCM always overestimates the residual queue, with the amount of the overestimation depending on the cycle position that coincides with the period demarcation point. If the period demarcation point were to coincide with the first end of red then the HCM approach would produce a residual queue of 17, which is 10 greater than the true residual queue of 7 since the thruput is not deducted in the HCM approach. However, if the period demarcation point were to coincide with the start of red then the HCM approach would produce a residual queue of 11, which is 4 greater than the true residual queue of 7. The HCM approach mistakenly includes the 4 arrivals on green as part of the residual queue. Furthermore, if the period demarcation point were to coincide with the end of the second red then the HCM approach would produce a residual queue of 19, which is 10 greater than the true residual queue of 9. Consequently, depending on the exact location of the demarcation point, the HCM approach produces a residual queue for this example that is too large by a minimum value of 4 and a maximum value of 10. **The residual queue bias is always upward when the HCM approach is used with the maximum amount of the bias being equal to the thruput and the minimum amount of the bias being equal to the number of arrivals during the green indication.**

As its name implies, the value of the initial queue delay term (d_3) is heavily dependent on the size of the initial (residual) queue. Consequently, an upward bias in the residual queue can be expected to produce an upward bias in the initial queue delay, and a corresponding upward bias in the control delay. This will only occur when volume exceeds capacity since the initial queue delay is zero if volume is less than capacity. Also, since the amount of this upward bias does not increase as the over-saturated volume-to-capacity ratio increases, but rather stays "constant" at a value that fluctuates between the arrivals on green and the thruput, the relative error will be greatest near a v/c ratio of 1.0 and will decrease as the v/c ratio increases. This effect is clearly evident in Figure 4-23.

Detailed Example of Cycle-Period Issues in Calculating d_3

In this research, rather easily obtainable departure information from stop line counts, along with historical peak hour factors, are used to estimate both a minimum and a maximum cumulative arrival curve. These curves are then used as a theoretical envelope to bracket the real-time delay prediction results. Because cumulative curves are used in the theoretical bracketing of the delay, it is very important to understand the difference in the "delay" produced by cumulative arrival curves and the true delay associated with trajectory analysis. To do so, a one-hour (3600 second) example has been developed that is summarized in Tables 7-3 through 7-6.

An important point needs to be made about capacity. Keeping things simple, capacity is usually considered to be the number of vehicles that CAN pass the stop bar during a certain time period given current operating conditions (including the most important operating condition, g/C ratio). However, for the purposes of accurate queue accumulation, which is critical in calculating the d_3 term, capacity needs to be replaced by "thruput", the number of vehicles that DO pass the stop bar during a certain time period given current operating conditions. Let's say

that, due to previous periods of over-saturated flow, we have accumulated a residual queue of 80 vehicles. The next 15-minute period has a flow rate of 400 vph and a capacity of 600 vph, with capacity being calculated using the standard formula c = s(g/C). Using this definition of capacity, the queue would shrink by 50 vehicles ([400-600]/4 = -50) during this period and the initial (residual) queue for the next period would be 30 vehicles. However, because some wasted green time occurs at the end of a few of the cycles, let's say that only 120 vehicles actually pass the stop bar during this 15-minute period - which is an effective capacity of only 480 vph (120 x 4 = 480). The end result is that the queue actually shrinks by only 20 vehicles ([400-480]/4 = -20), producing a residual queue of 60 vehicles. The corresponding value for d_3 will have considerable error if thruput is not used instead of the standard definition of capacity.

Tables 7-3 through 7-6 summarize the comprehensive example. A 90-second cycle is used in this example with the start of the green offset by about 15 seconds from the 15-minute period demarcation points. At time zero, the signal is green and there is no queue. Since there is no queue of any type (let al.one a residual queue), the value of d_3 for period 1 is simply zero.

The signal turns green at time 75 (seconds). This is the first start-of-green (or end-of-red). 23 vehicles have arrived at the stop bar or back of queue by time 75 and 7 vehicles have departed from the stop bar. These 7 vehicles departed the stop bar during the green interval that was in operation when period 1 began. At time 900, the demarcation point between periods 1 and 2, 178 vehicles have arrived and 156 vehicles have departed. So, on a period basis, we have 178 arrivals and 156 departures in period 1, with a resulting "queue" of 22 vehicles. In this example, 9 of the 22 caged vehicles are moving (between the stop bar and the front of the queue) and 13 vehicles are truly queued at time 900. In any event, 178 would be the volume counted by a traffic technician who was instructed to begin counting at the top of the hour, and it is the

volume that would be used for period 1, the first 15-minute period, in an HCM multi-period analysis. If we also allow **capacity** to vary on a 15-minute basis, as reflected by actual thruput, then we would enter a value of 156 (which equals **624 vph**) and, using equation F16-6 from the HCM, the resulting residual queue at the end of the first period would be **22 vehicles.** This matches the number of caged vehicles at time 900. Using equation F16-1 from the HCM with 22 for the initial (residual) queue (Q_b), d_3 for period 2 would then be calculated as **126 sec/veh** by the HCM. It should be noted that the HCS+ software does not allow capacity to vary by 15-minute interval but instead requires a single capacity for the entire hour.

Unfortunately, these calculations are not correct because 22 is not the residual queue. The period demarcation point does not occur at the start-of-green and the thruput has not been deducted. The closest start-of-green time to the demarcation point between periods 1 and 2 (time 900) occurs at time 885. 176 vehicles have arrived by this time and 149 vehicles have departed. The queue at this point is 27 vehicles in length (176-149) and, since it occurs at the start-of-green, it is a true queue; all vehicles are stopped. However, although it is a true queue, it is not the residual queue. To calculate the residual queue we must subtract out the number of vehicles that depart the stop bar during the subsequent green period (the thruput). The subsequent end-of-green occurs at time 915. 183 vehicles have arrived by this time and 165 vehicles have departed. The "queue" at this point is 18 vehicles in length (183-165). However, it is neither a true queue (15 of the 18 vehicles are moving) nor is it the residual queue. Subtracting the 149 cumulative departing vehicles at the start-of-green (time 885) from the 165 cumulative departing vehicles from the end-of-green (time 916) yields a thruput of 16 vehicles. Subtracting this thruput (16) from the start-of-green queue (27) produces the true residual queue of **11 vehicles** at the end of period 1.

The capacity for the 900-second interval from time 885 to time 1785 is simply the thruput for this period, which is obtained by subtracting the cumulative departures for these two times: 306-149 = 157. Since this thruput occurs over a 900-second interval, the equivalent hourly capacity is calculated as: 157 x 3600/900 = 628 vph. Using equation F16-1 from the HCM with 11 for the residual queue (Q_b) and 628 for the capacity, d_3 for period 2 is correctly calculated as only **69 sec/veh,** not 126 sec/veh.

It should be noted that all yellow time is treated as green time in this example and that, for our purposes, the end-of-green is actually the end-of-yellow. When the approach is operating under capacity conditions, it is not uncommon for a CORSIM vehicle to cross the stop bar even after the indication has turned red. Consequently, the accuracy of the departures at the end-of-green is improved by using the departures that occur 1 second after the end-of green; time 916 in this example.

At time 1800, the demarcation point between periods 2 and 3, 352 vehicles have arrived and 313 vehicles have departed. On a period basis, we have 174 arrivals (352-178) and 157 departures (313-156) in period 2, with a resulting "queue" of 39 vehicles (352-313). In this example, 7 of the 39 caged vehicles are moving (between the stop bar and the front of the queue) and 32 vehicles are truly queued at time 1800. 174 would be the volume counted by a traffic technician who was instructed to count at 15-minute intervals, and it is the value that would be entered into an HCM multi-period analysis for period 2, the second 15-minute period. If we also enter **capacity**, as reflected by actual thruput, into the HCM analysis, then we would enter a value of 157 (which equals **628 vph**) and, using equation F16-6 from the HCM, the resulting residual queue at the end of the second period calculated by HCS+ would be **39 vehicles.** This matches the number of caged vehicles at time 1800. Using equation F16-1 from the HCM with

39 for the initial (residual) queue (Q_b), d_3 for period 3 would then be calculated as **225 sec/veh** by the HCM.

These calculations are once again wrong because 39 is not the residual queue. As before, the problem is twofold; the period demarcation point does not occur at the start-of-green and the thruput has not been deducted. The closest start-of-green time to the demarcation point between periods 2 and 3 (1800) occurs at time 1785. 351 vehicles have arrived by this time and 306 vehicles have departed. The queue at this point is 45 vehicles in length (351-306) and, since it occurs at the start-of-green, it is a true queue; all vehicles are stopped. However, although it is a true queue, it is not the residual queue. The number of vehicles that depart the stop bar during the subsequent green period (the thruput) must be subtracted to calculate the residual queue. The subsequent end-of-green occurs at time 1815. 353 vehicles have arrived by this time and, 1 second later, 320 vehicles have departed. The "queue" at this point is 33 vehicles in length (353-320). However, it is neither a true queue (15 of the 33 vehicles are moving) nor is it the residual queue. Subtracting the 306 cumulative departing vehicles at the start-of-green (time 1785) from the 320 cumulative departing vehicles from the end-of-green (time 1816) yields a thruput of 14 vehicles. Subtracting this thruput (14) from the start-of-green queue (45) produces the true residual queue of **31 vehicles** at the end of period 2.

The capacity for the 900-second interval from time 1785 to time 2685 is the thruput for this period, which is obtained by subtracting the cumulative departures for these two times: 459-306 = 153. Since this thruput occurs over a 900-second interval, the equivalent hourly capacity is calculated as: 153 x 3600/900 = 612 vph. Using equation F16-1 from the HCM with 31 for the initial (residual) queue (Q_b) and 612 for the capacity, d_3 for period 3 is correctly calculated as only **173 sec/veh,** not 225 sec/veh.

At time 2700, the demarcation point between periods 3 and 4, 502 vehicles have arrived and 465 vehicles have departed. On a period basis, we have 150 arrivals (502-352) and 152 departures (465-313) in period 3, with a resulting "queue" of 37 vehicles (502-465). In this example, 6 of the 37 caged vehicles are moving (between the stop bar and the front of the queue) and 31 vehicles are truly queued at time 2700. 150 would be the volume counted by a traffic technician who was instructed to count at 15-minute intervals, and it is the value that would be entered into the multi-period HCM analysis for period 3, the third 15-minute period. If we also enter **capacity**, as reflected by actual thruput, into the HCM analysis, then we would enter a value of 152 (which equals **608 vph**) and, using equation F16-6 from the HCM, the resulting residual queue at the end of the third period calculated by the HCM would be **37 vehicles.** This matches the number of caged vehicles at time 2700. Using equation F16-1 from the HCM with 37 for the initial (residual) queue (Q_b), d_3 for period 4 would then be calculated as **155 sec/veh** by the HCM.

As before, these calculations are incorrect because 37 is not the residual queue. The period demarcation point does not occur at the start-of-green and the thruput has not been deducted. The closest start-of-green time to the demarcation point between periods 3 and 4 (2700) occurs at time 2685. 502 vehicles have arrived by this time and 459 vehicles have departed. The queue at this point is 43 vehicles in length (502-459) and, since it occurs at the start-of-green, it is a true queue; all vehicles are stopped. However, although it is a true queue, it is not the residual queue. To calculate the residual queue we must subtract out the number of vehicles that depart the stop bar (the thruput) during the subsequent green period. The subsequent end-of-green occurs at time 2715. 506 vehicles have arrived by this time and, 1 second later, 474 vehicles have departed. The "queue" at this point is 32 vehicles in length (506-474). However, it is neither a

true queue (12 of the 33 vehicles are moving) nor is it the residual queue. Subtracting the 459 cumulative departing vehicles at the start-of-green (time 2685) from the 474 cumulative departing vehicles from the end-of-green (time 2716) yields a thruput of 15 vehicles. Subtracting this thruput (15) from the start-of-green queue (43) produces the true residual queue of **28 vehicles** at the end of period 3.

The capacity for the 900-second interval from time 2685 to time 3554, the start of the last full green in period 4, is the thruput for this period, which is obtained by subtracting the cumulative departures for these two times: 588-459 = 129. Since this thruput occurs over an 869-second interval, the equivalent hourly capacity is calculated as: 129 x 3600/869 = 534 vph. Using equation F16-1 from the HCM with 28 for the initial (residual) queue (Q_b) and 534 for the capacity, d_3 for period 4 is correctly calculated as only **64 sec/veh,** not 155 sec/veh.

This example clearly demonstrates that the delay error caused by using period-based arrivals and capacities instead of cycle-based arrivals and capacities can be quite large. The period-based method simply does not produce the correct residual queue.

The situation becomes even worse when we use the period-based method with a constant capacity value as is required by the HCS+ software. The thruput for the entire hour in this example is 590 vehicles. If we calculate the hourly capacity using the standard c = s(g/C) formula, the result is 594 vehicle per hour, which is very close. Using a single value of 590 for the hourly capacity produces residual queue lengths of 31 at the start of period 2, 57 at the start of period 3 and 60 at the start of period 4, with a final queue of 6 at the end of period 4. The associated values of d_3 are 186 sec/veh for period 2, 348 sec/veh for period 3, and 200 sec/veh for period 4. All of these values are much higher than they should be. The situation can be remedied somewhat by using a single capacity value that is calculated using information taken

only from over-saturated periods. If this is done for our example, the d_3 delay results are close to those obtained for the variable capacity period-based scenario: 134 sec/veh for period 2, 229 sec/veh for period 3, and 65 sec/veh for period 4.

Table 7-3 documents the calculation of the arrivals and departures on both a period basis and a cycle basis and also provides the associated queue length calculations. The wide disparity in the calculation of the residual queue is clearly evident from a review of the values contained in the last three columns.

Table 7-4 provides the d_1, d_2 and d_3 results for both a period-based and cycle-based approach. Summing these values, the total control delay for each period and the cumulative control delay are also calculated and a comparison made to CORSIM control delay. A review of this table shows that the largest deviation from the CORSIM results occurs when a period-based analysis with a single (fixed) hourly capacity is used (the HCS+ software approach). The period-based analysis can be improved significantly by allowing capacity to vary over the four 15-minute periods; the period-based variable capacity approach. However, to approach the CORSIM results, a cycle-based analysis must be used to calculate d_3, an approach which uses the correct definition of the residual queue. A tremendous improvement is made in the calculation of control delay when the correct approach is taken.

As was discussed previously in Chapter 6, d_2 requires adjustment when the residual queue is not zero to eliminate the delay effects associated with random arrivals. As is shown in Table 7-5, when this additional correction is made, a further improvement in the delay results occurs, especially for intermediate periods. However, the effect of the d_2 adjustment in this particular case is minor in comparison to the cycle-based correction.

As was also discussed in Chapter 6, the d_3 term is based on a cumulative curve approach. Consequently, a further adjustment is warranted to convert cumulative curve delay to control delay. This adjustment to d_3 is provided in Table 7-6 and, in this particular case, has minimal effect. (The adjustment percentages were obtained from a BuckTraj analysis of CORSIM-generated vehicle trajectories.)

This example clearly demonstrates that the accuracy of the delay calculations is greatly increased under the preferred option, a cycle-based approach with proper definition of residual queue, varying capacity by period, and a d_2 term that eliminates the effect of randomness during over-saturated conditions.

Previously, in Tables 6-7 through 6-15, a comparison was made between stopped delay obtained from simulation and "actual" stopped delay obtained from cumulative curves for our four examples. Although the delay obtained from these two sources were generally in close agreement, there were instances where discrepancies arose. The use of a period-based approach instead of a cycle-based approach may be the cause of these discrepancies.

Table 7-1. Generalized example of cycle-period delay discrepancies - data

Cycle Length:	60 seconds									78 seconds									162 seconds								
Red/Green Pattern:	Start on Full Red				Start on Full Green				Start on Half Green				Start on Full Red				Start on Full Green				Start on Half Green				Start on Full Red				Start on Full Green				Start on Half Green			
Period 1																																						
Actual Arrivals & Departures/Thruput (vph):	720	600			720	576			720	588			720	572			vph	720	593		vph	720	582		vph	720	540			vph	720	583			vph	720	562	
Actual Arrivals & Departures/Thruput (@15min):	180	150			180	144			180	147			180	143				180	148			180	146			180	135				180	146				180	140	
Period 2																																						
Actual Arrivals & Departures/Thruput (vph):	520	600			520	600			520	600			520	624			vph	520	584		vph	520	610		vph	520	648			vph	520	576			vph	520	630	
Actual Arrivals, Dep/Thruput (veh per 15min):	130	150			130	150			130	150			130	156				130	146			130	153			130	162				130	144				130	158	
Actual Arrivals & Dep/Thruput (@30min):	310	300			310	294			310	297			310	299				310	294			310	298			310	297				310	290				310	298	
A=Arrivals, D=Departures, Q=Queue:	A	D	Q		A	D	Q		A	D	Q		A	D	Q			A	D	Q		A	D	Q		A	D	Q			A	D	Q			A	D	Q
Time (sec)																																						
0		0	0			0	0			0	0			0	0				0	0			0	0			0	0				0	0				0	0	
1	R	0	0	0	G	0	0	0	G	0	0	0	R	0	0	0	G		0	0	0	G	0	0	0	R	0	0	0	G		0	0	0	G		0	0	0
2	R	0	0	0	G	0	0	0	G	0	0	0	R	0	0	0	G		0	0	0	G	0	0	0	R	0	0	0	G		0	0	0	G		0	0	0
3	R	1	0	1	G	1	1	0	G	1	1	0	R	1	0	1	G		1	1	0	G	1	1	0	R	1	0	1	G		1	1	0	G		1	1	0
4	R	1	0	1	G	1	1	0	G	1	1	0	R	1	0	1	G		1	1	0	G	1	1	0	R	1	0	1	G		1	1	0	G		1	1	0
5	R	1	0	1	G	1	1	0	G	1	1	0	R	1	0	1	G		1	1	0	G	1	1	0	R	1	0	1	G		1	1	0	G		1	1	0
6	R	1	0	1	G	1	1	0	G	1	1	0	R	1	0	1	G		1	1	0	G	1	1	0	R	1	0	1	G		1	1	0	G		1	1	0
7	R	1	0	1	G	1	1	0	G	1	1	0	R	1	0	1	G		1	1	0	G	1	1	0	R	1	0	1	G		1	1	0	G		1	1	0
8	R	2	0	2	G	2	2	0	G	2	2	0	R	2	0	2	G		2	2	0	G	2	2	0	R	2	0	2	G		2	2	0	G		2	2	0
9	R	2	0	2	G	2	2	0	G	2	2	0	R	2	0	2	G		2	2	0	G	2	2	0	R	2	0	2	G		2	2	0	G		2	2	0
10	R	2	0	2	G	2	2	0	G	2	2	0	R	2	0	2	G		2	2	0	G	2	2	0	R	2	0	2	G		2	2	0	G		2	2	0
11	R	2	0	2	G	2	2	0	R	2	2	0	R	2	0	2	G		2	2	0	G	2	2	0	R	2	0	2	G		2	2	0	G		2	2	0
12	R	2	0	2	G	2	2	0	R	2	2	0	R	2	0	2	G		2	2	0	G	2	2	0	R	2	0	2	G		2	2	0	G		2	2	0
13	R	3	0	3	G	3	3	0	R	3	2	1	R	3	0	3	G		3	3	0	G	3	3	0	R	3	0	3	G		3	3	0	G		3	3	0
14	R	3	0	3	G	3	3	0	R	3	2	1	R	3	0	3	G		3	3	0	R	3	3	0	R	3	0	3	G		3	3	0	G		3	3	0
15	R	3	0	3	G	3	3	0	R	3	2	1	R	3	0	3	G		3	3	0	R	3	3	0	R	3	0	3	G		3	3	0	G		3	3	0
16	R	3	0	3	G	3	3	0	R	3	2	1	R	3	0	3	G		3	3	0	R	3	3	1	R	3	0	3	G		3	3	0	G		3	3	0
17	R	3	0	3	G	3	3	0	R	3	2	1	R	3	0	3	G		3	3	0	R	3	3	1	R	3	0	3	G		3	3	0	G		3	3	0
18	R	4	0	4	G	4	4	0	R	4	2	2	R	4	0	4	G		4	4	0	R	4	3	1	R	4	0	4	G		4	4	0	G		4	4	0
19	R	4	0	4	G	4	4	0	R	4	2	2	R	4	0	4	G		4	4	0	R	4	3	1	R	4	0	4	G		4	4	0	G		4	4	0
20	R	4	0	4	G	4	4	0	R	4	2	2	R	4	0	4	G		4	4	0	R	4	3	1	R	4	0	4	G		4	4	0	G		4	4	0
21	R	4	0	4	R	4	4	0	R	4	2	2	R	4	0	4	G		4	4	0	R	4	3	2	R	4	0	4	G		4	4	0	G		4	4	0
22	R	4	0	4	R	4	4	0	R	4	2	2	R	4	0	4	G		4	4	0	R	4	3	2	R	4	0	4	G		4	4	0	G		4	4	0
23	R	5	0	5	R	5	4	1	R	5	2	3	R	5	0	5	G		5	5	0	R	5	3	2	R	5	0	5	G		5	5	0	G		5	5	0
24	R	5	0	5	R	5	4	1	R	5	2	3	R	5	0	5	G		5	5	0	R	5	3	2	R	5	0	5	G		5	5	0	G		5	5	0
25	R	5	0	5	R	5	4	1	R	5	2	3	R	5	0	5	G		5	5	0	R	5	3	2	R	5	0	5	G		5	5	0	G		5	5	0
26	R	5	0	5	R	5	4	1	R	5	2	3	R	5	0	5	G		5	5	0	R	5	3	3	R	5	0	5	G		5	5	0	G		5	5	0
27	R	5	0	5	R	5	4	1	R	5	2	3	R	5	0	5	R		5	5	0	R	5	3	3	R	5	0	5	G		5	5	0	G		5	5	0
28	R	6	0	6	R	6	4	2	R	6	2	4	R	6	0	6	R		6	5	0	R	6	3	3	R	6	0	6	G		6	6	0	R		6	5	0
29	R	6	0	6	R	6	4	2	R	6	2	4	R	6	0	6	R		6	5	1	R	6	3	3	R	6	0	6	G		6	6	0	R		6	5	0
30	R	6	0	6	R	6	4	2	R	6	2	4	R	6	0	6	R		6	5	1	R	6	3	3	R	6	0	6	G		6	6	0	R		6	5	1
31	R	6	0	6	R	6	4	2	R	6	2	4	R	6	0	6	R		6	5	1	R	6	3	4	R	6	0	6	G		6	6	0	R		6	5	1
32	R	6	0	6	R	6	4	2	R	6	2	4	R	6	0	6	R		6	5	1	R	6	3	4	R	6	0	6	G		6	6	0	R		6	5	1
33	R	7	0	7	R	7	4	3	R	7	2	5	R	7	0	7	R		7	5	1	R	7	3	4	R	7	0	7	G		7	7	0	R		7	5	1
34	R	7	0	7	R	7	4	3	R	7	2	5	R	7	0	7	R		7	5	2	R	7	3	4	R	7	0	7	G		7	7	0	R		7	5	1
35	R	7	0	7	R	7	4	3	R	7	2	5	R	7	0	7	R		7	5	2	R	7	3	4	R	7	0	7	G		7	7	0	R		7	5	2
36	R	7	0	7	R	7	4	3	R	7	2	5	R	7	0	7	R		7	5	2	R	7	3	5	R	7	0	7	G		7	7	0	R		7	5	2
37	R	7	0	7	R	7	4	3	R	7	2	5	R	7	0	7	R		7	5	2	R	7	3	5	R	7	0	7	G		7	7	0	R		7	5	2
38	R	8	0	8	R	8	4	4	R	8	2	6	R	8	0	8	R		8	5	2	R	8	3	5	R	8	0	8	G		8	8	0	R		8	5	2
39	R	8	0	8	R	8	4	4	R	8	2	6	R	8	0	8	R		8	5	3	R	8	3	5	R	8	0	8	G		8	8	0	R		8	5	2
40	R	8	0	8	R	8	4	4	R	8	2	6	R	8	0	8	R		8	5	3	R	8	3	5	R	8	0	8	G		8	8	0	R		8	5	3
41	G	8	1	8	R	8	4	4	R	8	2	6	R	8	0	8	R		8	5	3	R	8	3	6	R	8	0	8	G		8	8	0	R		8	5	3
42	G	8	1	7	R	8	4	4	R	8	2	6	R	8	0	8	R		8	5	3	R	8	3	6	R	8	0	8	G		8	8	0	R		8	5	3
43	G	9	2	7	R	9	4	5	R	9	2	7	R	9	0	9	R		9	5	3	R	9	3	6	R	9	0	9	G		9	9	0	R		9	5	3
44	G	9	2	7	R	9	4	5	R	9	2	7	R	9	0	9	R		9	5	4	R	9	3	6	R	9	0	9	G		9	9	0	R		9	5	3
45	G	9	3	7	R	9	4	5	R	9	2	7	R	9	0	9	R		9	5	4	R	9	3	6	R	9	0	9	G		9	9	0	R		9	5	4
46	G	9	3	6	R	9	4	5	R	9	2	7	R	9	0	9	R		9	5	4	R	9	3	7	R	9	0	9	G		9	9	0	R		9	5	4
47	G	9	4	6	R	9	4	5	R	9	2	7	R	9	0	9	R		9	5	4	R	9	3	7	R	9	0	9	G		9	9	0	R		9	5	4
48	G	10	4	6	R	10	4	6	R	10	2	8	R	10	0	10	R		10	5	4	R	10	3	7	R	10	0	10	G		10	10	0	R		10	5	4
49	G	10	5	5	R	10	4	6	R	10	2	8	R	10	0	10	R		10	5	5	R	10	3	7	R	10	0	10	G		10	10	0	R		10	5	4
50	G	10	5	5	R	10	4	6	R	10	2	8	R	10	0	10	R		10	5	5	R	10	3	7	R	10	0	10	G		10	10	0	R		10	5	5
51	G	10	6	5	R	10	4	6	G	10	3	8	R	10	0	10	R		10	5	5	R	10	3	8	R	10	0	10	G		10	10	0	R		10	5	5
52	G	10	6	4	R	10	4	6	G	10	3	7	R	10.4	0.0	10.4	R		10	5	5	R	10	3	8	R	10	0	10	G		10	10	0	R		10	5	5
53	G	11	7	4	R	11	4	7	G	11	4	7	G	11	1	10	R		11	5	5	R	11	3	8	R	11	0	11	G		11	11	0	R		11	5	5
54	G	11	7	4	R	11	4	7	G	11	4	7	G	11	1	10	R		11	5	6	R	11	3	8	R	11	0	11	G		11	11	0	R		11	5	5
55	G	11	8	3	R	11	4	7	G	11	5	6	G	11	2	9	R		11	5	6	R	11	3	8	R	11	0	11	R		11	11	0	R		11	5	6
56	G	11	8	3	R	11	4	7	G	11	5	6	G	11	2	9	R		11	5	6	R	11	3	9	R	11	0	11	R		11	11	0	R		11	5	6

Table 7-2. Generalized example of cycle-period delay discrepancies – summary

A		B	C	D	E	F	G	H	I	J	K	L	M	N	O	P	Q	R	S	T	U	V	W	X	Y	Z	AA	AB	AC	AD	AE
Cycle Length:		**60 seconds**															**78 seconds**														
Red/Green Pattern:		Start on Full Red					Start on Full Green					Start on Half Green					Start on Full Red					Start on Full Green					Start on Half Green				
Cycle Length (sec):	C	60			Thruput		60					60					78					78					78				
Green Time (sec):	g = G	20			10		20			10		20			10		26			13		26			13		26			13	
Red Time (sec):		40					40					40					52					52					52				
g/C = G/C		0.33					0.33					0.33					0.33					0.33					0.33				
A=Arrivals, D=Departures, Q=Queue:	Cumulative		A	D	Q	d		A	D	Q	d		A	D	Q	d		A	D	Q	d		A	D	Q	d		A	D	Q	d
Theoretical Arrivals & Dep/Capacity (vph)	X = v_1/c_1	v_1=	720	600	= c_1			720	600				720	600				720	600				720	600				720	600		
PERIOD-BASED ANALYSIS	T = 0.25																														
Actual Arrivals & Departures/Thruput (vph):	**Period 1**		720	600				720	576				720	588				720	572			vph	720	593			vph	720	582.4		
Actual Arrivals, Dep/Thruput & Q_b (@15min):			180	150	30			180	144	36			180	147	33			180	143	37			180	148	32			180	146	34	
Actual Arrivals & Departures/Thruput (vph):	**Period 2**		520	600	= c			520	600				520	600				520	624			vph	520	584			vph	520	610		
Actual Arrivals, Dep/Thruput & Q_b (15min):			130	150				130	150				130	150				130	156				130	146				130	153		
Actual Arrivals, Dep/Thruput & Q_b (@30min):			310	300	10			310	294	16			310	297	13			310	299	11			310	294	16			310	298	12	
u & t			1.00	0.25	False Q_b			1.00	0.25				1.00	0.25				1.00	0.25				1.00	0.25				1.00	0.25		
Calc. d_3 & Q_b=c_1T(X-1) based on theoretical capacity:					30	**180**				30	**180**				30	**180**				30	**180**				30	**180**				30	**180**
Calc. d_3=1800Q_b(1+u)t/CT & Q_b based on actual thruput:					30	**180**				36	**216**				33	**198**				37	**213**				31.8	**196**				34.4	**203**
CYCLE-BASED ANALYSIS		Time																													
Actual Arrivals, Departures/Thruput & Q_b at end of 1st red:		40	8	0	True Q_b		60	12	4			50	10	2			52	10.4	0			78	15.6	5.2			65	13.0	2.6		
Actual Arrivals, Departures/Thruput & Q_b at end of last red:		880	176	140	26		900	180	144	26		890	178	142	26		832	166.4	130.0	23.4		858	171.6	135.2	23.4		845	169.0	132.6	23.4	
Actual Arrival & Dep/Thruput For Time Shown:	**Period 1**	840	168	140	(176-140-10)		840	168	140			840	168	140			780	156	130			780	156	130			780	156	130		
Adjusted Arrivals & Dep/Thruput (15min):		900	180	150			900	180	150			900	180	150			900	180	150			900	180	150			900	180	150		
Adjusted Arrivals & Departures/Thruput (vph):			720	600				720	600				720	600				720	600				720	600				720	600		
Actual Arr, Dep/Thruput & Q_b For Time Shown at end of last red:		1780	307	290	7		1800	310	294	6		1790	309	292	7		1768	305	286	6		1794	309	291	5		1781	307	289	6	
Actual Arrival & Dep/Thruput For Time Shown:		900	131	150			900	130	150			900	131	150			936	139	156			936	138	156			936	138	156		
Adj Arrival & Dep/Thruput (15 min)		900	131	150			900	130	150			900	131	150			900	134	150			900	132	150			900	133	150		
Adj Arrival & Dep/Thruput (vph)			524	600	= c			520	600				522	600				535	600				529	600				532	600		
u & t:	**Period 2**		1.00	0.25				1.00	0.25				1.00	0.25				1.00	0.25				1.00	0.25				1.00	0.25		
Calculated d_3 = 1800Q_b(1+u)t/cT based on actual thruput:						**156**					**156**					**156**					**140**					**140**					**140**
Calculated d_1=0.5C[1-g/C]^2/[1-g/C]:						20					20					20					26					26					26
Period 2 Actual "Control" Delay (d_1 + d_3) in sec:					20990					20390					20690					21899					21180				21576	
Period 2 Actual "Control" Delay (d_1 + d_3) in sec/veh:						**140**					**136**					**138**					**140**					**145**					**141**

A		AF	AG	AH	AI	AJ	AK	AL	AM	AN	AO	AP	AQ	AR	AS	AT
Cycle Length:		**162 seconds**														
Red/Green Pattern:		Start on Full Red					Start on Full Green					Start on Half Green				
Cycle Length (sec):	C	162					162					162				
Green Time (sec):	g = G	54			27		54			27		54			27	
Red Time (sec):		108					108					108				
g/C = G/C		0.33					0.33					0.33				
Cumulative A=Arrivals, D=Departures, Q=Queue:			A	D	Q	d		A	D	Q	d		A	D	Q	d
Theoretical Arrivals & Dep/Capacity (vph)	X = v_1/c_1		720	600				720	600				720	600		
PERIOD-BASED ANALYSIS	T = 0.25															
Actual Arrivals & Departures/Thruput (vph):	**Period 1**	vph	720	540			vph	720	583.2			vph	720	561.6		
Actual Arrivals, Dep/Thruput & Q_b (@15min):			180	135	45			180	146	34			180	140	40	
Actual Arrivals & Departures/Thruput (vph):	**Period 2**	vph	520	648			vph	520	576			vph	520	630		
Actual Arrivals, Dep/Thruput & Q_b (15min):			130	162				130	144				130	158		
Actual Arrivals, Dep/Thruput & Q_b (@30min):			310	297	13			310	290	20			310	298	12	
u & t			1.00	0.25				1.00	0.25				1.00	0.25		
Calc. d_3 & Q_b=c_1T(X-1) based on theoretical capacity:					30	**180**				30	**180**				30	**180**
Calc. d_3=1800Q_b(1+u)t/CT & Q_b based on actual thruput:					45	**250**				34.2	**214**				39.6	**226**
CYCLE-BASED ANALYSIS																
Actual Arrivals, Departures/Thruput & Q_b at end of 1st red:		108	21.6	0.0			162	32.4	10.8			135	27.0	5.4		
Actual Arrivals, Departures/Thruput & Q_b at end of last red:		756	151.2	108.0	16.2		810	162.0	118.8	16.2		783	156.6	113.4	16.2	
Actual Arrival & Dep/Thruput For Time Shown:	**Period 1**	648	129.6	108			648	129.6	108			648	129.6	108		
Adjusted Arrivals & Dep/Thruput (15min):		900	180	150			900	180	150			900	180	150		
Adjusted Arrivals & Departures/Thruput (vph):			720	600				720	600				720	600		
Actual Arr, Dep/Thruput & Q_b For Time Shown at end of last red:		1728	300	270	3		1782	307	281	0		1755	303	275	1	
Actual Arrival & Dep/Thruput For Time Shown:		972	148	162			972	145	162			972	147	162		
Adj Arrival & Dep/Thruput (15 min)		900	137	150			900	135	150			900	136	150		
Adj Arrival & Dep/Thruput (vph)			550	600				539	600				544	600		
u & t:	**Period 2**		1.00	0.25				1.00	0.25				1.00	0.25		
Calculated d_3 = 1800Q_b(1+u)t/cT based on actual thruput:						**97**					**97**					**97**
Calculated d_1=0.5C[1-g/C]^2/[1-g/C]:						54					54					54
Period 2 Actual "Control" Delay (d_1 + d_3) in sec:					26084					24797					25580	
Period 2 Actual "Control" Delay (d_1 + d_3) in sec/veh:						**161**					**172**					**162**

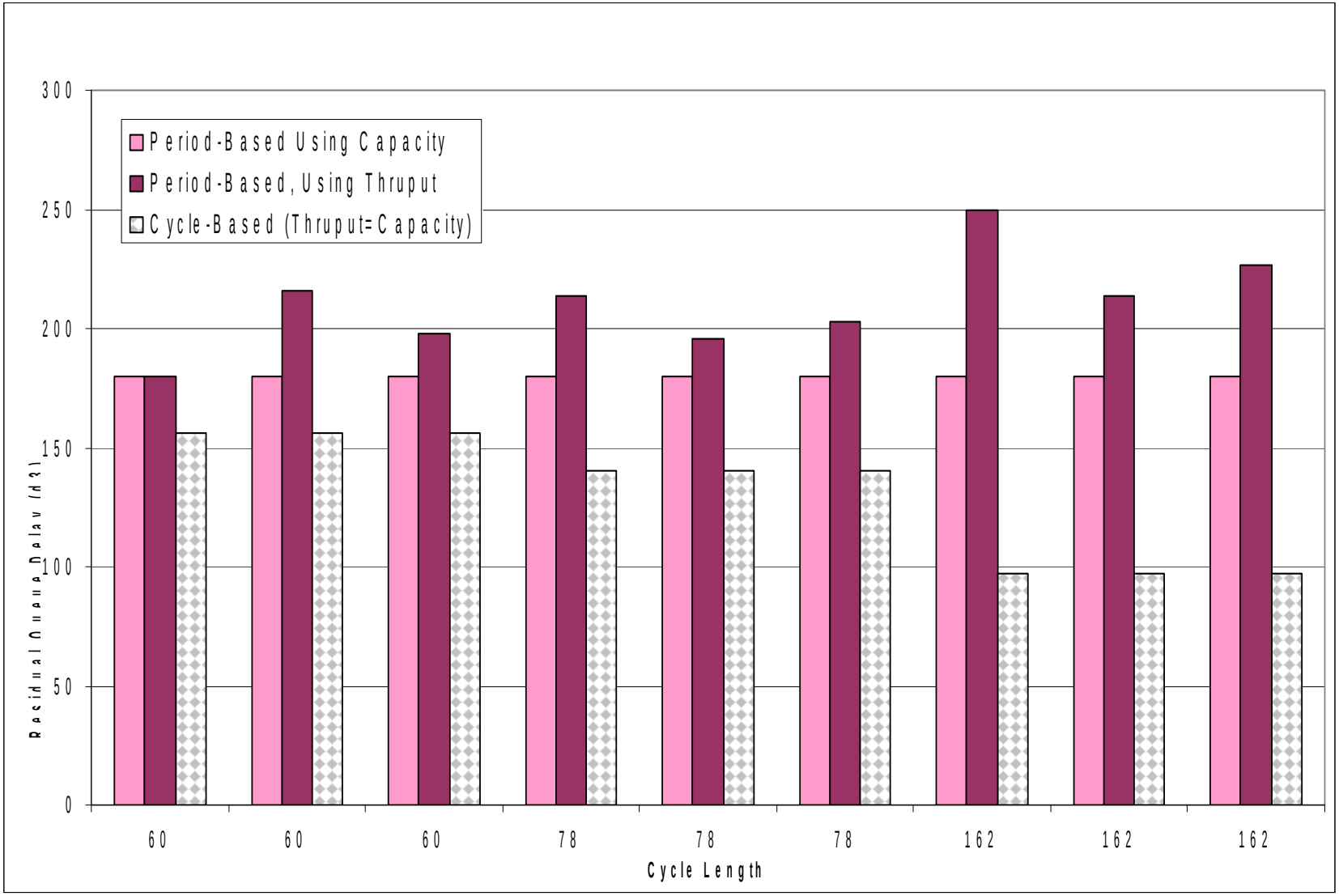

Figure 7-1. Cycle v. period initial queue delay analysis

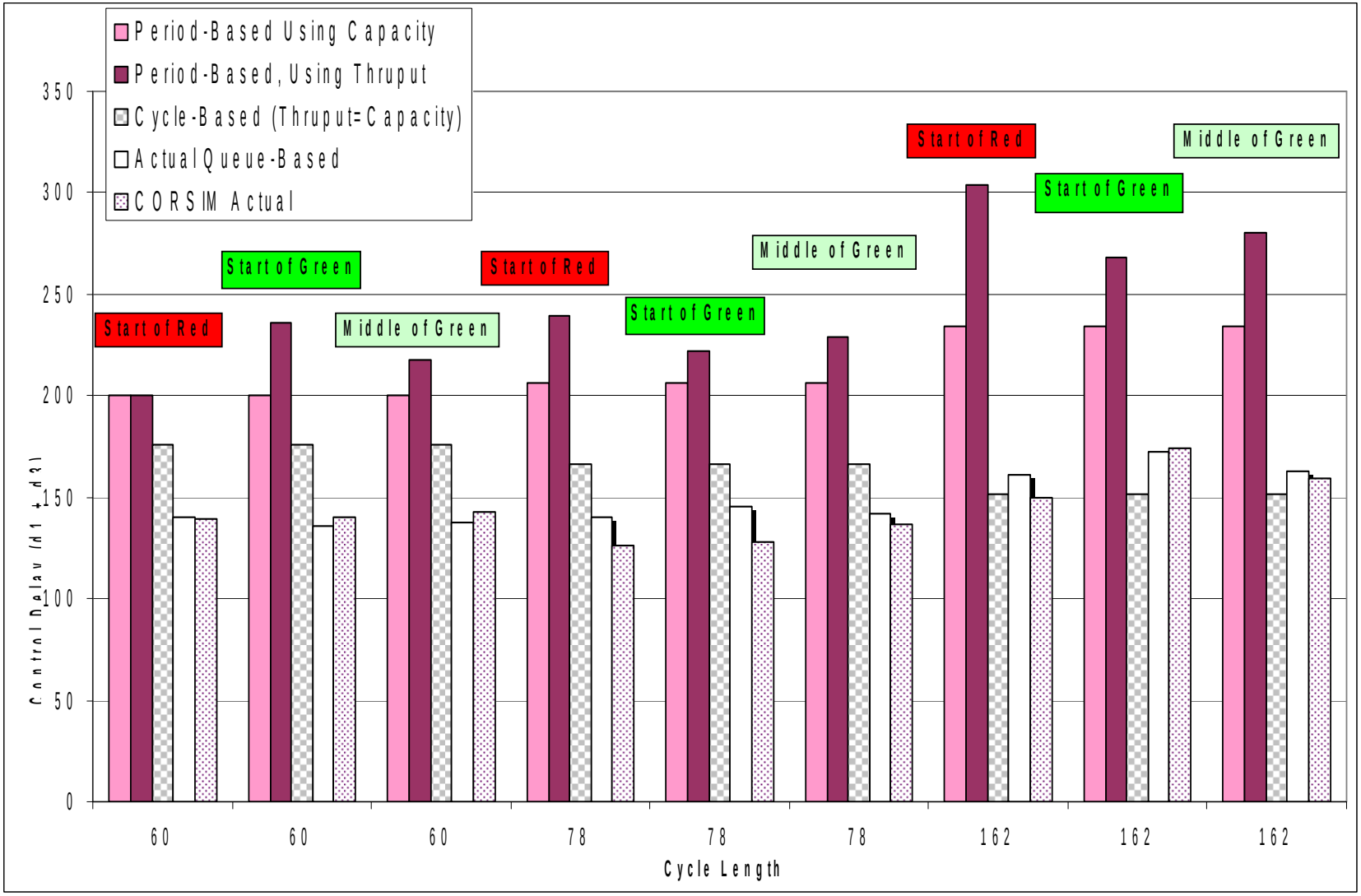

Figure 7-2. Cycle v. period "control delay" analysis

Table 7-3. Detailed example of cycle-period delay discrepancies, residual queue determination

90 sec cycle length Volume Pattern: 690_690_590_345 Random Number Set 3	Time Point	Cumulative Arrivals at BOQ	Cumulative Departures From SB	Arrivals (Volume) Time Period	Arrivals (Volume) Vehicles Arriving at BOQ	Arrivals (Volume) Cycle Basis	Arrivals (Volume) Period Basis	Departures (Capacity) Time Period	Departures (Capacity) Vehicles Departing Stop Bar	Departures (Capacity) Cycle Basis	Departures (Capacity) Period Basis	P Cycle Thruput	Total Caged at EOR	Residual Queue Cycle Basis Var Cap	Residual Queue Period Basis Var Cap	Residual Queue Period Basis Fixed Cap
Start of Period 1	0	0	0											**0**	**0**	**0**
Start of First Full Green	75	**23**	**7**		23				7				**16**			
				810	153	**153**	**178**	**900**	142	**142**	**156**		11			
Start of Last Green in Period 1	885	176	149										**27**			
					2				7							
Start of Period 2	900	178	156												**22**	**31**
				900	5	**175**			9	**157**			18			
End of Last Green (+1s) in Period 1	916	183	165									16	**45**	**11**		
					168		**174**	**900**	141		**157**					
Start of Last Green in Period 2	1785	351	306													
					1				7							
Start of Period 3	1800	352	313												**39**	**57**
				900	1	**151**			7	**153**			-2			
End of Last Green (+1s) in Period 2	1816	353	320									14	**43**	**31**		
					149		**150**	**900**	139		**152**					
Start of Last Green in Period 3	2685	502	459													
					0				6							
Start of Period 4	2700	502	465												**37**	**60**
				869	4	**88**			9	**129**			-41			
End of Last Green (+1s) in Period 3	2716	506	474									15	**2**	**28**		
					84		**94**	**900**	114		**125**					
Start of Last Full Green	3554	590	588													
				13	0	**0**			2	**2**			-2			
End of Last Green	3567	590	590									2	**0**	**0**		
					6				0							
End of Period 4	3600	596	590												**6**	**6**
TOTALS:					**596**	**567**	**596**		**590**	**583**	**590**					
Initial Vehicles Ignored						23				7						
Final Vehicles Ignored						6				0						
						596				**590**						

Table 7-4. Detailed example of cycle-period delay discrepancies, delay comparison

PERIOD	d_3			d_2			d_1			Total Delay (sec/veh)				Cumulative Total Delay (sec/veh)			
	Cycle Basis	Period Basis		Cycle Basis	Period Basis		Cycle Basis	Period Basis		Cycle Basis	Period Basis			Cycle Basis	Period Basis		
	Var Cap	Var Cap	Fixed Cap	Var Cap	Var Cap	Fixed Cap	Var Cap	Var Cap	Fixed Cap	Var Cap	Var Cap	Fixed Cap	Corsim	Var Cap	Var Cap	Fixed Cap	Corsim
1	**0**	0	0	**54**	82	108	**31**	31	31	86	113	140	82	86	113	140	82
2	**69**	126	186	**72**	69	97	**31**	31	31	172	227	315	132	132	169	226	120
3	**173**	225	348	**33**	33	41	**31**	31	31	237	289	420	168	157	205	284	151
4	**64**	155	200	**4**	6	2	**30**	31	31	98	192	233	89	139	203	276	150

Table 7-5. Detailed example of cycle-period delay discrepancies, delay comparison with modified d2 term

PERIOD	d_3		d_2		d_1		Total Delay (sec/veh)			Cumulative Total Delay (sec/veh)		
	Cycle Basis		Cycle Basis		Cycle Basis		Cycle Basis			Cycle Basis		
	Original d_2	Modified d_2	Original d_2	Modified d_2	Original d_2	Modified d_2	Original d_2	Modified d_2	Corsim	Original d_2	Modified d_2	Corsim
1	**0**	0	**54**	54	**31**	31	86	86	82	86	86	82
2	**69**	69	**72**	52	**31**	31	172	152	132	132	121	120
3	**173**	173	**33**	0	**31**	31	237	204	168	157	147	151
4	**64**	64	**4**	1	**30**	30	98	96	89	139	139	150

Table 7-6. Detailed example of cycle-period delay discrepancies, delay comparison with d3 adjustment

PERIOD	d_3	d_2	d_1	Total Delay (sec/veh)		A_{CC} to D_C	Cumulative Total Delay (sec/veh)		
	Cycle Basis	Cycle Basis	Cycle Basis	Cycle Basis		Conversion	Cycle Basis		
	Modified d_2	Modified d_2	Modified d_2	Modified d_2	Corsim	Percentage	Modified d_2	With d3 Adjustment	Corsim
1	**0**	**54**	**31**	**86**	82	108%	**86**	92	82
2	**69**	**52**	**31**	**152**	132	102%	**121**	123	120
3	**173**	**0**	**31**	**204**	168	100%	**147**	147	151
4	**64**	**1**	**30**	**96**	89	99%	**139**	138	150

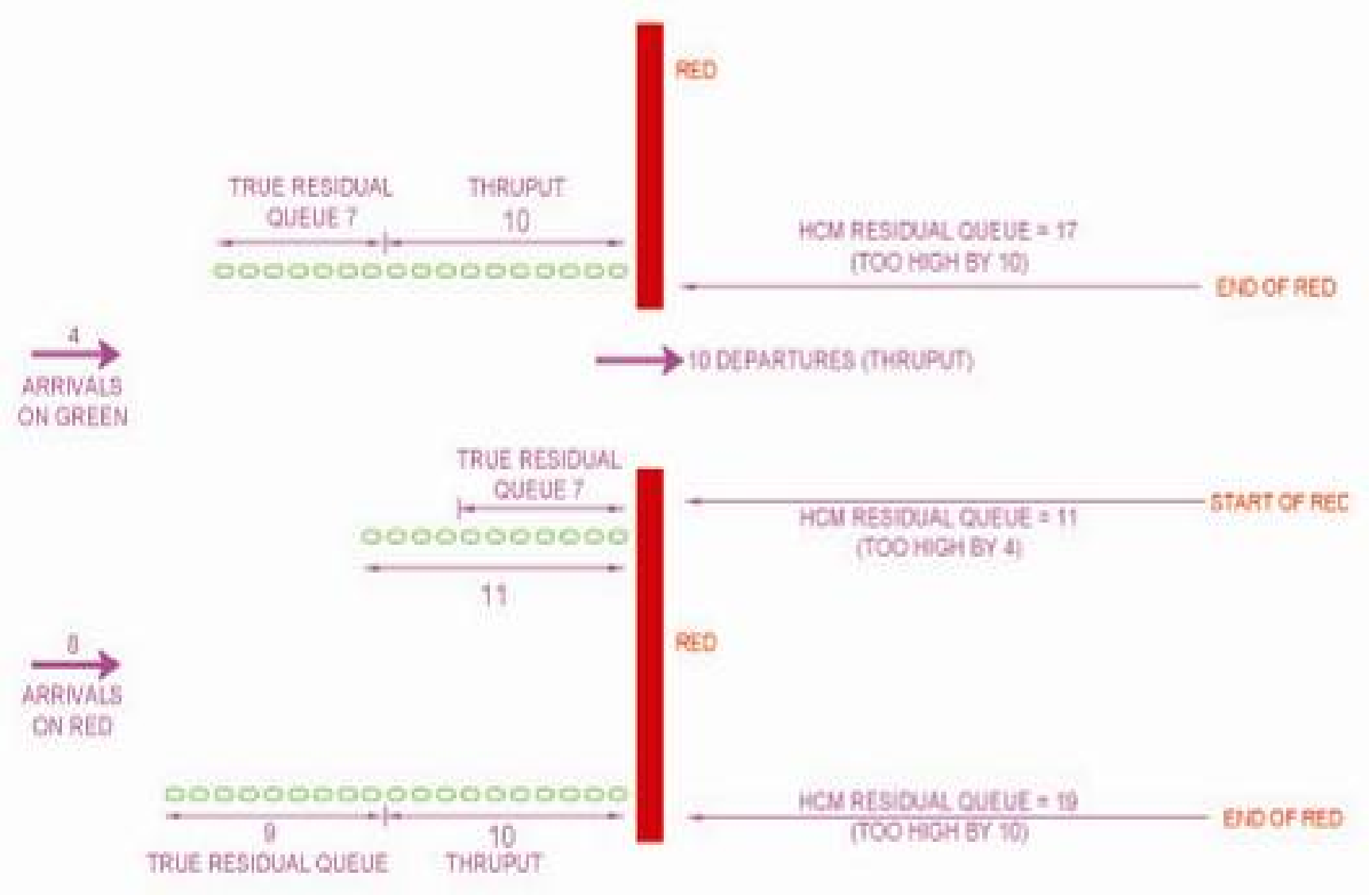

Figure 7-3. Upward bias in HCM residual queue calculation

CHAPTER 8
CONCLUSIONS, APPLICATIONS, AND RECOMMENDATIONS

Conclusions drawn from the research effort, along with potential applications of the real-time delay estimation procedure that was developed as the core element of this research, are presented in this chapter.

Research Findings

The following findings have resulted from the research at hand:

1. The research has demonstrated that it is possible to develop a reasonably accurate real-time procedure for estimating actual stopped delay under conditions of limited information. The procedure developed, which utilizes a series of adjustments to the measured arrival rate entering the field of view to estimate the true arrival rate at the back of the queue, is capable of predicting the unseen component of delay for both under-saturated conditions and over-saturated conditions.

2. The research indicates that there are two important variables for predicted non-visible delay: the number of consecutive cycles during which the end of the queue remains outside the field of view, and the speed at which the queue propagates towards its source.

3. The importance of the queue propagation effect increases as the over-saturated volume-to-capacity ratio increases. At lower over-saturated v/c ratios queue propagation has little effect on the predicted delay but at higher v/c ratios it has a substantial effect.

4. This research demonstrates that it is possible to identify both minimum and maximum cumulative arrival curves for the entire analysis time frame. These curves are established through the use of arrival information obtained at the end of the analysis period when all queues are visible, along with historical minimum peak hour factors.

5. A series of equations are presented which allow these minimum and maximum curves to be calculated for any set of arrival conditions, and for any number of 15-minute analysis periods. The concept of a peak period factor is introduced to handle analysis time frames greater than one hour.

6. Given these minimum and maximum cumulative arrival curves, the research demonstrates that it is possible to calculate a set of theoretical upper and lower bounds on the solution space for overflow delay. A series of equations are presented which allow these bounds to be calculated.

7. The research demonstrates that these theoretical bounds can be used, in an ex post facto manner, to bracket the real-time stopped delay estimation procedure. They can also be used to identify an independent "most probable" arrival pattern by selecting an intermediate curve between the upper and lower bounds that minimizes the maximum percent error between the estimate and the actual delay.

8. This research demonstrates that, contrary to popular belief, the area between the arrival and departure curves is not the delay (either stopped or control) incurred by approaching vehicles. It is rather a mixture of delay and non-delay time elements. Consequently, the Highway Capacity Manual (HCM) assertion that the area between the cumulative arrival curve and the uniform departure curve can be added to the d_1 term and the random portion of the d_2 term to obtain control delay is not quite right.

9. An evaluation of trajectory analysis during over-saturated conditions is used to reconcile the difference between stopped delay and the area between the cumulative arrival and cumulative departure curves. Typical factors for converting cumulative curve delay (overflow delay) into stopped delay are presented.

10. It is demonstrated that the operational definition of an initial (residual) queue as presented in the HCM is not correct. The research shows that, in order to identify the true residual queue on an approach, the situation must be evaluated at the end of the red period for the approach, and the expected thruput during the subsequent green period must be subtracted from the observed "queue". Failure to do so leads to an overestimation of the initial queue and a corresponding overestimation of the initial queue delay.

11. It is shown that, all other things being equal, the degree of delay overestimation stemming from the HCM's improper definition of the residual queue tends to increase as the cycle length increases.

12. It is also shown that, all other things being equal, the degree of overestimation by the HCM is highest during over-saturated periods having v/c ratios slightly above 1.0

13. The 2000 Highway Capacity Manual's multi-period signalized intersection analysis procedure uses a period-based technique for queue accumulation. This technique has certain drawbacks that can produce substantial errors when calculating control delay during over-saturated conditions. The degree of error increases with increasing cycle length. A cycle-based counting technique is proposed to remedy this deficiency.

14. As presented in the 2000 Highway Capacity Manual, the random delay component of the incremental delay term incorrectly contributes to control delay even during over-saturated periods that are preceded by an initial queue. The result is an artificial increase in control delay. The amount of the increase is highest when the random delay component is greatest, which once again occurs at over-saturated v/c ratios close to 1.0 A modification to the d_2 delay term is proposed to remedy this situation.

15. During over-saturated conditions, variability in capacity due to cycle-to-cycle changes in driver aggressiveness is more important with respect to delay than variations in the arrival pattern at the back of the queue. The single hour-long capacity value found in the HCS+ software represents an artificial restriction on capacity variation that contributes to incorrect delay results during congested conditions.

Application of the Research

The major accomplishment of this research was the development of a theoretically constrained delay estimation technique that is based on limited information. Use of the technique to estimate control delay on an over-saturated intersection approach for a one-hour analysis time frame would proceed as follows:

10. Using the vehicle detection equipment for the approach of interest, real-time second-by-second data were collected on the number of vehicles crossing the stop bar, the number of vehicles entering the field of view, the length of the visible queue, and the presence or absence of a stationary vehicle in the last queue position of the field of view.

11. This data set is entered into the BuckQ module of the BuckGO delay estimation software, which measures the length of the visible queue and estimates the length of the non-visible queue at every second of the one-hour analysis time frame. Second-by-second cumulative stopped delay is then calculated using this queue information.

12. The stopped delay prediction is converted by BuckQ to control delay using a series of conversion ratios that vary by cycle length and v/c ratio. The conversion ratio varies between 1.2 and 1.4 with 1.3 being a typical value. The BuckQ predicted control delay is considered the final control delay for use in real-time traffic control.

13. The time during the last 15-minute period at which the end of the queue becomes visible is recorded, as is the cumulative number of vehicles that have crossed the stop bar at that time. At the end of the one-hour analysis time frame, the cumulative number of vehicles that have crossed the stop bar is also recorded. This information is used to calculate the arrival rate during the last 15-minute period.

14. The minimum reasonable Peak Hour Factor (PHF) for the approach and time period in question is obtained from historical traffic counts. The BuckBOUND module of the BuckGO delay estimation software constructs a theoretical set of upper and lower bounds using this minimum PHF and the calculated arrival rate during the last 15-minute period.

15. The BuckCURVE module of the BuckGO delay estimation software then calculates the cumulative curve delay associated with both the upper and lower bounds.

16. The cumulative curve delay is then converted to stopped delay by the application of a correction factor (approximately 0.75).

17. The corrected maximum theoretical stopped delay associated with the upper bound, and the minimum theoretical stopped delay associated with the lower bound, are compared to the predicted stopped delay. If the predicted stopped delay falls outside

of the theoretical bounds during any of the four 15-minute periods, then the predicted delay is appropriately adjusted to remain within the bounds. The resulting "hybrid" stopped delay is considered the final stopped delay prediction. Note that the theoretical bracketing of the predicted stopped delay is carried-out in an ex post facto manner, after the analysis time frame has expired.

18. The hybrid stopped delay results are converted to control delay using a series of conversion ratios that vary by cycle length and v/c ratio. The conversion ratio varies between 1.2 and 1.4 with 1.3 being a typical value. The hybrid control delay is considered the final control delay prediction for project evaluation purposes.

Using this process, the proposed delay estimation technique proves useful for both real-time traffic control and project evaluation.

Three examples are provided to demonstrate how the delay estimation procedure developed in this research might be used in real world applications to improve the results obtained.

Example 1: Signal System Retiming Evaluation

A consultant has been hired to retime 10 traffic signals that are part of a closed-loop system along a busy arterial (SR 4) in Pahokee, Florida. Initial (before) travel time runs are conducted along SR 4 during all analysis periods of interest; including the weekday AM and PM peak periods. New signal timings are developed, implemented, and fine-tuned. Final (after) travel time runs are then conducted along SR 4 during the same periods as the initial runs. All periods show a significant reduction in travel time along SR 4 with implementation of the new timings. Unfortunately, the citizens of Pahokee are not happy with the retiming project so a new consultant is hired to check the work.

It quickly becomes evident to the new consultant that, although traffic flow along SR 4 seems pretty good, side street delay is excessive at many critical locations with repeated phase failures and extensive recurring queues. The new consultant repeats the "after" SR 4 travel time runs, but this time with the BuckGO suite of delay estimation software installed as an add-on to

the closed-loop software. BuckGO is used to measure actual side street stopped delay when queue lengths do not exceed the field of view, and to estimate stopped delay when they do. Appropriate ratios, based on cycle length and v/c ratio, are then applied to the stopped delay values to obtain control delay.

To the pleasure of the citizens of Pahokee, the new consultant reinstalls the initial timings. The "before" travel time runs are then repeated, this time with BuckGO in operation. The new consultant obtains almost exactly the same "before" and "after" travel time results along SR 4 as the original consultant; the improvement along SR 4 was indeed real. However, after reviewing the BuckGO results, the new consultant realizes that side street delay skyrocketed when the new timings were installed.

Example 2: Real-Time Traffic Signal Control

A real-time adaptive traffic signal control program has been installed at the "T" intersection of Main Street and Elm Street in Clewiston, Florida. The adaptive software uses volume information obtained from upstream inductance loop detectors to optimize signal timings at this isolated signal. Unfortunately, the local traffic engineer has received numerous citizen complaints that not enough green time is being provided to the side street approach during peak periods. The engineer investigates and determines that multiple cycle failures and recurring queues occur on the side street during the weekday PM peak hour. The engineer calls in a consultant for assistance.

The consultant reviews the situation and determines that, during the PM peak hour, side street queues extend well past the upstream inductance loop, which is located a healthy 400 feet from the stop bar. Because of this, the loop is not counting the true demand on the approach and is, therefore, not allocating green time based on a delay determination that is derived from the true arrival rate.

The consultant addresses the problem by adding the BuckGO module to the adaptive software. When queues extend beyond the upstream loop, BuckGO estimates the true (higher) arrival rate and associated (greater) delay based on the number of adjacent blind periods that occur. This improved estimate of delay results in a reallocation of green time that greatly reduces the extent and duration of the recurring side street queues. Complaints from the citizens of Clewiston concerning the signal timing at this intersection disappear.

Example 3: Signalized Intersection Capacity Analysis

A traffic engineer would like to determine the delay on various approaches to an existing signalized intersection that is experiencing severe congestion. However, the queues are so long on some of the approaches (over 1/2 mile), and build so rapidly, that counting arriving vehicles is virtually impossible. The engineer is smart enough to know that merely counting vehicles crossing the stop bar will not produce a true picture of delay since these counts do not measure the true demand on the approach, only the supply. The engineer, once again, calls in a consultant for assistance.

The consultant reviews the situation and determines that BuckQ could be used to estimate the arriving volume on the over-saturated approaches. The appropriate 15-minute count data are collected and, for the under-saturated, near-saturated, and slightly over-saturated movements, a multi-period analysis based on HCM principals is conducted to determine approach control delay. However, for the grossly over-saturated movements, BuckGO is used.

Potential Areas of Extended Research

The following areas of additional research have been identified:

1. **Extension of the procedure to examine other cycle lengths and other fields of view** – Although preliminary analyses were made that involved three cycle lengths (80, 120 and 160 seconds) and two fields of view (8 and 12), the final detailed analysis included only one cycle length (120 seconds) and one field of view (12). It would be of interest to expand the range for both of these important items to quantify their effect. In addition,

the g/C ratio was held constant at about 0.30 Varying this value and examining the results would also be of interest.

2. **Investigation of other methods for adjusting the arrival rate during adjacent blind periods** – Although it appears to work rather well over the range of simulation conditions investigated in this dissertation, the use of a power function based on the number of adjacent blind periods is only one of many possible methods for adjusting the arrival rate at the back of the queue. Other options could be investigated, including the use of a logarithmic function instead of a power function, or the use of the length of the adjacent blind period in seconds as the input to the function rather than the number of adjacent blind periods. We could also develop logic that would ignore any isolated break in the number of vehicles entering the field of view when determining whether or not the non-visible queue had dissipated. This would eliminate false termination of the blind period due to "sleepers", queued motorists who failed to advance into the field of view in a timely manner due to some distraction.

3. **Accounting for the effect of trucks in the traffic stream** – Trucks have a twofold effect on queue formation and discharge: 1.) They have a discharge headway that is greater than that of passenger cars (CORSIM assumes 120%), and 2.) They are longer than passenger cars, which causes fewer vehicles to be observable within a given field of view. Also, as both Tarko [29] and Cohen [31] discovered, in the real world trucks have a third effect on queue formation and discharge, their presence lengthens the headways of passenger cars in the traffic stream. All of these effects could be examined in future work, especially as they relate to our choice of a 5 second headway for re-setting the non-visible queue to zero.

4. **Accounting for the effect of arrival type** – Vehicles typically arrive at an approach in one of three basic ways: 1. They arrive randomly, 2. They arrive in platoons that reach the approach at the same time every cycle (since the approach is "fed" by an upstream signal with an equivalent cycle length), or 3. They arrive in platoons that reach the approach at different times during the cycle (since the approach is "fed" by an upstream signal with a different cycle length). The sensitivity of our delay estimation procedure to arrival type is another fertile area for future simulation-based research.

5. **Accounting for the effect of multiple approach lanes** – The queue arrival and discharge situation is complicated when lane-changes can occur, as is the case for side streets with multiple approach lanes. Modifying the delay estimation procedure to handle queue accumulation under such conditions would be of practical benefit.

6. **Accounting for the effect of queue mixing** – Vehicle queues often mix together on an approach under high-volume or over-saturated conditions. For example, it is not uncommon for queues from a left turn lane to spillback into the adjacent thru lane during peak periods. This mixing of queues offers a particularly challenging problem if one desires to apportion delay by movement, rather than by approach.

7. **Field application of the delay estimation procedure** – Application of the delay estimation procedure described in this document to an intersection approach would probably be the most enlightening extension to the research. The logical place to start would be with the simplest possible case, a single lane approach where left turns are not permitted (such as in a downtown area) having very few trucks and random arrivals. During our research efforts, some time was spent experimenting with video taken on a multi-lane main street approach in Gainesville, Florida and on a multi-lane side street approach in Jacksonville, Florida. Work was begun on a software program for producing queue length and count information from the video. This is a challenging endeavor in and of itself given the peculiarities of video detection.

8. **Development of additional examples** – In order to illustrate the calculation of the theoretical upper and lower bounds, and associated overflow delay, for the 5-period and n-period cases, additional examples could be developed.

9. **Use of other measures of effectiveness (MOE)** – It may be that other MOEs besides delay are of interest when evaluating intersection performance. Such MOEs might include variables mentioned in this document, including: predicted queue length, predicted back-of-queue position, number of phase failures, number of vehicle re-queues, number of adjacent blind periods, or percent of time that the queue is not visible. Or they might involve totally new variables. A 2004 paper by Zhang and Prevedouros [51], which was based on a web-survey with 2017 responses, suggests that "waiting time" (a.k.a. "delay") is not as important to motorists as other factors. These factors include: traffic signal responsiveness (related to the delay when no vehicles are present on conflicting movements), extent of phase failures, availability of left turn lanes and phasing, and pavement quality. In addition, as discussed by Tarnoff and Ordonez [1], the use of alternative MOEs may be particularly appropriate when over-saturated conditions prevail:

   "*When saturation exists, different measures of effectiveness should be used for evaluating system performance. During under-saturated conditions, stops and delays are the MOEs typically used. When saturated conditions exist, the objective is to minimize the time period during which these conditions exist, and the MOEs in use include queue lengths, number of cycle failures and the percent of time that intersections are congested. This is accomplished by controlling the direction of queue build-up to avoid spillback and minimize cycle failures.*"

10. **Use of other simulation programs** - If may prove beneficial to make use of a second simulation program (such as SYNCHRO/SIMTRAFFIC, VISSIM, PARAMICS or AIMSUN) to check the results obtained with CORSIM and to make use of features inherent in these programs that may be superior to those in CORSIM. For example, when dealing with a multiple lane approach, CORSIM often has the first few vehicles in the queue starting simultaneously, which is quite a deviation from reality.

11. **Closely spaced intersections** – The usefulness of any procedure that is developed would be enhanced if it could be applied to closely spaced intersections, including those that occur in the vicinity of freeway ramp terminals.

12. **Arterial evaluation -** The procedures developed in this research should prove useful for arterial evaluation, at least as far as side street approach delay and delay in the main street left turn lane are concerned. The value of the procedures would be maximized where significant periods of over-saturated operation occur. Consequently, integrating the results of this research into a larger arterial evaluation tool would be of interest.

13. **Development of an automated delay estimation module** - Finally, the ultimate extension of this research would be the development of a closed-loop or traffic signal controller module that would automate the delay estimation procedure. The module would provide real-time delay estimation, even during over-saturated conditions, and would apply ex post facto delay adjustments once queues have cleared. The module night be patented and marketed to both traffic signal controller manufacturers and traffic signal software development firms.

APPENDIX A
DATA SETS FOR BUCKQ TESTING

CORSIM 5.1

216 Total Runs

12 volume levels

3 random number sets per volume level

3 cycle lengths

2 fields of view

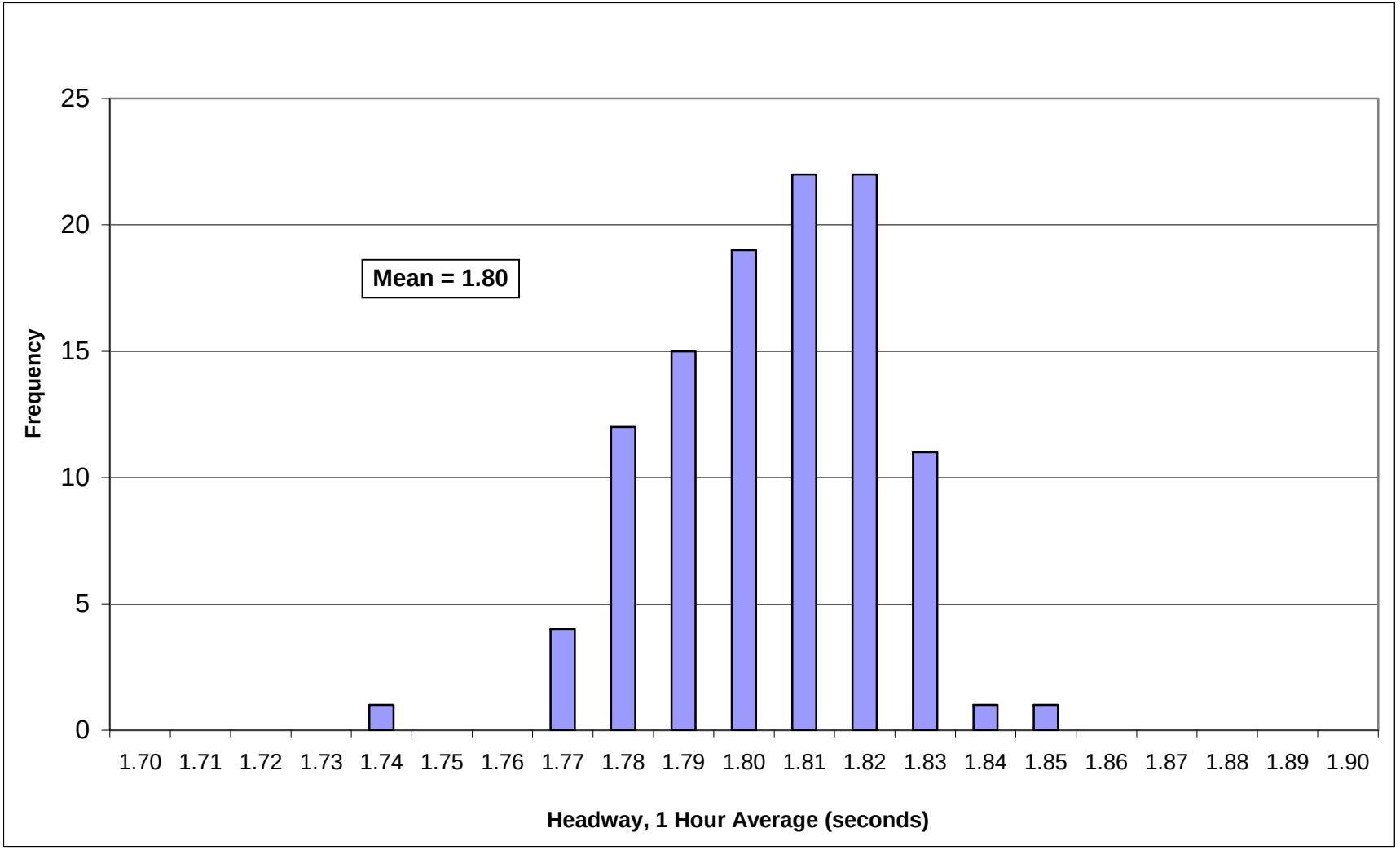

Figure A-1. Queue discharge headway histogram

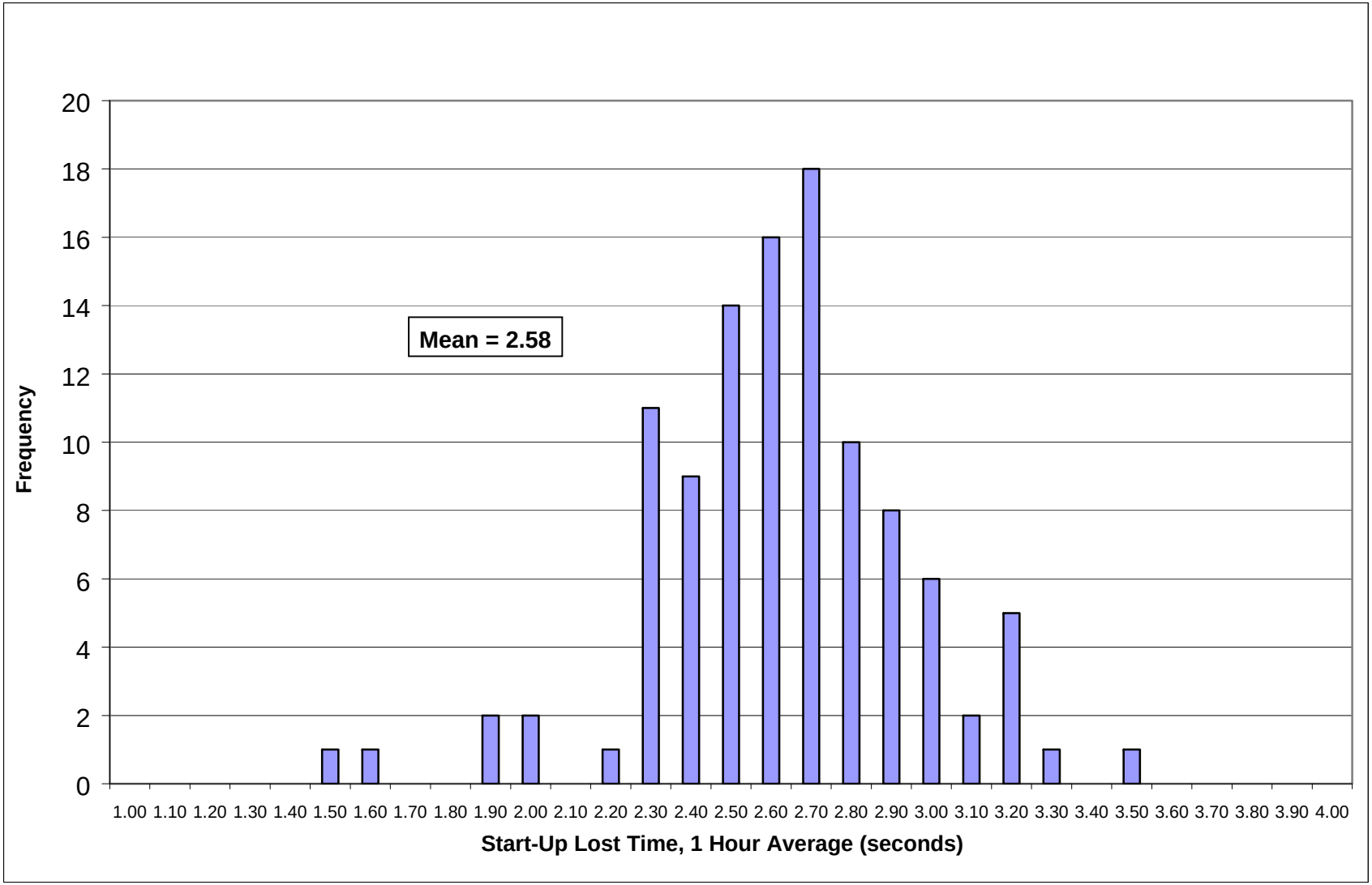

Figure A-2. Start-up lost time histogram

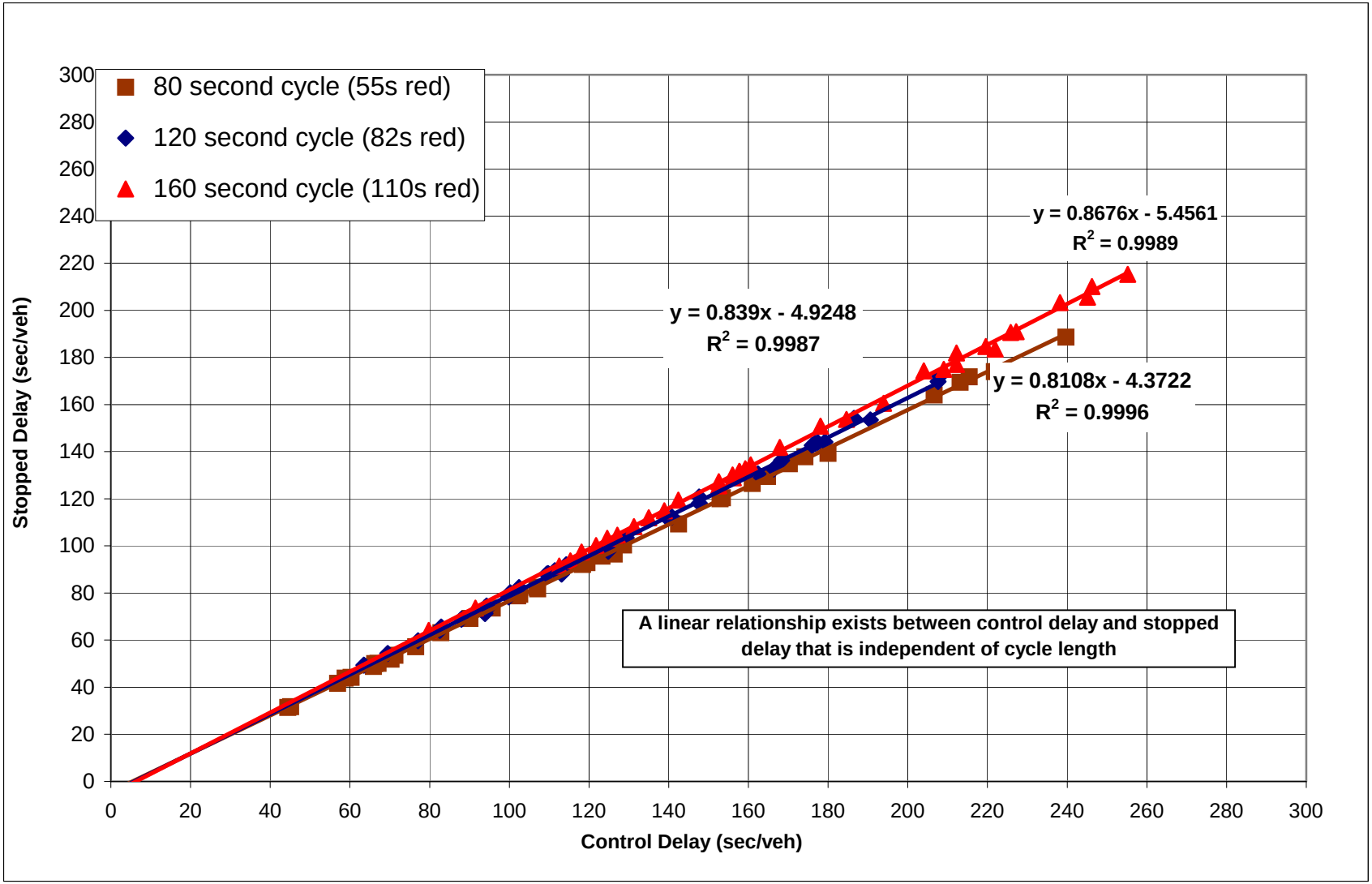

Figure A-3. Comparison of control delay and stopped delay by cycle length (g/C =0.30)

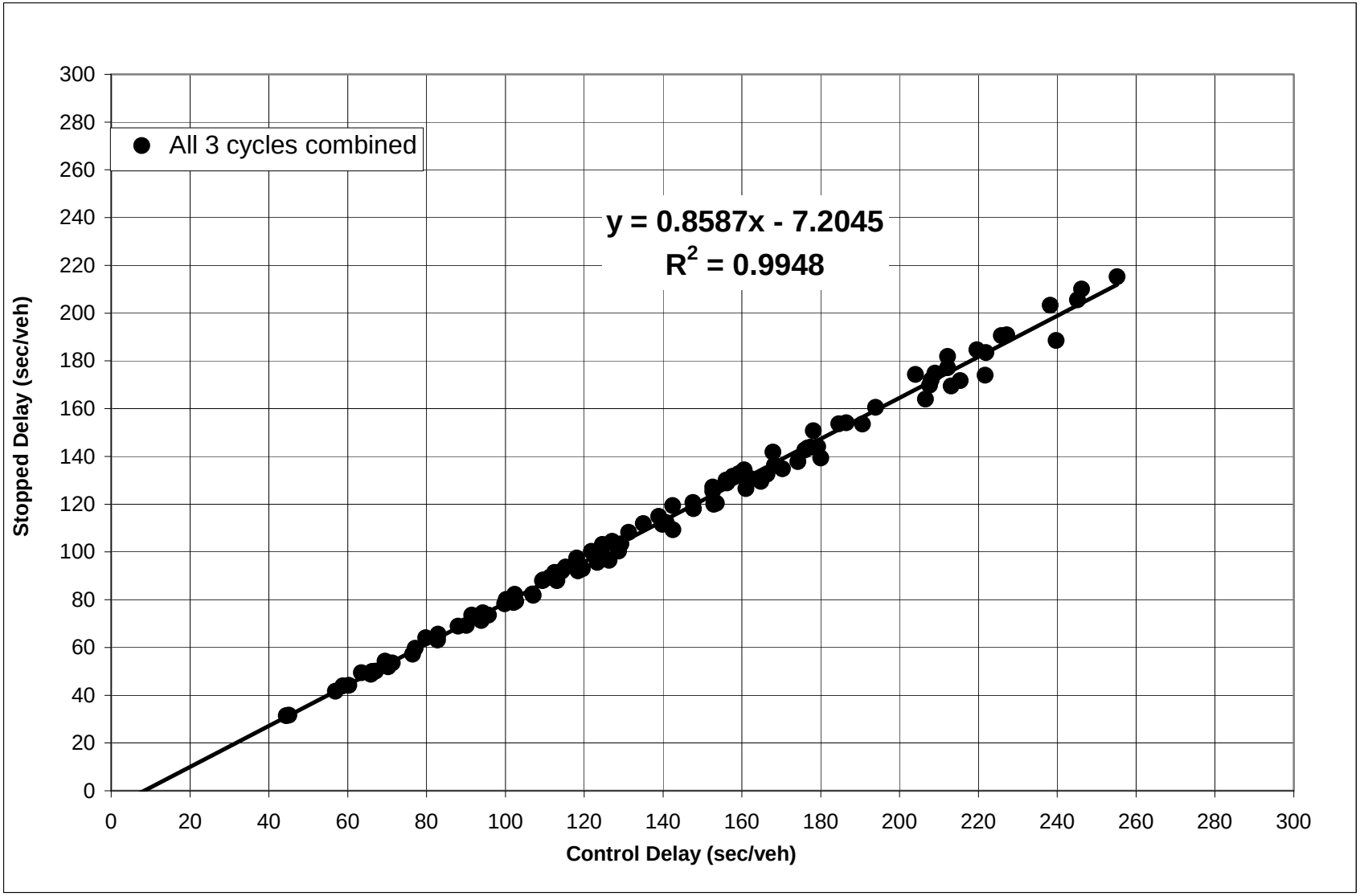

Figure A-4. Comparison of control delay and stopped delay (g/C =0.30)

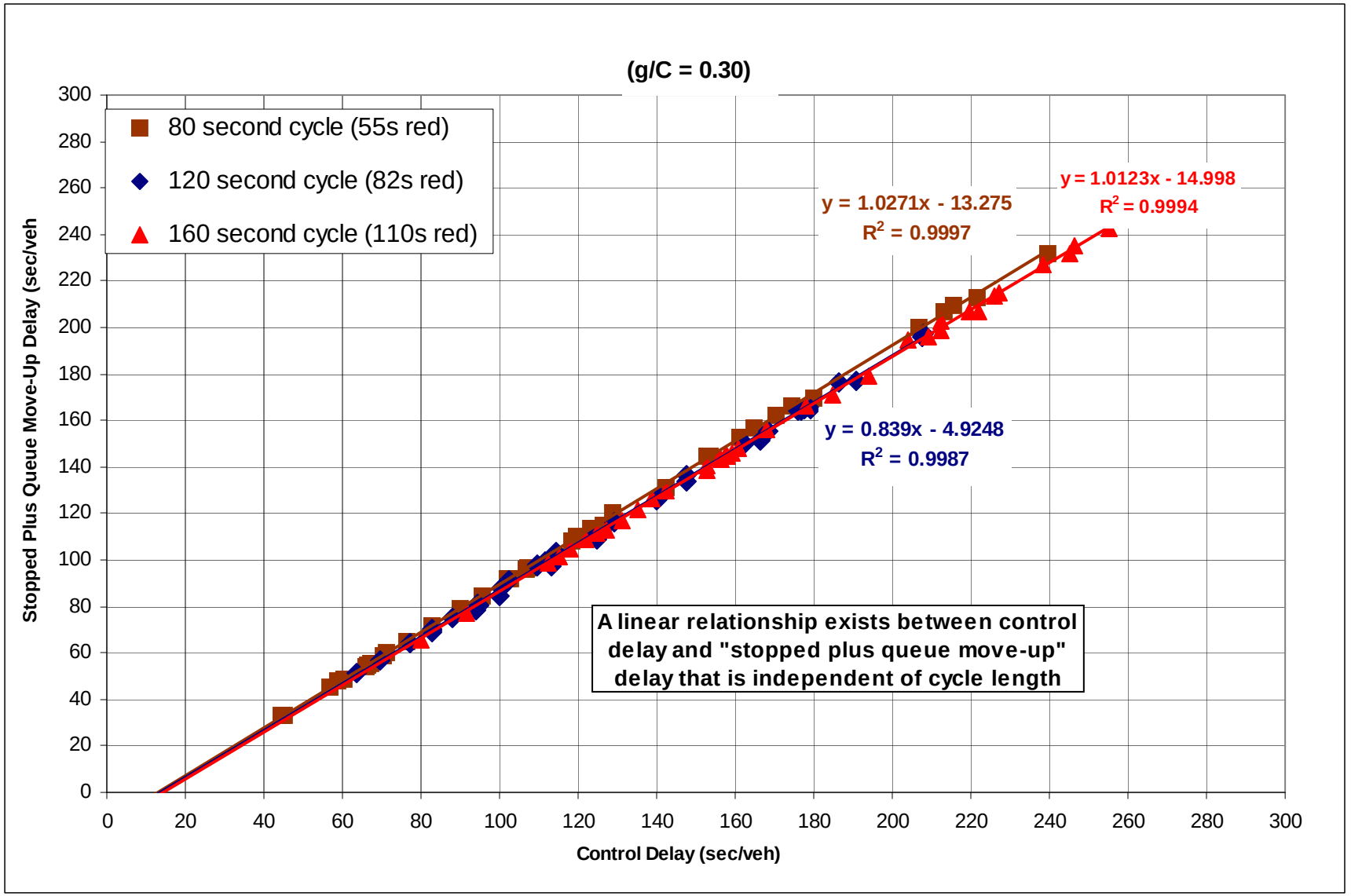

Figure A-5. Comparison of control delay and stopped plus queue move-up delay by cycle length (g/C = 0.30)

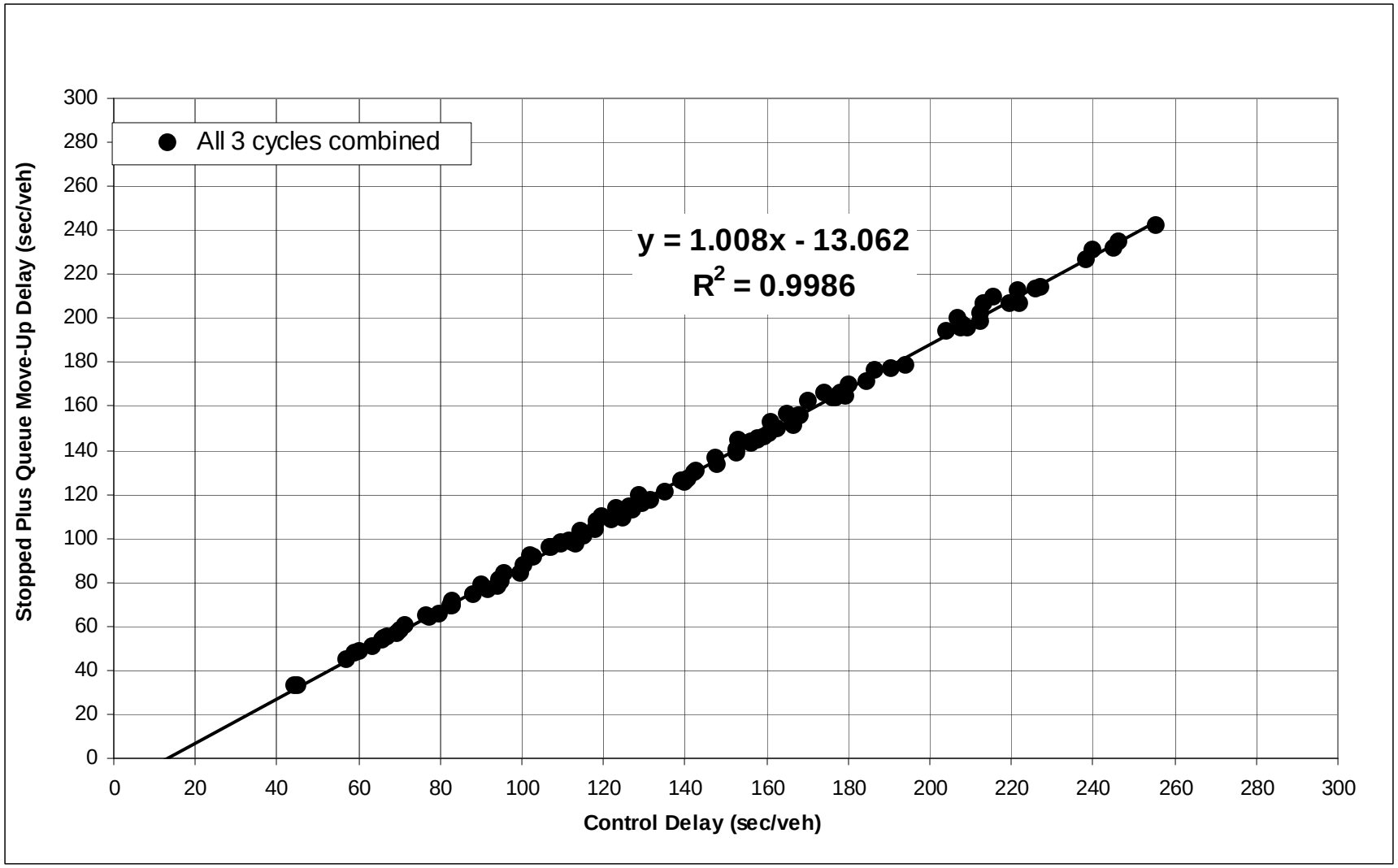

Figure A-6. Comparison of control delay and stopped delay plus queue move-up delay (g/C =0.30)

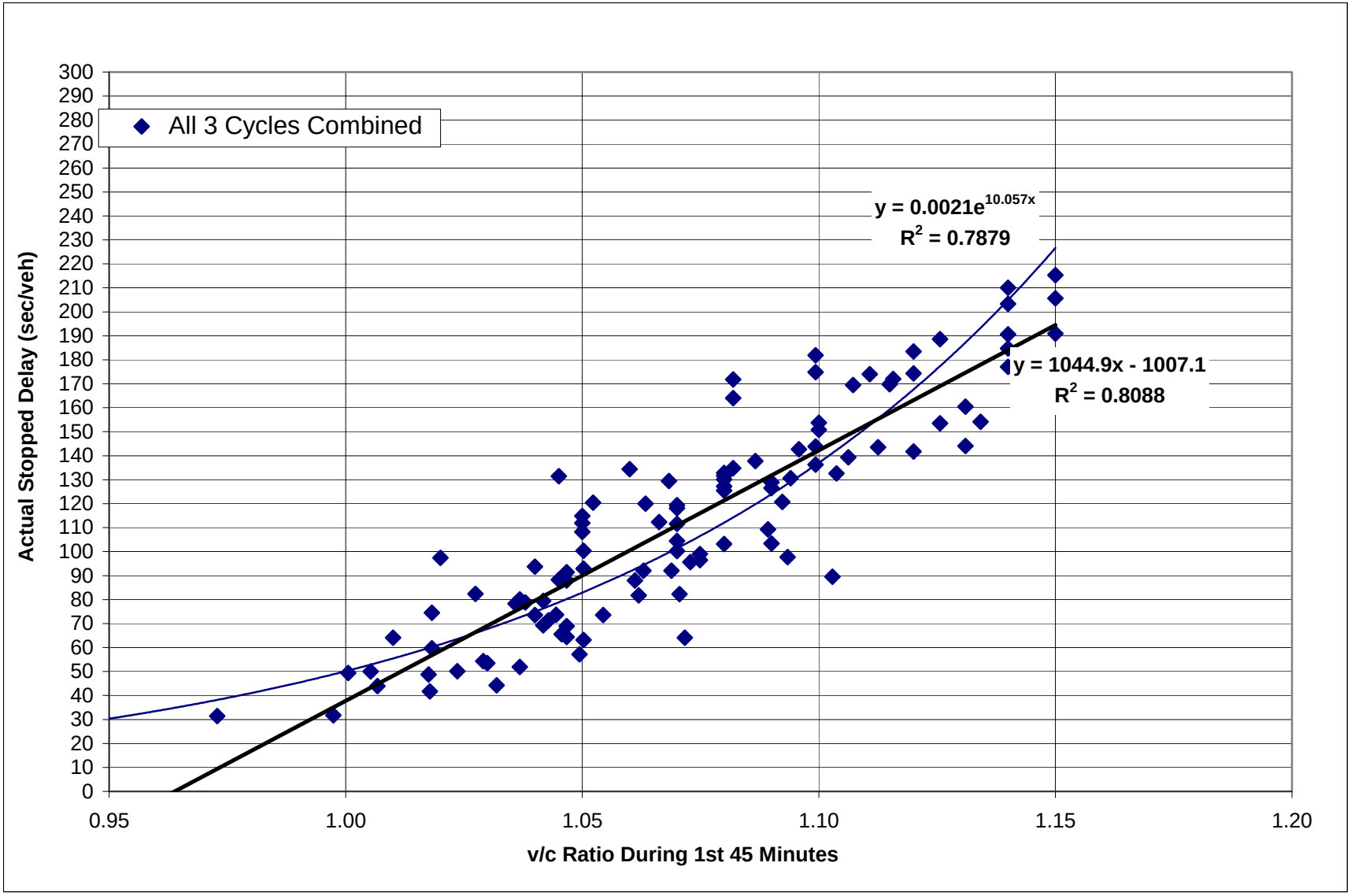

Figure A-7. Relationship between v/c ratio and stopped delay

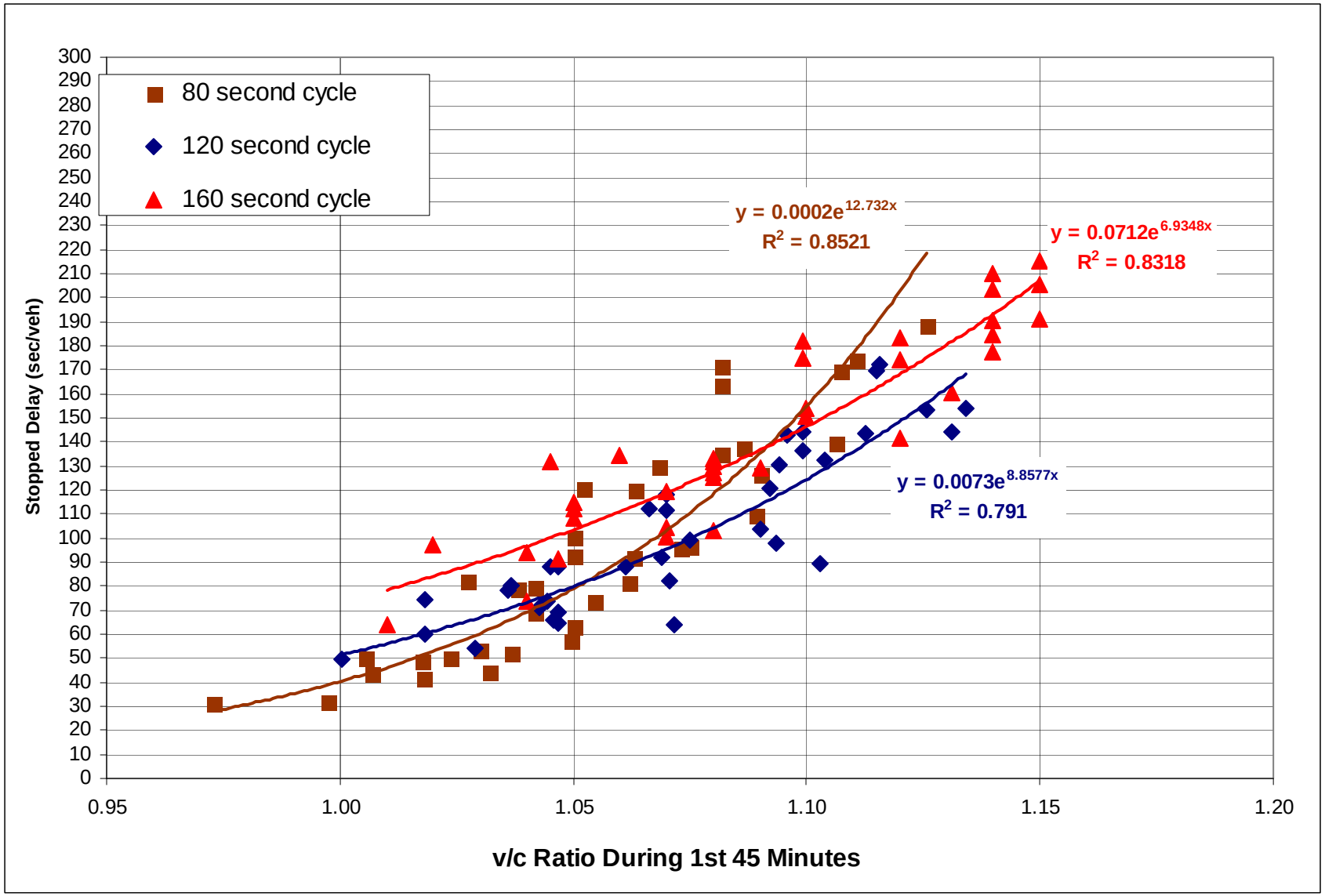

Figure A-8. Relationship between v/c ratio and stopped delay by cycle length

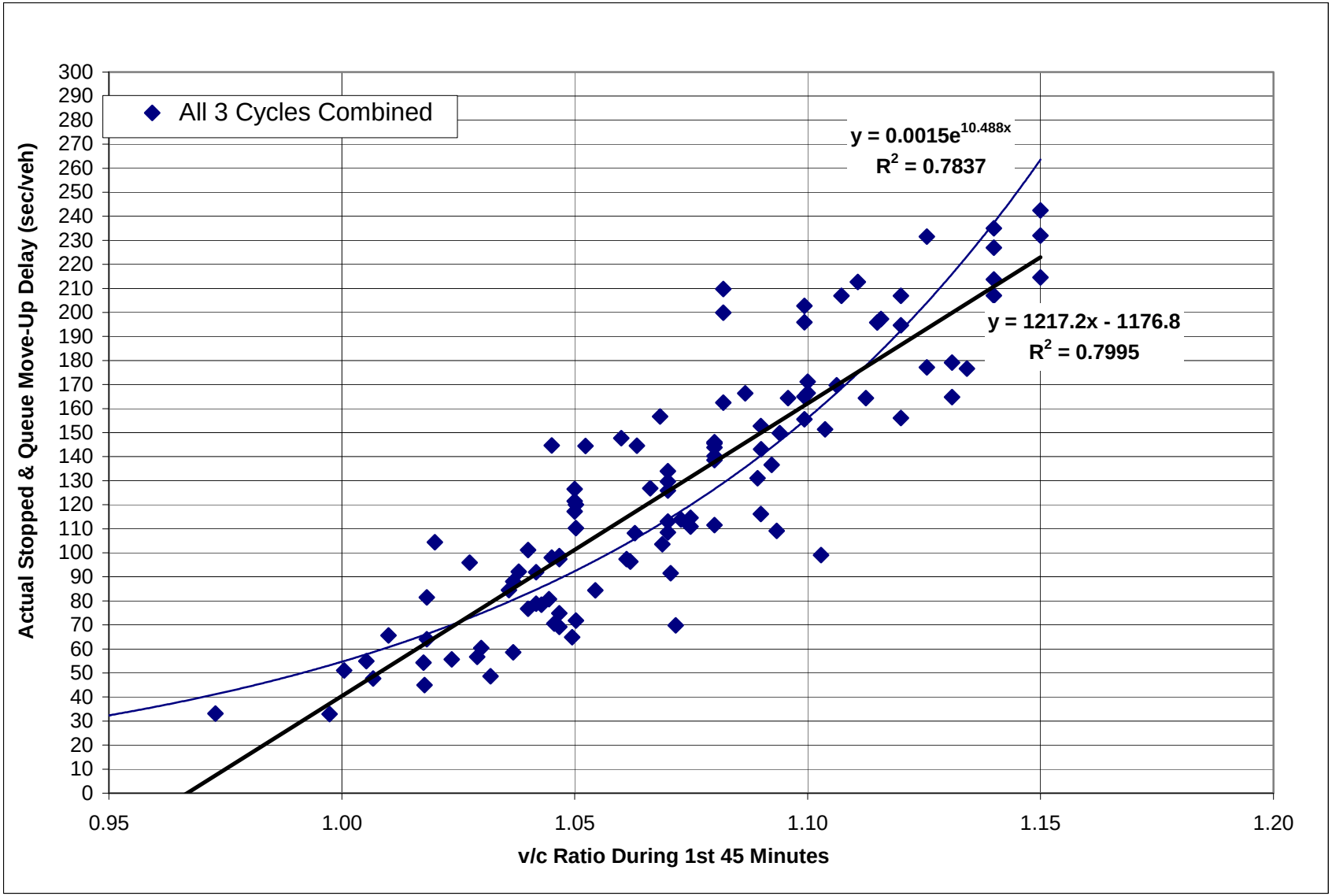

Figure A-9. Relationship between v/c ratio and stopped plus queue move-up delay

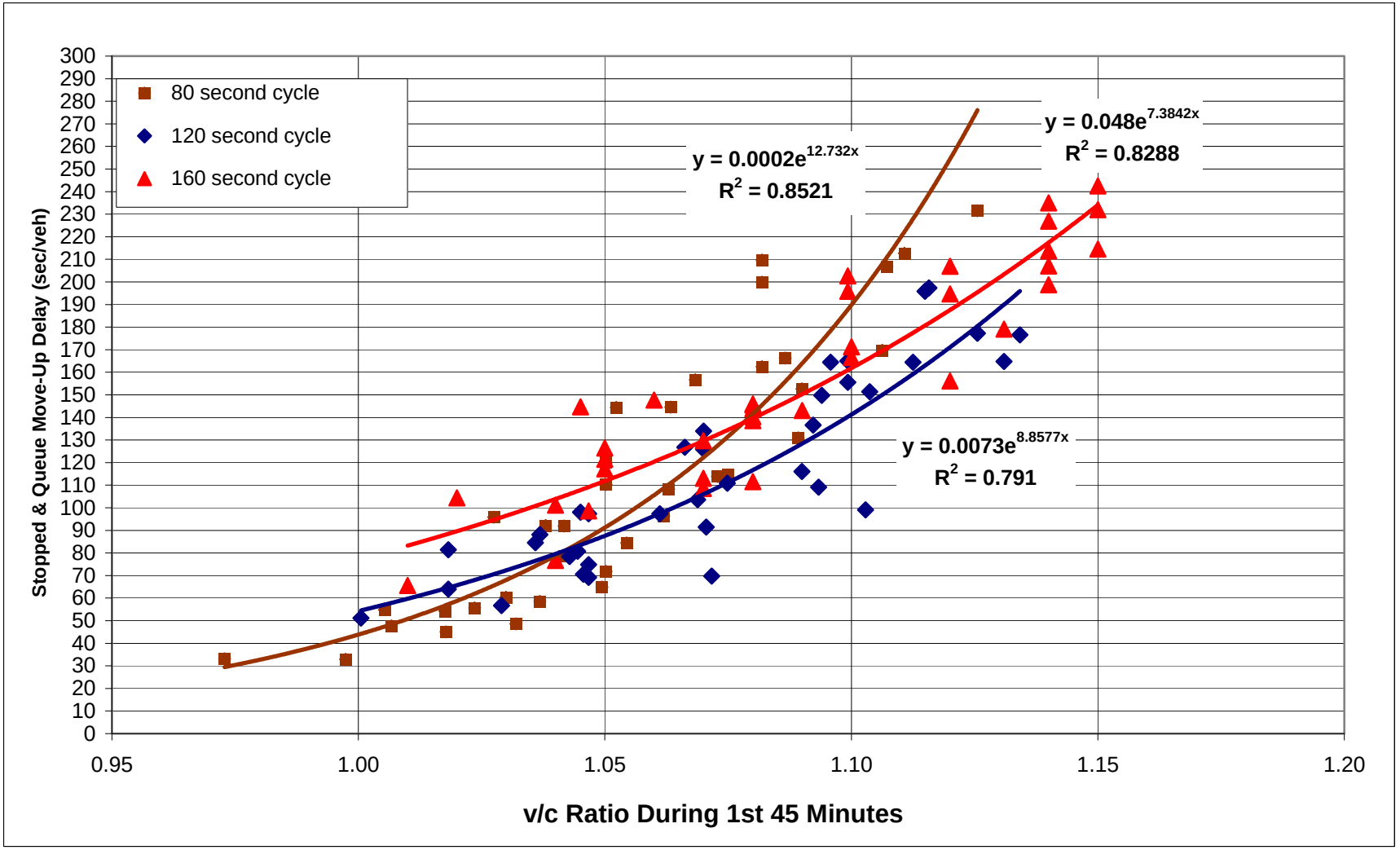

Figure A-10. Relationship between v/c ratio and stopped plus queue move-up delay by cycle length

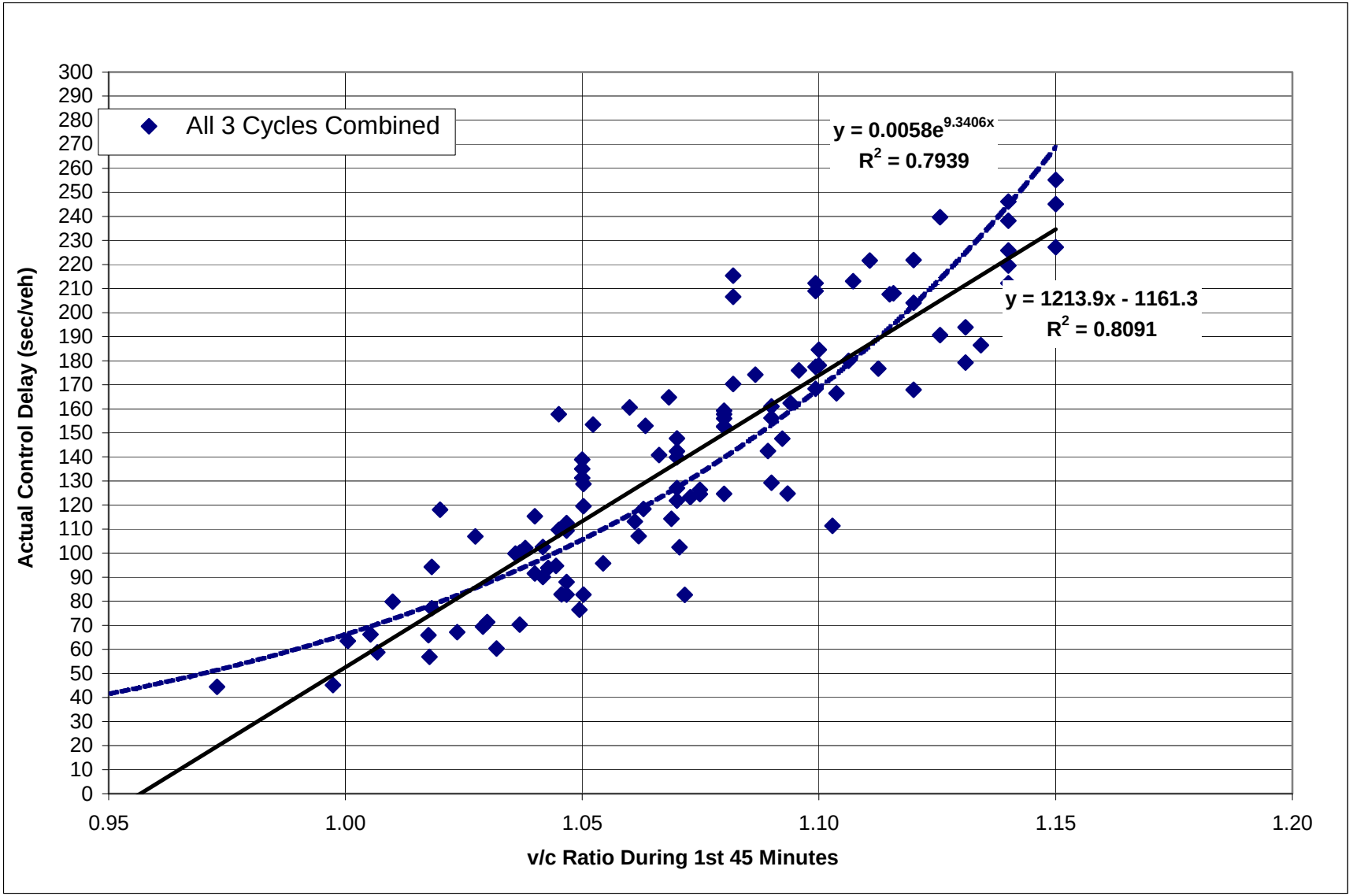

Figure A-11. Relationship between v/c ratio and control delay

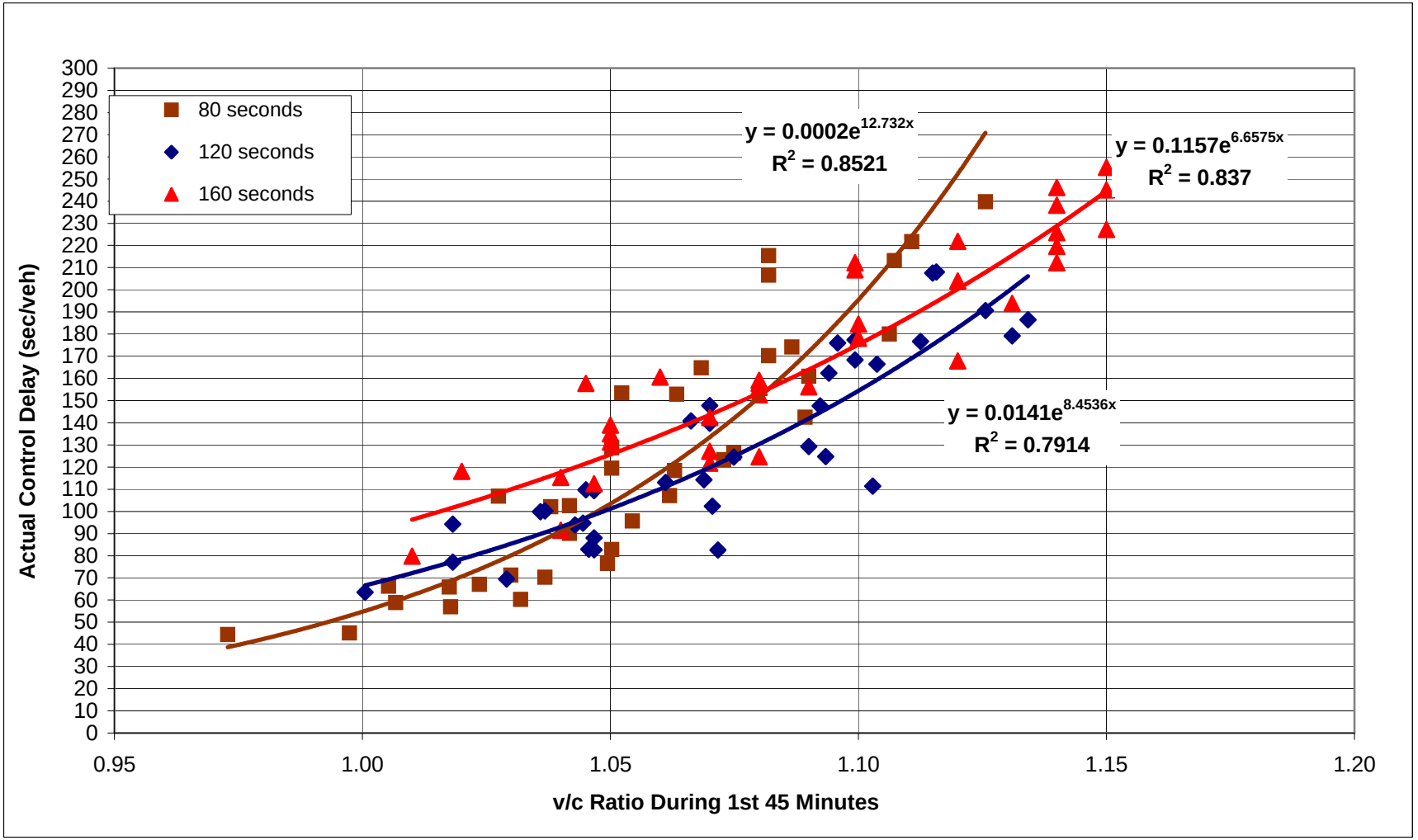

Figure A-12. Relationship between v/c ratio and control delay by cycle length

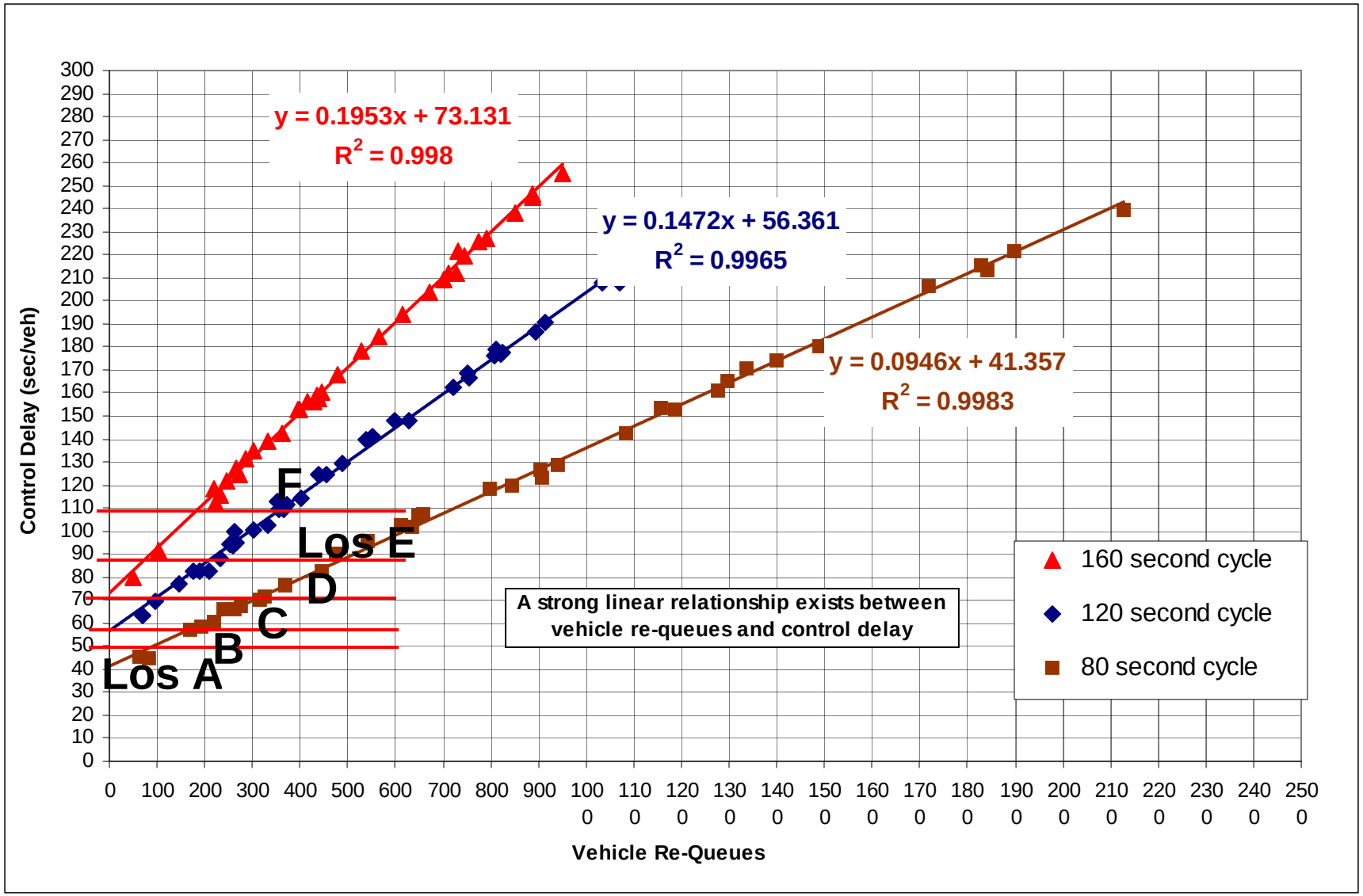

Figure A-13. Relationship between vehicle re-queues and control delay

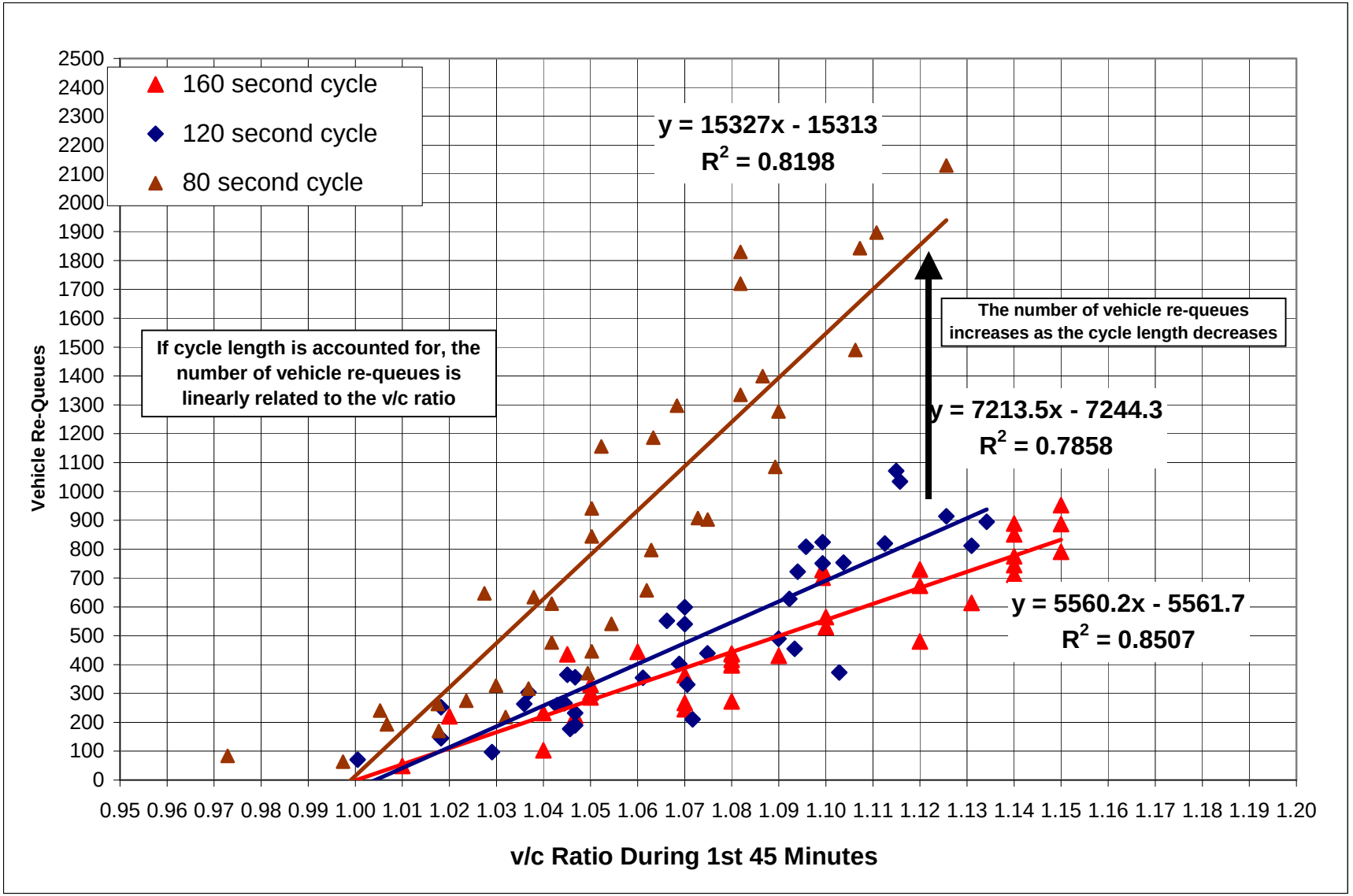

Figure A-14. Relationship between v/c ratio and vehicle re-queues

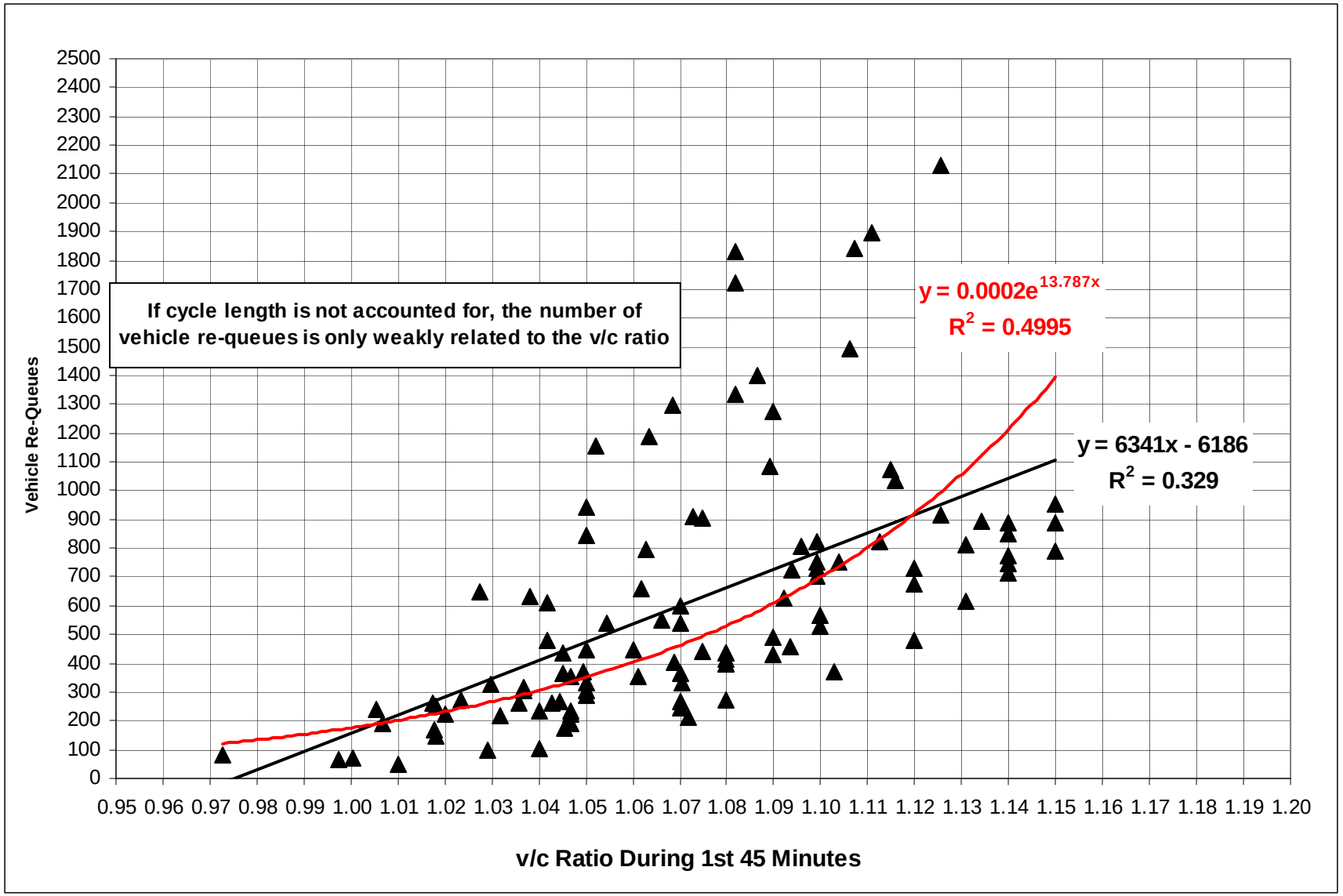

Figure A-15. Relationship between v/c ratio and vehicle re-queues by cycle length

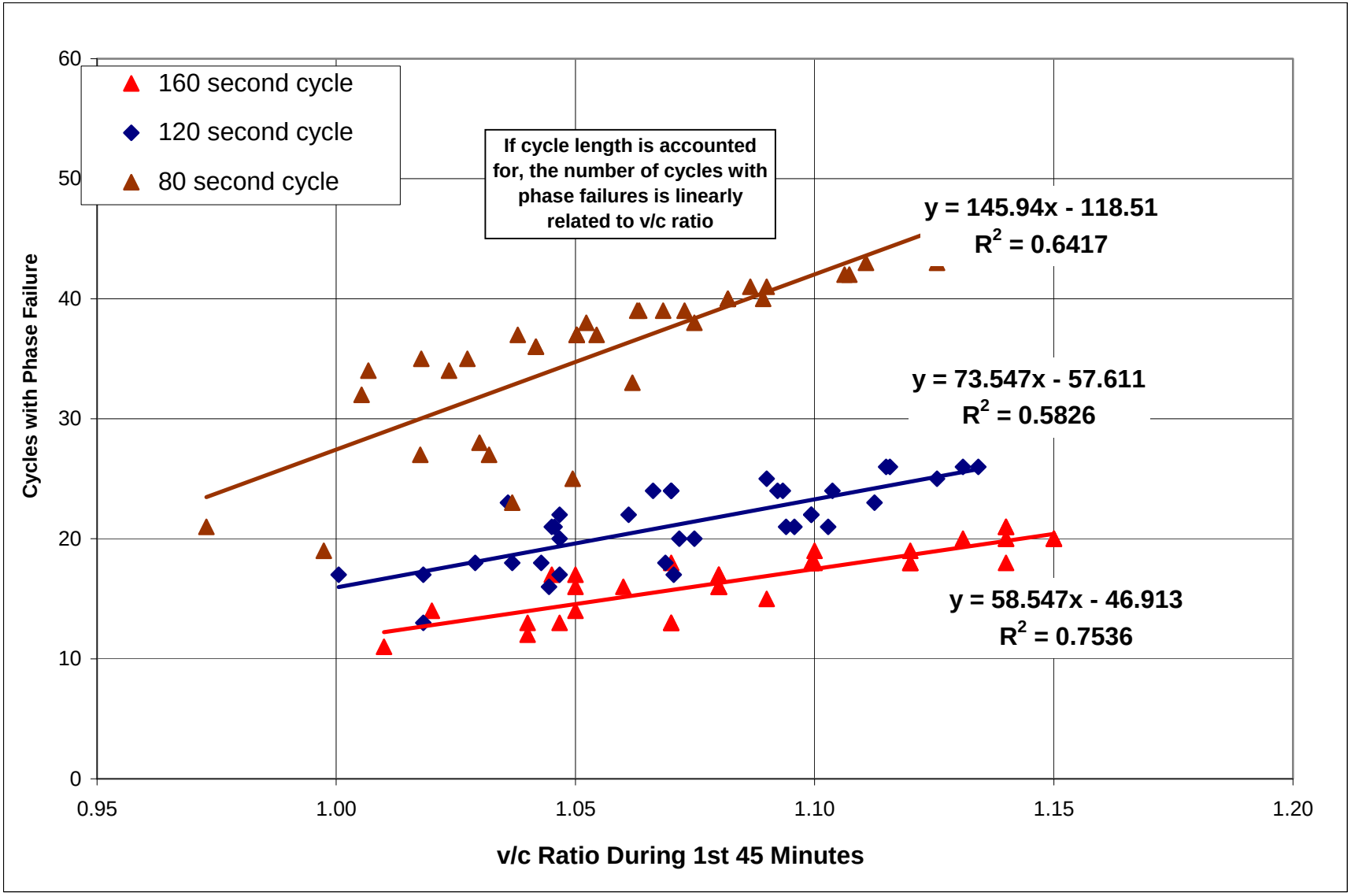

Figure A-16. Relationship between v/c ratio and cycles with phase failure

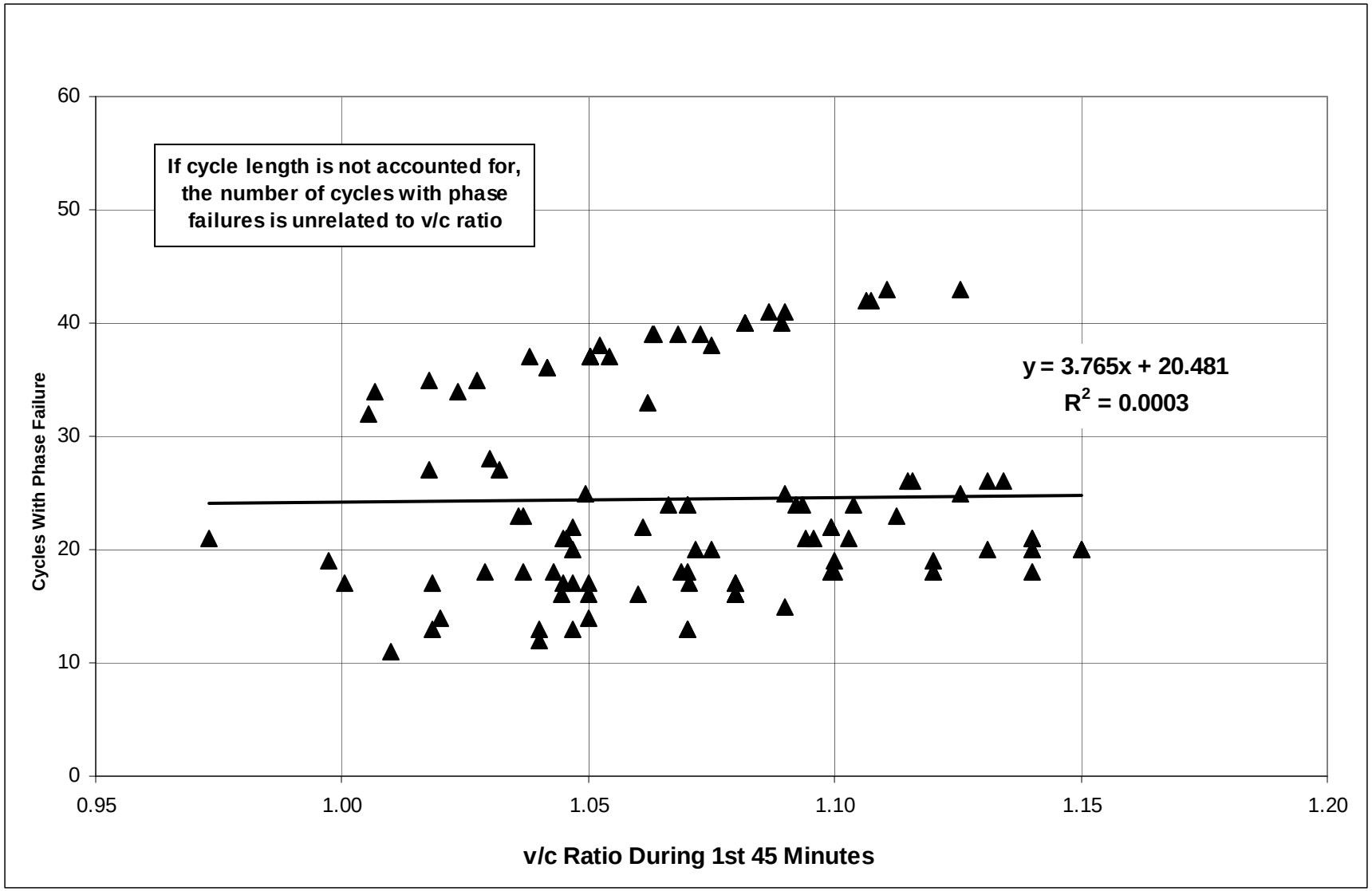

Figure A-17. Relationship between v/c ratio and cycles with phase failure by cycle length

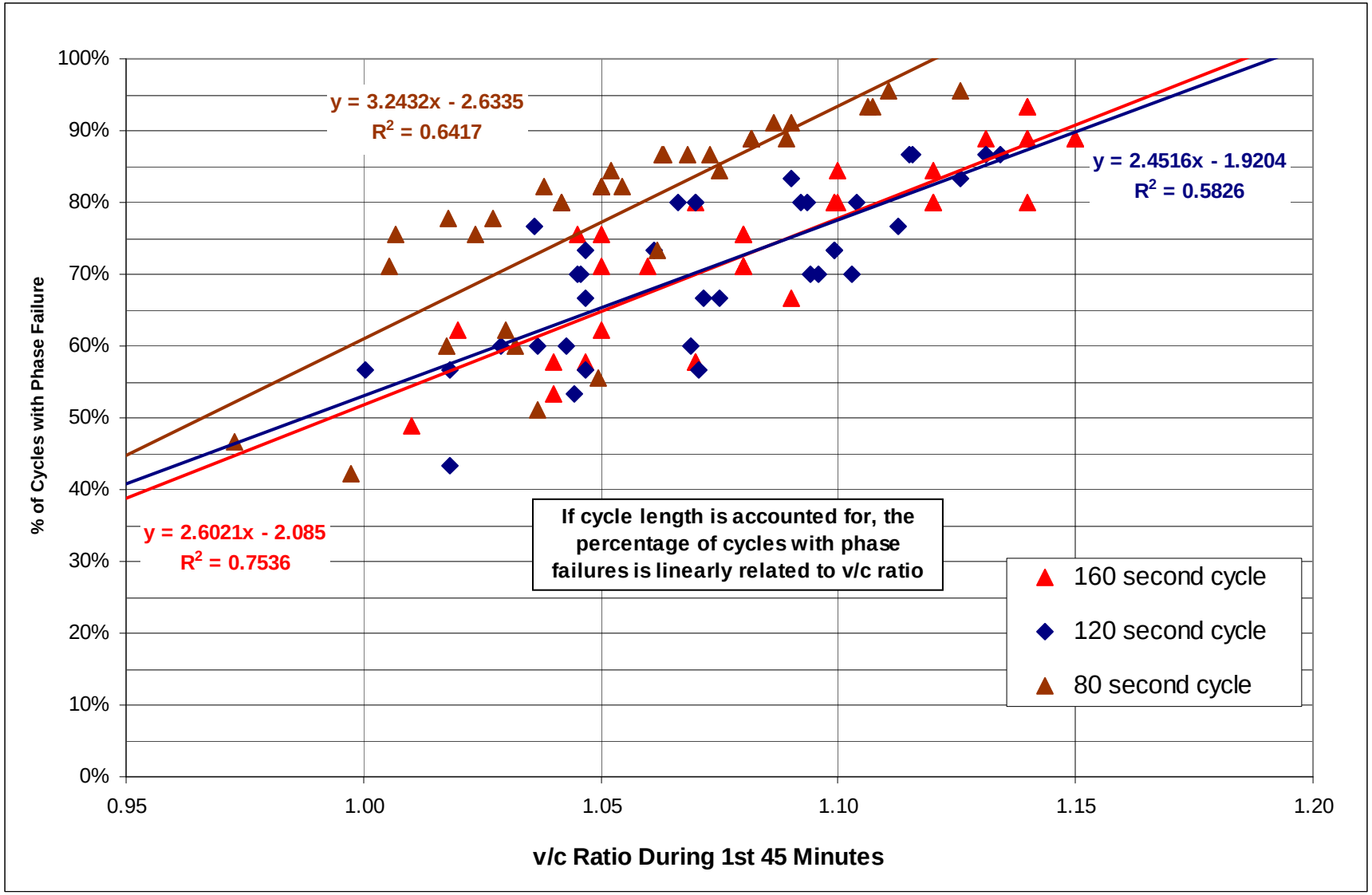

Figure A-18. Percentage of cycles in 1 hour with phase failure by cycle length

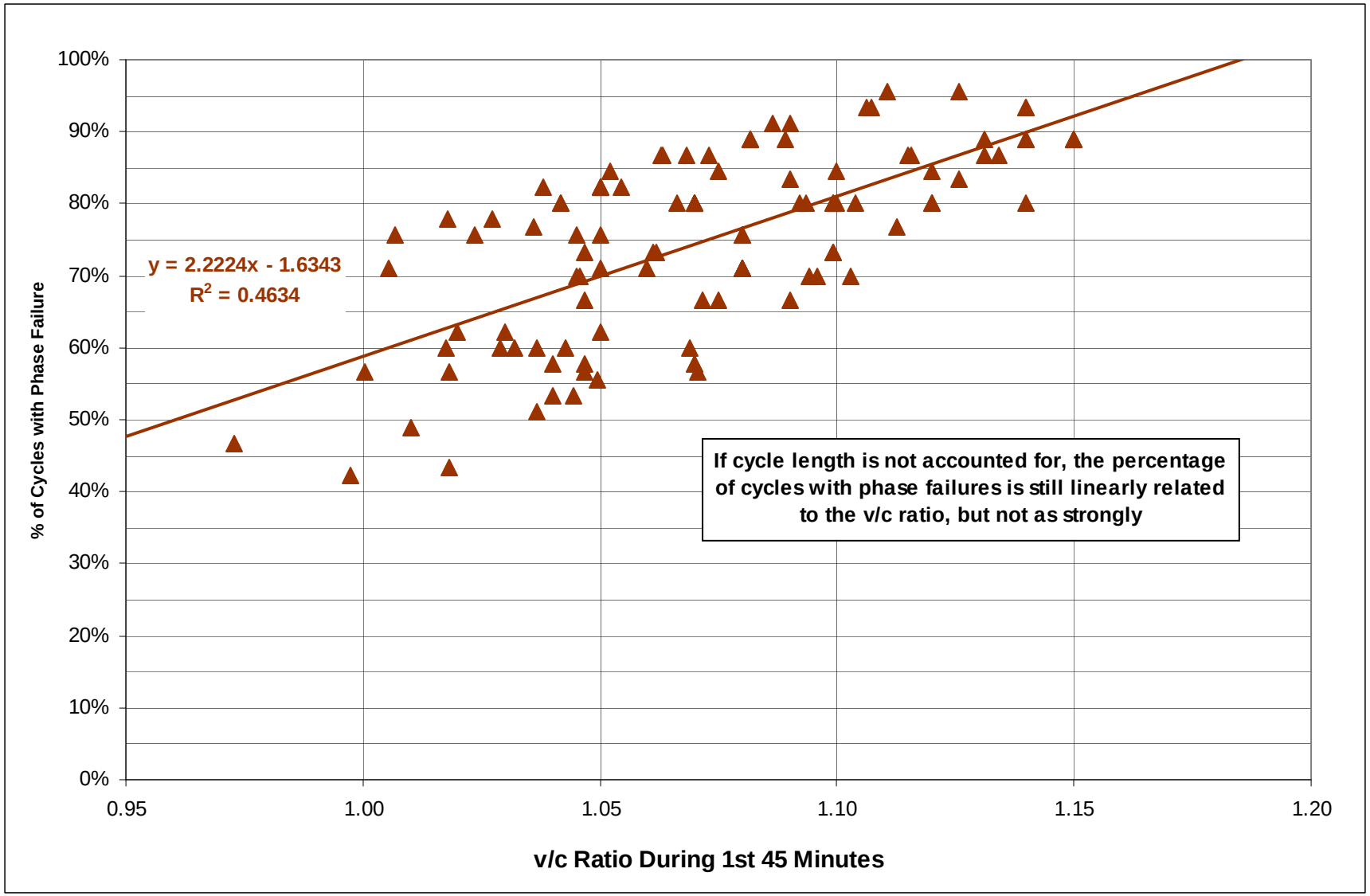

Figure A-19. Percentage of cycles in 1 hour with phase failure

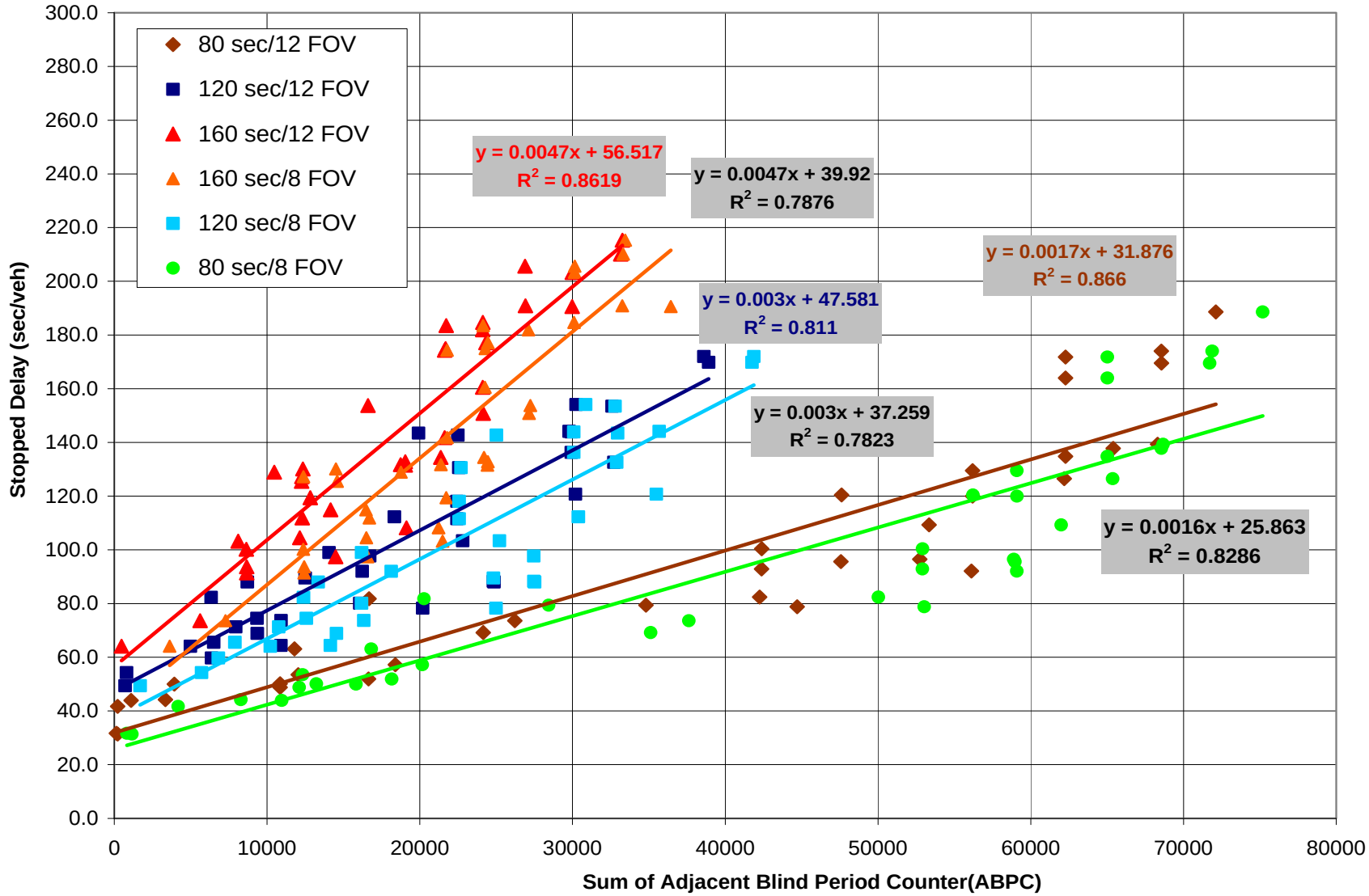

Figure A-20. Linear relationship between ABPC and stopped delay

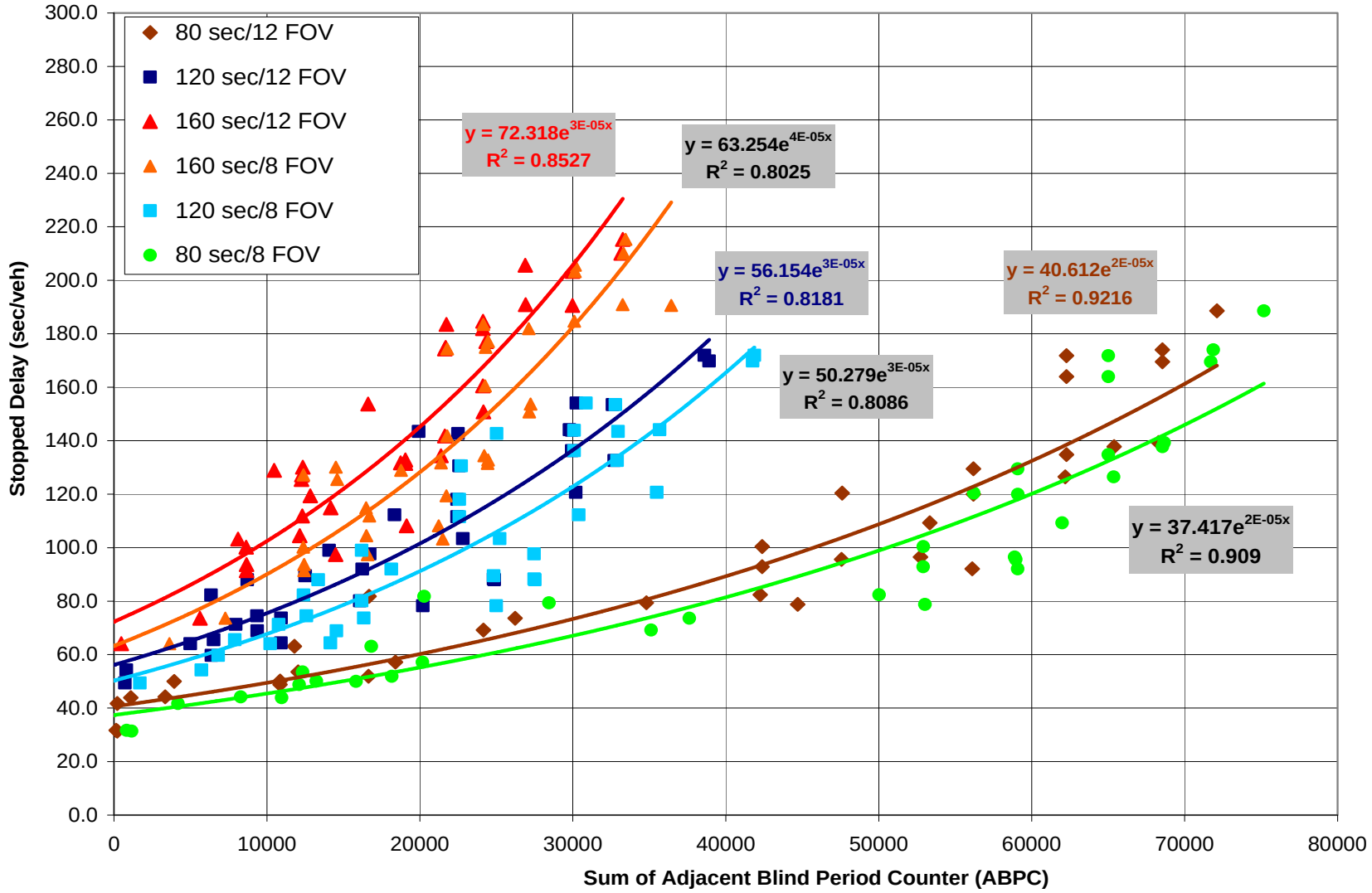

Figure A-21. Exponential relationship between ABPC and stopped delay

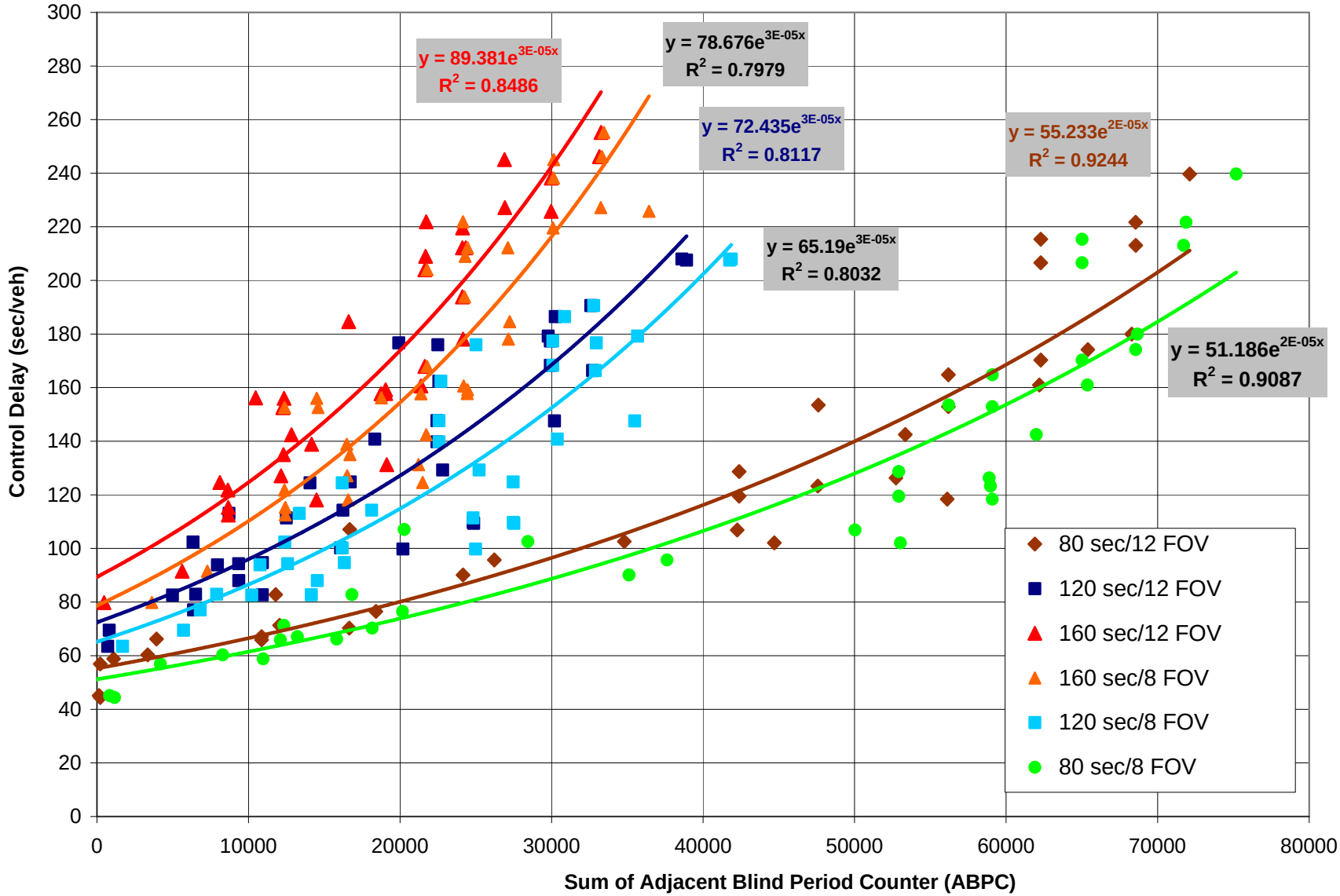

Figure A-22. Relationship between ABPC and control delay

APPENDIX B
TYPICAL PEAK HOUR FACTORS

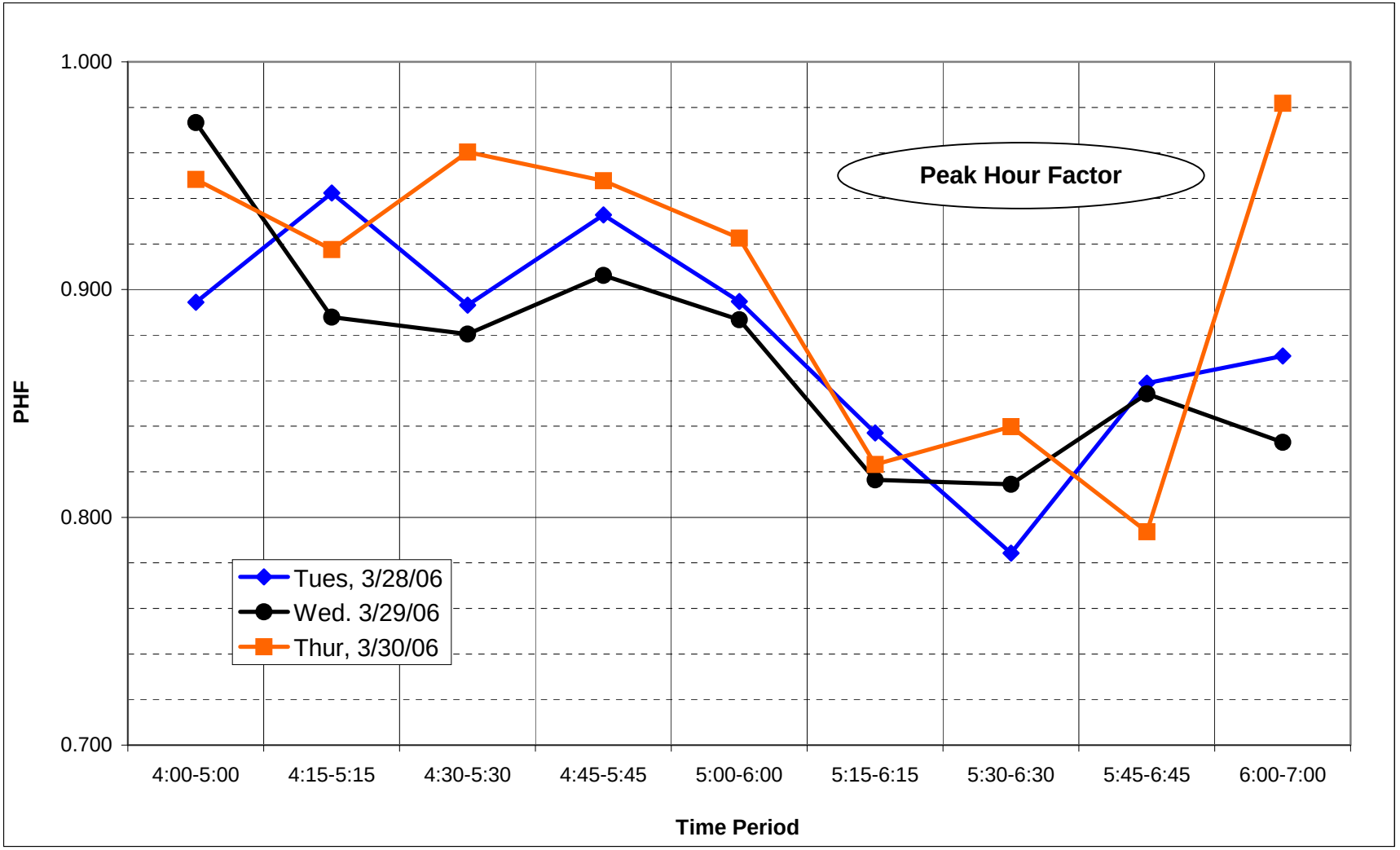

Figure B-1. US 1 S. PM peak hour factor, southbound (outbound) flow

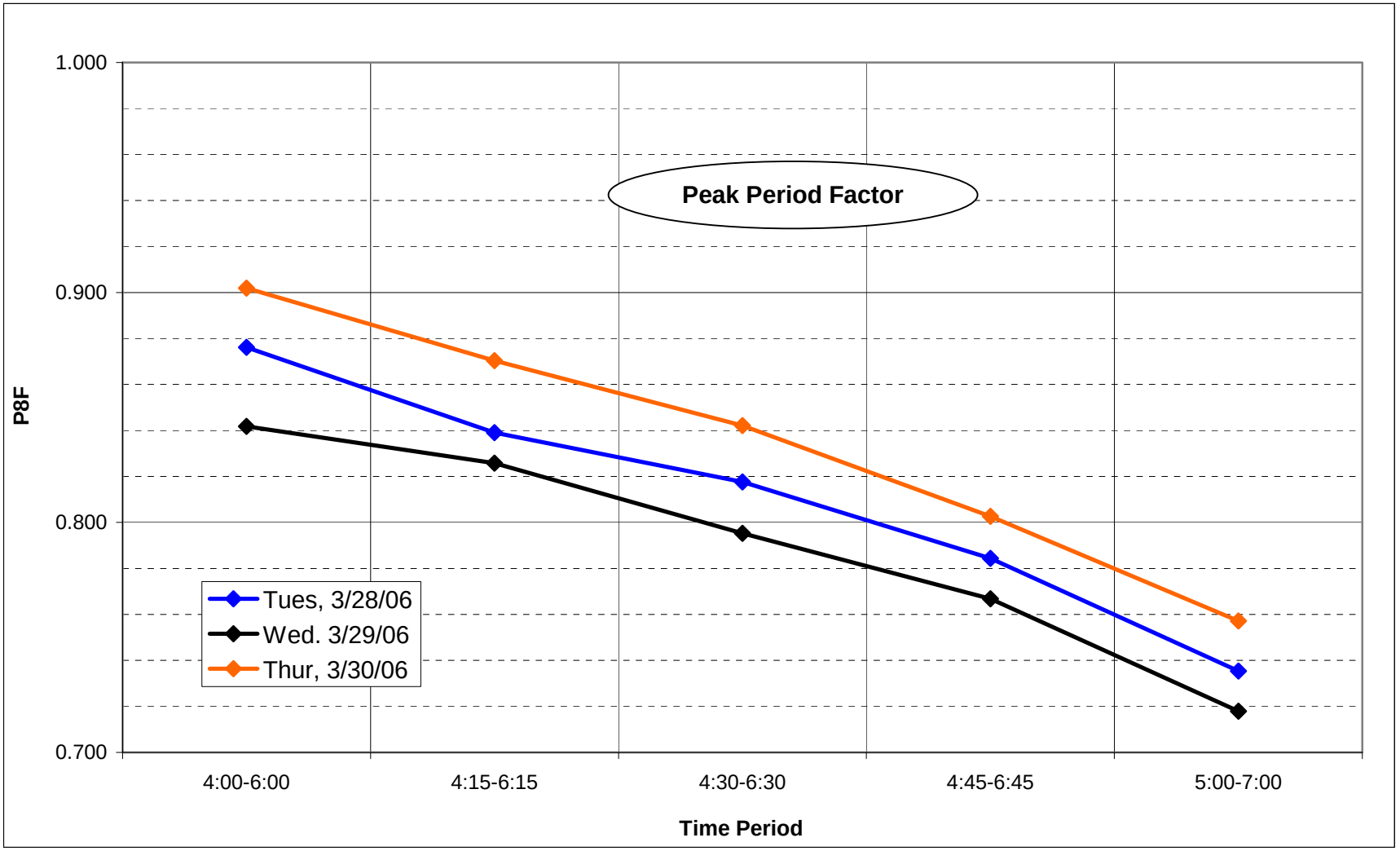

Figure B-2. US 1 S. PM peak period factor, southbound (outbound) flow

Table B1. US 1 machine counts (Southern St. Johns County)

		North of SR 206									
		Tuesday, 3/28/06				**1-Hour**	**PHF**		**2-Hour**	**PPF**	
Start Time	End Time	Southbound	Northbound	Both		**Period**	SB	NB	**Period**	SB	NB
4:00	4:15	303	176	479	1	4:00-5:00	0.894	0.924	4:00-6:00	0.876	0.892
4:15	4:30	250	188	438	2	4:15-5:15	0.942	0.917	4:15-6:15	0.839	0.869
4:30	4:45	249	197	446	3	4:30-5:30	0.893	0.940	4:30-6:30	0.818	0.835
4:45	**5:00**	**282**	**167**	**449**	4	4:45-5:45	0.933	0.935	4:45-6:45	0.784	0.809
5:00	**5:15**	**282**	**207**	**489**	5	5:00-6:00	0.895	0.926	5:00-7:00	0.735	0.768
5:15	**5:30**	**316**	**207**	**523**	6	5:15-6:15	0.837	0.842			
5:30	**5:45**	**299**	**212**	**511**	7	5:30-6:30	0.784	0.754			
5:45	6:00	234	159	393	8	5:45-6:45	0.859	0.910			
6:00	6:15	209	136	345	9	6:00-7:00	0.871	0.852			
6:15	6:30	196	132	328							
6:30	6:45	165	152	317							
6:45	7:00	158	98	256							
Peak Hour:		1179	793	**1972**							

Table B-1. Continued.

		Wednesday, 3/29/06				1-Hour	PHF		2-Hour	PPF	
Start Time	End Time	SB	NB	Both		Period	SB	NB	Period	SB	NB
4:00	4:15	252	151	403	1	4:00-5:00	0.973	0.836	4:00-6:00	0.842	0.841
4:15	4:30	262	215	477	2	4:15-5:15	0.888	0.877	4:15-6:15	0.826	0.859
4:30	4:45	246	169	415	3	4:30-5:30	0.880	0.874	4:30-6:30	0.795	0.817
4:45	**5:00**	**260**	**184**	**444**	4	4:45-5:45	0.906	0.890	4:45-6:45	0.767	0.799
5:00	**5:15**	**301**	**186**	**487**	5	5:00-6:00	0.887	0.896	5:00-7:00	0.718	0.770
5:15	**5:30**	**320**	**216**	**536**	6	5:15-6:15	0.816	0.894			
5:30	**5:45**	**279**	**229**	**508**	7	5:30-6:30	0.815	0.810			
5:45	6:00	235	190	425	8	5:45-6:45	0.854	0.853			
6:00	6:15	211	184	395	9	6:00-7:00	0.833	0.800			
6:15	6:30	184	139	323							
6:30	6:45	173	135	308							
6:45	7:00	135	131	266							
Peak Hour:		1160	815	**1975**							

Table B-1. Continued.

		Thursday, 3/30/06				1-Hour	PHF		2-Hour	PPF	
Start Time	End Time	SB	NB	Both		Period	SB	NB	Period	SB	NB
4:00	4:15	254	205	459	1	4:00-5:00	0.948	0.901	4:00-6:00	0.902	0.916
4:15	4:30	246	187	433	2	4:15-5:15	0.918	0.963	4:15-6:15	0.870	0.887
4:30	4:45	271	185	456	3	4:30-5:30	0.960	0.930	4:30-6:30	0.842	0.898
4:45	**5:00**	**276**	**162**	**438**	4	4:45-5:45	0.948	0.913	4:45-6:45	0.803	0.872
5:00	**5:15**	**297**	**186**	**483**	5	5:00-6:00	0.923	0.932	5:00-7:00	0.757	0.849
5:15	**5:30**	**297**	**196**	**493**	6	5:15-6:15	0.823	0.896			
5:30	**5:45**	**256**	**205**	**461**	7	5:30-6:30	0.840	0.906			
5:45	6:00	246	177	423	8	5:45-6:45	0.794	0.835			
6:00	6:15	179	157	336	9	6:00-7:00	0.982	0.770			
6:15	6:30	179	204	383							
6:30	6:45	177	143	320							
6:45	7:00	168	124	292							
Peak Hour:		1126	749	**1875**							
						Lowest	0.784	0.754		0.718	0.768
						Highest	0.982	0.963		0.902	0.916
						Average	**0.885**	0.881		**0.812**	0.845

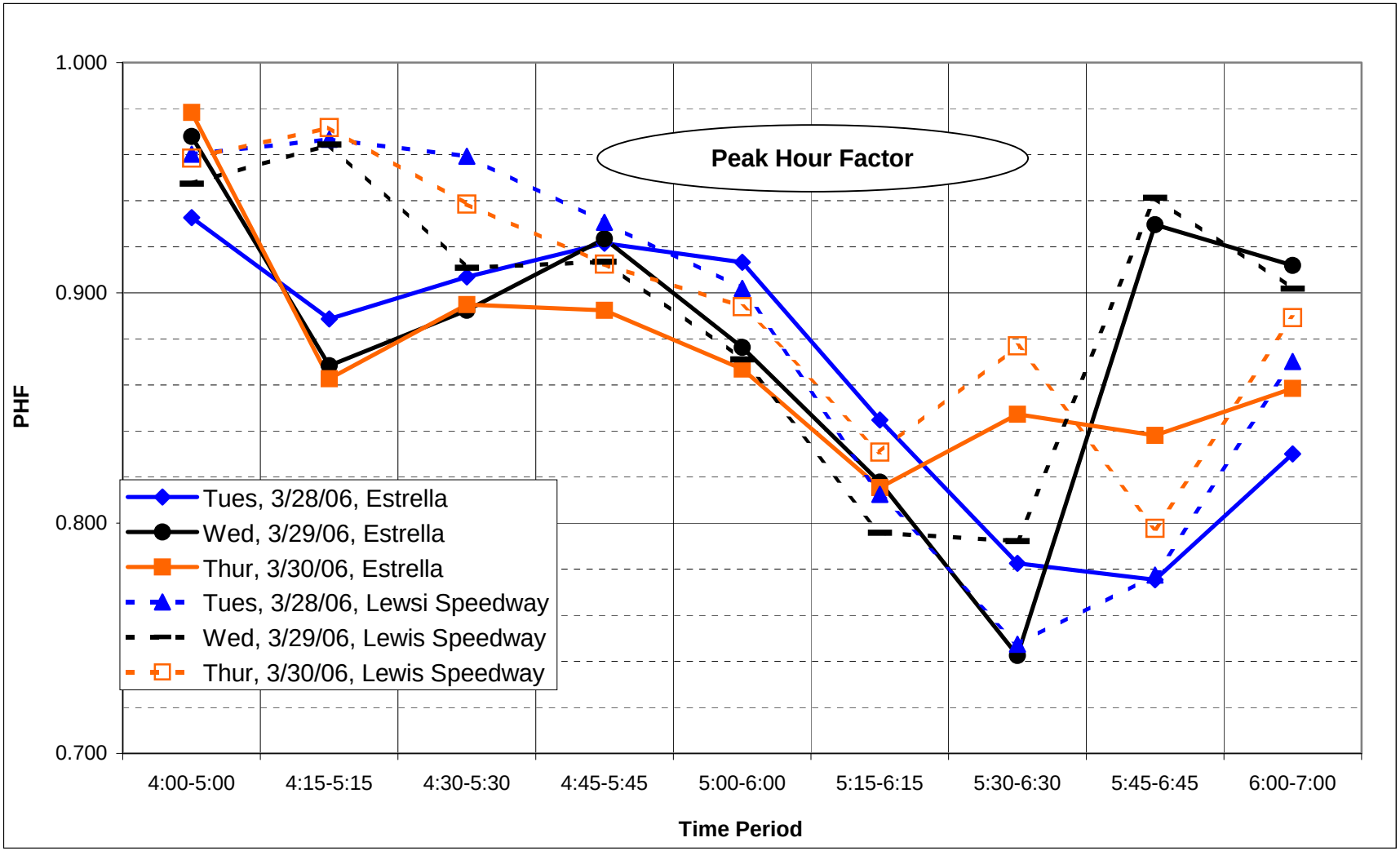

Figure B-3. US 1 N. PM peak hour factor, northbound (outbound) flow

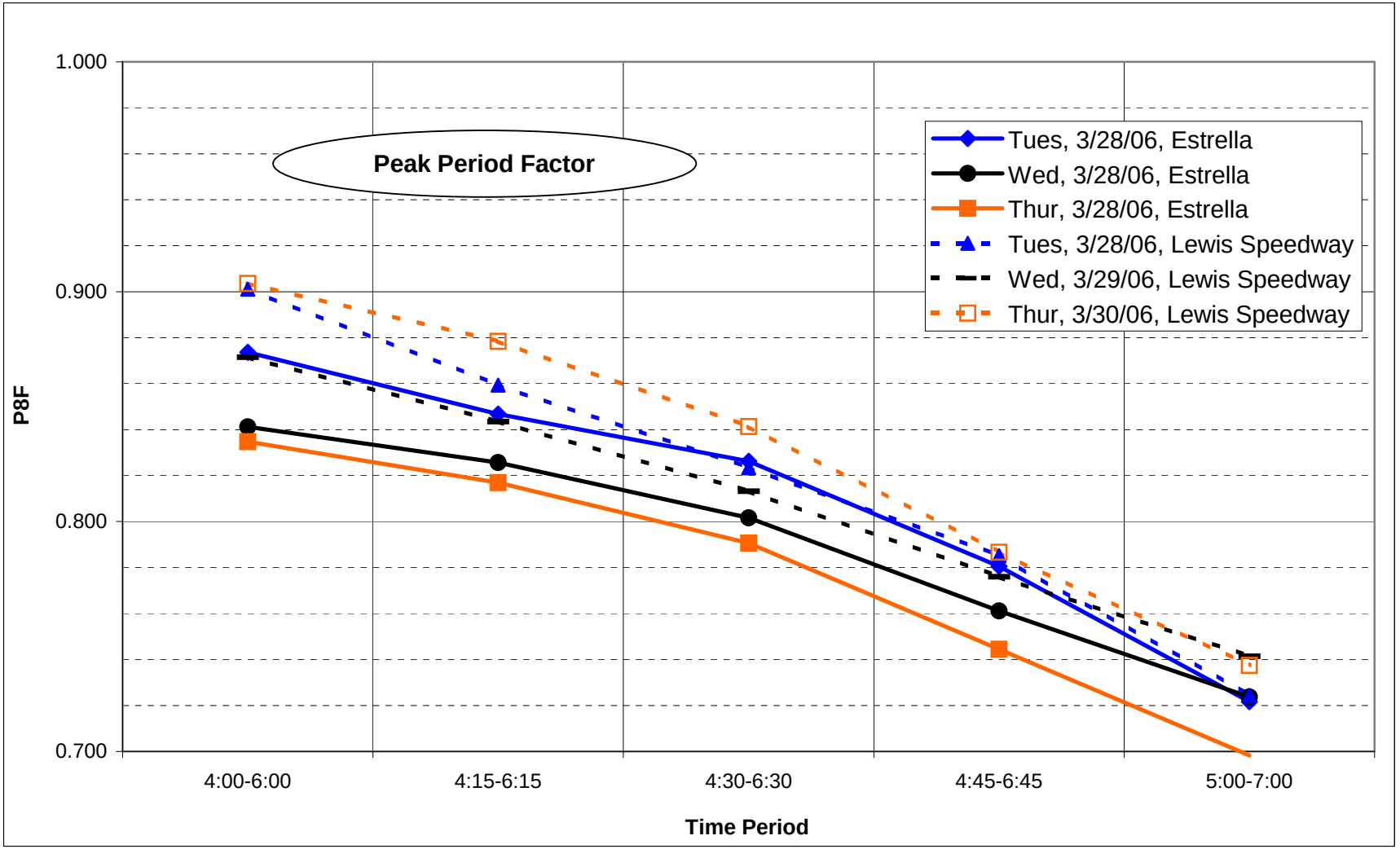

Figure B-4. US 1 N. PM peak period factor, northbound (outbound) flow

Table B-2. US1 Machine counts (northern St. Johns County)

North of Estrella Avenue

Tuesday, 3/28/06

Start Time	End Time	Northbound	Southbound	Both
4:00	4:15	214	251	465
4:15	4:30	220	216	436
4:30	**4:45**	**245**	**320**	**565**
4:45	**5:00**	**235**	**231**	**466**
5:00	**5:15**	**274**	**261**	**535**
5:15	**5:30**	**240**	**249**	**489**
5:30	5:45	261	258	519
5:45	6:00	226	202	428
6:00	6:15	155	167	322
6:15	6:30	175	176	351
6:30	6:45	145	158	303
6:45	7:00	106	110	216
Peak Hour:		994	1061	**2055**

	1-Hour Period	PHF NB	PHF SB	2-Hour Period	PPF NB	PPF SB
1	4:00-5:00	0.933	0.795	4:00-6:00	0.874	0.777
2	4:15-5:15	0.889	0.803	4:15-6:15	0.847	0.744
3	4:30-5:30	0.907	0.829	4:30-6:30	0.826	0.728
4	4:45-5:45	0.922	0.957	4:45-6:45	0.781	0.815
5	5:00-6:00	0.913	0.929	5:00-7:00	0.722	0.757
6	5:15-6:15	0.845	0.849			
7	5:30-6:30	0.783	0.778			
8	5:45-6:45	0.775	0.870			
9	6:00-7:00	0.830	0.868			

Wednesday, 3/29/06

Start Time	End Time	Northbound	Southbound	Both
4:00	4:15	211	238	449
4:15	4:30	227	242	469
4:30	4:45	234	276	510
4:45	**5:00**	**234**	**250**	**484**
5:00	**5:15**	**281**	**286**	**567**
5:15	**5:30**	**254**	**237**	**491**
5:30	**5:45**	**269**	**241**	**510**
5:45	6:00	181	179	360
6:00	6:15	176	192	368
6:15	6:30	173	177	350
6:30	6:45	143	164	307
6:45	7:00	150	132	282
Peak Hour:		1038	1014	**2052**

	1-Hour Period	PHF NB	PHF SB	2-Hour Period	PPF NB	PPF SB
1	4:00-5:00	0.968	0.911	4:00-6:00	0.841	0.852
2	4:15-5:15	0.868	0.921	4:15-6:15	0.826	0.832
3	4:30-5:30	0.892	0.917	4:30-6:30	0.802	0.803
4	4:45-5:45	0.923	0.886	4:45-6:45	0.761	0.754
5	5:00-6:00	0.876	0.824	5:00-7:00	0.724	0.703
6	5:15-6:15	0.818	0.881			
7	5:30-6:30	0.743	0.818			
8	5:45-6:45	0.930	0.927			
9	6:00-7:00	0.912	0.866			

Thursday, 3/30/06

Start Time	End Time	Northbound	Southbound	Both
4:00	4:15	224	233	457
4:15	4:30	241	226	467
4:30	**4:45**	**242**	**277**	**519**
4:45	**5:00**	**240**	**254**	**494**
5:00	**5:15**	**295**	**252**	**547**
5:15	**5:30**	**279**	**231**	**510**
5:30	5:45	239	241	480
5:45	6:00	210	220	430
6:00	6:15	182	198	380
6:15	6:30	179	157	336
6:30	6:45	133	171	304
6:45	7:00	131	153	284
Peak Hour:		1056	1014	**2070**

	1-Hour Period	PHF NB	PHF SB	2-Hour Period	PPF NB	PPF SB
1	4:00-5:00	0.978	0.894	4:00-6:00	0.835	0.873
2	4:15-5:15	0.863	0.911	4:15-6:15	0.817	0.857
3	4:30-5:30	0.895	0.915	4:30-6:30	0.791	0.826
4	4:45-5:45	0.892	0.963	4:45-6:45	0.744	0.848
5	5:00-6:00	0.867	0.937	5:00-7:00	0.698	0.805
6	5:15-6:15	0.815	0.923			
7	5:30-6:30	0.847	0.846			
8	5:45-6:45	0.838	0.848			
9	6:00-7:00	0.859	0.857			

Lowest	0.743	0.778	0.698	0.703
Highest	0.978	0.963	0.874	0.873
Average	**0.873**	0.879	**0.792**	0.798
Lowest	0.743	0.731	0.698	0.597
Highest	0.978	0.963	0.904	0.873
Average	**0.882**	0.860	**0.806**	0.752

South of Lewis Speedway

Tuesday, 3/28/06

Start Time	End Time	Northbound	Southbound	Both
4:00	4:15	251	291	542
4:15	**4:30**	**264**	**288**	**552**
4:30	**4:45**	**252**	**378**	**630**
4:45	**5:00**	**270**	**250**	**520**
5:00	**5:15**	**258**	**338**	**596**
5:15	5:30	256	263	519
5:30	5:45	288	262	550
5:45	6:00	237	211	448
6:00	6:15	155	191	346
6:15	6:30	181	191	372
6:30	6:45	164	165	329
6:45	7:00	130	141	271
Peak Hour:		1300	1517	**2817**

	1-Hour Period	PHF NB	PHF SB	2-Hour Period	PPF NB	PPF SB
1	4:00-5:00	0.960	0.798	4:00-6:00	0.901	0.754
2	4:15-5:15	0.967	0.829	4:15-6:15	0.859	0.721
3	4:30-5:30	0.959	0.813	4:30-6:30	0.823	0.689
4	4:45-5:45	0.931	0.823	4:45-6:45	0.785	0.692
5	5:00-6:00	0.902	0.794	5:00-7:00	0.724	0.652
6	5:15-6:15	0.813	0.881			
7	5:30-6:30	0.747	0.816			
8	5:45-6:45	0.777	0.898			
9	6:00-7:00	0.870	0.901			

Wednesday, 3/29/06

Start Time	End Time	Northbound	Southbound	Both
4:00	4:15	245	321	566
4:15	4:30	266	273	539
4:30	**4:45**	**258**	**364**	**622**
4:45	**5:00**	**239**	**276**	**515**
5:00	**5:15**	**267**	**345**	**612**
5:15	**5:30**	**289**	**269**	**558**
5:30	5:45	261	271	532
5:45	6:00	190	216	406
6:00	6:15	180	188	368
6:15	6:30	196	186	382
6:30	6:45	172	179	351
6:45	7:00	159	143	302
Peak Hour:		1053	1254	**2307**

	1-Hour Period	PHF NB	PHF SB	2-Hour Period	PPF NB	PPF SB
1	4:00-5:00	0.947	0.848	4:00-6:00	0.872	0.802
2	4:15-5:15	0.964	0.864	4:15-6:15	0.843	0.756
3	4:30-5:30	0.911	0.861	4:30-6:30	0.813	0.726
4	4:45-5:45	0.913	0.841	4:45-6:45	0.776	0.699
5	5:00-6:00	0.871	0.798	5:00-7:00	0.741	0.651
6	5:15-6:15	0.796	0.871			
7	5:30-6:30	0.792	0.794			
8	5:45-6:45	0.941	0.890			
9	6:00-7:00	0.902	0.926			

Thursday, 3/30/06

Start Time	End Time	Northbound	Southbound	Both
4:00	4:15	252	332	584
4:15	**4:30**	**282**	**331**	**613**
4:30	***4:45***	***283***	***426***	***709***
4:45	**5:00**	**268**	**331**	**599**
5:00	**5:15**	**267**	**411**	**678**
5:15	5:30	297	270	567
5:30	5:45	252	290	542
5:45	6:00	246	230	476
6:00	6:15	192	220	412
6:15	6:30	194	178	372
6:30	6:45	153	181	334
6:45	7:00	151	182	333
Peak Hour:		1100	1499	**2599**

	1-Hour Period	PHF NB	PHF SB	2-Hour Period	PPF NB	PPF SB
1	4:00-5:00	0.958	0.833	4:00-6:00	0.904	0.769
2	4:15-5:15	0.972	0.880	4:15-6:15	0.878	0.736
3	*4:30-5:30*	*0.939*	*0.844*	*4:30-6:30*	*0.841*	*0.691*
4	4:45-5:45	0.912	0.792	4:45-6:45	0.787	0.642
5	5:00-6:00	0.894	0.731	5:00-7:00	0.737	0.597
6	5:15-6:15	0.831	0.871			
7	5:30-6:30	0.877	0.791			
8	5:45-6:45	0.798	0.879			
9	6:00-7:00	0.889	0.865			

Lowest	0.747	0.731	0.724	0.597
Highest	0.972	0.926	0.904	0.802
Average	**0.890**	0.842	**0.819**	0.705

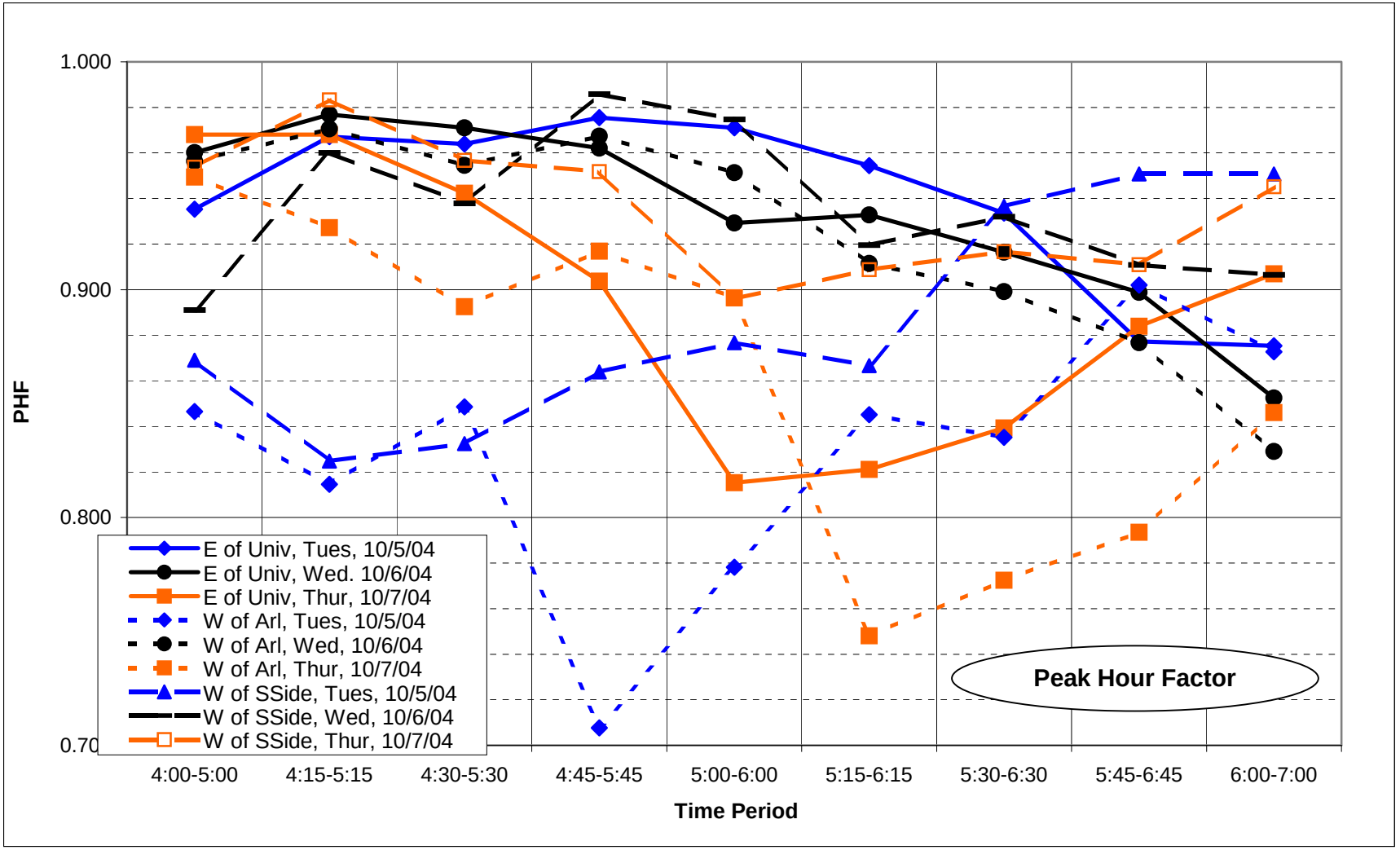

Figure B-5. Atlantic Boulevard PM peak hour factor, eastbound (outbound) flow

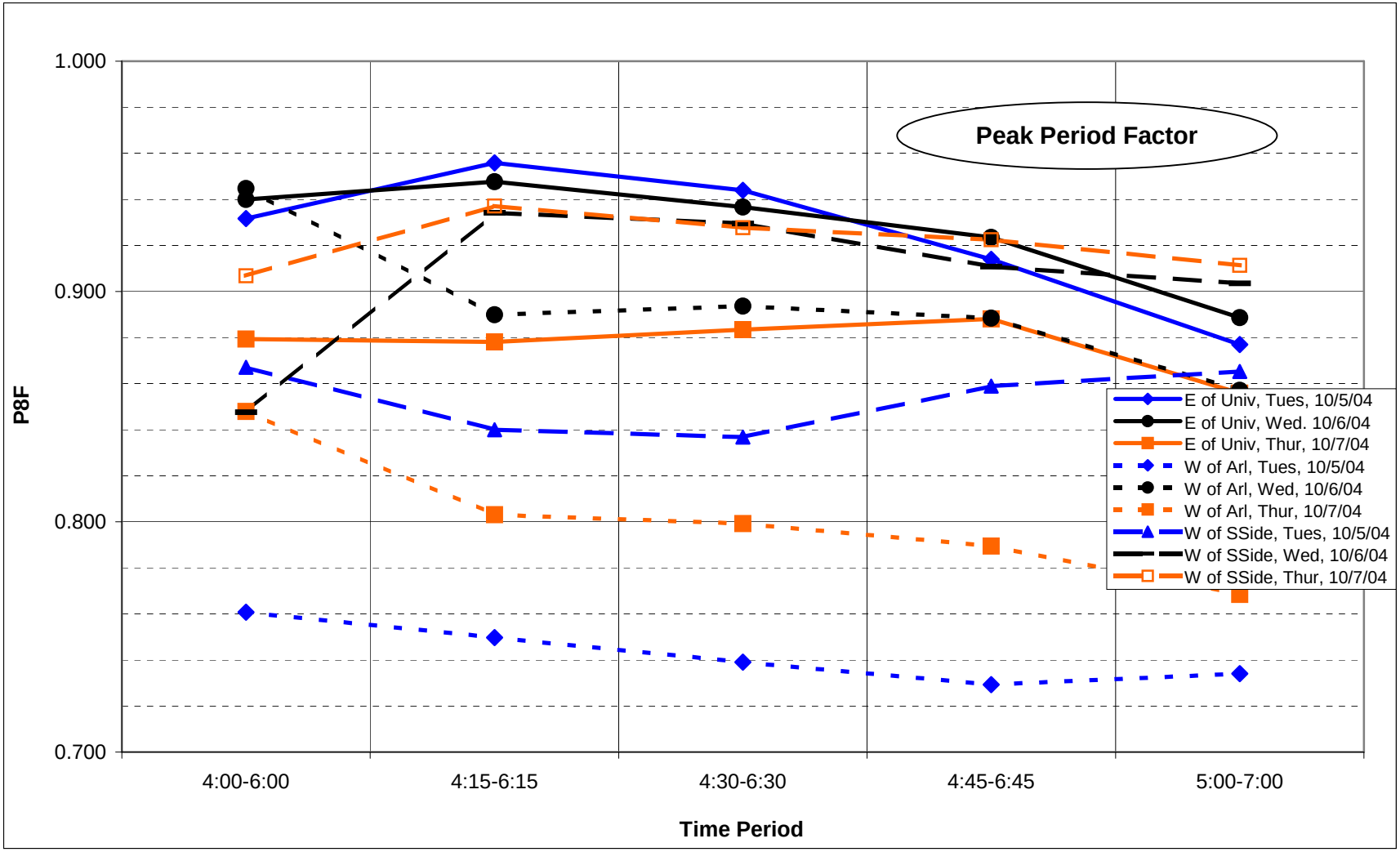

Figure B-6. Atlantic Boulevard PM peak period factor, eastbound (outbound) flow

Table B-3. Atlantic Boulevard machine counts

East of University Boulevard

Tuesday, 10/5/04

Start Time	End Time	Eastbound	Westbound	Both
4:00	4:15	406	290	696
4:15	4:30	363	317	680
4:30	4:45	366	307	673
4:45	**5:00**	**384**	**309**	**693**
5:00	**5:15**	**388**	**293**	**681**
5:15	**5:30**	**358**	**369**	**727**
5:30	**5:45**	**384**	**347**	**731**
5:45	6:00	377	295	672
6:00	6:15	347	314	661
6:15	6:30	326	278	604
6:30	6:45	273	229	502
6:45	7:00	269	267	536
Peak Hour:		1514	1318	**2832**

	1-Hour Period	PHF EB	PHF WB	2-Hour Period	PPF EB	PPF WB
1	4:00-5:00	0.935	0.965	4:00-6:00	0.932	0.856
2	4:15-5:15	0.967	0.967	4:15-6:15	0.956	0.864
3	4:30-5:30	0.964	0.866	4:30-6:30	0.944	0.851
4	4:45-5:45	0.976	0.893	4:45-6:45	0.914	0.825
5	5:00-6:00	0.971	0.883	5:00-7:00	0.877	0.810
6	5:15-6:15	0.954	0.898			
7	5:30-6:30	0.934	0.889			
8	5:45-6:45	0.877	0.889			
9	6:00-7:00	0.875	0.866			

West of Arlington Road

Tuesday, 10/5/04

Start Time	End Time	Eastbound	Westbound	Both
4:00	4:15	482	298	780
4:15	4:30	441	296	737
4:30	4:45	407	311	718
4:45	5:00	302	286	588
5:00	5:15	287	282	569
5:15	**5:30**	**416**	**316**	**732**
5:30	**5:45**	**549**	**300**	**849**
5:45	**6:00**	**457**	**283**	**740**
6:00	**6:15**	**434**	**286**	**720**
6:15	6:30	394	281	675
6:30	6:45	364	231	595
6:45	7:00	323	281	604
Peak Hour:		1856	1185	**3041**

	1-Hour Period	PHF EB	PHF WB	2-Hour Period	PPF EB	PPF WB
1	4:00-5:00	0.846	0.957	4:00-6:00	0.761	0.938
2	4:15-5:15	0.815	0.945	4:15-6:15	0.750	0.934
3	4:30-5:30	0.849	0.945	4:30-6:30	0.739	0.928
4	4:45-5:45	0.708	0.937	4:45-6:45	0.729	0.896
5	5:00-6:00	0.778	0.934	5:00-7:00	0.734	0.894
6	5:15-6:15	0.845	0.938			
7	5:30-6:30	0.835	0.958			
8	5:45-6:45	0.902	0.945			
9	6:00-7:00	0.873	0.943			

West of Southside Boulevard

Tuesday, 10/5/04

Start Time	End Time	Eastbound	Westbound	Both
4:00	**4:15**	**375**	**325**	**700**
4:15	**4:30**	**378**	**320**	**698**
4:30	**4:45**	**267**	**341**	**608**
4:45	**5:00**	**294**	**292**	**586**
5:00	5:15	308	300	608
5:15	5:30	373	302	675
5:30	5:45	314	262	576
5:45	6:00	313	282	595
6:00	6:15	293	262	555
6:15	6:30	335	272	607
6:30	6:45	333	261	594
6:45	7:00	313	247	560
Peak Hour:		1314	1278	**2592**

	1-Hour Period	PHF EB	PHF WB	2-Hour Period	PPF EB	PPF WB
1	4:00-5:00	0.869	0.937	4:00-6:00	0.867	0.889
2	4:15-5:15	0.825	0.919	4:15-6:15	0.840	0.865
3	4:30-5:30	0.832	0.905	4:30-6:30	0.837	0.848
4	4:45-5:45	0.864	0.957	4:45-6:45	0.859	0.924
5	5:00-6:00	0.877	0.949	5:00-7:00	0.865	0.906
6	5:15-6:15	0.867	0.917			
7	5:30-6:30	0.937	0.956			
8	5:45-6:45	0.951	0.955			
9	6:00-7:00	0.951	0.958			

Wednesday, 10/6/04

Start Time	End Time	Eastbound	Westbound	Both
4:00	4:15	359	285	644
4:15	4:30	382	259	641
4:30	**4:45**	**364**	**300**	**664**
4:45	**5:00**	**389**	**314**	**703**
5:00	**5:15**	**385**	**339**	**724**
5:15	**5:30**	**373**	**320**	**693**
5:30	5:45	350	310	660
5:45	6:00	323	306	629
6:00	6:15	383	281	664
6:15	6:30	348	248	596
6:30	6:45	323	206	529
6:45	7:00	252	228	480
Peak Hour:		1511	1273	**2784**

	1-Hour Period	PHF EB	PHF WB	2-Hour Period	PPF EB	PPF WB
1	4:00-5:00	0.960	0.922	4:00-6:00	0.940	0.897
2	4:15-5:15	0.977	0.894	4:15-6:15	0.948	0.896
3	4:30-5:30	0.971	0.939	4:30-6:30	0.937	0.892
4	4:45-5:45	0.962	0.946	4:45-6:45	0.924	0.857
5	5:00-6:00	0.929	0.940	5:00-7:00	0.889	0.825
6	5:15-6:15	0.933	0.951			
7	5:30-6:30	0.916	0.923			
8	5:45-6:45	0.899	0.850			
9	6:00-7:00	0.852	0.857			

Wednesday, 10/6/04

Start Time	End Time	Eastbound	Westbound	Both
4:00	4:15	459	272	731
4:15	4:30	428	242	670
4:30	**4:45**	**428**	**304**	**732**
4:45	**5:00**	**441**	**302**	**743**
5:00	**5:15**	**450**	**305**	**755**
5:15	**5:30**	**468**	**313**	**781**
5:30	5:45	452	261	713
5:45	6:00	411	284	695
6:00	6:15	503	281	784
6:15	6:30	443	241	684
6:30	6:45	407	214	621
6:45	7:00	315	216	531
Peak Hour:		1787	1224	**3011**

	1-Hour Period	PHF EB	PHF WB	2-Hour Period	PPF EB	PPF WB
1	4:00-5:00	0.956	0.921	4:00-6:00	0.945	0.912
2	4:15-5:15	0.971	0.945	4:15-6:15	0.890	0.915
3	4:30-5:30	0.955	0.978	4:30-6:30	0.894	0.915
4	4:45-5:45	0.967	0.943	4:45-6:45	0.888	0.879
5	5:00-6:00	0.951	0.929	5:00-7:00	0.857	0.845
6	5:15-6:15	0.912	0.910			
7	5:30-6:30	0.899	0.939			
8	5:45-6:45	0.877	0.898			
9	6:00-7:00	0.829	0.847			

Wednesday, 10/6/04

Start Time	End Time	Eastbound	Westbound	Both
4:00	**4:15**	**383**	**302**	**685**
4:15	**4:30**	**329**	**287**	**616**
4:30	**4:45**	**338**	**346**	**684**
4:45	**5:00**	**315**	**326**	**641**
5:00	5:15	316	307	623
5:15	5:30	299	305	604
5:30	5:45	316	286	602
5:45	6:00	301	334	635
6:00	6:15	342	270	612
6:15	6:30	316	257	573
6:30	6:45	287	261	548
6:45	7:00	295	268	563
Peak Hour:		1365	1261	**2626**

	1-Hour Period	PHF EB	PHF WB	2-Hour Period	PPF EB	PPF WB
1	4:00-5:00	0.891	0.911	4:00-6:00	0.848	0.901
2	4:15-5:15	0.960	0.915	4:15-6:15	0.934	0.889
3	4:30-5:30	0.938	0.928	4:30-6:30	0.929	0.878
4	4:45-5:45	0.986	0.939	4:45-6:45	0.911	0.878
5	5:00-6:00	0.975	0.922	5:00-7:00	0.904	0.856
6	5:15-6:15	0.920	0.894			
7	5:30-6:30	0.932	0.859			
8	5:45-6:45	0.911	0.840			
9	6:00-7:00	0.906	0.978			

Thursday, 10/7/04

Start Time	End Time	Eastbound	Westbound	Both
4:00	4:15	387	288	675
4:15	4:30	375	257	632
4:30	**4:45**	**399**	**287**	**686**
4:45	**5:00**	**384**	**305**	**689**
5:00	**5:15**	**387**	**358**	**745**
5:15	**5:30**	**334**	**327**	**661**
5:30	5:45	294	314	608
5:45	6:00	247	336	583
6:00	6:15	383	282	665
6:15	6:30	392	277	669
6:30	6:45	364	272	636
6:45	7:00	283	257	540
Peak Hour:		1504	1277	**2781**

	1-Hour Period	PHF EB	PHF WB	2-Hour Period	PPF EB	PPF WB
1	4:00-5:00	0.968	0.932	4:00-6:00	0.879	0.863
2	4:15-5:15	0.968	0.843	4:15-6:15	0.878	0.861
3	4:30-5:30	0.942	0.892	4:30-6:30	0.883	0.868
4	4:45-5:45	0.904	0.911	4:45-6:45	0.888	0.863
5	5:00-6:00	0.815	0.932	5:00-7:00	0.856	0.846
6	5:15-6:15	0.821	0.937			
7	5:30-6:30	0.839	0.900			
8	5:45-6:45	0.884	0.868			
9	6:00-7:00	0.907	0.965			

Thursday, 10/7/04

Start Time	End Time	Eastbound	Westbound	Both
4:00	4:15	446	293	739
4:15	4:30	460	262	722
4:30	**4:45**	**484**	**287**	**771**
4:45	**5:00**	**448**	**281**	**729**
5:00	**5:15**	**403**	**319**	**722**
5:15	**5:30**	**393**	**270**	**663**
5:30	5:45	399	278	677
5:45	6:00	250	246	496
6:00	6:15	523	249	772
6:15	6:30	444	256	700
6:30	6:45	443	255	698
6:45	7:00	360	243	603
Peak Hour:		1728	1157	**2885**

	1-Hour Period	PHF EB	PHF WB	2-Hour Period	PPF EB	PPF WB
1	4:00-5:00	0.949	0.958	4:00-6:00	0.848	0.876
2	4:15-5:15	0.927	0.900	4:15-6:15	0.803	0.859
3	4:30-5:30	0.893	0.907	4:30-6:30	0.799	0.857
4	4:45-5:45	0.917	0.900	4:45-6:45	0.789	0.844
5	5:00-6:00	0.896	0.872	5:00-7:00	0.768	0.829
6	5:15-6:15	0.748	0.938			
7	5:30-6:30	0.772	0.925			
8	5:45-6:45	0.793	0.982			
9	6:00-7:00	0.846	0.979			

Thursday, 10/7/04

Start Time	End Time	Eastbound	Westbound	Both
4:00	**4:15**	**373**	**329**	**702**
4:15	**4:30**	**355**	**312**	**667**
4:30	**4:45**	**343**	**321**	**664**
4:45	**5:00**	**352**	**299**	**651**
5:00	5:15	358	321	679
5:15	5:30	317	287	604
5:30	5:45	336	303	639
5:45	6:00	272	269	541
6:00	6:15	351	299	650
6:15	6:30	328	287	615
6:30	6:45	328	256	584
6:45	7:00	320	266	586
Peak Hour:		1423	1261	**2684**

	1-Hour Period	PHF EB	PHF WB	2-Hour Period	PPF EB	PPF WB
1	4:00-5:00	0.954	0.958	4:00-6:00	0.907	0.927
2	4:15-5:15	0.983	0.976	4:15-6:15	0.937	0.939
3	4:30-5:30	0.957	0.956	4:30-6:30	0.928	0.929
4	4:45-5:45	0.952	0.942	4:45-6:45	0.922	0.904
5	5:00-6:00	0.896	0.919	5:00-7:00	0.911	0.891
6	5:15-6:15	0.909	0.955			
7	5:30-6:30	0.917	0.955			
8	5:45-6:45	0.911	0.929			
9	6:00-7:00	0.945	0.926			

Lowest	0.815	0.843		0.856	0.810
Highest	0.977	0.967		0.956	0.897
Average	0.922	0.908		0.910	0.858
Lowest	0.708	0.840		0.729	0.810
Highest	0.986	0.982		0.956	0.939
Average	**0.904**	0.924		**0.872**	0.880

Lowest	0.708	0.847		0.729	0.829
Highest	0.971	0.982		0.945	0.938
Average	0.871	0.932		0.813	0.888

Lowest	0.825	0.840		0.837	0.848
Highest	0.986	0.978		0.937	0.939
Average	0.919	0.932		0.893	0.895

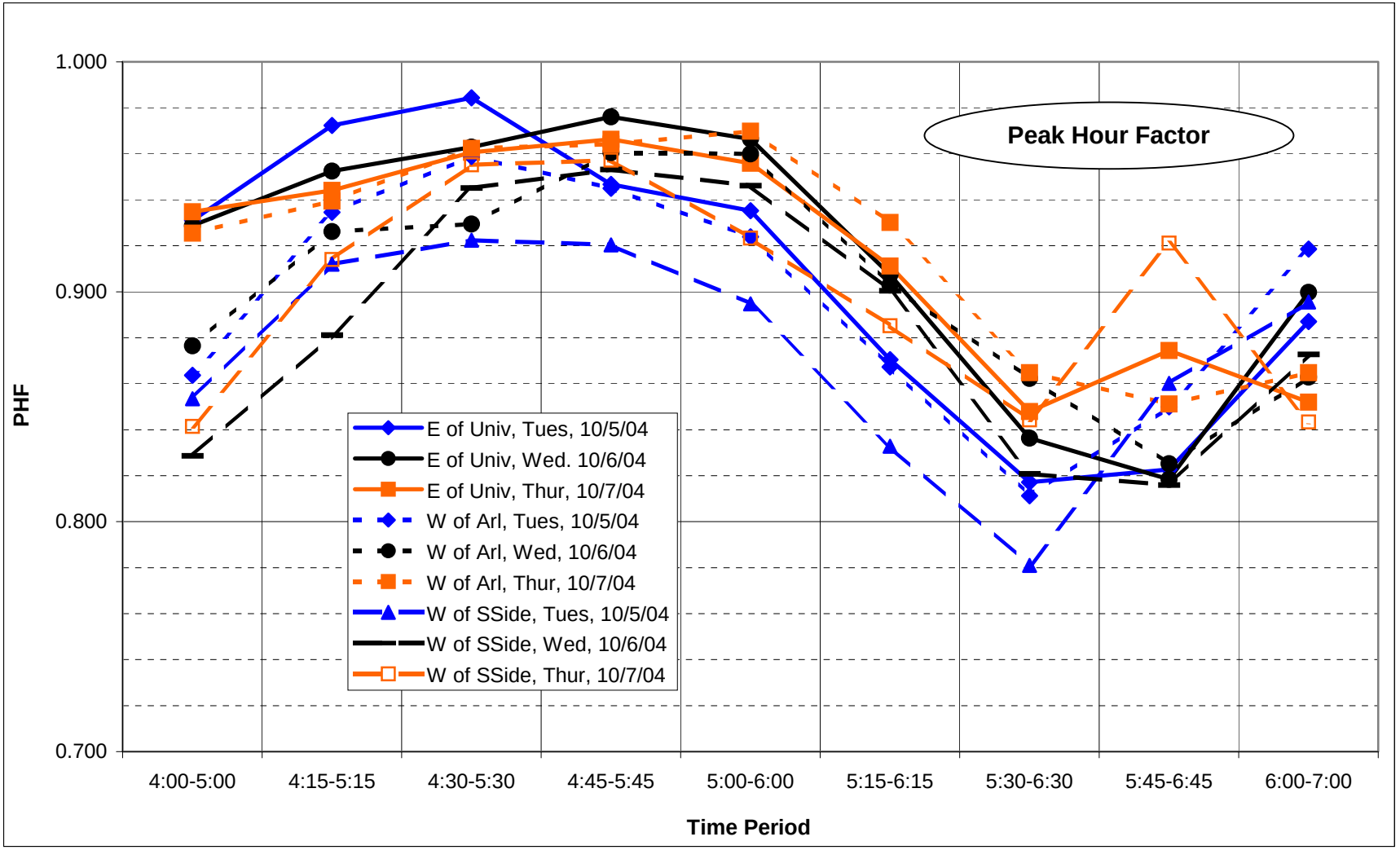

Figure B-7. University Blvd. PM peak hour factor, northbound (outbound) flow

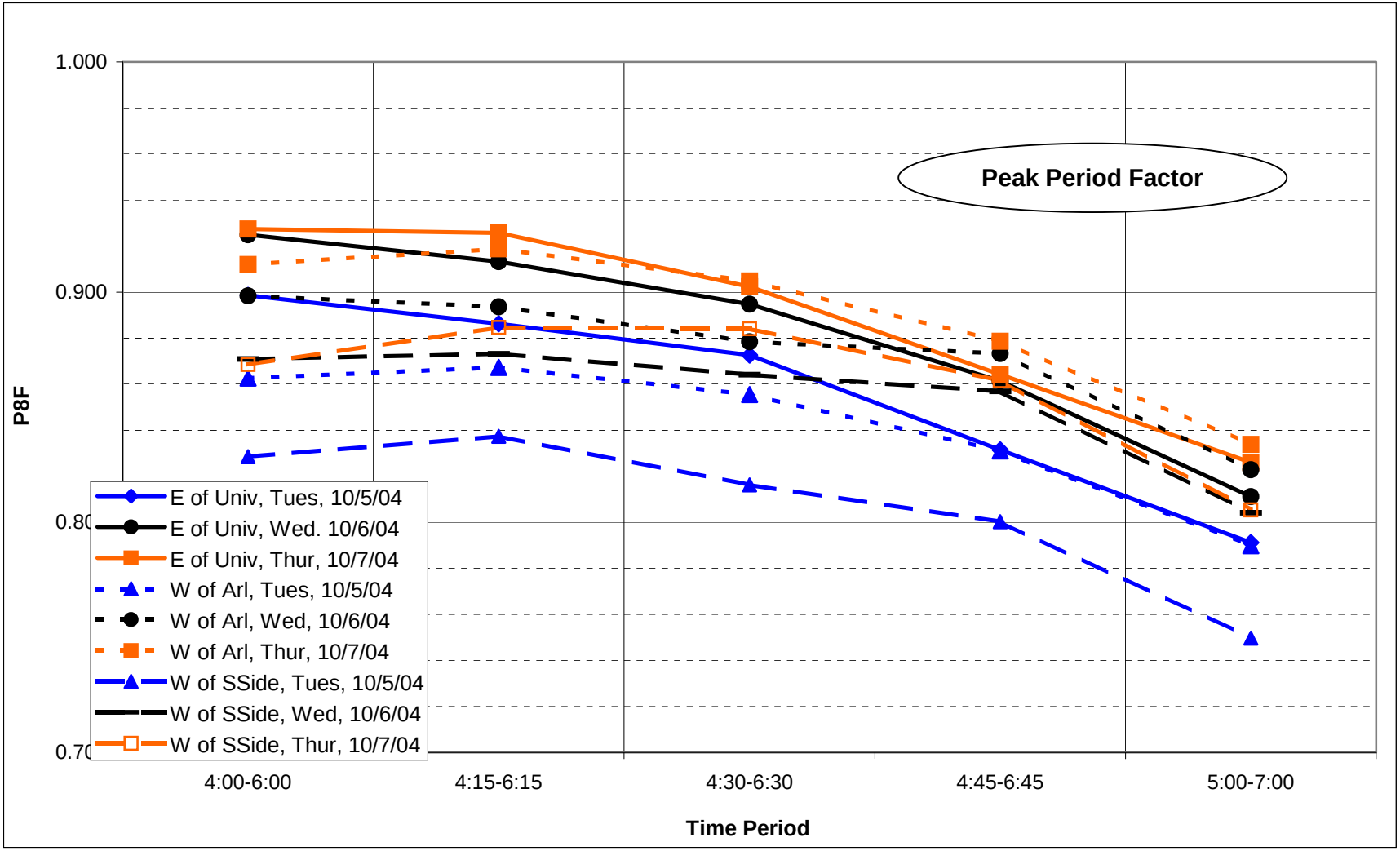

Figure B-8. University Blvd. PM peak period factor, northbound (outbound) flow

Table B-4. University Boulevard machine counts (Jacksonville).

South of Los Santos Drive

Tuesday, 8/19/03

Start Time	End Time	Northbound	Southbound	Both
4:00	4:15	403	237	640
4:15	4:30	440	270	710
4:30	4:45	486	301	787
4:45	**5:00**	**481**	**311**	**792**
5:00	**5:15**	**487**	**309**	**796**
5:15	**5:30**	**495**	**305**	**800**
5:30	**5:45**	**525**	**268**	**793**
5:45	6:00	457	281	738
6:00	6:15	351	255	606
6:15	6:30	383	271	654
6:30	6:45	313	229	542
6:45	7:00	312	202	514
Peak Hour:		1988	1193	**3181**

	1-Hour Period	PHF NB	PHF SB	2-Hour Period	PPF NB	PPF SB
1	4:00-5:00	0.931	0.900	4:00-6:00	0.899	0.917
2	4:15-5:15	0.972	0.957	4:15-6:15	0.886	0.924
3	4:30-5:30	0.984	0.986	4:30-6:30	0.873	0.925
4	4:45-5:45	0.947	0.959	4:45-6:45	0.831	0.896
5	5:00-6:00	0.935	0.941	5:00-7:00	0.791	0.858
6	5:15-6:15	0.870	0.909			
7	5:30-6:30	0.817	0.956			
8	5:45-6:45	0.823	0.922			
9	6:00-7:00	0.887	0.883			

North of Arlington Road

Tuesday, 8/19/03

Start Time	End Time	Northbound	Southbound	Both
4:00	4:15	316		316
4:15	4:30	393		393
4:30	4:45	398		398
4:45	**5:00**	**451**		**451**
5:00	**5:15**	**444**		**444**
5:15	**5:30**	**456**		**456**
5:30	**5:45**	**486**		**486**
5:45	6:00	410		410
6:00	6:15	334		334
6:15	6:30	347		347
6:30	6:45	303		303
6:45	7:00	291		291
Peak Hour:		1837	0	**1837**

	1-Hour Period	PHF NB	PHF SB	2-Hour Period	PPF NB	PPF SB
1	4:00-5:00	0.864		4:00-6:00	0.863	
2	4:15-5:15	0.935		4:15-6:15	0.867	
3	4:30-5:30	0.959		4:30-6:30	0.855	
4	4:45-5:45	0.945		4:45-6:45	0.831	
5	5:00-6:00	0.924		5:00-7:00	0.790	
6	5:15-6:15	0.867				
7	5:30-6:30	0.811				
8	5:45-6:45	0.850				
9	6:00-7:00	0.919				

South of Baywood Road

Tuesday, 8/19/03

Start Time	End Time	Northbound	Southbound	Both
4:00	4:15	283	184	467
4:15	4:30	387	242	629
4:30	4:45	339	235	574
4:45	**5:00**	**418**	**232**	**650**
5:00	**5:15**	**432**	**220**	**652**
5:15	**5:30**	**405**	**270**	**675**
5:30	**5:45**	**468**	**243**	**711**
5:45	6:00	370	200	570
6:00	6:15	316	231	547
6:15	6:30	308	231	539
6:30	6:45	279	210	489
6:45	7:00	229	211	440
Peak Hour:		1723	965	**2688**

	1-Hour Period	PHF NB	PHF SB	2-Hour Period	PPF NB	PPF SB
1	4:00-5:00	0.853	0.923	4:00-6:00	0.829	0.845
2	4:15-5:15	0.912	0.960	4:15-6:15	0.837	0.867
3	4:30-5:30	0.922	0.886	4:30-6:30	0.816	0.862
4	4:45-5:45	0.920	0.894	4:45-6:45	0.800	0.850
5	5:00-6:00	0.895	0.864	5:00-7:00	0.750	0.841
6	5:15-6:15	0.833	0.874			
7	5:30-6:30	0.781	0.931			
8	5:45-6:45	0.860	0.944			
9	6:00-7:00	0.896	0.956			

Wednesday, 8/20/03

Start Time	End Time	Northbound	Southbound	Both
4:00	4:15	422	266	688
4:15	4:30	423	245	668
4:30	**4:45**	**480**	**296**	**776**
4:45	**5:00**	**488**	**278**	**766**
5:00	**5:15**	**495**	**282**	**777**
5:15	**5:30**	**513**	**285**	**798**
5:30	5:45	507	251	758
5:45	6:00	468	258	726
6:00	6:15	374	278	652
6:15	6:30	347	246	593
6:30	6:45	343	292	635
6:45	7:00	282	232	514
Peak Hour:		1976	1141	**3117**

	1-Hour Period	PHF NB	PHF SB	2-Hour Period	PPF NB	PPF SB
1	4:00-5:00	0.929	0.916	4:00-6:00	0.925	0.913
2	4:15-5:15	0.953	0.930	4:15-6:15	0.913	0.918
3	4:30-5:30	0.963	0.964	4:30-6:30	0.895	0.918
4	4:45-5:45	0.976	0.961	4:45-6:45	0.861	0.929
5	5:00-6:00	0.966	0.944	5:00-7:00	0.811	0.909
6	5:15-6:15	0.907	0.940			
7	5:30-6:30	0.836	0.929			
8	5:45-6:45	0.818	0.920			
9	6:00-7:00	0.900	0.897			

Wednesday, 8/20/03

Start Time	End Time	Northbound	Southbound	Both
4:00	4:15	327		327
4:15	4:30	363		363
4:30	4:45	370		370
4:45	**5:00**	**423**		**423**
5:00	**5:15**	**411**		**411**
5:15	**5:30**	**443**		**443**
5:30	**5:45**	**425**		**425**
5:45	6:00	422		422
6:00	6:15	310		310
6:15	6:30	309		309
6:30	6:45	352		352
6:45	7:00	244		244
Peak Hour:		1702	0	**1702**

	1-Hour Period	PHF NB	PHF SB	2-Hour Period	PPF NB	PPF SB
1	4:00-5:00	0.876		4:00-6:00	0.898	
2	4:15-5:15	0.926		4:15-6:15	0.894	
3	4:30-5:30	0.929		4:30-6:30	0.878	
4	4:45-5:45	0.960		4:45-6:45	0.873	
5	5:00-6:00	0.960		5:00-7:00	0.823	
6	5:15-6:15	0.903				
7	5:30-6:30	0.862				
8	5:45-6:45	0.825				
9	6:00-7:00	0.863				

Wednesday, 8/20/03

Start Time	End Time	Northbound	Southbound	Both
4:00	4:15	295	200	495
4:15	4:30	305	188	493
4:30	4:45	349	222	571
4:45	**5:00**	**410**	**216**	**626**
5:00	**5:15**	**381**	**222**	**603**
5:15	**5:30**	**410**	**235**	**645**
5:30	**5:45**	**427**	**225**	**652**
5:45	6:00	398	216	614
6:00	6:15	303	231	534
6:15	6:30	274	247	521
6:30	6:45	324	245	569
6:45	7:00	230	219	449
Peak Hour:		1628	898	**2526**

	1-Hour Period	PHF NB	PHF SB	2-Hour Period	PPF NB	PPF SB
1	4:00-5:00	0.829	0.930	4:00-6:00	0.871	0.917
2	4:15-5:15	0.881	0.955	4:15-6:15	0.873	0.934
3	4:30-5:30	0.945	0.952	4:30-6:30	0.864	0.918
4	4:45-5:45	0.953	0.955	4:45-6:45	0.857	0.930
5	5:00-6:00	0.946	0.955	5:00-7:00	0.804	0.931
6	5:15-6:15	0.900	0.965			
7	5:30-6:30	0.821	0.930			
8	5:45-6:45	0.816	0.950			
9	6:00-7:00	0.873	0.953			

Thursday, 8/21/03

Start Time	End Time	Northbound	Southbound	Both
4:00	4:15	414	243	657
4:15	4:30	443	290	733
4:30	**4:45**	**479**	**301**	**780**
4:45	**5:00**	**455**	**260**	**715**
5:00	**5:15**	**496**	**293**	**789**
5:15	**5:30**	**476**	**277**	**753**
5:30	5:45	498	280	778
5:45	6:00	434	243	677
6:00	6:15	407	279	686
6:15	6:30	350	279	629
6:30	6:45	327	243	570
6:45	7:00	303	249	552
Peak Hour:		1906	1131	**3037**

	1-Hour Period	PHF NB	PHF SB	2-Hour Period	PPF NB	PPF SB
1	4:00-5:00	0.935	0.909	4:00-6:00	0.927	0.908
2	4:15-5:15	0.944	0.950	4:15-6:15	0.926	0.923
3	4:30-5:30	0.961	0.939	4:30-6:30	0.902	0.919
4	4:45-5:45	0.966	0.947	4:45-6:45	0.864	0.919
5	5:00-6:00	0.956	0.933	5:00-7:00	0.826	0.914
6	5:15-6:15	0.911	0.963			
7	5:30-6:30	0.848	0.965			
8	5:45-6:45	0.874	0.935			
9	6:00-7:00	0.852	0.941			

Lowest	0.817	0.883	0.791	0.858
Highest	0.984	0.986	0.927	0.929
Average	0.913	0.937	0.875	0.913
Lowest	0.781	0.864	0.750	0.841
Highest	0.984	0.986	0.927	0.939
Average	**0.902**	0.936	**0.861**	0.908

Thursday, 8/21/03

Start Time	End Time	Northbound	Southbound	Both
4:00	4:15	331		331
4:15	4:30	366		366
4:30	4:45	406		406
4:45	5:00	400		400
5:00	**5:15**	**425**		**425**
5:15	**5:30**	**432**		**432**
5:30	**5:45**	**440**		**440**
5:45	**6:00**	**410**		**410**
6:00	6:15	355		355
6:15	6:30	317		317
6:30	6:45	314		314
6:45	7:00	242		242
Peak Hour:		1707	0	**1707**

	1-Hour Period	PHF NB	PHF SB	2-Hour Period	PPF NB	PPF SB
1	4:00-5:00	0.925		4:00-6:00	0.912	
2	4:15-5:15	0.939		4:15-6:15	0.919	
3	4:30-5:30	0.962		4:30-6:30	0.905	
4	4:45-5:45	0.964		4:45-6:45	0.879	
5	5:00-6:00	0.970		5:00-7:00	0.834	
6	5:15-6:15	0.930				
7	5:30-6:30	0.865				
8	5:45-6:45	0.851				
9	6:00-7:00	0.865				

Lowest	0.811	0.790		
Highest	0.970	0.919		
Average	0.906	0.868		

Thursday, 8/21/03

Start Time	End Time	Northbound	Southbound	Both
4:00	4:15	293	209	502
4:15	4:30	314	214	528
4:30	4:45	370	206	576
4:45	**5:00**	**413**	**216**	**629**
5:00	**5:15**	**413**	**236**	**649**
5:15	**5:30**	**382**	**207**	**589**
5:30	**5:45**	**427**	**227**	**654**
5:45	6:00	355	223	578
6:00	6:15	348	239	587
6:15	6:30	312	236	548
6:30	6:45	293	212	505
6:45	7:00	221	198	419
Peak Hour:		1635	886	**2521**

	1-Hour Period	PHF NB	PHF SB	2-Hour Period	PPF NB	PPF SB
1	4:00-5:00	0.841	0.978	4:00-6:00	0.869	0.921
2	4:15-5:15	0.914	0.924	4:15-6:15	0.885	0.925
3	4:30-5:30	0.955	0.916	4:30-6:30	0.884	0.936
4	4:45-5:45	0.957	0.939	4:45-6:45	0.862	0.939
5	5:00-6:00	0.923	0.946	5:00-7:00	0.805	0.930
6	5:15-6:15	0.885	0.937			
7	5:30-6:30	0.844	0.968			
8	5:45-6:45	0.921	0.952			
9	6:00-7:00	0.843	0.926			

Lowest	0.781	0.864	0.750	0.841
Highest	0.957	0.978	0.885	0.939
Average	0.886	0.936	0.840	0.903

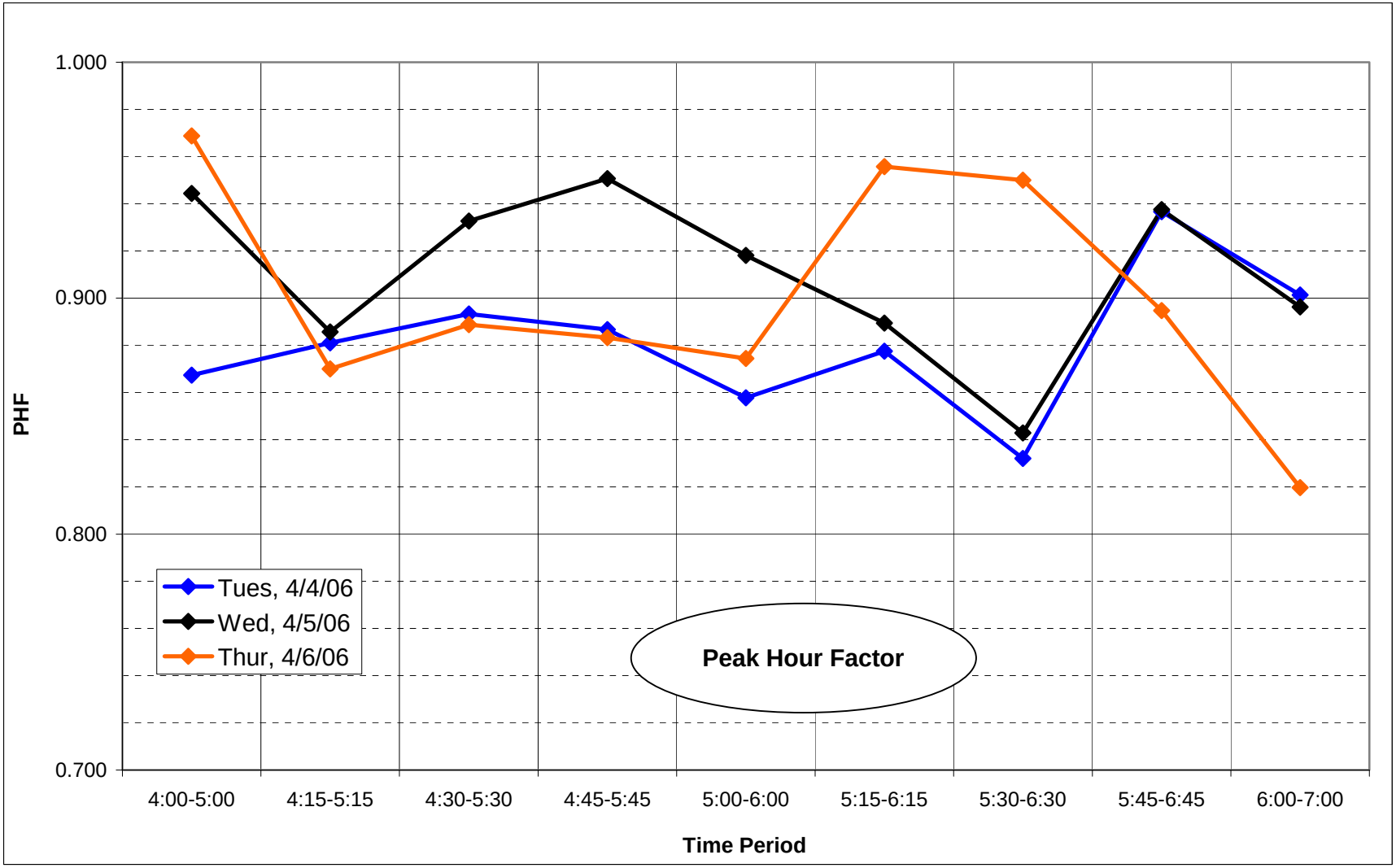

Figure B-9. SR A1A S. PM peak hour factor, southbound (outbound) flow

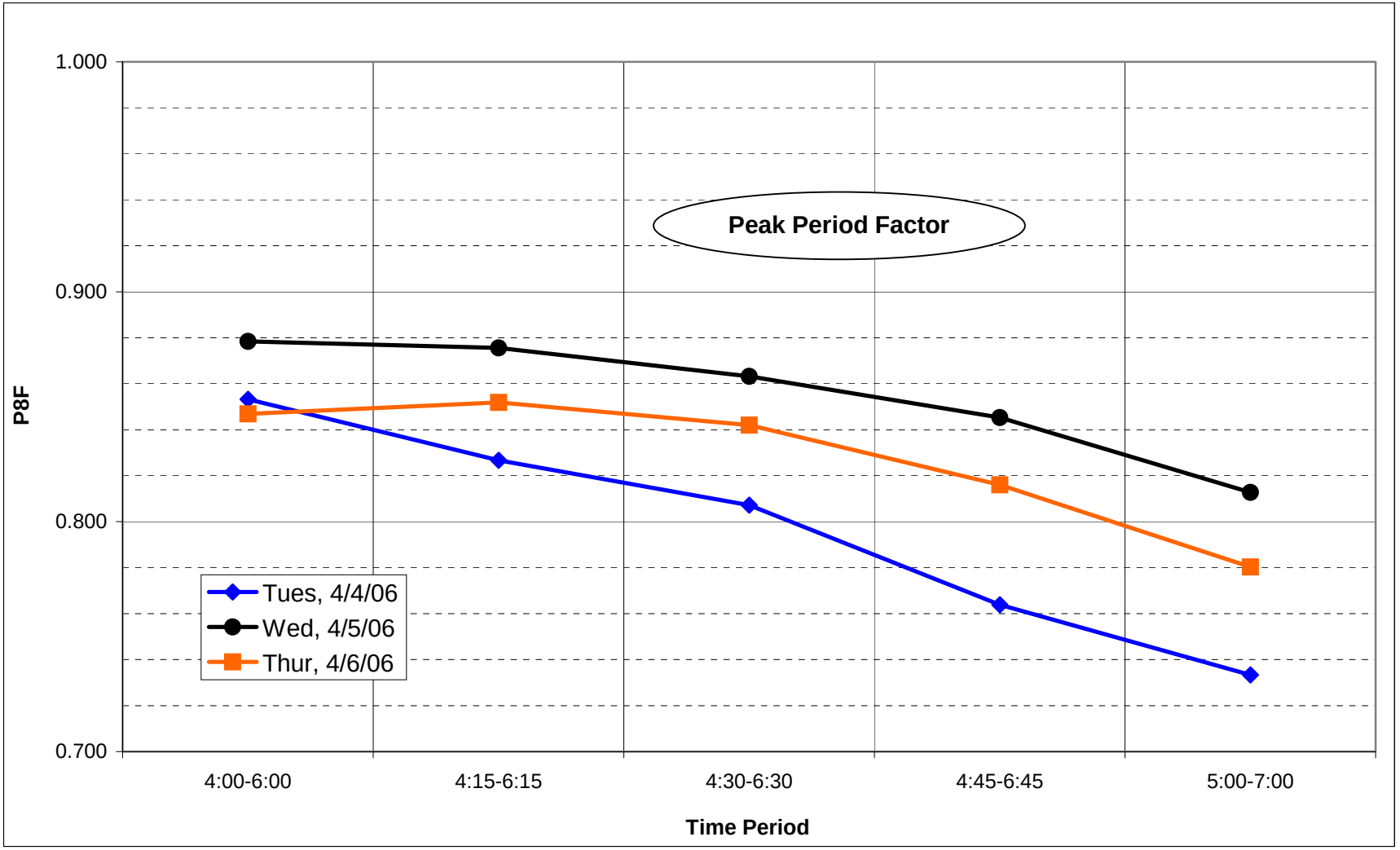

Figure B-10. SR A1A S. PM peak period factor, southbound (outbound) flow

Table B-5. SR A1A machine counts (Crescent Beach)

North of Riverside Boulevard

Tuesday, 4/4/06

Start Time	End Time	Southbound	Northbound	Both
4:00	4:15	230	149	379
4:15	4:30	187	161	348
4:30	**4:45**	**201**	**151**	**352**
4:45	**5:00**	**180**	**166**	**346**
5:00	**5:15**	**225**	**158**	**383**
5:15	**5:30**	**198**	**154**	**352**
5:30	5:45	195	154	349
5:45	6:00	154	146	300
6:00	6:15	148	122	270
6:15	6:30	152	151	303
6:30	6:45	123	134	257
6:45	7:00	125	118	243
Peak Hour:		804	629	**1433**

Wednesday, 4/5/06

Start Time	End Time	Southbound	Northbound	Both
4:00	4:15	181	195	376
4:15	4:30	175	177	352
4:30	4:45	194	171	365
4:45	**5:00**	**198**	**159**	**357**
5:00	**5:15**	**223**	**171**	**394**
5:15	**5:30**	**217**	**167**	**384**
5:30	**5:45**	**210**	**163**	**373**
5:45	6:00	169	161	330
6:00	6:15	176	149	325
6:15	6:30	153	132	285
6:30	6:45	162	151	313
6:45	7:00	140	128	268
Peak Hour:		848	660	**1508**

Thursday, 4/6/06

Start Time	End Time	Southbound	Northbound	Both
4:00	4:15	181	200	381
4:15	**4:30**	**181**	**188**	**369**
4:30	**4:45**	**192**	**162**	**354**
4:45	**5:00**	**190**	**191**	**381**
5:00	**5:15**	**227**	**171**	**398**
5:15	5:30	198	153	351
5:30	5:45	187	174	361
5:45	6:00	182	158	340
6:00	6:15	190	150	340
6:15	6:30	163	137	300
6:30	6:45	145	141	286
6:45	7:00	125	122	247
Peak Hour:		790	712	**1502**

	1-Hour Period	PHF SB	PHF NB	2-Hour Period	PPF SB	PPF NB
1	4:00-5:00	0.867	0.944	4:00-6:00	0.853	0.933
2	4:15-5:15	0.881	0.958	4:15-6:15	0.827	0.913
3	4:30-5:30	0.893	0.947	4:30-6:30	0.807	0.905
4	4:45-5:45	0.887	0.952	4:45-6:45	0.764	0.892
5	5:00-6:00	0.858	0.968	5:00-7:00	0.733	0.900
6	5:15-6:15	0.878	0.935			
7	5:30-6:30	0.832	0.930			
8	5:45-6:45	0.937	0.916			
9	6:00-7:00	0.901	0.869			

	1-Hour Period	PHF SB	PHF NB	2-Hour Period	PPF SB	PPF NB
1	4:00-5:00	0.944	0.900	4:00-6:00	0.878	0.874
2	4:15-5:15	0.886	0.958	4:15-6:15	0.876	0.931
3	4:30-5:30	0.933	0.977	4:30-6:30	0.863	0.931
4	4:45-5:45	0.951	0.965	4:45-6:45	0.845	0.916
5	5:00-6:00	0.918	0.968	5:00-7:00	0.813	0.893
6	5:15-6:15	0.889	0.958			
7	5:30-6:30	0.843	0.928			
8	5:45-6:45	0.938	0.921			
9	6:00-7:00	0.896	0.927			

	1-Hour Period	PHF SB	PHF NB	2-Hour Period	PPF SB	PPF NB
1	4:00-5:00	0.969	0.926	4:00-6:00	0.847	0.873
2	4:15-5:15	0.870	0.932	4:15-6:15	0.852	0.882
3	4:30-5:30	0.889	0.886	4:30-6:30	0.842	0.848
4	4:45-5:45	0.883	0.902	4:45-6:45	0.816	0.834
5	5:00-6:00	0.874	0.943	5:00-7:00	0.780	0.866
6	5:15-6:15	0.956	0.912			
7	5:30-6:30	0.950	0.889			
8	5:45-6:45	0.895	0.927			
9	6:00-7:00	0.820	0.917			

	PHF SB	PHF NB	PPF SB	PPF NB
Lowest	0.820	0.869	0.733	0.834
Highest	0.969	0.977	0.878	0.933
Average	0.898	0.932	0.826	0.893

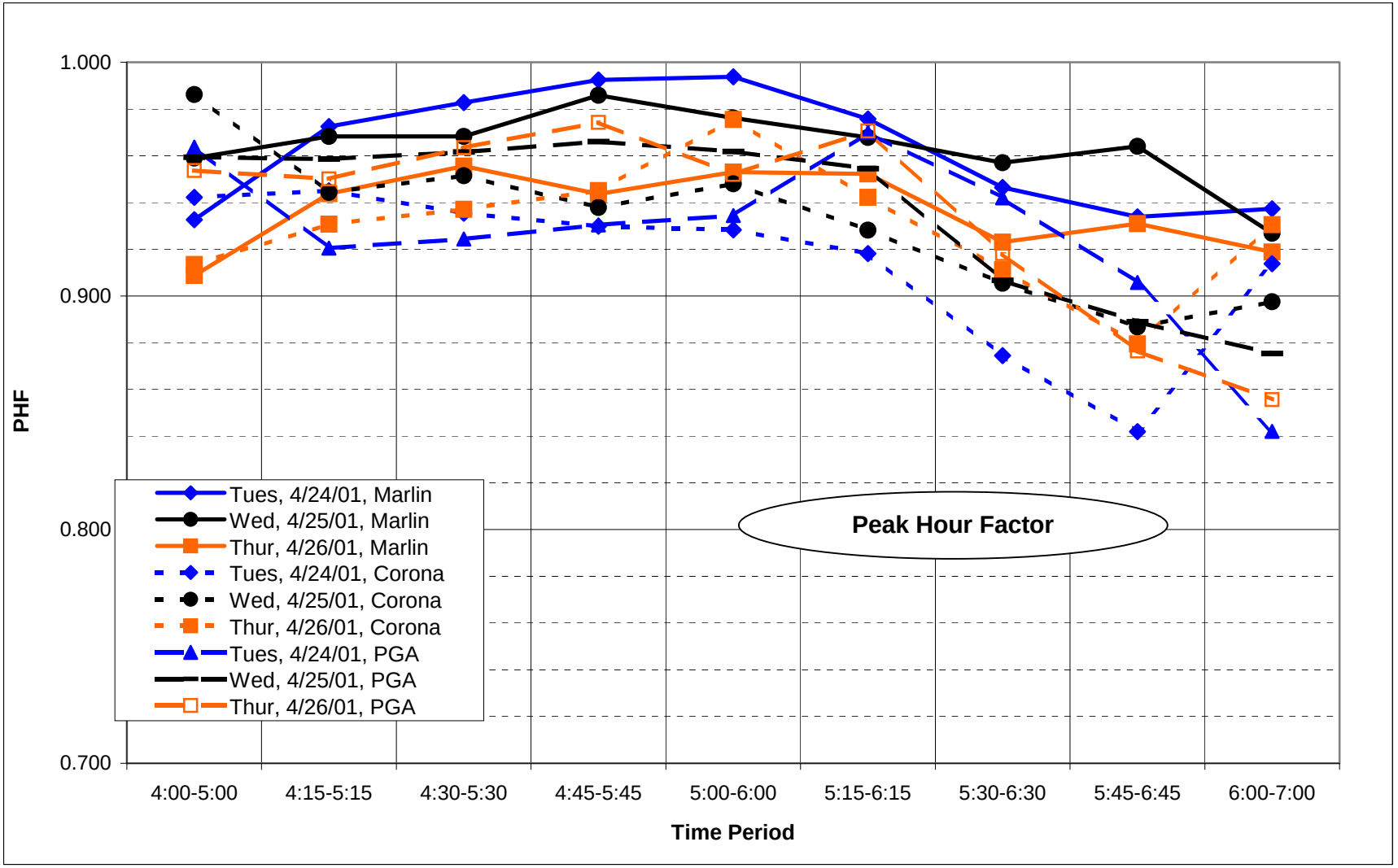

Figure B-11 - SR A1A N. PM peak hour factor, southbound (outbound) flow

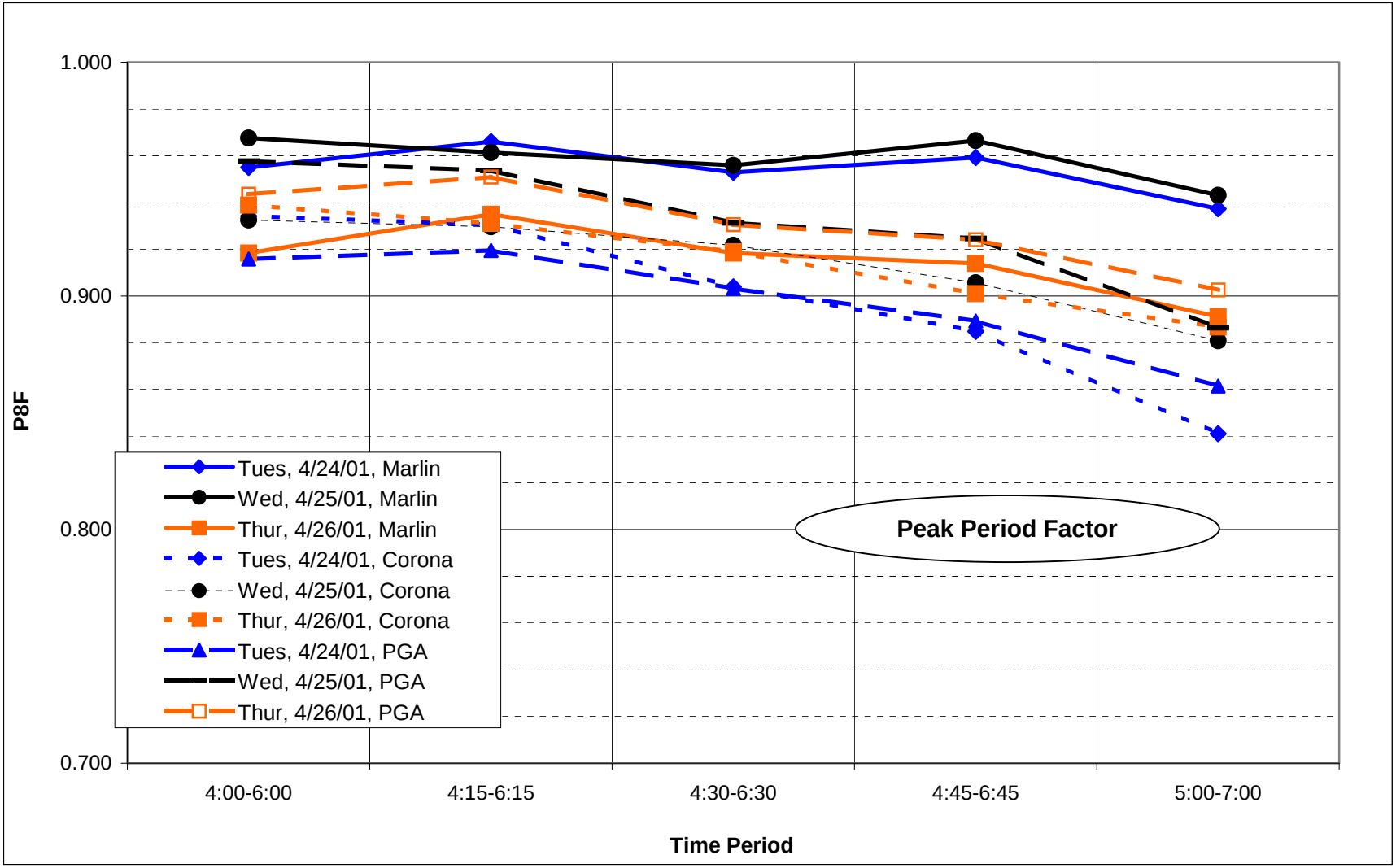

Figure B-12. SR A1A N. PM peak period factor, southbound (outbound) flow

Table B-6. SR A1A machine counts (Ponte Vedra) PDF 17 KB

North of Marlin Avenue

Tuesday, 4/24/01

Start Time	End Time	Southbound	Northbound	Both		1-Hour Period	PHF SB	PHF NB	2-Hour Period	PPF SB	PPF NB
4:00	4:15	497	533	1030	1	4:00-5:00	0.933	0.922	4:00-6:00	0.955	0.873
4:15	4:30	573	481	1054	2	4:15-5:15	0.972	0.847	4:15-6:15	0.966	0.855
4:30	4:45	608	450	1058	3	4:30-5:30	0.983	0.889	4:30-6:30	0.953	0.843
4:45	5:00	590	502	1092	4	4:45-5:45	0.992	0.926	4:45-6:45	0.959	0.829
5:00	**5:15**	**594**	**600**	**1194**	5	5:00-6:00	0.994	0.927	5:00-7:00	0.937	0.805
5:15	**5:30**	**598**	**582**	**1180**	6	5:15-6:15	0.976	0.890			
5:30	**5:45**	**592**	**539**	**1131**	7	5:30-6:30	0.946	0.887			
5:45	**6:00**	**593**	**504**	**1097**	8	5:45-6:45	0.934	0.872			
6:00	6:15	551	446	997	9	6:00-7:00	0.937	0.919			
6:15	6:30	509	423	932							
6:30	6:45	562	384	946							
6:45	7:00	485	387	872							
Peak Hour:		2377	2225	**4602**							

Wednesday, 4/25/01

Start Time	End Time	Southbound	Northbound	Both							
4:00	4:15	542	469	1011	1	4:00-5:00	0.959	0.960	4:00-6:00	0.968	0.905
4:15	4:30	567	418	985	2	4:15-5:15	0.968	0.876	4:15-6:15	0.961	0.897
4:30	4:45	513	456	969	3	4:30-5:30	0.968	0.917	4:30-6:30	0.956	0.906
4:45	5:00	553	458	1011	4	4:45-5:45	0.986	0.941	4:45-6:45	0.966	0.883
5:00	**5:15**	**563**	**532**	**1095**	5	5:00-6:00	0.976	0.964	5:00-7:00	0.943	0.844
5:15	**5:30**	**567**	**505**	**1072**	6	5:15-6:15	0.968	0.963			
5:30	**5:45**	**553**	**507**	**1060**	7	5:30-6:30	0.957	0.940			
5:45	**6:00**	**531**	**507**	**1038**	8	5:45-6:45	0.964	0.867			
6:00	6:15	575	434	1009	9	6:00-7:00	0.927	0.840			
6:15	6:30	542	459	1001							
6:30	6:45	577	358	935							
6:45	7:00	445	292	737							
Peak Hour:		2214	2051	**4265**							

Thursday, 4/26/01

Start Time	End Time	Southbound	Northbound	Both							
4:00	4:15	475	551	1026	1	4:00-5:00	0.909	0.920	4:00-6:00	0.918	0.882
4:15	4:30	600	488	1088	2	4:15-5:15	0.944	0.908	4:15-6:15	0.935	0.866
4:30	4:45	543	497	1040	3	4:30-5:30	0.956	0.893	4:30-6:30	0.918	0.865
4:45	5:00	563	492	1055	4	4:45-5:45	0.944	0.905	4:45-6:45	0.914	0.850
5:00	**5:15**	**559**	**561**	**1120**	5	5:00-6:00	0.953	0.922	5:00-7:00	0.891	0.829
5:15	**5:30**	**590**	**603**	**1193**	6	5:15-6:15	0.952	0.886			
5:30	**5:45**	**617**	**528**	**1145**	7	5:30-6:30	0.923	0.948			
5:45	**6:00**	**586**	**533**	**1119**	8	5:45-6:45	0.931	0.900			
6:00	6:15	557	474	1031	9	6:00-7:00	0.919	0.910			
6:15	6:30	518	487	1005							
6:30	6:45	521	424	945							
6:45	7:00	451	387	838							
Peak Hour:		2352	2225	**4577**							

Lowest	0.909	0.840	0.891	0.805
Highest	0.994	0.964	0.968	0.906
Average	0.954	0.909	0.943	0.862
Lowest	0.842	0.796	0.841	0.793
Highest	0.994	0.972	0.968	0.915
Average	**0.937**	0.901	**0.924**	0.856

North of Corona Road

Tuesday, 4/24/01

Start Time	End Time	Southbound	Northbound	Both		1-Hour Period	PHF SB	PHF NB	2-Hour Period	PPF SB	PPF NB
4:00	4:15	381	362	743	1	4:00-5:00	0.942	0.881	4:00-6:00	0.934	0.890
4:15	4:30	436	340	776	2	4:15-5:15	0.945	0.909	4:15-6:15	0.930	0.876
4:30	4:45	415	369	784	3	4:30-5:30	0.935	0.932	4:30-6:30	0.904	0.863
4:45	**5:00**	**445**	**424**	**869**	4	4:45-5:45	0.930	0.949	4:45-6:45	0.885	0.834
5:00	**5:15**	**386**	**408**	**794**	5	5:00-6:00	0.928	0.934	5:00-7:00	0.841	0.816
5:15	**5:30**	**419**	**379**	**798**	6	5:15-6:15	0.918	0.899			
5:30	**5:45**	**405**	**398**	**803**	7	5:30-6:30	0.874	0.845			
5:45	6:00	446	340	786	8	5:45-6:45	0.842	0.898			
6:00	6:15	368	314	682	9	6:00-7:00	0.914	0.905			
6:15	6:30	341	294	635							
6:30	6:45	347	273	620							
6:45	7:00	289	256	545							
Peak Hour:		1655	1609	**3264**							

Wednesday, 4/25/01

Start Time	End Time	Southbound	Northbound	Both							
4:00	4:15	398	298	696	1	4:00-5:00	0.986	0.861	4:00-6:00	0.933	0.867
4:15	4:30	397	323	720	2	4:15-5:15	0.944	0.897	4:15-6:15	0.930	0.884
4:30	4:45	387	344	731	3	4:30-5:30	0.951	0.932	4:30-6:30	0.922	0.867
4:45	**5:00**	**388**	**395**	**783**	4	4:45-5:45	0.938	0.943	4:45-6:45	0.906	0.838
5:00	**5:15**	**422**	**356**	**778**	5	5:00-6:00	0.948	0.899	5:00-7:00	0.881	0.793
5:15	**5:30**	**409**	**377**	**786**	6	5:15-6:15	0.928	0.896			
5:30	**5:45**	**364**	**407**	**771**	7	5:30-6:30	0.905	0.830			
5:45	6:00	428	324	752	8	5:45-6:45	0.887	0.850			
6:00	6:15	388	351	739	9	6:00-7:00	0.898	0.796			
6:15	6:30	370	269	639							
6:30	6:45	332	249	581							
6:45	7:00	303	249	552							
Peak Hour:		1583	1535	**3118**							

Thursday, 4/26/01

Start Time	End Time	Southbound	Northbound	Both							
4:00	4:15	394	371	765	1	4:00-5:00	0.913	0.842	4:00-6:00	0.939	0.842
4:15	4:30	390	383	773	2	4:15-5:15	0.931	0.840	4:15-6:15	0.931	0.839
4:30	4:45	433	335	768	3	4:30-5:30	0.937	0.854	4:30-6:30	0.919	0.821
4:45	**5:00**	**365**	**460**	**825**	4	4:45-5:45	0.945	0.900	4:45-6:45	0.901	0.808
5:00	**5:15**	**424**	**368**	**792**	5	5:00-6:00	0.975	0.923	5:00-7:00	0.887	0.826
5:15	**5:30**	**401**	**408**	**809**	6	5:15-6:15	0.942	0.917			
5:30	**5:45**	**428**	**420**	**848**	7	5:30-6:30	0.911	0.863			
5:45	6:00	417	355	772	8	5:45-6:45	0.879	0.920			
6:00	6:15	367	358	725	9	6:00-7:00	0.931	0.855			
6:15	6:30	348	317	665							
6:30	6:45	335	287	622							
6:45	7:00	316	262	578							
Peak Hour:		1618	1656	**3274**							

Lowest	0.842	0.796	0.841	0.793
Highest	0.986	0.949	0.939	0.890
Average	0.925	0.888	0.909	0.844

North of PGA Tour Boulevard

Tuesday, 4/24/01

Start Time	End Time	Southbound	Northbound	Both		1-Hour Period	PHF SB	PHF NB	2-Hour Period	PPF SB	PPF NB
4:00	4:15	342	327	669	1	4:00-5:00	0.964	0.911	4:00-6:00	0.916	0.892
4:15	4:30	351	263	614	2	4:15-5:15	0.920	0.925	4:15-6:15	0.919	0.876
4:30	4:45	326	335	661	3	4:30-5:30	0.924	0.970	4:30-6:30	0.903	0.883
4:45	**5:00**	**334**	**350**	**684**	4	4:45-5:45	0.930	0.949	4:45-6:45	0.889	0.852
5:00	**5:15**	**377**	**347**	**724**	5	5:00-6:00	0.934	0.913	5:00-7:00	0.861	0.810
5:15	**5:30**	**357**	**326**	**683**	6	5:15-6:15	0.970	0.868			
5:30	**5:45**	**335**	**366**	**701**	7	5:30-6:30	0.942	0.837			
5:45	6:00	340	298	638	8	5:45-6:45	0.906	0.927			
6:00	6:15	353	281	634	9	6:00-7:00	0.842	0.922			
6:15	6:30	302	281	583							
6:30	6:45	284	245	529							
6:45	7:00	250	229	479							
Peak Hour:		1403	1389	**2792**							

Wednesday, 4/25/01

Start Time	End Time	Southbound	Northbound	Both							
4:00	4:15	326	250	576	1	4:00-5:00	0.959	0.896	4:00-6:00	0.958	0.909
4:15	4:30	333	322	655	2	4:15-5:15	0.959	0.936	4:15-6:15	0.954	0.915
4:30	4:45	300	278	578	3	4:30-5:30	0.962	0.972	4:30-6:30	0.931	0.881
4:45	5:00	338	304	642	4	4:45-5:45	0.966	0.935	4:45-6:45	0.925	0.867
5:00	**5:15**	**325**	**301**	**626**	5	5:00-6:00	0.962	0.943	5:00-7:00	0.886	0.836
5:15	**5:30**	**337**	**299**	**636**	6	5:15-6:15	0.954	0.917			
5:30	**5:45**	**306**	**330**	**636**	7	5:30-6:30	0.907	0.866			
5:45	**6:00**	**340**	**315**	**655**	8	5:45-6:45	0.889	0.837			
6:00	6:15	315	266	581	9	6:00-7:00	0.875	0.904			
6:15	6:30	272	232	504							
6:30	6:45	282	241	523							
6:45	7:00	234	223	457							
Peak Hour:		1308	1245	**2553**							

Thursday, 4/26/01

Start Time	End Time	Southbound	Northbound	Both							
4:00	4:15	327	350	677	1	4:00-5:00	0.954	0.941	4:00-6:00	0.943	0.881
4:15	4:30	330	327	657	2	4:15-5:15	0.950	0.874	4:15-6:15	0.951	0.862
4:30	4:45	356	335	691	3	4:30-5:30	0.963	0.878	4:30-6:30	0.930	0.850
4:45	5:00	345	306	651	4	4:45-5:45	0.974	0.876	4:45-6:45	0.924	0.821
5:00	**5:15**	**322**	**388**	**710**	5	5:00-6:00	0.952	0.914	5:00-7:00	0.903	0.803
5:15	**5:30**	**349**	**333**	**682**	6	5:15-6:15	0.971	0.906			
5:30	**5:45**	**344**	**333**	**677**	7	5:30-6:30	0.918	0.876			
5:45	**6:00**	**314**	**364**	**678**	8	5:45-6:45	0.876	0.816			
6:00	6:15	348	289	637	9	6:00-7:00	0.856	0.929			
6:15	6:30	272	289	561							
6:30	6:45	286	246	532							
6:45	7:00	285	250	535							
Peak Hour:		1329	1418	**2747**							

Lowest	0.842	0.816	0.861	0.803
Highest	0.974	0.972	0.958	0.915
Average	0.933	0.905	0.920	0.862

Table B-7. Appendix B data summary.

			Peak Direction	3-Day Minimum PHF	3-Day Average PHF	3-Day Maximum PHF
	Atlantic Boulevard	West of Arlington Road	Eastbound	0.708	0.871	0.971
> 0.70	US 1 North	North of Estrella Avenue	Northbound	0.743	0.873	0.978
	US 1 North	South of Lewis Speedway	Northbound	0.747	0.890	0.972
> 0.75	University Boulevard	South of Baywood Road	Northbound	0.781	0.886	0.957
	US 1 South	North of SR 206	Southbound	0.784	0.885	0.982
	University Boulevard	North of Arlington Road	Northbound	0.811	0.906	0.970
	Atlantic Boulevard	East of University Boulevard	Eastbound	0.815	0.922	0.977
	University Boulevard	South of Los Santos Drive	Northbound	0.817	0.913	0.984
> 0.80	SR A1A	North of Riverside Boulevard	Southbound	0.820	0.898	0.969
	Atlantic Boulevard	West of Southside Boulevard	Eastbound	0.825	0.919	0.986
	SR A1A	North of Corona Road	Southbound	0.842	0.925	0.986
	SR A1A	North of PGA Tour Boulevard	Southbound	0.842	0.933	0.974
	SR A1A	North of Marlin Avenue	Southbound	0.909	0.954	0.994
			Overall Minimum	**0.71**	0.87	0.96
			Overall Average	0.80	**0.91**	0.98
			Overall Maximum	0.91	0.95	**0.99**

APPENDIX C
GENERALIZED CYCLE-PERIOD DELAY EXAMPLE:

Table C-1. Generalized example of cycle-period delay discrepancies – data.

A	B	C	D	E	F	G	H	I	J	K	L	M	N	O	P	Q	R	S	T	U	V	W	X	Y	Z	AA	AB	AC	AD	AE	AF	AG	AH	AI	AJ	AK	AL	AM	AN	AO	AP	AQ	AR	AS	AT
Cycle Length:	**60 seconds**																																													
Red/Green Pattern:	Start on Full Red						Start on Full Green					Start on Half Green					Start on Full Red					Start on Full Green					Start on Half Green					Start on Full Red					Start on Full Green					Start on Half Green				
Period 1																																													
Actual Arrivals & Departures/Thruput (vph):		720	600				720	576				720	588				720	572			vph	720	593			vph	720	582			vph	720	540			vph	720	583			vph	720	562		
Actual Arrivals & Departures/Thruput (@15min):		180	150				180	144				180	147				180	143				180	148				180	146				180	135				180	146				180	140		
Period 2																																													
Actual Arrivals & Departures/Thruput (vph):		520	600				520	600				520	600				520	624			vph	520	584			vph	520	610			vph	520	648			vph	520	576			vph	520	630		
Actual Arrivals, Dep/Thruput (veh per 15min):		130	150				130	150				130	150				130	156				130	146				130	153				130	162				130	144				130	158		
Actual Arrivals & Dep/Thruput (@30min):		310	300				310	284				310	297				310	299				310	294				310	288				310	287				310	290				310	298		
A=Arrivals, D=Departures, Q=Queue:		A	D	Q			A	D	Q			A	D	Q			A	D	Q			A	D	Q			A	D	Q			A	D	Q			A	D	Q			A	D	Q		
Time (sec)																																													
0		0	0				0	0				0	0				0	0				0	0				0	0				0	0				0	0				0	0		
1	R	0	0	0	G	0	0	0	G	0	0	0	R	0	0	0	G	0	0	0	G	0	0	0	R	0	0	0	G	0	0	0	G	0	0	0	G	0	0	0	G	0	0	0	G	0	0	0
2	R	0	0	0	G	0	0	0	G	0	0	0	R	0	0	0	G	0	0	0	G	0	0	0	R	0	0	0	G	0	0	0	G	0	0	0	G	0	0	0	G	0	0	0	G	0	0	0
3	R	1	0	1	G	1	1	0	G	1	1	0	R	1	0	1	G	1	1	0	G	1	1	0	R	1	0	1	G	1	1	0	G	1	1	0	G	1	1	0	G	1	1	0	G	1	1	0
4	R	1	0	1	G	1	1	0	G	1	1	0	R	1	0	1	G	1	1	0	G	1	1	0	R	1	0	1	G	1	1	0	G	1	1	0	G	1	1	0	G	1	1	0	G	1	1	0
5	R	1	0	1	G	1	1	0	G	1	1	0	R	1	0	1	G	1	1	0	G	1	1	0	R	1	0	1	G	1	1	0	G	1	1	0	G	1	1	0	G	1	1	0	G	1	1	0
6	R	1	0	1	G	1	1	0	G	1	1	0	R	1	0	1	G	1	1	0	G	1	1	0	R	1	0	1	G	1	1	0	G	1	1	0	G	1	1	0	G	1	1	0	G	1	1	0
7	R	1	0	1	G	1	1	0	G	1	1	0	R	1	0	1	G	1	1	0	G	1	1	0	R	1	0	1	G	1	1	0	G	1	1	0	G	1	1	0	G	1	1	0	G	1	1	0
8	R	2	0	2	G	2	2	0	G	2	2	0	R	2	0	2	G	2	2	0	G	2	2	0	R	2	0	2	G	2	2	0	G	2	2	0	G	2	2	0	G	2	2	0	G	2	2	0
9	R	2	0	2	G	2	2	0	G	2	2	0	R	2	0	2	G	2	2	0	G	2	2	0	R	2	0	2	G	2	2	0	G	2	2	0	G	2	2	0	G	2	2	0	G	2	2	0
10	R	2	0	2	G	2	2	0	G	2	2	0	R	2	0	2	G	2	2	0	G	2	2	0	R	2	0	2	G	2	2	0	G	2	2	0	G	2	2	0	G	2	2	0	G	2	2	0
11	R	2	0	2	G	2	2	0	R	2	2	0	R	2	0	2	G	2	2	0	G	2	2	0	R	2	0	2	G	2	2	0	G	2	2	0	G	2	2	0	G	2	2	0	G	2	2	0
12	R	2	0	2	G	2	2	0	R	2	2	0	R	2	0	2	G	2	2	0	G	2	2	0	R	2	0	2	G	2	2	0	G	2	2	0	G	2	2	0	G	2	2	0	G	2	2	0
13	R	3	0	3	G	3	3	0	R	3	2	1	R	3	0	3	G	3	3	0	G	3	3	0	R	3	0	3	G	3	3	0	G	3	3	0	G	3	3	0	G	3	3	0	G	3	3	0
14	R	3	0	3	G	3	3	0	R	3	2	1	R	3	0	3	G	3	3	0	G	3	3	0	R	3	0	3	G	3	3	0	G	3	3	0	G	3	3	0	G	3	3	0	G	3	3	0
15	R	3	0	3	G	3	3	0	R	3	2	1	R	3	0	3	G	3	3	0	G	3	3	0	R	3	0	3	G	3	3	0	G	3	3	0	G	3	3	0	G	3	3	0	G	3	3	0
16	R	3	0	3	G	3	3	0	R	3	2	1	R	3	0	3	G	3	3	0	G	3	3	0	R	3	0	3	G	3	3	0	G	3	3	0	G	3	3	0	G	3	3	0	G	3	3	0
17	R	3	0	3	G	3	3	0	R	3	2	1	R	3	0	3	G	3	3	0	G	3	3	0	R	3	0	3	G	3	3	0	G	3	3	0	G	3	3	0	G	3	3	0	G	3	3	0
18	R	4	0	4	G	4	4	0	R	4	2	2	R	4	0	4	G	4	4	0	G	4	4	0	R	4	0	4	G	4	4	0	G	4	4	0	G	4	4	0	G	4	4	0	G	4	4	0
19	R	4	0	4	G	4	4	0	R	4	2	2	R	4	0	4	G	4	4	0	G	4	4	0	R	4	0	4	G	4	4	0	G	4	4	0	G	4	4	0	G	4	4	0	G	4	4	0
20	R	4	0	4	G	4	4	0	R	4	2	2	R	4	0	4	G	4	4	0	G	4	4	0	R	4	0	4	G	4	4	0	G	4	4	0	G	4	4	0	G	4	4	0	G	4	4	0
21	R	4	0	4	R	4	4	0	R	4	2	2	R	4	0	4	G	4	4	0	G	4	4	0	R	4	0	4	G	4	4	0	G	4	4	0	G	4	4	0	G	4	4	0	G	4	4	0
22	R	4	0	4	R	4	4	0	R	4	2	2	R	4	0	4	G	4	4	0	G	4	4	0	R	4	0	4	G	4	4	0	G	4	4	0	G	4	4	0	G	4	4	0	G	4	4	0
23	R	5	0	5	R	5	4	1	R	5	2	3	R	5	0	5	G	5	5	0	G	5	5	0	R	5	0	5	G	5	5	0	G	5	5	0	G	5	5	0	G	5	5	0	G	5	5	0
24	R	5	0	5	R	5	4	1	R	5	2	3	R	5	0	5	G	5	5	0	G	5	5	0	R	5	0	5	G	5	5	0	G	5	5	0	G	5	5	0	G	5	5	0	G	5	5	0
25	R	5	0	5	R	5	4	1	R	5	2	3	R	5	0	5	G	5	5	0	G	5	5	0	R	5	0	5	G	5	5	0	G	5	5	0	G	5	5	0	G	5	5	0	G	5	5	0
26	R	5	0	5	R	5	4	1	R	5	2	3	R	5	0	5	G	5	5	0	G	5	5	0	R	5	0	5	G	5	5	0	G	5	5	0	G	5	5	0	G	5	5	0	G	5	5	0
27	R	5	0	5	R	5	4	1	R	5	2	3	R	5	0	5	R	5	5	0	R	5	5	0	R	5	0	5	G	5	5	0	G	5	5	0	G	5	5	0	G	5	5	0	G	5	5	0
28	R	6	0	6	R	6	4	2	R	6	2	4	R	6	0	6	R	6	5	0	R	6	5	0	R	6	0	6	G	6	6	0	G	6	6	0	G	6	6	0	G	6	6	0	R	6	5	0
29	R	6	0	6	R	6	4	2	R	6	2	4	R	6	0	6	R	6	5	1	R	6	5	1	R	6	0	6	G	6	6	0	G	6	6	0	G	6	6	0	G	6	6	0	R	6	5	0
30	R	6	0	6	R	6	4	2	R	6	2	4	R	6	0	6	R	6	5	1	R	6	5	1	R	6	0	6	G	6	6	0	G	6	6	0	G	6	6	0	G	6	6	0	R	6	5	1
31	R	6	0	6	R	6	4	2	R	6	2	4	R	6	0	6	R	6	5	1	R	6	5	1	R	6	0	6	G	6	6	0	G	6	6	0	G	6	6	0	G	6	6	0	R	6	5	1
32	R	6	0	6	R	6	4	2	R	6	2	4	R	6	0	6	R	6	5	1	R	6	5	1	R	6	0	6	G	6	6	0	G	6	6	0	G	6	6	0	G	6	6	0	R	6	5	1
33	R	7	0	7	R	7	4	3	R	7	2	5	R	7	0	7	R	7	5	1	R	7	5	1	R	7	0	7	G	7	7	0	G	7	7	0	G	7	7	0	G	7	7	0	R	7	5	1
34	R	7	0	7	R	7	4	3	R	7	2	5	R	7	0	7	R	7	5	2	R	7	5	2	R	7	0	7	G	7	7	0	G	7	7	0	G	7	7	0	G	7	7	0	R	7	5	1
35	R	7	0	7	R	7	4	3	R	7	2	5	R	7	0	7	R	7	5	2	R	7	5	2	R	7	0	7	G	7	7	0	G	7	7	0	G	7	7	0	G	7	7	0	R	7	5	2
36	R	7	0	7	R	7	4	3	R	7	2	5	R	7	0	7	R	7	5	2	R	7	5	2	R	7	0	7	G	7	7	0	G	7	7	0	G	7	7	0	G	7	7	0	R	7	5	2
37	R	7	0	7	R	7	4	3	R	7	2	5	R	7	0	7	R	7	5	2	R	7	5	2	R	7	0	7	G	7	7	0	G	7	7	0	G	7	7	0	G	7	7	0	R	7	5	2
38	R	8	0	8	R	8	4	4	R	8	2	6	R	8	0	8	R	8	5	2	R	8	5	2	R	8	0	8	G	8	8	0	G	8	8	0	G	8	8	0	G	8	8	0	R	8	5	2
39	R	8	0	8	R	8	4	4	R	8	2	6	R	8	0	8	R	8	5	3	R	8	5	3	R	8	0	8	G	8	8	0	G	8	8	0	G	8	8	0	G	8	8	0	R	8	5	2
40	R	8	0	8	R	8	4	4	R	8	2	6	R	8	0	8	R	8	5	3	R	8	5	3	R	8	0	8	G	8	8	0	G	8	8	0	G	8	8	0	G	8	8	0	R	8	5	3
41	G	8	1	8	R	8	4	4	R	8	2	6	R	8	0	8	R	8	5	3	R	8	5	3	R	8	0	8	G	8	8	0	G	8	8	0	G	8	8	0	G	8	8	0	R	8	5	3
42	G	8	1	7	R	8	4	4	R	8	2	6	R	8	0	8	R	8	5	3	R	8	5	3	R	8	0	8	G	8	8	0	G	8	8	0	G	8	8	0	G	8	8	0	R	8	5	3
43	G	9	2	7	R	9	4	5	R	9	2	7	R	9	0	9	R	9	5	3	R	9	5	3	R	9	0	9	G	9	9	0	G	9	9	0	G	9	9	0	G	9	9	0	R	9	5	3
44	G	9	2	7	R	9	4	5	R	9	2	7	R	9	0	9	R	9	5	4	R	9	5	4	R	9	0	9	G	9	9	0	G	9	9	0	G	9	9	0	G	9	9	0	R	9	5	3
45	G	9	3	7	R	9	4	5	R	9	2	7	R	9	0	9	R	9	5	4	R	9	5	4	R	9	0	9	G	9	9	0	G	9	9	0	G	9	9	0	G	9	9	0	R	9	5	4
46	G	9	3	6	R	9	4	5	R	9	2	7	R	9	0	9	R	9	5	4	R	9	5	4	R	9	0	9	G	9	9	0	G	9	9	0	G	9	9	0	G	9	9	0	R	9	5	4
47	G	9	4	6	R	9	4	5	R	9	2	7	R	9	0	9	R	9	5	4	R	9	5	4	R	9	0	9	G	9	9	0	G	9	9	0	G	9	9	0	G	9	9	0	R	9	5	4
48	G	10	4	6	R	10	4	6	R	10	2	8	R	10	0	10	R	10	5	4	R	10	5	4	R	10	3	7	R	10	0	10	G	10	10	0	G	10	10	0	G	10	10	0	R	10	5	4
49	G	10	5	5	R	10	4	6	R	10	2	8	R	10	0	10	R	10	5	5	R	10	5	5	R	10	3	7	R	10	0	10	G	10	10	0	G	10	10	0	G	10	10	0	R	10	5	4
50	G	10	5	5	R	10	4	6	R	10	2	8	R	10	0	10	R	10	5	5	R	10	5	5	R	10	3	7	R	10	0	10	G	10	10	0	G	10	10	0	G	10	10	0	R	10	5	5
51	G	10	6	5	R	10	4	6	G	10	3	8	R	10	0	10	R	10	5	5	R	10	5	5	R	10	3	8	R	10	0	10	G	10	10	0	G	10	10	0	G	10	10	0	R	10	5	5
52	G	10	6	4	R	10	4	6	G	10	3	7	R	10.4	0.0	10.4	R	10	5	5	R	10	5	5	R	10	3	8	R	10	0	10	G	10	10	0	G	10	10	0	G	10	10	0	R	10	5	5
53	G	11	7	4	R	11	4	7	G	11	4	7	G	11	1	10	R	11	5	5	R	11	5	5	R	11	3	8	R	11	0	11	G	11	11	0	R	11	5	5	R	11	5	5	R	11	5	5
54	G	11	7	4	R	11	4	7	G	11	4	7	G	11	1	10	R	11	5	6	R	11	5	6	R	11	3	8	R	11	0	11	G	11	11	0	R	11	5	5	R	11	5	5	R	11	5	5
55	G	11	8	3	R	11	4	7	G	11	5	6	G	11	2	9	R	11	5	6	R	11	5	6	R	11	3	8	R	11	0	11	R	11	11	0	R	11	5	6	R	11	5	6	R	11	5	6
56	G	11	8	3	R	11	4	7	G	11	5	6	G	11	2	9	R	11	5	6	R	11	5	6	R	11	3	9	R	11	0	11	R	11	11	0	R	11	5	6	R	11	5	6	R	11	5	6
57	G	11	9	3	R	11	4	7	G	11	6	6	G	11	3	9	R	11	5	6	R	11	5	6	R	11	3	9	R	11	0	11	R	11	11	1	R	11	5	6	R	11	5	6	R	11	5	6
58	G	12	9	3	R	12	4	8	G	12	6	6	G	12	3	9	R	12	5	6	R	12	5	6	R	12	3	9	R	12	0	12	R	12	11	1	R	12	5	6	R	12	5	6	R	12	5	6
59	G	12	10	2	R	12	4	8	G	12	7	5	G	12	4	8	R	12	5	7	R	12	5	7	R	12	3	9	R	12	0	12	R	12	11	1	R	12	5	6	R	12	5	6	R	12	5	6
60	G	12	10	2	R	12	4	8	G	12	7	5	G	12	4	8	R	12	5	7	R	12	5	7	R	12	3	9	R	12	0	12	R	12	11	1	R	12	5	7	R	12	5	7	R	12	5	7
61	R	12	10	2	G	12	5	8	G	12	8	5	G	12	5	8	R	12	5	7	R	12	5	7	R	12	3	10	R	12	0	12	R	12	11	1	R	12	5	7	R	12	5	7	R	12	5	7
62	R	12	10	2	G	12	5	7	G	12	8	4	G	12	5	7	R	12	5	7	R	12	5	7	R	12	3	10	R	12	0	12	R	12	11	2	R	12	5	7	R	12	5	7	R	12	5	7
63	R	13	10	3	G	13	6	7	G	13	9	4	G	13	6	7	R	13	5	7	R	13	5	7	R	13	3	10	R	13	0	13	R	13	11	2	R	13	5	7	R	13	5	7	R	13	5	7
64	R	13	10	3	G	13	6	7	G	13	9	4	G	13	6	7	R	13	5	8	R	13	5	8	R	13	3	10	R	13	0	13	R	13	11	2	R	13	5	7	R	13	5	7	R	13	5	7
65	R	13	10	3	G	13	7	6	G	13	10	3	G	13	7	6	R	13	5	8	R	13	5	8	R	13.0	2.6	10.4	R	13	0	13	R	13	11	2	R	13	5	8	R	13	5	8	R	13	5	8
66	R	13	10	3	G	13	7	8	G	13	10	3	G	13	7	6	R	13	5	8	R	13	5	8	G	13	3	10	R	13	0	13	R	13	11	2	R	13	5	8	R	13	5	8	R	13	5	8
67	R	13	10	3	G	13	8	6	G	13	11	3	G	13	8	6	R	13	5	8	G	13	4	10	R	13	0	13	R	13	11	3	R	13	5	8	R	13	5	8	R	13	5	8	R	13	5	8
68	R	14	10	4	G	14	8	6	G	14	11	3	G	14	8	6	R	14	5	8	G	14	4	9	R	14	0	14	R	14	11	3	R	14	5	8	R	14	5	8	R	14	5	8	R	14	5	8

Table C-1. Continued

A=Arrivals, D=Departures, Q=Queue:

Time (sec)

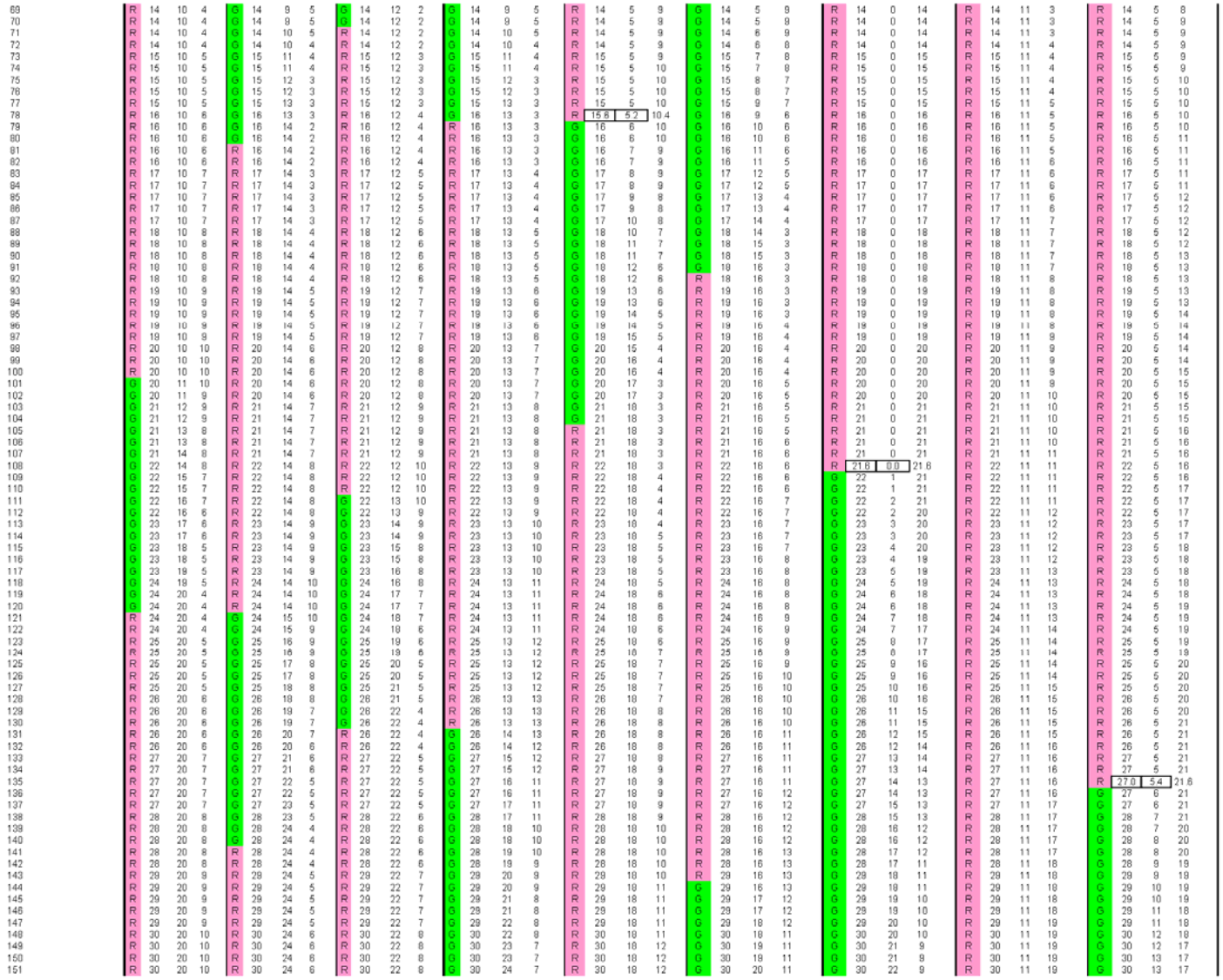

Table C-1. Continued

A=Arrivals, D=Departures, Q=Queue:

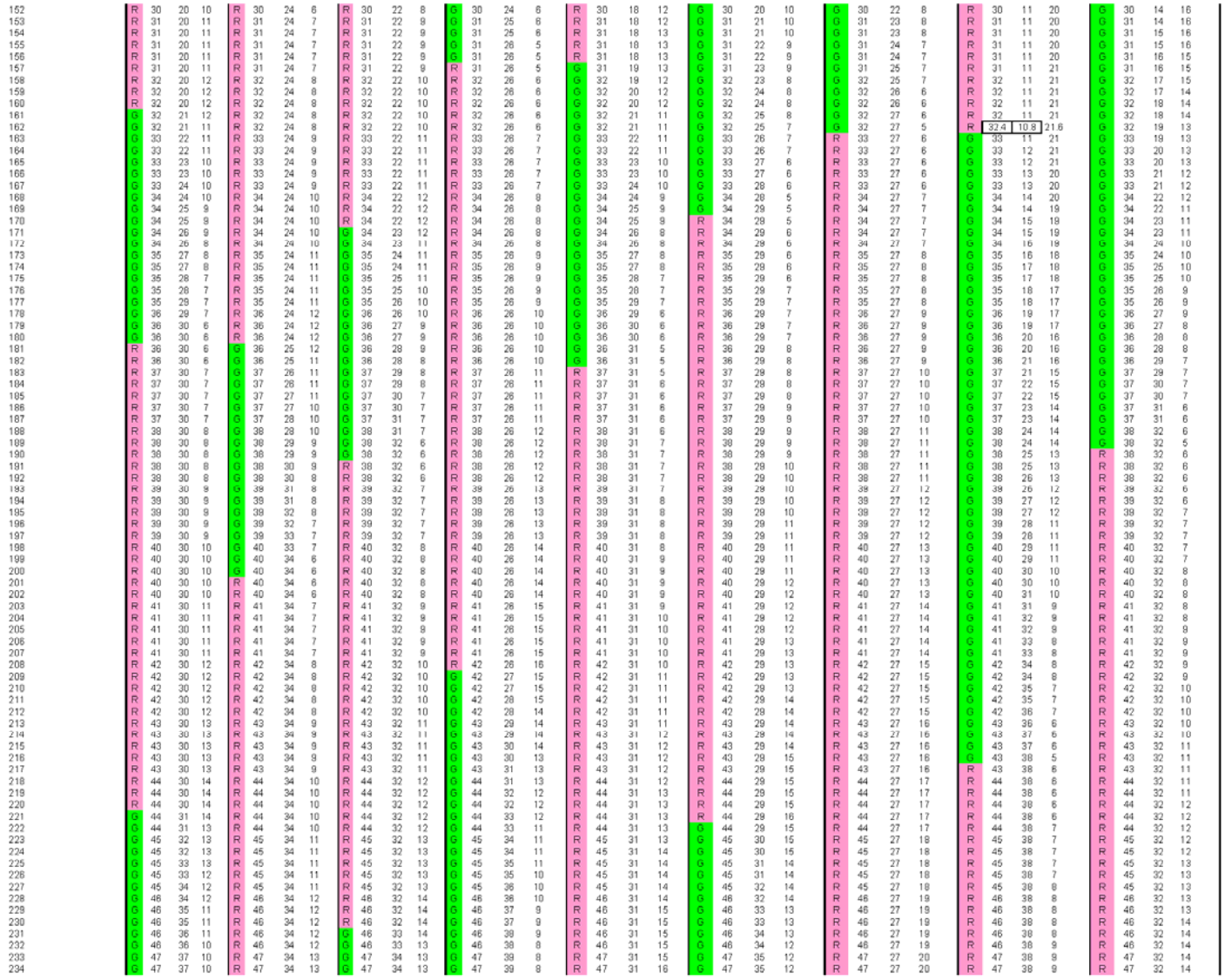

Table C-1. Continued

A=Arrivals, D=Departures, Q=Queue:

Time (sec)	A	D	Q	A	D	Q	A	D	Q	A	D	Q	A	D	Q	A	D	Q	A	D	Q	A	D	Q	A	D	Q
235	G	47	38	10	R	47	34	13	G	47	35	13	R	47	39	8	G	47	32	15	G	47	36	11	R	47	27	20	R	47	38	9	R	47	32	15
236	G	47	38	9	R	47	34	13	G	47	35	12	R	47	39	8	G	47	32	15	G	47	36	11	R	47	27	20	R	47	38	9	R	47	32	15
237	G	47	39	9	R	47	34	13	G	47	36	12	R	47	39	8	G	47	33	15	G	47	37	11	R	47	27	20	R	47	38	10	R	47	32	15
238	G	48	39	9	R	48	34	14	G	48	36	12	R	48	39	9	G	48	33	14	G	48	37	11	R	48	27	21	R	48	38	10	R	48	32	15
239	G	48	40	8	R	48	34	14	G	48	37	11	R	48	39	9	G	48	34	14	G	48	38	10	R	48	27	21	R	48	38	10	R	48	32	15
240	G	48	40	8	R	48	34	14	G	48	37	11	R	48	39	9	G	48	34	14	G	48	38	10	R	48	27	21	R	48	38	10	R	48	32	16
241	R	48	40	8	G	48	35	14	G	48	38	11	R	48	39	9	G	48	35	14	G	48	39	10	R	48	27	21	R	48	38	10	R	48	32	16
242	R	48	40	8	G	48	35	13	G	48	38	10	R	48	39	9	G	48	35	13	G	48	39	9	R	48	27	21	R	48	38	11	R	48	32	16
243	R	49	40	9	G	49	36	13	G	49	39	10	R	49	39	10	G	49	36	13	G	49	40	9	R	49	27	22	R	49	38	11	R	49	32	16
244	R	49	40	9	G	49	36	13	G	49	39	10	R	49	39	10	G	49	36	13	G	49	40	9	R	49	27	22	R	49	38	11	R	49	32	16
245	R	49	40	9	G	49	37	13	G	49	40	10	R	49	39	10	G	49	37	12	G	49	41	8	R	49	27	22	R	49	38	11	R	49	32	17
246	R	49	40	9	G	49	37	12	G	49	40	9	R	49	39	10	G	49	37	12	G	49	41	8	R	49	27	22	R	49	38	11	R	49	32	17
247	R	49	40	9	G	49	38	12	G	49	41	9	R	49	39	10	G	49	38	12	G	49	42	8	R	49	27	22	R	49	38	12	R	49	32	17
248	R	50	40	10	G	50	38	12	G	50	41	9	R	50	39	11	G	50	38	11	R	50	42	8	R	50	27	23	R	50	38	12	R	50	32	17
249	R	50	40	10	G	50	39	11	G	50	42	8	R	50	39	11	G	50	39	11	R	50	42	8	R	50	27	23	R	50	38	12	R	50	32	17
250	R	50	40	10	G	50	39	11	G	50	42	8	R	50	39	11	G	50	39	11	R	50	42	8	R	50	27	23	R	50	38	12	R	50	32	18
251	R	50	40	10	G	50	40	11	R	50	42	8	R	50	39	11	G	50	40	11	R	50	42	9	R	50	27	23	R	50	38	12	R	50	32	18
252	R	50	40	10	G	50	40	10	R	50	42	8	R	50	39	11	G	50	40	10	R	50	42	9	R	50	27	23	R	50	38	13	R	50	32	18
253	R	51	40	11	G	51	41	10	R	51	42	9	R	51	39	12	G	51	41	10	R	51	42	9	R	51	27	24	R	51	38	13	R	51	32	18
254	R	51	40	11	G	51	41	10	R	51	42	9	R	51	39	12	G	51	41	10	R	51	42	9	R	51	27	24	R	51	38	13	R	51	32	18
255	R	51	40	11	G	51	42	10	R	51	42	9	R	51	39	12	G	51	42	9	R	51	42	9	R	51	27	24	R	51	38	13	R	51	32	19
256	R	51	40	11	G	51	42	9	R	51	42	9	R	51	39	12	G	51	42	9	R	51	42	10	R	51	27	24	R	51	38	13	R	51	32	19
257	R	51	40	11	G	51	43	9	R	51	42	9	R	51	39	12	G	51	43	9	R	51	42	10	R	51	27	24	R	51	38	14	R	51	32	19
258	R	52	40	12	G	52	43	9	R	52	42	10	R	52	39	13	G	52	43	8	R	52	42	10	R	52	27	25	R	52	38	14	R	52	32	19
259	R	52	40	12	G	52	44	8	R	52	42	10	R	52	39	13	G	52	44	8	R	52	42	10	R	52	27	25	R	52	38	14	R	52	32	19
260	R	52	40	12	G	52	44	8	R	52	42	10	R	52	39	13	G	52	44	8	R	52	42	10	R	52	27	25	R	52	38	14	R	52	32	20
261	R	52	40	12	R	52	44	9	R	52	42	10	R	52	39	13	R	52	44	9	R	52	42	11	R	52	27	25	R	52	38	14	R	52	32	20
262	R	52	40	12	R	52	44	8	R	52	42	10	R	52	39	13	R	52	44	8	R	52	42	11	R	52	27	25	R	52	38	15	R	52	32	20
263	R	53	40	13	R	53	44	9	R	53	42	11	R	53	39	14	R	53	44	8	R	53	42	11	R	53	27	26	R	53	38	15	R	53	32	20
264	R	53	40	13	R	53	44	9	R	53	42	11	R	53	39	14	R	53	44	9	R	53	42	11	R	53	27	26	R	53	38	15	R	53	32	20
265	R	53	40	13	R	53	44	9	R	53	42	11	R	53	39	14	R	53	44	9	R	53	42	11	R	53	27	26	R	53	38	15	R	53	32	21
266	R	53	40	13	R	53	44	9	R	53	42	11	R	53	39	14	R	53	44	9	R	53	42	12	R	53	27	26	R	53	38	15	R	53	32	21
267	R	53	40	13	R	53	44	9	R	53	42	11	R	53	39	14	R	53	44	9	R	53	42	12	R	53	27	26	R	53	38	16	R	53	32	21
268	R	54	40	14	R	54	44	10	R	54	42	12	R	54	39	15	R	54	44	9	R	54	42	12	R	54	27	27	R	54	38	16	R	54	32	21
269	R	54	40	14	R	54	44	10	R	54	42	12	R	54	39	15	R	54	44	10	R	54	42	12	R	54	27	27	R	54	38	16	R	54	32	21
270	R	54	40	14	R	54	44	10	R	54	42	12	R	54	39	15	R	54	44	10	R	54	42	12	R	54	27	27	R	54	38	16	R	54	32	22
271	R	54	40	14	R	54	44	10	R	54	42	12	R	54	39	15	R	54	44	10	R	54	42	13	G	54	28	27	R	54	38	16	R	54	32	22
272	R	54	40	14	R	54	44	10	R	54	42	12	R	54	39	15	R	54	44	10	R	54	42	13	G	54	29	26	R	54	38	17	R	54	32	22
273	R	55	40	15	R	55	44	11	R	55	42	13	R	55	39	16	R	55	44	10	R	55	42	13	G	55	29	26	R	55	38	17	R	55	32	22
274	R	55	40	15	R	55	44	11	R	55	42	13	R	55	39	16	R	55	44	11	R	55	42	13	G	55	29	26	R	55	38	17	R	55	32	22
275	R	55	40	15	R	55	44	11	R	55	42	13	R	55	39	16	R	55	44	11	R	55	42	13	G	55	30	26	R	55	38	17	R	55	32	23
276	R	55	40	15	R	55	44	11	R	55	42	13	R	55	39	16	R	55	44	11	R	55	42	14	G	55	30	25	R	55	38	17	R	55	32	23
277	R	55	40	15	R	55	44	11	R	55	42	13	R	55	39	16	R	55	44	11	R	55	42	14	G	55	31	25	R	55	38	18	R	55	32	23
278	R	56	40	16	R	56	44	12	R	56	42	14	R	56	39	17	R	56	44	11	R	56	42	14	G	56	31	25	R	56	38	18	R	56	32	23
279	R	56	40	16	R	56	44	12	R	56	42	14	R	56	39	17	R	56	44	12	R	56	42	14	G	56	32	24	R	56	38	18	R	56	32	23
280	R	56	40	16	R	56	44	12	R	56	42	14	R	56	39	17	R	56	44	12	R	56	42	14	G	56	32	24	R	56	38	18	R	56	32	24
281	G	56	41	16	R	56	44	12	R	56	42	14	R	56	39	17	R	56	44	12	R	56	42	15	G	56	33	24	R	56	38	18	R	56	32	24
282	G	56	41	15	R	56	44	12	R	56	42	14	R	56	39	17	R	56	44	12	R	56	42	15	G	56	33	23	R	56	38	19	R	56	32	24
283	G	57	42	15	R	57	44	13	R	57	42	15	R	57	39	18	R	57	44	12	R	57	42	15	G	57	34	23	R	57	38	19	R	57	32	24
284	G	57	42	15	R	57	44	13	R	57	42	15	R	57	39	18	R	57	44	13	R	57	42	15	G	57	34	23	R	57	38	19	R	57	32	24
285	G	57	43	15	R	57	44	13	R	57	42	15	R	57	39	18	R	57	44	13	R	57	42	15	G	57	35	23	R	57	38	19	R	57	32	25
286	G	57	43	14	R	57	44	13	R	57	42	15	R	57	39	18	R	57	44	13	R	57	42	16	G	57	35	22	R	57	38	19	R	57	32	25
287	G	57	44	14	R	57	44	13	R	57	42	15	G	57	40	18	R	57	44	13	R	57	42	16	G	57	36	22	R	57	38	20	R	57	32	25
288	G	58	44	14	R	58	44	14	R	58	42	16	G	58	40	18	R	58	44	13	R	58	42	16	G	58	36	22	R	58	38	20	R	58	32	25
289	G	58	45	13	R	58	44	14	R	58	42	16	G	58	41	17	R	58	44	14	R	58	42	16	G	58	37	21	R	58	38	20	R	58	32	25
290	G	58	45	13	R	58	44	14	R	58	42	16	G	58	41	17	R	58	44	14	R	58	42	16	G	58	37	21	R	58	38	20	R	58	32	26
291	G	58	46	13	R	58	44	14	G	58	43	16	G	58	42	17	R	58	44	14	R	58	42	17	G	58	38	21	R	58	38	20	R	58	32	26
292	G	58	46	12	R	58	44	14	G	58	43	15	G	58	42	16	R	58	44	14	R	58	42	17	G	58	38	20	R	58	38	21	R	58	32	26
293	G	59	47	12	R	59	44	15	G	59	44	15	G	59	43	16	R	59	44	14	R	59	42	17	G	59	39	20	R	59	38	21	R	59	32	26
294	G	59	47	12	R	59	44	15	G	59	44	15	G	59	43	16	R	59	44	15	R	59	42	17	G	59	39	20	R	59	38	21	R	59	32	26
295	G	59	48	12	R	59	44	15	G	59	45	15	G	59	44	16	R	59	44	15	R	59	42	17	G	59	40	20	R	59	38	21	R	59	32	27
296	G	59	48	11	R	59	44	15	G	59	45	14	G	59	44	15	R	59	44	15	R	59	42	18	G	59	40	19	R	59	38	21	R	59	32	27
297	G	59	48	11	R	59	44	15	G	59	46	14	G	59	45	15	R	59	44	16	R	59	42	18	G	59	41	19	R	59	38	22	R	59	32	27
298	G	60	48	11	R	60	44	16	G	60	46	14	G	60	45	15	R	60	44	15	R	60	42	18	G	60	41	19	R	60	38	22	G	60	33	27
299	G	60	50	10	R	60	44	16	G	60	47	13	G	60	46	14	R	60	44	16	R	60	42	18	G	60	42	18	R	60	38	22	G	60	33	26
300	G	60	50	10	R	60	44	16	G	60	47	13	G	60	46	14	R	60	44	16	G	60	42	18	G	60	42	18	R	60	38	22	G	60	34	26
301	R	60	50	10	G	60	45	16	G	60	48	13	G	60	47	14	R	60	44	16	G	60	43	18	G	60	43	18	R	60	38	22	G	60	34	26
302	R	60	50	10	G	60	45	15	G	60	48	12	G	60	47	13	R	60	44	16	G	60	43	17	G	60	43	17	R	60	38	23	G	60	35	26
303	R	61	50	11	G	61	46	15	G	61	49	12	G	61	48	13	R	61	44	16	G	61	44	17	G	61	44	17	R	61	38	23	G	61	35	25
304	R	61	50	11	G	61	46	15	G	61	49	12	G	61	48	13	R	61	44	17	G	61	44	17	G	61	44	17	R	61	38	23	G	61	36	25
305	R	61	50	11	G	61	47	15	G	61	50	12	G	61	49	13	R	61	44	17	G	61	45	16	G	61	45	17	R	61	38	23	G	61	36	25
306	R	61	50	11	G	61	47	14	G	61	50	11	G	61	49	12	R	61	44	17	G	61	45	16	G	61	45	16	R	61	38	23	G	61	37	24
307	R	61	50	11	G	61	48	14	G	61	51	11	G	61	50	12	R	61	44	17	G	61	46	16	G	61	46	16	R	61	38	24	G	61	37	24
308	R	62	50	12	G	62	48	14	G	62	51	11	G	62	50	12	R	62	44	17	G	62	46	16	G	62	46	16	R	62	38	24	G	62	38	24
309	R	62	50	12	G	62	49	13	G	62	52	10	G	62	51	11	R	62	44	18	G	62	47	15	G	62	47	15	R	62	38	24	G	62	38	23
310	R	62	50	12	G	62	49	13	G	62	52	10	G	62	51	11	R	62	44	18	G	62	47	15	G	62	47	15	R	62	38	24	G	62	39	23
311	R	62	50	12	G	62	50	13	R	62	52	10	G	62	52	11	R	62	44	18	G	62	48	15	G	62	48	15	R	62	38	24	G	62	39	23
312	R	62	50	12	G	62	50	12	R	62	52	10	G	62	52	10	R	62	44	18	G	62	48	14	G	62	48	14	R	62	38	25	G	62	40	23
313	R	63	50	13	G	63	51	12	R	63	52	11	R	63	52	11	G	63	45	18	G	63	49	14	G	63	49	14	R	63	38	25	G	63	40	22
314	R	63	50	13	G	63	51	12	R	63	52	11	R	63	52	11	G	63	45	18	G	63	49	14	G	63	49	14	R	63	38	25	G	63	41	22
315	R	63	50	13	G	63	52	12	R	63	52	11	R	63	52	11	G	63	46	17	G	63	50	13	G	63	50	14	R	63	38	25	G	63	41	22
316	R	63	50	13	G	63	52	11	R	63	52	11	R	63	52	11	G	63	46	17	G	63	50	13	G	63	50	13	R	63	38	25	G	63	42	21
317	R	63	50	13	G	63	53	11	R	63	52	11	R	63	52	11	G	63	47	17	G	63	51	13	G	63	51	13	R	63	38	26	G	63	42	21

Table C-1. Continued

A=Arrivals, D=Departures, Q=Queue:

Time (sec)	A	D	Q	A	D	Q	A	D	Q	A	D	Q	A	D	Q	A	D	Q	A	D	Q	A	D	Q	A	D	Q
318	R 64	50	14	G 64	53	11	R 64	52	12	R 64	52	12	G 64	47	16	G 64	51	13	G 64	51	13	R 64	38	26	G 64	43	21
319	R 64	50	14	G 64	54	10	R 64	52	12	R 64	52	12	G 64	48	16	G 64	52	12	G 64	52	12	R 64	38	26	G 64	43	20
320	R 64	50	14	G 64	54	10	R 64	52	12	R 64	52	12	G 64	48	16	G 64	52	12	G 64	52	12	R 64	38	26	G 64	44	20
321	R 64	50	14	R 64	54	10	R 64	52	12	R 64	52	12	G 64	49	16	G 64	53	12	G 64	53	12	R 64	38	26	G 64	44	20
322	R 64	50	14	R 64	54	10	R 64	52	12	R 64	52	12	G 64	49	15	G 64	53	11	G 64	53	11	R 64	38	27	G 64	45	20
323	R 65	50	15	R 65	54	11	R 65	52	13	R 65	52	13	G 65	50	15	G 65	54	11	G 65	54	11	R 65	38	27	G 65	45	19
324	R 65	50	15	R 65	54	11	R 65	52	13	R 65	52	13	G 65	50	15	G 65	54	11	G 65	54	11	R 65	38	27	G 65	46	19
325	R 65	50	15	R 65	54	11	R 65	52	13	R 65	52	13	G 65	51	14	G 65	55	10	R 65	54	11	G 65	38	27	G 65	46	19
326	R 65	50	15	R 65	54	11	R 65	52	13	R 65	52	13	G 65	51	14	R 65	55	11	R 65	54	11	G 65	39	26	G 65	47	18
327	R 65	50	15	R 65	54	11	R 65	52	13	R 65	52	13	G 65	52	14	R 65	55	11	R 65	54	11	G 65	39	26	G 65	47	18
328	R 66	50	16	R 66	54	12	R 66	52	14	R 66	52	14	G 66	52	13	R 66	55	11	R 66	54	12	G 66	40	26	G 66	48	18
329	R 66	50	16	R 66	54	12	R 66	52	14	R 66	52	14	G 66	53	13	R 66	55	11	R 66	54	12	G 66	40	26	G 66	48	17
330	R 66	50	16	R 66	54	12	R 66	52	14	R 66	52	14	G 66	53	13	R 66	55	11	R 66	54	12	G 66	41	25	G 66	49	17
331	R 66	50	16	R 66	54	12	R 66	52	14	R 66	52	14	G 66	54	13	R 66	55	12	R 66	54	12	G 66	41	25	G 66	49	17
332	R 66	50	16	R 66	54	12	R 66	52	14	R 66	52	14	G 66	54	12	R 66	55	12	R 66	54	12	G 66	42	25	G 66	50	17
333	R 67	50	17	R 67	54	13	R 67	52	15	R 67	52	15	G 67	55	12	R 67	55	12	R 67	54	13	G 67	42	24	G 67	50	16
334	R 67	50	17	R 67	54	13	R 67	52	15	R 67	52	15	G 67	55	12	R 67	55	12	R 67	54	13	G 67	43	24	G 67	51	16
335	R 67	50	17	R 67	54	13	R 67	52	15	R 67	52	15	G 67	56	11	R 67	55	12	R 67	54	13	G 67	43	24	G 67	51	16
336	R 67	50	17	R 67	54	13	R 67	52	15	R 67	52	15	G 67	56	11	R 67	55	13	R 67	54	13	G 67	44	23	G 67	52	15
337	R 67	50	17	R 67	54	13	R 67	52	15	R 67	52	15	G 67	57	11	R 67	55	13	R 67	54	13	G 67	44	23	G 67	52	15
338	R 68	50	18	R 68	54	14	R 68	52	16	R 68	52	16	G 68	57	10	R 68	55	13	R 68	54	14	G 68	45	23	G 68	53	15
339	R 68	50	18	R 68	54	14	R 68	52	16	R 68	52	16	R 68	57	11	R 68	55	13	R 68	54	14	G 68	45	23	G 68	53	14
340	R 68	50	18	R 68	54	14	R 68	52	16	R 68	52	16	R 68	57	11	R 68	55	13	R 68	54	14	G 68	46	22	G 68	54	14
341	G 68	51	18	R 68	54	14	R 68	52	16	R 68	52	16	R 68	57	11	R 68	55	14	R 68	54	14	G 68	46	22	G 68	54	14
342	G 68	51	17	R 68	54	14	R 68	52	16	R 68	52	16	R 68	57	11	R 68	55	14	R 68	54	14	G 68	47	22	G 68	55	14
343	G 69	52	17	R 69	54	15	R 69	52	17	R 69	52	17	R 69	57	11	R 69	55	14	R 69	54	15	G 69	47	21	G 69	55	13
344	G 69	52	17	R 69	54	15	R 69	52	17	R 69	52	17	R 69	57	12	R 69	55	14	R 69	54	15	G 69	48	21	G 69	56	13
345	G 69	53	17	R 69	54	15	R 69	52	17	R 69	52	17	R 69	57	12	R 69	55	14	R 69	54	15	G 69	48	21	G 69	56	13
346	G 69	53	16	R 69	54	15	R 69	52	17	R 69	52	17	R 69	57	12	R 69	55	15	R 69	54	15	G 69	49	20	G 69	57	12
347	G 69	54	16	R 69	54	15	R 69	52	17	R 69	52	17	R 69	57	12	R 69	55	15	R 69	54	15	G 69	49	20	G 69	57	12
348	G 70	54	16	R 70	54	16	R 70	52	18	R 70	52	18	R 70	57	12	R 70	55	15	R 70	54	16	G 70	50	20	G 70	58	12
349	G 70	55	15	R 70	54	16	R 70	52	18	R 70	52	18	R 70	57	13	R 70	55	15	R 70	54	16	G 70	50	20	G 70	58	11
350	G 70	55	15	R 70	54	16	R 70	52	18	R 70	52	18	R 70	57	13	R 70	55	15	R 70	54	16	G 70	51	19	G 70	59	11
351	G 70	56	15	R 70	54	16	G 70	53	18	R 70	52	18	R 70	57	13	R 70	55	16	R 70	54	16	G 70	51	19	G 70	59	11
352	G 70	56	14	R 70	54	16	G 70	53	17	R 70	52	18	R 70	57	13	R 70	55	16	R 70	54	16	G 70	52	19	R 70	59	11
353	G 71	57	14	R 71	54	17	G 71	54	17	R 71	52	18	R 71	57	13	R 71	55	16	R 71	54	17	G 71	52	18	R 71	59	11
354	G 71	57	14	R 71	54	17	G 71	54	17	R 71	52	19	R 71	57	14	R 71	55	16	R 71	54	17	G 71	53	18	R 71	59	11
355	G 71	58	14	R 71	54	17	G 71	55	17	R 71	52	19	R 71	57	14	R 71	55	16	R 71	54	17	G 71	53	18	R 71	59	12
356	G 71	58	13	R 71	54	17	G 71	55	16	R 71	52	19	R 71	57	14	R 71	55	17	R 71	54	17	G 71	54	17	R 71	59	12
357	G 71	58	13	R 71	54	17	G 71	56	16	R 71	52	19	R 71	57	14	R 71	55	17	R 71	54	17	G 71	54	17	R 71	59	12
358	G 72	59	13	R 72	54	18	G 72	56	16	R 72	52	20	R 72	57	14	R 72	55	17	R 72	54	18	G 72	55	17	R 72	59	12
359	G 72	60	12	R 72	54	18	G 72	57	15	R 72	52	20	R 72	57	15	R 72	55	17	R 72	54	18	G 72	55	17	R 72	59	12
360	G 72	60	12	R 72	54	18	G 72	57	15	R 72	52	20	R 72	57	15	R 72	55	17	R 72	54	18	G 72	56	16	R 72	59	13
361	R 72	60	12	G 72	55	18	G 72	58	15	R 72	52	20	R 72	57	15	R 72	55	18	R 72	54	18	G 72	56	16	R 72	59	13
362	R 72	60	12	G 72	55	17	G 72	58	14	R 72	52	20	R 72	57	15	R 72	55	18	R 72	54	18	G 72	57	16	R 72	59	13
363	R 73	60	13	G 73	56	17	G 73	59	14	R 73	52	21	R 73	57	15	R 73	55	18	R 73	54	19	G 73	57	15	R 73	59	13
364	R 73	60	13	G 73	56	17	G 73	59	14	R 73	52	21	R 73	57	16	R 73	55	18	R 73	54	19	G 73	58	15	R 73	59	13
365	R 73	60	13	G 73	57	17	G 73	60	14	G 73	53	21	R 73	57	16	R 73	55	19	R 73	54	19	G 73	58	15	R 73	59	14
366	R 73	60	13	G 73	57	16	G 73	60	13	G 73	53	20	R 73	57	16	R 73	55	19	R 73	54	19	G 73	59	14	R 73	59	14
367	R 73	60	13	G 73	58	16	G 73	61	13	G 73	54	20	R 73	57	16	R 73	55	19	R 73	54	19	G 73	59	14	R 73	59	14
368	R 74	60	14	G 74	58	16	G 74	61	13	G 74	54	20	R 74	57	16	R 74	55	19	R 74	54	20	G 74	60	14	R 74	59	14
369	R 74	60	14	G 74	59	15	G 74	62	12	G 74	55	19	R 74	57	17	R 74	55	19	R 74	54	20	G 74	60	14	R 74	59	14
370	R 74	60	14	G 74	59	15	G 74	62	12	G 74	55	19	R 74	57	17	R 74	55	19	R 74	54	20	G 74	61	13	R 74	59	15
371	R 74	60	14	G 74	60	15	R 74	62	12	G 74	56	19	R 74	57	17	R 74	55	20	R 74	54	20	G 74	61	13	R 74	59	15
372	R 74	60	14	G 74	60	14	R 74	62	12	G 74	56	19	R 74	57	17	R 74	55	20	R 74	54	20	G 74	62	13	R 74	59	15
373	R 75	60	15	G 75	61	14	R 75	62	13	G 75	57	18	R 75	57	17	R 75	55	20	R 75	54	21	G 75	62	12	R 75	59	15
374	R 75	60	15	G 75	61	14	R 75	62	13	G 75	57	18	R 75	57	18	R 75	55	20	R 75	54	21	G 75	63	12	R 75	59	15
375	R 75	60	15	G 75	62	14	R 75	62	13	G 75	58	18	R 75	57	18	R 75	55	20	R 75	54	21	G 75	63	12	R 75	59	16
376	R 75	60	15	G 75	62	13	R 75	62	13	G 75	58	17	R 75	57	18	R 75	55	21	R 75	54	21	G 75	64	11	R 75	59	16
377	R 75	60	15	G 75	63	13	R 75	62	13	G 75	59	17	R 75	57	18	R 75	55	21	R 75	54	21	G 75	64	11	R 75	59	16
378	R 76	60	16	G 76	63	13	R 76	62	14	G 76	59	17	R 76	57	18	G 76	55	21	R 76	54	22	R 76	65	11	R 76	59	16
379	R 76	60	16	G 76	64	12	R 76	62	14	G 76	60	16	R 76	57	19	G 76	56	20	R 76	54	22	R 76	65	11	R 76	59	16
380	R 76	60	16	G 76	64	12	R 76	62	14	G 76	60	16	R 76	57	19	G 76	56	20	R 76	54	22	R 76	65	11	R 76	59	17
381	R 76	60	16	R 76	64	12	R 76	62	14	G 76	61	16	R 76	57	19	G 76	57	20	R 76	54	22	R 76	65	11	R 76	59	17
382	R 76	60	16	R 76	64	12	R 76	62	14	G 76	61	15	R 76	57	19	G 76	57	19	R 76	54	22	R 76	65	12	R 76	59	17
383	R 77	60	17	R 77	64	13	R 77	62	15	G 77	62	15	R 77	57	19	G 77	58	19	R 77	54	23	R 77	65	12	R 77	59	17
384	R 77	60	17	R 77	64	13	R 77	62	15	G 77	62	15	R 77	57	20	G 77	58	19	R 77	54	23	R 77	65	12	R 77	59	17
385	R 77	60	17	R 77	64	13	R 77	62	15	G 77	63	15	R 77	57	20	G 77	59	18	R 77	54	23	R 77	65	12	R 77	59	18
386	R 77	60	17	R 77	64	13	R 77	62	15	G 77	63	14	R 77	57	20	G 77	59	18	R 77	54	23	R 77	65	12	R 77	59	18
387	R 77	60	17	R 77	64	13	R 77	62	15	G 77	64	14	R 77	57	20	G 77	60	18	R 77	54	23	R 77	65	13	R 77	59	18
388	R 78	60	18	R 78	64	14	R 78	62	16	G 78	64	14	R 78	57	20	G 78	60	18	R 78	54	24	R 78	65	13	R 78	59	18
389	R 78	60	18	R 78	64	14	R 78	62	16	G 78	65	13	R 78	57	21	G 78	61	17	R 78	54	24	R 78	65	13	R 78	59	18
390	R 78	60	18	R 78	64	14	R 78	62	16	G 78	65	13	R 78	57	21	G 78	61	17	R 78	54	24	R 78	65	13	R 78	59	19
391	R 78	60	18	R 78	64	14	R 78	62	16	R 78	65	13	G 78	58	21	G 78	62	17	R 78	54	24	R 78	65	13	R 78	59	19
392	R 78	60	18	R 78	64	14	R 78	62	16	R 78	65	13	G 78	58	20	G 78	62	18	R 78	54	24	R 78	65	14	R 78	59	19
393	R 79	60	19	R 79	64	15	R 79	62	17	R 79	65	14	G 79	59	20	G 79	63	16	R 79	54	25	R 79	65	14	R 79	59	19
394	R 79	60	19	R 79	64	15	R 79	62	17	R 79	65	14	G 79	59	20	G 79	63	16	R 79	54	25	R 79	65	14	R 79	59	19
395	R 79	60	19	R 79	64	15	R 79	62	17	R 79	65	14	G 79	60	19	G 79	64	15	R 79	54	25	R 79	65	14	R 79	59	20
396	R 79	60	19	R 79	64	15	R 79	62	17	R 79	65	14	G 79	60	19	G 79	64	15	R 79	54	25	R 79	65	14	R 79	59	20
397	R 79	60	19	R 79	64	15	R 79	62	17	R 79	65	14	G 79	61	19	G 79	65	15	R 79	54	25	R 79	65	15	R 79	59	20
398	R 80	60	20	R 80	64	16	R 80	62	18	R 80	65	15	G 80	61	18	G 80	65	15	R 80	54	26	R 80	65	15	R 80	59	20
399	R 80	60	20	R 80	64	16	R 80	62	18	R 80	65	15	G 80	62	18	G 80	66	14	R 80	54	26	R 80	65	15	R 80	59	20
400	R 80	60	20	R 80	64	16	R 80	62	18	R 80	65	15	G 80	62	18	G 80	66	14	R 80	54	26	R 80	65	15	R 80	59	21

Table C-1. Continued

A=Arrivals, D=Departures, Q=Queue:

Time (sec)	A	D	Q	A	D	Q	A	D	Q	A	D	Q	A	D	Q	A	D	Q	A	D	Q	A	D	Q	A	D	Q
401	G 80	61	20	R 80	64	16	R 80	62	18	R 80	65	15	G 80	63	18	G 80	67	14	R 80	54	26	R 80	65	15	R 80	59	21
402	G 80	61	19	R 80	64	16	R 80	62	18	R 80	65	15	G 80	63	17	G 80	67	13	R 80	54	26	R 80	65	16	R 80	59	21
403	G 81	62	19	R 81	64	17	R 81	62	19	R 81	65	16	G 81	64	17	G 81	68	13	R 81	54	27	R 81	65	16	R 81	59	21
404	G 81	62	19	R 81	64	17	R 81	62	19	R 81	65	16	G 81	64	17	R 81	68	13	R 81	54	27	R 81	65	16	R 81	59	21
405	G 81	63	18	R 81	64	17	R 81	62	19	R 81	65	16	G 81	65	16	R 81	68	13	R 81	54	27	R 81	65	16	R 81	59	22
406	G 81	63	18	R 81	64	17	R 81	62	19	R 81	65	16	G 81	65	16	R 81	68	14	R 81	54	27	R 81	65	16	R 81	59	22
407	G 81	64	18	R 81	64	17	R 81	62	19	R 81	65	16	G 81	66	16	R 81	68	14	R 81	54	27	R 81	65	17	R 81	59	22
408	G 82	64	18	R 82	64	18	R 82	62	20	R 82	65	17	G 82	66	15	R 82	68	14	R 82	54	28	R 82	65	17	R 82	59	22
409	G 82	65	17	R 82	64	18	R 82	62	20	R 82	65	17	G 82	67	15	R 82	68	14	R 82	54	28	R 82	65	17	R 82	59	22
410	G 82	65	17	R 82	64	18	R 82	62	20	R 82	65	17	G 82	67	15	R 82	68	14	R 82	54	28	R 82	65	17	R 82	59	23
411	G 82	66	17	R 82	64	18	G 82	63	20	R 82	65	17	G 82	68	15	R 82	68	15	R 82	54	28	R 82	65	17	R 82	59	23
412	G 82	66	16	R 82	64	18	G 82	63	19	R 82	65	17	G 82	68	14	R 82	68	15	R 82	54	28	R 82	65	18	R 82	59	23
413	G 83	67	16	R 83	64	19	G 83	64	19	R 83	65	18	G 83	69	14	R 83	68	15	R 83	54	29	R 83	65	18	R 83	59	23
414	G 83	67	16	R 83	64	19	G 83	64	19	R 83	65	18	G 83	69	14	R 83	68	15	R 83	54	29	R 83	65	18	R 83	59	23
415	G 83	68	16	R 83	64	19	G 83	65	19	R 83	65	18	G 83	70	13	R 83	68	15	R 83	54	29	R 83	65	18	R 83	59	24
416	G 83	68	15	R 83	64	19	G 83	65	18	R 83	65	18	G 83	70	13	R 83	68	16	R 83	54	29	R 83	65	18	R 83	59	24
417	G 83	69	15	R 83	64	19	G 83	66	18	R 83	65	18	R 83	70	13	R 83	68	16	R 83	54	29	R 83	65	19	R 83	59	24
418	G 84	69	15	R 84	64	20	G 84	66	18	R 84	65	19	R 84	70	13	R 84	68	16	R 84	54	30	R 84	65	19	R 84	59	24
419	G 84	70	14	R 84	64	20	G 84	67	17	R 84	65	19	R 84	70	14	R 84	68	16	R 84	54	30	R 84	65	19	R 84	59	24
420	G 84	70	14	R 84	64	20	G 84	67	17	R 84	65	19	R 84	70	14	R 84	68	16	R 84	54	30	R 84	65	19	R 84	59	25
421	R 84	70	14	G 84	65	20	G 84	68	17	R 84	65	19	R 84	70	14	R 84	68	17	R 84	54	30	R 84	65	19	R 84	59	25
422	R 84	70	14	G 84	65	19	G 84	68	16	R 84	65	19	R 84	70	14	R 84	68	17	R 84	54	30	R 84	65	20	R 84	59	25
423	R 85	70	15	G 85	66	19	G 85	69	16	R 85	65	20	R 85	70	14	R 85	68	17	R 85	54	31	R 85	65	20	R 85	59	25
424	R 85	70	15	G 85	66	19	G 85	69	16	R 85	65	20	R 85	70	15	R 85	68	17	R 85	54	31	R 85	65	20	R 85	59	25
425	R 85	70	15	G 85	67	19	G 85	70	16	R 85	65	20	R 85	70	15	R 85	68	17	R 85	54	31	R 85	65	20	R 85	59	26
426	R 85	70	15	G 85	67	18	G 85	70	15	R 85	65	20	R 85	70	15	R 85	68	18	R 85	54	31	R 85	65	20	R 85	59	26
427	R 85	70	15	G 85	68	18	G 85	71	15	R 85	65	20	R 85	70	15	R 85	68	18	R 85	54	31	R 85	65	21	R 85	59	26
428	R 86	70	16	G 86	68	18	G 86	71	15	R 86	65	21	R 86	70	15	R 86	68	18	R 86	54	32	R 86	65	21	R 86	59	26
429	R 86	70	16	G 86	69	17	G 86	72	14	R 86	65	21	R 86	70	16	R 86	68	18	R 86	54	32	R 86	65	21	R 86	59	26
430	R 86	70	16	G 86	69	17	G 86	72	14	R 86	65	21	R 86	70	16	R 86	68	18	R 86	54	32	R 86	65	21	R 86	59	27
431	R 86	70	16	G 86	70	17	R 86	72	14	R 86	65	21	R 86	70	16	R 86	68	19	R 86	54	32	R 86	65	21	R 86	59	27
432	R 86	70	16	G 86	70	16	R 86	72	14	R 86	65	21	R 86	70	16	R 86	68	19	R 86	54	32	R 86	65	22	R 86	59	27
433	R 87	70	17	G 87	71	16	R 87	72	15	R 87	65	22	R 87	70	16	R 87	68	19	G 87	55	32	R 87	65	22	R 87	59	27
434	R 87	70	17	G 87	71	16	R 87	72	15	R 87	65	22	R 87	70	17	R 87	68	19	G 87	55	32	R 87	65	22	R 87	59	27
435	R 87	70	17	G 87	72	16	R 87	72	15	R 87	65	22	R 87	70	17	R 87	68	19	G 87	56	32	R 87	65	22	R 87	59	28
436	R 87	70	17	G 87	72	15	R 87	72	15	R 87	65	22	R 87	70	17	R 87	68	20	G 87	56	31	R 87	65	22	R 87	59	28
437	R 87	70	17	G 87	73	15	R 87	72	15	R 87	65	22	R 87	70	17	R 87	68	20	G 87	57	31	R 87	65	23	R 87	59	28
438	R 88	70	18	G 88	73	15	R 88	72	16	R 88	65	23	R 88	70	17	R 88	68	20	G 88	57	31	R 88	65	23	R 88	59	29
439	R 88	70	18	G 88	74	14	R 88	72	16	R 88	65	23	R 88	70	18	R 88	68	20	G 88	58	30	R 88	65	23	R 88	59	29
440	R 88	70	18	G 88	74	14	R 88	72	16	R 88	65	23	R 88	70	18	R 88	68	20	G 88	58	30	R 88	65	23	R 88	59	29
441	R 88	70	18	R 88	74	14	R 88	72	16	R 88	65	23	R 88	70	18	R 88	68	21	G 88	59	30	R 88	65	23	R 88	59	29
442	R 88	70	18	R 88	74	14	R 88	72	16	R 88	65	23	R 88	70	18	R 88	68	21	G 88	59	29	R 88	65	24	R 88	59	29
443	R 89	70	19	R 89	74	15	R 89	72	17	G 89	68	23	R 88	70	18	R 89	68	21	G 89	60	29	R 89	65	24	R 89	59	29
444	R 89	70	19	R 89	74	15	R 89	72	17	G 89	68	23	R 89	70	19	R 89	68	21	G 89	60	29	R 89	65	24	R 89	59	29
445	R 89	70	19	R 89	74	15	R 89	72	17	G 89	67	23	R 89	70	19	R 89	68	21	G 89	61	29	R 89	65	24	R 89	59	30
446	R 89	70	19	R 89	74	15	R 89	72	17	G 89	67	22	R 89	70	19	R 89	68	22	G 89	61	28	R 89	65	24	R 89	59	30
447	R 89	70	19	R 89	74	15	R 89	72	17	G 89	68	22	R 89	70	19	R 89	68	22	G 89	62	28	R 89	65	25	R 89	59	30
448	R 90	70	20	R 90	74	16	R 90	72	18	G 90	68	22	R 90	70	19	R 90	68	22	G 90	62	28	R 90	65	25	R 90	59	30
449	R 90	70	20	R 90	74	16	R 90	72	18	G 90	69	21	R 90	70	20	R 90	68	22	G 90	63	27	R 90	65	25	R 90	59	30
450	R 90	70	20	R 90	74	16	R 90	72	18	G 90	69	21	R 90	70	20	R 90	68	22	G 90	63	27	R 90	65	25	R 90	59	31
451	R 90	70	20	R 90	74	16	R 90	72	18	G 90	70	21	R 90	70	20	R 90	68	23	G 90	64	27	R 90	65	25	R 90	59	31
452	R 90	70	20	R 90	74	16	R 90	72	18	G 90	70	20	R 90	70	20	R 90	68	23	G 90	64	26	R 90	65	26	R 90	59	31
453	R 91	70	21	R 91	74	17	R 91	72	19	G 91	71	20	R 91	70	20	R 91	68	23	G 91	65	26	R 91	65	26	R 91	59	31
454	R 91	70	21	R 91	74	17	R 91	72	19	G 91	71	20	R 91	70	21	R 91	68	23	G 91	65	26	R 91	65	26	R 91	59	31
455	R 91	70	21	R 91	74	17	R 91	72	19	G 91	72	20	R 91	70	21	R 91	68	23	G 91	66	26	R 91	65	26	R 91	59	32
456	R 91	70	21	R 91	74	17	R 91	72	19	G 91	72	19	R 91	70	21	G 91	68	23	G 91	66	25	R 91	65	26	R 91	59	32
457	R 91	70	21	R 91	74	17	R 91	72	19	G 91	73	19	R 91	70	21	G 91	69	23	G 91	67	25	R 91	65	27	R 91	59	32
458	R 92	70	22	R 92	74	18	R 92	72	20	G 92	73	19	R 92	70	21	G 92	69	23	G 92	67	25	R 92	65	27	R 92	59	32
459	R 92	70	22	R 92	74	18	R 92	72	20	G 92	74	18	R 92	70	22	G 92	70	22	G 92	68	24	R 92	65	27	R 92	59	32
460	R 92	70	22	R 92	74	18	R 92	72	20	G 92	74	18	R 92	70	22	G 92	70	22	G 92	68	24	R 92	65	27	G 92	60	32
461	G 92	71	22	R 92	74	18	R 92	72	20	G 92	75	18	R 92	70	22	G 92	71	22	G 92	69	24	R 92	65	27	G 92	60	32
462	G 92	71	21	R 92	74	18	R 92	72	20	G 92	75	17	R 92	70	22	G 92	71	21	G 92	69	23	R 92	65	28	G 92	61	32
463	G 93	72	21	R 93	74	19	R 93	72	21	G 93	76	17	R 93	70	22	G 93	72	21	G 93	70	23	R 93	65	28	G 93	61	31
464	G 93	72	21	R 93	74	19	R 93	72	21	G 93	76	17	R 93	70	23	G 93	72	21	G 93	70	23	R 93	65	28	G 93	62	31
465	G 93	73	21	R 93	74	19	R 93	72	21	G 93	77	17	R 93	70	23	G 93	73	20	G 93	71	23	R 93	65	28	G 93	62	31
466	G 93	73	20	R 93	74	19	R 93	72	21	G 93	77	16	R 93	70	23	G 93	73	20	G 93	71	22	R 93	65	28	G 93	63	30
467	G 93	74	20	R 93	74	19	R 93	72	21	G 93	78	16	R 93	70	23	G 93	74	20	G 93	72	22	R 93	65	29	G 93	63	30
468	G 94	74	20	R 94	74	20	R 94	72	22	G 94	78	16	R 94	70	23	G 94	74	20	G 94	72	22	R 94	65	29	G 94	64	30
469	G 94	75	19	R 94	74	20	R 94	72	22	R 94	78	16	G 94	71	23	G 94	75	19	G 94	73	21	R 94	65	29	G 94	64	29
470	G 94	75	19	R 94	74	20	R 94	72	22	R 94	78	16	G 94	71	23	G 94	75	19	G 94	73	21	R 94	65	29	G 94	65	29
471	G 94	76	19	R 94	74	20	G 94	73	22	R 94	78	16	G 94	72	23	G 94	76	19	G 94	74	21	R 94	65	29	G 94	65	29
472	G 94	76	18	R 94	74	20	G 94	73	21	R 94	78	16	G 94	72	22	G 94	76	18	G 94	74	20	R 94	65	30	G 94	66	29
473	G 95	77	18	R 95	74	21	G 95	74	21	R 95	78	17	G 95	73	22	G 95	77	18	G 95	75	20	R 95	65	30	G 95	66	28
474	G 95	77	18	R 95	74	21	G 95	74	21	R 95	78	17	G 95	73	22	G 95	77	18	G 95	75	20	R 95	65	30	G 95	67	28
475	G 95	78	18	R 95	74	21	G 95	75	21	R 95	78	17	G 95	74	21	G 95	78	17	G 95	76	20	R 95	65	30	G 95	67	28
476	G 95	78	17	R 95	74	21	G 95	75	20	R 95	78	17	G 95	74	21	G 95	78	17	G 95	76	19	R 95	65	30	G 95	68	27
477	G 95	79	17	R 95	74	21	G 95	76	20	R 95	78	17	G 95	75	21	G 95	79	17	G 95	77	19	R 95	65	31	G 95	68	27
478	G 96	79	17	R 96	74	22	G 96	76	20	R 96	78	18	G 96	75	20	G 96	79	17	G 96	77	19	R 96	65	31	G 96	69	27
479	G 96	80	16	R 96	74	22	G 96	77	19	R 96	78	18	G 96	76	20	G 96	80	16	G 96	78	18	R 96	65	31	G 96	69	26
480	G 96	80	16	R 96	74	22	G 96	77	19	R 96	78	18	G 96	76	20	G 96	80	16	G 96	78	18	R 96	65	31	G 96	70	26
481	R 96	80	16	G 96	75	22	G 96	78	19	R 96	78	18	G 96	77	20	G 96	81	16	G 96	79	18	R 96	65	31	G 96	70	26
482	R 96	80	16	G 96	75	21	G 96	78	18	R 96	78	18	G 96	77	19	R 96	81	16	G 96	79	17	R 96	65	32	G 96	71	26
483	R 97	80	17	G 97	76	21	G 97	79	18	R 97	78	19	G 97	78	19	R 97	81	16	G 97	80	17	R 97	65	32	G 97	71	25

Table C-1. Continued

A=Arrivals, D=Departures, Q=Queue:

Time (sec)	A	D	Q	A	D	Q	A	D	Q	A	D	Q	A	D	Q	A	D	Q	A	D	Q	A	D	Q	A	D	Q
484	R 97	80	17	G 97	76	21	G 97	79	18	R 97	78	19	G 97	78	19	R 97	81	16	G 97	80	17	R 97	65	32	G 97	72	25
485	R 97	80	17	G 97	77	21	G 97	80	18	R 97	78	19	G 97	79	18	R 97	81	16	R 97	81	17	R 97	65	32	G 97	72	25
486	R 97	80	17	G 97	77	20	G 97	80	17	R 97	78	19	G 97	79	18	R 97	81	17	R 97	81	16	R 97	65	32	G 97	73	24
487	R 97	80	17	G 97	78	20	G 97	81	17	R 97	78	19	G 97	80	18	R 97	81	17	R 97	81	17	R 97	65	32	G 97	73	24
488	R 98	80	18	G 98	78	20	G 98	81	17	R 98	78	20	G 98	80	17	R 98	81	17	R 98	81	17	G 98	66	32	G 98	74	24
489	R 98	80	18	G 98	79	19	G 98	82	16	R 98	78	20	G 98	81	17	R 98	81	17	R 98	81	17	G 98	66	32	G 98	74	23
490	R 98	80	18	G 98	79	19	G 98	82	16	R 98	78	20	G 98	81	17	R 98	81	17	R 98	81	17	G 98	67	31	G 98	75	23
491	R 98	80	18	G 98	80	19	R 98	82	16	R 98	78	20	G 98	82	17	R 98	81	18	R 98	81	17	G 98	67	31	G 98	75	23
492	R 98	80	18	G 98	80	18	R 98	82	16	R 98	78	20	G 98	82	16	R 98	81	18	R 98	81	17	G 98	68	31	G 98	76	23
493	R 99	80	19	G 99	81	18	R 99	82	17	R 99	78	21	G 99	83	16	R 99	81	18	R 99	81	18	G 99	68	30	G 99	76	22
494	R 99	80	19	G 99	81	18	R 99	82	17	R 99	78	21	G 99	83	16	R 99	81	18	R 99	81	18	G 99	69	30	G 99	77	22
495	R 99	80	19	G 99	82	18	R 99	82	17	R 99	78	21	R 99	83	16	R 99	81	18	R 99	81	18	G 99	69	30	G 99	77	22
496	R 99	80	19	G 99	82	17	R 99	82	17	R 99	78	21	R 99	83	16	R 99	81	19	R 99	81	18	G 99	70	29	G 99	78	21
497	R 99	80	19	G 99	83	17	R 99	82	17	R 99	78	21	R 99	83	16	R 99	81	19	R 99	81	18	G 99	70	29	G 99	78	21
498	R 100	80	20	G 100	83	17	R 100	82	18	R 100	78	22	R 100	83	16	R 100	81	19	R 100	81	19	G 100	71	29	G 100	79	21
499	R 100	80	20	G 100	84	16	R 100	82	18	R 100	78	22	R 100	83	17	R 100	81	19	R 100	81	19	G 100	71	29	G 100	79	20
500	R 100	80	20	G 100	84	16	R 100	82	18	R 100	78	22	R 100	83	17	R 100	81	19	R 100	81	19	G 100	72	28	G 100	80	20
501	R 100	80	20	R 100	84	16	R 100	82	18	R 100	78	22	R 100	83	17	R 100	81	20	R 100	81	19	G 100	72	28	G 100	80	20
502	R 100	80	20	R 100	84	16	R 100	82	18	R 100	78	22	R 100	83	17	R 100	81	20	R 100	81	19	G 100	73	28	G 100	81	20
503	R 101	80	21	R 101	84	17	R 101	82	19	R 101	78	23	R 101	83	17	R 101	81	20	R 101	81	20	G 101	73	27	G 101	81	19
504	R 101	80	21	R 101	84	17	R 101	82	19	R 101	78	23	R 101	83	18	R 101	81	20	R 101	81	20	G 101	74	27	G 101	82	19
505	R 101	80	21	R 101	84	17	R 101	82	19	R 101	78	23	R 101	83	18	R 101	81	20	R 101	81	20	G 101	74	27	G 101	82	19
506	R 101	80	21	R 101	84	17	R 101	82	19	R 101	78	23	R 101	83	18	R 101	81	21	R 101	81	20	G 101	75	26	G 101	83	18
507	R 101	80	21	R 101	84	17	R 101	82	19	R 101	78	23	R 101	83	18	R 101	81	21	R 101	81	20	G 101	75	26	G 101	83	18
508	R 102	80	22	R 102	84	18	R 102	82	20	R 102	78	24	R 102	83	18	R 102	81	21	R 102	81	21	G 102	76	26	G 102	84	18
509	R 102	80	22	R 102	84	18	R 102	82	20	R 102	78	24	R 102	83	19	R 102	81	21	R 102	81	21	G 102	76	26	G 102	84	17
510	R 102	80	22	R 102	84	18	R 102	82	20	R 102	78	24	R 102	83	19	R 102	81	21	R 102	81	21	G 102	77	25	G 102	85	17
511	R 102	80	22	R 102	84	18	R 102	82	20	R 102	78	24	R 102	83	19	R 102	81	22	R 102	81	21	G 102	77	25	G 102	85	17
512	R 102	80	22	R 102	84	18	R 102	82	20	R 102	78	24	R 102	83	19	R 102	81	22	R 102	81	21	G 102	78	25	G 102	86	17
513	R 103	80	23	R 103	84	19	R 103	82	21	R 103	78	25	R 103	83	19	R 103	81	22	R 103	81	22	G 103	78	24	G 103	86	16
514	R 103	80	23	R 103	84	19	R 103	82	21	R 103	78	25	R 103	83	20	R 103	81	22	R 103	81	22	G 103	79	24	R 103	86	16
515	R 103	80	23	R 103	84	19	R 103	82	21	R 103	78	25	R 103	83	20	R 103	81	22	R 103	81	22	G 103	79	24	R 103	86	17
516	R 103	80	23	R 103	84	19	R 103	82	21	R 103	78	25	R 103	83	20	R 103	81	23	R 103	81	22	G 103	80	23	R 103	86	17
517	R 103	80	23	R 103	84	19	R 103	82	21	R 103	78	25	R 103	83	20	R 103	81	23	R 103	81	22	G 103	80	23	R 103	86	17
518	R 104	80	24	R 104	84	20	R 104	82	22	R 104	78	26	R 104	83	20	R 104	81	23	R 104	81	23	G 104	81	23	R 104	86	17
519	R 104	80	24	R 104	84	20	R 104	82	22	R 104	78	26	R 104	83	21	R 104	81	23	R 104	81	23	G 104	81	23	R 104	86	17
520	R 104	80	24	R 104	84	20	R 104	82	22	R 104	78	26	R 104	83	21	R 104	81	23	R 104	81	23	G 104	82	22	R 104	86	18
521	G 104	81	24	R 104	84	20	R 104	82	22	G 104	79	26	R 104	83	21	R 104	81	24	R 104	81	23	G 104	82	22	R 104	86	18
522	G 104	81	23	R 104	84	20	R 104	82	22	G 104	79	25	R 104	83	21	R 104	81	24	R 104	81	23	G 104	83	22	R 104	86	18
523	G 105	82	23	R 105	84	21	R 105	82	23	G 105	80	25	R 105	83	21	R 105	81	24	R 105	81	24	G 105	83	21	R 105	86	18
524	G 105	82	23	R 105	84	21	R 105	82	23	G 105	80	25	R 105	83	22	R 105	81	24	R 105	81	24	G 105	84	21	R 105	86	18
525	G 105	83	23	R 105	84	21	R 105	82	23	G 105	81	25	R 105	83	22	R 105	81	24	R 105	81	24	G 105	84	21	R 105	86	19
526	G 105	83	22	R 105	84	21	R 105	82	23	G 105	81	24	R 105	83	22	R 105	81	25	R 105	81	24	G 105	85	20	R 105	86	19
527	G 105	84	22	R 105	84	21	R 105	82	23	G 105	82	24	R 105	83	22	R 105	81	25	R 105	81	24	G 105	85	20	R 105	86	19
528	G 106	84	22	R 106	84	22	R 106	82	24	G 106	82	24	R 106	83	22	R 106	81	25	R 106	81	25	G 106	86	20	R 106	86	19
529	G 106	85	21	R 106	84	22	R 106	82	24	G 106	83	23	R 106	83	23	R 106	81	25	R 106	81	25	G 106	86	20	R 106	86	19
530	G 106	85	21	R 106	84	22	R 106	82	24	G 106	83	23	R 106	83	23	R 106	81	25	R 106	81	25	G 106	87	19	R 106	86	20
531	G 106	86	21	R 106	84	22	G 106	83	24	G 106	84	23	R 106	83	23	R 106	81	26	R 106	81	25	G 106	87	19	R 106	86	20
532	G 106	86	20	R 106	84	22	G 106	83	23	G 106	84	22	R 106	83	23	R 106	81	26	R 106	81	25	G 106	88	19	R 106	86	20
533	G 107	87	20	R 107	84	23	G 107	84	23	G 107	85	22	R 107	83	23	R 107	81	26	R 107	81	26	G 107	88	18	R 107	86	20
534	G 107	87	20	R 107	84	23	G 107	84	23	G 107	85	22	R 107	83	24	G 107	81	26	R 107	81	26	G 107	89	18	R 107	86	20
535	G 107	88	20	R 107	84	23	G 107	85	23	G 107	86	22	R 107	83	24	G 107	82	25	R 107	81	26	G 107	89	18	R 107	86	21
536	G 107	88	19	R 107	84	23	G 107	85	22	G 107	86	21	R 107	83	24	G 107	82	25	R 107	81	26	G 107	90	17	R 107	86	21
537	G 107	88	19	R 107	84	23	G 107	86	22	G 107	87	21	R 107	83	24	G 107	83	25	R 107	81	26	G 107	90	17	R 107	86	21
538	G 108	89	19	R 108	84	24	G 108	86	22	G 108	87	21	R 108	83	24	G 108	83	25	R 108	81	27	G 108	91	17	R 108	86	21
539	G 108	90	18	R 108	84	24	G 108	87	21	G 108	88	20	R 108	83	25	G 108	84	24	R 108	81	27	G 108	91	17	R 108	86	21
540	G 108	90	18	R 108	84	24	G 108	87	21	G 108	88	20	R 108	83	25	G 108	84	24	R 108	81	27	G 108	92	16	R 108	86	22
541	R 108	90	18	G 108	85	24	G 108	88	21	G 108	89	20	R 108	83	25	G 108	85	24	R 108	81	27	R 108	92	16	R 108	86	22
542	R 109	90	18	G 108	85	23	G 109	88	20	G 108	89	19	R 108	83	25	G 108	85	23	R 108	81	27	R 108	92	17	R 108	86	22
543	R 109	90	19	G 109	86	23	G 109	89	20	G 109	90	19	R 109	83	25	G 109	86	23	R 109	81	28	R 109	92	17	R 109	86	22
544	R 109	90	19	G 109	86	23	G 109	89	20	G 109	90	19	R 109	83	26	G 109	86	23	R 109	81	28	R 109	92	17	R 109	86	22
545	R 109	90	19	G 109	87	23	G 109	90	20	G 109	91	19	R 109	83	26	G 109	87	22	R 109	81	28	R 109	92	17	R 109	86	23
546	R 109	90	19	G 109	87	22	G 109	90	19	G 109	91	18	R 109	83	26	G 109	87	22	R 109	81	28	R 109	92	17	R 109	86	23
547	R 109	90	19	G 109	88	22	G 109	91	19	R 109	91	18	G 109	84	26	G 109	88	22	R 109	81	28	R 109	92	18	R 109	86	23
548	R 110	90	20	G 110	88	22	G 110	91	19	R 110	91	19	G 110	84	25	G 110	88	22	R 110	81	29	R 110	92	18	R 110	86	23
549	R 110	90	20	G 110	89	21	G 110	92	18	R 110	91	19	G 110	85	25	G 110	89	21	R 110	81	29	R 110	92	18	R 110	86	23
550	R 110	90	20	G 110	89	21	G 110	92	18	R 110	91	19	G 110	85	25	G 110	89	21	R 110	81	29	R 110	92	18	R 110	86	24
551	R 110	90	20	G 110	90	21	R 110	92	18	R 110	91	19	G 110	86	25	G 110	90	21	R 110	81	29	R 110	92	18	R 110	86	24
552	R 110	90	20	G 110	90	20	R 110	92	18	R 110	91	19	G 110	86	24	G 110	90	20	R 110	81	29	R 110	92	19	R 110	86	24
553	R 111	90	21	G 111	91	20	R 111	92	19	R 111	91	20	G 111	87	24	G 111	91	20	R 111	81	30	R 111	92	19	R 111	86	24
554	R 111	90	21	G 111	91	20	R 111	92	19	R 111	91	20	G 111	87	24	G 111	91	20	R 111	81	30	R 111	92	19	R 111	86	24
555	R 111	90	21	G 111	92	20	R 111	92	19	R 111	91	20	G 111	88	23	G 111	92	19	R 111	81	30	R 111	92	19	R 111	86	25
556	R 111	90	21	G 111	92	19	R 111	92	19	R 111	91	20	G 111	88	23	G 111	92	19	R 111	81	30	R 111	92	19	R 111	86	25
557	R 111	90	21	G 111	93	19	R 111	92	19	R 111	91	20	G 111	89	23	G 111	93	19	R 111	81	30	R 111	92	20	R 111	86	25
558	R 112	90	22	G 112	93	19	R 112	92	20	R 112	91	21	G 112	89	22	G 112	93	19	R 112	81	31	R 112	92	20	R 112	86	25
559	R 112	90	22	G 112	94	18	R 112	92	20	R 112	91	21	G 112	90	22	G 112	94	18	R 112	81	31	R 112	92	20	R 112	86	25
560	R 112	90	22	G 112	94	18	R 112	92	20	R 112	91	21	G 112	90	22	R 112	94	18	R 112	81	31	R 112	92	20	R 112	86	26
561	R 112	90	22	R 112	94	18	R 112	92	20	R 112	91	21	G 112	91	22	R 112	94	19	R 112	81	31	R 112	92	20	R 112	86	26
562	R 112	90	22	R 112	94	18	R 112	92	20	R 112	91	21	G 112	91	21	R 112	94	19	R 112	81	31	R 112	92	21	R 112	86	26
563	R 113	90	23	R 113	94	19	R 113	92	21	R 113	91	22	G 113	92	21	R 113	94	19	R 113	81	32	R 113	92	21	R 113	86	26
564	R 113	90	23	R 113	94	19	R 113	92	21	R 113	91	22	G 113	92	21	R 113	94	19	R 113	81	32	R 113	92	21	R 113	86	26
565	R 113	90	23	R 113	94	19	R 113	92	21	R 113	91	22	G 113	93	20	R 113	94	19	R 113	81	32	R 113	92	21	R 113	86	27
566	R 113	90	23	R 113	94	19	R 113	92	21	R 113	91	22	G 113	93	20	R 113	94	20	R 113	81	32	R 113	92	21	R 113	86	27

Table C-1. Continued

A=Arrivals, D=Departures, Q=Queue:

Time (sec)	A	D	Q	A	D	Q	A	D	Q	A	D	Q	A	D	Q	A	D	Q	A	D	Q	A	D	Q	A	D	Q
567	113	90	23	113	94	19	113	92	21	113	91	22	113	94	20	113	94	20	113	81	32	113	92	22	113	86	27
568	114	90	24	114	94	20	114	92	22	114	91	23	114	94	19	114	94	20	114	81	33	114	92	22	114	86	27
569	114	90	24	114	94	20	114	92	22	114	91	23	114	95	19	114	94	20	114	81	33	114	92	22	114	86	27
570	114	90	24	114	94	20	114	92	22	114	91	23	114	95	19	114	94	20	114	81	33	114	92	22	114	86	28
571	114	90	24	114	94	20	114	92	22	114	91	23	114	96	19	114	94	21	114	81	33	114	92	22	114	86	28
572	114	90	24	114	94	20	114	92	22	114	91	23	114	96	19	114	94	21	114	81	33	114	92	23	114	86	28
573	115	90	25	115	94	21	115	92	23	115	91	24	115	96	18	115	94	21	115	81	34	115	92	23	115	86	28
574	115	90	25	115	94	21	115	92	23	115	91	24	115	96	19	115	94	21	115	81	34	115	92	23	115	86	28
575	115	90	25	115	94	21	115	92	23	115	91	24	115	96	19	115	94	21	115	81	34	115	92	23	115	86	29
576	115	90	25	115	94	21	115	92	23	115	91	24	115	96	19	115	94	22	115	81	34	115	92	23	115	86	29
577	115	90	25	115	94	21	115	92	23	115	91	24	115	96	19	115	94	22	115	81	34	115	92	24	115	86	29
578	116	90	26	116	94	22	116	92	24	116	91	25	116	96	19	116	94	22	116	81	35	116	92	24	116	86	29
579	116	90	26	116	94	22	116	92	24	116	91	25	116	96	20	116	94	22	116	81	35	116	92	24	116	86	29
580	116	90	26	116	94	22	116	92	24	116	91	25	116	96	20	116	94	22	116	81	35	116	92	24	116	86	30
581	116	91	26	116	94	22	116	92	24	116	91	25	116	96	20	116	94	23	116	81	35	116	92	24	116	86	30
582	116	91	25	116	94	22	116	92	24	116	91	25	116	96	20	116	94	23	116	81	35	116	92	25	116	86	30
583	117	92	25	117	94	23	117	92	25	117	91	26	117	96	20	117	94	23	117	81	36	117	92	25	117	86	30
584	117	92	25	117	94	23	117	92	25	117	91	26	117	96	21	117	94	23	117	81	36	117	92	25	117	86	30
585	117	93	25	117	94	23	117	92	25	117	91	26	117	96	21	117	94	23	117	81	36	117	92	25	117	86	31
586	117	93	24	117	94	23	117	92	25	117	91	26	117	96	21	117	94	24	117	81	36	117	92	25	117	86	31
587	117	94	24	117	94	23	117	92	25	117	91	26	117	96	21	117	94	24	117	81	36	117	92	26	117	86	31
588	118	94	24	118	94	24	118	92	26	118	91	27	118	96	21	118	94	24	118	81	37	118	92	26	118	86	31
589	118	95	23	118	94	24	118	92	26	118	91	27	118	96	22	118	94	24	118	81	37	118	92	26	118	86	31
590	118	95	23	118	94	24	118	92	26	118	91	27	118	96	22	118	94	24	118	81	37	118	92	26	118	86	32
591	118	96	23	118	94	24	118	93	26	118	91	27	118	96	22	118	94	25	118	81	37	118	92	26	118	86	32
592	118	96	22	118	94	24	118	93	25	118	91	27	118	96	22	118	94	25	118	81	37	118	92	27	118	86	32
593	119	97	22	119	94	25	119	94	25	119	91	28	119	96	22	119	94	25	119	81	38	119	92	27	119	86	32
594	119	97	22	119	94	25	119	94	25	119	91	28	119	96	23	119	94	25	119	81	38	119	92	27	119	86	32
595	119	98	22	119	94	25	119	95	25	119	91	28	119	96	23	119	94	25	119	82	38	119	92	27	119	86	33
596	119	98	21	119	94	25	119	95	24	119	91	28	119	96	23	119	94	26	119	82	37	119	92	27	119	86	33
597	119	99	21	119	94	25	119	96	24	119	91	28	119	96	23	119	94	26	119	83	37	119	92	28	119	86	33
598	120	99	21	120	94	26	120	96	24	120	91	29	120	96	23	120	94	26	120	83	37	120	92	28	120	86	33
599	120	100	20	120	94	26	120	97	23	120	92	28	120	96	24	120	94	26	120	84	36	120	92	28	120	86	33
600	120	100	20	120	94	26	120	97	23	120	92	28	120	96	24	120	94	26	120	84	36	120	92	28	120	86	34
601	120	100	20	120	95	26	120	98	23	120	93	28	120	96	24	120	94	27	120	85	36	120	92	28	120	86	34
602	120	100	20	120	95	25	120	98	22	120	93	27	120	96	24	120	94	27	120	85	35	120	92	29	120	86	34
603	121	100	21	121	96	25	121	99	22	121	94	27	121	96	24	121	94	27	121	86	35	121	92	29	121	86	34
604	121	100	21	121	96	25	121	99	22	121	94	27	121	96	25	121	94	27	121	86	35	121	92	29	121	86	34
605	121	100	21	121	97	25	121	100	22	121	95	27	121	96	25	121	94	27	121	87	35	121	92	29	121	86	35
606	121	100	21	121	97	24	121	100	21	121	95	28	121	96	25	121	94	28	121	87	34	121	92	29	121	86	35
607	121	100	21	121	98	24	121	101	21	121	96	28	121	96	25	121	94	28	121	88	34	121	92	30	121	86	35
608	122	100	22	122	98	24	122	101	21	122	96	26	122	96	25	122	94	28	122	88	34	122	92	30	122	86	35
609	122	100	22	122	99	23	122	102	20	122	97	25	122	96	26	122	94	28	122	88	33	122	92	30	122	86	35
610	122	100	22	122	99	23	122	102	20	122	97	25	122	96	26	122	94	28	122	89	33	122	92	30	122	86	36
611	122	100	22	122	100	23	122	102	20	122	98	25	122	96	26	122	94	29	122	90	33	122	92	30	122	86	36
612	122	100	22	122	100	22	122	102	20	122	98	24	122	96	26	122	94	28	122	90	32	122	92	31	122	86	36
613	123	100	23	123	101	22	123	102	21	123	99	24	123	96	26	123	95	28	123	91	32	123	92	31	123	86	36
614	123	100	23	123	101	22	123	102	21	123	99	24	123	96	27	123	95	28	123	91	32	123	92	31	123	86	36
615	123	100	23	123	102	22	123	102	21	123	100	24	123	96	27	123	96	27	123	92	32	123	92	31	123	86	37
616	123	100	23	123	102	21	123	102	21	123	100	23	123	96	27	123	96	27	123	92	31	123	92	31	123	86	37
617	123	100	23	123	103	21	123	102	21	123	101	23	123	96	27	123	97	27	123	93	31	123	92	32	123	86	37
618	124	100	24	124	103	21	124	102	22	124	101	23	124	96	27	124	97	27	124	93	31	124	92	32	124	86	37
619	124	100	24	124	104	20	124	102	22	124	102	22	124	96	28	124	98	26	124	94	30	124	92	32	124	86	37
620	124	100	24	124	104	20	124	102	22	124	102	22	124	96	28	124	98	26	124	94	30	124	92	32	124	86	38
621	124	100	24	124	104	20	124	102	22	124	103	22	124	96	28	124	99	26	124	95	30	124	92	32	124	86	38
622	124	100	24	124	104	20	124	102	22	124	103	21	124	96	28	124	99	25	124	95	29	124	92	33	124	87	38
623	125	100	25	125	104	21	125	102	23	125	104	21	125	96	28	125	100	25	125	96	29	125	92	33	125	87	37
624	125	100	25	125	104	21	125	102	23	125	104	21	125	96	29	125	100	25	125	96	29	125	92	33	125	88	37
625	125	100	25	125	104	21	125	102	23	125	104	21	125	97	28	125	101	24	125	97	29	125	92	33	125	88	37
626	125	100	25	125	104	21	125	102	23	125	104	21	125	97	28	125	101	24	125	97	28	125	92	33	125	89	36
627	125	100	25	125	104	21	125	102	23	125	104	21	125	98	28	125	102	24	125	98	28	125	92	34	125	89	36
628	126	100	26	126	104	22	126	102	24	126	104	22	126	98	27	126	102	24	126	99	28	126	92	34	126	90	36
629	126	100	26	126	104	22	126	102	24	126	104	22	126	99	27	126	103	23	126	99	27	126	92	34	126	90	35
630	126	100	26	126	104	22	126	102	24	126	104	22	126	99	27	126	103	23	126	99	27	126	92	34	126	91	35
631	126	100	26	126	104	22	126	102	24	126	104	22	126	100	27	126	104	23	126	100	27	126	92	34	126	91	35
632	126	100	26	126	104	22	126	102	24	126	104	22	126	100	26	126	104	22	126	100	26	126	92	35	126	92	35
633	127	100	27	127	104	23	127	102	25	127	104	23	127	101	26	127	105	22	127	101	26	127	92	35	127	92	34
634	127	100	27	127	104	23	127	102	25	127	104	23	127	101	26	127	105	22	127	101	26	127	92	35	127	93	34
635	127	100	27	127	104	23	127	102	25	127	104	23	127	102	25	127	106	21	127	102	26	127	92	35	127	93	34
636	127	100	27	127	104	23	127	102	25	127	104	23	127	102	25	127	106	21	127	102	25	127	92	35	127	94	33
637	127	100	27	127	104	23	127	102	25	127	104	23	127	103	25	127	107	21	127	103	25	127	92	36	127	94	33
638	128	100	28	128	104	24	128	102	26	128	104	24	128	103	24	128	107	21	128	103	25	128	92	36	128	95	33
639	128	100	28	128	104	24	128	102	26	128	104	24	128	104	24	128	107	21	128	104	24	128	92	36	128	95	32
640	128	100	28	128	104	24	128	102	26	128	104	24	128	104	24	128	107	21	128	104	24	128	92	36	128	96	32
641	128	101	28	128	104	24	128	102	26	128	104	24	128	105	24	128	107	22	128	105	24	128	92	36	128	96	32
642	129	101	27	129	104	24	129	102	26	129	104	24	129	105	23	129	107	22	129	105	23	129	92	37	129	97	32
643	129	102	27	129	104	25	129	102	27	129	104	25	129	106	23	129	107	22	129	106	23	129	92	37	129	97	31
644	129	102	27	129	104	25	129	102	27	129	104	25	129	106	23	129	107	22	129	106	23	129	92	37	129	98	31
645	129	103	27	129	104	25	129	102	27	129	104	25	129	107	22	129	107	23	129	107	22	129	92	37	129	98	31
646	129	103	26	129	104	25	129	102	27	129	104	25	129	107	22	129	107	23	129	107	22	129	92	37	129	99	30
647	129	104	26	129	104	25	129	102	27	129	104	25	129	108	22	129	107	23	129	108	22	129	92	38	129	99	30
648	130	104	26	130	104	26	130	102	28	130	104	26	130	108	21	130	107	23	130	108	22	130	92	38	130	100	30
649	130	105	25	130	104	26	130	102	28	130	104	26	130	109	21	130	107	23	130	108	22	130	92	38	130	100	29

Table C-1. Continued

A=Arrivals, D=Departures, Q=Queue:

Time (sec)	A	D	Q	A	D	Q	A	D	Q	A	D	Q	A	D	Q	A	D	Q	A	D	Q	A	D	Q	A	D	Q
650	G	130	105	25	R	130	104	26	R	130	102	28	R	130	104	26	G	130	109	21	R	130	107	23	R	130	108	22	G	130	93	37	G	130	101	29
651	G	130	106	25	R	130	104	26	G	130	103	28	R	130	104	26	R	130	109	21	R	130	107	24	R	130	108	22	G	130	93	37	G	130	101	29
652	G	130	106	24	R	130	104	26	G	130	103	27	R	130	104	26	R	130	109	21	R	130	107	24	R	130	108	22	G	130	94	37	G	130	102	29
653	G	131	107	24	R	131	104	27	G	131	104	27	R	131	104	27	R	131	109	21	R	131	107	24	R	131	108	23	G	131	94	36	G	131	102	28
654	G	131	107	24	R	131	104	27	G	131	104	27	R	131	104	27	R	131	109	22	R	131	107	24	R	131	108	23	G	131	95	36	G	131	103	28
655	G	131	108	24	R	131	104	27	G	131	105	27	R	131	104	27	R	131	109	22	R	131	107	24	R	131	108	23	G	131	95	36	G	131	103	28
656	G	131	108	23	R	131	104	27	G	131	105	26	R	131	104	27	R	131	109	22	R	131	107	25	R	131	108	23	G	131	96	35	G	131	104	27
657	G	131	109	23	R	131	104	27	G	131	106	26	R	131	104	27	R	131	109	22	R	131	107	25	R	131	108	23	G	131	96	35	G	131	104	27
658	G	132	109	23	R	132	104	28	G	132	106	26	R	132	104	28	R	132	109	22	R	132	107	25	R	132	108	24	G	132	97	35	G	132	105	27
659	G	132	110	22	R	132	104	28	G	132	107	25	R	132	104	28	R	132	109	23	R	132	107	25	R	132	108	24	G	132	97	35	G	132	105	26
660	G	132	110	22	R	132	104	28	G	132	107	25	R	132	104	28	R	132	109	23	R	132	107	25	R	132	108	24	G	132	98	34	G	132	106	26
661	R	132	110	22	G	132	105	28	G	132	108	25	R	132	104	28	R	132	109	23	R	132	107	26	R	132	108	24	G	132	98	34	G	132	106	26
662	R	132	110	22	G	132	105	27	G	132	108	24	R	132	104	28	R	132	109	23	R	132	107	26	R	132	108	24	G	132	99	34	G	132	107	26
663	R	133	110	23	G	133	106	27	G	133	109	24	R	133	104	28	R	133	109	23	R	133	107	26	R	133	108	25	G	133	99	33	G	133	107	25
664	R	133	110	23	G	133	106	27	G	133	109	24	R	133	104	28	R	133	109	24	R	133	107	26	R	133	108	25	G	133	100	33	G	133	108	25
665	R	133	110	23	G	133	107	27	G	133	110	24	R	133	104	28	R	133	109	24	R	133	107	26	R	133	108	25	G	133	100	33	G	133	108	25
666	R	133	110	23	G	133	107	26	G	133	110	23	R	133	104	29	R	133	109	24	R	133	107	27	R	133	108	25	G	133	101	32	G	133	109	24
667	R	133	110	23	G	133	108	26	G	133	111	23	R	133	104	29	R	133	109	24	R	133	107	27	R	133	108	25	G	133	101	32	G	133	109	24
668	R	134	110	24	G	134	108	26	G	134	111	23	R	134	104	30	R	134	109	24	R	134	107	27	R	134	108	26	G	134	102	32	G	134	110	24
669	R	134	110	24	G	134	109	25	G	134	112	22	R	134	104	30	R	134	109	25	R	134	107	27	R	134	108	26	G	134	102	32	G	134	110	23
670	R	134	110	24	G	134	109	25	G	134	112	22	R	134	104	30	R	134	109	25	R	134	107	27	R	134	108	26	G	134	103	31	G	134	111	23
671	R	134	110	24	G	134	110	25	R	134	112	22	R	134	104	30	R	134	109	25	R	134	107	28	R	134	108	26	G	134	103	31	G	134	111	23
672	R	134	110	24	G	134	110	24	R	134	112	22	R	134	104	30	R	134	109	25	R	134	107	28	R	134	108	26	G	134	104	31	G	134	112	23
673	R	135	110	25	G	135	111	24	R	135	112	23	R	135	104	31	R	135	109	25	R	135	107	28	R	135	108	27	G	135	104	30	G	135	112	22
674	R	135	110	25	G	135	111	24	R	135	112	23	R	135	104	31	R	135	109	26	R	135	107	28	R	135	108	27	G	135	105	30	G	135	113	22
675	R	135	110	25	G	135	112	24	R	135	112	23	R	135	104	31	R	135	109	26	R	135	107	28	R	135	108	27	G	135	105	30	G	135	113	22
676	R	135	110	25	C	135	112	23	R	135	112	23	R	135	104	31	R	135	109	26	R	135	107	29	R	135	108	27	G	135	106	29	R	135	113	22
677	R	135	110	25	G	135	113	23	R	135	112	23	G	135	105	31	R	135	109	26	R	135	107	29	R	135	108	27	G	135	106	29	R	135	113	22
678	R	136	110	26	G	136	113	23	R	136	112	24	G	136	105	31	R	136	109	26	R	136	107	29	R	136	108	28	G	136	107	29	R	136	113	22
679	R	136	110	26	G	136	114	22	R	136	112	24	G	136	106	30	R	136	109	27	R	136	107	29	R	136	108	28	G	136	107	29	R	136	113	22
680	R	136	110	26	G	136	114	22	R	136	112	24	G	136	106	30	R	136	109	27	R	136	107	29	R	136	108	28	G	136	108	28	R	136	113	23
681	R	136	110	26	R	136	114	22	R	136	112	24	G	136	107	30	R	136	109	27	R	136	107	30	R	136	108	28	G	136	108	28	R	136	113	23
682	R	136	110	26	R	136	114	22	R	136	112	24	G	136	107	28	R	136	109	27	R	136	107	30	R	136	108	28	G	136	109	28	R	136	113	23
683	R	137	110	27	R	137	114	23	R	137	112	25	G	137	108	29	R	137	109	27	R	137	107	30	R	137	109	29	G	137	109	27	R	137	113	23
684	R	137	110	27	R	137	114	23	R	137	112	25	G	137	108	29	R	137	109	28	R	137	107	30	R	137	109	29	G	137	110	27	R	137	113	23
685	R	137	110	27	R	137	114	23	R	137	112	25	G	137	109	29	R	137	109	28	R	137	107	30	R	137	108	29	G	137	110	27	R	137	113	24
686	R	137	110	27	R	137	114	23	R	137	112	25	G	137	109	29	R	137	109	28	R	137	107	31	R	137	108	29	G	137	111	26	R	137	113	24
687	R	137	110	27	R	137	114	23	R	137	112	25	G	137	110	29	R	137	109	29	R	137	107	31	R	137	108	29	G	137	111	26	R	137	113	24
688	R	138	110	28	R	138	114	24	R	138	112	26	G	138	110	28	R	138	109	29	R	138	107	31	R	138	108	30	G	138	112	26	R	138	113	24
689	R	138	110	28	R	138	114	24	R	138	112	26	G	138	111	27	R	138	109	29	R	138	107	31	R	138	108	30	G	138	112	26	R	138	113	24
690	R	138	110	28	R	138	114	24	R	138	112	26	G	138	111	27	R	138	109	29	G	138	107	31	R	138	108	30	G	138	113	25	R	138	113	25
691	R	138	110	28	R	138	114	24	R	138	112	26	G	138	112	27	R	138	109	29	G	138	108	31	R	138	108	30	G	138	113	25	R	138	113	25
692	R	138	110	28	R	138	114	24	R	138	112	26	G	138	112	28	R	138	109	29	G	138	108	30	R	138	108	30	G	138	114	25	R	138	113	25
693	R	139	110	29	R	139	114	25	R	139	112	27	G	139	113	28	R	139	109	29	G	139	109	30	R	139	108	31	G	139	114	24	R	139	113	25
694	R	139	110	29	R	139	114	25	R	139	112	27	G	139	113	28	R	139	109	30	G	139	109	30	R	139	108	31	G	139	115	24	R	139	113	25
695	R	139	110	29	R	139	114	25	R	139	112	27	G	139	114	28	R	139	109	30	G	139	110	29	R	139	108	31	G	139	115	24	R	139	113	26
696	R	139	110	29	R	139	114	25	R	139	112	27	G	139	114	25	R	139	109	30	G	139	110	29	R	139	108	31	G	139	116	23	R	139	113	26
697	R	139	110	29	R	139	114	25	R	139	112	27	G	139	115	25	R	139	109	30	G	139	111	29	R	139	108	31	G	139	116	23	R	139	113	26
698	R	140	110	30	R	140	114	26	R	140	112	28	G	140	115	25	R	140	109	30	G	140	111	29	R	140	108	32	G	140	117	23	R	140	113	26
699	R	140	110	30	R	140	114	26	R	140	112	28	G	140	116	24	R	140	109	31	G	140	112	28	R	140	108	32	G	140	117	23	R	140	113	26
700	R	140	110	30	R	140	114	26	R	140	112	28	G	140	116	24	R	140	109	31	G	140	112	28	R	140	108	32	G	140	118	22	R	140	113	27
701	G	140	111	30	R	140	114	26	R	140	112	28	G	140	117	24	R	140	109	31	G	140	113	28	R	140	108	32	G	140	118	22	R	140	113	27
702	G	140	111	29	R	140	114	26	R	140	112	28	G	140	117	23	R	140	109	31	G	140	113	27	R	140	108	32	G	140	119	22	R	140	113	27
703	G	141	112	29	R	141	114	27	R	141	112	29	R	141	117	24	G	141	110	31	G	141	114	27	R	141	108	33	R	141	119	22	R	141	113	27
704	G	141	112	29	R	141	114	27	R	141	112	29	R	141	117	24	G	141	110	31	G	141	114	27	R	141	108	33	R	141	119	22	R	141	113	27
705	G	141	113	29	R	141	114	27	R	141	112	29	R	141	117	24	G	141	111	30	G	141	115	26	R	141	108	33	R	141	119	22	R	141	113	28
706	G	141	113	28	R	141	114	27	R	141	112	29	R	141	117	24	G	141	111	30	G	141	115	26	R	141	108	33	R	141	119	22	R	141	113	28
707	G	141	114	28	R	141	114	27	R	141	112	29	R	141	117	24	G	141	112	30	G	141	116	26	R	141	108	33	R	141	119	23	R	141	113	28
708	G	142	114	28	R	142	114	28	R	142	112	30	R	142	117	25	G	142	112	29	G	142	116	26	R	142	108	34	R	142	119	23	R	142	113	28
709	G	142	115	27	R	142	114	28	R	142	112	30	R	142	117	25	G	142	113	29	G	142	117	25	R	142	108	34	R	142	119	23	R	142	113	28
710	G	142	115	27	R	142	114	28	R	142	112	30	R	142	117	25	G	142	113	29	G	142	117	25	R	142	108	34	R	142	119	23	R	142	113	29
711	G	142	116	27	R	142	114	28	G	142	113	30	R	142	117	25	G	142	114	29	G	142	118	25	R	142	108	34	R	142	119	23	R	142	113	29
712	G	142	116	26	R	142	114	28	G	142	113	29	R	142	117	25	G	142	114	28	G	142	118	24	R	142	108	34	R	142	119	24	R	142	113	29
713	G	143	117	26	R	143	114	29	G	143	114	29	R	143	117	26	G	143	115	28	G	143	118	24	R	143	108	35	R	143	119	24	R	143	113	29
714	G	143	117	26	R	143	114	29	G	143	114	29	R	143	117	26	G	143	115	28	G	143	118	24	R	143	108	35	R	143	119	24	R	143	113	29
715	G	143	118	26	R	143	114	29	G	143	115	29	R	143	117	26	G	143	116	27	G	143	120	23	R	143	108	35	R	143	119	24	R	143	113	30
716	G	143	118	25	R	143	114	29	G	143	115	28	R	143	117	26	G	143	116	27	R	143	120	24	R	143	108	35	R	143	119	24	R	143	113	30
717	G	143	119	25	R	143	114	29	G	143	116	28	R	143	117	26	G	143	117	27	R	143	120	24	R	143	108	35	R	143	119	25	R	143	113	30
718	G	144	119	25	R	144	114	30	G	144	116	28	R	144	117	27	G	144	117	26	R	144	120	24	R	144	108	36	R	144	119	25	R	144	113	30
719	G	144	120	24	R	144	114	30	G	144	117	27	R	144	117	27	G	144	118	26	R	144	120	24	R	144	108	36	R	144	119	25	R	144	113	30
720	G	144	120	24	R	144	114	30	G	144	117	27	R	144	117	27	G	144	118	26	R	144	120	24	R	144	108	36	R	144	119	25	R	144	113	31
721	R	144	120	24	G	144	115	30	G	144	118	27	R	144	117	27	G	144	119	26	R	144	120	25	R	144	108	36	R	144	119	25	R	144	113	31
722	R	144	120	24	G	144	115	29	G	144	118	26	R	144	117	27	G	144	119	25	R	144	120	25	R	144	108	36	R	144	119	26	R	144	113	31
723	R	145	120	25	G	145	116	29	G	145	119	26	R	145	117	28	G	145	120	25	R	145	120	25	R	145	108	37	R	145	119	26	R	145	113	31
724	R	145	120	25	G	145	116	29	G	145	119	26	R	145	117	28	G	145	120	25	R	145	120	25	R	145	108	37	R	145	119	26	R	145	113	31
725	R	145	120	25	C	145	117	29	G	145	120	26	R	145	117	28	G	145	121	24	R	145	120	25	R	145	108	37	R	145	119	26	R	145	113	32
726	R	145	120	25	G	145	117	28	G	145	120	25	R	145	117	28	G	145	121	24	R	145	120	26	R	145	108	37	R	145	119	26	R	145	113	32
727	R	145	120	25	G	145	118	28	G	145	121	25	R	145	117	28	G	145	122	24	R	145	120	26	R	145	108	37	R	145	119	27	R	145	113	32
728	R	146	120	26	G	146	118	28	G	146	121	25	R	146	117	29	G	146	122	23	R	146	120	26	R	146	108	38	R	146	119	27	R	146	113	32
729	R	146	120	26	G	146	119	27	G	146	122	24	R	146	117	29	R	146	122	24	R	146	120	26	R	146	108	38	R	146	119	27	R	146	113	32
730	R	146	120	26	G	146	119	27	G	146	122	24	R	146	117	29	R	146	122	24	R	146	120	26	R	146	108	38	R	146	119	27	R	146	113	33
731	R	146	120	26	G	146	120	27	R	146	122	24	R	146	117	29	R	146	122	24	R	146	120	27	R	146	108	38	R	146	119	27	R	146	113	33
732	R	146	120	26	G	146	120	26	R	146	122	24	R	146	117	29	R	146	122	24	R	146	120	27	R	146	108	38	R	146	119	28	R	146	113	33

Table C-1. Continued

A=Arrivals, D=Departures, Q=Queue:

Time (sec)	A	D	Q	A	D	Q	A	D	Q	A	D	Q	A	D	Q	A	D	Q	A	D	Q	A	D	Q	A	D	Q
733	R 147	120	27	G 147	121	26	R 147	122	25	R 147	117	30	R 147	122	24	R 147	120	27	R 147	108	39	R 147	119	28	R 147	113	33
734	R 147	120	27	G 147	121	26	R 147	122	25	R 147	117	30	R 147	122	25	R 147	120	27	R 147	108	39	R 147	119	28	R 147	113	33
735	R 147	120	27	G 147	122	26	R 147	122	25	R 147	117	30	R 147	122	25	R 147	120	27	R 147	108	39	R 147	119	28	R 147	113	34
736	R 147	120	27	G 147	122	25	R 147	122	25	R 147	117	30	R 147	122	25	R 147	120	28	R 147	108	39	R 147	119	28	R 147	113	34
737	R 147	120	27	G 147	123	25	R 147	122	25	R 147	117	30	R 147	122	25	R 147	120	28	R 147	108	39	R 147	119	29	R 147	113	34
738	R 148	120	28	G 148	123	25	R 148	122	26	R 148	117	31	R 148	122	25	R 148	120	28	R 148	108	40	R 148	119	29	R 148	113	34
739	R 148	120	28	G 148	124	24	R 148	122	26	R 148	117	31	R 148	122	26	R 148	120	28	R 148	108	40	R 148	119	29	R 148	113	34
740	R 148	120	28	G 148	124	24	R 148	122	26	R 148	117	31	R 148	122	26	R 148	120	28	R 148	108	40	R 148	119	29	R 148	113	35
741	R 148	120	28	R 148	124	24	R 148	122	26	R 148	117	31	R 148	122	26	R 148	120	29	R 148	108	40	R 148	119	29	R 148	113	35
742	R 148	120	28	R 148	124	24	R 148	122	26	R 148	117	31	R 148	122	26	R 148	120	29	R 148	108	40	R 148	119	30	R 148	113	35
743	R 149	120	28	R 149	124	25	R 149	122	27	R 149	117	32	R 149	122	26	R 149	120	29	R 149	108	41	R 149	119	30	R 149	113	35
744	R 149	120	28	R 149	124	25	R 149	122	27	R 149	117	32	R 149	122	27	R 149	120	29	R 149	108	41	R 149	119	30	R 149	113	35
745	R 149	120	29	R 149	124	25	R 149	122	27	R 149	117	32	R 149	122	27	R 149	120	29	R 149	108	41	R 149	119	30	R 149	113	36
746	R 149	120	29	R 149	124	25	R 149	122	27	R 149	117	32	R 149	122	27	R 149	120	30	R 149	108	41	R 149	119	30	R 149	113	36
747	R 149	120	29	R 149	124	25	R 149	122	27	R 149	117	32	R 149	122	27	R 149	120	30	R 149	108	41	R 149	119	31	R 149	113	36
748	R 150	120	30	R 150	124	26	R 150	122	28	R 150	117	33	R 150	122	27	R 150	120	30	R 150	108	42	R 150	119	31	R 150	113	36
749	R 150	120	30	R 150	124	26	R 150	122	28	R 150	117	33	R 150	122	28	R 150	120	30	R 150	108	42	R 150	119	31	R 150	113	36
750	R 150	120	30	R 150	124	26	R 150	122	28	R 150	117	33	R 150	122	28	R 150	120	30	R 150	108	42	R 150	119	31	R 150	113	37
751	R 150	120	30	R 150	124	26	R 150	122	28	R 150	117	33	R 150	122	28	R 150	120	31	R 150	108	42	R 150	119	31	R 150	113	37
752	R 150	120	30	R 150	124	26	R 150	122	28	R 150	117	33	R 150	122	28	R 150	120	31	R 150	108	42	R 150	119	32	R 150	113	37
753	R 151	120	31	R 151	124	27	R 151	122	29	R 151	117	34	R 151	122	28	R 151	120	31	R 151	108	43	R 151	119	32	R 151	113	37
754	R 151	120	31	R 151	124	27	R 151	122	29	R 151	117	34	R 151	122	29	R 151	120	31	R 151	108	43	R 151	119	32	R 151	113	37
755	R 151	120	31	R 151	124	27	R 151	122	29	G 151	118	34	R 151	122	29	R 151	120	31	R 151	108	43	R 151	119	32	R 151	113	38
756	R 151	120	31	R 151	124	27	R 151	122	29	G 151	118	33	R 151	122	29	R 151	120	32	R 151.2	108.0	43.2	R 151	119	32	R 151	113	38
757	R 151	120	31	R 151	124	27	R 151	122	29	G 151	119	33	R 151	122	29	R 151	120	32	G 151	109	43	R 151	119	33	R 151	113	38
758	R 152	120	32	R 152	124	28	R 152	122	30	G 152	119	33	R 152	122	29	R 152	120	32	G 152	109	43	R 152	119	33	R 152	113	38
759	R 152	120	32	R 152	124	28	R 152	122	30	G 152	120	32	R 152	122	30	R 152	120	32	G 152	110	42	R 152	119	33	R 152	113	39
760	R 152	120	32	R 152	124	28	R 152	122	30	G 152	120	32	R 152	122	30	R 152	120	32	G 152	110	42	R 152	119	33	R 152	113	39
761	G 152	121	32	R 152	124	28	R 152	122	30	G 152	121	32	R 152	122	30	R 152	120	33	G 152	111	42	R 152	119	33	R 152	113	39
762	G 152	121	31	R 152	124	28	R 152	122	30	G 152	121	31	R 152	122	30	R 152	120	33	G 152	111	41	R 152	119	34	R 152	113	39
763	G 153	122	31	R 153	124	29	R 153	122	31	G 153	122	31	R 153	122	30	R 153	120	33	G 153	112	41	R 153	119	34	R 153	113	39
764	G 153	122	31	R 153	124	29	R 153	122	31	G 153	122	31	R 153	122	31	R 153	120	33	G 153	112	41	R 153	119	34	R 153	113	39
765	G 153	123	30	R 153	124	29	R 153	122	31	G 153	123	30	R 153	122	31	R 153	120	33	G 153	113	40	R 153	119	34	R 153	113	40
766	G 153	123	30	R 153	124	29	R 153	122	31	G 153	123	30	R 153	122	31	R 153	120	34	G 153	113	40	R 153	119	34	R 153	113	40
767	G 153	124	30	R 153	124	29	R 153	122	31	G 153	124	30	R 153	122	31	R 153	120	34	G 153	114	40	R 153	119	35	R 153	113	40
768	G 154	124	30	R 154	124	30	R 154	122	32	G 154	124	30	R 154	122	31	G 154	120	33	G 154	114	40	R 154	119	35	R 154	113	40
769	G 154	125	29	R 154	124	30	R 154	122	32	G 154	125	29	R 154	122	32	G 154	121	33	G 154	115	39	R 154	119	35	R 154	113	40
770	G 154	125	29	R 154	124	30	R 154	122	32	G 154	125	29	R 154	122	32	G 154	121	33	G 154	115	39	R 154	119	35	R 154	113	41
771	G 154	126	29	R 154	124	30	G 154	123	32	G 154	126	29	R 154	122	32	G 154	122	33	G 154	116	39	R 154	119	35	R 154	113	41
772	G 154	126	28	R 154	124	30	G 154	123	31	G 154	126	28	R 154	122	32	G 154	122	32	G 154	116	38	R 154	119	36	R 154	113	41
773	G 155	127	28	R 155	124	31	G 155	124	31	G 155	127	28	R 155	122	32	G 155	123	32	G 155	117	38	R 155	119	36	R 155	113	41
774	G 155	127	28	R 155	124	31	G 155	124	31	G 155	127	28	R 155	122	33	G 155	123	32	G 155	117	38	R 155	119	36	R 155	113	41
775	G 155	128	27	R 155	124	31	G 155	125	30	G 155	128	27	R 155	122	33	G 155	124	31	G 155	118	37	R 155	119	36	R 155	113	42
776	G 155	128	27	R 155	124	31	G 155	125	30	G 155	128	27	R 155	122	33	G 155	124	31	G 155	118	37	R 155	119	36	R 155	113	42
777	G 155	129	27	R 155	124	31	G 155	126	30	G 155	129	27	R 155	122	33	G 155	125	31	G 155	119	37	R 155	119	37	R 155	113	42
778	G 156	129	27	R 156	124	32	G 156	126	30	G 156	129	27	R 156	122	33	G 156	125	30	G 156	119	37	R 156	119	37	R 156	113	42
779	G 156	130	26	R 156	124	32	G 156	127	29	G 156	130	26	R 156	122	34	G 156	126	30	G 156	120	36	R 156	119	37	R 156	113	42
780	G 156	130	26	R 156	124	32	G 156	127	29	G 156	130	26	R 156	122	34	G 156	126	30	G 156	120	36	R 156	119	37	R 156	113	43
781	R 156	130	26	G 156	125	32	G 156	128	29	R 156	130	26	G 156	123	33	G 156	127	30	G 156	121	36	R 156	119	37	R 156	113	43
782	R 156	130	26	G 156	125	31	G 156	128	28	R 156	130	26	G 156	123	33	G 156	127	29	G 156	121	35	R 156	119	38	R 156	113	43
783	R 157	130	27	G 157	126	31	G 157	129	28	R 157	130	27	G 157	124	33	G 157	128	29	G 157	122	35	R 157	119	38	R 156.8	113.4	43.2
784	R 157	130	27	G 157	126	31	G 157	129	28	R 157	130	27	G 157	124	33	G 157	128	29	G 157	122	35	R 157	119	38	G 157	114	43
785	R 157	130	27	G 157	127	30	G 157	130	27	R 157	130	27	G 157	125	32	G 157	128	28	G 157	123	34	R 157	119	38	G 157	114	43
786	R 157	130	27	G 157	127	30	G 157	130	27	R 157	130	27	G 157	125	32	G 157	128	28	G 157	123	34	R 157	119	38	G 157	115	42
787	R 157	130	27	G 157	128	30	G 157	131	27	R 157	130	27	G 157	126	32	G 157	130	28	G 157	124	34	R 157	119	39	G 157	115	42
788	R 158	130	28	G 158	128	30	G 158	131	27	R 158	130	28	G 158	126	31	G 158	130	27	G 158	124	34	R 158	119	39	G 158	116	42
789	R 158	130	28	G 158	129	29	G 158	132	26	R 158	130	28	G 158	127	31	G 158	131	27	G 158	125	33	R 158	119	39	G 158	116	41
790	R 158	130	28	G 158	129	29	G 158	132	26	R 158	130	28	G 158	127	31	G 158	131	27	G 158	125	33	R 158	119	39	G 158	117	41
791	R 159	130	28	G 158	130	29	R 158	132	26	R 158	130	28	G 158	128	30	G 158	132	27	G 158	126	33	R 158	119	39	G 159	117	41
792	R 159	130	28	G 158	130	28	R 158	132	26	R 158	130	28	G 158	128	30	G 158	132	26	G 158	126	32	R 158	119	40	G 159	118	40
793	R 159	130	28	G 159	131	28	R 159	132	27	R 159	130	29	G 159	129	30	G 159	133	26	G 159	127	32	R 159	119	40	G 159	118	40
794	R 159	130	29	G 159	131	28	R 159	132	27	R 159	130	29	G 159	129	30	R 159	133	26	G 159	127	32	R 159	119	40	G 159	119	40
795	R 159	130	29	G 159	132	27	R 159	132	27	R 159	130	29	G 159	130	29	R 159	133	26	G 159	128	31	R 159	119	40	G 159	119	40
796	R 159	130	29	G 159	132	27	R 159	132	27	R 159	130	29	G 159	130	29	R 159	133	27	G 159	128	31	R 159	119	40	G 159	120	39
797	R 159	130	29	G 159	133	27	R 159	132	27	R 159	130	29	G 159	131	29	R 160	133	27	G 159	129	31	R 159	119	41	G 159	120	39
798	R 160	130	30	G 160	133	27	R 160	132	28	R 160	130	30	G 160	131	28	R 160	133	27	G 160	129	31	R 160	119	41	G 160	121	39
799	R 160	130	30	G 160	134	26	R 160	132	28	R 160	130	30	G 160	132	28	R 160	133	27	G 160	130	30	R 160	119	41	G 160	121	38
800	R 160	130	30	G 160	134	26	R 160	132	28	R 160	130	30	G 160	132	28	R 160	133	27	G 160	130	30	R 160	119	41	G 160	122	38
801	R 160	130	30	R 160	134	26	R 160	132	28	R 160	130	30	G 160	133	27	R 160	133	28	G 160	131	30	R 160	119	41	G 160	122	38
802	R 160	130	30	R 160	134	26	R 160	132	28	R 160	130	30	G 160	133	27	R 160	133	28	G 160	131	29	R 160	119	42	G 160	123	37
803	R 161	130	31	R 161	134	27	R 161	132	29	R 161	130	31	G 161	134	27	R 161	133	28	G 161	132	29	R 161	119	42	G 161	123	37
804	R 161	130	31	R 161	134	27	R 161	132	29	R 161	130	31	G 161	134	27	R 161	133	28	G 161	132	29	R 161	119	42	G 161	124	37
805	R 161	130	31	R 161	134	27	R 161	132	29	R 161	130	31	G 161	135	26	R 161	133	28	G 161	133	28	R 161	119	42	G 161	124	37
806	R 161	130	31	R 161	134	27	R 161	132	29	R 161	130	31	G 161	135	26	R 161	133	29	G 161	133	28	R 161	119	42	G 161	125	36
807	R 161	130	31	R 161	134	27	R 161	132	29	R 161	130	31	R 161	135	26	R 161	133	29	G 161	134	28	R 161	119	43	G 161	125	36
808	R 162	130	32	R 162	134	28	R 162	132	30	R 162	130	32	R 162	135	26	R 162	133	29	G 162	134	28	R 162	119	43	G 162	126	36
809	R 162	130	32	R 162	134	28	R 162	132	30	R 162	130	32	R 162	135	27	R 162	133	29	G 162	135	27	R 162	119	43	G 162	126	35
810	R 162	130	32	R 162	134	28	R 162	132	30	R 162	130	32	R 162	135	27	R 162	133	29	G 162	135	27	R 162.0	118.8	43.2	G 162	127	35
811	R 162	130	32	R 162	134	28	R 162	132	30	R 162	130	32	R 162	135	27	R 162	133	30	R 162	135	27	G 162	119	43	G 162	127	35
812	R 162	130	32	R 162	134	28	R 162	132	30	R 162	130	32	R 162	135	27	R 162	133	30	R 162	135	27	G 162	120	43	G 162	128	34
813	R 163	130	33	R 163	134	29	R 163	132	31	R 163	130	33	R 163	135	27	R 163	133	30	R 163	135	28	G 163	120	42	G 163	128	34
814	R 163	130	33	R 163	134	29	R 163	132	31	R 163	130	33	R 163	135	28	R 163	133	30	R 163	135	28	G 163	121	42	G 163	129	34
815	R 163	130	33	R 163	134	29	R 163	132	31	R 163	130	33	R 163	135	28	R 163	133	30	R 163	135	28	G 163	121	42	G 163	129	34

Table C-1. Continued

A=Arrivals, D=Departures, Q=Queue:

Time (sec)	A	D	Q	A	D	Q	A	D	Q	A	D	Q	A	D	Q	A	D	Q	A	D	Q	A	D	Q	A	D	Q
816	R	163	130	33	R	163	134	29	R	163	132	31	R	163	130	33	R	163	135	28	R	163	133	31	R	163	135	28	G	163	122	41	G	163	130	33
817	R	163	130	33	R	163	134	29	R	163	132	31	R	163	130	33	R	163	135	28	R	163	133	31	R	163	135	28	G	163	122	41	G	163	130	33
818	R	164	130	34	R	164	134	30	R	164	132	32	R	164	130	34	R	164	135	28	R	164	133	31	R	164	135	29	G	164	123	41	G	164	131	33
819	R	164	130	34	R	164	134	30	R	164	132	32	R	164	130	34	R	164	135	29	R	164	133	31	R	164	135	29	G	164	123	40	G	164	131	32
820	R	164	130	34	R	164	134	30	R	164	132	32	R	164	130	34	R	164	135	29	R	164	133	31	R	164	135	29	G	164	124	40	G	164	132	32
821	G	164	131	34	R	164	134	30	R	164	132	32	R	164	130	34	R	164	135	29	R	164	133	32	R	164	135	29	G	164	124	40	G	164	132	32
822	G	164	131	33	R	164	134	30	R	164	132	32	R	164	130	34	R	164	135	29	R	164	133	32	R	164	135	29	G	164	125	40	G	164	133	31
823	G	165	132	33	R	165	134	31	R	165	132	33	R	165	130	35	R	165	135	29	R	165	133	32	R	165	135	30	G	165	125	39	G	165	133	31
824	G	165	132	33	R	165	134	31	R	165	132	33	R	165	130	35	R	165	135	30	R	165	133	32	R	165	135	30	G	165	126	39	G	165	134	31
825	G	165	133	32	R	165	134	31	R	165	132	33	R	165	130	35	R	165	135	30	R	165	133	32	R	165	135	30	G	165	126	39	G	165	134	31
826	G	165	133	32	R	165	134	31	R	165	132	33	R	165	130	35	R	165	135	30	R	165	133	33	R	165	135	30	G	165	127	38	G	165	135	30
827	G	165	134	32	R	165	134	31	R	165	132	33	R	165	130	35	R	165	135	30	R	165	133	33	R	165	135	30	G	165	127	38	G	165	135	30
828	G	166	134	32	R	166	134	32	R	166	132	34	R	166	130	36	R	166	135	30	R	166	133	33	R	166	135	31	G	166	128	38	G	166	136	30
829	G	166	135	31	R	166	134	32	R	166	132	34	R	166	130	36	R	166	135	31	R	166	133	33	R	166	135	31	G	166	128	37	G	166	136	29
830	G	166	135	31	R	166	134	32	R	166	132	34	R	166	130	36	R	166	135	31	R	166	133	33	R	166	135	31	G	166	129	37	G	166	137	29
831	G	166	136	31	R	166	134	32	G	166	133	34	R	166	130	36	R	166	135	31	R	166	133	34	R	166	135	31	G	166	129	37	G	166	137	29
832	G	166	136	30	R	166	134	32	G	166	133	33	R	168.4	130.0	36.4	R	166	135	31	R	166	133	34	R	166	135	31	G	166	130	37	G	166	138	28
833	G	167	137	30	R	167	134	33	G	167	134	33	G	167	131	36	R	167	135	31	R	167	133	34	R	167	135	32	G	167	130	36	G	167	138	28
834	G	167	137	30	R	167	134	33	G	167	134	33	G	167	131	36	R	167	135	32	R	167	133	34	R	167	135	32	G	167	131	36	G	167	139	28
835	G	167	138	29	R	167	134	33	G	167	135	32	G	167	132	35	R	167	135	32	R	167	133	34	R	167	135	32	G	167	131	36	G	167	139	28
836	G	167	138	29	R	167	134	33	G	167	135	32	G	167	132	35	R	167	135	32	R	167	133	35	R	167	135	32	G	167	132	35	G	167	140	27
837	G	167	139	29	R	167	134	33	G	167	136	32	G	167	133	35	R	167	135	32	R	167	133	35	R	167	135	32	G	167	132	35	G	167	140	27
838	G	168	139	29	R	168	134	34	G	168	136	32	G	168	133	35	R	168	135	32	R	168	133	35	R	168	135	33	G	168	133	35	R	168	140	27
839	G	168	140	28	R	168	134	34	G	168	137	31	G	168	134	34	R	168	135	33	R	168	133	35	R	168	135	33	G	168	133	34	R	168	140	27
840	G	168	140	28	R	168	134	34	G	168	137	31	G	168	134	34	R	168	135	33	R	168	133	35	R	168	135	33	G	168	134	34	R	168	140	28
841	R	168	140	28	G	168	135	34	G	168	138	31	G	168	135	34	R	168	135	33	R	168	133	36	R	168	135	33	G	168	134	34	R	168	140	28
842	R	169	140	29	C	169	135	33	G	169	139	30	G	169	135	33	R	169	135	33	R	169	133	36	R	169	135	34	G	169	135	34	R	169	140	28
843	R	169	140	29	G	169	136	33	G	169	139	30	G	169	136	33	R	169	135	33	R	169	133	36	R	169	135	34	G	169	135	33	R	169	140	28
844	R	169	140	29	G	169	136	33	G	169	139	30	G	169	136	33	R	169	135	34	R	169	133	36	R	169	135	34	G	169	136	33	R	169	140	28
845	R	169	140	29	G	169	137	32	G	169	140	29	G	169	137	32	R	169	135	34	R	169.0	132.8	36.4	R	169	135	34	G	169	136	33	R	169	140	29
846	R	169	140	29	G	169	137	32	G	169	140	29	G	169	137	32	R	169	135	34	G	169	133	36	R	169	135	34	G	169	137	32	R	169	140	29
847	R	169	140	29	G	169	138	32	G	169	141	29	G	169	138	32	R	169	135	34	G	169	134	36	R	169	135	34	G	169	137	32	R	169	140	29
848	R	170	140	30	G	170	138	32	G	170	141	29	G	170	138	32	R	170	135	34	G	170	134	35	R	170	135	35	G	170	138	32	R	170	140	29
849	R	170	140	30	C	170	139	31	G	170	142	28	G	170	139	31	R	170	135	35	C	170	135	35	R	170	135	35	G	170	138	31	R	170	140	29
850	R	170	140	30	G	170	139	31	G	170	142	28	G	170	139	31	R	170	135	35	C	170	135	35	R	170	135	35	G	170	139	31	R	170	140	30
851	R	170	140	30	G	170	140	31	R	170	142	28	G	170	140	31	R	170	135	35	C	170	136	35	R	170	135	35	G	170	139	31	R	170	140	30
852	R	170	140	30	G	170	140	30	R	170	142	28	G	170	140	30	R	170	135	35	C	170	136	34	R	170	135	35	G	170	140	31	R	170	140	30
853	R	171	140	31	G	171	141	30	R	171	142	29	G	171	141	30	R	171	135	35	C	171	137	34	R	171	135	36	G	171	140	30	R	171	140	30
854	R	171	140	31	G	171	141	30	R	171	142	29	G	171	141	30	R	171	135	36	C	171	137	34	R	171	135	36	G	171	141	30	R	171	140	30
855	R	171	140	31	G	171	142	29	R	171	142	29	G	171	142	29	R	171	135	36	G	171	138	33	R	171	135	36	G	171	141	30	R	171	140	31
856	R	171	140	31	G	171	142	29	R	171	142	29	G	171	142	29	R	171	135	36	G	171	138	33	R	171	135	36	G	171	142	29	R	171	140	31
857	R	171	140	31	G	171	143	29	R	171	142	29	G	171	143	29	R	171	135	36	G	171	139	33	R	171	135	36	G	171	142	29	R	171	140	31
858	R	172	140	32	G	172	143	29	R	172	142	30	G	172	143	29	R	171.6	135.2	36.4	G	172	139	32	R	172	135	37	G	172	143	29	R	172	140	31
859	R	172	140	32	G	172	144	28	R	172	142	30	R	172	143	29	G	172	138	36	G	172	140	32	R	172	135	37	G	172	143	28	R	172	140	31
860	R	172	140	32	G	172	144	28	R	172	142	30	R	172	143	29	G	172	138	36	G	172	140	32	R	172	135	37	G	172	144	28	R	172	140	32
861	R	172	140	32	R	172	144	28	R	172	142	30	R	172	143	29	G	172	137	35	G	172	141	32	R	172	135	37	G	172	144	28	R	172	140	32
862	R	172	140	32	R	172	144	28	R	172	142	30	R	172	143	29	G	172	137	35	G	172	141	31	R	172	135	37	G	172	145	28	R	172	140	32
863	R	173	140	33	R	173	144	29	R	173	142	31	R	173	143	30	C	173	139	35	G	173	142	31	R	173	135	38	G	173	145	27	R	173	140	32
864	R	173	140	33	R	173	144	29	R	173	142	31	R	173	143	30	G	173	138	35	G	173	142	31	R	173	135	38	G	173	146	27	R	173	140	32
865	R	173	140	33	R	173	144	29	R	173	142	31	R	173	143	30	C	173	139	34	G	173	143	30	R	173	135	38	R	173	146	27	R	173	140	33
866	R	173	140	33	R	173	144	29	R	173	142	31	R	173	143	30	G	173	139	34	G	173	143	30	R	173	135	38	R	173	146	27	R	173	140	33
867	R	173	140	33	R	173	144	29	R	173	142	31	R	173	143	30	G	173	140	34	G	173	144	30	R	174	135	39	R	174	146	28	R	174	140	33
868	R	174	140	34	R	174	144	30	R	174	142	32	R	174	143	31	G	174	140	33	G	174	144	29	R	174	135	39	R	174	146	28	R	174	140	33
869	R	174	140	34	R	174	144	30	R	174	142	32	R	174	143	31	G	174	141	33	G	174	145	29	R	174	135	39	R	174	146	28	R	174	140	34
870	R	174	140	34	R	174	144	30	R	174	142	32	R	174	143	31	C	174	141	33	G	174	145	29	R	174	135	39	R	174	146	28	R	174	140	34
871	R	174	140	34	R	174	144	30	R	174	142	32	R	174	143	31	G	174	142	32	G	174	146	29	R	174	135	39	R	174	146	28	R	174	140	34
872	R	174	140	34	R	174	144	30	R	174	142	32	R	174	143	31	G	174	142	32	R	174	146	29	R	174	135	39	R	174	146	29	R	174	140	34
873	R	175	140	35	R	175	144	31	R	175	142	33	R	175	143	32	G	175	143	32	R	175	146	29	R	175	135	40	R	175	146	29	R	175	140	34
874	R	175	140	35	R	175	144	31	R	175	142	33	R	175	143	32	G	175	143	32	R	175	146	29	R	175	135	40	R	175	146	29	R	175	140	34
875	R	175	140	35	R	175	144	31	R	175	142	33	R	175	143	32	G	175	144	31	R	175	146	29	R	175	135	40	R	175	146	29	R	175	140	35
876	R	175	140	35	R	175	144	31	R	175	142	33	R	175	143	32	G	175	144	31	R	175	146	30	R	175	135	40	R	175	146	29	R	175	140	35
877	R	175	140	35	R	175	144	31	R	175	142	33	R	175	143	32	G	175	145	31	R	175	146	30	R	175	135	40	R	175	146	30	R	175	140	35
878	R	176	140	36	R	176	144	32	R	176	142	34	R	176	143	33	G	176	145	30	R	176	146	30	R	176	135	41	R	176	146	30	R	176	140	35
879	R	176	140	36	R	176	144	32	R	176	142	34	R	176	143	33	G	176	146	30	R	176	146	30	R	176	135	41	R	176	146	30	R	176	140	35
880	R	176	140	36	R	176	144	32	R	176	142	34	R	176	143	33	G	176	146	30	R	176	146	30	R	176	135	41	R	176	146	30	R	176	140	36
881	G	176	141	36	R	176	144	32	R	176	142	34	R	176	143	33	G	176	147	29	R	176	146	31	R	176	135	41	R	176	146	30	R	176	140	36
882	G	176	141	35	R	176	144	32	R	176	142	34	R	176	143	33	G	176	147	29	R	176	146	31	R	176	135	41	R	176	146	31	R	176	140	36
883	G	177	142	35	R	177	144	33	R	177	142	35	R	177	143	34	G	177	148	29	R	177	146	31	R	177	135	42	R	177	146	31	R	177	140	36
884	G	177	142	35	R	177	144	33	R	177	142	35	R	177	143	34	C	177	149	29	R	177	146	31	R	177	135	42	R	177	146	31	R	177	140	36
885	G	177	143	34	R	177	144	33	R	177	142	35	R	177	143	34	R	177	148	29	R	177	146	31	R	177	135	42	R	177	146	31	R	177	140	37
886	G	177	143	34	R	177	144	33	R	177	142	35	R	177	143	34	R	177	148	29	R	177	146	32	R	177	135	42	R	177	146	31	R	177	140	37
887	G	177	144	34	R	177	144	33	R	177	142	35	R	177	143	34	R	177	148	29	R	177	146	32	R	177	135	42	R	177	146	32	R	177	140	37
888	G	178	144	34	R	178	144	34	R	178	142	36	R	178	143	35	R	178	148	29	R	178	146	32	R	178	135	43	R	178	146	32	R	178	140	37
889	G	178	145	33	R	178	144	34	R	178	142	36	R	178	143	35	R	178	148	30	R	178	146	32	R	178	135	43	R	178	146	32	R	178	140	37
890	G	178	145	33	R	178	144	34	R	178	142	36	R	178	143	35	R	178	148	30	R	178	146	32	R	178	135	43	R	178	146	32	R	178	140	38
891	G	178	146	33	R	178	144	34	G	178	143	36	R	178	143	35	R	178	149	30	R	178	146	33	R	178	135	43	R	178	146	32	R	178	140	38
892	G	178	146	32	R	178	144	34	G	178	143	35	R	178	143	35	R	178	148	30	R	178	146	33	R	178	135	43	R	178	146	33	R	178	140	38
893	G	179	147	32	R	179	144	35	G	179	144	35	R	179	143	36	R	179	148	30	R	179	146	33	R	179	135	44	R	179	146	33	R	179	140	38
894	G	179	147	32	R	179	144	35	G	179	144	35	R	179	143	36	R	179	148	31	R	179	146	33	R	179	135	44	R	179	146	33	R	179	140	39
895	G	179	148	31	R	179	144	35	G	179	145	34	R	179	143	36	R	179	148	31	R	179	146	33	R	179	135	44	R	179	146	33	R	179	140	39
896	G	179	148	31	R	179	144	35	G	179	145	34	R	179	143	36	R	179	148	31	R	179	146	34	R	179	135	44	R	179	146	33	R	179	140	39
897	G	179	149	31	R	179	144	35	G	179	146	34	R	179	143	36	R	179	148	31	R	179	146	34	R	179	135	44	R	179	146	34	R	179	140	39
898	G	180	149	31	R	180	144	36	G	180	146	34	R	180	143	37	R	180	148	31	R	180	146	34	R	180	135	45	R	180	146	34	R	180	140	39

Table C-1. Continued

A=Arrivals, D=Departures, Q=Queue:

Time (sec)	A	D	Q	A	D	Q	A	D	Q	A	D	Q	A	D	Q	A	D	Q	A	D	Q	A	D	Q	A	D	Q
899	G	180	150	30	R	180	144	36	G	180	147	33	R	180	143	37	R	180	148	32	R	180	146	34	R	180	135	45	R	180	146	34	R	180	140	39
900	G	180	150	30	R	180	144	36	G	180	147	33	R	180	143	37	R	180	148	32	R	180	146	34	R	180	135	45	R	180	146	34	R	180	140	40
901	R	180	150	30	G	180	145	36	G	180	148	33	R	180	143	37	R	180	148	32	R	180	146	35	R	180	135	45	R	180	146	34	R	180	140	40
902	R	180	150	30	G	180	145	35	G	180	148	32	R	180	143	37	R	180	148	32	R	180	146	35	R	180	135	45	R	180	146	34	R	180	140	40
903	R	180	150	30	G	180	146	35	G	180	149	32	R	180	143	37	R	180	148	32	R	180	146	35	R	180	135	45	R	180	146	35	R	180	140	40
904	R	181	150	31	G	181	146	35	G	181	149	32	R	181	143	38	R	181	148	32	R	181	146	35	R	181	135	46	R	181	146	35	R	181	140	40
905	R	181	150	31	G	181	147	34	G	181	150	31	R	181	143	38	R	181	148	33	R	181	146	35	R	181	135	46	R	181	146	35	R	181	140	40
906	R	181	150	31	G	181	147	34	G	181	150	31	R	181	143	38	R	181	148	33	R	181	146	35	R	181	135	46	R	181	146	35	R	181	140	40
907	R	181	150	31	G	181	148	34	G	181	151	31	R	181	143	38	R	181	148	33	R	181	146	35	R	181	135	46	R	181	146	35	R	181	140	41
908	R	181	150	31	G	181	148	33	G	181	151	30	R	181	143	38	R	181	148	33	R	181	146	36	R	181	135	46	R	181	146	35	R	181	140	41
909	R	181	150	31	G	181	149	33	G	181	152	30	R	181	143	38	R	181	148	33	R	181	146	36	R	181	135	46	R	181	146	35	R	181	140	41
910	R	181	150	31	G	181	149	32	G	181	152	29	R	181	143	38	R	181	148	33	R	181	146	36	R	181	135	46	R	181	146	36	R	181	140	41
911	R	182	150	32	G	182	150	32	R	182	152	30	G	182	144	39	R	182	149	33	R	182	146	36	R	182	135	47	R	182	146	36	R	182	140	41
912	R	182	150	32	G	182	150	32	R	182	152	30	G	182	144	38	R	182	148	34	R	182	146	36	R	182	135	47	R	182	146	36	R	182	140	41
913	R	182	150	32	G	182	151	31	R	182	152	30	G	182	145	37	R	182	148	34	R	182	146	36	R	182	135	47	R	182	146	36	R	182	140	41
914	R	182	150	32	G	182	151	31	R	182	152	30	G	182	145	37	R	182	148	34	R	182	146	36	R	182	135	47	R	182	146	36	R	182	140	42
915	R	182	150	32	G	182	152	31	R	182	152	30	G	182	146	37	R	182	148	34	R	182	146	37	R	182	135	47	R	182	146	36	R	182	140	42
916	R	182	150	32	G	182	152	30	R	182	152	30	G	182	146	36	R	182	148	34	R	182	146	37	R	182	135	47	R	182	146	37	R	182	140	42
917	R	182	150	32	G	182	153	30	R	182	152	30	G	182	147	36	R	182	148	34	R	182	146	37	R	182	135	47	R	182	146	37	R	182	140	42
918	R	183	150	33	G	183	153	30	R	183	152	31	G	183	147	36	R	183	149	34	R	183	146	37	R	183	135	48	R	183	146	37	R	183	140	42
919	R	183	150	33	G	183	154	29	R	183	152	31	G	183	148	35	R	183	148	35	R	183	146	37	R	183	136	47	G	183	146	37	R	183	140	42
920	R	183	150	33	G	183	154	29	R	183	152	31	G	183	148	35	R	183	148	35	R	183	146	37	G	183	136	47	R	183	146	37	R	183	140	42
921	R	183	150	33	R	183	154	29	R	183	152	31	G	183	149	35	R	183	148	35	R	183	146	37	G	183	137	47	R	183	146	37	R	183	140	43
922	R	183	150	33	R	183	154	29	R	183	152	31	G	183	149	34	R	183	148	35	R	183	146	38	G	183	137	46	R	183	146	37	R	183	140	43
923	R	183	150	33	R	183	154	29	R	183	152	31	G	183	150	34	R	183	148	35	R	183	146	38	G	183	138	46	R	183	146	38	R	183	140	43
924	R	183	150	33	R	183	154	29	R	183	152	31	G	183	150	33	R	183	148	35	G	183	146	37	G	183	138	45	R	183	146	38	R	183	140	43
925	R	184	150	34	R	184	154	30	R	184	152	32	G	184	151	33	R	184	149	35	G	184	147	37	G	184	139	45	R	184	146	38	R	184	140	43
926	R	184	150	34	R	184	154	30	R	184	152	32	G	184	151	33	R	184	148	36	G	184	147	37	G	184	139	45	R	184	146	38	R	184	140	43
927	R	184	150	34	R	184	154	30	R	184	152	32	G	184	152	32	R	184	148	36	G	184	148	36	G	184	140	44	R	184	146	38	R	184	140	43
928	R	184	150	34	R	184	154	30	R	184	152	32	G	184	152	32	R	184	148	36	G	184	148	36	G	184	140	44	R	184	146	38	R	184	140	44
929	R	184	150	34	R	184	154	30	R	184	152	32	G	184	153	32	R	184	148	36	G	184	149	36	G	184	141	44	R	184	146	38	R	184	140	44
930	R	184	150	34	R	184	154	30	R	184	152	32	G	184	153	31	R	184	148	36	G	184	149	35	G	184	141	43	R	184	146	39	R	184	140	44
931	R	184	150	34	R	184	154	30	R	184	152	32	G	184	154	31	R	184	148	36	G	184	150	35	G	184	142	43	R	184	146	39	R	184	140	44
932	R	185	150	35	R	185	154	31	R	185	152	33	G	185	154	31	R	185	149	36	G	185	150	35	G	185	142	43	R	185	146	39	R	185	140	44
933	R	185	150	35	R	185	154	31	R	185	152	33	G	185	155	30	R	185	148	37	G	185	151	34	G	185	143	42	R	185	146	39	R	185	140	44
934	R	185	150	35	R	185	154	31	R	185	152	33	G	185	155	30	R	185	148	37	G	185	151	34	G	185	143	42	R	185	146	39	R	185	140	45
935	R	185	150	35	R	185	154	31	R	185	152	33	G	185	156	30	R	185	148	37	G	185	152	33	G	185	144	42	R	185	146	39	R	185	140	45
936	R	185	150	35	R	185	154	31	R	185	152	33	G	185	156	29	R	185	149	37	G	185	152	33	G	185	144	41	R	185	146	39	R	185	140	45
937	R	185	150	35	R	185	154	31	R	185	152	33	R	185	156	29	G	185	149	37	G	185	153	33	G	185	145	41	R	185	146	40	R	185	140	45
938	R	185	150	35	R	185	154	31	R	185	152	33	R	185	156	28	G	185	149	38	G	185	153	32	G	185	146	40	R	185	146	40	R	185	140	45
939	R	186	150	36	R	186	154	32	R	186	152	34	R	186	156	30	G	186	150	36	G	186	154	32	G	186	146	40	R	186	146	40	R	186	140	45
940	R	186	150	36	R	186	154	32	R	186	152	34	R	186	156	30	G	186	150	36	G	186	154	32	G	186	146	40	R	186	146	40	R	186	140	45
941	G	186	151	35	R	186	154	32	R	186	152	34	R	186	156	30	G	186	151	35	G	186	155	31	G	186	147	39	R	186	146	40	R	186	140	46
942	G	186	151	35	R	186	154	32	R	186	152	34	R	186	156	30	G	186	151	35	G	186	155	31	G	186	147	39	R	186	146	40	R	186	140	46
943	G	186	152	35	R	186	154	32	R	186	152	34	R	186	156	30	G	186	152	35	G	186	156	31	G	186	148	39	R	186	146	40	R	186	140	46
944	G	186	152	34	R	186	154	32	R	186	152	34	R	186	156	30	G	186	152	34	G	186	156	30	G	186	148	38	R	186	146	41	R	186	140	46
945	G	186	153	34	R	186	154	32	R	186	152	34	R	186	156	30	G	186	153	34	G	186	157	30	G	186	149	38	R	186	146	41	R	186	140	46
946	G	187	153	34	R	187	154	33	R	187	152	35	R	187	156	31	G	187	153	33	G	187	157	30	G	187	149	38	R	187	146	41	G	187	141	46
947	G	187	154	33	R	187	154	33	R	187	152	35	R	187	156	31	G	187	154	33	G	187	158	29	G	187	150	37	R	187	146	41	G	187	141	45
948	G	187	154	33	R	187	154	33	R	187	152	35	R	187	156	31	G	187	154	33	G	187	158	29	G	187	150	37	R	187	146	41	G	187	142	45
949	G	187	155	33	R	187	154	33	R	187	152	35	R	187	156	31	G	187	155	32	G	187	159	28	G	187	151	37	R	187	146	41	G	187	142	45
950	G	187	155	32	R	187	154	33	R	187	152	35	R	187	156	31	G	187	155	32	R	187	159	29	G	187	151	36	R	187	146	41	G	187	143	44
951	G	187	156	32	R	187	154	33	G	188	153	35	R	187	156	31	G	187	156	32	R	187	159	29	G	187	152	36	R	187	146	42	G	187	143	44
952	G	188	156	32	R	188	154	34	G	188	153	35	R	188	156	32	G	188	156	31	R	188	159	29	G	188	152	36	R	188	146	42	G	188	144	44
953	G	188	157	31	R	188	154	34	G	188	154	34	R	188	156	32	G	188	157	31	R	188	159	29	G	188	153	35	R	188	146	42	G	188	144	43
954	G	188	157	31	R	188	154	34	G	188	154	34	R	188	156	32	G	188	157	31	R	188	159	29	G	188	153	35	R	188	146	42	G	188	145	43
955	G	188	158	30	R	188	154	34	G	188	155	33	R	188	156	32	G	188	158	30	R	188	159	29	G	188	154	34	R	188	146	42	G	188	145	43
956	G	188	158	30	R	188	154	34	G	188	155	33	R	188	156	32	G	188	158	30	R	188	159	29	G	188	154	34	R	188	146	42	G	188	146	42
957	G	188	159	30	R	188	154	34	G	188	156	33	R	188	156	32	G	188	159	30	R	188	159	30	G	188	155	34	R	188	146	42	G	188	146	42
958	G	188	159	29	R	188	154	34	G	188	156	32	R	188	156	32	G	188	159	29	R	188	159	30	G	188	155	33	R	188	146	43	G	188	147	41
959	G	189	160	29	R	189	154	35	G	189	157	32	R	189	156	33	G	189	160	29	R	189	159	30	G	189	156	33	R	189	146	43	G	189	147	41
960	G	189	160	29	R	189	154	35	G	189	157	32	R	189	156	33	G	189	160	29	R	189	159	30	G	189	156	33	R	189	146	43	G	189	148	41
961	R	189	160	29	G	189	155	34	G	189	158	31	R	189	156	33	G	189	161	28	R	189	159	30	G	189	157	32	R	189	146	43	G	189	148	40
962	R	189	160	29	G	189	155	34	G	189	158	31	R	189	156	33	G	189	161	28	R	189	159	30	G	189	157	32	R	189	146	43	G	189	149	40
963	R	189	160	29	G	189	156	34	G	189	159	31	R	189	156	33	R	189	161	28	R	189	159	30	G	189	158	32	R	189	146	43	G	189	149	40
964	R	189	160	29	G	189	156	33	G	189	159	30	R	189	156	33	R	189	161	28	R	189	159	31	G	189	158	31	R	189	146	43	G	189	150	39
965	R	189	160	29	G	189	157	33	G	189	160	30	R	189	156	33	R	189	161	28	R	189	159	31	G	189	159	31	R	189	146	44	G	189	150	39
966	R	190	160	30	G	190	157	33	G	190	160	30	R	190	156	34	R	190	161	28	R	190	159	31	G	190	159	31	R	190	146	44	G	190	151	39
967	R	190	160	30	G	190	158	32	G	190	161	29	R	190	156	34	R	190	161	29	R	190	159	31	G	190	160	30	R	190	146	44	G	190	151	38
968	R	190	160	30	G	190	158	32	G	190	161	29	R	190	156	34	R	190	161	29	R	190	159	31	G	190	160	30	R	190	146	44	G	190	152	38
969	R	190	160	30	G	190	159	31	G	190	162	28	R	190	156	34	R	190	161	29	R	190	159	31	G	190	161	29	R	190	146	44	G	190	152	38
970	R	190	160	30	G	190	159	31	G	190	162	28	R	190	156	34	R	190	161	29	R	190	159	32	G	190	161	29	R	190	146	44	G	190	153	37
971	R	190	160	30	G	190	160	31	R	190	162	28	R	190	156	34	R	190	161	29	R	190	159	32	G	190	162	29	R	190	146	44	G	190	153	37
972	R	190	160	30	G	190	160	30	R	190	162	28	R	190	156	34	R	190	161	29	R	190	159	32	G	190	162	28	R	190	146	45	G	190	154	36
973	R	191	160	31	G	191	161	30	R	191	162	29	R	191	156	35	R	191	161	29	R	191	159	32	R	191	162	28	G	191	146	44	G	191	154	36
974	R	191	160	31	G	191	161	30	R	191	162	29	R	191	156	35	R	191	161	29	R	191	159	32	R	191	162	29	G	191	147	44	G	191	155	36
975	R	191	160	31	G	191	162	29	R	191	162	29	R	191	156	35	R	191	161	30	R	191	159	32	R	191	162	29	G	191	147	44	G	191	155	35
976	R	191	160	31	G	191	162	29	R	191	162	29	R	191	156	35	R	191	161	30	R	191	159	32	R	191	162	29	G	191	148	43	G	191	156	35
977	R	191	160	31	G	191	163	29	R	191	162	29	R	191	156	35	R	191	161	30	R	191	159	33	R	191	162	29	G	191	148	43	G	191	156	35
978	R	191	160	31	G	191	163	28	R	191	162	29	R	191	156	35	R	191	161	30	R	191	159	33	R	191	162	29	G	191	149	42	G	191	157	34
979	R	191	160	31	G	191	164	28	R	191	162	29	R	191	156	35	R	191	161	30	R	191	159	33	R	191	162	29	G	191	149	42	G	191	157	34
980	R	192	160	32	G	192	164	28	R	192	162	30	R	192	156	36	R	192	161	30	R	192	159	33	R	192	162	30	G	192	150	42	G	192	158	34
981	R	192	160	32	R	192	164	28	R	192	162	30	R	192	156	36	R	192	161	30	R	192	159	33	R	192	162	30	G	192	150	41	G	192	158	33

Table C-1. Continued

A=Arrivals, D=Departures, Q=Queue:

Time (sec)	A	D	Q	A	D	Q	A	D	Q	A	D	Q	A	D	Q	A	D	Q	A	D	Q	A	D	Q	A	D	Q
982	R	192	160	32	R	192	164	28	R	192	162	30	R	192	156	36	R	192	161	31	R	192	159	33	R	192	162	30	G	192	151	41	G	192	159	33
983	R	192	160	32	R	192	164	28	R	192	162	30	R	192	156	36	R	192	161	31	R	192	159	33	R	192	162	30	G	192	151	41	G	192	159	33
984	R	192	160	32	R	192	164	28	R	192	162	30	R	192	156	36	R	192	161	31	R	192	159	34	R	192	162	30	G	192	152	40	G	192	160	32
985	R	192	160	32	R	192	164	28	R	192	162	30	R	192	156	36	R	192	161	31	R	192	159	34	R	192	162	30	G	192	152	40	G	192	160	32
986	R	192	160	32	R	192	164	28	R	192	162	30	R	192	156	36	R	192	161	31	R	192	159	34	R	192	162	30	G	192	153	40	G	192	161	32
987	R	193	160	33	R	193	164	29	R	193	162	31	R	193	156	37	R	193	161	31	R	193	159	34	R	193	162	31	G	193	153	39	G	193	161	31
988	R	193	160	33	R	193	164	29	R	193	162	31	R	193	156	37	R	193	161	32	R	193	159	34	R	193	162	31	G	193	154	39	G	193	162	31
989	R	193	160	33	R	193	164	29	R	193	162	31	G	193	157	36	R	193	161	32	R	193	159	34	R	193	162	31	G	193	154	39	G	193	162	30
990	R	193	160	33	R	193	164	29	R	193	162	31	G	193	157	36	R	193	161	32	R	193	159	34	R	193	162	31	G	193	155	38	G	193	163	30
991	R	193	160	33	R	193	164	29	R	193	162	31	G	193	158	36	R	193	161	32	R	193	159	35	R	193	162	31	G	193	155	38	G	193	163	30
992	R	193	160	33	R	193	164	29	R	193	162	31	G	193	158	35	R	193	161	32	R	193	159	35	R	193	162	31	G	193	156	37	G	193	164	29
993	R	193	160	33	R	193	164	29	R	193	162	31	G	193	159	35	R	193	161	32	R	193	159	35	R	193	162	31	G	193	156	37	G	193	164	29
994	R	194	160	34	R	194	164	30	R	194	162	32	G	194	159	35	R	194	161	32	R	194	159	35	R	194	162	32	G	194	157	37	G	194	165	29
995	R	194	160	34	R	194	164	30	R	194	162	32	G	194	160	34	R	194	161	33	R	194	159	35	R	194	162	32	G	194	157	36	G	194	165	28
996	R	194	160	34	R	194	164	30	R	194	162	32	G	194	160	34	R	194	161	33	R	194	159	35	R	194	162	32	G	194	158	36	G	194	166	28
997	R	194	160	34	R	194	164	30	R	194	162	32	G	194	161	34	R	194	161	33	R	194	159	35	R	194	162	32	G	194	158	36	G	194	166	28
998	R	194	160	34	R	194	164	30	R	194	162	32	G	194	161	33	R	194	161	33	R	194	159	36	R	194	162	32	G	194	159	35	G	194	167	27
999	R	194	160	34	R	194	164	30	R	194	162	32	G	194	162	33	R	194	161	33	R	194	159	36	R	194	162	32	G	194	159	35	G	194	167	27
1000	R	194	160	34	R	194	164	30	R	194	162	32	G	194	162	32	R	194	161	33	R	194	159	36	R	194	162	32	G	194	160	35	R	194	167	27
1001	G	195	161	34	R	195	164	31	R	195	162	33	G	195	163	32	R	195	161	33	R	195	159	36	R	195	162	33	G	195	160	34	R	195	167	27
1002	G	195	161	34	R	195	164	31	R	195	162	33	G	195	163	32	R	195	161	34	G	195	159	36	R	195	162	33	G	195	161	34	R	195	167	27
1003	G	195	162	33	R	195	164	31	R	195	162	33	G	195	164	31	R	195	161	34	G	195	160	35	R	195	162	33	G	195	161	34	R	195	167	27
1004	G	195	162	33	R	195	164	31	R	195	162	33	G	195	164	31	R	195	161	34	G	195	160	35	R	195	162	33	G	195	162	33	R	195	167	28
1005	G	195	163	33	R	195	164	31	R	195	162	33	G	195	165	31	R	195	161	34	G	195	161	35	R	195	162	33	G	195	162	33	R	195	167	28
1006	G	195	163	32	R	195	164	31	R	195	162	33	G	195	165	30	R	195	161	34	G	195	161	34	R	195	162	33	G	195	163	33	R	195	167	28
1007	G	195	164	32	R	195	164	31	R	195	162	33	G	195	166	30	R	195	161	34	G	195	162	34	R	195	162	33	G	195	163	32	R	195	167	28
1008	G	196	164	32	R	196	164	32	R	196	162	34	G	196	166	30	R	196	161	34	G	196	162	33	R	196	162	34	G	196	164	32	R	196	167	28
1009	G	196	165	31	R	196	164	32	R	196	162	34	G	196	167	29	R	196	161	35	G	196	163	33	R	196	162	34	G	196	164	31	R	196	167	28
1010	G	196	165	31	R	196	164	32	R	196	162	34	G	196	167	29	R	196	161	35	G	196	163	33	R	196	162	34	G	196	165	31	R	196	167	28
1011	G	196	166	31	R	196	164	32	G	196	163	34	G	196	169	29	R	196	161	35	G	196	164	32	R	196	162	34	G	196	165	31	R	196	167	29
1012	G	196	166	30	R	196	164	32	G	196	163	33	G	196	168	28	R	196	161	35	G	196	164	32	R	196	162	34	G	196	166	30	R	196	167	29
1013	G	196	167	30	R	196	164	32	G	196	164	33	G	196	169	28	R	196	161	35	G	196	165	32	R	196	162	34	G	196	166	30	R	196	167	29
1014	G	196	167	29	R	196	164	32	G	196	164	32	G	196	169	27	R	196	161	35	G	196	165	31	R	196	162	34	G	196	167	30	R	196	167	29
1015	G	197	168	29	R	197	164	33	G	197	165	32	R	197	169	28	G	197	162	35	G	197	166	31	R	197	162	35	G	197	167	29	R	197	167	29
1016	G	197	168	29	R	197	164	33	G	197	165	32	R	197	169	28	G	197	162	35	G	197	166	31	R	197	162	35	G	197	168	29	R	197	167	29
1017	G	197	169	28	R	197	164	33	G	197	166	31	R	197	169	28	G	197	163	34	G	197	167	30	R	197	162	35	G	197	168	29	R	197	167	29
1018	G	197	169	28	R	197	164	33	G	197	166	31	R	197	169	28	G	197	163	34	G	197	167	30	R	197	162	35	G	197	169	28	R	197	167	30
1019	G	197	170	28	R	197	164	33	G	197	167	31	R	197	169	28	G	197	164	33	G	197	168	30	R	197	162	35	G	197	169	28	R	197	167	30
1020	G	197	170	27	R	197	164	33	G	197	167	30	R	197	169	28	G	197	164	33	G	197	168	29	R	197	162	35	G	197	170	28	R	197	167	30
1021	R	197	170	27	G	197	165	33	G	197	168	30	R	197	169	28	G	197	165	33	G	197	168	29	R	197	162	35	G	197	170	27	R	197	167	30
1022	R	198	170	28	G	198	165	33	G	198	168	30	R	198	169	29	G	198	165	32	G	198	169	29	R	198	162	36	G	198	171	27	R	198	167	30
1023	R	198	170	28	G	198	166	32	G	198	169	29	R	198	169	29	G	198	166	32	G	198	170	28	R	198	162	36	G	198	171	26	R	198	167	30
1024	R	198	170	28	G	198	166	32	G	198	169	29	R	198	169	29	G	198	166	32	G	198	170	28	R	198	162	36	G	198	172	26	R	198	167	31
1025	R	198	170	28	G	198	167	32	G	198	170	29	R	198	169	29	G	198	167	31	G	198	171	27	R	198	162	36	G	198	172	26	R	198	167	31
1026	R	198	170	28	G	198	167	31	G	198	170	28	R	198	169	29	G	198	167	31	G	198	171	27	R	198	162	36	G	198	173	25	R	198	167	31
1027	R	198	170	28	G	198	168	31	G	198	171	28	R	198	169	29	G	198	168	31	G	198	172	27	R	198	162	36	R	198	173	26	R	198	167	31
1028	R	198	170	28	G	198	168	30	G	198	171	27	R	198	169	29	G	198	168	30	R	198	172	27	R	198	162	36	R	198	173	26	R	198	167	31
1029	R	199	170	29	C	199	169	30	C	199	172	27	R	199	169	30	C	199	169	30	R	199	172	27	R	199	162	37	R	199	173	26	R	199	167	31
1030	R	199	170	29	G	199	169	30	G	199	172	27	R	199	169	30	G	199	169	30	R	199	172	27	R	199	162	37	R	199	173	26	R	199	167	31
1031	R	199	170	29	G	199	170	29	R	199	172	27	R	199	169	30	G	199	170	29	R	199	172	27	R	199	162	37	R	199	173	26	R	199	167	32
1032	R	199	170	29	G	199	170	29	R	199	172	27	R	199	169	30	G	199	170	29	R	199	172	27	R	199	162	37	R	199	173	26	R	199	167	32
1033	R	199	170	29	G	199	171	29	R	199	172	27	R	199	169	30	G	199	171	29	R	199	172	28	R	199	162	37	R	199	173	26	R	199	167	32
1034	R	199	170	29	G	199	171	28	R	199	172	27	R	199	169	30	G	199	171	28	R	199	172	28	R	199	162	37	R	199	173	27	R	199	167	32
1035	R	199	170	29	G	199	172	28	R	199	172	27	R	199	169	30	G	199	172	28	R	199	172	28	R	199	162	37	R	199	173	27	R	199	167	32
1036	R	200	170	30	G	200	172	28	R	200	172	28	R	200	169	31	G	200	172	27	R	200	172	28	R	200	162	38	R	200	173	27	R	200	167	32
1037	R	200	170	30	G	200	173	27	R	200	172	28	R	200	169	31	G	200	173	27	R	200	172	28	R	200	162	38	R	200	173	27	R	200	167	32
1038	R	200	170	30	G	200	173	27	R	200	172	28	R	200	169	31	G	200	173	27	R	200	172	28	R	200	162	38	R	200	173	27	R	200	167	33
1039	R	200	170	30	G	200	174	27	R	200	172	28	R	200	169	31	G	200	174	26	R	200	172	28	R	200	162	38	R	200	173	27	R	200	167	33
1040	R	200	170	30	G	200	174	26	R	200	172	28	R	200	169	31	G	200	174	26	R	200	172	29	R	200	162	38	R	200	173	27	R	200	167	33
1041	R	200	170	30	R	200	174	26	R	200	172	28	R	200	169	31	R	200	174	26	R	200	172	29	R	200	162	38	R	200	173	28	R	200	167	33
1042	R	201	170	31	R	201	174	27	R	201	172	29	R	201	169	32	R	201	174	26	R	201	172	29	R	201	162	39	R	201	173	28	R	201	167	33
1043	R	201	170	31	R	201	174	27	R	201	172	29	R	201	169	32	R	201	174	26	R	201	172	29	R	201	162	39	R	201	173	28	R	201	167	33
1044	R	201	170	31	R	201	174	27	R	201	172	29	R	201	169	32	R	201	174	27	R	201	172	29	R	201	162	39	R	201	173	28	R	201	167	33
1045	R	201	170	31	R	201	174	27	R	201	172	29	R	201	169	32	R	201	174	27	R	201	172	29	R	201	162	39	R	201	173	28	R	201	167	34
1046	R	201	170	31	R	201	174	27	R	201	172	29	R	201	169	32	R	201	174	27	R	201	172	29	R	201	162	39	R	201	173	28	R	201	167	34
1047	R	201	170	31	R	201	174	27	R	201	172	29	R	201	169	32	R	201	174	27	R	201	172	30	R	201	162	39	R	201	173	28	R	201	167	34
1048	R	201	170	31	R	201	174	27	R	201	172	29	R	201	169	32	R	201	174	27	R	201	172	30	R	201	162	39	R	201	173	29	R	201	167	34
1049	R	202	170	32	R	202	174	28	R	202	172	30	R	202	169	33	R	202	174	27	R	202	172	30	R	202	162	40	R	202	173	29	R	202	167	34
1050	R	202	170	32	R	202	174	28	R	202	172	30	R	202	169	33	R	202	174	27	R	202	172	30	R	202	162	40	R	202	173	29	R	202	167	34
1051	R	202	170	32	R	202	174	28	R	202	172	30	R	202	169	33	R	202	174	28	R	202	172	30	R	202	162	40	R	202	173	29	R	202	167	34
1052	R	202	170	32	R	202	174	28	R	202	172	30	R	202	169	33	R	202	174	28	R	202	172	30	R	202	162	40	R	202	173	29	R	202	167	35
1053	R	202	170	32	R	202	174	28	R	202	172	30	R	202	169	33	R	202	174	28	R	202	172	30	R	202	162	40	R	202	173	29	R	202	167	35
1054	R	202	170	32	R	202	174	28	R	202	172	30	R	202	169	33	R	202	174	28	R	202	172	31	R	202	162	40	R	202	173	29	R	202	167	35
1055	R	202	170	32	R	202	174	28	R	202	172	30	R	202	169	33	R	202	174	28	R	202	172	31	R	202	162	40	R	202	173	30	R	202	167	35
1056	R	203	170	33	R	203	174	29	R	203	172	31	R	203	169	34	R	203	174	28	R	203	172	31	R	203	162	41	R	203	173	30	R	203	167	35
1057	R	203	170	33	R	203	174	29	R	203	172	31	R	203	169	34	R	203	174	29	R	203	172	31	R	203	162	41	R	203	173	30	R	203	167	35
1058	R	203	170	33	R	203	174	29	R	203	172	31	R	203	169	34	R	203	174	29	R	203	172	31	R	203	162	41	R	203	173	30	R	203	167	35
1059	R	203	170	33	R	203	174	29	R	203	172	31	R	203	169	34	R	203	174	29	R	203	172	31	R	203	162	41	R	203	173	30	R	203	167	36
1060	R	203	170	33	R	203	174	29	R	203	172	31	R	203	169	34	R	203	174	29	R	203	172	32	R	203	162	41	R	203	173	30	R	203	167	36
1061	G	203	171	33	R	203	174	29	R	203	172	31	R	203	169	34	R	203	174	29	R	203	172	32	R	203	162	41	R	203	173	30	R	203	167	36
1062	G	203	171	32	R	203	174	29	R	203	172	31	R	203	169	34	R	203	174	29	R	203	172	32	R	203	162	41	R	203	173	31	R	203	167	36
1063	G	204	172	32	R	204	174	30	R	204	172	32	R	204	169	35	R	204	174	29	R	204	172	32	R	204	162	42	R	204	173	31	R	204	167	36
1064	G	204	172	32	R	204	174	30	R	204	172	32	R	204	169	35	R	204	174	29	R	204	172	32	R	204	162	42	R	204	173	31	R	204	167	36

Table C-1. Continued

A=Arrivals, D=Departures, Q=Queue:

Time (sec)	A	D	Q	A	D	Q	A	D	Q	A	D	Q	A	D	Q	A	D	Q	A	D	Q	A	D	Q	A	D	Q
1065	G	204	173	31	R	204	174	30	R	204	172	32	R	204	169	35	R	204	174	30	R	204	172	32	R	204	162	42	R	204	173	31	R	204	167	36
1066	G	204	173	31	R	204	174	30	R	204	172	32	R	204	169	35	R	204	174	30	R	204	172	32	R	204	162	42	R	204	173	31	R	204	167	37
1067	G	204	174	31	R	204	174	30	R	204	172	32	G	204	170	35	R	204	174	30	R	204	172	33	R	204	162	42	R	204	173	31	R	204	167	37
1068	G	204	174	30	R	204	174	30	R	204	172	32	G	204	170	34	R	204	174	30	R	204	172	33	R	204	162	42	R	204	173	31	R	204	167	37
1069	G	204	175	30	R	204	174	30	R	204	172	32	G	204	171	34	R	204	174	30	R	204	172	33	R	204	162	42	R	204	173	32	R	204	167	37
1070	G	205	175	30	R	205	174	31	R	205	172	33	G	205	171	34	R	205	174	30	R	205	172	33	R	205	162	43	R	205	173	32	R	205	167	37
1071	G	205	176	29	R	205	174	31	G	205	173	32	G	205	172	33	R	205	174	30	R	205	172	33	R	205	162	43	R	205	173	32	R	205	167	37
1072	G	205	176	29	R	205	174	31	G	205	173	32	G	205	172	33	R	205	174	31	R	205	172	33	R	205	162	43	R	205	173	32	R	205	167	37
1073	G	205	177	28	R	205	174	31	G	205	174	31	G	205	173	32	R	205	174	31	R	205	172	33	R	205	162	43	R	205	173	32	R	205	167	38
1074	G	205	177	28	R	205	174	31	G	205	174	31	G	205	173	32	R	205	174	31	R	205	172	34	R	205	162	43	R	205	173	32	R	205	167	38
1075	G	205	178	28	R	205	174	31	G	205	175	31	G	205	174	32	R	205	174	31	R	205	172	34	R	205	162	43	R	205	173	32	R	205	167	38
1076	G	205	178	27	R	205	174	31	G	205	175	30	G	205	174	31	R	205	174	31	R	205	172	34	R	205	162	43	R	205	173	33	R	205	167	38
1077	G	206	179	27	R	206	174	32	G	206	176	30	G	206	175	31	R	206	174	31	R	206	172	34	R	206	162	44	R	206	173	33	R	206	167	39
1078	G	206	179	27	R	206	174	32	G	206	176	30	G	206	175	31	R	206	174	32	R	206	172	34	R	206	162	44	R	206	173	33	R	206	167	38
1079	G	206	180	26	R	206	174	32	G	206	177	29	G	206	176	30	R	206	174	32	R	206	172	34	R	206	162	44	R	206	173	33	R	206	167	38
1080	G	206	180	26	R	206	174	32	G	206	177	29	G	206	176	30	R	206	174	32	G	206	172	34	R	206	162	44	R	206	173	33	R	206	167	39
1081	R	206	180	26	G	206	175	32	G	206	178	29	G	206	177	30	R	206	174	32	G	206	173	34	G	206	163	44	R	206	173	33	R	206	167	39
1082	R	206	180	26	G	206	175	31	G	206	178	28	G	206	177	29	R	206	174	32	G	206	173	33	G	206	163	43	R	206	173	33	R	206	167	39
1083	R	206	180	26	G	206	176	31	G	206	178	28	G	206	178	29	R	206	174	32	G	206	174	33	G	206	164	43	R	206	173	34	R	206	167	39
1084	R	207	180	27	G	207	176	31	G	207	179	28	G	207	178	29	R	207	174	32	G	207	174	32	G	207	164	43	R	207	173	34	R	207	167	39
1085	R	207	180	27	G	207	177	30	G	207	180	27	G	207	179	28	R	207	174	33	G	207	175	32	G	207	165	42	R	207	173	34	R	207	167	39
1086	R	207	180	27	G	207	177	30	G	207	180	27	G	207	179	28	R	207	174	33	G	207	175	32	G	207	165	42	R	207	173	34	R	207	167	39
1087	R	207	180	27	G	207	178	30	G	207	181	27	G	207	180	28	R	207	174	33	G	207	176	31	G	207	166	42	R	207	173	34	R	207	167	40
1088	R	207	180	27	G	207	178	29	G	207	181	26	G	207	180	27	R	207	174	33	G	207	176	31	G	207	166	41	R	207	173	34	R	207	167	40
1089	R	207	180	27	G	207	179	29	G	207	182	26	G	207	181	27	R	207	174	33	G	207	177	31	G	207	167	41	R	207	173	34	R	207	167	40
1090	R	207	180	27	G	207	179	28	G	207	182	25	G	207	181	26	R	207	174	33	G	207	177	30	G	207	167	40	R	207	173	35	R	207	167	40
1091	R	208	180	26	G	208	180	28	R	208	182	26	G	208	182	26	R	208	174	33	G	208	178	30	G	208	168	40	R	208	173	35	R	208	167	40
1092	R	208	180	28	G	208	180	28	R	208	182	26	G	208	182	26	R	208	174	34	G	208	178	30	G	208	168	40	R	208	173	35	R	208	167	40
1093	R	208	180	28	G	208	181	27	R	208	182	26	R	208	182	26	G	208	175	33	G	208	179	29	G	208	169	39	R	208	173	35	R	208	167	40
1094	R	208	180	28	G	208	181	27	R	208	182	26	R	208	182	26	G	208	175	33	G	208	179	29	G	208	169	39	R	208	173	35	R	208	167	41
1095	R	208	180	28	G	208	182	27	R	208	182	26	R	208	182	26	G	208	176	32	G	208	180	28	G	208	170	39	R	208	173	35	R	208	167	41
1096	R	208	180	28	G	208	182	26	R	208	182	26	R	208	182	26	G	208	176	32	G	208	180	28	G	208	170	38	R	208	173	36	R	208	167	41
1097	R	208	180	28	G	208	183	26	R	208	182	26	R	208	182	26	G	208	177	32	G	208	181	28	G	208	171	38	R	208	173	36	R	208	167	41
1098	R	209	180	29	C	209	183	26	R	209	182	27	R	209	182	27	G	209	177	31	C	209	181	27	G	209	171	38	R	209	173	36	R	209	167	41
1099	R	209	180	29	G	209	184	25	R	209	182	27	R	209	182	27	G	209	178	31	G	209	182	27	G	209	172	37	R	209	173	36	R	209	167	41
1100	R	209	180	29	G	209	184	25	R	209	182	27	R	209	182	27	G	209	178	31	G	209	182	27	G	209	172	37	R	209	173	36	R	209	167	41
1101	R	209	180	29	R	209	184	25	R	209	182	27	R	209	182	27	G	209	179	30	G	209	183	26	G	209	173	37	R	209	173	36	R	209	167	42
1102	R	209	180	29	R	209	184	25	R	209	182	27	R	209	182	27	G	209	179	30	G	209	183	26	G	209	173	36	R	209	173	36	R	209	167	42
1103	R	209	180	29	R	209	184	25	R	209	182	27	R	209	182	27	G	209	180	30	G	209	184	26	G	209	174	36	R	209	173	37	R	209	167	42
1104	R	209	180	29	R	209	184	25	R	209	182	27	R	209	182	27	G	209	180	29	G	209	184	25	G	209	174	35	R	209	173	37	R	209	167	42
1105	R	210	180	30	R	210	184	26	R	210	182	28	R	210	182	28	G	210	181	29	G	210	185	25	G	210	175	35	R	210	173	37	R	210	167	42
1106	R	210	180	30	R	210	184	26	R	210	182	28	R	210	182	28	G	210	181	29	R	210	185	25	G	210	175	35	R	210	173	37	R	210	167	42
1107	R	210	180	30	R	210	184	26	R	210	182	28	R	210	182	28	G	210	182	28	R	210	185	25	G	210	176	34	R	210	173	37	R	210	167	42
1108	R	210	180	30	R	210	184	26	R	210	182	28	R	210	182	28	G	210	182	28	R	210	185	25	G	210	176	34	R	210	173	37	G	210	168	42
1109	R	210	180	30	R	210	184	26	R	210	182	28	R	210	182	28	G	210	183	27	R	210	185	26	G	210	177	34	R	210	173	37	G	210	168	42
1110	R	210	180	30	R	210	184	26	R	210	182	28	R	210	182	28	G	210	183	27	R	210	185	26	G	210	177	33	R	210	173	38	G	210	169	41
1111	R	210	180	30	R	210	184	26	R	210	182	28	R	210	182	28	G	210	184	27	R	210	185	26	G	210	178	33	R	210	173	38	G	210	169	41
1112	R	211	180	31	R	211	184	27	R	211	182	29	R	211	182	29	C	211	184	26	R	211	185	26	G	211	178	33	R	211	173	38	G	211	170	41
1113	R	211	180	31	R	211	184	27	R	211	182	29	R	211	182	29	G	211	185	26	R	211	185	26	G	211	179	32	R	211	173	38	G	211	170	40
1114	R	211	180	31	R	211	184	27	R	211	182	29	R	211	182	29	C	211	185	26	R	211	185	26	G	211	179	32	R	211	173	38	G	211	171	40
1115	R	211	180	31	R	211	184	27	R	211	182	29	R	211	182	29	G	211	186	25	R	211	185	26	G	211	180	32	R	211	173	38	G	211	171	40
1116	R	211	180	31	R	211	184	27	R	211	182	29	R	211	182	29	G	211	186	25	R	211	185	27	G	211	180	31	R	211	173	38	G	211	172	39
1117	R	211	180	31	R	211	184	27	R	211	182	29	R	211	182	29	G	211	187	25	R	211	185	27	G	211	181	31	R	211	173	39	G	211	172	39
1118	R	211	180	31	R	211	184	27	R	211	182	29	R	211	182	29	C	211	187	24	R	211	185	27	G	211	181	30	R	211	173	39	G	211	173	39
1119	R	212	180	32	R	212	184	28	R	212	182	30	R	212	182	30	R	212	187	24	R	212	185	27	G	212	182	30	R	212	173	39	G	212	173	39
1120	R	212	180	32	R	212	184	28	R	212	182	30	R	212	182	30	R	212	187	25	R	212	185	27	G	212	182	30	R	212	173	39	G	212	174	38
1121	G	212	181	31	R	212	184	28	R	212	182	30	R	212	182	30	R	212	187	25	R	212	185	27	G	212	183	29	R	212	173	39	G	212	174	38
1122	G	212	181	31	R	212	184	28	R	212	182	30	R	212	182	30	R	212	187	25	R	212	185	27	G	212	183	29	R	212	173	39	G	212	175	37
1123	G	212	182	31	R	212	184	28	R	212	182	30	R	212	182	30	R	212	187	25	R	212	185	28	G	212	184	29	R	212	173	39	G	212	175	37
1124	G	212	182	30	R	212	184	28	R	212	182	30	R	212	182	30	R	212	187	25	R	212	185	28	G	212	184	28	R	212	173	40	G	212	176	36
1125	G	212	183	30	R	212	184	28	R	212	182	30	R	212	182	30	R	212	187	25	R	212	185	28	G	212	185	28	R	212	173	40	G	212	176	36
1126	G	213	183	30	R	213	184	29	R	213	182	31	R	213	182	31	R	213	187	25	R	213	185	28	G	213	185	28	R	213	173	40	G	213	177	36
1127	G	213	184	29	R	213	184	29	R	213	182	31	R	213	182	31	R	213	187	26	R	213	185	28	G	213	186	27	R	213	173	40	G	213	177	35
1128	G	213	184	29	R	213	184	29	R	213	182	31	R	213	182	31	R	213	187	26	R	213	185	28	G	213	186	27	R	213	173	40	G	213	178	35
1129	G	213	185	29	R	213	184	29	R	213	182	31	R	213	182	31	R	213	187	26	R	213	185	28	G	213	187	27	R	213	173	40	G	213	178	35
1130	G	213	185	28	R	213	184	29	R	213	182	31	R	213	182	31	R	213	187	26	R	213	185	29	G	213	187	26	R	213	173	40	G	213	179	34
1131	G	213	186	28	R	213	184	29	C	213	183	31	R	213	182	31	R	213	187	26	R	213	185	29	G	213	188	26	R	213	173	41	G	213	179	34
1132	G	214	186	28	R	214	184	30	C	214	183	31	R	214	182	32	R	214	187	26	R	214	185	29	G	214	188	26	R	214	173	41	G	214	180	34
1133	G	214	187	27	R	214	184	30	C	214	184	30	R	214	182	32	R	214	187	26	R	214	185	29	G	214	189	25	R	214	173	41	G	214	180	33
1134	G	214	187	27	R	214	184	30	G	214	184	30	R	214	182	32	R	214	187	27	R	214	185	29	G	214	189	25	R	214	173	41	G	214	181	33
1135	G	214	188	26	R	214	184	30	G	214	185	29	R	214	182	32	R	214	187	27	R	214	185	29	R	214	189	25	G	214	173	41	G	214	181	33
1136	G	214	188	26	R	214	184	30	G	214	185	29	R	214	182	32	R	214	187	27	R	214	185	29	R	214	189	25	G	214	174	40	G	214	182	32
1137	G	214	189	26	R	214	184	30	G	214	186	29	R	214	182	32	R	214	187	27	R	214	185	30	R	214	189	25	G	214	174	40	G	214	182	32
1138	G	214	189	25	R	214	184	30	G	214	186	28	R	214	182	32	R	214	187	27	R	214	185	30	R	214	189	25	G	214	175	40	G	214	183	31
1139	G	215	190	25	R	215	184	31	G	215	187	28	R	215	182	33	R	215	187	27	R	215	185	30	R	215	189	26	G	215	175	39	G	215	183	31
1140	G	215	190	25	R	215	184	31	G	215	187	28	R	215	182	33	R	215	187	27	R	215	185	30	R	215	189	26	G	215	176	39	G	215	184	31
1141	R	215	190	25	G	215	185	30	G	215	188	27	R	215	182	33	R	215	187	28	R	215	185	30	R	215	189	26	G	215	176	39	G	215	184	30
1142	R	215	190	25	G	215	185	30	G	215	188	27	R	215	182	33	R	215	187	28	R	215	185	30	R	215	189	26	G	215	177	38	G	215	185	30
1143	R	215	190	25	G	215	186	30	G	215	189	27	R	215	182	33	R	215	187	28	R	215	185	30	R	215	189	26	G	215	177	38	G	215	185	30
1144	R	215	190	25	G	215	186	29	G	215	189	26	R	215	182	33	R	215	187	28	R	215	185	31	R	215	189	26	G	215	178	37	G	215	186	29
1145	R	215	190	25	G	215	187	29	G	215	190	26	G	215	183	33	R	215	187	28	R	215	185	31	R	215	189	26	G	215	178	37	G	215	186	29
1146	R	216	190	26	G	216	187	29	G	216	190	26	G	216	183	33	R	216	187	28	R	216	185	31	R	216	189	27	G	216	178	37	G	216	187	29
1147	R	216	190	26	G	216	188	28	G	216	191	25	G	216	184	32	R	216	187	28	R	216	185	31	R	216	189	27	G	216	179	36	G	216	187	28

Table C-1. Continued

A=Arrivals, D=Departures, Q=Queue:

Time (sec)	A	D	Q	A	D	Q	A	D	Q	A	D	Q	A	D	Q	A	D	Q	A	D	Q	A	D	Q	A	D	Q
1148	R	216	190	26	G	216	188	28	G	216	191	25	G	216	184	32	R	216	187	29	R	216	185	31	R	216	189	27	G	216	180	36	G	216	188	28
1149	R	216	190	26	G	216	189	27	G	216	192	24	G	216	185	31	R	216	187	29	R	216	185	31	R	216	189	27	G	216	180	36	G	216	188	28
1150	R	216	190	26	G	216	189	27	G	216	192	24	G	216	185	31	R	216	187	29	R	216	185	32	R	216	189	27	G	216	181	35	G	216	189	27
1151	R	216	190	26	G	216	190	27	R	216	192	24	G	216	186	31	R	216	187	29	R	216	185	32	R	216	189	27	G	216	181	35	G	216	189	27
1152	R	216	190	26	G	216	190	26	R	216	192	24	G	216	186	30	R	216	187	29	R	216	185	32	R	216	189	27	G	216	182	35	G	216	190	26
1153	R	217	190	27	G	217	191	26	R	217	192	25	G	217	187	30	R	217	187	29	R	217	185	32	R	217	189	28	G	217	182	34	G	217	190	26
1154	R	217	190	27	G	217	191	26	R	217	192	25	G	217	187	30	R	217	187	29	R	217	185	32	R	217	189	28	G	217	183	34	G	217	191	26
1155	R	217	190	27	G	217	192	25	R	217	192	25	G	217	188	29	R	217	187	30	R	217	185	32	R	217	189	28	G	217	183	34	G	217	191	25
1156	R	217	190	27	G	217	192	25	R	217	192	25	G	217	188	29	R	217	187	30	R	217	185	32	R	217	189	28	G	217	184	33	G	217	192	25
1157	R	217	190	27	G	217	193	25	R	217	192	25	G	217	189	29	R	217	187	30	R	217	185	33	R	217	189	28	G	217	184	33	G	217	192	25
1158	R	217	190	27	G	217	193	24	R	217	192	25	G	217	189	28	R	217	187	30	G	217	185	32	R	217	189	28	G	217	185	32	G	217	193	24
1159	R	217	190	27	G	217	194	24	R	217	192	25	G	217	190	28	R	217	187	30	G	217	186	32	R	217	189	28	G	217	185	32	G	217	193	24
1160	R	218	190	28	G	218	194	24	R	218	192	26	G	218	190	28	R	218	187	30	G	218	186	31	R	218	189	29	G	218	186	32	G	218	194	24
1161	R	218	190	28	R	218	194	24	R	218	192	26	G	218	191	27	R	218	187	30	G	218	187	31	R	218	189	29	G	218	186	31	G	218	194	23
1162	R	218	190	28	R	218	194	24	R	218	192	26	G	218	191	27	R	218	187	31	G	218	187	31	R	218	189	29	G	218	187	31	R	218	194	23
1163	R	218	190	28	R	218	194	24	R	218	192	26	G	218	192	26	R	218	187	31	G	218	188	30	R	218	189	29	G	218	187	31	R	218	194	24
1164	R	218	190	28	R	218	194	24	R	218	192	26	G	218	192	26	R	218	187	31	G	218	188	30	R	218	189	29	G	218	188	30	R	218	194	24
1165	R	218	190	28	R	218	194	24	R	218	192	26	G	218	193	26	R	218	187	31	G	218	189	30	R	218	189	29	G	218	188	30	R	218	194	24
1166	R	218	190	28	R	218	194	24	R	218	192	26	G	218	193	25	R	218	187	31	G	218	189	29	R	218	189	29	G	218	188	30	R	218	194	24
1167	R	219	190	29	R	219	194	25	R	219	192	27	G	219	194	25	R	219	187	31	G	219	190	29	R	219	189	30	G	219	189	29	R	219	194	24
1168	R	219	190	29	R	219	194	25	R	219	192	27	G	219	194	25	R	219	187	32	G	219	190	29	R	219	189	30	G	219	190	29	R	219	194	24
1169	R	219	190	29	R	219	194	25	R	219	192	27	G	219	195	24	R	219	187	32	G	219	191	28	R	219	189	30	G	219	190	29	R	219	194	24
1170	R	219	190	29	R	219	194	25	R	219	192	27	G	219	195	24	R	219	187	32	G	219	191	28	R	219	189	30	G	219	191	28	R	219	194	25
1171	R	219	190	29	R	219	194	25	R	219	192	27	R	219	195	24	G	219	188	31	G	219	192	28	R	219	189	30	G	219	191	28	R	219	194	25
1172	R	219	190	29	R	219	194	25	R	219	192	27	R	219	195	24	G	219	188	31	G	219	192	27	R	219	189	30	G	219	192	27	R	219	194	25
1173	R	219	190	29	R	219	194	25	R	219	192	27	R	219	195	24	G	219	189	31	G	219	193	27	R	219	189	30	G	219	192	27	R	219	194	25
1174	R	220	190	30	R	220	194	26	R	220	192	28	R	220	195	25	G	220	189	30	G	220	193	26	R	220	189	31	G	220	193	27	R	220	194	25
1175	R	220	190	30	R	220	194	26	R	220	192	28	R	220	195	25	G	220	190	30	G	220	194	26	R	220	189	31	G	220	193	26	R	220	194	25
1176	R	220	190	30	R	220	194	26	R	220	192	28	R	220	195	25	G	220	190	30	G	220	194	26	R	220	189	31	G	220	194	26	R	220	194	25
1177	R	220	190	30	R	220	194	26	R	220	192	28	R	220	195	25	G	220	191	29	G	220	195	25	R	220	189	31	G	220	194	26	R	220	194	26
1178	R	220	190	30	R	220	194	26	R	220	192	28	R	220	195	25	G	220	191	29	G	220	195	25	R	220	189	31	G	220	195	26	R	220	194	26
1179	R	220	190	30	R	220	194	26	R	220	192	28	R	220	195	25	G	220	192	29	G	220	196	25	R	220	189	31	G	220	195	25	R	220	194	26
1180	R	220	190	30	R	220	194	26	R	220	192	28	R	220	195	25	G	220	192	28	G	220	196	24	R	220	189	31	G	220	196	25	R	220	194	26
1181	G	221	191	30	R	221	194	27	R	221	192	29	R	221	195	26	G	221	193	28	G	221	197	24	R	221	189	32	G	221	196	24	R	221	194	26
1182	G	221	191	30	R	221	194	27	R	221	192	29	R	221	195	26	G	221	193	28	G	221	197	24	R	221	189	32	G	221	197	24	R	221	194	26
1183	G	221	192	29	R	221	194	27	R	221	192	29	R	221	195	26	G	221	194	27	G	221	198	23	R	221	189	32	G	221	197	24	R	221	194	26
1184	G	221	192	29	R	221	194	27	R	221	192	29	R	221	195	26	G	221	194	27	R	221	198	23	R	221	189	32	G	221	198	23	R	221	194	27
1185	G	221	193	29	R	221	194	27	R	221	192	29	R	221	195	26	G	221	195	26	R	221	198	24	R	221	189	32	G	221	198	23	R	221	194	27
1186	G	221	193	28	R	221	194	27	R	221	192	29	R	221	195	26	G	221	195	26	R	221	198	24	R	221	189	32	G	221	198	23	R	221	194	27
1187	G	221	194	28	R	221	194	27	R	221	192	29	R	221	195	26	G	221	196	26	R	221	198	24	R	221	189	32	G	221	198	22	R	221	194	27
1188	G	222	194	28	R	222	194	28	R	222	192	30	R	222	195	27	G	222	196	25	R	222	198	24	R	222	189	33	G	222	200	22	R	222	194	27
1189	G	222	195	27	R	222	194	28	R	222	192	30	R	222	195	27	G	222	197	25	R	222	198	24	R	222	189	33	R	222	200	22	R	222	194	27
1190	G	222	195	27	R	222	194	28	R	222	192	30	R	222	195	27	G	222	197	25	R	222	198	24	R	222	189	33	R	222	200	22	R	222	194	27
1191	G	222	196	27	R	222	194	28	G	222	193	30	R	222	195	27	G	222	198	24	R	222	198	24	R	222	189	33	R	222	200	22	R	222	194	28
1192	G	222	196	26	R	222	194	28	G	222	193	29	R	222	195	27	G	222	198	24	R	222	198	25	R	222	189	33	R	222	200	22	R	222	194	28
1193	G	222	197	26	R	222	194	28	G	222	194	29	R	222	195	27	G	222	199	24	R	222	198	25	R	222	189	33	R	222	200	23	R	222	194	28
1194	G	222	197	25	R	222	194	28	G	222	194	28	R	222	195	27	G	222	199	23	R	222	198	25	R	222	189	33	R	222	200	23	R	222	194	28
1195	G	223	198	25	R	223	194	29	G	223	195	28	R	223	195	28	G	223	200	23	R	223	198	25	R	223	189	34	R	223	200	23	R	223	194	28
1196	G	223	198	25	R	223	194	29	G	223	195	28	R	223	195	28	G	223	200	23	R	223	198	25	R	223	189	34	R	223	200	23	R	223	194	28
1197	G	223	199	24	R	223	194	29	G	223	196	27	R	223	195	28	R	223	200	23	R	223	198	25	R	223	189	34	R	223	200	23	R	223	194	28
1198	G	223	199	24	R	223	194	29	G	223	196	27	R	223	195	28	R	223	200	23	R	223	198	25	R	223	189	34	R	223	200	23	R	223	194	29
1199	G	223	200	24	R	223	194	29	G	223	197	27	R	223	195	28	R	223	200	23	R	223	198	26	R	223	189	34	R	223	200	23	R	223	194	29
1200	G	223	200	23	R	223	194	29	G	223	197	26	R	223	195	28	R	223	200	23	R	223	198	26	R	223	189	34	R	223	200	24	R	223	194	29
1201	R	223	200	23	G	223	195	29	G	223	198	26	R	223	195	28	R	223	200	23	R	223	198	26	R	223	189	34	R	223	200	24	R	223	194	29
1202	R	224	200	24	G	224	195	29	G	224	198	26	R	224	195	29	R	224	200	23	R	224	198	26	R	224	189	35	R	224	200	24	R	224	194	29
1203	R	224	200	24	G	224	196	28	G	224	199	25	R	224	195	29	R	224	200	24	R	224	198	26	R	224	189	35	R	224	200	24	R	224	194	29
1204	R	224	200	24	G	224	196	28	G	224	199	25	R	224	195	29	R	224	200	24	R	224	198	26	R	224	189	35	R	224	200	24	R	224	194	30
1205	R	224	200	24	G	224	197	28	G	224	200	25	R	224	195	29	R	224	200	24	R	224	198	26	R	224	189	35	R	224	200	24	R	224	194	30
1206	R	224	200	24	C	224	197	27	G	224	200	24	R	224	195	29	R	224	200	24	R	224	198	27	R	224	189	35	R	224	200	24	R	224	194	30
1207	R	224	200	24	G	224	198	27	G	224	201	24	R	224	195	29	R	224	200	24	R	224	198	27	R	224	189	35	R	224	200	25	R	224	194	30
1208	R	224	200	24	G	224	198	26	G	224	201	23	R	224	195	29	R	224	200	24	R	224	198	27	R	224	189	35	R	224	200	25	R	224	194	30
1209	R	225	200	25	G	225	199	26	G	225	202	23	R	225	195	30	R	225	200	24	R	225	198	27	R	225	189	36	R	225	200	25	R	225	194	30
1210	R	225	200	25	G	225	199	26	G	225	202	23	R	225	195	30	R	225	200	25	R	225	198	27	R	225	189	36	R	225	200	25	R	225	194	30
1211	R	225	200	25	G	225	200	25	R	225	202	23	R	225	195	30	R	225	200	25	R	225	198	27	R	225	189	36	R	225	200	25	R	225	194	31
1212	R	225	200	25	G	225	200	25	R	225	202	23	R	225	195	30	R	225	200	25	R	225	198	27	R	225	189	36	R	225	200	25	R	225	194	31
1213	R	225	200	25	G	225	201	25	R	225	202	23	R	225	195	30	R	225	200	25	R	225	198	28	R	225	189	36	R	225	200	25	R	225	194	31
1214	R	225	200	25	G	225	201	24	R	225	202	23	R	225	195	30	R	225	200	25	R	225	198	28	R	225	189	36	R	225	200	26	R	225	194	31
1215	R	225	200	25	G	225	202	24	R	225	202	23	R	225	195	30	R	225	200	25	R	225	198	28	R	225	189	36	R	225	200	26	R	225	194	31
1216	R	226	200	26	C	226	202	24	R	226	202	24	R	226	195	31	R	226	200	25	R	226	198	28	R	226	189	37	R	226	200	26	R	226	194	31
1217	R	226	200	26	G	226	203	23	R	226	202	24	R	226	195	31	R	226	200	26	R	226	198	28	R	226	189	37	R	226	200	26	R	226	194	31
1218	R	226	200	26	G	226	203	23	R	226	202	24	R	226	195	31	R	226	200	26	R	226	198	28	R	226	189	37	R	226	200	26	R	226	194	32
1219	R	226	200	26	G	226	204	23	R	226	202	24	R	226	195	31	R	226	200	26	R	226	198	28	R	226	189	37	R	226	200	26	R	226	194	32
1220	R	226	200	26	G	226	204	22	R	226	202	24	R	226	195	31	R	226	200	26	R	226	198	29	R	226	189	37	R	226	200	26	R	226	194	32
1221	R	226	200	26	R	226	204	22	R	226	202	24	R	226	195	31	R	226	200	26	R	226	198	29	R	226	189	37	R	226	200	27	R	226	194	32
1222	R	227	200	27	R	227	204	23	R	227	202	25	R	227	195	32	R	227	200	26	R	227	198	29	R	227	189	38	R	227	200	27	R	227	194	32
1223	R	227	200	27	R	227	204	23	R	227	202	25	G	227	196	31	R	227	200	26	R	227	198	29	R	227	189	38	R	227	200	27	R	227	194	32
1224	R	227	200	27	R	227	204	23	R	227	202	25	G	227	196	31	R	227	200	27	R	227	198	29	R	227	189	38	R	227	200	27	R	227	194	32
1225	R	227	200	27	R	227	204	23	R	227	202	25	G	227	197	30	R	227	200	27	R	227	198	29	R	227	189	38	R	227	200	27	R	227	194	33
1226	R	227	200	27	R	227	204	23	R	227	202	25	G	227	197	30	R	227	200	27	R	227	198	29	R	227	189	38	R	227	200	27	R	227	194	33
1227	R	227	200	27	R	227	204	23	R	227	202	25	G	227	198	30	R	227	200	27	R	227	198	30	R	227	189	38	R	227	200	27	R	227	194	33
1228	R	227	200	27	R	227	204	23	R	227	202	25	G	227	198	29	R	227	200	27	R	227	198	30	R	227	189	38	R	227	200	28	R	227	194	33
1229	R	228	200	28	R	228	204	24	R	228	202	26	G	228	199	29	R	228	200	27	R	228	198	30	R	228	189	39	R	228	200	28	R	228	194	33
1230																																				

Table C-1. Continued

A=Arrivals, D=Departures, Q=Queue:

Time (sec)	A	D	Q	A	D	Q	A	D	Q	A	D	Q	A	D	Q	A	D	Q	A	D	Q	A	D	Q	A	D	Q
1231	R	228	200	28	R	228	204	24	R	228	202	26	G	228	200	28	R	228	200	28	R	228	198	30	R	228	189	39	R	228	200	28	R	228	194	33
1232	R	228	200	28	R	228	204	24	R	228	202	26	G	228	200	28	R	228	200	28	R	228	198	30	R	228	189	39	R	228	200	28	R	228	194	34
1233	R	228	200	28	R	228	204	24	R	228	202	26	G	228	201	28	R	228	200	28	R	228	198	30	R	228	189	39	R	228	200	28	R	228	194	34
1234	R	228	200	28	R	228	204	24	R	228	202	26	G	228	201	27	R	228	200	28	R	228	198	31	R	228	189	39	R	228	200	28	R	228	194	34
1235	R	228	200	28	R	228	204	24	R	228	202	26	G	228	202	27	R	228	200	28	R	228	198	31	R	228	189	39	R	228	200	29	R	228	194	34
1236	R	229	200	29	R	228	204	25	R	229	202	27	G	229	202	27	R	229	200	28	G	229	198	30	R	229	189	40	R	228	200	29	R	229	194	34
1237	R	229	200	29	R	228	204	25	R	229	202	27	G	229	203	26	R	229	200	28	G	229	198	30	R	229	189	40	R	228	200	29	R	229	194	34
1238	R	229	200	29	R	228	204	25	R	229	202	27	G	229	203	26	R	229	200	29	G	229	198	30	R	229	189	40	R	228	200	29	R	229	194	34
1239	R	229	200	29	R	228	204	25	R	229	202	27	G	229	204	25	R	229	200	29	G	229	200	29	R	229	189	40	R	228	200	29	R	229	194	35
1240	R	229	200	29	R	228	204	25	R	229	202	27	G	229	204	25	R	229	200	29	G	229	200	29	R	229	189	40	R	228	200	29	R	229	194	35
1241	G	229	201	28	R	228	204	25	R	229	202	27	G	229	205	25	R	229	200	29	G	229	201	29	R	228	189	40	R	228	200	29	R	229	194	35
1242	G	229	201	28	R	229	204	25	R	229	202	27	G	229	205	24	R	229	200	29	G	229	201	28	R	228	189	40	R	228	200	30	R	229	194	35
1243	G	230	202	28	R	230	204	26	R	230	202	28	G	230	206	24	R	230	200	29	G	230	202	28	G	230	190	40	R	230	200	30	R	230	194	35
1244	G	230	202	28	R	230	204	26	R	230	202	28	G	230	206	24	R	230	200	29	G	230	202	28	G	230	190	40	R	230	200	30	R	230	194	35
1245	G	230	203	27	R	230	204	26	R	230	202	28	G	230	207	23	R	230	200	30	G	230	203	27	G	230	191	39	R	230	200	30	R	230	194	35
1246	G	230	203	27	R	230	204	26	R	230	202	28	G	230	207	23	R	230	200	30	G	230	203	27	G	230	191	39	R	230	200	30	R	230	194	36
1247	G	230	204	27	R	230	204	26	R	230	202	28	G	230	208	23	R	230	200	30	G	230	204	27	G	230	192	39	R	230	200	30	R	230	194	36
1248	G	230	204	26	R	230	204	26	R	230	202	28	G	230	208	22	R	230	200	30	G	230	204	26	G	230	192	38	R	230	200	30	R	230	194	36
1249	G	230	205	26	R	230	204	26	R	230	202	28	R	230	208	22	G	230	201	30	G	230	205	26	G	230	193	38	R	230	200	31	R	230	194	36
1250	G	231	205	26	R	231	204	27	R	231	202	29	R	231	208	23	G	231	201	29	G	231	205	25	G	231	193	38	R	231	200	31	R	231	194	36
1251	G	231	206	25	R	231	204	27	G	231	203	28	R	231	208	23	G	231	202	29	G	231	206	25	G	231	194	37	R	231	200	31	R	231	194	36
1252	G	231	206	25	R	231	204	27	G	231	203	28	R	231	208	23	G	231	202	29	G	231	206	25	G	231	194	37	R	231	200	31	R	231	194	36
1253	G	231	207	24	R	231	204	27	G	231	204	27	R	231	208	23	G	231	203	28	G	231	207	24	G	231	195	36	R	231	200	31	R	231	194	37
1254	G	231	207	24	R	231	204	27	G	231	204	27	R	231	208	23	G	231	203	28	G	231	207	24	G	231	195	36	R	231	200	31	R	231	194	37
1255	G	231	208	24	R	231	204	27	G	231	205	27	R	231	208	23	G	231	204	28	G	231	208	24	G	231	196	36	R	231	200	31	R	231	194	37
1256	G	231	208	23	R	231	204	27	G	231	205	26	R	231	208	23	G	231	204	27	G	231	208	23	G	231	196	35	R	231	200	32	R	231	194	37
1257	G	232	209	23	R	232	204	28	G	232	206	26	R	232	208	24	G	232	205	27	G	232	209	23	G	232	197	35	R	232	200	32	R	232	194	37
1258	G	232	209	23	R	232	204	28	G	232	206	26	R	232	208	24	G	232	205	27	G	232	209	23	G	232	197	35	R	232	200	32	R	232	194	37
1259	G	232	210	22	R	232	204	28	G	232	207	25	R	232	208	24	G	232	206	26	G	232	210	22	G	232	198	34	R	232	200	32	R	232	194	38
1260	G	232	210	22	R	232	204	28	G	232	207	25	R	232	208	24	G	232	206	26	G	232	210	22	G	232	198	34	R	232	200	32	R	232	194	38
1261	R	232	210	22	G	232	205	28	G	232	208	25	R	232	208	24	G	232	207	25	G	232	211	22	G	232	199	34	R	232	200	32	R	232	194	38
1262	R	232	210	22	G	232	205	27	G	232	208	24	R	232	208	24	G	232	207	25	R	232	211	22	G	232	199	33	R	232	200	32	R	232	194	38
1263	R	232	210	22	G	232	208	27	G	232	209	24	R	232	208	24	G	232	208	25	R	232	211	22	G	232	200	33	R	232	200	33	R	232	194	38
1264	R	233	210	23	G	233	206	27	G	233	209	24	R	233	208	25	G	233	209	24	R	233	211	22	G	233	200	33	R	233	200	33	R	233	194	38
1265	R	233	210	23	G	233	207	26	G	233	210	23	R	233	208	25	G	233	209	24	R	233	211	22	G	233	201	32	R	233	200	33	R	233	194	38
1266	R	233	210	23	G	233	207	26	G	233	210	23	R	233	208	25	G	233	209	24	R	233	211	22	G	233	201	32	R	233	200	33	R	233	194	38
1267	R	233	210	23	G	233	208	26	G	233	211	23	R	233	208	25	G	233	210	23	R	233	211	22	G	233	202	32	R	233	200	33	R	233	194	39
1268	R	233	210	23	G	233	208	25	G	233	211	22	R	233	208	25	G	233	210	23	R	233	211	23	G	233	202	31	R	233	200	33	R	233	194	39
1269	R	233	210	23	G	233	208	25	G	233	212	22	R	233	208	25	G	233	211	23	R	233	211	23	G	233	203	31	R	233	200	33	R	233	194	39
1270	R	233	210	23	G	233	208	24	G	233	212	21	R	233	208	25	G	233	211	22	R	233	211	23	G	233	203	30	R	233	200	34	G	233	195	39
1271	R	234	210	24	G	234	210	24	R	234	212	22	R	234	208	26	G	234	212	22	R	234	211	23	G	234	204	30	R	234	200	34	G	234	195	38
1272	R	234	210	24	G	234	210	24	R	234	212	22	R	234	208	26	G	234	212	22	R	234	211	23	G	234	204	30	R	234	200	34	G	234	196	38
1273	R	234	210	24	G	234	211	23	R	234	212	22	R	234	208	26	G	234	213	21	R	234	211	23	G	234	205	29	R	234	200	34	G	234	196	37
1274	R	234	210	24	G	234	211	23	R	234	212	22	R	234	208	26	G	234	213	21	R	234	211	23	G	234	205	29	R	234	200	34	G	234	197	37
1275	R	234	210	24	G	234	212	23	R	234	212	22	R	234	208	26	R	234	213	21	R	234	211	24	G	234	206	29	R	234	200	34	G	234	197	37
1276	R	234	210	24	G	234	212	22	R	234	212	22	R	234	208	26	R	234	213	21	R	234	211	24	G	234	206	28	R	234	200	35	G	234	198	36
1277	R	234	210	24	G	234	213	22	R	234	212	22	R	234	208	26	R	234	213	21	R	234	211	24	G	234	207	28	R	234	200	35	G	234	198	36
1278	R	235	210	25	G	235	213	22	R	235	212	23	R	235	208	27	R	235	213	21	R	235	211	24	G	235	207	28	R	235	200	35	G	235	199	36
1279	R	235	210	25	G	235	214	21	R	235	212	23	R	235	208	27	R	235	213	22	R	235	211	24	G	235	208	27	R	235	200	35	G	235	199	35
1280	R	235	210	25	G	235	214	21	R	235	212	23	R	235	208	27	R	235	213	22	R	235	211	24	G	235	208	27	R	235	200	35	G	235	200	35
1281	R	235	210	25	R	235	214	21	R	235	212	23	R	235	208	27	R	235	213	22	R	235	211	24	G	235	209	27	R	235	200	35	G	235	200	35
1282	R	235	210	25	R	235	214	21	R	235	212	23	R	235	208	27	R	235	213	22	R	235	211	25	G	235	209	26	R	235	200	35	G	235	201	34
1283	R	235	210	25	R	235	214	21	R	235	212	23	R	235	208	27	R	235	213	22	R	235	211	25	G	235	210	26	R	235	200	36	G	235	201	34
1284	R	235	210	25	R	235	214	21	R	235	212	23	R	235	208	27	R	235	213	22	R	235	211	25	G	235	210	25	R	235	200	36	G	235	202	34
1285	R	236	210	26	R	236	214	22	R	236	212	24	R	236	209	28	R	236	213	22	R	236	211	25	G	236	211	25	R	236	200	36	G	236	202	33
1286	R	236	210	26	R	236	214	22	R	236	212	24	R	236	208	28	R	236	213	23	R	236	211	25	G	236	211	25	R	236	200	36	G	236	203	33
1287	R	236	210	26	R	236	214	22	R	236	212	24	R	236	208	28	R	236	213	23	R	236	211	25	G	236	212	24	R	236	200	36	G	236	203	32
1288	R	236	210	26	R	236	214	22	R	236	212	24	R	236	208	28	R	236	213	23	R	236	211	25	G	236	212	24	R	236	200	36	G	236	204	32
1289	R	236	210	26	R	236	214	22	R	236	212	24	R	236	208	28	R	236	213	23	R	236	211	26	G	236	213	24	R	236	200	36	G	236	204	32
1290	R	236	210	26	R	236	214	22	R	236	212	24	R	236	208	28	R	236	213	23	R	236	211	26	G	236	213	23	R	236	200	37	G	236	205	31
1291	R	236	210	26	R	236	214	22	R	236	212	24	R	236	208	28	R	236	213	23	R	236	211	26	G	236	214	23	R	236	200	37	G	236	205	31
1292	R	237	210	27	R	237	214	23	R	237	212	25	R	237	208	29	R	237	213	23	R	237	211	26	G	237	214	23	R	237	200	37	G	237	206	31
1293	R	237	210	27	R	237	214	23	R	237	212	25	R	237	208	29	R	237	213	24	R	237	211	26	G	237	215	22	R	237	200	37	G	237	206	30
1294	R	237	210	27	R	237	214	23	R	237	212	25	R	237	208	29	R	237	213	24	R	237	211	26	G	237	215	22	R	237	200	37	G	237	207	30
1295	R	237	210	27	R	237	214	23	R	237	212	25	R	237	208	29	R	237	213	24	R	237	211	26	G	237	216	22	R	237	200	37	G	237	207	30
1296	R	237	210	27	R	237	214	23	R	237	212	25	R	237	208	29	R	237	213	24	R	237	211	27	G	237	216	21	R	237	200	37	G	237	208	29
1297	R	237	210	27	R	237	214	23	R	237	212	25	R	237	208	29	R	237	213	24	R	237	211	27	R	237	216	21	G	237	200	37	G	237	208	29
1298	R	237	210	27	R	237	214	23	R	237	212	25	R	237	208	29	R	237	213	24	R	237	211	27	R	237	216	21	G	237	201	37	G	237	209	29
1299	R	238	210	28	R	238	214	24	R	238	212	26	R	238	208	30	R	238	213	24	R	238	211	27	R	238	216	22	G	238	201	36	G	238	209	28
1300	R	238	210	28	R	238	214	24	R	238	212	26	R	238	208	30	R	238	213	25	R	238	211	27	R	238	216	22	G	238	202	36	G	238	210	28
1301	G	238	211	27	R	238	214	24	R	238	212	26	G	238	209	29	R	238	213	25	R	238	211	27	R	238	216	22	G	238	202	36	G	238	210	28
1302	G	238	211	27	R	238	214	24	R	238	212	26	G	238	209	29	R	238	213	25	R	238	211	27	R	238	216	22	G	238	203	35	G	238	211	27
1303	G	238	212	27	R	238	214	24	R	238	212	26	G	238	210	29	R	238	213	25	R	238	211	28	R	238	216	22	G	238	203	35	G	238	211	27
1304	G	238	212	26	R	238	214	24	R	238	212	26	G	238	210	28	R	238	213	25	R	238	211	28	R	238	216	22	G	238	204	35	G	238	212	26
1305	G	238	213	26	R	238	214	24	R	238	212	26	G	238	211	28	R	238	213	25	R	238	211	28	R	238	216	22	G	238	204	34	G	238	212	26
1306	G	239	213	26	R	239	214	25	R	239	212	27	G	239	211	28	R	239	213	25	R	239	211	28	R	239	216	23	G	239	205	34	G	239	213	26
1307	G	239	214	25	R	239	214	25	R	239	212	27	G	239	212	27	R	239	213	26	R	239	211	28	R	239	216	23	G	239	205	33	G	239	213	25
1308	G	239	214	25	R	239	214	25	R	239	212	27	G	239	212	27	R	239	213	26	R	239	211	28	R	239	216	23	G	239	206	33	G	239	214	25
1309	G	239	215	25	R	239	214	25	R	239	212	27	G	239	213	27	R	239	213	26	R	239	211	28	R	239	216	23	G	239	206	33	G	239	214	25
1310	G	239	215	24	R	239	214	25	R	239	212	27	G	239	213	26	R	239	213	26	R	239	211	29	R	239	216	23	G	239	207	32	G	239	215	24
1311	G	239	216	24	R	239	214	25	G	239	213	27	G	239	214	26	R	239	213	26	R	239	211	29	R	239	216	23	G	239	207	32	G	239	215	24
1312	G	240	216	24	R	240	214	26	G	240	213	27	G	240	214	26	R	240	213	26	R	240	211	29	R	240	216	24	G	240	208	32	G	240	216	24
1313	G	240	217	23	R	240	214	26	G	240	214	26	G	240	215	25	R	240	213	26	R	240	211	29	R	240	216	24	G	240	208	31	G	240	216	23

Table C-1. Continued

A=Arrivals, D=Departures, Q=Queue:

Time (sec)	A	D	Q	A	D	Q	A	D	Q	A	D	Q	A	D	Q	A	D	Q	A	D	Q	A	D	Q	A	D	Q
1314	G	240	217	23	R	240	214	26	G	240	214	26	G	240	215	25	R	240	213	27	G	240	211	29	R	240	216	24	G	240	209	31	G	240	217	23
1315	G	240	218	22	R	240	214	26	G	240	215	25	G	240	216	24	R	240	213	27	G	240	212	28	R	240	216	24	G	240	209	31	G	240	217	23
1316	G	240	218	22	R	240	214	26	G	240	215	25	G	240	216	24	R	240	213	27	G	240	212	28	R	240	216	24	G	240	210	30	G	240	218	22
1317	G	240	219	22	R	240	214	26	G	240	216	25	G	240	217	24	R	240	213	27	G	240	213	28	R	240	216	24	G	240	210	30	G	240	218	22
1318	G	240	219	21	R	240	214	26	G	240	216	24	G	240	217	23	R	240	213	27	G	240	213	27	R	240	216	24	G	240	211	30	G	240	219	21
1319	G	241	220	21	R	241	214	27	G	241	217	24	G	241	219	23	R	241	213	27	G	241	214	27	R	241	216	25	G	241	211	29	G	241	219	21
1320	G	241	220	21	R	241	214	27	G	241	217	24	G	241	218	23	R	241	213	27	G	241	214	27	R	241	216	25	G	241	212	29	G	241	220	21
1321	R	241	220	21	G	241	215	26	G	241	216	23	G	241	219	22	R	241	213	28	G	241	215	26	R	241	216	25	G	241	212	29	G	241	220	20
1322	R	241	220	21	G	241	215	26	G	241	216	23	G	241	219	22	R	241	213	28	G	241	215	26	R	241	216	25	G	241	213	28	G	241	221	20
1323	R	241	220	21	G	241	216	26	G	241	219	23	G	241	220	22	R	241	213	28	G	241	216	25	R	241	216	25	G	241	213	28	G	241	221	20
1324	R	241	220	21	G	241	216	25	G	241	219	22	G	241	220	21	R	241	213	28	G	241	216	25	R	241	216	25	G	241	214	27	R	241	221	20
1325	R	241	220	21	G	241	217	25	G	241	220	22	G	241	221	21	R	241	213	28	G	241	217	25	R	241	216	25	G	241	214	27	R	241	221	20
1326	R	242	220	22	G	242	217	25	G	242	220	22	G	242	221	21	R	242	213	28	G	242	217	24	R	242	216	26	G	242	215	27	R	242	221	20
1327	R	242	220	22	G	242	218	24	G	242	221	21	R	242	221	21	G	242	214	28	G	242	218	24	R	242	216	26	G	242	215	26	R	242	221	20
1328	R	242	220	22	G	242	218	24	G	242	221	21	R	242	221	21	G	242	214	28	G	242	218	24	R	242	216	26	G	242	216	26	R	242	221	20
1329	R	242	220	22	G	242	219	23	G	242	222	20	R	242	221	21	G	242	215	27	G	242	219	23	R	242	216	26	G	242	216	26	R	242	221	21
1330	R	242	220	22	G	242	219	23	G	242	222	20	R	242	221	21	G	242	215	27	G	242	219	23	R	242	216	26	G	242	217	25	R	242	221	21
1331	R	242	220	22	G	242	220	23	R	242	222	20	R	242	221	21	G	242	216	27	G	242	220	23	R	242	216	26	G	242	217	25	R	242	221	21
1332	R	242	220	22	G	242	220	22	R	242	222	20	R	242	221	21	G	242	216	28	G	242	220	22	R	242	216	26	G	242	218	25	R	242	221	21
1333	R	243	220	23	G	243	221	22	R	243	222	21	R	243	221	22	G	243	217	26	G	243	221	22	R	243	216	27	G	243	218	24	R	243	221	21
1334	R	243	220	23	G	243	221	22	R	243	222	21	R	243	221	22	G	243	217	25	G	243	221	22	R	243	216	27	G	243	219	24	R	243	221	21
1335	R	243	220	23	G	243	222	21	R	243	222	21	R	243	221	22	G	243	218	25	G	243	222	21	R	243	216	27	G	243	219	24	R	243	221	21
1336	R	243	220	23	G	243	222	21	R	243	222	21	R	243	221	22	G	243	218	25	G	243	222	21	R	243	216	27	G	243	220	23	R	243	221	22
1337	R	243	220	23	G	243	223	21	R	243	222	21	R	243	221	22	G	243	219	24	G	243	223	21	R	243	216	27	G	243	220	23	R	243	221	22
1338	R	243	220	23	G	243	223	20	R	243	222	21	R	243	221	22	G	243	219	24	G	243	223	20	R	243	216	27	G	243	221	22	R	243	221	22
1339	R	243	220	23	G	243	224	20	R	243	222	21	R	243	221	22	G	243	220	24	G	243	224	20	R	243	216	27	G	243	221	22	R	243	221	22
1340	R	244	220	24	G	244	224	20	R	244	222	22	R	244	221	23	G	244	220	23	R	244	224	20	R	244	216	28	G	244	222	22	R	244	221	22
1341	R	244	220	24	R	244	224	20	R	244	222	22	R	244	221	23	G	244	221	23	R	244	224	20	R	244	216	28	G	244	222	21	R	244	221	22
1342	R	244	220	24	R	244	224	20	R	244	222	22	R	244	221	23	G	244	221	23	R	244	224	20	R	244	216	28	G	244	223	21	R	244	221	22
1343	R	244	220	24	R	244	224	20	R	244	222	22	R	244	221	23	G	244	222	22	R	244	224	20	R	244	216	28	G	244	223	21	R	244	221	23
1344	R	244	220	24	R	244	224	20	R	244	222	22	R	244	221	23	G	244	222	22	R	244	224	21	R	244	216	28	G	244	224	20	R	244	221	23
1345	R	244	220	24	R	244	224	20	R	244	222	22	R	244	221	23	G	244	223	22	R	244	224	21	R	244	216	28	G	244	224	20	R	244	221	23
1346	R	244	220	24	R	244	224	20	R	244	222	22	R	244	221	23	G	244	223	21	R	244	224	21	R	244	216	28	G	244	225	20	R	244	221	23
1347	R	245	220	25	R	245	224	21	R	245	222	23	R	245	221	24	G	245	224	21	R	245	224	21	R	245	216	29	G	245	225	19	R	245	221	23
1348	R	245	220	25	R	245	224	21	R	245	222	23	R	245	221	24	G	245	224	21	R	245	224	21	R	245	216	29	G	245	226	19	R	245	221	23
1349	R	245	220	25	R	245	224	21	R	245	222	23	R	245	221	24	G	245	225	20	R	245	224	21	R	245	216	29	G	245	226	19	R	245	221	23
1350	R	245	220	25	R	245	224	21	R	245	222	23	R	245	221	24	G	245	225	20	R	245	224	21	R	245	216	29	G	245	227	18	R	245	221	24
1351	R	245	220	25	R	245	224	21	R	245	222	23	R	245	221	24	G	245	226	19	R	245	224	22	R	245	216	29	R	245	227	18	R	245	221	24
1352	R	245	220	25	R	245	224	21	R	245	222	23	R	245	221	24	G	245	226	19	R	245	224	22	R	245	216	29	R	245	227	18	R	245	221	24
1353	R	245	220	25	R	245	224	21	R	245	222	23	R	245	221	24	R	245	226	19	R	245	224	22	R	245	216	29	R	245	227	18	R	245	221	24
1354	R	246	220	26	R	246	224	22	R	246	222	24	R	246	221	25	R	246	226	19	R	246	224	22	R	246	216	30	R	246	227	19	R	246	221	24
1355	R	246	220	26	R	246	224	22	R	246	222	24	R	246	221	25	R	246	226	20	R	246	224	22	R	246	216	30	R	246	227	19	R	246	221	24
1356	R	246	220	26	R	246	224	22	R	246	222	24	R	246	221	25	R	246	226	20	R	246	224	22	R	246	216	30	R	246	227	19	R	246	221	24
1357	R	246	220	26	R	246	224	22	R	246	222	24	R	246	221	25	R	246	226	20	R	246	224	22	R	246	216	30	R	246	227	19	R	246	221	25
1358	R	246	220	26	R	246	224	22	R	246	222	24	R	246	221	25	R	246	226	20	R	246	224	23	R	246	216	30	R	246	227	19	R	246	221	25
1359	R	246	220	26	R	246	224	22	R	246	222	24	R	246	221	25	R	246	226	20	R	246	224	23	R	246	216	30	R	246	227	19	R	246	221	25
1360	R	246	220	26	R	246	224	22	R	246	222	24	R	246	221	25	R	246	226	20	R	246	224	23	R	246	216	30	R	246	227	20	R	246	221	25
1361	G	247	221	26	R	247	224	23	R	247	222	25	R	247	221	26	R	247	226	20	R	247	224	23	R	247	216	31	R	247	227	20	R	247	221	25
1362	G	247	221	26	R	247	224	23	R	247	222	25	R	247	221	26	R	247	226	21	R	247	224	23	R	247	216	31	R	247	227	20	R	247	221	25
1363	G	247	222	25	R	247	224	23	R	247	222	25	R	247	221	26	R	247	226	21	R	247	224	23	R	247	216	31	R	247	227	20	R	247	221	25
1364	G	247	222	25	R	247	224	23	R	247	222	25	R	247	221	26	R	247	226	21	R	247	224	23	R	247	216	31	R	247	227	20	R	247	221	26
1365	G	247	223	25	R	247	224	23	R	247	222	25	R	247	221	26	R	247	226	21	R	247	224	24	R	247	216	31	R	247	227	20	R	247	221	26
1366	G	247	223	24	R	247	224	23	R	247	222	25	R	247	221	26	R	247	226	21	R	247	224	24	R	247	216	31	R	247	227	21	R	247	221	26
1367	G	247	224	24	R	247	224	23	R	247	222	25	R	247	221	26	R	247	226	21	R	247	224	24	R	247	216	31	R	247	227	21	R	247	221	26
1368	G	248	224	24	R	248	224	24	R	248	222	26	R	248	221	27	R	248	226	21	R	248	224	24	R	248	216	32	R	248	227	21	R	248	221	26
1369	G	248	225	23	R	248	224	24	R	248	222	26	R	248	221	27	R	248	226	22	R	248	224	24	R	248	216	32	R	248	227	21	R	248	221	26
1370	G	248	225	23	R	248	224	24	R	248	222	26	R	248	221	27	R	248	226	22	R	248	224	24	R	248	216	32	R	248	227	21	R	248	221	26
1371	G	248	226	23	R	248	224	24	G	248	223	26	R	248	221	27	R	248	226	22	R	248	224	24	R	248	216	32	R	248	227	21	R	248	221	27
1372	G	248	226	22	R	248	224	24	G	248	223	25	R	248	221	27	R	248	226	22	R	248	224	25	R	248	216	32	R	248	227	21	R	248	221	27
1373	G	248	227	22	R	248	224	24	G	248	224	25	R	248	221	27	R	248	226	22	R	248	224	25	R	248	216	32	R	248	227	22	R	248	221	27
1374	G	248	227	21	R	248	224	24	G	248	224	24	R	248	221	27	R	248	226	22	R	248	224	25	R	248	216	32	R	248	227	22	R	248	221	27
1375	G	249	228	21	R	249	224	25	G	249	225	24	R	249	221	28	R	249	226	22	R	249	224	25	R	249	216	33	R	249	227	22	R	249	221	27
1376	G	249	228	21	R	249	224	25	G	249	225	24	R	249	221	28	R	249	226	23	R	249	224	25	R	249	216	33	R	249	227	22	R	249	221	27
1377	G	249	229	20	R	249	224	25	G	249	226	23	R	249	221	28	R	249	226	23	R	249	224	25	R	249	216	33	R	249	227	22	R	249	221	27
1378	G	249	229	20	R	249	224	25	G	249	226	23	R	249	221	28	R	249	226	23	R	249	224	25	R	249	216	33	R	249	227	22	R	249	221	28
1379	G	249	230	20	R	249	224	25	G	249	227	23	G	249	222	28	R	249	226	23	R	249	224	26	R	249	216	33	R	249	227	22	R	249	221	28
1380	G	249	230	19	R	249	224	25	G	249	227	22	G	249	222	27	R	249	226	23	R	249	224	26	R	249	216	33	R	249	227	23	R	249	221	28
1381	R	249	230	19	G	249	225	25	G	249	228	22	G	249	223	27	R	249	226	23	R	249	224	26	R	249	216	33	R	249	227	23	R	249	221	28
1382	R	250	230	20	G	250	225	25	G	250	228	22	G	250	223	27	R	250	226	24	R	250	224	26	R	250	216	34	R	250	227	23	R	250	221	28
1383	R	250	230	20	G	250	226	24	G	250	228	21	G	250	224	26	R	250	226	24	R	250	224	26	R	250	216	34	R	250	227	23	R	250	221	28
1384	R	250	230	20	G	250	226	24	G	250	229	21	G	250	224	26	R	250	226	24	R	250	224	26	R	250	216	34	R	250	227	23	R	250	221	29
1385	R	250	230	20	G	250	227	24	G	250	230	21	G	250	225	26	R	250	226	24	R	250	224	26	R	250	216	34	R	250	227	23	R	250	221	29
1386	R	250	230	20	G	250	227	23	G	250	230	20	G	250	225	25	R	250	226	24	R	250	224	27	R	250	216	34	R	250	227	23	R	250	221	29
1387	R	250	230	20	G	250	228	23	G	250	231	20	G	250	226	25	R	250	226	24	R	250	224	27	R	250	216	34	R	250	227	24	R	250	221	29
1388	R	250	230	20	G	250	228	22	G	250	231	19	G	250	226	24	R	250	226	24	R	250	224	27	R	250	216	34	R	250	227	24	R	250	221	29
1389	R	251	230	21	G	251	229	22	G	251	232	19	G	251	227	24	R	251	226	24	R	251	224	27	R	251	216	35	R	251	227	24	R	251	221	29
1390	R	251	230	21	G	251	229	22	G	251	232	19	G	251	227	24	R	251	226	25	R	251	224	27	R	251	216	35	R	251	227	24	R	251	221	29
1391	R	251	230	21	G	251	230	21	R	251	232	19	G	251	228	23	R	251	226	25	R	251	224	27	R	251	216	35	R	251	227	24	R	251	221	30
1392	R	251	230	21	G	251	230	21	R	251	232	19	G	251	228	23	R	251	226	25	G	251	224	27	R	251	216	35	R	251	227	24	R	251	221	30
1393	R	251	230	21	G	251	231	21	R	251	232	19	G	251	229	23	R	251	226	25	G	251	225	27	R	251	216	35	R	251	227	24	R	251	221	30
1394	R	251	230	21	G	251	231	20	R	251	232	19	G	251	229	22	R	251	226	25	G	251	225	26	R	251	216	35	R	251	227	25	R	251	221	30
1395	R	251	230	21	G	251	232	20	R	251	232	19	G	251	230	22	R	251	226	25	G	251	226	26	R	251	216	35	R	251	227	25	R	251	221	30
1396	R	252	230	22	G	252	232	20	R	252	232	20	G	252	230	22	R	252	226	25	G	252	226	26	R	252	216	36	R	252	227	25	R	252	221	30

Table C-1. Continued

A=Arrivals, D=Departures, Q=Queue:

Time (sec)	A	D	Q	A	D	Q	A	D	Q	A	D	Q	A	D	Q	A	D	Q	A	D	Q	A	D	Q	A	D	Q
1397	R	252	230	22	G	252	233	19	R	252	232	20	G	252	231	21	R	252	228	28	G	252	227	25	R	252	218	36	R	252	227	25	R	252	221	30
1398	R	252	230	22	G	252	233	19	R	252	232	20	G	252	231	21	R	252	226	26	G	252	227	25	R	252	216	36	R	252	227	25	R	252	221	31
1399	R	252	230	22	G	252	234	19	R	252	232	20	G	252	232	21	R	252	226	26	G	252	228	24	R	252	216	36	R	252	227	25	R	252	221	31
1400	R	252	230	22	G	252	234	18	R	252	232	20	G	252	232	20	R	252	226	26	G	252	228	24	R	252	216	36	R	252	227	25	R	252	221	31
1401	R	252	230	22	R	252	234	18	R	252	232	20	G	252	233	20	R	252	226	26	G	252	229	24	R	252	216	36	R	252	227	26	R	252	221	31
1402	R	253	230	23	R	253	234	19	R	253	232	21	G	253	233	20	R	253	226	26	G	253	229	23	R	253	216	37	R	253	227	26	R	253	221	31
1403	R	253	230	23	R	253	234	19	R	253	232	21	G	253	234	19	R	253	226	26	G	253	230	23	R	253	216	37	R	253	227	26	R	253	221	31
1404	R	253	230	23	R	253	234	19	R	253	232	21	G	253	234	19	R	253	226	27	G	253	230	23	R	253	216	37	R	253	227	26	R	253	221	31
1405	R	253	230	23	R	253	234	18	R	253	232	21	R	253	234	19	G	253	227	26	G	253	231	22	G	253	217	36	R	253	227	26	R	253	221	32
1406	R	253	230	23	R	253	234	19	R	253	232	21	R	253	234	19	G	253	227	26	G	253	231	22	G	253	217	36	R	253	227	26	R	253	221	32
1407	R	253	230	23	R	253	234	18	R	253	232	21	R	253	234	19	G	253	228	26	G	253	232	22	G	253	218	36	R	253	227	26	R	253	221	32
1408	R	253	230	23	R	253	234	19	R	253	232	21	R	253	234	19	G	253	228	25	G	253	232	21	G	253	218	35	R	253	227	27	R	253	221	32
1409	R	254	230	24	R	254	234	20	R	254	232	22	R	254	234	20	G	254	228	25	G	254	233	21	G	254	218	35	R	254	227	27	R	254	221	32
1410	R	254	230	24	R	254	234	20	R	254	232	22	R	254	234	20	G	254	229	24	G	254	233	21	G	254	219	35	R	254	227	27	R	254	221	32
1411	R	254	230	24	R	254	234	20	R	254	232	22	R	254	234	20	G	254	230	24	G	254	234	20	G	254	220	34	R	254	227	27	R	254	221	32
1412	R	254	230	24	R	254	234	20	R	254	232	22	R	254	234	20	G	254	230	24	G	254	234	20	G	254	220	34	R	254	227	27	R	254	221	33
1413	R	254	230	24	R	254	234	20	R	254	232	22	R	254	234	20	G	254	231	23	G	254	235	19	G	254	221	34	R	254	227	27	R	254	221	33
1414	R	254	230	24	R	254	234	20	R	254	232	22	R	254	234	20	G	254	231	23	G	254	235	18	G	254	221	33	R	254	227	27	R	254	221	33
1415	R	254	230	24	R	254	234	20	R	254	232	22	R	254	234	20	G	254	232	23	G	254	236	19	G	254	222	33	R	254	227	28	R	254	221	33
1416	R	255	230	25	R	255	234	21	R	255	232	23	R	255	234	21	G	255	232	22	G	255	236	18	G	255	222	33	R	255	227	28	R	255	221	33
1417	R	255	230	25	R	255	234	21	R	255	232	23	R	255	234	21	G	255	233	22	G	255	237	18	G	255	223	32	R	255	227	28	R	255	221	33
1418	R	255	230	25	R	255	234	21	R	255	232	23	R	255	234	21	G	255	233	22	R	255	237	18	G	255	223	32	R	255	227	28	R	255	221	33
1419	R	255	230	25	R	255	234	21	R	255	232	23	R	255	234	21	G	255	234	21	R	255	237	18	G	255	224	31	R	255	227	28	R	255	221	34
1420	R	255	230	25	R	255	234	21	R	255	232	23	R	255	234	21	G	255	234	21	R	255	237	19	G	255	224	31	R	255	227	28	R	255	221	34
1421	G	255	231	25	R	255	234	21	R	255	232	23	R	255	234	21	G	255	235	21	R	255	237	19	G	255	225	31	R	255	227	28	R	255	221	34
1422	G	255	231	24	R	255	234	21	R	255	232	23	R	255	234	21	G	255	235	20	R	255	237	19	G	255	225	30	R	255	227	29	R	255	221	34
1423	G	256	232	24	R	256	234	22	R	256	232	24	R	256	234	22	G	256	236	20	R	256	237	18	G	256	226	30	R	256	227	29	R	256	221	34
1424	G	256	232	24	R	256	234	22	R	256	232	24	R	256	234	22	G	256	236	19	R	256	237	18	G	256	226	30	R	256	227	29	R	256	221	34
1425	G	256	233	23	R	256	234	22	R	256	232	24	R	256	234	22	G	256	237	19	R	256	237	18	G	256	227	29	R	256	227	29	R	256	221	34
1426	G	256	233	23	R	256	234	22	R	256	232	24	R	256	234	22	G	256	237	19	R	256	237	19	G	256	227	29	R	256	227	29	R	256	221	35
1427	G	256	234	23	R	256	234	22	R	256	232	24	R	256	234	22	G	256	238	19	R	256	237	20	G	256	228	29	R	256	227	29	R	256	221	35
1428	G	256	234	22	R	256	234	22	R	256	232	24	R	256	234	22	G	256	238	18	R	256	237	20	G	256	228	28	R	256	227	29	R	256	221	35
1429	G	256	235	22	R	256	234	22	R	256	232	24	R	256	234	22	G	256	239	18	R	256	237	20	G	256	229	28	R	256	227	30	R	256	221	35
1430	G	257	235	22	R	257	234	23	R	257	232	25	R	257	234	23	G	257	239	17	R	257	237	20	G	257	229	28	R	257	227	30	R	257	221	35
1431	G	257	236	21	R	257	234	23	G	257	233	24	R	257	234	23	R	257	239	17	R	257	237	20	G	257	230	27	R	257	227	30	R	257	221	35
1432	G	257	236	21	R	257	234	23	G	257	233	24	R	257	234	23	R	257	239	18	R	257	237	20	G	257	230	27	R	257	227	30	G	257	222	35
1433	G	257	237	20	R	257	234	23	G	257	234	23	R	257	234	23	R	257	239	18	R	257	237	20	G	257	231	26	R	257	227	30	G	257	222	35
1434	G	257	237	20	R	257	234	23	G	257	234	23	R	257	234	23	R	257	239	18	R	257	237	21	G	257	231	26	R	257	227	30	G	257	223	34
1435	G	257	238	20	R	257	234	23	G	257	235	23	R	257	234	23	R	257	239	18	R	257	237	21	G	257	232	26	R	257	227	30	G	257	223	34
1436	G	257	238	19	R	257	234	23	G	257	235	22	R	257	234	23	R	257	239	18	R	257	237	21	G	257	232	25	R	257	227	31	G	257	224	34
1437	G	258	239	19	R	258	234	24	G	258	236	22	R	258	234	24	R	258	239	18	R	258	237	21	G	258	233	25	R	258	227	31	G	258	224	33
1438	G	258	239	18	R	258	234	24	G	258	236	22	R	258	234	24	R	258	239	19	R	258	237	21	G	258	233	25	R	258	227	31	G	258	225	33
1439	G	258	240	18	R	258	234	24	G	258	237	21	R	258	234	24	R	258	239	19	R	258	237	21	G	258	234	24	R	258	227	31	G	258	225	32
1440	G	258	240	18	R	258	234	24	G	258	237	21	R	258	234	24	R	258	239	19	R	258	237	21	G	258	234	24	R	258	227	31	G	258	226	32
1441	R	258	240	18	G	258	235	24	G	258	238	21	R	258	234	24	R	258	239	19	R	258	237	22	G	258	235	24	R	258	227	31	G	258	226	32
1442	R	258	240	18	G	258	235	23	G	258	238	20	R	258	234	24	R	258	239	19	R	258	237	22	G	258	235	23	R	258	227	31	G	258	227	31
1443	R	258	240	18	G	258	236	23	G	258	239	20	R	258	234	24	R	258	239	19	R	258	237	22	G	258	236	23	R	258	227	32	G	258	227	31
1444	R	259	240	19	G	259	236	23	G	259	239	20	R	259	234	25	R	259	239	19	R	259	237	22	G	259	236	23	R	259	227	32	G	259	228	31
1445	R	259	240	19	G	259	237	22	G	259	240	19	R	259	234	25	R	259	239	20	R	259	237	22	G	259	237	22	R	259	227	32	G	259	228	30
1446	R	259	240	19	G	259	237	22	G	259	240	19	R	259	234	25	R	259	239	20	R	259	237	22	G	259	237	22	R	259	227	32	G	259	229	30
1447	R	259	240	19	G	259	238	22	G	259	241	19	R	259	234	25	R	259	239	20	R	259	237	22	G	259	238	22	R	259	227	32	G	259	229	30
1448	R	259	240	19	G	259	238	21	G	259	241	18	R	259	234	25	R	259	239	20	R	259	237	23	G	259	238	21	R	259	227	32	G	259	230	29
1449	R	259	240	19	G	259	238	21	G	259	242	18	R	259	234	25	R	259	239	20	R	259	237	23	G	259	239	21	R	259	227	33	G	259	231	29
1450	R	259	240	19	G	259	239	20	G	259	242	17	R	259	234	25	R	259	239	20	R	260	237	23	G	260	240	20	R	260	227	33	G	260	231	28
1451	R	260	240	20	G	260	240	20	R	260	242	18	R	260	234	26	R	260	239	20	R	260	237	23	G	260	240	20	R	260	227	33	G	260	232	28
1452	R	260	240	20	G	260	240	20	R	260	242	18	R	260	234	26	R	260	239	21	R	260	237	23	G	260	240	20	R	260	227	33	G	260	232	27
1453	R	260	240	20	G	260	241	19	R	260	242	18	R	260	234	26	R	260	239	21	R	260	237	23	G	260	241	19	R	260	227	33	G	260	232	27
1454	R	260	240	20	G	260	241	19	R	260	242	18	R	260	234	26	R	260	239	21	R	260	237	23	G	260	241	19	R	260	227	33	G	260	233	27
1455	R	260	240	20	G	260	242	19	R	260	242	18	R	260	234	26	R	260	239	21	R	260	237	24	G	260	242	19	R	260	227	33	G	260	233	27
1456	R	260	240	20	G	260	242	18	R	260	242	18	R	260	234	26	R	260	239	21	R	260	237	24	G	260	242	18	R	260	227	34	G	260	234	26
1457	R	260	240	20	G	260	243	18	R	260	242	18	G	260	235	26	R	260	239	21	R	260	237	24	G	260	243	18	R	260	227	34	G	260	234	26
1458	R	261	240	21	G	261	243	18	R	261	242	19	G	261	235	26	R	261	239	21	R	261	237	24	G	261	243	18	R	261	227	34	G	261	235	26
1459	R	261	240	21	G	261	244	17	R	261	242	19	G	261	236	25	R	261	239	22	R	261	237	24	R	261	243	18	G	261	227	33	G	261	235	25
1460	R	261	240	21	G	261	244	17	R	261	242	19	G	261	236	25	R	261	239	22	R	261	237	24	R	261	243	18	G	261	228	33	G	261	236	25
1481	R	261	240	21	R	261	244	17	R	261	242	19	G	261	237	25	R	261	239	22	R	261	237	24	R	261	243	18	G	261	228	33	G	261	238	25
1462	R	261	240	21	R	261	244	17	R	261	242	19	G	261	237	24	R	261	239	22	R	261	237	25	R	261	243	18	G	261	229	32	G	261	237	24
1483	R	261	240	21	R	261	244	17	R	261	242	19	G	261	238	24	R	261	239	22	R	261	237	25	R	261	243	18	G	261	229	32	G	261	237	24
1464	R	261	240	21	R	261	244	17	R	261	242	19	G	261	238	23	R	261	239	22	R	261	237	25	R	261	243	18	G	261	230	32	G	261	238	24
1465	R	262	240	22	R	262	244	18	R	262	242	20	G	262	238	23	R	262	239	22	R	262	237	25	R	262	243	18	G	262	230	31	G	262	238	23
1466	R	262	240	22	R	262	244	18	R	262	242	20	G	262	239	23	R	262	239	23	R	262	237	25	R	262	243	19	G	262	231	31	G	262	239	23
1467	R	262	240	22	R	262	244	18	R	262	242	20	G	262	240	22	R	262	239	23	R	262	237	25	R	262	243	18	G	262	231	31	G	262	239	22
1488	R	262	240	22	R	262	244	18	R	262	242	20	G	262	240	22	R	262	239	23	R	262	237	25	R	262	243	19	G	262	232	30	G	262	240	22
1468	R	262	240	22	R	262	244	18	R	262	242	20	G	262	241	22	R	262	239	23	R	262	237	26	R	262	243	18	G	262	232	30	G	262	240	22
1470	R	262	240	22	R	262	244	18	R	262	242	20	G	262	241	21	R	262	239	23	G	262	237	25	R	262	243	19	G	262	233	30	G	262	241	21
1471	R	262	240	22	R	262	244	18	R	262	242	20	G	262	242	21	R	262	239	23	C	262	238	25	R	262	243	19	C	262	233	29	C	262	241	21
1472	R	263	240	23	R	263	244	19	R	263	242	21	G	263	242	21	R	263	239	23	G	263	238	25	R	263	243	20	G	263	234	29	G	263	242	21
1473	R	263	240	23	R	263	244	19	R	263	242	21	G	263	243	20	R	263	239	24	G	263	239	24	R	263	243	20	G	263	234	28	G	263	242	20
1474	R	263	240	23	R	263	244	18	R	263	242	21	G	263	243	20	R	263	239	24	G	263	238	24	R	263	243	20	G	263	235	28	G	263	243	20
1475	R	263	240	23	R	263	244	18	R	263	242	21	G	263	244	20	R	263	239	24	G	263	240	23	R	263	243	20	G	263	235	28	G	263	243	20
1476	R	263	240	23	R	263	244	18	R	263	242	21	G	263	244	18	R	263	239	24	G	263	240	23	R	263	243	20	G	263	236	27	G	263	244	19
1477	R	263	240	23	R	263	244	18	R	263	242	21	G	263	245	19	R	263	239	24	G	263	241	23	R	263	243	20	G	263	236	27	G	263	244	19
1478	R	263	240	23	R	263	244	18	R	263	242	21	G	263	245	18	R	263	239	24	G	263	241	22	R	263	243	20	G	263	237	27	G	263	245	19
1479	R	264	240	24	R	264	244	20	R	264	242	22	G	264	248	18	R	264	239	24	G	264	242	22	R	264	243	21	G	264	237	26	G	264	245	18

Table C-1. Continued

A=Arrivals, D=Departures, Q=Queue:

Time (sec)		A	D	Q		A	D	Q		A	D	Q		A	D	Q		A	D	Q		A	D	Q		A	D	Q		A	D	Q
1480	R	264	240	24	R	264	244	20	R	264	242	22	G	264	246	18	R	264	239	25	G	264	242	22	R	264	243	21	G	264	238	26	G	264	246	18
1481	G	264	241	23	R	264	244	20	R	264	242	22	G	264	247	17	R	264	239	25	G	264	243	21	R	264	243	21	G	264	238	26	G	264	246	18
1482	G	264	241	23	R	264	244	20	R	264	242	22	G	264	247	17	R	264	239	25	G	264	243	21	R	264	243	21	G	264	239	25	G	264	247	17
1483	G	264	242	23	R	264	244	20	R	264	242	22	R	264	247	17	G	264	240	25	G	264	244	21	R	264	243	21	G	264	239	25	G	264	247	17
1484	G	264	242	22	R	264	244	20	R	264	242	22	R	264	247	17	G	264	240	24	G	264	244	20	R	264	243	21	G	264	240	25	G	264	248	16
1485	G	264	243	22	R	264	244	20	R	264	242	22	R	264	247	17	G	264	241	24	G	264	245	20	R	264	243	21	G	264	240	24	G	264	248	16
1486	G	265	243	22	R	265	244	21	R	265	242	23	R	265	247	18	G	265	241	23	G	265	245	20	R	265	243	22	G	265	241	24	R	265	248	16
1487	G	265	244	21	R	265	244	21	R	265	242	23	R	265	247	18	G	265	242	23	G	265	246	19	R	265	243	22	G	265	241	23	R	265	248	16
1488	G	265	244	21	R	265	244	21	R	265	242	23	R	265	247	18	G	265	242	23	G	265	246	19	R	265	243	22	G	265	242	23	R	265	248	17
1489	G	265	245	21	R	265	244	21	R	265	242	23	R	265	247	18	G	265	243	22	G	265	247	18	R	265	243	22	G	265	242	23	R	265	248	17
1490	G	265	245	20	R	265	244	21	R	265	242	23	R	265	247	18	G	265	243	22	G	265	247	18	R	265	243	22	G	265	243	22	R	265	248	17
1491	G	265	246	20	R	265	244	21	G	265	243	23	R	265	247	18	G	265	244	22	G	265	248	18	R	265	243	22	G	265	243	22	R	265	248	17
1492	G	266	246	20	R	266	244	22	G	266	243	23	R	266	247	19	G	266	244	21	G	266	248	17	R	266	243	23	G	266	244	22	R	266	248	17
1493	G	266	247	19	R	266	244	22	G	266	244	22	R	266	247	19	G	266	245	21	G	266	249	17	R	266	243	23	G	266	244	21	R	266	248	17
1494	G	266	247	19	R	266	244	22	G	266	244	22	R	266	247	19	G	266	245	21	G	266	249	17	R	266	243	23	G	266	245	21	R	266	248	18
1495	G	266	248	18	R	266	244	22	G	266	245	21	R	266	247	19	G	266	246	20	G	266	250	16	R	266	243	23	G	266	245	21	R	266	248	18
1496	G	266	248	18	R	266	244	22	G	266	245	21	R	266	247	19	G	266	246	20	R	266	250	16	R	266	243	23	G	266	246	20	R	266	248	18
1497	G	266	249	18	R	266	244	22	G	266	246	21	R	266	247	19	G	266	247	20	R	266	250	17	R	266	243	23	G	266	246	20	R	266	248	18
1498	G	266	249	17	R	266	244	22	G	266	246	20	R	266	247	19	G	266	247	19	R	266	250	17	R	266	243	23	G	266	247	20	R	266	248	18
1499	G	267	250	17	R	267	244	23	G	267	247	20	R	267	247	20	G	267	248	19	R	267	250	17	R	267	243	24	G	267	247	19	R	267	248	18
1500	G	267	250	17	R	267	244	23	G	267	247	20	R	267	247	20	G	267	248	18	R	267	250	17	R	267	243	24	G	267	248	19	R	267	248	18
1501	R	267	250	17	G	267	245	22	G	267	248	19	R	267	247	20	G	267	249	18	R	267	250	17	R	267	243	24	G	267	248	19	R	267	248	18
1502	R	267	250	17	G	267	245	22	G	267	248	19	R	267	247	20	G	267	249	18	R	267	250	17	R	267	243	24	G	267	248	18	R	267	248	19
1503	R	267	250	17	G	267	246	22	G	267	249	19	R	267	247	20	G	267	250	17	R	267	250	17	R	267	243	24	G	267	249	18	R	267	248	19
1504	R	267	250	17	G	267	246	21	G	267	249	18	R	267	247	20	G	267	250	17	R	267	250	18	R	267	243	24	G	267	250	17	R	267	248	19
1505	R	267	250	17	G	267	247	21	G	267	250	18	R	267	247	20	G	267	251	17	R	267	250	18	R	267	243	24	G	267	250	17	R	267	248	19
1506	R	268	250	18	G	268	247	21	G	268	250	18	R	268	247	21	G	268	251	16	R	268	250	18	R	268	243	25	G	268	251	17	R	268	248	19
1507	R	268	250	18	G	268	248	20	G	268	251	17	R	268	247	21	G	268	252	16	R	268	250	18	R	268	243	25	G	268	251	16	R	268	248	19
1508	R	268	250	18	G	268	248	20	G	268	251	17	R	268	247	21	G	268	252	16	R	268	250	18	R	268	243	25	G	268	252	16	R	268	248	19
1509	R	268	250	18	G	268	249	19	G	268	252	16	R	268	247	21	R	268	252	16	R	268	250	18	R	268	243	25	G	268	252	16	R	268	248	20
1510	R	268	250	18	G	268	249	19	G	268	252	16	R	268	247	21	R	268	252	16	R	268	250	19	R	268	243	25	G	268	253	15	R	268	248	20
1511	R	268	250	18	G	268	250	19	R	268	252	16	R	268	247	21	R	268	252	16	R	268	250	19	R	268	243	25	G	268	253	15	R	268	248	20
1512	R	268	250	18	G	268	250	18	R	268	252	16	R	268	247	21	R	268	252	16	R	268	250	19	R	268	243	25	G	268	254	15	R	268	248	20
1513	R	269	250	19	G	269	251	18	R	269	252	17	R	269	247	22	R	269	252	16	R	269	250	19	R	269	243	26	R	269	254	15	R	269	248	20
1514	R	269	250	19	G	269	251	18	R	269	252	17	R	269	247	22	R	269	252	16	R	269	250	19	R	269	243	26	R	269	254	15	R	269	248	20
1515	R	269	250	19	G	269	252	17	R	269	252	17	R	269	247	22	R	269	252	17	R	269	250	19	R	269	243	26	R	269	254	15	R	269	248	20
1516	R	269	250	19	G	269	252	17	R	269	252	17	R	269	247	22	R	269	252	17	R	269	250	19	R	269	243	26	R	269	254	15	R	269	248	21
1517	R	269	250	19	G	269	253	17	R	269	252	17	R	269	247	22	R	269	252	17	R	269	250	20	R	269	243	26	R	269	254	15	R	269	248	21
1518	R	269	250	19	G	269	253	16	R	269	252	17	R	269	247	22	R	269	252	17	R	269	250	20	R	269	243	26	R	269	254	15	R	269	248	21
1519	R	269	250	19	G	269	254	16	R	269	252	17	R	269	247	22	R	269	252	17	R	269	250	20	R	269	243	26	R	269	254	16	R	269	248	21
1520	R	270	250	20	G	270	254	16	R	270	252	18	R	270	247	23	R	270	252	17	R	270	250	20	R	270	243	27	R	270	254	16	R	270	248	21
1521	R	270	250	20	R	270	254	16	R	270	252	18	R	270	247	23	R	270	252	17	R	270	250	20	R	270	243	27	R	270	254	16	R	270	248	21
1522	R	270	250	20	R	270	254	16	R	270	252	18	R	270	247	23	R	270	252	18	R	270	250	20	R	270	243	27	R	270	254	16	R	270	248	21
1523	R	270	250	20	R	270	254	16	R	270	252	18	R	270	247	23	R	270	252	18	R	270	250	20	R	270	243	27	R	270	254	16	R	270	248	22
1524	R	270	250	20	R	270	254	16	R	270	252	18	R	270	247	23	R	270	252	18	R	270	250	21	R	270	243	27	R	270	254	16	R	270	248	22
1525	R	270	250	20	R	270	254	16	R	270	252	18	R	270	247	23	R	270	252	18	R	270	250	21	R	270	243	27	R	270	254	16	R	270	248	22
1526	R	270	250	20	R	270	254	16	R	270	252	18	R	270	247	23	R	270	252	18	R	270	250	21	R	270	243	27	R	270	254	17	R	270	248	22
1527	R	271	250	21	R	271	254	17	R	271	252	19	R	271	247	24	R	271	252	18	R	271	250	21	R	271	243	28	R	271	254	17	R	271	248	22
1528	R	271	250	21	R	271	254	17	R	271	252	19	R	271	247	24	R	271	252	19	R	271	250	21	R	271	243	28	R	271	254	17	R	271	248	22
1529	R	271	250	21	R	271	254	17	R	271	252	19	R	271	247	24	R	271	252	19	R	271	250	21	R	271	243	28	R	271	254	17	R	271	248	22
1530	R	271	250	21	R	271	254	17	R	271	252	19	R	271	247	24	R	271	252	19	R	271	250	21	R	271	243	28	R	271	254	17	R	271	248	23
1531	R	271	250	21	R	271	254	17	R	271	252	19	R	271	247	24	R	271	252	19	R	271	250	22	R	271	243	28	R	271	254	17	R	271	248	23
1532	R	271	250	21	R	271	254	17	R	271	252	19	R	271	247	24	R	271	252	19	R	271	250	22	R	271	243	28	R	271	254	17	R	271	248	23
1533	R	271	250	21	R	271	254	17	R	271	252	19	R	271	247	24	R	271	252	19	R	271	250	22	R	271	243	28	R	271	254	18	R	271	248	23
1534	R	272	250	22	R	272	254	18	R	272	252	20	R	272	247	25	R	272	252	19	R	272	250	22	R	272	243	29	R	272	254	18	R	272	248	23
1535	R	272	250	22	R	272	254	18	R	272	252	20	G	272	248	24	R	272	252	20	R	272	250	22	R	272	243	29	R	272	254	18	R	272	248	23
1536	R	272	250	22	R	272	254	18	R	272	252	20	G	272	248	24	R	272	252	20	R	272	250	22	R	272	243	29	R	272	254	18	R	272	248	23
1537	R	272	250	22	R	272	254	18	R	272	252	20	G	272	249	24	R	272	252	20	R	272	250	22	R	272	243	29	R	272	254	18	R	272	248	24
1538	R	272	250	22	R	272	254	18	R	272	252	20	G	272	249	23	R	272	252	20	R	272	250	23	R	272	243	29	R	272	254	18	R	272	248	24
1539	R	272	250	22	R	272	254	18	R	272	252	20	G	272	250	23	R	272	252	20	R	272	250	23	R	272	243	29	R	272	254	18	R	272	248	24
1540	R	272	250	22	R	272	254	18	R	272	252	20	G	272	250	22	R	272	252	20	R	272	250	23	R	272	243	29	R	272	254	19	R	272	248	24
1541	G	273	251	22	R	273	254	19	R	273	252	21	G	273	251	22	R	273	252	20	R	273	250	23	R	273	243	30	R	273	254	19	R	273	248	24
1542	G	273	251	22	R	273	254	19	R	273	252	21	G	273	251	22	R	273	252	21	R	273	250	23	R	273	243	30	R	273	254	19	R	273	248	24
1543	G	273	252	21	R	273	254	19	R	273	252	21	G	273	252	21	R	273	252	21	R	273	250	23	R	273	243	30	R	273	254	19	R	273	248	24
1544	G	273	252	21	R	273	254	19	R	273	252	21	G	273	252	21	R	273	252	21	R	273	250	23	R	273	243	30	R	273	254	19	R	273	248	25
1545	G	273	253	21	R	273	254	19	R	273	252	21	G	273	253	21	R	273	252	21	R	273	250	24	R	273	243	30	R	273	254	19	R	273	248	25
1546	G	273	253	20	R	273	254	19	R	273	252	21	G	273	253	20	R	273	252	21	R	273	250	24	R	273	243	30	R	273	254	20	R	273	248	25
1547	G	273	254	20	R	273	254	19	R	273	252	21	G	273	254	20	R	273	252	21	R	273	250	24	R	273	243	30	R	273	254	20	R	273	248	25
1548	G	274	254	20	R	274	254	20	R	274	252	22	G	274	254	20	R	274	252	21	G	274	250	23	R	274	243	31	R	274	254	20	R	274	248	25
1549	G	274	255	19	R	274	254	20	R	274	252	22	G	274	255	19	R	274	252	22	G	274	251	23	R	274	243	31	R	274	254	20	R	274	248	25
1550	G	274	255	19	R	274	254	20	R	274	252	22	G	274	255	19	R	274	252	22	G	274	251	23	R	274	243	31	R	274	254	20	R	274	248	25
1551	G	274	256	19	R	274	254	20	G	274	253	22	G	274	256	19	R	274	252	22	G	274	252	22	R	274	243	31	R	274	254	20	R	274	248	26
1552	G	274	256	18	R	274	254	20	G	274	253	21	G	274	256	18	R	274	252	22	G	274	252	22	R	274	243	31	R	274	254	20	R	274	248	26
1553	G	274	257	18	R	274	254	20	G	274	254	21	G	274	257	18	R	274	252	22	G	274	253	22	R	274	243	31	R	274	254	21	R	274	248	26
1554	G	274	257	17	R	274	254	20	G	274	254	20	G	274	257	17	R	274	252	22	G	274	253	21	R	274	243	31	R	274	254	21	R	274	248	26
1555	G	275	258	17	R	275	254	21	G	275	255	20	G	275	258	17	R	275	252	22	G	275	254	21	R	275	243	32	R	275	254	21	R	275	248	26
1556	G	275	258	17	R	275	254	21	G	275	255	20	G	275	258	17	R	275	252	23	G	275	254	21	R	275	243	32	R	275	254	21	R	275	248	26
1557	G	275	259	16	R	275	254	21	G	275	256	19	G	275	259	16	R	275	252	23	G	275	255	20	R	275	243	32	R	275	254	21	R	275	248	26
1558	G	275	259	16	R	275	254	21	G	275	256	19	G	275	259	16	R	275	252	23	G	275	255	20	R	275	243	32	R	275	254	21	R	275	248	27
1559	G	275	260	16	R	275	254	21	G	275	257	19	G	275	260	16	R	275	252	23	G	275	256	20	R	275	243	32	R	275	254	21	R	275	248	27
1560	G	275	260	15	R	275	254	21	G	275	257	18	G	275	260	15	R	275	252	23	G	275	256	19	R	275	243	32	R	275	254	22	R	275	248	27
1561	R	275	260	15	G	275	255	21	G	275	258	18	R	275	260	15	G	275	253	23	G	275	257	19	R	275	243	32	R	275	254	22	R	275	248	27
1562	R	276	260	16	G	276	255	21	G	276	258	18	R	276	260	16	G	276	253	22	G	276	257	19	R	276	243	33	R	276	254	22	R	276	248	27

Table C-1. Continued

A=Arrivals, D=Departures, Q=Queue:

Time (sec)		A	D	Q		A	D	Q		A	D	Q		A	D	Q		A	D	Q		A	D	Q		A	D	Q		A	D	Q		A	D	Q
1563	R	276	260	16	G	276	256	20	G	276	259	17	R	276	260	16	G	276	254	22	G	276	258	18	R	276	243	33	R	276	254	22	R	276	248	27
1564	R	276	260	16	G	276	256	20	G	276	259	17	R	276	260	16	G	276	254	22	G	276	258	18	R	276	243	33	R	276	254	22	R	276	248	28
1565	R	276	260	16	G	276	257	20	G	276	260	17	R	276	260	16	G	276	255	21	G	276	259	17	R	276	243	33	R	276	254	22	R	276	248	28
1566	R	276	260	16	G	276	257	19	G	276	260	16	R	276	260	16	G	276	255	21	G	276	259	17	R	276	243	33	R	276	254	22	R	276	248	28
1567	R	276	260	16	G	276	258	19	G	276	261	16	R	276	260	16	G	276	256	21	G	276	260	17	G	276	244	33	R	276	254	23	R	276	248	28
1568	R	276	260	16	G	276	258	18	G	276	261	15	R	276	260	16	G	276	256	20	G	276	260	16	G	276	244	32	R	276	254	23	R	276	248	28
1569	R	277	260	17	G	277	259	18	G	277	262	15	R	277	260	17	G	277	257	20	G	277	261	16	G	277	245	32	R	277	254	23	R	277	248	28
1570	R	277	260	17	G	277	259	18	G	277	262	15	R	277	260	17	G	277	257	20	G	277	261	16	G	277	245	32	R	277	254	23	R	277	248	28
1571	R	277	260	17	G	277	260	17	R	277	262	15	R	277	260	17	G	277	258	19	G	277	262	15	G	277	246	31	R	277	254	23	R	277	248	29
1572	R	277	260	17	G	277	260	17	R	277	262	15	R	277	260	17	G	277	258	19	G	277	262	15	G	277	246	31	R	277	254	23	R	277	248	29
1573	R	277	260	17	G	277	261	17	R	277	262	15	R	277	260	17	G	277	259	19	G	277	263	15	G	277	247	31	R	277	254	23	R	277	248	29
1574	R	277	260	17	G	277	261	16	R	277	262	15	R	277	260	17	G	277	259	18	R	277	263	15	G	277	247	30	R	277	254	24	R	277	248	29
1575	R	277	260	17	G	277	262	16	R	277	262	15	R	277	260	17	G	277	260	18	R	277	263	15	G	277	248	30	R	277	254	24	R	277	248	29
1576	R	278	260	18	G	278	262	16	R	278	262	16	R	278	260	18	G	278	260	17	R	278	263	15	G	278	248	30	R	278	254	24	R	278	248	29
1577	R	278	260	18	G	278	263	15	R	278	262	16	R	278	260	18	G	278	261	17	R	278	263	15	G	278	249	29	R	278	254	24	R	278	248	29
1578	R	278	260	18	G	278	263	15	R	278	262	16	R	278	260	18	G	278	261	17	R	278	263	15	G	278	249	29	R	278	254	24	R	278	248	30
1579	R	278	260	18	G	278	264	15	R	278	262	16	R	278	260	18	G	278	262	16	R	278	263	15	G	278	250	29	R	278	254	24	R	278	248	30
1580	R	278	260	18	G	278	264	14	R	278	262	16	R	278	260	18	G	278	262	16	R	278	263	16	G	278	250	28	R	278	254	24	R	278	248	30
1581	R	278	260	18	R	278	264	14	R	278	262	16	R	278	260	18	G	278	263	16	R	278	263	16	G	278	251	28	R	278	254	25	R	278	248	30
1582	R	279	260	19	R	279	264	15	R	279	262	17	R	279	260	19	G	279	263	15	R	279	263	16	G	279	251	28	R	279	254	25	R	279	248	30
1583	R	279	260	19	R	279	264	15	R	279	262	17	R	279	260	19	G	279	264	15	R	279	263	16	G	279	252	27	R	279	254	25	R	279	248	30
1584	R	279	260	19	R	279	264	15	R	279	262	17	R	279	260	19	G	279	264	15	R	279	263	16	G	279	252	27	R	279	254	25	R	279	248	30
1585	R	279	260	19	R	279	264	15	R	279	262	17	R	279	260	19	G	279	265	14	R	279	263	16	G	279	253	26	R	279	254	25	R	279	248	31
1586	R	279	260	19	R	279	264	15	R	279	262	17	R	279	260	19	G	279	265	14	R	279	263	16	G	279	253	26	R	279	254	25	R	279	248	31
1587	R	279	260	19	R	279	264	15	R	279	262	17	R	279	260	19	R	279	265	14	R	279	263	17	G	279	254	26	R	279	254	25	R	279	248	31
1588	R	279	260	19	R	279	264	15	R	279	262	17	R	279	260	19	R	279	265	14	R	279	263	17	G	279	254	25	R	279	254	26	R	279	248	31
1589	R	280	260	20	R	280	264	16	R	280	262	18	R	280	260	20	R	280	265	14	R	280	263	17	G	280	255	25	R	280	254	26	R	280	248	31
1590	R	280	260	20	R	280	264	16	R	280	262	18	R	280	260	20	R	280	265	14	R	280	263	17	G	280	255	25	R	280	254	26	R	280	248	31
1591	R	280	260	20	R	280	264	16	R	280	262	18	R	280	260	20	R	280	265	15	R	280	263	17	G	280	256	24	R	280	254	26	R	280	248	31
1592	R	280	260	20	R	280	264	16	R	280	262	18	R	280	260	20	R	280	265	15	R	280	263	17	G	280	256	24	R	280	254	26	R	280	248	32
1593	R	280	260	20	R	280	264	16	R	280	262	18	R	280	260	20	R	280	265	15	R	280	263	17	G	280	257	24	R	280	254	26	R	280	248	32
1594	R	280	260	20	R	280	264	16	R	280	262	18	R	280	260	20	R	280	265	15	R	280	263	18	G	280	257	23	R	280	254	26	G	280	249	31
1595	R	280	260	20	R	280	264	16	R	280	262	18	R	280	260	20	R	280	265	15	R	280	263	18	G	280	258	23	R	280	254	27	G	280	249	31
1596	R	281	260	21	R	281	264	17	R	281	262	19	R	281	260	21	R	281	265	15	R	281	263	18	G	281	258	23	R	281	254	27	G	281	250	31
1597	R	281	260	21	R	281	264	17	R	281	262	19	R	281	260	21	R	281	265	15	R	281	263	18	G	281	259	22	R	281	254	27	G	281	250	30
1598	R	281	260	21	R	281	264	17	R	281	262	19	R	281	260	21	R	281	265	16	R	281	263	18	G	281	259	22	R	281	254	27	G	281	251	30
1599	R	281	260	21	R	281	264	17	R	281	262	19	R	281	260	21	R	281	265	16	R	281	263	18	G	281	260	21	R	281	254	27	G	281	251	30
1600	R	281	260	21	R	281	264	17	R	281	262	19	R	281	260	21	R	281	265	16	R	281	263	19	G	281	260	21	R	281	254	27	G	281	252	29
1601	G	281	261	21	R	281	264	17	R	281	262	19	R	281	260	21	R	281	265	16	R	281	263	19	G	281	261	21	R	281	254	27	G	281	252	29
1602	G	281	261	20	R	281	264	17	R	281	262	19	R	281	260	21	R	281	265	16	R	281	263	19	G	281	261	20	R	281	254	28	G	281	253	28
1603	G	282	262	20	R	282	264	18	R	282	262	20	R	282	260	22	R	282	265	16	R	282	263	19	G	282	262	20	R	282	254	28	G	282	253	28
1604	G	282	262	20	R	282	264	18	R	282	262	20	R	282	260	22	R	282	265	16	R	282	263	19	G	282	262	20	R	282	254	28	G	282	254	28
1605	G	282	263	19	R	282	264	18	R	282	262	20	R	282	260	22	R	282	265	17	R	282	263	19	G	282	263	19	R	282	254	28	G	282	254	27
1606	G	282	263	19	R	282	264	18	R	282	262	20	R	282	260	22	R	282	265	17	R	282	263	19	G	282	263	19	R	282	254	28	G	282	255	27
1607	G	282	264	19	R	282	264	18	R	282	262	20	R	282	260	22	R	282	265	17	R	282	263	20	G	282	264	19	R	282	254	28	G	282	255	27
1608	G	282	264	18	R	282	264	18	R	282	262	20	R	282	260	22	R	282	265	17	R	282	263	20	G	282	264	18	R	282	254	28	G	282	256	26
1609	G	282	265	18	R	282	264	18	R	282	262	20	R	282	260	22	R	282	265	17	R	282	263	20	G	282	265	18	R	282	254	29	G	282	256	26
1610	G	283	265	18	R	283	264	19	R	283	262	21	R	283	260	23	R	283	265	17	R	283	263	20	G	283	265	18	R	283	254	29	G	283	257	26
1611	G	283	266	17	R	283	264	19	G	283	263	20	R	283	260	23	R	283	265	17	R	283	263	20	G	283	266	17	R	283	254	29	G	283	257	25
1612	G	283	266	17	R	283	264	19	G	283	263	20	R	283	260	23	R	283	265	18	R	283	263	20	G	283	266	17	R	283	254	29	G	283	258	25
1613	G	283	267	16	R	283	264	19	G	283	264	19	G	283	261	22	R	283	265	18	R	283	263	20	G	283	267	16	R	283	254	29	G	283	258	25
1614	G	283	267	16	R	283	264	19	G	283	264	19	C	283	261	22	R	283	265	18	R	283	263	21	G	283	267	16	R	283	254	29	G	283	259	24
1615	G	283	268	16	R	283	264	19	G	283	265	19	C	283	262	22	R	283	265	18	R	283	263	21	G	283	268	16	R	283	254	29	G	283	259	24
1616	G	283	268	15	R	283	264	19	G	283	265	18	G	283	262	21	R	283	265	18	R	283	263	21	G	283	268	15	R	283	254	30	G	283	260	24
1617	G	284	269	15	R	284	264	20	G	284	266	18	G	284	263	21	R	284	265	18	R	284	263	21	G	284	269	15	R	284	254	30	G	284	260	23
1618	G	284	269	15	R	284	264	20	G	284	266	18	G	284	263	21	R	284	265	19	R	284	263	21	G	284	269	15	R	284	254	30	G	284	261	23
1619	G	284	270	14	R	284	264	20	G	284	267	17	G	284	264	20	R	284	265	19	R	284	263	21	G	284	270	14	R	284	254	30	G	284	261	22
1620	G	284	270	14	R	284	264	20	G	284	267	17	G	284	264	20	R	284	265	19	R	284	263	21	G	284	270	14	R	284	254	30	G	284	262	22
1621	R	284	270	14	G	284	265	20	G	284	268	17	G	284	265	20	R	284	265	19	R	284	263	22	R	284	270	14	G	284	254	30	G	284	262	22
1622	R	284	270	14	G	284	265	19	G	284	268	16	G	284	265	19	R	284	265	19	R	284	263	22	R	284	270	14	G	284	255	29	G	284	263	21
1623	R	284	270	14	G	284	266	19	G	284	269	16	G	284	266	19	R	284	265	19	R	284	263	22	R	284	270	14	G	284	255	29	G	284	263	21
1624	R	285	270	15	G	285	266	19	G	285	269	16	G	285	266	19	R	285	265	19	R	285	263	22	R	285	270	15	G	285	256	29	G	285	264	21
1625	R	285	270	15	G	285	267	18	G	285	270	15	G	285	267	18	R	285	265	20	R	285	263	22	R	285	270	15	G	285	256	28	G	285	264	20
1626	R	285	270	15	G	285	267	18	G	285	270	15	G	285	267	18	R	285	265	20	G	285	263	22	R	285	270	15	G	285	257	28	G	285	265	20
1627	R	285	270	15	G	285	268	18	G	285	271	15	G	285	268	18	R	285	265	20	G	285	264	21	R	285	270	15	G	285	257	28	G	285	265	20
1628	R	285	270	15	G	285	268	17	G	285	271	14	G	285	268	17	R	285	265	20	G	285	264	21	R	285	270	15	G	285	258	27	G	285	266	19
1629	R	285	270	15	G	285	269	17	G	285	272	14	G	285	269	17	R	285	265	20	G	285	265	21	R	285	270	15	G	285	258	27	G	285	266	19
1630	R	285	270	15	G	285	269	16	G	285	272	13	G	285	269	16	R	285	265	20	G	285	265	20	R	285	270	15	G	285	259	27	G	285	267	19
1631	R	286	270	16	G	286	270	16	R	286	272	14	G	286	270	16	R	286	265	20	G	286	266	20	R	286	270	16	G	286	259	26	G	286	267	18
1632	R	286	270	16	G	286	270	16	R	286	272	14	G	286	270	16	R	286	265	21	G	286	266	20	R	286	270	16	G	286	260	26	G	286	268	18
1633	R	286	270	16	G	286	271	15	R	286	272	14	G	286	271	15	R	286	265	21	G	286	267	19	R	286	270	16	G	286	260	26	G	286	268	17
1634	R	286	270	16	G	286	271	15	R	286	272	14	G	286	271	15	R	286	265	21	G	286	267	19	R	286	270	16	G	286	261	25	G	286	269	17
1635	R	286	270	16	G	286	272	15	R	286	272	14	G	286	272	15	R	286	265	21	G	286	268	19	R	286	270	16	G	286	261	25	G	286	269	17
1636	R	286	270	16	G	286	272	14	R	286	272	14	G	286	272	14	R	286	265	21	G	286	268	18	R	286	270	16	G	286	262	25	G	286	270	16
1637	R	286	270	16	G	286	273	14	R	286	272	14	G	286	273	14	R	286	265	21	G	286	269	18	R	286	270	16	G	286	262	24	G	286	270	16
1638	R	287	270	17	G	287	273	14	R	287	272	15	G	287	273	14	R	287	265	21	G	287	269	17	R	287	270	17	G	287	263	24	G	287	271	16
1639	R	287	270	17	G	287	274	13	R	287	272	15	R	287	273	14	G	287	266	21	G	287	270	17	R	287	270	17	G	287	263	23	G	287	271	15
1640	R	287	270	17	G	287	274	13	R	287	272	15	R	287	273	14	G	287	266	21	G	287	270	17	R	287	270	17	G	287	264	23	G	287	272	15
1641	R	287	270	17	R	287	274	13	R	287	272	15	R	287	273	14	G	287	267	20	G	287	271	16	R	287	270	17	G	287	264	23	G	287	272	15
1642	R	287	270	17	R	287	274	13	R	287	272	15	R	287	273	14	G	287	267	20	G	287	271	16	R	287	270	17	G	287	265	22	G	287	273	14
1643	R	287	270	17	R	287	274	13	R	287	272	15	R	287	273	14	G	287	268	20	G	287	272	16	R	287	270	17	G	287	265	22	G	287	273	14
1644	R	287	270	17	R	287	274	13	R	287	272	15	R	287	273	14	G	287	268	19	G	287	272	15	R	287	270	17	G	287	266	22	G	287	274	14
1645	R	288	270	18	R	288	274	14	R	288	272	16	R	288	273	15	G	288	269	19	G	288	273	15	R	288	270	18	G	288	266	21	G	288	274	13

Table C-1. Continued

A=Arrivals, D=Departures, Q=Queue:

Time (sec)		A	D	Q		A	D	Q		A	D	Q		A	D	Q		A	D	Q		A	D	Q		A	D	Q		A	D	Q		A	D	Q
1646	R	288	270	18	R	288	274	14	R	288	272	16	R	288	273	15	G	288	269	19	G	288	273	15	R	288	270	18	G	288	267	21	G	288	275	13
1647	R	288	270	18	R	288	274	14	R	288	272	16	R	288	273	15	G	288	270	18	G	288	274	14	R	288	270	18	G	288	267	21	G	288	275	12
1648	R	288	270	18	R	288	274	14	R	288	272	16	R	288	273	15	G	288	270	18	G	288	274	14	R	288	270	18	G	288	268	20	R	288	275	13
1649	R	288	270	18	R	288	274	14	R	288	272	16	R	288	273	15	G	288	271	17	G	288	275	14	R	288	270	18	G	288	268	20	R	288	275	13
1650	R	289	270	19	R	288	274	14	R	288	272	16	R	288	273	15	G	288	271	17	G	288	275	13	R	289	270	19	G	288	269	20	R	288	275	13
1651	R	288	270	18	R	288	274	14	R	288	272	16	R	288	273	15	G	288	272	17	G	288	276	13	R	288	270	18	G	288	269	19	R	288	275	13
1652	R	289	270	19	R	289	274	15	R	289	272	17	R	289	273	16	G	289	272	16	R	289	276	13	R	289	270	19	G	289	270	19	R	289	275	13
1653	R	289	270	19	R	289	274	15	R	289	272	17	R	289	273	16	G	289	273	16	R	289	276	13	R	289	270	19	G	289	270	18	R	289	275	13
1654	R	289	270	19	R	289	274	15	R	289	272	17	R	289	273	16	G	289	273	16	R	289	276	13	R	289	270	19	G	289	271	18	R	289	275	14
1655	R	289	270	19	R	289	274	15	R	289	272	17	R	289	273	16	G	289	274	15	R	289	276	13	R	289	270	19	G	289	271	18	R	289	275	14
1656	R	289	270	19	R	289	274	15	R	289	272	17	R	289	273	16	G	289	274	15	R	289	276	14	R	289	270	19	G	289	272	17	R	289	275	14
1657	R	289	270	19	R	289	274	15	R	289	272	17	R	289	273	16	G	289	275	15	R	289	276	14	R	289	270	19	G	289	272	17	R	289	275	14
1658	R	289	270	19	R	289	274	15	R	289	272	17	R	289	273	16	G	289	275	14	R	289	276	14	R	289	270	19	G	289	273	17	R	289	275	14
1659	R	290	270	20	R	290	274	16	R	290	272	18	R	290	273	17	G	290	276	14	R	290	276	14	R	290	270	20	G	290	273	16	R	290	275	14
1660	R	290	270	20	R	290	274	16	R	290	272	18	R	290	273	17	G	290	276	14	R	290	276	14	R	290	270	20	G	290	274	16	R	290	275	14
1661	G	290	271	19	R	290	274	16	R	290	272	18	R	290	273	17	G	290	277	13	R	290	276	14	R	290	270	20	G	290	274	16	R	290	275	15
1662	G	290	271	19	R	290	274	16	R	290	272	18	R	290	273	17	G	290	277	13	R	290	276	14	R	290	270	20	G	290	275	15	R	290	275	15
1663	G	290	272	19	R	290	274	16	R	290	272	18	R	290	273	17	G	290	278	13	R	290	276	15	R	290	270	20	G	290	275	15	R	290	275	15
1664	G	290	272	18	R	290	274	16	R	290	272	18	R	290	273	17	G	290	278	12	R	290	276	15	R	290	270	20	G	290	276	15	R	290	275	15
1665	G	290	273	18	R	290	274	16	R	290	272	18	R	290	273	17	R	290	278	12	R	290	276	15	R	290	270	20	G	290	276	14	R	290	275	15
1666	G	291	273	18	R	291	274	17	R	291	272	19	R	291	273	18	R	291	278	12	R	291	276	15	R	291	270	21	G	291	277	14	R	291	275	15
1667	G	291	274	17	R	291	274	17	R	291	272	19	R	291	273	18	R	291	278	13	R	291	276	15	R	291	270	21	G	291	277	13	R	291	275	15
1668	G	291	274	17	R	291	274	17	R	291	272	19	R	291	273	18	R	291	278	13	R	291	276	15	R	291	270	21	G	291	278	13	R	291	275	16
1669	G	291	275	17	R	291	274	17	R	291	272	19	R	291	273	18	R	291	278	13	R	291	276	15	R	291	270	21	G	291	278	13	R	291	275	16
1670	G	291	275	16	R	291	274	17	R	291	272	19	R	291	273	18	R	291	278	13	R	291	276	16	R	291	270	21	G	291	279	12	R	291	275	16
1671	G	291	276	16	R	291	274	17	G	291	273	19	R	291	273	18	R	291	278	13	R	291	276	16	R	291	270	21	G	291	279	12	R	291	275	16
1672	G	292	276	16	R	292	274	18	G	292	273	19	R	292	273	19	R	292	278	13	R	292	276	16	R	292	270	22	G	292	280	12	R	292	275	16
1673	G	292	277	15	R	292	274	18	G	292	274	18	R	292	273	19	R	292	278	13	R	292	276	16	R	292	270	22	G	292	280	11	R	292	275	16
1674	G	292	277	15	R	292	274	18	G	292	274	18	R	292	273	19	R	292	278	14	R	292	276	16	R	292	270	22	G	292	281	11	R	292	275	16
1675	G	292	278	14	R	292	274	18	G	292	275	17	R	292	273	19	R	292	278	14	R	292	276	16	R	292	270	22	R	292	281	11	R	292	275	17
1676	G	292	278	14	R	292	274	18	G	292	275	17	R	292	273	19	R	292	278	14	R	292	276	16	R	292	270	22	R	292	281	11	R	292	275	17
1677	G	292	279	14	R	292	274	18	G	292	276	17	R	292	273	19	R	292	278	14	R	292	276	17	R	292	270	22	R	292	281	11	R	292	275	17
1678	G	292	279	13	R	292	274	18	G	292	276	16	R	292	273	19	R	292	278	14	R	292	276	17	R	292	270	22	R	292	281	12	R	292	275	17
1679	G	293	280	13	R	293	274	19	G	293	277	16	R	293	273	20	R	293	278	14	R	293	276	17	R	293	270	23	R	293	281	12	R	293	275	17
1680	G	293	280	13	R	293	274	19	G	293	277	16	R	293	273	20	R	293	278	14	R	293	276	17	R	293	270	23	R	293	281	12	R	293	275	17
1681	R	293	280	13	G	293	275	18	G	293	278	15	R	293	273	20	R	293	278	15	R	293	276	17	R	293	270	23	R	293	281	12	R	293	275	17
1682	R	293	280	13	G	293	275	18	G	293	278	15	R	293	273	20	R	293	278	15	R	293	276	17	R	293	270	23	R	293	281	12	R	293	275	18
1683	R	293	280	13	G	293	276	18	G	293	279	15	R	293	273	20	R	293	278	15	R	293	276	17	R	293	270	23	R	293	281	12	R	293	275	18
1684	R	293	280	13	G	293	276	17	G	293	279	14	R	293	273	20	R	293	278	15	R	293	276	18	R	293	270	23	R	293	281	12	R	293	275	18
1685	R	293	280	13	G	293	277	17	G	293	280	14	R	293	273	20	R	293	278	15	R	293	276	18	R	293	270	23	R	293	281	13	R	293	275	18
1686	R	294	280	14	G	294	277	17	G	294	280	14	R	294	273	21	R	294	278	15	R	294	276	18	R	294	270	24	R	294	281	13	R	294	275	18
1687	R	294	280	14	G	294	278	16	G	294	281	13	R	294	273	21	R	294	278	15	R	294	276	18	R	294	270	24	R	294	281	13	R	294	275	18
1688	R	294	280	14	G	294	278	16	G	294	281	13	R	294	273	21	R	294	278	16	R	294	276	18	R	294	270	24	R	294	281	13	R	294	275	18
1689	R	294	280	14	G	294	279	15	G	294	282	12	R	294	273	21	R	294	278	16	R	294	276	18	R	294	270	24	R	294	281	13	R	294	275	19
1690	R	294	280	14	G	294	279	15	G	294	282	12	R	294	273	21	R	294	278	16	R	294	276	19	R	294	270	24	R	294	281	13	R	294	275	19
1691	R	294	280	14	G	294	280	15	R	294	282	12	G	294	274	21	R	294	278	16	R	294	276	19	R	294	270	24	R	294	281	13	R	294	275	19
1692	R	294	280	14	G	294	280	14	R	294	282	12	G	294	274	20	R	294	278	16	R	294	276	19	R	294	270	24	R	294	281	14	R	294	275	19
1693	R	295	280	15	G	295	281	14	R	295	282	13	G	295	275	20	R	295	278	16	R	295	276	19	R	295	270	25	R	295	281	14	R	295	275	19
1694	R	295	280	15	G	295	281	14	R	295	282	13	G	295	275	20	R	295	278	16	R	295	276	19	R	295	270	25	R	295	281	14	R	295	275	19
1695	R	295	280	15	G	295	282	13	R	295	282	13	G	295	276	19	R	295	278	17	R	295	276	19	R	295	270	25	R	295	281	14	R	295	275	19
1696	R	295	280	15	G	295	282	13	R	295	282	13	G	295	276	19	R	295	278	17	R	295	276	19	R	295	270	25	R	295	281	14	R	295	275	20
1697	R	295	280	15	G	295	283	13	R	295	282	13	G	295	277	18	R	295	278	17	R	295	276	20	R	295	270	25	R	295	281	14	R	295	275	20
1698	R	295	280	15	G	295	283	12	R	295	282	13	G	295	277	18	R	295	278	17	R	295	276	20	R	295	270	25	R	295	281	14	R	295	275	20
1699	R	295	280	15	G	295	284	12	R	295	282	13	G	295	278	18	R	295	278	17	R	295	276	20	R	295	270	25	R	295	281	15	R	295	275	20
1700	R	296	280	16	G	296	284	12	R	296	282	14	G	296	278	18	R	296	278	17	R	296	276	20	R	296	270	26	R	296	281	15	R	296	275	20
1701	R	296	280	16	R	296	284	12	R	296	282	14	G	296	279	17	R	296	278	17	R	296	276	20	R	296	270	26	R	296	281	15	R	296	275	20
1702	R	296	280	16	R	296	284	12	R	296	282	14	G	296	279	17	R	296	278	18	R	296	276	20	R	296	270	26	R	296	281	15	R	296	275	20
1703	R	296	280	16	R	296	284	12	R	296	282	14	G	296	280	16	R	296	278	18	R	296	276	20	R	296	270	26	R	296	281	15	R	296	275	21
1704	R	296	280	16	R	296	284	12	R	296	282	14	G	296	280	16	R	296	278	18	G	296	276	20	R	296	270	26	R	296	281	15	R	296	275	21
1705	R	296	280	16	R	296	284	12	R	296	282	14	G	296	281	16	R	296	278	18	G	296	277	20	R	296	270	26	R	296	281	15	R	296	275	21
1706	R	296	280	16	R	296	284	12	R	296	282	14	G	296	281	15	R	296	278	18	G	296	277	19	R	296	270	26	R	296	281	16	R	296	275	21
1707	R	297	280	17	R	297	284	13	R	297	282	15	G	297	282	15	R	297	278	18	G	297	278	19	R	297	270	27	R	297	281	16	R	297	275	21
1708	R	297	280	17	R	297	284	13	R	297	282	15	G	297	282	15	R	297	278	19	G	297	278	19	R	297	270	27	R	297	281	16	R	297	275	21
1709	R	297	280	17	R	297	284	13	R	297	282	15	G	297	283	14	R	297	278	19	G	297	279	18	R	297	270	27	R	297	281	16	R	297	275	21
1710	R	297	280	17	R	297	284	13	R	297	282	15	G	297	283	14	R	297	278	19	G	297	279	18	R	297	270	27	R	297	281	16	R	297	275	22
1711	R	297	280	17	R	297	284	13	R	297	282	15	G	297	284	14	R	297	278	19	G	297	280	18	R	297	270	27	R	297	281	16	R	297	275	22
1712	R	297	280	17	R	297	284	13	R	297	282	15	G	297	284	13	R	297	278	19	G	297	280	17	R	297	270	27	R	297	281	16	R	297	275	22
1713	R	297	280	17	R	297	284	13	R	297	282	15	G	297	285	13	R	297	278	19	G	297	281	17	R	297	270	27	R	297	281	17	R	297	275	22
1714	R	298	280	18	R	298	284	14	R	298	282	16	G	298	285	13	R	298	278	19	G	298	281	16	R	298	270	28	R	298	281	17	R	298	275	22
1715	R	298	280	18	R	298	284	14	R	298	282	16	G	298	286	12	R	298	278	20	G	298	282	16	R	298	270	28	R	298	281	17	R	298	275	22
1716	R	298	280	18	R	298	284	14	R	298	282	16	G	298	286	12	R	298	278	20	G	298	282	16	R	298	270	28	R	298	281	17	R	298	275	22
1717	R	298	280	18	R	298	284	14	R	298	282	16	R	298	286	12	G	298	279	19	G	298	283	15	R	298	270	28	R	298	281	17	R	298	275	23
1718	R	298	280	18	R	298	284	14	R	298	282	16	R	298	286	12	G	298	279	19	G	298	283	15	R	298	270	28	R	298	281	17	R	298	275	23
1719	R	298	280	18	R	298	284	14	R	298	282	16	R	298	286	12	G	298	280	19	G	298	284	15	R	298	270	28	R	298	281	17	R	298	275	23
1720	R	298	280	18	R	298	284	14	R	298	282	16	R	298	286	12	G	298	280	18	G	298	284	14	R	298	270	28	R	298	281	18	R	298	275	23
1721	G	299	281	18	R	299	284	15	R	299	282	17	R	299	286	13	G	299	281	18	G	299	285	14	R	299	270	29	R	299	281	18	R	299	275	23
1722	G	299	281	18	R	299	284	15	R	299	282	17	R	299	286	13	G	299	281	18	G	299	285	14	R	299	270	29	R	299	281	18	R	299	275	23
1723	G	299	282	17	R	299	284	15	R	299	282	17	R	299	286	13	G	299	282	17	G	299	286	13	R	299	270	29	R	299	281	18	R	299	275	23
1724	G	299	282	17	R	299	284	15	R	299	282	17	R	299	286	13	G	299	282	17	G	299	286	13	R	299	270	29	R	299	281	18	R	299	275	24
1725	G	299	283	17	R	299	284	15	R	299	282	17	R	299	286	13	G	299	283	16	G	299	287	13	R	299	270	29	R	299	281	18	R	299	275	24
1726	G	299	283	16	R	299	284	15	R	299	282	17	R	299	286	13	G	299	283	16	G	299	287	12	R	299	270	29	R	299	281	19	R	299	275	24
1727	G	299	284	16	R	299	284	15	R	299	282	17	R	299	286	13	G	299	284	16	G	299	288	12	R	299	270	29	R	299	281	19	R	299	275	24
1728	G	300	284	16	R	300	284	16	R	300	282	18	R	300	286	14	G	300	284	15	G	300	288	11	R	300	270	30	R	300	281	19	R	300	275	24

Table C-1. Continued

A=Arrivals, D=Departures, Q=Queue:

Time (sec)	A	D	Q	A	D	Q	A	D	Q	A	D	Q	A	D	Q	A	D	Q	A	D	Q	A	D	Q	A	D	Q	A	D	Q
1729	G	300	285	15	R	300	284	16	R	300	282	18	R	300	286	14	G	300	285	15	G	300	289	11	G	300	271	29	R	300	281	19	R	300	275	24
1730	G	300	285	15	R	300	284	16	R	300	282	18	R	300	286	14	G	300	285	15	R	300	289	11	G	300	271	29	R	300	281	19	R	300	275	24
1731	G	300	286	15	R	300	284	16	G	300	283	18	R	300	286	14	G	300	286	14	R	300	289	11	G	300	272	29	R	300	281	19	R	300	275	25
1732	G	300	286	14	R	300	284	16	G	300	283	17	R	300	286	14	G	300	286	14	R	300	289	12	G	300	272	28	R	300	281	19	R	300	275	25
1733	G	300	287	14	R	300	284	16	G	300	284	17	R	300	286	14	G	300	287	14	R	300	289	12	G	300	273	28	R	300	281	20	R	300	275	25
1734	G	300	287	13	R	300	284	16	G	300	284	16	R	300	286	14	G	300	287	13	R	300	289	12	G	300	273	27	R	300	281	20	R	300	275	25
1735	G	301	288	13	R	301	284	17	G	301	285	16	R	301	286	15	G	301	288	13	R	301	289	12	G	301	274	27	R	301	281	20	R	301	275	25
1736	G	301	288	13	R	301	284	17	G	301	285	16	R	301	286	15	G	301	288	13	R	301	289	12	G	301	274	27	R	301	281	20	R	301	275	25
1737	G	301	289	12	R	301	284	17	G	301	286	15	R	301	286	15	G	301	289	12	R	301	289	12	G	301	275	26	R	301	281	20	R	301	275	25
1738	G	301	289	12	R	301	284	17	G	301	286	15	R	301	286	15	G	301	289	12	R	301	289	12	G	301	275	26	R	301	281	20	R	301	275	26
1739	G	301	290	12	R	301	284	17	G	301	287	15	R	301	286	15	G	301	290	11	R	301	289	13	G	301	276	26	R	301	281	20	R	301	275	26
1740	G	301	290	11	R	301	284	17	G	301	287	14	R	301	286	15	G	301	290	11	R	301	288	13	G	301	276	25	R	301	281	21	R	301	275	26
1741	R	301	290	11	G	301	285	17	G	301	288	14	R	301	286	15	G	301	291	11	R	301	289	13	G	301	277	25	R	301	281	21	R	301	275	26
1742	R	302	290	12	G	302	285	17	G	302	288	14	R	302	286	16	G	302	291	10	R	302	289	13	G	302	277	25	R	302	281	21	R	302	275	26
1743	R	302	290	12	G	302	286	16	G	302	289	13	R	302	286	16	R	302	291	11	R	302	289	13	G	302	278	24	R	302	281	21	R	302	275	26
1744	R	302	290	12	G	302	286	16	G	302	289	13	R	302	286	16	R	302	291	11	R	302	289	13	G	302	278	24	R	302	281	21	R	302	275	27
1745	R	302	290	12	G	302	287	16	G	302	290	13	R	302	286	16	R	302	291	11	R	302	289	13	G	302	278	24	R	302	281	21	R	302	275	27
1746	R	302	290	12	G	302	287	15	G	302	290	12	R	302	286	16	R	302	291	11	R	302	289	14	G	302	278	23	R	302	281	21	R	302	275	27
1747	R	302	290	12	G	302	288	15	G	302	291	12	R	302	286	16	R	302	291	11	R	302	289	14	G	302	280	23	R	302	281	22	R	302	275	27
1748	R	302	290	12	G	302	288	14	G	302	291	11	R	302	286	16	R	302	291	11	R	302	289	14	G	302	280	22	R	302	281	22	R	302	275	27
1749	R	303	290	13	G	303	289	14	G	303	292	11	R	303	286	17	R	303	291	11	R	303	289	14	G	303	281	22	R	303	281	22	R	303	275	27
1750	R	303	290	13	G	303	289	14	G	303	292	11	R	303	286	17	R	303	291	12	R	303	289	14	G	303	281	22	R	303	281	22	R	303	275	27
1751	R	303	290	13	G	303	290	13	R	303	292	11	R	303	286	17	R	303	291	12	R	303	289	14	G	303	282	21	R	303	281	22	R	303	275	28
1752	R	303	290	13	G	303	290	13	R	303	292	11	R	303	286	17	R	303	291	12	R	303	289	14	G	303	282	21	R	303	281	22	R	303	275	28
1753	R	303	290	13	G	303	291	13	R	303	292	11	R	303	286	17	R	303	291	12	R	303	289	15	G	303	283	21	R	303	281	22	R	303	275	28
1754	R	303	290	13	G	303	291	12	R	303	292	11	R	303	286	17	R	303	291	12	R	303	289	15	G	303	283	20	R	303	281	23	R	303	275	28
1755	R	303	290	13	C	303	292	12	R	303	292	11	R	303	286	17	R	303	291	12	R	303	289	15	C	303	284	20	R	303	281	23	R	303	275	28
1756	R	304	290	14	G	304	292	12	R	304	292	12	R	304	286	18	R	304	291	12	R	304	289	15	G	304	284	20	R	304	281	23	G	304	276	28
1757	R	304	290	14	G	304	293	11	R	304	292	12	R	304	286	18	R	304	291	13	R	304	289	15	G	304	285	19	R	304	281	23	G	304	276	27
1758	R	304	290	14	G	304	293	11	R	304	292	12	R	304	286	18	R	304	291	13	R	304	289	15	G	304	285	19	R	304	281	23	G	304	277	27
1759	R	304	290	14	G	304	294	11	R	304	292	12	R	304	286	18	R	304	291	13	R	304	289	15	G	304	286	19	R	304	281	23	G	304	277	27
1760	R	304	290	14	C	304	294	10	R	304	292	12	R	304	286	10	R	304	291	13	R	304	289	16	C	304	286	18	R	304	281	23	C	304	278	26
1761	R	304	290	14	R	304	294	10	R	304	292	12	R	304	286	10	R	304	291	13	R	304	289	16	C	304	287	18	R	304	281	24	C	304	278	26
1762	R	305	290	15	R	305	294	11	R	305	292	13	R	305	286	18	R	305	291	13	R	305	289	16	G	305	287	18	R	305	281	24	G	305	278	26
1763	R	305	290	15	R	305	294	11	R	305	292	13	R	305	286	18	R	305	291	13	R	305	289	16	G	305	288	17	R	305	281	24	G	305	278	25
1764	R	305	290	15	R	305	294	11	R	305	292	13	R	305	286	18	R	305	291	14	R	305	289	16	G	305	288	17	R	305	281	24	G	305	280	25
1765	R	305	290	15	R	305	294	11	R	305	292	13	R	305	286	19	R	305	291	14	R	305	289	16	C	305	289	16	R	305	281	24	G	305	280	25
1766	R	305	290	15	R	305	294	11	R	305	292	13	R	305	286	19	R	305	291	14	R	305	289	16	C	305	289	16	R	305	281	24	G	305	281	24
1767	R	305	290	15	R	305	294	11	R	305	292	13	R	305	286	19	R	305	291	14	R	305	289	17	C	305	290	16	R	305	281	24	G	305	281	24
1768	R	305	290	15	R	305	294	11	R	305	292	13	R	305	286	19	R	305	291	14	R	305	289	17	G	305	290	15	R	305	281	25	G	305	282	23
1769	R	306	290	16	R	306	294	12	R	306	292	14	G	306	287	19	R	306	291	14	R	306	289	17	G	306	291	15	R	306	281	25	G	306	282	23
1770	R	306	290	16	R	306	294	12	R	306	292	14	G	306	287	19	R	306	291	14	R	306	289	17	G	306	291	15	R	306	281	25	G	306	283	23
1771	R	306	290	16	R	306	294	12	R	306	292	14	C	306	288	10	R	306	291	15	R	306	289	17	C	306	292	14	R	306	281	25	C	306	283	22
1772	R	306	290	16	R	306	294	12	R	306	292	14	C	306	288	10	R	306	291	15	R	306	289	17	C	306	292	14	R	306	281	25	C	306	284	22
1773	R	306	290	16	R	306	294	12	R	306	292	14	C	306	289	10	R	306	291	15	R	306	289	17	C	306	293	14	R	306	281	25	C	306	284	22
1774	R	306	290	16	R	306	294	12	R	306	292	14	G	306	289	17	R	306	291	15	R	306	289	18	G	306	293	13	R	306	281	25	G	306	285	21
1775	R	308	290	18	R	308	294	12	R	308	292	14	G	308	290	17	R	308	291	15	R	308	289	18	G	308	294	13	R	308	281	26	G	308	285	21
1776	R	307	290	17	R	307	294	13	R	307	292	15	G	307	290	17	R	307	291	15	R	307	289	18	G	307	294	13	R	307	281	26	G	307	288	21
1777	R	307	290	17	R	307	294	13	R	307	292	15	G	307	291	16	R	307	291	15	R	307	289	18	G	307	295	12	R	307	281	26	G	307	286	20
1778	R	307	290	17	R	307	294	13	R	307	292	15	G	307	291	16	R	307	291	16	R	307	289	18	G	307	295	12	R	307	281	26	G	307	287	20
1779	R	307	290	17	R	307	294	13	R	307	292	15	G	307	292	15	R	307	291	16	R	307	289	18	G	307	296	11	R	307	281	26	G	307	287	20
1780	R	307	290	17	R	307	294	13	R	307	292	15	G	307	292	15	R	307	291	16	R	307	289	19	G	307	296	11	R	307	281	26	G	307	288	19
1781	G	307	291	17	R	307	294	13	R	307	292	15	G	307	293	15	R	307	291	16	R	307	289	19	G	307	297	11	R	307	281	26	G	307	288	19
1782	G	307	291	16	R	307	294	13	R	307	292	15	G	307	293	14	R	307	291	16	G	307	289	18	G	307	297	10	R	307	281	27	G	307	289	18
1783	G	308	292	16	R	308	294	14	R	308	292	16	G	308	294	14	R	308	291	16	G	308	290	18	R	308	297	11	G	308	281	26	G	308	289	18
1784	G	308	292	16	R	308	294	14	R	308	292	16	G	308	294	14	R	308	291	16	G	308	290	18	R	308	297	11	G	308	282	26	G	308	290	18
1785	G	308	293	15	R	308	294	14	R	308	292	16	G	308	295	13	R	308	291	17	G	308	291	17	R	308	297	11	G	308	282	26	G	308	290	17
1786	G	308	293	15	R	308	294	14	R	308	292	16	G	308	295	13	R	308	291	17	G	308	291	17	R	308	297	11	G	308	283	25	G	308	291	17
1787	G	308	294	15	R	308	294	14	R	308	292	16	G	308	296	13	R	308	291	17	G	308	292	17	R	308	297	11	G	308	283	25	G	308	291	17
1788	G	308	294	14	R	308	294	14	R	308	292	16	G	308	296	12	R	308	291	17	G	308	292	16	R	308	297	11	G	308	284	24	G	308	292	16
1789	G	308	295	14	R	308	294	14	R	308	292	16	G	308	297	12	R	308	291	17	G	308	293	16	R	308	297	11	G	308	284	24	G	308	292	16
1790	G	309	295	14	R	309	294	15	R	309	292	17	G	309	297	12	R	309	291	17	G	309	293	15	R	309	297	12	G	309	285	24	G	309	293	16
1791	G	309	296	13	R	309	294	15	G	309	293	16	G	309	298	11	R	309	291	17	G	309	294	15	R	309	297	12	G	309	285	23	G	309	293	15
1792	C	309	296	13	R	309	294	15	C	309	293	16	G	309	298	11	R	309	291	16	C	309	294	15	R	309	297	12	C	309	286	23	C	309	294	15
1793	C	309	297	12	R	309	294	15	C	309	294	15	G	309	299	10	R	309	291	16	C	309	295	14	R	309	297	12	C	309	286	23	C	309	294	15
1794	C	309	297	12	R	309	294	15	C	309	294	15	G	309	299	10	R	309	291	16	C	309	295	14	R	309	297	12	C	309	287	22	C	309	295	14
1795	G	309	298	12	R	309	294	15	G	309	295	15	R	309	299	10	G	309	292	18	G	309	296	14	R	309	297	12	G	309	287	22	G	309	295	14
1796	G	309	298	11	R	309	294	15	G	309	295	14	R	309	299	10	G	309	292	17	G	309	296	13	R	309	297	12	G	309	288	22	G	309	296	14
1797	G	310	299	11	R	310	294	16	G	310	296	14	R	310	299	11	G	310	293	17	G	310	297	13	R	310	297	13	G	310	288	21	G	310	296	13
1798	C	310	299	11	R	310	294	16	C	310	296	14	R	310	299	11	C	310	293	17	G	310	297	13	R	310	297	13	C	310	289	21	C	310	297	13
1799	G	310	300	10	R	310	294	16	G	310	297	13	R	310	299	11	G	310	294	16	G	310	298	12	R	310	297	13	G	310	289	21	G	310	297	12
1800	G	310	300	10	R	310	294	16	G	310	297	13	R	310	299	11	G	310	294	16	G	310	298	12	R	310	297	13	G	310	290	20	G	310	298	12

REFERENCES

1. P. Tarnoff and J. Ordonez, Signal Timing Practices and Procedures, Institute of Transportation Engineers, March 2004, pp. 1-3,

2. Hurdle, V.F., Signalized Intersection Delay Models – A Primer for the Uninitiated, *Transportation Research Record 971*, TRB, National Research Council, Washington, D.C., 1984, pp. 96-105.

3. Dowling, R. G., Definition, Interpretation and Calculation of Traffic Analysis Tools Measures of Effectiveness, Final Report, Dowling Associates, Inc., November 2006

4. *Highway Capacity Manual*. TRB, National Research Council, Washington, D.C., 2000

5. M. Saito, J. Walker and A. Zundel, Use of Image Analysis to Estimate Average Stopped Delays Per Vehicle at Signalized Intersections, *Transportation Research Record 1776*, National Research Council, Washington, D.C., 2001, pp. 106-112,

6. Engelbrecht, R.J., Fambro, D. B., Rouphail, N.M. and Barkawi, A.A., Validation of Generalized Delay Model for Oversaturated Conditions, *Transportation Research Record 1572*, TRB, National Research Council, Washington, D.C., 1997, pp.122-130

7. Potts, I. B., Bauer, K. M., Harwood, D. W., Ringert, J. F., Zeeger, J. D., Gilmore, D. K., Relationship of Lane Width to Saturation Flow Rate on Urban and Suburban Signalized Intersection Approaches, Transportation Research Board 2007 Annual Meeting Compendium of Papers

8. Lin, F., Chang, C., Tseng, P., Errors in Capacity and Timing Design Analyses of Signalized Intersections in the Absence of Steady Queue Discharge Rates, Transportation Research Board 2007 Annual Meeting Compendium of Papers

9. Maddula, S. M*onitoting the Performance of a Signalized Intersection by Video Image Detection.* Masters Thesis, August 1994, Department of Civil Engineering, University of Florida.

10. Lall, K.B., Berka, S., Eghtedari, A.G. and Fowler, J. Intersection Delay Measurement Using Video Detection Systems. In proceedings of the *Third International Symposium on Highway Capacity*, Volume 2, Copenhagen, Denmark, June 1998, pp.711-727.

11. Quiroga, C.A. and Bullock, D. Measuring Control Delay at Signalized Intersections. July/August 1999, Journal of Transportation Engineering, Vol. 125, No. 4, pp. 271-280

12. Zheng, J., Wang, Y., Niahan, N.L., Hallenbeck, M.E., Detecting Cycle Failures at Signalized Intersections Using Video Image Processing, *Transportation Research Board 84th Annual Meeting*, TRB, National Research Council, Washington, D.C., January, 2005

13. Hoeschen, B., Bullock, D., and Schlappi, M., A Systematic Procedure for Estimating Intersection Control Delay from Large GPS Travel Time Data Sets. *Transportation Research Board 84th Annual Meeting*, TRB, National Research Council, Washington, D.C., January, 2005

14. Sun, C., Ritchie, S.G., Tsai, K., and Jayakrishnan, R. Use of Vehicle Signature Analysis and Lexicographic Optimization for Vehicle Reidentification on Freeways. In *Transportation Research*, Part C, 1999, pp.168-185.

15. Palen, J., Coifman, B., Sun, C., Ritchie, S., and Varaiya, P. California Partners for Advanced Transit and Highways (PATH) Enhanced Loop-Based Traffic Surveillance Program. In *ITS Quarterly*, Fall 2000, pp.17-25.

16. Liu, H.X., Oh, J. and Recker, W. *Adaptive Signal Control System with On-Line Performance Measure*. December 2001, Institute of Transportation Studies, University of California, Irvine

17. Sun, C., Arr, G., Ramachandran, R.P. and Ritchie, S.G. Vehicle Reidentification Using Multi-Detector Fusion. July 2002, IEEE Transactions (forthcoming)

18. Oh, C. and Ritchie, S.G. *Real-Time Inductive-Signature-Based Level of Service for Signalized Intersections*, December 2001, Institute of Transportation Studies, University of California, Irvine

19. Coifman, B. and Ergueta, E. *Improved Vehicle Reidentification and Travel Time Measurement on Congested Freeways*, September/October 2003, Journal of Transportation Engineering, Vol. 129, No. 5, pp. 475-483

20. Coifman, B. and Dhoorjaty, S. *Event Data-Based Traffic Detector Validation Tests*, May/June 2004, Journal of Transportation Engineering, Vol. 130, No. 3, pp. 313-321

21. Jeng, S., Ritchie, S. G., Tok, Y. C., Freeway Corridor Performance Measurement Based on Vehicle Reidentification, Transportation Research Board 2007 Annual Meeting Compendium of Papers, Washington D.C.

22. Washburn, S. and Nihan, N., *Estimating Link Travel Time with the Mobilizer Video Image Tracking System*, January/February 1999, Journal of Transportation Engineering, Vol. 125, No. 1, pp. 15-20

23. Grenard, J.L., Bullock, D. and Tarko, A.P. *Evaluation of Selected Video Detection Systems at Signalized Intersections*, November 2001, School of Civil Engineering, Purdue University

24. Bonneson, J and Abbas, M. *Video Detection for Intersection and Interchange Control*, September 2002, Texas Transportation Institute, Texas A&M University

25. Oh, J. and Leonard, J.D. Ve*hicle Detection Using Video Image Processing System: Evaluation of PEEK VideoTrak*, July/August 2003, Journal of Transportation Engineering, Vol. 129, No. 4, pp. 462-465

26. Riley, W. R. and Gardner, C. Technique for Measuring Delay at Intersections, *Transportation Research Record 644*, TRB, National Research Council, Washington, D.C.,1977, pp. 1-7

27. Bonneson, J, Modeling Queued Driver Behavior at Signalized Junctions, In *Transportation Research Record 1365*, TRB, National Research Council, Washington, D.C., 1992, pp.99-107.

28. Fambro, D. and Rouphail, N. Generalized Delay Model for Signalized Intersections and Arterial Streets. In *Transportation Research Record 1572*, TRB, National Research Council, Washington, D.C., 1997, pp.112-121.

29. Tarko, A.P. and Tracz, M., Uncertainty in saturation Flow Predictions, In *Transportation Research Circular E-C018*, TRB, National Research Council, Washington, D.C., June 2000, pp.310-321.

30. Li, H. and Prevedouros, P.D., Detailed Observations of Saturation Headways and Start-Up Lost Times. In *Transportation Research Record 1802*, TRB, National Research Council, Washington, D.C., 2002, pp.44-53.

31. Cohen, S.L., Application of Car-Following Systems to Queue Discharge Problem at Signalized Intersections. In *Transportation Research Record 1802*, TRB, National Research Council, Washington, D.C., 2002, pp.205-213.

32. Mousa, R.M., Simulation Modeling and Variability Assessment of Delays at Traffic Signals, March/April 2003, Journal of Transportation Engineering, Vol. 129, No 2, pp. 177-185

33. Rakha, H. and Zhang, W., Consistency of Shock-wave and Queuing Theory Procedures for Analysis of roadway Bottlenecks, *Transportation Research Board 84th Annual Meeting*, TRB, National Research Council, Washington, D.C., January, 2005

34. Perez-Cartagena, R.I. and Tarko, A.P., Calibration of Capacity Parameters for Signalized Intersections in Indiana, *Transportation Research Board 84th Annual Meeting*, TRB, National Research Council, Washington, D.C., January, 2005

35. Kebab, W., Dixon, M., and Abdel-Raheim, A., Field Measurement of Approach Delay at Signalized Intersections Using Point Data, Transportation Research Board 2007 Annual Meeting Compendium of Papers, Washington D.C.

36. Brilon, W., Geistefeldt, J., and Zurlinden, H., Implementing the Concept of Reliability for Highway Capacity Analysis, *Transportation Research Board 86th Annual Meeting*, TRB, National Research Council, Washington, D.C., January, 2007

37. Jiang, Y., Li, S., and Zhu, K.Q., "Traffic Delay Studies at Signalized Intersections with Global Positioning System Devices", ITE Journal, August 2005

38. Ko, J., Hunter, M., and Guensler, R., Measuring Control Delay Using Second-By-Second GPS Speed Data, *Transportation Research Board 86th Annual Meeting*, TRB, National Research Council, Washington, D.C., January, 2007

39. Comert, G. and Certin, M., Queue Length Estimation from Probe Vehicle Location: Undersaturated Conditions, Transportation Research Board 2007 Annual Meeting Compendium of Papers, Washington D.C.

40. Wunnava, S., Yen, K., Babji, T., Zavaletta, R. Romero, R. and Archilla, C., Travel Time Estimation Using Cell Phones (TTECP) for Highways and Roadways, Final Report, Florida Atlantic University, January 29, 2007

41. Buckholz, J. and Lee, S., TSDViewer Program Documentation, Unpublished Research Report, University of Florida, October 3, 2007

42. Buckholz, J. and Lee, S., DTDiagram Program Documentation, Unpublished Research Report, University of Florida, October 3, 2007

43. Buckholz, J, BuckTRAJ Program Documentation, Unpublished Research Report, University of Florida, October 3, 2007

44. A Policy on Geometric Design of Highways and Streets, Fifth Edition, 2004, American Association of State Highway and Transportation Officials

45. Courage, K. G., Fambro, D. B., Akcelik, R, Lin, P. S., Anwar, M., & Viloria, F., Capacity Analysis of Traffic-Actuated Intersections, December 1996, University of Florida, NCHRP Project 3-48 Final Report

46. Long, G., Startup Delays of Queued Vehicles, *Transportation Research Board 84th Annual Meeting*, TRB, National Research Council, Washington, D.C., January, 2005

47. Akcelik, R, Time-Dependent Expressions for Delay, Stop Rate and Queue Length at Traffic Signals, October 1980, Australian Road Research Board Internal Report AIR 367-1

48. Courage, K. G., Summary of HCM Procedure Inputs, Process and Outputs, University of Florida Transportation Research Center, Draft Working Paper 385-2, January 2007

49. Tarko, A. P., Perez-Cartagena, R.I., 2005, Variability of Peak Hour Factors at Intersections, Transportation Research Record: Journal of the Transportation Research Board No.1920, pp 125-130

50. Hellinga, B., and Abdy, Z., Impact of Day-to-Day Variability of Peak Hour Volumes on Signalized Intersection Performance, Transportation Research Board 2007 Annual Meeting Compendium of Papers, Washington D.C.

51. Zhang, L. and Prevedouros, P.D., User Perceptions of Signalized Intersection Level of Service, *Transportation Research Board 84th Annual Meeting*, TRB, National Research Council, Washington, D.C., January, 2005

BIOGRAPHICAL SKETCH

Jeffrey W. Buckholz is president and chief traffic engineer for JW Buckholz Traffic Engineering Inc of Jacksonville Florida as well as an adjunct professor at the University of North Florida. Mr. Buckholz holds a masters degree in civil engineering with a transportation major from the University of California at Berkeley and both a masters of business administration degree and a bachelor of science degree in civil engineering from the University of Toledo. He is a registered civil engineer in Florida, Georgia, Massachusetts, Ohio, Michigan and California and is a state-certified unlimited electrical contractor in Florida and Georgia

Mr. Buckholz is a senior level traffic engineer with 26 years of wide-ranging experience in the transportation profession. This experience includes transportation planning and traffic impact analysis, highway capacity analysis, advanced signal system design, traffic signal construction, traffic signal timing, and ITS design. He is a court certified expert witness in the field of traffic engineering and is also certified by the International Municipal Signal Association as a Level II Traffic Signal Technician. In addition, he has authored three training manuals on traffic signal design, construction, and inspection for the International Municipal Signal Association.